

ornl

**OAK RIDGE
NATIONAL
LABORATORY**

LOCKHEED MARTIN



MANAGED AND OPERATED BY
LOCKHEED MARTIN ENERGY RESEARCH CORPORATION
FOR THE UNITED STATES
DEPARTMENT OF ENERGY

ORNL-27 (3-96)

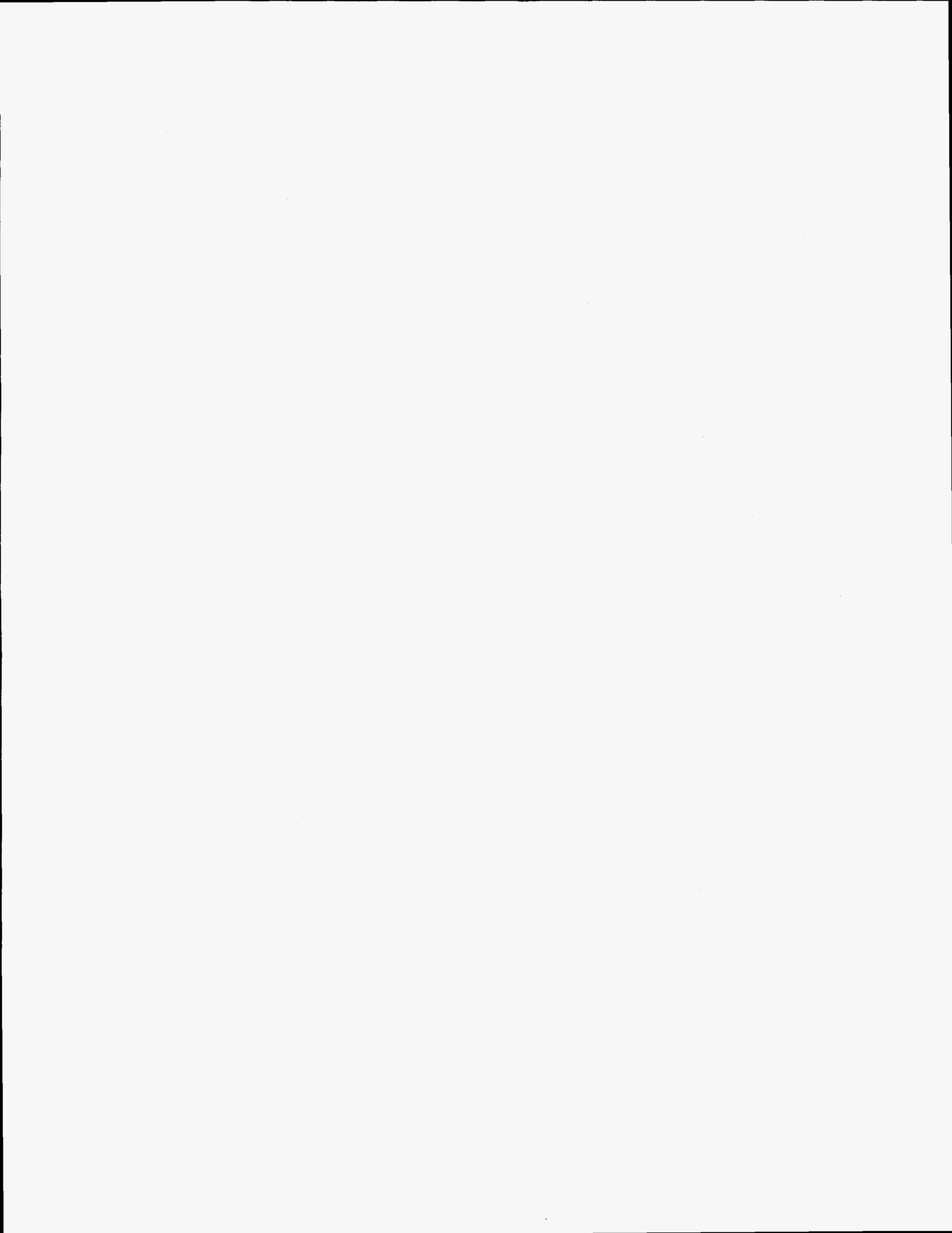
RECEIVED

OCT 27 1998

OSTI

ORNL/TM-11778/R1

A User's Manual for MASH v1.5 — A Monte Carlo Adjoint Shielding Code System



Computational Physics and Engineering Division

**A USER'S MANUAL FOR MASH v1.5 - A MONTE
CARLO ADJOINT SHIELDING CODE SYSTEM**

Editor:

Jeffrey O. Johnson

Primary Contributors:

Charles O. Slater, Johnnie M. Barnes, James D. Drischler, and Jeffrey O. Johnson
Oak Ridge National Laboratory

DATE PUBLISHED – October 1998

This work is sponsored by the Defense Special Weapons Agency,
DSWA Order No. 98-3020, DOE Interagency Agreement No. 0046-I121-A1,
and the U. S. Army National Ground Intelligence Center,
MIPR No. 3397, DOE Interagency Agreement No. 1205-E097-A1

Prepared by
Oak Ridge National Laboratory
Oak Ridge, Tennessee 37831
managed by
Lockheed Martin Energy Research
for the
U. S. DEPARTMENT OF ENERGY
under Contract No. DE-AC05-96OR22464

This report has been reproduced directly from the best available copy.

Available to DOE and DOE contractors from the Office of Scientific and Technical Information, P. O. Box 62, Oak Ridge, TN 37831; prices available from (423) 576-8401.

This report was prepared as an account of work sponsored by an agency of the United States Government. Neither the United States Government nor any agency thereof, nor any of their employees, makes any warranty, express or implied, or assumes any legal liability or responsibility for the accuracy, completeness, or usefulness of any information, apparatus, product, or process disclosed, or represents that its use would not infringe privately owned rights. Reference herein to any specific commercial product, process, or service by trade name, trademark, manufacturer, or otherwise, does not necessarily constitute or imply its endorsement, recommendation, or favoring by the United States Government or any agency thereof. The views and opinions of authors expressed herein do not necessarily state or reflect those of the United States Government of any agency thereof.

DISCLAIMER

Portions of this document may be illegible in electronic image products. Images are produced from the best available original document.

TABLE OF CONTENTS

	Page
LIST OF FIGURES	ix
LIST OF TABLES	xiii
PREFACE	xv
ABSTRACT	xvii
1.0 MASH: A MONTE CARLO ADJOINT SHIELDING CODE SYSTEM	1-1
1.1 INTRODUCTION TO MASH	1-1
1.1.1 Background	1-1
1.1.2 History of MASH v1.0 Development	1-1
1.1.3 Summary of Corrections and Improvements to MASH V1.0	1-5
1.2 STRUCTURE OF MASH v1.5	1-7
1.3 STRUCTURE OF MASH USER'S MANUAL	1-7
1.3.1 The Main Text	1-7
1.3.2 The Appendices	1-12
1.3.3 The Sample Problem	1-12
1.4 REFERENCES	1-12
2.0 GIP: A GROUP-ORGANIZED CROSS SECTION INPUT PROGRAM ..	2-1
2.1 INTRODUCTION TO GIP	2-1
2.1.1 Background	2-1
2.1.2 Method Used	2-1
2.2 GIP INPUT REQUIREMENTS	2-2
2.3 GIP INPUT DATA NOTES	2-3
2.3.1 Special Diffusion Theory Option	2-7
2.3.2 Upscatter Option	2-7
2.3.3 Adjoint Reordering Example	2-7
2.4 INPUT LIBRARY FORMAT	2-8
2.4.1 ANISN Nuclide Format Cross-Section File	2-10
2.5 GIP OUTPUT FILE	2-11
2.6 LOGICAL UNIT REQUIREMENTS	2-13
2.7 REFERENCES	2-13
2.8 SAMPLE PROBLEM	2-14
3.0 GRTUNCL: A TWO-DIMENSIONAL ANALYTIC FIRST COLLISION SOURCE CODE	3-1
3.1 INTRODUCTION TO GRTUNCL	3-1
3.1.1 Background	3-1
3.1.2 Method Used	3-2
3.2 GRTUNCL INPUT REQUIREMENTS	3-4

TABLE OF CONTENTS
(continued)

		Page
3.3	GRTUNCL INPUT DATA NOTES	3-6
	3.3.1 Adjoint Reordering Example	3-12
3.4	INPUT LIBRARY FORMAT	3-13
	3.4.1 ALC1 Formatted Cross-Section Input File	3-13
	3.4.2 ANISN Nuclide Format Cross-Section File	3-14
	3.4.3 GIP Formatted Cross-Section Input File	3-16
3.5	GRTUNCL OUTPUT FILE	3-18
3.6	LOGICAL UNIT REQUIREMENTS	3-21
3.7	REFERENCES	3-21
3.8	SAMPLE PROBLEM	3-22
4.0	GRTUNCL3D - A THREE DIMENSIONAL ANALYTIC FIRST COLLISION SOURCE CODE.....	4-1
5.0	DORT; A TWO-DIMENSIONAL DISCRETE ORDINATES TRANSPORT CODE.....	5-1
5.1	INTRODUCTION TO DORT	5-1
	5.1.1 Background	5-1
	5.1.2 The Problem Solved	5-1
	5.1.3 Code Structure	5-2
5.2	THEORETICAL BASIS	5-3
	5.2.1 The Integro-Differential Transport Equation	5-3
	5.2.2 The Finite Difference Formulation	5-4
	5.2.3 Fluence Evaluation Strategy	5-8
	5.2.4 Additional Theory Information	5-10
5.3	DORT INPUT DATA SPECIFICATIONS	5-11
	5.3.1 Card-Image Format	5-11
	5.3.2 Space Meshes	5-12
	5.3.3 Variable Space Mesh	5-13
	5.3.4 Variable Directional Quadrature	5-13
	5.3.5 Variable Legendre Expansion	5-13
	5.3.6 Adjoint Data	5-13
	5.3.7 Card-Image Input Specifications	5-14
5.4	DORT INPUT REQUIREMENTS	5-14
5.5	DORT INPUT DATA NOTES	5-25
	5.5.1 Special Geometry Features	5-25
	5.5.2 Special Theory Options	5-26
	5.5.3 Cross Section Input and Mixing	5-27
	5.5.4 Activity Edits	5-29
	5.5.5 Negative Source Removal	5-30
	5.5.6 Problem Type Specification	5-30
	5.5.7 Iteration Limits and Convergence	5-31
	5.5.8 Search Strategy	5-33
	5.5.9 Upscatter Rebalance	5-34
	5.5.10 Fission Rescaling	5-34

TABLE OF CONTENTS
(continued)

		Page
	5.5.11 Fission Extrapolation	5-35
	5.5.12 Error-Mode Extrapolation	5-35
	5.5.13 Fluence Iteration Acceleration	5-36
	5.5.14 Stabilization	5-37
	5.5.15 Input Source and Fluence Specification	5-38
	5.5.16 Key Fluence Monitoring	5-38
	5.5.17 Energy Boundary Input	5-38
	5.5.18 Fluence Extrapolation Model	5-39
	5.5.19 Alternate Zone Map Input	5-40
	5.5.20 Note on DORT Mesh for an Air-Over-Ground Problem	5-40
5.6	DORT INPUT AND OUTPUT FILE FORMATS	5-42
5.7	LOGICAL UNIT REQUIREMENTS	5-52
	5.7.1 Input and Output Data Files	5-52
	5.7.2 Scratch Data Sets	5-52
5.8	DETAILS OF DORT JOB REQUIREMENTS	5-54
	5.8.1 CPU Time Usage	5-54
	5.8.2 Problem Printed Output	5-54
5.9	REFERENCES	5-58
5.10	SAMPLE PROBLEM	5-59
6.0 TORT:	3-DIMENSIONAL DISCRETE ORDINATES NEUTRON-PHOTON TRANSPORT CODE	6-1
7.0 VISTA:	A VARIABLE INPUT SOURCE TRANSFORMATION AND ASSEMBLY CODE	7-1
7.1	INTRODUCTION TO VISTA	7-1
	7.1.1 Background	7-1
	7.1.2 Method Used	7-1
7.2	VISTA INPUT REQUIREMENTS	7-2
7.3	VISTA INPUT DATA NOTES	7-4
7.4	VISTA INPUT FLUENCE FILE FORMAT	7-5
7.5	VISTA OUTPUT FILE	7-8
7.6	LOGICAL UNIT REQUIREMENTS	7-9
7.7	REFERENCES	7-10
7.8	SAMPLE PROBLEM	7-10
8.0 VISTA3D:	A VARIABLE INPUT SOURCE TRANSFORMATION AND ASSEMBLY CODE FOR TORT FLUX DATA	8-1
9.0 MORSE:	A MULTIGROUP OAK RIDGE STOCHASTIC EXPERIMENT CODE	9-1
9.1	INTRODUCTION TO MORSE	9-1
	9.1.1 Theoretical Basis	9-2

TABLE OF CONTENTS
(continued)

		Page
	9.1.2 In-Group Energy Biasing	9-6
9.2	MORSE CODE STRUCTURE	9-7
	9.2.1 Random Walk Module	9-8
	9.2.2 Multigroup Cross-Section Module	9-12
	9.2.3 The GIFT5 Geometry Package	9-17
	9.2.4 Modifications to MORSE for In-Group Biasing	9-21
	9.2.5 Modifications to MORSE-CG for the MASH Code System	9-22
9.3	MORSE INPUT REQUIREMENTS	9-22
	9.3.1 Random Walk Input Instructions	9-25
	9.3.2 Cross Section Module Input Instructions	9-31
	9.3.3 Special MASH Input Instructions	9-33
	9.3.4 GIFT5 Geometry Input Instructions	9-34
9.4	ANISN NUCLIDE FORMAT CROSS-SECTION FILE	9-39
9.5	MORSE LEAKAGE TAPE OUTPUT FILE FOR DRC2	9-41
9.6	LOGICAL UNIT REQUIREMENTS	9-44
9.7	REFERENCES	9-45
9.8	SAMPLE PROBLEM	9-47
10.0	DRC2: A CODE WITH SPECIALIZED APPLICATIONS FOR COUPLING LOCALIZED MONTE CARLO ADJOINT CALCULATIONS WITH FLUENCES FROM TWO-DIMENSIONAL R-Z DORT DISCRETE ORDINATES AIR-OVER-GROUND CALLCULATIONS.....	10-1
10.1	INTRODUCTION TO DRC2	10-1
	10.1.1 History	10-1
	10.1.2 Background	10-1
	10.1.3 Method Used	10-2
10.2	DRC2 INPUT REQUIREMENTS	10-7
10.3	DRC2 INPUT DATA NOTES	10-9
	10.3.1 Common Block Information	10-11
10.4	DRC2 INPUT FILE FORMATS	10-14
10.5	DRC2 OUTPUT FILES AND LOGICAL UNIT REQUIREMENTS .	10-17
10.6	CODE SYSTEM	10-19
10.7	TEST PROBLEMS	10-20
10.8	CONCLUSIONS	10-20
10.9	REFERENCES	10-20
10.10	SAMPLE PROBLEMS.....	10-21
11.0	DRC3 -- A CODE WITH SPECIALIZED APPLICATIONS FOR COUPLING LOCALIZED MONTE CARLO ADJOINT CALCULATIONS WITH FLUENCES FROM THREE-DIMENSIONAL X-Y-Z TORT DISCRETE ORDINATES AIR-OVER-GROUND CALLCULATIONS	11-1
	APPENDIX A: FIDO INPUT	A-1

TABLE OF CONTENTS
(continued)

	Page
APPENDIX B: IN-GROUP ENERGY BIASING	B-1
INTRODUCTION	B-2
BACKGROUND	B-3
THEORETICAL BASIS FOR IN-GROUP ENERGY BIASING	B-3
Markov Chain Analysis of the Forward	
Three-Group Infinite Medium Problem	B-4
Adjoint Three-Group Analysis	B-8
In-Group Energy Bias Analysis	B-10
IN-GROUP BIASING CODE MODIFICATIONS FOR MORSE	B-15
DEMONSTRATION CALCULATIONS	B-16
REFERENCES ..	B-16
APPENDIX C: THE GIFT5 GEOMETRY PACKAGE	C-1
BACKGROUND	C-2
INTRODUCTION	C-3
TARGET DESCRIPTION DATA	C-3
PRELIMINARY STEPS	C-3
SOLIDS	C-4
SOLID TABLE ..	C-27
"COMBINATION" OF SOLIDS	C-27
REGION TABLE	C-30
RECOMMENDED PROCEDURES FOR THE REGION TABLE	C-33
REGION IDENTIFICATION TABLE	C-33
SPECIAL REGION IDENTIFICATION NUMBERS	C-36
USING IDENTIFICATION NUMBERS TO "COMBINE" REGIONS	C-36
RULES FOR REGIONS	C-37
GIFT5 GEOMETRY PACKAGE MEMORY REQUIREMENTS	
AND REGION TOLERANCES	C-39
REGION RPP TABLE	C-40
THE TITLE AND TARGET SPECIFICATION CARDS	C-40
CARD ORDER FOR THE TARGET DESCRIPTION INPUT	C-43
REFERENCES ..	C-43
APPENDIX D: DRC2 VERIFICATION AND VALIDATION	
TEST PROBLEM SUITE	D-1
TEST PROBLEM 1: FREE-FIELD FLUENCE CALCULATION	D-2
TEST PROBLEM 2: METRIC DOGHOUSE	D-2
TEST PROBLEM 3: LARGE (30 m x 6m x 3m) STEEL-TOPPED	
CONCRETE BUILDING.....	D-3
TEST PROBLEM 4: BREN SIX-HOUSE CLUSTER	D-4
TEST PROBLEM 5: LARGE RADIUS, AIR-FILLED, ANNULAR,	
CYLINDRICAL CONCRETE TUNNEL	D-5
REFERENCES ..	D-7

TABLE OF CONTENTS
(continued)

	Page
APPENDIX E: MASH 1.0 CODE SYSTEM ABSTRACT	E-1
APPENDIX F: USER NOTES	F-1
INTRODUCTION	F-1
QUESTIONS AND ANSWERS ON AIR-OVER-GROUND ENVIRONMENT CALCULATIONS WITH GRTUNCL/DORT	F-1
QUESTIONS AND ANSWERS ON ADJOINT MONTE CARLO CALCULATIONS WITH MORSE	F-5

LIST OF FIGURES

Figure		Page
1-1.	Typical MASH Problem Involving an Armored Vehicle	1-2
1-2.	Typical MASH Problem Involving an Enclosed Structure	1-3
1-3.	General Structure of the MASH Code System	1-8
1-4.	Data Flow Diagram of the MASH Code System Environment Calculation.	1-9
1-5.	Data Flow Diagram of the MASH Code System Target Calculation.....	1-10
1-6.	Data Flow Diagram of the MASH Code System Folding of the Environment Calculation and Target Calculation.....	1-11
2-1.	Sample GIP Input for the Two-Meter Box Air-Over-Ground Analysis	2-15
2-2.	Sample GIP Output for the Two-Meter Box Air-Over-Ground Analysis	2-17
3-1.	Schematic Diagram of the Air-Over-Ground Geometry Model Used in the GRTUNCL Analysis	3-23
3-2.	Sample GRTUNCL Input for the Two-Meter Box Air-Over-Ground Analysis	3-24
3-3.	Sample GRTUNCL Output for the Two-Meter Box Air-Over-Ground Analysis	3-26
5-1.	Triangular Geometry Options	5-27
5-2.	Schematic Diagram of the Air-Over-Ground Geometry Model Used in the DORT Analysis	5-61
5-3.	Sample DORT Input for the Two-Meter Box Air-Over-Ground Analysis	5-62
5-4.	Sample DORT Output for the Two-Meter Box Air-Over-Ground Analysis	5-65
7-1.	Schematic Diagram of the Air-Over-Ground Geometry Model Used in the VISTA Analysis	7-12
7-2.	Sample VISTA Input for the Two-Meter Box Air-Over-Ground Analysis	7-13
7-3.	Sample VISTA Output for the Two-Meter Box Air-Over-Ground Analysis	7-14

LIST OF FIGURES

Figure		Page
9-1.	Schematic Diagram of the Two-Meter Box Geometry Model Used in the MORSE Analysis	9-51
9-2.	Sample MORSE Input for the Two-Meter Box Analysis	9-52
10-1	Sample DRC2 Input for the Two-Meter Box Protection Factor Analysis.....	10-23
10-2	Sample DRC2 Output (Unit ft06) For the Two-Miter Box Protection Factor Analysis	10-24
10-3	Sample DRC2 Output (Unit ft10) for the Two-Meter Box Protection Factor Analysis	10-39
10-4	Sample DRC2 Output (Unit ft11) For the Two-Meter Box Protection Factor Analysis	10-44
B-1.	Characteristics of Functions in Equation (27)	B-14
C-1.	Four-faced, Four Vertices, Convex Polyhedron (ARB4) Input	C-6
C-2.	Five-faced, Five Vertices, Convex Polyhedron (ARB5) Input	C-7
C-3.	Five-faced, Six Vertices, Convex Polyhedron (ARB6) Input	C-8
C-4.	Six-faced, Seven Vertices, Convex Polyhedron (ARB7) Input	C-9
C-5.	Six-faces, Eight Vertices, Convex Polyhedron (ARB8) Input	C-10
C-6.	N-faces, Convex Polyhedron (ARBN) Input	C-11
C-7.	Triangular Surfaced (ARS) Polyhedron Input	C-12
C-8.	Box (BOX) Input	C-14
C-9.	Ellipsoid of Revolution (ELL) Input	C-15
C-10.	Input for Ellipsoid with Elliptical Cross Section (ELL G)	C-16
C-11.	Half Space (HAF) Input	C-17
C-12.	Right Angle Wedge (RAW) Input	C-18
C-13.	Right Circular Cylinder (RCC) Input	C-19
C-14.	Right Elliptical Cylinder (REC) Input	C-20
C-15.	Rectangular Parallelepiped (RPP) Input	C-21

LIST OF FIGURES

Figure		Page
C-16.	Sphere (SPH) Input	C-22
C-17.	Truncated Elliptical Cone (TEC) Input	C-23
C-18.	Truncated General Cone (TGC) Input	C-24
C-19.	Torus (TOR) Input	C-25
C-20.	Truncated Right Angle Cone (TRC) Input	C-26
C-21.	Intersection, Subtraction, and Union Between Two Solids	C-29
C-22.	Intersection, Subtraction, and Union Between Three Solids	C-31
C-23.	Card Input for the Region Cards and the Region Table for the Sample Target	C-32
C-24.	Card Input for the Region Identification Table and a Region Identification Table for the Sample Target	C-36
C-25.	Illustrations for Region Rules	C-38
C-26.	Card Input for the Region RPP Table and the Region RPP Table for the Sample Target	C-41
C-27.	Card Input for the Title Card and Target Specification Card	C-42
D-1	Geometry for Test Problem 2: Metric Doghouse	D-8
D-2	Exterior View of the Geometry for Test Problem 3: Large, Steel-Topped Concrete Building	D-9
D-3	Interior View of the Geometry for Test Problems 3: Large, Steel-Topped Concrete Building	D-10
D-4	Geometry for Test Problem 4: BREN Six-House Cluster.....	D-11
D-5	View of the Geometry for Test Problem 4: BREN Six-House Cluster.	D-12
D-6	Sketch of the Geometry for Test Problem 5: Large-Radius, Air-Filled, Annular, Cylindrical Concrete Tunnel.....	D-13

LIST OF TABLES

Table		Page
5-1.	Directional Properties of the Geometries	5-5
5-2.	Typical Stabilization Values	5-37
5-3.	Radial Mesh Away from Source	5-41
5-4.	Mesh Upward from Source	5-41
5-5.	Mesh Downward from Source	5-42
5-6.	Mesh Upward from Ground	5-42
5-7	DORT Scratch Data Set Record Information	5-53
9-1.	BANKR Arguments	9-10
9-2.	Variables that may be Written on Collision Tape (NBIND)	9-11
9-3.	Examples of the Relationship Between Random Walk and Cross-Section Module Group Input Parameters	9-13
9-4.	Location of MASH Arrays in BLANK COMMON	9-23
9-5.	Definition of Variables in Common IVCS	9-24
9-6	Summary Description of Input for Solids Table	9-37
9-7	Definition of Variables in USER COMMON	9-45
10-1	Detector Response Definitions in DRC	10-6
10-2	Definitions of Parameters and Protection Factors used to Characterize the Effectiveness of Shields	10-6
10-3.	Location of DRC Arrays in BLANK COMMON	10-11
10-4.	Definitions of Variables in Common TDT1	10-12
10-5.	Definitions of Variables in Common IDRC	10-13
10-6.	Definitions of Variables in USER COMMON	10-18
C-1.	List of 20 Geometric Solids Used by the GIFT5 Geometry Package	C-5
C-2.	Solid Table for the Sample Target	C-28

LIST OF TABLES

Table	Page
C-3	Identification Numbers Used for Vehicles and Air Regions Within the Vehicles in the GIFT5 Geometry Package C-34
D-1	Comparison of DORT and DRC2 Calculated Fluxes for Test Problem 1: Free-Field Fluence Calculations D-14
D-2	Comparison of DRC 2 Calculated Protection Factors for Test Problem 2: Metric Doghouse..... D-15
D-3	Comparison of DRC2 Calculated Neutron and Gamma-Ray Tissue Dose Protection Factors for Test Problem 3: Large, Steel-Topped Concrete Building D-16
D-4	Comparison of DRC2 Calculated Neutron Tissue Dose Protection Factors for Test Problem 3: Large, Steel-Topped Concrete Building..... D-17
D-5	Comparison of DRC2 Calculated Soft Tissue Kerma Total Protection Factors for Test Problem 4: BREN Six-House Cluster..... D-18
D-6	Comparison of DRC and DRC2 Calculated Soft Tissue Kerma Protection Factors for Test Problem 4: BREN Six-House Cluster D-19
D-7	Comparison of DRC and DRC2 Calculated Soft Tissue Kerma For Test Problem 4: BREN Six-House Cluster. D-20
D-8	Comparison of DRC2 and DORT Calculated Fluences and Doses For Test Problem 5: Large-Radius, Air-Filled, Cylindrical Concrete Tunnel..... D-21
D-9	Maximum Percent Differences Between the Above-Ground Perturbed and Unperturbed Neutron and Gamma-Ray Total Fluences As a Function of a Leakage Surface for Test Problem 5: Large-Radius, Air-Filled, Cylindrical Concrete Tunnel..... D-22

PREFACE

The development of the MASH code system has been due to the efforts of numerous people over a period of several years. All of those involved in the MASH effort would like to express their gratitude to the Defense Special Weapons Agency and the U.S. Army National Ground Intelligence Center who have continuously supported and monitored the project. Since MASH represents a collection of codes, and parts of this manual are extracted from other documents supporting these various codes, the major contributors to the MASH effort deserve mention. Ballistic Research Laboratory (BRL) contributed the GIFT5 geometry package (along with much of its documentation) utilized in the MORSE component of MASH. Science Applications International Corporation (SAIC) contributed the in-group energy biasing methodology incorporated in MORSE (along with much of its documentation) and the programming required to couple the GIFT5 geometry package into the MORSE component of MASH. Furthermore, SAIC collaborated with the extensive programming changes, error debugging, and code testing throughout the development phase of the MASH project. Oak Ridge National Laboratory (ORNL) contributed most of the codes which make up the MASH code system. The ORNL investigators have incorporated the many contributions from within ORNL along with the contributions from the other investigators at BRL and SAIC into the MASH code system and are responsible for the final version of MASH to be released along with the supporting documentation.

Each section within this manual contains its own set of references to acknowledge the principal sources of the contributions to that particular section. These references acknowledge the contributions of those not directly involved with the MASH project, but without their efforts MASH would not exist. Here it is sufficient to state that the efforts of all those who aided this project through technical consultation, code programming and testing, review, manuscript preparation, and administrative support are gratefully acknowledged.

Jeffrey O. Johnson, editor

ABSTRACT

The Monte Carlo Adjoint Shielding Code System, MASH, calculates neutron and gamma-ray environments and radiation protection factors for armored military vehicles, structures, trenches, and other shielding configurations by coupling a forward discrete ordinates air-over-ground transport calculation with an adjoint Monte Carlo treatment of the shielding geometry. Efficiency and optimum use of computer time are emphasized. The code system includes the GRTUNCL and DORT codes for air-over-ground transport calculations, the MORSE code with the GIFT5 combinatorial geometry package for adjoint shielding calculations, and several peripheral codes that perform the required data preparations, transformations, and coupling functions. The current version, MASH v1.5, is the successor to the original MASH v1.0 code system initially developed at Oak Ridge National Laboratory (ORNL).

The discrete ordinates calculation determines the fluence on a coupling surface surrounding the shielding geometry due to an external neutron/gamma-ray source. The Monte Carlo calculation determines the effectiveness of the fluence at that surface in causing a response in a detector within the shielding geometry, i.e., the "dose importance" of the coupling surface fluence. A coupling code folds the fluence together with the dose importance, giving the desired dose response. The coupling code can determine the dose response as a function of the shielding geometry orientation relative to the source, distance from the source, and energy response of the detector.

This user's manual includes a short description of each code, the input required to execute the code along with some helpful input data notes, and a representative sample problem (input data and selected output edits) for each code.

1.0 MASH: A MONTE CARLO ADJOINT SHIELDING CODE SYSTEM

1.1 INTRODUCTION TO MASH

1.1.1 Background

An armored vehicle can provide important protection against the effects of a nuclear weapon. In the case of a tactical weapon, prompt radiation may be the dominant effect over a considerable area surrounding the detonation. The Monte Carlo Adjoint Shielding Code System (MASH) was developed by Oak Ridge National Laboratory (ORNL) to facilitate the calculation of radiation protection factors for a given vehicle; i.e., the ratio by which the free-field radiation is reduced due to the presence of the vehicle.¹ MASH was constructed by linking together a discrete-ordinates air-over-ground transport calculation and an adjoint Monte Carlo vehicle dose-importance calculation. A typical problem involving an armored vehicle is shown in Figure 1-1. While the code system was principally designed to be used for vehicles, MASH is also applicable to other shielded structures. A typical problem involving a shielded structure, such as a house, is shown in Figure 1-2.

The typical MASH problem involves the detonation of a low-kiloton yield tactical nuclear weapon within a kilometer of the target (vehicle). The air-over-ground transport calculation determines the neutron and photon fluence as a function of energy on a coupling surface surrounding the target (vehicle). The dose-importance calculation determines the effectiveness of particles at the coupling surface in contributing to dose at a detector position within the target (vehicle). A coupling code folds the fluence together with the dose importance, giving the dose response. The coupling code can also rotate the vehicle, move it to different distances from the source, and perturb the energy response of the detector.

1.1.2 History of MASH v1.0 Development

MASH was developed as an improvement/extension of the Vehicle Code System (VCS)^{2,3} originally developed at ORNL. VCS was initially developed as a four-code system including MORSE, DOT, DRC, and VISA. MORSE⁴ is both a forward and an adjoint Monte Carlo transport code which can calculate the fluence in the complicated three-dimensional vehicle geometry. DOT⁵ is a two-dimensional discrete ordinates radiation transport code which calculates the energy- and angle-dependent free-field initial radiation environment. DRC couples the adjoint fluences from MORSE with the free-field environments from DOT to calculate the radiation environments or protection factors at "detector" locations in the vehicle or structure. VISA is used to format the DOT angular fluence into a data file for use by DRC.

VCS was regularly used at ORNL, the Ballistic Research Laboratory (BRL), Science Applications International Corporation (SAIC), Lawrence Livermore National Laboratory (LLNL), and Wehrwissenschaftliche Dienststelle der Bundeswehr fur ABC-Schutz (WWD), West Germany⁶ for the calculations of neutron and gamma-ray protection factors of military vehicles, structures, trenches, and other shield configurations. VCS represented a powerful tool for coupling complex geometry calculations into single free-field environments, and as such, had applications to a great many shielding problems. Past applications included a wide variety of Army vehicles, house shielding at Hiroshima and Nagasaki, trench shielding factors at the Nevada Test Site, and in-missile radiation environments.

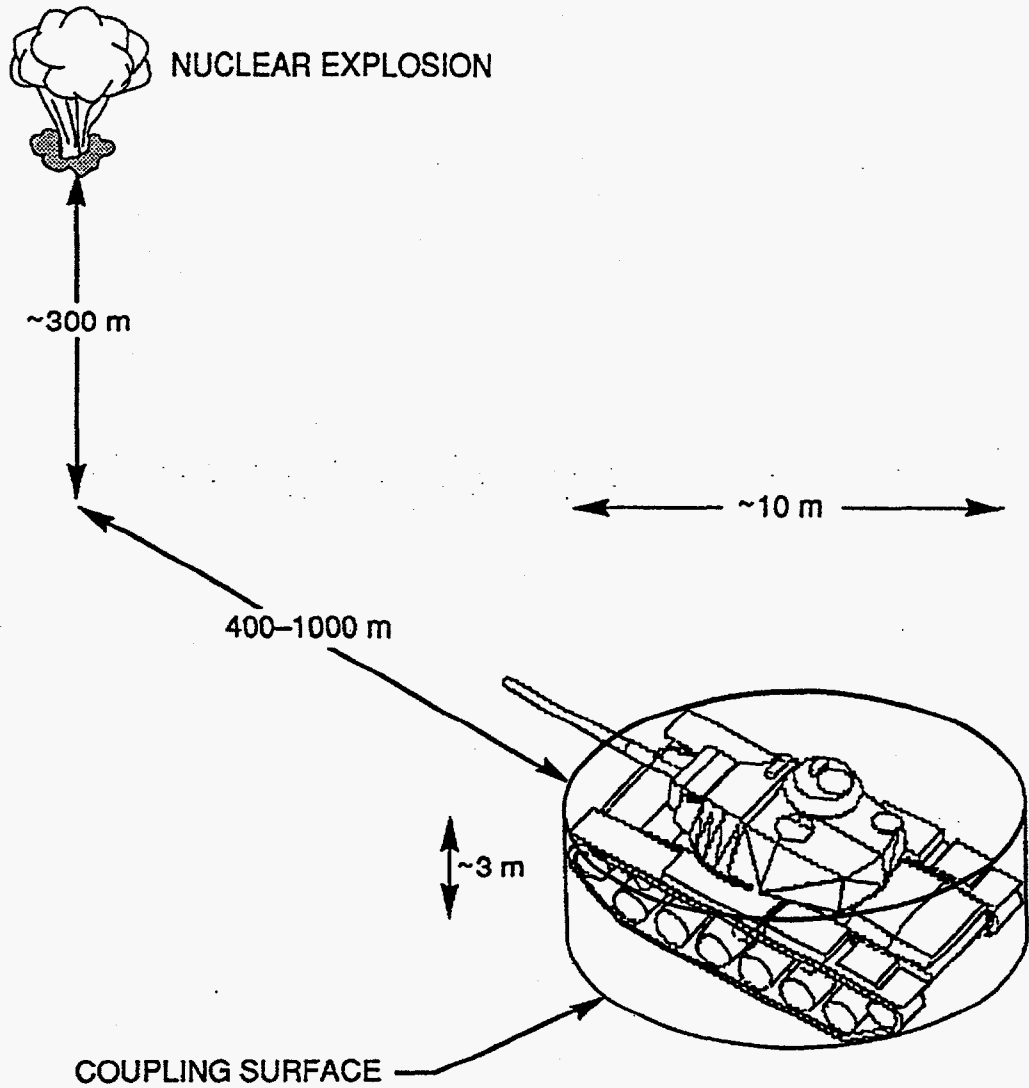


Figure 1-1. Typical MASH Problem Involving an Armored Vehicle.

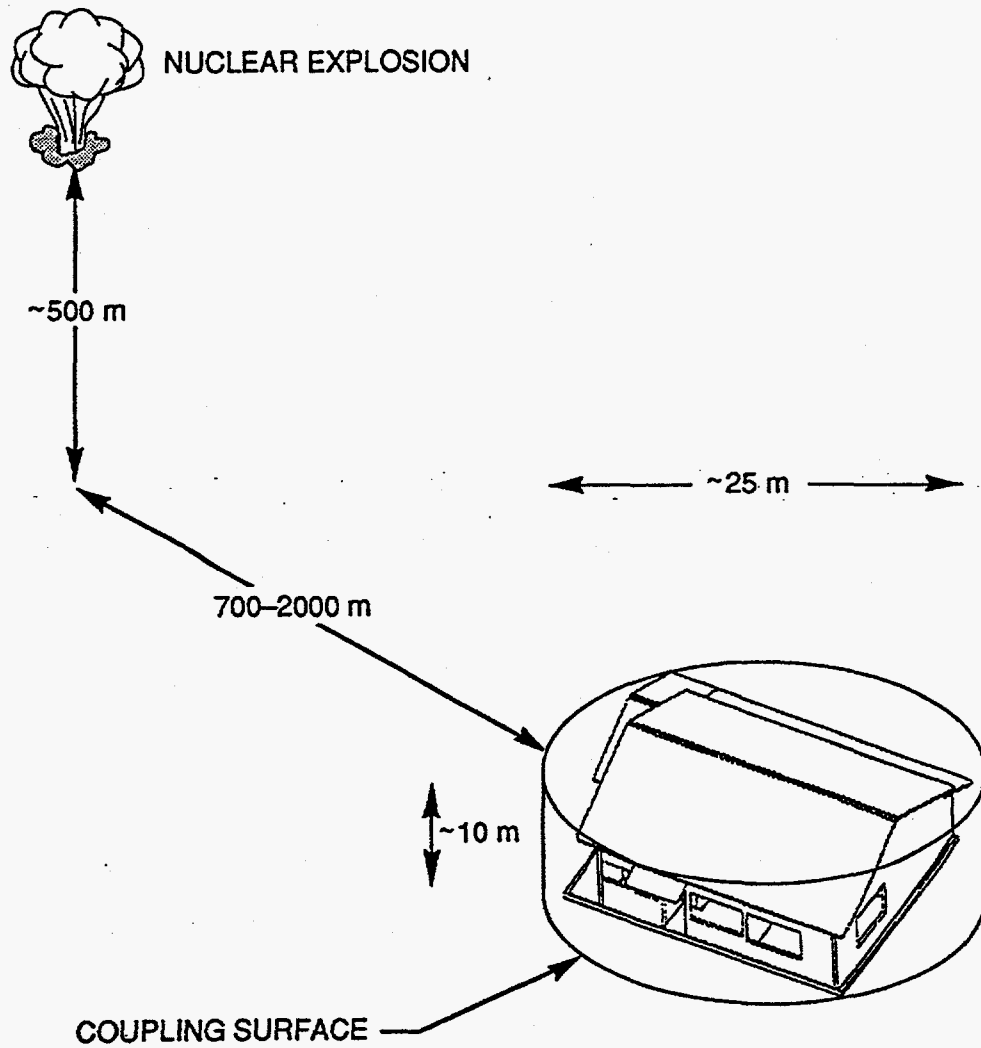


Figure 1-2. Typical MASH Problem Involving an Enclosed Structure.

Over the course of time, different versions of VCS were created due to the different installations tailoring the code to suit their particular purpose. At ORNL, the DOT III code was replaced with the DOT IV^{7,8} code, and VISA was replaced with VISTA. BRL, which has been a major user and source of funding for the VCS code, made a number of modifications to the MORSE and DRC parts of VCS in 1976-1977. The major change to MORSE was the replacement of the combinatorial geometry model, which SAIC had previously installed in MORSE,⁹ with GIFT combinatorial geometry, which was similar to the MORSE combinatorial geometry but which had been further developed at BRL.¹⁰⁻¹² After those modifications, BRL contracted SAIC to evaluate and document some aspects of the VCS. That effort concluded that "*VCS is a sophisticated and well-planned code package capable of accurate, state-of-the-art radiation transport in complex, three-dimensional vehicles*" and suggested a new "within-group" energy biasing scheme for adjoint MORSE.¹³ In two subsequent efforts, one for the WWD,¹⁴ and the other for BRL,¹⁵ SAIC installed and tested the new in-group energy bias methodology in the adjoint MORSE part of VCS. The study for WWD demonstrated that this scheme could provide a factor of four increase in the efficiency of VCS for a shielding calculation with 10 cm of steel.

The result of all this independent development of VCS was a proliferation of different versions of the code, of which most were not compatible. The Defense Special Weapons Agency (DSWA), formally the Defense Nuclear Agency, expressed concern over the potential for disagreement between independent analyses of the same armored vehicle. Consequently, BRL, ORNL, and SAIC were tasked to identify the problems associated with the "current" version(s) of VCS, incorporate the various modifications (which would improve the VCS code) that have been added to the different versions, and create a singularly referenced version of VCS. In particular, the purpose of this project was to establish and verify a version of VCS which was generally acceptable to the user community, and to place this version of VCS under responsible custody on the DSWA computing network for use on the CRAY computer system at Los Alamos National Laboratory (LANL) under the CRAY Time Sharing System (CTSS). In this effort, SAIC took the lead in the selection of the geometry model and in the development and testing of the in-group energy biasing; ORNL developed a new reference cross section data set, modified DRC to couple MORSE and DOT calculations made with different energy group sets, and compiled the new version of VCS. SAIC and ORNL shared the task of code verification and validation.

In years prior to the original MASH code system development effort, three problems with VCS and the primary cross section library used in VCS analyses were identified. These three problems included:

1. The biasing treatment used in the MORSE adjoint calculation of VCS did not favorably sample the most important regions of energy space, especially for calculations involving steel and polyethylene. These two materials are potentially important shielding components of armored vehicles. Furthermore, theoretical analyses of the standard adjoint scattering treatment indicated inherent large variances for adjoint Monte Carlo analyses of thick media.
2. The energy group structure of the 58 group (37 neutron groups, 21 gamma groups) DLC 31 cross section library,¹⁵ had suspected deficiencies for transport in steel and air, especially near 1 MeV and at epithermal energies.

3. The more recent GIFT5¹⁶ geometry routines used by BRL for constructing vehicle models have certain incompatibilities with the geometry routines in MORSE. Vehicle models developed by BRL for various analyses other than nuclear survivability/shielding effectiveness had to be revised, at a significant cost in man power and elapsed time, for VCS analyses.

As a result of this effort, SAIC installed a "user community compatible" geometry package and in-group energy biasing into VCS by incorporating the GIFT5 geometry package and a revised in-group energy bias package into the BRL MIFT version of MORSE. After a significant verification effort, this package was released to ORNL for further verification and validation. SAIC called this version of MORSE "MIFT2",¹⁸ indicating that it was an update of the BRL MIFT code. ORNL developed the new Defense Applications Broad-group Library (DABL69),¹⁹ with 46 neutron energy groups and 23 gamma-ray groups, made several modifications to many of the code system modules, and incorporated the SAIC changes to the MORSE component into the new version of VCS called MASH (Monte Carlo Adjoint Shielding). The final result, MASH v1.0, was compiled and tested in 1992 and placed under responsible custody of DSWA on the DSWA computing network for use on the CRAY computer system at LANL under the CTSS operating system. A MASH v1.0 User's Workshop was conducted in Oak Ridge, Tennessee in 1993 and the code system was released to the U. S. military organizations and contractors, and NATO allies with a need for such a computational tool.

1.1.3 Summary of Corrections and Improvements to MASH v1.0

With respect to the MASH code system as a whole, the most significant change was to port the code system from the LANL Cray over to an IBM RISC-6000 workstation to be run under the UNIX operating system. There were only minor changes in the modules associated with the environment calculation, i.e. GIP, GRTUNCL, DORT, and VISTA. These changes were primarily in the DORT code and involved modifications designed to speed up the code. The changes did not effect typical user input data and should be transparent to the MASH code system user. The two major changes to MASH involved the MORSE module and the DRC module.

The MORSE module was modified to include several features identified in the MASH v1.0 Workshop as options which would either enhance the functionality of the code or make it more "user friendly". The major changes include:

1. Added a failed job recovery capability. This allows the user to process the number of batches already completed in a DRC2 calculation even though the MORSE job had an abnormal termination. For example, if you are processing 1000 batches and the MORSE calculation fails on batch number 936, you can still analyze the 935 completed batches in DRC2. This was recommended since minor glitches in the geometry routines will sometimes abort the MORSE run, even though the geometry file/model is correct.
2. Improved the geometry/material input. In MASH v1.0, the user had to input the material by zone data (Card GH) in separate arrays, even though this information was also being read in from the GIFT5 geometry file. This input was eliminated. Now the user uses the material field on the Region Identification card in the GIFT5 input stream to specify the materials for each region in the geometry. As in MASH v1.0, the user must take care that the cross-section materials match the geometry materials.

3. Added a reduced material density capability. This feature was added because most of the vehicle models are constructed with many regions defined as material X at Y%. For any given vehicle, there could be multiple percentages of material X. In MASH v1.0, each different material X at Y% had to be created as a separate cross-section material. This led to large cross-section data sets. In MASH v1.5, only one material X at 100% has to be created. The percentages are then read in from the Region Identification card in the GIFT5 input stream to specify the percentage of material for each region in the geometry and this information is used to modify the transport cross sections as needed. This simplifies the cross-section mixing, reduces the amount of core needed, and simplifies the material by zone input.
4. Moved the MORSE region importance assignment data. In MASH v1.0, the importance region assignment data was read in on Card GI. This input has been eliminated and the importance region assignment data is now read in on the Region Identification card in the GIFT5 input stream to specify the importance parameters to be assigned for each region in the geometry.
5. Modified the parameter list written on the MORSE leakage file to be read by DRC2. In MASH v1.0, only the Z height of the detector location was included in the MASH leakage file. In MASH v1.5, all three coordinates of the detector location (X, Y, and Z) are included. Furthermore, three additional parameters relating geometry information were included for future use in the graphical analysis/display of the MASH results.

The DRC2 module, developed by C. O. Slater²¹, was added and represents an extensive modification of the DRC code used in MASH v1.0 for coupling. With DRC, the spatial dependence of the fluence was limited to axial variation. Linear interpolation was used to obtain the fluence at axial locations falling between the DORT fluence locations. However, since radial variation of the DORT fluences could be important for large vehicle systems or other large structures, the DRC2 code was developed to incorporate coupling with axially and radially varying DORT forward fluence fields. An option was included for specifying either linear or logarithmic interpolation or extrapolation of the fluences. In either case, linear is used when negatives are encountered.

DRC2 is set up to use the MASH file either with or without X-Y dependence or the MASH file with its fewer collision file parameters (8 vs 13 defined parameters). In addition, DRC2 can calculate results for several range/orientations in a single pass through the code. Titles written to unit 11 are constructed from the input range and orientation data and the first 56 characters of the case title. The format is the expected one for an unpublished text-formatting and transmission-factor-calculating code (TFX).

The inclusion of X-Y dependent fluence fields in the DRC2 calculation and the calculation of results for several ranges and orientations in one pass through the code results in considerably more data in core than was the case with the DRC code. Therefore, if the allocated memory is not large enough to store all data in core, the code will perform the calculation "ex-core" with group blocking (i.e., the calculation is performed for a portion of the groups at a time until all group calculations are finished), provided data for at least one group will fit in core.

All components of MASH v1.5, except the GIFT5 input module to MORSE, use a form of the FIDO free-form input data described in detail in Appendix A. The GIFT5 geometry input for the MORSE component currently is in fixed format, however, future efforts will convert this input over to the FIDO free-form method.

1.2 STRUCTURE OF MASH v1.5

The general structure of the MASH code system is shown in Figure 1-3, while the data flow is detailed in Figures 1-4 through 1-6. A typical MASH calculation can be broken up into three distinct sections, the environment calculation (Figure 1-4), the target calculation (Figure 1-5), and the folding calculation (Figure 1-6). The GIP code is used to create and mix the materials required to run the air-over-ground transport analysis. The compositions and source data for the air-over-ground transport calculation are input into both the GRTUNCL and DORT codes. In order to maintain particle balance and reduce ray effects, GRTUNCL calculates the uncollided fluence and first-collision source throughout the problem space. This information is input to DORT which calculates the resulting collided fluence, and merges the two results. All fluence information is passed to VISTA, where it is condensed and reordered for convenient processing. Only a few ground ranges from the radiation source are normally processed at this step. Additional ground ranges may be obtained by rerunning the VISTA code at a minimal cost.

The complex three-dimensional target (vehicle) geometry description and material compositions are input to the MORSE code. MORSE records the required information for each adjoint track leaving the coupling surface on a leakage data set which is input to the Detector Response Code, DRC2. DRC2 folds the adjoint leakage data together with the reformatted DORT fluence at the coupling surface, i.e., the VISTA code output fluence file, for the selected orientation, range, and detector response. It also provides edits of estimated variances of the results as requested by the user. The protection factor itself is obtained by dividing the free-field dose, available from DORT, by the dose response at the detector position within the target (vehicle) given by DRC2.

Most of the cost of MASH is incurred in the DORT and MORSE codes. Therefore, it is advantageous to save the VISTA output for use with many MORSE runs. Likewise, it is practical to use a single MORSE leakage tape for a target (vehicle) to examine a number of target orientations, source ranges and types, and detector response functions.

1.3 STRUCTURE OF MASH USER'S MANUAL

1.3.1 The Main Text

The remainder of the main text of this manual (Sections 2.0 through 10.0) gives a detailed description of each of the codes in the current release of MASH. Some sections only include a title page denoting a module to be added in a later release of MASH. Included in each section is a brief description of the code and its theory (if applicable), the input requirements, detailed input data notes, the input and output file formats, the logical unit requirements, a list of references pertaining to that particular section, and a sample problem. For the two major codes within MASH, i.e., DORT and MORSE, the section is not intended to be a complete description and the interested user might consider obtaining the reference documents for these two codes. However, the information in each of the sections should be sufficient for understanding and using MASH.

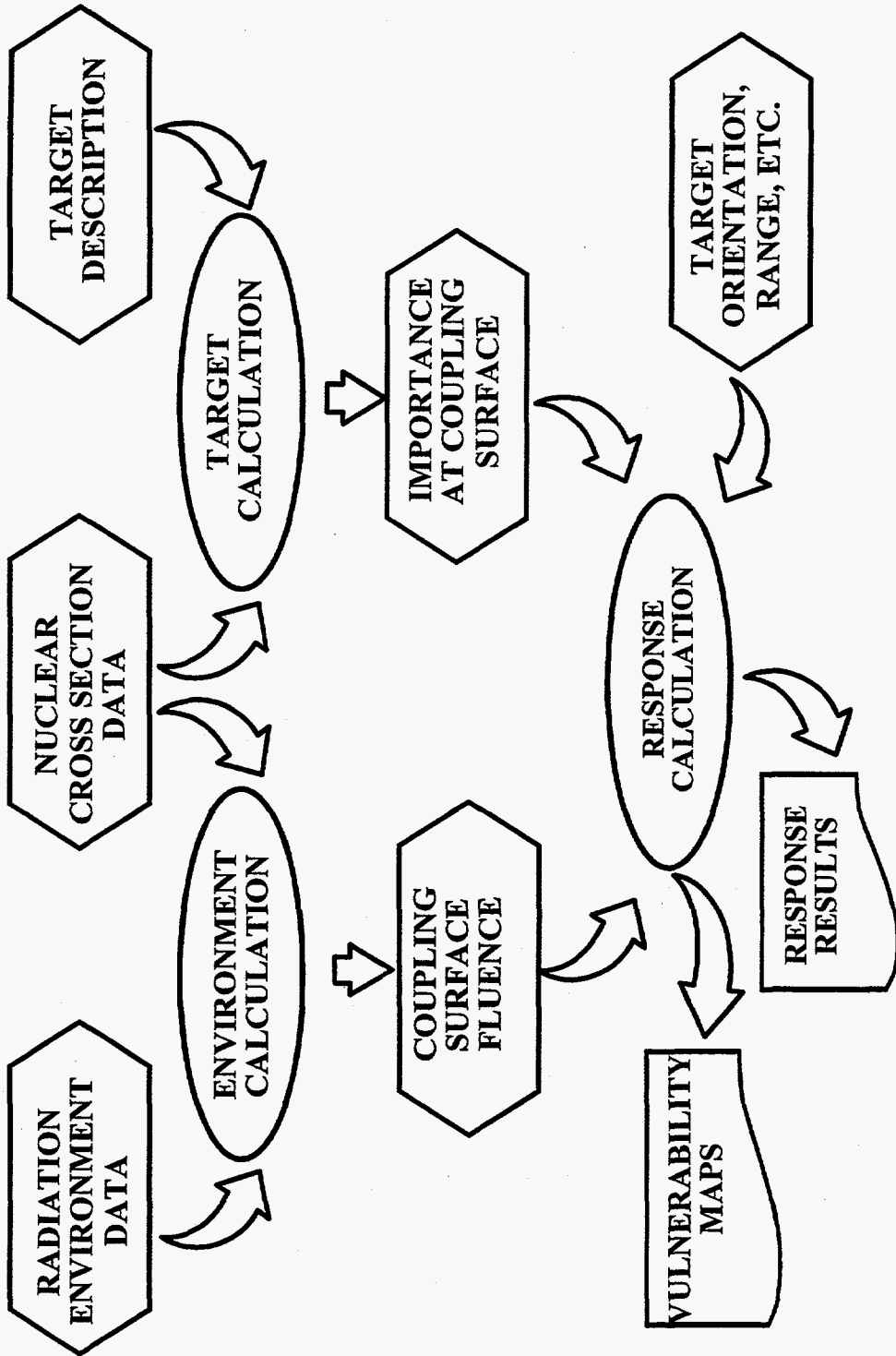


Figure 1-3. General Structure of the MASH Code System.

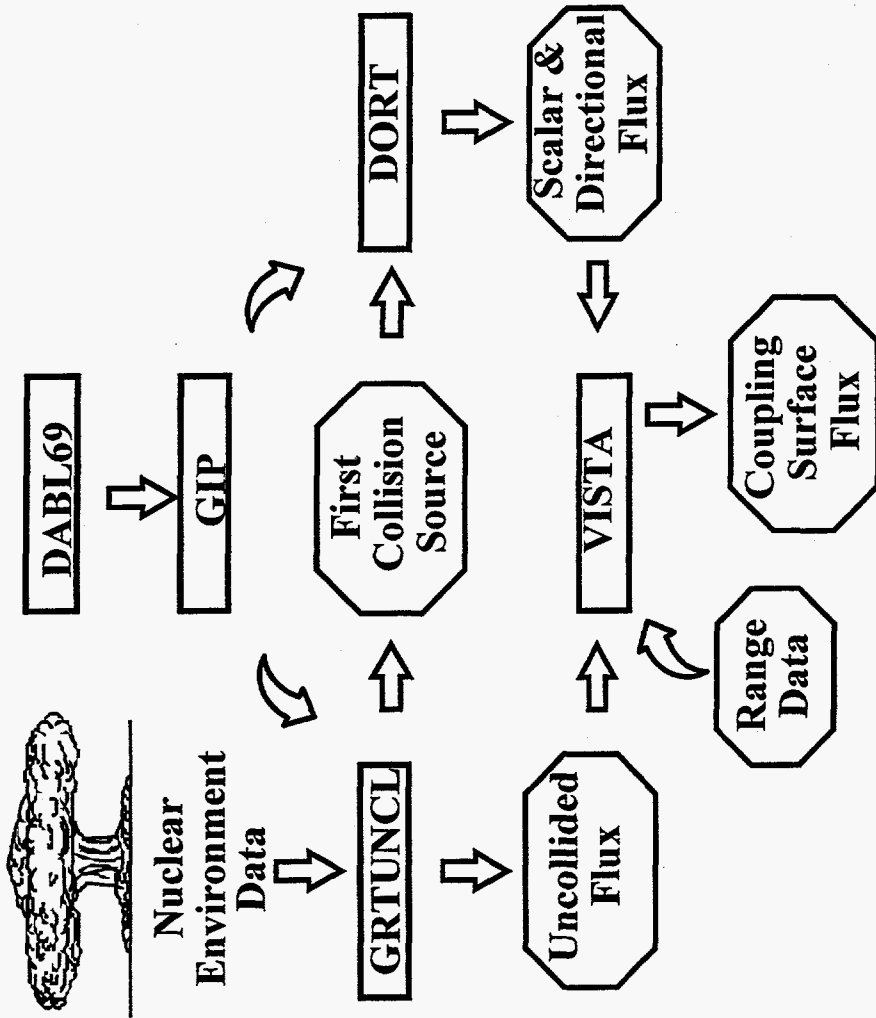


Figure 1-4. Data Flow Diagram of the MASH Code System Environment Calculation.

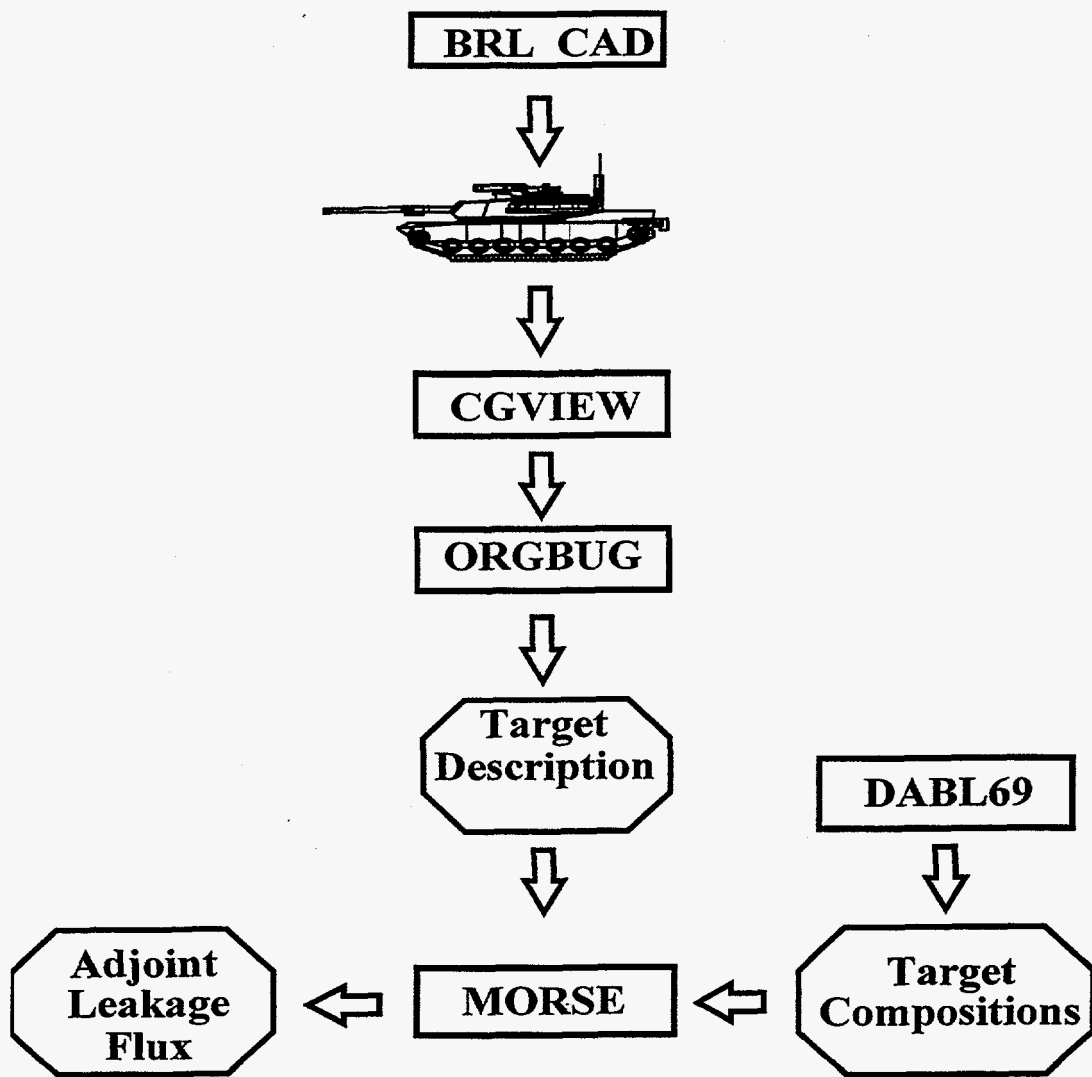


Figure 1-5. Data Flow Diagram of the MASH Code System Target Calculation.

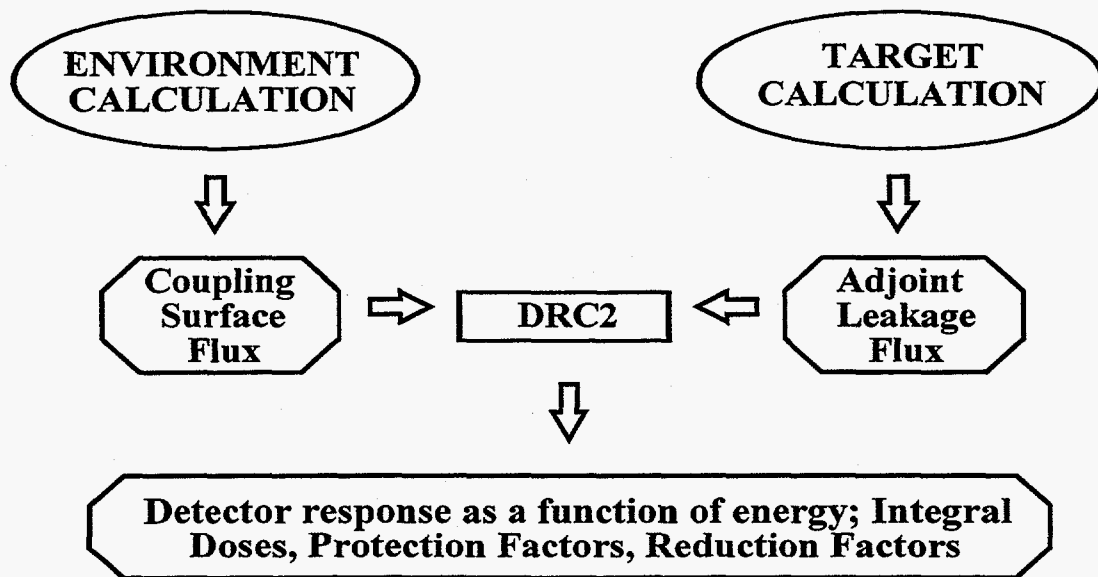


Figure 1-6. Data Flow Diagram of the MASH Code System Folding of the Environment Calculation and Target Calculation.

1.3.2 The Appendices

The Appendices include detailed descriptions of FIDO input (Appendix A), the theory behind in-group energy biasing (Appendix B), a detailed description for the GIFT5 geometry package (Appendix C), a detailed discussion on the comparisons used to validate the DRC2 coupling code and differences associated with using single point and/or multiple point coupling files (Appendix D), a listing of the MASH v1.5 computer code abstract (Appendix E), and a short, informal "user notes" section (Appendix F) which addresses some of the caveats of performing the MASH analysis of the sample problem as determined through the experience of the MASH v1.5 manual's editor. The inclusion of the in-group biasing theory in Appendix B (rather than in the MORSE section) and the DRC2 code validation in Appendix D (rather than the DRC2 section) was due to the format chosen for the "user's" manual. The detailed description of the GIFT5 geometry package was included for completeness since this package is unpublished.

1.3.3 The Sample Problem

The sample problem represents a "benchmark" calculation of MASH v1.0 on the Two-Meter Box Test Bed experiments performed at APRF.^{22,23} The results of the MASH analysis were generally within 15% of the experimental measurements for both differential and integral free-field and in-box neutron and gamma-ray dose. There was also excellent agreement in the protection factor analysis for the box. This sample problem was independently analyzed by both SAIC and ORNL with C/C ratios, i.e., SAIC calculations/ORNL calculations, typically within 5%. The sample problem input and output for each code is given in the respective sections of the report. However, each part of the sample problem fits into the data flow shown in Figures 1-4, 1-5, and 1-6, and the user should take time to see which parameters in one code depend on parameters from the previous code, i.e., the axial and radial mesh between DORT and GRTUNCL. In the discussion of the sample problem in each section, most of these dependencies are identified.

1.4 REFERENCES

1. J. O. Johnson, ed. "A User's Manual for MASH 1.0 - A Monte Carlo Adjoint Shielding Code System," ORNL/TM-11778, Oak Ridge National Laboratory, (March 1992).
2. W. A. Rhoades and M. B. Emmett et al., "Vehicle Code System (VCS User's Manual)," ORNL/TM-4648, Oak Ridge National Laboratory (August 1974).
3. W. A. Rhoades et al., "Development of a Code System for Determining Radiation Protection of Armored Vehicles (The VCS Code)," ORNL/TM-4664, Oak Ridge National Laboratory, (October 1974).
4. M. B. Emmett, "The MORSE Monte Carlo Radiation Transport Code System," ORNL-4972 (1975), ORNL-4972/R1 (1983), ORNL-4972/R2 (1984), Oak Ridge National Laboratory.

5. W. A. Rhoades and F. R. Mynatt, "The DOT III Two-Dimensional Discrete Ordinates Transport Code," ORNL-TM-4280, Oak Ridge National Laboratory, (September 1973).
6. L. F. Schanzler and F. W. Bucholz et al., "Protection Factors of the Leopard 1A1 Comparison of Calculated Results with Measured Values," Wehrwissenschaftliche Dienststelle der Bundeswehr fur ABC-Schutz, 3042 Munster, Federal Republic of Germany. Paper presented at the meeting on Protection Factors of Armored Vehicles, German Ministry of Defense, Bonn, Germany (22-25 June 1982).
7. W. A. Rhoades, D. B. Simpson, R. L. Childs, and W. W. Engle, Jr. "The DOT IV Two-Dimensional Discrete Ordinates Transport Code with Space-Dependent Mesh and Quadrature," ORNL/TM-6529, Oak Ridge National Laboratory (January 1979).
8. W. A. Rhoades and R. L. Childs, "An Updated Version of the DOT 4 One- and Two-Dimensional Neutron/Photon Transport Code," ORNL-5851, Oak Ridge National Laboratory (1982).
9. E. A. Straker, W. H. Scott, Jr., and N. R. Byrn, "The MORSE Code with Combinatorial Geometry," Defense Nuclear Agency DNA 2860T, SAI-72-511-LJ, Science Applications International Corporation, (May 1972).
10. Lawrence W. Bain, Jr. and Mathew J. Reisinger, "The GIFT Code User Manual; Volume I. Introduction and Input Requirements," BRL 1802, Ballistic Research Laboratory, (July 1975).
11. Gary G. Kuehl, Lawrence W. Bain, Jr. and Mathew J. Reisinger, "The GIFT Code User Manual; Volume II. The Output Options," ARBRL-TR-02189, Ballistic Research Laboratory, (September 1979).
12. A. E. Rainis and Ralph E. Rexroad, "MIFT: GIFT Combinatorial Geometry Input to VCS Code," BRL Report No. 1967, Ballistic Research Laboratory, (March 1977).
13. W. H. Scott, Jr., "Vehicle Code System (VCS) Documentation and Uncertainty Analysis," SAI Report SAI-133-79-977-LJ, Science Applications International Corporation, (December 1979).
14. W. H. Scott, Jr., and V. E. Staggs, "Adjoint Energy Biasing and Thermal Neutron Diffusion in the MORSE and VCS Codes," SAI-133-81-384-LJ Science Applications International Corporation, (November 1981).
15. W. H. Scott, Jr., et al., "Predictive Algorithm for Radiation Protection," Volume 1, "VCS In-Group Energy Bias, The DACM Code and DOT Calculations," SAIC-85/1710, Science Applications International Corporation, (May 1985).
16. D. E. Bartine, et al., "Production and Testing of the DNA Few-Group Coupled Neutron-Gamma Cross-Section Library," ORNL/TM-4840, Oak Ridge National Laboratory, (March 1977).
17. "The GIFT5 Geometry Package", Ballistic Research Laboratory, (No formal documentation exists for GIFT5.)

18. J. A. Stoddard, S. D. Egbert, and W. H. Scott, Jr., "The Vehicle Code System with In-Group Energy Bias and GIFT5 Geometry," DNA-TR-87-23, Science Applications International Corporation, (January 1987).
19. D. T. Ingersoll, R. W. Roussin, C. Y. Fu, and J. E. White, "DABL69: A Broad-Group Neutron/Photon Cross-Section Library for Defense Nuclear Applications," ORNL/TM-10568, Oak Ridge National Laboratory, (June 1989).
20. W. A. Rhoades and R. L. Childs, "The DORT Two-Dimensional Discrete-Ordinates Transport Code," Nuclear Science & Engineering 99, 1, pp. 88-89, (May 1988).
21. C. O. Slater, "DRC2: A Code with Specialized Applications for Coupling Localized Monte Carlo Adjoint Calculations with Fluences from Two-Dimensional R-Z Discrete Ordinates Air-Over-Ground Calculations," ORNL/TM-11873, Oak Ridge National Laboratory, (January 1992).
22. J. O. Johnson, J. D. Drischler, and J. M. Barnes, "Analysis of the Fall-1989 Two-Meter Box Test Bed Experiments Performed at the Army Pulse Radiation Facility (APRF)," ORNL/TM-11777, Oak Ridge National Laboratory, (May 1991).
23. R. T. Santoro et al., "DNA Radiation Environments Program Fall 1989 2-Meter Box Experiments and Analysis," ORNL/TM-11840, Oak Ridge National Laboratory, (May 1991).

2.0 GIP: A GROUP-ORGANIZED CROSS SECTION INPUT PROGRAM*

2.1 INTRODUCTION TO GIP

2.1.1 Background

GIP is an auxiliary code used to pre-mix the material cross-section sets for very large discrete ordinates calculations (relative to available core space). The motivation for developing GIP was due to complications arising when the amount of core space required for the mixing table exceeded the available core storage. GIP was written to treat each component of the Legendre expansion, i.e., P_L term, of a cross-section set as a separate nuclide. This data processing treatment was seen as a requirement in the 1960's, when the code originated. Although certain features of the mixing table expedite the mixing of P_L sets, there is little doubt the code would be more convenient for present-day problems if all of the components of the Legendre expansion for a cross-section set were treated as a unit.

GIP accepts nuclide-organized microscopic cross-section data from either the input stream in card-image format or from a data library prepared by the ALC1¹ program. Macroscopic cross section mixtures can be prepared as specified by a mixing table similar to that of DORT². The total upscatter cross section can be calculated and inserted into the set. The result is a "GIP" cross section library file (defined in Section 2.5). Microscopic and/or macroscopic cross-section data can be included in the output cross-section library file and/or printed output file.

The chief virtues of GIP are its extreme simplicity and its high compatibility with DORT, ANISN³, and related codes. It is operable on virtually any type computer that provides sequential scratch files. It uses the FIDO card-image input processor described in Appendix A, and shares many subroutines with DORT.

2.1.2 Method Used

The cross sections specified in the input stream are selected, and the number of energy groups which can be processed at one time is decided. The groups for the amount of core allocated, i.e., "one corefull," are selected as each nuclide is read and dumped onto a source file. The remaining groups, if any, are written to a holding file. When all nuclides have been located, the data are read from the source file into core and written in group-ordered format onto a sorting file. A new corefull of data is then moved from the holding file to the source file, and then to the sorting file as before. Unprocessed groups, if any, are spilled to a second holding file, which is processed like the first holding file. This sequence continues until all groups have been processed. Efficiency is improved when one group of data can be written directly to the sorting file each time the source file is loaded. In the final step, the group-organized data are read, mixed, edited, and written to the output file.

The advantages of the GIP system are that it can process a cross section volume of several corefulls with inconsequential cost, using only sequential files, and that it is easily adapted

*W. A. Rhodes and M. B. Emmett, "DOS: The Discrete Ordinates System," ORNL/TM-8362, Oak Ridge National Laboratory, (September 1982).

to new or different computing environments. Unfortunately, if the cross section volume increases to ten or more corefills, for example, the sorting process may become inefficient.

The GIP method was originated by W. W. Engle, Jr. in a program called TAPEMAKER³, the predecessor to the ALC1 program, which operated on the IBM 7090 before the days of random access files. The basic procedure has changed little since then.

2.2 GIP INPUT REQUIREMENTS

The following input cards are required to execute GIP. Default values are in brackets ([]).

Title Card (72 alphanumeric character description)

INPUT DATA BLOCK 1

1\$ Array - Integer Control Parameters

IGM	number of energy groups
IHT	position of total cross section in cross-section table
IHS	position of self-scatter cross section in cross-section table
IHM	cross-section table length per energy group (usually IHM = IHT + IGM)
MS	cross-section mixing table length

- 5 ---

MCR	number of materials read from cards
MTP	number of materials read from input cross-section library tape (nuclide or GIP format)
MTM	total number of materials (MCR+MTP+MIXTURES)
ITH	output cross-section library flag 0/1 = forward/adjoint cross-section library
ISCT	maximum order of Legendre expansion of cross sections

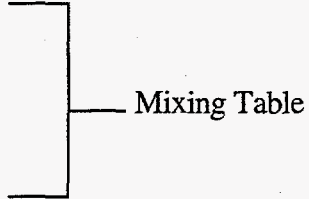
- 10 ---

IPRT	output cross-section print control flag 0/1/2 = print all materials/none/mixtures only
IOUT	output cross-section library control flag 0/1/2 = output all materials/none/mixtures only
IDOT	output cross-section library format flag 0/1/2 = ANISN/DOT III/DOT IV format
NBUF	number of k-bytes of core

E (terminate array with "E")

T (terminate block with "T") [T always required]

INPUT DATA BLOCK 2

- 10\$ Array - Material Numbers (MS entries)
 - 11\$ Array - Component Numbers (MS entries)
 - 12* Array - Density Multipliers (MS entries)
 - 7\$ Array - Mix Code (optional - MTM entries)
 - 13\$ Array - Nuclide ID Numbers on Library File (MTP entries required only if IDAT1 is not equal to 2)
- 

T (terminate block with "T") [T always required]

INPUT DATA BLOCK 3

- 14* Array - Cross Sections for Nuclide 1, ANISN format, all groups

[each new nuclide **must** start on a new card]

- Cross Sections for Nuclide MCR, ANISN format, all groups (IHM*IGM*MCR entries required)

T (terminate block with "T") [T required if MCR > 0]

2.3 GIP INPUT DATA NOTES

Except for the title card, all data are read using the FIDO input system. A detailed description of the FIDO input system is given in Appendix A. Data arrays are entered in blocks, each terminated by a "T". Unused data arrays (e.g., 10\$ if MS=0) are not entered, but a "T" must still be entered to signal the termination of each block. Multiple problems can be stacked with a blank card separating cases. Input data are not saved between stacked cases.

1\$ Array The meaning of the first eight input parameters of the 1\$ array are compatible with GRTUNCL (Section 3.0) and DORT (Section 5.0).

IHT, IHS, IHM The discussion of these input parameters is given in Section 2.4.1.

MCR, MTP, MTM GIP assigns storage space (IHM*IGM words/set) for MTM sets of cross sections, called "materials." The first MCR spaces are filled with data read from cards in the 14* array. The next MTP material spaces are filled with nuclide data read from the data set mounted on the input library logical unit (default=8) and stored in the order indicated by the 13\$ array. The remaining spaces between MCR+MTP and MTM are available for preparing mixtures.

NOTE: If MCR=0, the 14* array and corresponding data block terminator is not required.

ITH If ITH=1, two major reordering steps are carried out to produce an adjoint cross-section library:

1. The inscatter matrix is transposed, i.e., the table position associated with group g describing scattering from g' to g is changed to describe scattering from g to g' .
2. The ordering of the groups is reversed, i.e., data for group IGM appear first in the output file, followed by IGM-1, etc.

A simple three group example is illustrated in Section 2.3.3.

ISCT When the order of scatter is greater than zero, GIP expects the P_1 cross section to be material M+1, the P_2 cross section to be M+2, etc., where M is the P_0 material number:

```
P0 Data, Nuclide 1
P1
P2
.
.
.
PISCT Data, Nuclide 1

P0 Data, Nuclide 2
P1
P2
.
.
.
PISCT Data, Nuclide 2
.
.
.
```

For components other than P_0 , cross section positions other than positions IHT+1 through IHM may be zero.

IPRT, IOUT If IOUT=0, the output includes MCR+MTP microscopic cross sections, plus (MTM-MCR-MTP) mixtures. If IOUT=2, only the mixtures will be output. Printed cross-section edits are similarly controlled by IPRT.

For most DORT problems, I/O manipulation can be reduced by asking only for the output of the mixtures from GIP. They are then referred to in DORT such that material one is the first GIP mixture, etc. Any microscopic data to be used in DORT activity edits must be included as a mixture, as must nuclides whose concentrations are to be modified in a search.

IDOT This parameter identifies three possible output cross section library formats. Only the ANISN and DOT IV formats are discussed since they are used in present day applications. The DOT III format was retained from earlier versions of GIP, and although still operational, should be avoided, unless DOT III will be used for the final calculation.

NBUF This parameter defines the buffer space required for the data sets which are listed in Section 2.6.

10\$, 11\$, and 12* Arrays The cross section mixing table is used to combine elements into macroscopic mixtures. Experience will reveal that only the imagination limits its flexibility. As with DORT, the integers in the mixing table refer to a continuous array of MTM cross section sets of which the first MCR+MTP are nuclide data read from card-image input and a library file, respectively. All of the sets beyond MCR+MTP are preset to zero before the mixing table is executed. In non-search problems where cross-section storage is difficult, i.e., large problems that do not involve material buckling or concentration searches, material spaces originally used for input nuclides can be reused for mixtures. While the general rules for creating mixtures are equally applicable for GIP, GRTUNCL, and DORT, it should be noted that reference to eigenvalue modification in the DORT mixing table description has no application to GIP mixing. The interpretation rules applicable to GIP are as follows:

- a. If the mixture number is N and the component number is 0, then the cross sections in mixture N will be multiplied by the number entered in the density column:

$$\sigma_{\text{MIXTURE N(NEW)}} = \sigma_{\text{MIXTURE N(OLD)}} * \text{DENSITY}$$

- b. If the mixture number is N and the component number is M, then the cross sections in component M, multiplied by the density, will be added to the cross sections in mixture N:

$$\sigma_{\text{MIXTURE N(NEW)}} = \sigma_{\text{MIXTURE N(OLD)}} + \sigma_{\text{COMPONENT M}} * \text{DENSITY}$$

NOTE: Either a mixture or a component may be made up of microscopic or macroscopic cross sections for a single isotope or mixture of isotopes.

A sample mixing table showing the various options is given below.

MIXTURE (10\$ ARRAY)	COMPONENT (11\$ ARRAY)	DENSITY (12*ARRAY)
6	1	0.4
6	3	0.5
7	2	0.4
7	4	0.5
7	0	3.0

The mixture table given above would do the following:

- (1) Add components 1 and 3 with densities 0.4 and 0.5, respectively, to form mixture 6:

$$\sigma_6 = \sigma_1 * 0.4 + \sigma_3 * 0.5$$

- (2) Add components 2 and 4 with densities 0.4 and 0.5, respectively, to form mixture 7:

$$\sigma_7 = \sigma_2 * 0.4 + \sigma_4 * 0.5$$

- (3) Multiply mixture 7 by 3.0:

$$\sigma_7 = \sigma_7 * 3.0$$

10\$ Array If the 10\$ entry is tagged with a negative, the next ISCT components will be treated as P_L components. For example:

10\$	11\$	12*	(with ISCT = 3)
-13	1	1.0	

will be equivalent to

10\$	11\$	12*	(with ISCT = 0)
13	1	1.0	
14	2	1.0	
15	3	1.0	
16	4	1.0	

7\$ Array The numbers in the mixing table normally refer to positions in the material block, which contains MCR nuclides from cards, followed by MTP nuclides from tape and MTM-MCR-MTP mixtures. It is often convenient, however, when constructing the mixing table to refer to fictitious "mix code" numbers. The 7\$ array can be entered to define the list of fictitious mix codes corresponding to each material. If the 7\$ array is omitted, the mix code is equal to the material number.

13\$ Array A negative entry in the 13\$ array replaces the following ISCT entries with successive ID's. Thus:

13\$		13\$
-101		101
-101	is equivalent to	102
-101		103

14* Array The input of the 14* array is performed by subroutines which have certain restrictions in addition to those of normal FIDO input:

- a. The nuclide spaces are preset to 0.0, so that "E" or "F0" will have the effect of filling the remaining space with 0.0, but "E" and "F" must not be used in the input for the last nuclide.
- b. The 14* or 14** designation may precede each nuclide block, but is not required except in the first block.
- c. Entries, including operators such as "T", following the last data item for nuclides other than the last, and on the same card as the last item, will be ignored.
- d. The "T" which terminates this block must appear alone in column 3 of a separate card.

2.3.1 Special Diffusion Theory Option

If the cross-section set contains a transport cross section in position N, then setting ISCT = -N causes the total cross section (position IHT) to be replaced by the transport cross section and the self-scatter cross section (position IHS) to be reduced such as to maintain a constant absorption cross section. The resulting cross-section set is suitable for use in a P₀ DORT calculation, especially one using the diffusion package.

NOTE: Negative entries in the 10\$ array must not be used with this option.

2.3.2 Upscatter Option

If the self-scatter cross section position (IHS) is greater than IHT+1, the upscatter processor calculates the total upscattering cross section from each group and places it in the appropriate table position. No user action is required.

2.3.3 Adjoint Reordering Example

A three-group example showing the relationship between a forward and adjoint cross-section set is shown below. In this example, there is no upscatter, one activation cross section, IHT = 4, IHS = 5, and IHM = 7.

<u>Direct</u>	<u>Adjoint</u>
$\sigma^F(1)$	$\sigma^F(3)$
$\sigma^A(1)$	$\sigma^A(3)$
$v\sigma^F(1)$	$v\sigma^F(3)$
$\sigma^T(1)$	$\sigma^T(3)$

$\sigma(1 \rightarrow 1)$	$\sigma(3 \rightarrow 3)$
0	0
0	0
$\sigma^F(2)$	$\sigma^F(2)$
$\sigma^A(2)$	$\sigma^A(2)$
$v\sigma^F(2)$	$v\sigma^F(2)$
$\sigma^T(2)$	$\sigma^T(2)$
$\sigma(2 \rightarrow 2)$	$\sigma(2 \rightarrow 2)$
$\sigma(1 \rightarrow 2)$	$\sigma(2 \rightarrow 3)$
0	0
$\sigma^F(3)$	$\sigma^F(1)$
$\sigma^A(3)$	$\sigma^A(1)$
$v\sigma^F(3)$	$v\sigma^F(1)$
$\sigma^T(3)$	$\sigma^T(1)$
$\sigma(3 \rightarrow 3)$	$\sigma(1 \rightarrow 1)$
$\sigma(2 \rightarrow 3)$	$\sigma(1 \rightarrow 2)$
$\sigma(1 \rightarrow 3)$	$\sigma(1 \rightarrow 3)$

2.4 INPUT LIBRARY FORMAT

The input library format from which MTP nuclides are taken is defined in the following manner:

ALC Cross Section Library Format

```

C*****
C          PROPOSED 19 MAY 80
C
CF          ALC
CE          TRANSPORT CODE CROSS SECTION DATA
C
C*****
C
CD          THE TERMINATION RECORD DEFINES THE LENGTH OF
CD          THE DATA SET AND THE NUMBER OF NUCLIDES
C
CD          THE ID VALUES MUST BE IN ASCENDING ORDER
C
C-----
CS          FILE STRUCTURE
C
CS          RECORD TYPE          PRESENT IF

```



```

CS _____
CS ***** (REPEAT FOR ALL NUCLIDES)
CS * CONTROL DATA FOR A NUCLIDE ALWAYS
CS * CROSS SECTION DATA FOR A NUCLIDE ALWAYS
CS *****
C
CS TERMINATION ALWAYS
C
C-----
C
C-----
CR CONTROL DATA FOR A NUCLIDE
C
CL NOG,NCTL,NCC,NCID,(NAME(I),I=1,12)
C
CW 16=NUMBER OF WORDS
C
CD NOG NUMBER OF ENERGY GROUPS FOR THIS SET
CD NCTL LENGTH OF CROSS SECTION TABLE FOR THIS SET
CD NCC =0 SET WAS ADDED TO LIBRARY
CD =2 SET REPLACED AND EXISTING SET
CD NCID IDENTIFICATION NUMBER
CD NAME ARBITRARY DESCRIPTION, A4 FORMAT
C
C-----
C
C-----
CR CROSS SECTIONS FOR A NUCLIDE
C
CL ((CRX(IH,IG),IH=1,NCTL),IG=1,NOG)
C
CW NCTL*NOG=NUMBER OF WORDS
C
CD CRX CROSS SECTION DATA ORDERED
CD AS PER SECTION 2.4.1
CD NCTL AS SPECIFIED BY PREVIOUS RECORD
CD NOG AS SPECIFIED BY PREVIOUS RECORD
C
C-----
C
C-----
CR TERMINATION
C
CL NOG,NCTL,NCC,NCID,(NAME(I),I=1,12)
C
CW 16=NUMBER OF WORDS
C
CD NCC 7, ALWAYS
CD OTHER ITEMS ARBITRARY
C
C-----

```

2.4.1 ANISN Nuclide Format Cross-section File

In a normal GIP problem, cross sections are read from card input and/or from an external data set in nuclide-organized format, i.e., all the cross sections for one group of one nuclide, followed by other groups for that nuclide, and finally followed by data for other nuclides. Within a group, GIP expects the ordering of data in the cross section table in the following format:

Table Position	Entry	Cross Section Type
1	$\sigma^1(g)$	First activation cross section (if any)
.	.	
.	.	
.	.	
IHT-3	$\sigma^L(g)$	Last activation cross section (if any)
IHT-2	$\sigma^A(g)$	Absorption
IHT-1	$\nu\sigma^F(g)$	Neutron Production
IHT	$\sigma^T(g)$	Total removal
IHT+1	$\sigma^{TUS}(g)$	Total upscatter cross section from group g (omit this entry if NUS=0)
IHS-NUS	$\sigma(g+NUS \rightarrow g)$	Scattering from group g + NUS to g
.	.	
.	.	
.	.	
IHS-1	$\sigma(g+1 \rightarrow g)$	Scattering from group g+1 to g
IHS	$\sigma(g \rightarrow g)$	Scattering from group g to g
IHS+1	$\sigma(g-1 \rightarrow g)$	Scattering from group g-1 to g
.	.	
.	.	
.	.	
IHM	$\sigma(g-NDS \rightarrow g)$	Scattering from group g-NDS to g

From this, it can be seen that:

$NUS = IHS - IHT - 2 =$ number of upscatter groups, if greater than 0,

$NDS = IHM - IHS =$ number of downscatter groups,

$L = IHT - 3 =$ number of activation cross sections.

Special illustrations of interest are:

$$IHM = IGM + 3$$

$$IHS = 4$$

$$IHT = 3$$



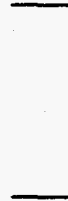
Full downscatter; no upscatter;
no activation cross section

and,

$$IHM = IGM + 5 + NUS$$

$$IHS = 6 + NUS$$

$$IHT = 4$$



Full downscatter; NUS upscatter;
room for an activation cross
section in position 1.

Thus the parameters IHT, IHS, and IHM completely describe the format of the cross sections. If there are no activity cross sections, $IHT=3$. If there is no upscatter $IHS = IHT + 1$. If there is no downscatter $IHM = IHS$ (i.e., a one group problem). If there is upscatter, GIP will compute a total upscatter cross section for each group of each material and place that cross section in position $IHT + 1$. The activity cross sections are only used for activity calculations and not used in the transport process itself.

2.5 GIP OUTPUT FILE

The GIP output file is group-ordered for transport codes and this format is compatible with both ANISN and DORT requirements. The groups are normally ordered from high to low neutron energy, then from high to low photon energy, if any photon groups are present.

GIP Cross Section Library Format

```

C-----
C
CR                PRINCIPAL CROSS SECTION DESCRIPTION
C
CL    (PCSD(IH),IH=1,IHT)
C
CW    NUMBER OF WORDS = MULT*IHT
C
CD    PCSD(IH)      PRINCIPAL CROSS SECTION LABELS - (A6)
C
C-----

C-----
C
CR                NUCLIDE IDENTIFICATION
C
CL    (NUC(MT),MT=1,MTM)
C
CW    NUMBER OF WORDS = MULT*MTM
C
CD    NUC(MT)      NUCLIDE LABELS - (A6)
C
C-----

C-----
C
CR                CROSS SECTION DATA
C
CL    ((SIG(IH,MT),IH=1,IHP),MT=1,MTM)
C
CW    NUMBER OF WORDS = IHP*MTM
C
CD    SIG(IH,MT)    CROSS SECTION DATA BY TABLE POSITION, THEN
CD                   BY NUCLIDE. TABLE POSITIONS CONTAIN:
CD    1  TO IHT-5   ARBITRARY DATA, SPECIFIED BY USER, OR ABSENT
CD                   IHT-4   FISSION YIELD FRACTION (RECOMMENDED)
CD                   IHT-3   FISSION CROSS SECTION (RECOMMENDED)
CD                   IHT-2   ABSORPTION CROSS SECTION
CD                   IHT-1   NEUTRON PRODUCTION CROSS SECTION
CD                   IHT-0   TOTAL CROSS SECTION
CD                   IHT+1   UPSCATTER FROM GROUP IG+(IHS-1-IHT) TO IG
CD    .....
CD    .....
CD                   IHS-1   UPSCATTER FROM GROUP IG+1 TO IG
CD                   IHS    SELF SCATTER FOR GROUP IG
CD                   IHT+1   DOWNSCATTER FROM GROUP IG-1 TO IG
CD    .....
CD    .....
CD                   IHM    DOWNSCATTER FROM GROUP IG+IHS-IHM TO IG
CD                   IHM+1   TOTAL SCATTER FROM GROUP G TO ALL GROUPS
CD                   (PRESENT ONLY IF IHS IS GREATER THAN IHT+1)

```

CD
 CD IHS MAY BE IHT+1 IF UPSCATTER IS ABSENT.
 CD TRANSFERS FROM GROUPS LESS THAN 1 OR
 CD GREATER THAN IGM ARE ZERO. POSITIONS
 CD LESS THAN OR EQUAL TO IHT ARE ZERO
 CD FOR PL COMPONENTS OTHER THAN THE 0TH.
 CD EACH COMPONENT OF A PL SET IS TREATED AS A
 CD SEPERATE NUCLIDE. THUS, M SETS WOULD
 CD COMPRISE M*NQUAD+M NUCLIDES
 CD IHP EQUALS IHM UNLESS IHS.GT.IHT+1, THEN IHM+1
 C
 C-----

2.6 LOGICAL UNIT REQUIREMENTS

Below is a listing of the files required to execute a GIP case along with the default values used in the code. In setting up a GIP case, efforts must be made for these units to be available.

1. Logical Unit 1 - SCRATCH
2. Logical Unit 2 - SCRATCH
3. Logical Unit 3 - SCRATCH
4. Logical Unit 8 - GIP formatted Cross-section Library Output
5. Logical Unit 9 - ANISN formatted Cross-section Library Input
6. Logical Unit 4 - SCRATCH
7. Logical Unit 6 - Printed Output
8. Logical Unit 5 - Card Input

Logical unit assignments for the first six data files can be modified by altering locations 15-20 of the 1\$ array (not shown in Section 2.2) to the new logical unit numbers. The new values will not be listed in the input edit, however.

2.7 REFERENCES

1. W. A. Rhoades, "The ALC1 Program for Cross-Section Library Management," ORNL-TM-4015, Oak Ridge National Laboratory, (December 1972).
2. W. A. Rhoades and R. L. Childs, "The DORT Two-Dimensional Discrete Ordinates Transport Code," Nuclear Science & Engineering 99, 1, pp. 88-89, (May 1988).
3. W. W. Engle, Jr., "A USER'S MANUAL FOR ANISN, A One-Dimensional Discrete-Ordinates Transport Code with Anisotropic Scattering," K-1693, Oak Ridge National Laboratory, (March 1967).

4. J. O. Johnson, J. D. Drischler, and J. M. Barnes, "Analysis of the Fall-1989 Two-Meter Box Test Bed Experiments Performed at the Army Pulse Radiation Facility (APRF)," ORNL/TM-11777, Oak Ridge National Laboratory, (May 1991).
5. R. T. Santoro et al., "DNA Radiation Environments Program Fall 1989 2-Meter Box Experiments and Analysis," ORNL/TM-11840, Oak Ridge National Laboratory, (May 1991).

2.8 SAMPLE PROBLEM

A complete listing of the input cards for the sample problem is given in Figure 2-1, and some selected output is shown in Figure 2-2. The sample problem demonstrates the processing of the materials for the air-over-ground analysis of the two-meter box experiments.^{4,5}

In viewing Figure 2-1, the input illustrates; 69 energy groups (IGM), a cross-section table length (IHM) of 72, no upscatter (IHT=3, and IHS=4), and a mixing table length (MS) of 558. No material data was read in from cards (MCR=0) and 144 materials were read in from tape (MTP=144). Since ISCT=5, there were actually 24 different nuclides read in from tape, each with a P_0 through P_5 component. The total number of mixtures (MTM) was 198, and only mixtures were output (IOUT=2) to the GIP library. No print was requested for the printed output (IPRT=1), and a DOT IV formatted cross-section file was output (IDOT=2). All comments after the slash (/) are ignored in FIDO input and are only useful for quick identification of the input parameters. The GIP sample input in Figure 2-1 shows multiple mixtures of the same material, i.e., ground and air, with different number densities. This allows mixing the cross sections for several different air-over-ground calculations in only one GIP case.

The selected GIP output shown in Figure 2-2 first illustrates the input parameters read in the first data block, followed by the memory requirements to run this particular GIP case, the input library record length, and an indication that the second data block has been successfully read. The output then produces the mixing table (10\$, 11\$, and 12* arrays) along with the mixing codes (7\$ array) and nuclide identification numbers (13\$ array). This output is useful for checking the input to make sure there are no errors in nuclides selected for mixtures, number densities used in mixtures, and nuclides selected from the input library. The mixing table is followed by a listing of the nuclides extracted from the input cross-section library file. This table is also useful for verifying the elements pulled off of the input cross-section library file. In this table, the user can also verify the P_L components used in the mixing. The output then shows some messages informing the user of the cross-section sorting process discussed in Section 2.1.2. Finally, the output lists the titles for the group-organized cross sections written to the output unit. If the print flag had been turned on (IPRT=0 or 2), the cross sections would have been printed after the titles. It should be noted that setting the print option to print either all elements and mixtures (IPRT=0) or only mixtures (IPRT=2) will produce a considerable amount of output for large group structures and high orders of scattering.

gip mixtures for the 10/89 two meter box experiments -- p5 forward

1\$\$ 69 3 4 72 558 /igm,iht,ihs,ihm,ms
0 144 198 0 5 /mcr,mtp,mtm,ith,isct
1 2 2 120 /iprt,iout,idot,nbuf

e t

10\$\$ 4i145 150 19q6 4i151 156 10q6 4i157 162 3q6 4i163 168 5q6
/ aprf ground borated concrete air 1020 steel

4i169 174 19q6 4i175 180 19q6 4i181 186 3q6 4i187 192 3q6
/ aprf ground aprf ground air air

4i193 198 3q6
/ air

11\$\$ 58i1 60 10i67 78 40i85 126 4i139 144 / aprf ground

16i1 18 4i31 36 16i43 60 4i91 96
4i103 108 10i127 138 / borated concrete

4i1 6 10i25 36 4i79 84 / air

4i19 24 16i55 72 10i97 108 / 1020 steel

58i1 60 10i67 78 40i85 126 4i139 144 / aprf ground

58i1 60 10i67 78 40i85 126 4i139 144 / aprf ground

4i1 6 10i25 36 4i79 84 / air

4i1 6 10i25 36 4i79 84 / air

4i1 6 10i25 36 4i79 84 / air

12** /number densities (atoms/b-cm)

6r4.236-02 6r9.586-09 6r3.509-08 6r3.775-04
6r4.752-05 6r4.178-02 6r1.427-04 6r9.126-05
6r1.377-03 6r9.514-03 6r3.610-06 6r3.537-06
6r2.048-04 6r2.599-05 6r7.199-06 6r3.213-04
6r2.783-07 6r2.793-07 6r4.858-07 6r7.315-08 /aprf ground-34% h2o

6r7.020-03 6r2.887-04 6r1.168-03 6r5.908-02
6r1.659-03 6r4.656-03 6r1.080-02 6r3.486-03
6r1.431-03 6r7.667-04 6r6.709-04 /borated concrete

Figure 2-1. Sample GIP Input for the
Two-Meter Box Air-Over-Ground Analysis.

6r6.122-07 6r3.985-05 6r1.100-05 6r2.383-07 /air - 10-24-89(a)

6r8.078-04 6r4.213-04 6r6.113-05 6r7.381-05
6r3.877-04 6r8.391-02 /1020 steel

6r2.653-02 6r1.162-08 6r4.254-08 6r4.576-04
6r5.760-05 6r3.823-02 6r1.729-04 6r1.106-04
6r1.669-03 6r1.153-02 6r4.376-06 6r4.288-06
6r2.482-04 6r3.151-05 6r8.727-06 6r3.895-04
6r3.373-07 6r3.386-07 6r5.889-07 6r8.867-08 /aprf ground-20% h2o

6r5.819-02 6r7.553-09 6r2.765-08 6r2.974-04
6r3.744-05 6r4.532-02 6r1.124-04 6r7.190-05
6r1.085-03 6r7.496-03 6r2.845-06 6r2.787-06
6r1.613-04 6r2.048-05 6r5.672-06 6r2.532-04
6r2.193-07 6r2.201-07 6r3.828-07 6r5.763-08 /aprf ground-48% h2o

6r3.278-07 6r4.021-05 6r1.095-05 6r2.405-07 /air - 11-01-89(h)

6r9.350-07 6r3.858-05 6r1.082-05 6r2.308-07 /air - 10-30-89(a)

6r5.596-07 6r3.948-05 6r1.087-05 6r2.361-07 /air - 10-25-89(a)

13\$\$ 1 2 3 4 5 6 43 44 45 46 47 48 49 50 51 52 53 54 55 56 57 58 59 60
61 62 63 64 65 66 67 68 69 70 71 72 79 80 81 82 83 84 85 86 87 88
89 90 91 92 93 94 95 96 97 98 99 100 101 102 103 104 105 106 107
108 109 110 111 112 113 114 115 116 117 118 119 120 121 122 123
124 125 126 127 128 129 130 131 132 133 134 135 136 137 138 157
158 159 160 161 162 163 164 165 166 167 168 169 170 171 172 173
174 175 176 177 178 179 180 181 182 183 184 185 186 199 200 201
202 203 204 205 206 207 208 209 210 223 224 225 226 227 228
/ h,b10,b11,c,n,o,na,mg,al,si,p,s,cl,ar,k,ca,mn,fe,co,ni,cu,zr,nb,sn

t

Figure 2-1. (continued)


```

** * execution began on 8/12/96 (225) at time 13:00:44
***** gip (ornl 17 may 90) *****
*** lhm aix configuration compiled 03/18/93 11:21:22
gip mixtures for the 10/89 two meter box experiments -- p5 forward
i$ array 21 entries read
0t

```

```

lcm no. of groups 69
lnt sigma(t) position 3
lms sigma(g-g) position 4
lhm table length 72
ms mixing table length 558
mcr no. of materials from cards 0
mtp no. of materials from lib. tape 144
mcm no. of materials (mcr+mcp+mixtures) 198
lth 0-direct solution, l=adjoin 0
lsc order of scattering expansion 5
lprt 0=print all, 1=no print, 2=print mixtures 1
lout 0=output all matls, 1=none, 2=mixt. only 2
ldot 0=anis output, 1=dotiii, 2=dotiv 2
nbuf no effect 120

```

```

16671 words memory required vs. available 100000
library record length = 4968, extended table length = 72

```

```

9 groups 2 through 10 go on unit 4
59 groups 11 through 69 go on unit 1

```

```

95726 words memory used
10$ array 558 entries read
11$ array 558 entries read
12* array 558 entries read
13$ array 144 entries read
0t

```

i	material (10\$)	component (11\$)	multiplier (12*)	mix code (7\$)	file id (13\$)
1	145	1	4.23600E-02	1	1
2	146	2	4.23600E-02	2	2
3	147	3	4.23600E-02	3	3
4	148	4	4.23600E-02	4	4
5	149	5	4.23600E-02	5	5
6	150	6	4.23600E-02	6	6
7	145	7	9.58600E-09	7	43
8	146	8	9.58600E-09	8	44
9	147	9	9.58600E-09	9	45
10	148	10	9.58600E-09	10	46
11	149	11	9.58600E-09	11	47
12	150	12	9.58600E-09	12	48
13	145	13	3.50900E-08	13	49
14	146	14	3.50900E-08	14	50
15	147	15	3.50900E-08	15	51
16	148	16	3.50900E-08	16	52
17	149	17	3.50900E-08	17	53
18	150	18	3.50900E-08	18	54
19	145	19	3.77500E-04	19	55
20	146	20	3.77500E-04	20	56
21	147	21	3.77500E-04	21	57
22	148	22	3.77500E-04	22	58
23	149	23	3.77500E-04	23	59
24	150	24	3.77500E-04	24	60

25	145	25	4.75200E-05	25	61
26	146	26	4.75200E-05	26	62
27	147	27	4.75200E-05	27	63
28	148	28	4.75200E-05	28	64
29	149	29	4.75200E-05	29	65
30	150	30	4.75200E-05	30	66
31	145	31	4.17800E-02	31	67
32	146	32	4.17800E-02	32	68
33	147	33	4.17800E-02	33	69
34	148	34	4.17800E-02	34	70
35	149	35	4.17800E-02	35	71
36	150	36	4.17800E-02	36	72
37	145	37	1.42700E-04	37	79
38	146	38	1.42700E-04	38	80
39	147	39	1.42700E-04	39	81
40	148	40	1.42700E-04	40	82

195	159	27	3.98500E-05	195	0
196	160	28	3.98500E-05	196	0
197	161	29	3.98500E-05	197	0
198	162	30	3.98500E-05	198	0
199	157	31	1.10000E-05		
200	158	32	1.10000E-05		
201	159	33	1.10000E-05		
202	160	34	1.10000E-05		

•
•
•

548	194	32	1.08700E-05		
549	195	33	1.08700E-05		
550	196	34	1.08700E-05		
551	197	35	1.08700E-05		
552	198	36	1.08700E-05		
553	193	79	2.36100E-07		
554	194	80	2.36100E-07		
555	195	81	2.36100E-07		
556	196	82	2.36100E-07		
557	197	83	2.36100E-07		
558	198	84	2.36100E-07		

elements from library file

matl	mix code	id	title
1	1	1	p0 h-1 minx(1301/1) xlags(1002) 08-14-85
2	2	2	p1 h-1 minx(1301/1) xlags(1002) 08-14-85
3	3	3	p2 h-1 minx(1301/1) xlags(1002) 08-14-85
4	4	4	p3 h-1 minx(1301/1) xlags(1002) 08-14-85
5	5	5	p4 h-1 minx(1301/1) xlags(1002) 08-14-85
6	6	6	p5 h-1 minx(1301/1) xlags(1002) 08-14-85
7	7	43	p0 b-10 1305 standard weighting
8	8	44	p1 b-10 1305 standard weighting
9	9	45	p2 b-10 1305 standard weighting
10	10	46	p3 b-10 1305 standard weighting
11	11	47	p4 b-10 1305 standard weighting
12	12	48	p5 b-10 1305 standard weighting

Figure 2-2. (continued)

13	13	p3	b-11	8811	standard weighting
14	14	p1	b-11	8811	standard weighting
15	15	p2	b-11	8811	standard weighting
16	16	p3	b-11	8811	standard weighting
17	17	p4	b-11	8811	standard weighting
18	18	p5	b-11	8811	standard weighting
19	19	p0	c	1306	standard weighting
20	20	p1	c	1306	standard weighting
21	21	p2	c	1306	standard weighting
22	22	p3	c	1306	standard weighting
23	23	p4	c	1306	standard weighting
24	24	p5	c	1306	standard weighting
25	25	p0	n-14	1275	standard weighting
26	26	p1	n-14	1275	standard weighting
27	27	p2	n-14	1275	standard weighting
28	28	p3	n-14	1275	standard weighting
29	29	p4	n-14	1275	standard weighting
30	30	p5	n-14	1275	standard weighting
31	31	p0	0-16	1276	standard weighting
32	32	p1	0-16	1276	standard weighting
33	33	p2	0-16	1276	standard weighting
34	34	p3	0-16	1276	standard weighting
35	35	p4	0-16	1276	standard weighting
36	36	p5	0-16	1276	standard weighting
37	37	p0	na-23	1311	standard weighting
38	38	p1	na-23	1311	standard weighting
39	39	p2	na-23	1311	standard weighting
40	40	p3	na-23	1311	standard weighting
41	41	p4	na-23	1311	standard weighting
42	42	p5	na-23	1311	standard weighting
43	43	p0	mg	1312	standard weighting
44	44	p1	mg	1312	standard weighting
45	45	p2	mg	1312	standard weighting
46	46	p3	mg	1312	standard weighting
47	47	p4	mg	1312	standard weighting
48	48	p5	mg	1312	standard weighting
49	49	p0	al-27	1313	standard weighting
50	50	p1	al-27	1313	standard weighting
51	51	p2	al-27	1313	standard weighting
52	52	p3	al-27	1313	standard weighting
53	53	p4	al-27	1313	standard weighting
54	54	p5	al-27	1313	standard weighting
55	55	p0	si	1314	standard weighting
56	56	p1	si	1314	standard weighting
57	57	p2	si	1314	standard weighting
58	58	p3	si	1314	standard weighting
59	59	p4	si	1314	standard weighting
60	60	p5	si	1314	standard weighting
61	61	p0	p-31	1315	standard weighting
62	62	p1	p-31	1315	standard weighting
63	63	p2	p-31	1315	standard weighting
64	64	p3	p-31	1315	standard weighting
65	65	p4	p-31	1315	standard weighting
66	66	p5	p-31	1315	standard weighting
67	67	p0	s	1347	standard weighting
68	68	p1	s	1347	standard weighting
69	69	p2	s	1347	standard weighting
70	70	p3	s	1347	standard weighting
71	71	p4	s	1347	standard weighting
72	72	p5	s	1347	standard weighting
73	73	p0	cl	1149	standard weighting

74	74	p1	cl	1149	standard weighting
75	75	p2	cl	1149	standard weighting
76	76	p3	cl	1149	standard weighting
77	77	p4	cl	1149	standard weighting
78	78	p5	cl	1149	standard weighting
79	79	p0	ar	8824	standard weighting
80	80	p1	ar	8824	standard weighting
81	81	p2	ar	8824	standard weighting
82	82	p3	ar	8824	standard weighting
83	83	p4	ar	8824	standard weighting
84	84	p5	ar	8824	standard weighting
85	85	p0	k	1150	standard weighting
86	86	p1	k	1150	standard weighting
87	87	p2	k	1150	standard weighting
88	88	p3	k	1150	standard weighting
89	89	p4	k	1150	standard weighting
90	90	p5	k	1150	standard weighting
91	91	p0	ca	1320	standard weighting
92	92	p1	ca	1320	standard weighting
93	93	p2	ca	1320	standard weighting
94	94	p3	ca	1320	standard weighting
95	95	p4	ca	1320	standard weighting
96	96	p5	ca	1320	standard weighting
97	97	p0	mn-55	1325	standard weighting
98	98	p1	mn-55	1325	standard weighting
99	99	p2	mn-55	1325	standard weighting
100	100	p3	mn-55	1325	standard weighting
101	101	p4	mn-55	1325	standard weighting
102	102	p5	mn-55	1325	standard weighting
103	103	p0	fe	9326	standard weighting
104	104	p1	fe	9326	standard weighting
105	105	p2	fe	9326	standard weighting
106	106	p3	fe	9326	standard weighting
107	107	p4	fe	9326	standard weighting
108	108	p5	fe	9326	standard weighting
109	109	p0	co-59	1327	standard weighting
110	110	p1	co-59	1327	standard weighting
111	111	p2	co-59	1327	standard weighting
112	112	p3	co-59	1327	standard weighting
113	113	p4	co-59	1327	standard weighting
114	114	p5	co-59	1327	standard weighting
115	115	p0	ni	1328	standard weighting
116	116	p1	ni	1328	standard weighting
117	117	p2	ni	1328	standard weighting
118	118	p3	ni	1328	standard weighting
119	119	p4	ni	1328	standard weighting
120	120	p5	ni	1328	standard weighting
121	121	p0	cu	1329	standard weighting
122	122	p1	cu	1329	standard weighting
123	123	p2	cu	1329	standard weighting
124	124	p3	cu	1329	standard weighting
125	125	p4	cu	1329	standard weighting
126	126	p5	cu	1329	standard weighting
127	127	p0	zr	8841	standard weighting
128	128	p1	zr	8841	standard weighting
129	129	p2	zr	8841	standard weighting
130	130	p3	zr	8841	standard weighting
131	131	p4	zr	8841	standard weighting
132	132	p5	zr	8841	standard weighting
133	133	p0	rb-93	1189	standard weighting
134	134	p1	rb-93	1189	standard weighting

```

135 135 207 p2 nb-93 1189 standard weighting
136 136 208 p3 nb-93 1189 standard weighting
137 137 209 p4 nb-93 1189 standard weighting
138 138 210 p5 nb-93 1189 standard weighting
139 139 223 p0 sn 8850 standard weighting
140 140 224 p1 sn 8850 standard weighting
141 141 225 p2 sn 8850 standard weighting
142 142 226 p3 sn 8850 standard weighting
143 143 227 p4 sn 8850 standard weighting
144 144 228 p5 sn 8850 standard weighting
*** all cross sections have been read from cards and library file 9, 1 group sorted directly to unit 3
*** 9 groups have been moved from unit 4 to unit 3

*** 1 group has been sorted from 3 to 1 a new corefull to 4, the balance, if any, to 2
*** 9 groups have been moved from unit 4 to unit 3

*** 1 group has been sorted from 3 to 2 a new corefull to 4, the balance, if any, to 1
*** 9 groups have been moved from unit 4 to unit 3

*** 1 group has been sorted from 3 to 1 a new corefull to 4, the balance, if any, to 2
*** 9 groups have been moved from unit 4 to unit 3

*** 1 group has been sorted from 3 to 2 a new corefull to 4, the balance, if any, to 1
*** 9 groups have been moved from unit 4 to unit 3

*** 1 group has been sorted from 3 to 1 a new corefull to 4, the balance, if any, to 2
*** 9 groups have been moved from unit 4 to unit 3

*** 9 groups have been moved from unit 2 to unit 3

cross sections for grp. 1
cross sections for grp. 2
cross sections for grp. 3
cross sections for grp. 4
cross sections for grp. 5
cross sections for grp. 6
cross sections for grp. 7
cross sections for grp. 8
.
.
.
cross sections for grp. 62
cross sections for grp. 63
cross sections for grp. 64
cross sections for grp. 65
cross sections for grp. 66
cross sections for grp. 67
cross sections for grp. 68
cross sections for grp. 69
*** accumulated charge = .1135 min. *** charge increment = .1135min.

```

Figure 2-2. (continued)

3.0 GRTUNCL: A TWO-DIMENSIONAL ANALYTIC FIRST COLLISION SOURCE CODE*

3.1 INTRODUCTION TO GRTUNCL

3.1.1 Background

In the development of DORT¹, a general method was obtained which was inherently capable of solving most two-dimensional neutron and gamma-ray transport problems, including deep penetration. The approximations of discrete ordinates theory are not limiting since, at least in principal, the number of energy groups, solid angle segments and space intervals, and the order of expansion of the differential scattering cross sections may be increased as necessary to obtain the desired solution. However, the problems which can be solved in practice are limited by the finite computer speed, memory size, and costs. In order to extend the capabilities of DORT, a combination of efficient programming and analytical "tools" were used. One of the analytical "tools" developed was the analytic first collision source code - GRTUNCL.

In two-dimensional r-z cylindrical geometry, the finite number of angles may result in an anomaly called the "ray effect." The problems in which ray effects are noticed are characterized by sources and detectors which are small compared to the total geometry, and a scattering mean free path which is long compared to the space mesh. Hence, if a problem such as a point source or point detector in a highly absorbing medium is approximated by the discrete ordinates difference equations, the fluences along a spherical surface centered about the source are observed to rise and fall in a wave-like pattern instead of being constant. Furthermore, the peaks in the distribution are observed to fall along rays following the polar angles of the quadrature centered at the source.

In the discrete ordinates solution of the two-dimensional cylindrical transport equation, the angles in the quadrature are arranged in levels which are comprised of directions having the same polar direction cosine, η . Within these levels, particles change angles due to both the curvature and scattering derivatives. However, transfers from a direction in one η level to one in another level occur only through scattering. Particles that start out in an η level tend to stay in the same level until scattered. Since there are only a finite number of η levels, particles tend to appear only at space intervals which are oriented with the source along a discrete η level. If the source region is distributed or if scattering is dominant, no ray effects appear. However, if the source is localized and spatial convection is dominant (i.e., the change in the particle fluence is governed by geometric attenuation), ray effects may be significant.

An obvious way to mitigate ray effects would be to increase the number of η levels. However, this approach is uneconomical and usually only slightly effective. Another technique is to employ an analytic first collision source. This method essentially removes

*R. L. Childs and J. V. Pace, III, "GRTUNCL: First Collision Source Program," Unpublished documentation (1982), included in the documentation of the Radiation Shielding Information Center CCC-484/DORT Code Package, Oak Ridge National Laboratory.

intermediate points a few mean free paths from the source, the fluence is dominated by the source from first collisions which, although emitted into the discrete mesh, is distributed smoothly in space due to the analytic uncollided fluence. For points many mean free paths from the source, the fluence is due to particles which have suffered many collisions, a situation in which ray effects would not normally appear.

Unfortunately, the technical problems involved in implementing the analytic first collision source in the general problem are prohibitive. For an arbitrary source distribution, the contribution to each space point from each source interval must be calculated. Furthermore, the cylindrical symmetry in r-z geometry must be accounted for by an azimuthal integration for each source interval. For example, a problem with 3000 space points and only 10 azimuthal intervals would require up to 9×10^7 calculations to determine the uncollided fluence. The point source on the cylindrical axis problem which produces the worst ray effects involves only 3×10^3 calculations for the same problem. Problems which have a co-axial parallel beam source may also be treated. Although these problems do not normally show severe ray effects, the source is usually input in the directions nearest the axis, which are usually 13° or more from the axis. This causes a slightly incorrect uncollided fluence and also makes it difficult to determine the collided fluence in the near axis angles.

3.1.2 Method Used²

An analytic first collision source technique has been developed for use with the two-dimensional code, DORT, for the simple sources described above. Basically, GRTUNCL is used to obtain the uncollided fluences and to generate space, angle, and energy dependent first collision source distributions for input into the DORT code. The actual calculational scheme in GRTUNCL for isotropic point sources consists of first calculating the uncollided fluence given by;

$$\phi_{u,g}(\mathbf{r}_i) = \sum_k S_g(\mathbf{r}_k) \frac{e^{-\beta_g(\mathbf{r}_k, \mathbf{r}_i)}}{4\pi|\mathbf{r}_i - \mathbf{r}_k|^2} \quad (3-1)$$

where $\phi_{u,g}(\mathbf{r}_i)$ is the uncollided fluence in energy group g at detector location \mathbf{r}_i due to an isotropic distributed source spanned at \mathbf{r}_k . Here $S_g(\mathbf{r}_k)$ is the number of source particles emitted at space point \mathbf{r}_k in energy group g per unit time and $\beta_g(\mathbf{r}_k, \mathbf{r}_i)$ is the number of mean-free-paths along the vector from \mathbf{r}_k to \mathbf{r}_i .

GRTUNCL then generates a space-, angle- and energy-dependent first collision source given by

$$\begin{aligned}
 S_g(\mathbf{r}_i, \Omega) = & \sum_l \sum_m \frac{A^{l,m}(\Omega)}{4\pi} \sum_{g'} \Sigma_{g' \rightarrow g}^l(\mathbf{r}_i) \\
 & \times \sum_k S_{g'}(\mathbf{r}_k) \frac{e^{-\beta_g(\mathbf{r}_k, \mathbf{r}_i)}}{4\pi |\mathbf{r}_i - \mathbf{r}_k|^2} \\
 & \times A^{l,m}(\Omega_k)
 \end{aligned} \tag{3-2}$$

where Ω_k represents the unit vector from \mathbf{r}_k to \mathbf{r}_i , the $A^{l,m}(\Omega)$ are reduced surface harmonics that result from two-dimensional symmetry, and the $\Sigma^l(g' \rightarrow g, \mathbf{r}_i)$ are the l 'th coefficients in Legendre expansions of the energy group-to-group scattering cross sections. The DORT code uses the first collision source distribution to calculate the distributions of the collided fluence moments throughout the geometry mesh.

The above procedure is implemented in GRTUNCL in the following manner:

1. The geometry is described with the same space mesh and material zones for the DORT problem.
2. The uncollided fluence (magnitude and angle) is calculated for each space point and energy group.
3. The first collision source, S , a function of radial interval, I , axial interval, J , angular moment, L , and group, G , is calculated for each space point, angular moment, and energy group.
4. The source array, S , and the scalar uncollided fluence are written to an output file.
5. DORT has been modified to use, as an option, the anisotropic source array, S , as the fixed source. The result of such a calculation is the collided fluence $\Phi_{c,g}(\mathbf{r})$. At the end of the calculation, an option is available to produce either the collided fluence or the total fluence (collided plus uncollided).

3.2 GRTUNCL INPUT REQUIREMENTS

The following input cards are required to execute GRTUNCL. Default values are in brackets (□).

Title Card (72 alphanumeric character description)

INPUT DATA BLOCK 1

1\$ Array - Integer Control Parameters

ITH input cross-section library flag
0/1 = forward/adjoint cross-section library
ISCT maximum order of Legendre expansion of cross sections
IZM number of material zones
IM number of radial intervals
JM number of axial intervals

- 5 ---

IGM number of energy groups
IHT position of total cross section in cross-section table
IHS position of self-scatter cross section in cross-section table
IHM cross-section table length per energy group (usually $IHM = IHT + IGM$)
MS cross-section mixing table length

- 10 ---

MCR number of materials read from cards
MTP number of materials read from input cross-section
library tape (nuclide or GIP format)
MT total number of materials (MCR+MTP+MIXTURES)
IDAT1 cross-section storage control flag
= 0 implies store cross sections in core
= 1 implies store cross sections on tape
= 2 implies cross sections on input GIP tape
NOA number of quadrature points in azimuthal spatial
integration for ring source (6* and 7* arrays required if > 0)

- 15 ---

IMODE output fluence file format flag
3/4 = DOT III/DOT IV format
IPRTC output cross-section print control flag
0/1 = print all materials/none
NFLSV uncollided fluence moments output control flag
= 0 implies no effect
> 0 implies write uncollided fluence moments on NFLSV
NPSO first collision source output control flag
= 0 implies no effect
> 0 implies write first collision source on NPSO
IPRTF number of groups of uncollided fluence to be printed

IPRTS number of groups of first collision source to be printed
 IZ3 source distribution table control flag
 = 0 implies no effect
 > 0 implies length of source distribution table
 IDFAC density factor control flag
 = 0 implies no effect
 > 0 implies density factors specified in 3* array
 NBUF number of k-bytes of core
 NTNPR = 0 implies no effect
 > 0 implies NTNPR is large scale print output unit

2* Array - Real Control Parameters

<p>XNF < 0 implies XNF is multiplication factor = 0 implies no normalization > 0 implies XNF is normalization factor</p>		<p>If IZ3 = 0</p>
<p>< 0 implies XNF is multiplication factor = 0 implies enter different $f(\eta)$ for each energy group in 14* array of INPUT DATA BLOCK 3 > 0 implies XNF is normalization factor</p>		<p>If IZ3 > 0</p>
<p>ZPT axial position of source (cm) RPT radial position of source (cm)</p>		

T (terminate block with "T") [T always required]

INPUT DATA BLOCK 2

13\$ Array - Nuclide ID Numbers on Library File (MTP entries required only if IDAT1 is not equal to 2)

14* Array - Cross Sections for Nuclide 1, ANISN³ format, all groups

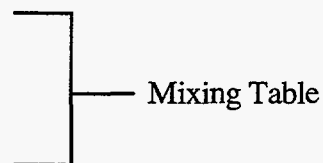
[each new nuclide must start on a new card]

- Cross Sections for Nuclide MCR, ANISN format, all groups (IHM*IGM*MCR entries required)

T (terminate block with "T") [T always required]

INPUT DATA BLOCK 3

- 1* Array - fission spectrum (IGM entries)
 - 2* Array - axial interval boundaries (JM+1 entries)
 - 3* Array - density factors by interval (IM*JM entries if IDFAC>0)
 - 4* Array - radial interval boundaries (IM+1 entries)
 - 6* Array - angular quadrature weights for azimuthal spatial integration (NOA entries)
 - 7* Array - discrete values of integrand for azimuthal spatial integration (NOA entries)
 - 8\$ Array - zone numbers by interval (IM*JM entries)
 - 9\$ Array - material numbers by zone (IZM entries)
 - 10\$ Array - Material Numbers (MS entries)
 - 11\$ Array - Component Numbers (MS entries)
 - 12* Array - Density Multipliers (MS entries)
 - 13* Array - direction cosines, η , for source input (IZ3 entries) (input negative η 's first)
 - 14* Array - input source shape, $f(\eta)$ (IZ3 or IZ3*IGM entries depending on XNF)
 - 15* Array - source by energy group (IGM entries)
- T (terminate block with "T") [T always required]



3.3 GRTUNCL INPUT DATA NOTES

Except for the title card, all data are read using the FIDO input system. A detailed description of the FIDO input system is given in Appendix A. Data arrays are entered in blocks, each terminated by a "T". Unused data arrays (e.g., 10\$ if MS=0) are not entered, but a "T" must still be entered to signal the termination of each block.

1\$ Array The definitions of many of the parameters in this array are compatible with GIP (Section 2.0) and DORT (Section 5.0).

ITH This flag only applies to the cross sections. If ITH=1, the source must be input in reverse order by energy group. If ITH=1, two major reordering steps are carried out to produce an adjoint cross-section library:

1. The inscatter matrix is transposed, i.e., the table position associated with group g describing scattering from g' to g is changed to describe scattering from g to g' .

2. The ordering of the groups is reversed, i.e., data for group IGM appear first in the output file, followed by IGM-1, etc.

A simple three group example is illustrated in Section 3.3.1.

ISCT When the order of scatter is greater than zero, GRTUNCL expects the P_1 cross section to be material $M+1$, the P_2 cross section to be $M+2$, etc., where M is the P_0 material number:

P_0 Data,	Nuclide 1
P_1	
P_2	
.	
.	
.	
P_{ISCT} Data,	Nuclide 1
P_0 Data,	Nuclide 2
P_1	
P_2	
.	
.	
.	
P_{ISCT} Data,	Nuclide 2
.	
.	
.	

For components other than P_0 , cross section positions other than positions IHT+1 through IHM may be zero.

IZM The number of material zones specified in GRTUNCL should correspond to the number of material zones specified in DORT. This is not a requirement, however, because in DORT the user has the option of specifying the convergence by zone and consequently may have more zones defined than are required in GRTUNCL. It is generally useful to set the number of material zones according to the DORT requirements and utilize the same input for GRTUNCL.

IM, JM The number of radial (IM) and axial (JM) intervals **must** correspond to the number of intervals utilized in DORT. Since GRTUNCL calculates the uncollided fluence and first collision source by interval, the number of intervals and interval boundaries must correspond to the DORT intervals. In setting up the interval boundaries, the position of the source (both axially and radially) must be considered so that the fluence does not differ by more than a factor of two between adjacent intervals. It should be noted that the interval next to the source interval will always exhibit greater than a factor of two difference in the fluence. A good rule of thumb for an air-over-ground calculation is to assume an initial

"source" interval size and apply a factor of 1.3 to that interval size to determine the interval boundaries. For example, assume the source is positioned at $r=0.0$ and the source interval is 10-cm wide. The radial interval boundaries will be 0.0, 10.0, 13.0 (10.0 x 1.3), 17.0 (13.0 x 1.3), 22.0 (17.0 x 1.3), 29.0 (22.0 x 1.3), etc., until the interval size reaches some predetermined maximum size, such as 25 meters for air. A similar sequence could be used for axial interval boundaries.

NOTE: GRTUNCL cannot handle a variable mesh. Therefore, in modeling the air-over-ground problem, ignore the DORT variable mesh option.

IHT, IHS, IHM The discussion of these input parameters is given in Section 3.4.2.

MCR, MTP, MT GRTUNCL assigns storage space (IHM*IGM words/set) for MT sets of cross sections, called "materials." The first MCR spaces are filled with data read from cards in the 14* array in INPUT DATA BLOCK 2. The next MTP material spaces are filled with nuclide data read from the data set mounted on the input library logical unit (default=4) and stored in the order indicated by the 13\$ array. The remaining spaces between MCR+MTP and MT are available for preparing mixtures.

NOTE: If MCR=0, and IDAT1=2, the 13\$ and 14* arrays in INPUT DATA BLOCK 2 and corresponding data block terminator are not required. This corresponds to pre-mixing the material cross sections in GIP and is the recommended method of supplying cross-section data to GRTUNCL.

IDAT1 This parameter controls the cross-section data storage. If IDAT1=0, MCR materials are read in from cards, MTP materials are read in from an ANISN formatted library on logical unit 4, and MT materials are stored in core. If IDAT1=1, MCR cross sections are read in from cards, MTP materials are read in from an ANISN formatted library on logical unit 4, and MCR+MTP materials are stored on logical unit one prior to mixing. MT materials (GIP formatted) are then stored on logical unit two after mixing. If IDAT1=2, MTP materials are read in from a GIP formatted library on logical unit four and stored on logical unit two. IDAT1=2 is the recommended option for cross-section storage.

NOA This parameter can be zero for on-centerline sources. Further discussion is given in the data notes for the 6* and 7* arrays.

IMODE This parameter identifies two possible output fluence file formats. Only the DOT IV format is discussed since it is used in present day applications. The DOT III format was retained from earlier versions of GRTUNCL, and although still operational, should be avoided, unless DOT III will be used in the final calculations.

IPRTC If IPRTC=0, printed cross-section edits for all materials will be output. It is recommended this parameter be set to one to avoid a large amount of output.

NFLSV If NFLSV is greater than zero, the uncollided fluence moment data are written on NFLSV. If IMODE = 4, the output is written in the VARSOR format, (see Section 3.5) which is suitable for use with DORT.

NPSO If NPSO is greater than zero, the first collision source data are written on NPSO. If IMODE=4, the output is written in the VARSOR format, (see Section 3.5) which is suitable for use as DORT input. If NPSO equals zero, the input parameters IPRTF and IPRTS are ignored.

IPRTF If IPRTF is greater than zero, IPRTF groups of uncollided fluence edits will be output. For a large number of intervals (IM*JM), it is recommended this parameter be set to a small number (less than five). Analyzing the first non-zero group of the uncollided fluence will indicate the adequacy of the interval boundaries in the spatial mesh.

IPRTS If IPRTS is greater than zero, IPRTS groups of first collision source edits will be output. It is recommended this parameter be set to zero because it generates a large volume of output.

IZ3 This parameter controls the number of direction cosines, η , used to describe the source input in the 13* array and the number of points used to describe the source shape, $f(\eta)$, input in the 14* array. If IZ3=0, only an energy dependent source distribution is entered in the 15* array, and the 13* and 14* arrays are omitted.

NBUF This parameter times 1000 is the initial memory objective of GRTUNCL. GRTUNCL divides the calculation into blocks where the number of blocks ranges from one to JM depending on how much memory has been allocated. A smaller number of blocks requires more memory. Consequently, a trade off between memory and I/O requirements results from the choice for NBUF. The minimum memory requirements (for JM blocks) will appear on the printed edits.

XNF This parameter is typically used as a normalization factor. For example, if the source distribution is per source particle, XNF can be used to obtain the absolute normalization if the total number of source particles is entered here. The meaning of the value of XNF is dependent on the parameter IZ3 and impacts additional input to GRTUNCL.

ZPT and RPT If RPT=0, the source will be a point source located axially at ZPT. If RPT>0, the source will be a ring source located axially at ZPT.

13\$ Array A negative entry in the 13\$ array replaces the following ISCT entries with successive ID's. Thus:

13\$		13\$
-101		101
-101	is equivalent to	102
-101		103

14* Array The input of the 14* array is performed by subroutines which have certain restrictions in addition to those of normal FIDO input:

- a. The nuclide spaces are preset to 0.0, so that "E" or "F0" will have the effect of filling the remaining space with 0.0, but "E" and "F" must not be used in the input for the last nuclide.
- b. The 14* or 14** designation may precede each nuclide block, but is not required except in the first block.

- c. Entries, including operators such as "T", following the last data item for nuclides other than the last, and on the same card as the last item, will be ignored.
- d. The "T" which terminates this block must appear alone in column 3 of a separate card.

7* Array The integration limits are assumed to be from -1 to 1 so $\int_{-1}^1 f(X) dX$ is assumed to be $\sum f(X_i) W_i$ where the W_i 's are entered in the 6* array and the X_i 's are entered in the 7* array.

8\$ Array The material zone numbers by interval are entered by IM entries by JM entries. For example, the material zone numbers are entered for the first axial interval, then the second axial interval, etc.

9\$ Array Negative numbers entered in this array indicates an anisotropic material and ISCT higher order moments must follow immediately on the cross-section unit. For example if a -1 and -7 are entered in this array for the first two material zones, and ISCT=5, GRTUNCL will expect to read the P_0 through P_5 components of the first material then the P_0 through P_5 components of the second material on the cross-section unit.

10\$, 11\$, and 12* Arrays The cross section mixing table is used to combine elements into macroscopic mixtures. Experience will reveal that only the imagination limits its flexibility. As with DORT, the integers in the mixing table refer to a continuous array of MT cross section sets of which the first MCR+MTP are nuclide data read from card-image input and a library file, respectively. All of the sets beyond MCR+MTP are preset to zero before the mixing table is executed. In non-search problems where cross-section storage is difficult, i.e., large problems that do not involve material buckling or concentration searches, material spaces originally used for input nuclides can be reused for mixtures. While the general rules for creating mixtures are equally applicable for GIP, GRTUNCL, and DORT, it should be noted that reference to eigenvalue modification in the DORT mixing table description has no application to GRTUNCL mixing. The interpretation rules applicable to GRTUNCL are as follows:

- a. If the mixture number is N and the component number is 0, then the cross sections in mixture N will be multiplied by the number entered in the density column:

$$\sigma_{\text{MIXTURE N(NEW)}} = \sigma_{\text{MIXTURE N(OLD)}} * \text{DENSITY}$$

- b. If the mixture number is N and the component number is M, then the cross sections in component M, multiplied by the density, will be added to the cross sections in mixture N:

$$\sigma_{\text{MIXTURE N(NEW)}} = \sigma_{\text{MIXTURE N(OLD)}} + \sigma_{\text{COMPONENT M}} * \text{DENSITY}$$

Note: Either a mixture or a component may be made up of microscopic or macroscopic cross sections for a single isotope or mixture of isotopes. A sample mixing table showing the various options is given below.

A sample mixing table showing the various options is given below.

MIXTURE (10\$ ARRAY)	COMPONENT (11\$ ARRAY)	DENSITY (12* ARRAY)
6	1	0.4
6	3	0.5
7	2	0.4
7	4	0.5
7	0	3.0

The mixture table given above would do the following:

- (1) Add components 1 and 3 with densities 0.4 and 0.5, respectively, to form mixture 6:

$$\sigma_6 = \sigma_1 * 0.4 + \sigma_3 * 0.5$$

- (2) Add components 2 and 4 with densities 0.4 and 0.5, respectively, to form mixture 7:

$$\sigma_7 = \sigma_2 * 0.4 + \sigma_4 * 0.5$$

- (3) Multiply mixture 7 by 3.0:

$$\sigma_7 = \sigma_7 * 3.0$$

10\$ Array If the 10\$ entry is tagged with a negative, the next ISCT components will be treated as P_L components. For example:

10\$	11\$	12*	(with ISCT = 3)
-13	1	1.0	

will be equivalent to

10\$	11\$	12*	(with ISCT = 0)
13	1	1.0	
14	2	1.0	
15	3	1.0	
16	4	1.0	

13*, 14*, and 15* Arrays These arrays control the source description in GRTUNCL. If IZ3=0, the source is entered only as a function of energy in the 15* array and the 13* and 14* arrays are omitted. This would be indicative of an isotropically emitted source spectrum. If IZ3>0, then the direction cosines, η , of the source are entered in the 13*

array (IZ3 entries with negative η 's entered first), and the source shape $f(\eta)$ is entered in the 14* array (IZ3 or IZ3*IGM entries depending on the value of XNF), and the energy dependence is entered in the 15* array (IGM entries). The units of the entries in the 14* array are particles/unit weight, i.e., 4π *particles/steradian. Typically, if IZ3>0 and XNF=0, the 13* array would contain IZ3 entries, the 14* array would contain IZ3*IGM entries, and the 15* array would be filled with IGM ones.

3.3.1 Adjoint Reordering Example

A three-group example showing the relationship between a forward and adjoint cross-section set is shown below. In this example, there is no upscatter, one activation cross section, IHT = 4, IHS = 5, and IHM = 7.

<u>Direct</u>	<u>Adjoint</u>
$\sigma^F(1)$	$\sigma^F(3)$
$\sigma^A(1)$	$\sigma^A(3)$
$v\sigma^F(1)$	$v\sigma^F(3)$
$\sigma^T(1)$	$\sigma^T(3)$
$\sigma(1 \rightarrow 1)$	$\sigma(3 \rightarrow 3)$
0	0
0	0
$\sigma^F(2)$	$\sigma^F(2)$
$\sigma^A(2)$	$\sigma^A(2)$
$v\sigma^F(2)$	$v\sigma^F(2)$
$\sigma^T(2)$	$\sigma^T(2)$
$\sigma(2 \rightarrow 2)$	$\sigma(2 \rightarrow 2)$
$\sigma(1 \rightarrow 2)$	$\sigma(2 \rightarrow 3)$
0	0
$\sigma^F(3)$	$\sigma^F(1)$
$\sigma^A(3)$	$\sigma^A(1)$
$v\sigma^F(3)$	$v\sigma^F(1)$
$\sigma^T(3)$	$\sigma^T(1)$
$\sigma(3 \rightarrow 3)$	$\sigma(1 \rightarrow 1)$
$\sigma(2 \rightarrow 3)$	$\sigma(1 \rightarrow 2)$
$\sigma(1 \rightarrow 3)$	$\sigma(1 \rightarrow 3)$

3.4 INPUT LIBRARY FORMAT

GRTUNCL inputs two different types of cross section files depending on the value of IDAT1. If IDAT1=0 or 1, the ACL1⁴ prepared input library format is expected. If IDAT1=2, the GIP formatted library format (see Section 3.4.3) is expected.

3.4.1 ACL1 Formatted Cross-section Input File

If IDAT1=0 or 1, the ACL1 prepared input library format from which MTP nuclides are taken is defined in the following manner:

ALC Cross Section Library Format

```
C*****
C          PROPOSED 19 MAY 80
C
C   CF      ALC
C   CE      TRANSPORT CODE CROSS SECTION DATA
C
C*****
C
C   CD          THE TERMINATION RECORD DEFINES THE LENGTH
C               OF THE DATA SET AND THE NUMBER OF NUCLIDES
C
C   CD          THE ID VALUES MUST BE IN ASCENDING ORDER
C
C-----
C   CS          FILE STRUCTURE
C
C   CS      RECORD TYPE                                PRESENT IF
C   CS      -----                                -----
C   CS ***** (REPEAT FOR ALL NUCLIDES)
C   CS *   CONTRAL DATA FOA A NUCLIDE                ALWAYS
C   CS *   CROSS SECTION DATA FOR A NUCLIDE         ALWAYS
C   CS *****
C
C   CS      TERMINATION                                ALWAYS
C
C-----
C
C-----
C   CR          CONTROL DATA FOR A NUCLIDE
C
C   CL      NOG,NCTL,NCC,NCID,(NAME(I),I=1,12)
C
C   CW      16=NUMBER OF WORDS
C
C   CD      NOG          NUMBER OF ENERGY GROUPS FOR THIS SET
C   CD      NCTL        LENGTH OF CROSS SECTION TABLE FOR THIS SET
```

```

CD   NCC           =0 SET WAS ADDED TO LIBRARY
CD           =2 SET REPLACED AND EXISTING SET
CD   NCID          IDENTIFICATION NUMBER
CD   NAME          ARBITRARY DESCRIPTION, A4 FORMAT

```

C

C

C

C

C

```

CR   CROSS SECTIONS FOR A NUCLIDE

```

C

```

CL   ((CRX(IH,IG),IH=1,NCTL),IG=1,NOG)

```

C

```

CW   NCTL*NOG=NUMBER OF WORDS

```

C

```

CD   CRX           CROSS SECTION DATA ORDERED

```

CD

AS PER SECTION 2.4.1

```

CD   NCTL          AS SPECIFIED BY PREVIOUS RECORD

```

CD

```

NOG          AS SPECIFIED BY PREVIOUS RECORD

```

C

C

C

C

```

CR   TERMINATION

```

C

```

CL   NOG,NCTL,NCC,NCID,(NAME(I),I=1,12)

```

C

```

CW   16=NUMBER OF WORDS

```

C

```

CD   NCC           7, ALWAYS

```

CD

```

OTHER ITEMS  ARBITRARY

```

C

C

3.4.2 ANISN Nuclide Format Cross-section File

In a normal GRTUNCL problem, cross sections are read from card input and/or from an external data set in nuclide-organized format, i.e., all the cross sections for one group of one nuclide, followed by other groups for that nuclide, and finally followed by data for other nuclides. Within a group, GRTUNCL expects the ordering of data in the cross section table in the following format:

Table Position	Entry	Cross Section Type
1	$\sigma^1(g)$	First activation cross section (if any)
.	.	.
.	.	.
IHT-3	$\sigma^L(g)$	Last activation cross section (if any)
IHT-2	$\sigma^A(g)$	Absorption
IHT-1	$\nu\sigma^F(g)$	Neutron Production
IHT	$\sigma^T(g)$	Total removal
IHT+1	$\sigma^{TUS}(g)$	Total upscatter cross section from group g (omit this entry if NUS=0)
IHS-NUS	$\sigma(g+NUS \rightarrow g)$	Scattering from group g+NUS to g
.	.	.
.	.	.
.	.	.
IHS-1	$\sigma(g+1 \rightarrow g)$	Scattering from group g+1 to g
IHS	$\sigma(g \rightarrow g)$	Scattering from group g to g
IHS+1	$\sigma(g-1 \rightarrow g)$	Scattering from group g-1 to g
.	.	.
.	.	.
.	.	.
IHM	$\sigma(g-NDS \rightarrow g)$	Scattering from group g-NDS to g

From this, it can be seen that:

NUS = IHS-IHT-2 = number of upscatter groups, if greater than 0,

NDS = IHM-IHS = number of downscatter groups,

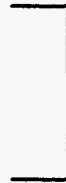
L = IHT-3 = number of activation cross sections.

Special illustrations of interest are:

$$IHM = IGM + 3$$

$$IHS = 4$$

$$IHT = 3$$



Full downscatter; no upscatter;
no activation cross section

and,

$$IHM = IGM + 5 + NUS$$

$$IHS = 6 + NUS$$

$$IHT = 4$$



Full downscatter; NUS upscatter;
room for an activation cross
section in position 1.

Thus the parameters IHT, IHS, and IHM completely describe the format of the cross sections. If there are no activity cross sections, IHT=3. If there is no upscatter IHS = IHT + 1. If there is no downscatter IHM = IHS (i.e., a one group problem). If there is upscatter, GRTUNCL will compute a total upscatter cross section for each group of each material and place that cross section in position IHT + 1. The activity cross sections are only used for activity calculations and not used in the transport process itself.

3.4.3 GIP Formatted Cross-section Input File

If IDAT1=2, GRTUNCL expects to read a GIP formatted library on logical unit four. Also, if IDAT1=0 or 1, GRTUNCL will create a GIP formatted cross-section file. The GIP input file is group-ordered for transport codes and this format is compatible with both ANISN, GRTUNCL, and DORT requirements. The groups are normally ordered from high to low neutron energy, then from high to low photon energy, if any photon groups are present.

GIP Cross Section Library Format

```

C-----
C
CR          PRINCIPAL CROSS SECTION DESCRIPTION
C
CL          (PCSD(IH),IH=1,IHT)
C
CW          NUMBER OF WORDS = MULT*IHT
C
CD          PCSD(IH)          PRINCIPAL CROSS SECTION LABELS - (A6)
C
C-----
C-----
C

```

CR NUCLIDE IDENTIFICATION
 C
 CL (NUC(MT),MT=1,MTM)
 C
 CW NUMBER OF WORDS = MULT*MTM
 C
 CD NUC(MT) NUCLIDE LABELS - (A6)
 C
 C

C
 C
 CR CROSS SECTION DATA
 C
 CL ((SIG(IH,MT),IH=1,IHP),MT=1,MTM)
 C
 CW NUMBER OF WORDS = IHP*MTM
 C
 CD SIG(IH,MT) CROSS SECTION DATA BY TABLE POSITION,
 CD THEN BY NUCLIDE. TABLE POSITIONS CONTAIN:
 CD 1 TO IHT-5 ARBITRARY DATA, SPECIFIED BY USER, OR ABSENT
 CD IHT-4 FISSION YIELD FRACTION (RECOMMENDED)
 CD IHT-3 FISSION CROSS SECTION (RECOMMENDED)
 CD IHT-2 ABSORPTION CROSS SECTION
 CD IHT-1 NEUTRON PRODUCTION CROSS SECTION
 CD IHT-0 TOTAL CROSS SECTION
 CD IHT+1 UPSCATTER FROM GROUP IG+(IHS-1-IHT) TO IG
 CD
 CD
 CD IHS-1 UPSCATTER FROM GROUP IG+1 TO IG
 CD IHS SELF SCATTER FOR GROUP IG
 CD IHT+1 DOWNSCATTER FROM GROUP IG-1 TO IG
 CD
 CD
 CD IHM DOWNSCATTER FROM GROUP IG+IHS-IHM TO IG
 CD IHM+1 TOTAL SCATTER FROM GROUP G TO ALL GROUPS
 CD (PRESENT ONLY IF IHS IS GREATER THAN IHT+1)
 CD
 CD IHS MAY BE IHT+1 IF UPSCATTER IS ABSENT.
 CD TRANSFERS FROM GROUPS LESS THAN 1 OR
 CD GREATER THAN IGM ARE ZERO. POSITIONS
 CD LESS THAN OR EQUAL TO IHT ARE ZERO FOR
 CD PL COMPONENTS OTHER THAN THE 0TH.
 CD EACH COMPONENT OF A PL SET IS TREATED AS A
 CD SEPERATE NUCLIDE. THUS, M SETS WOULD
 CD COMPRISE M*NQUAD+M NUCLIDES
 CD IHP EQUALS IHM UNLESS IHS.GT.IHT+1, THEN IHM+1
 C
 C

3.5 GRTUNCL OUTPUT FILE

GRTUNCL can output either a DOT III or DOT IV formatted file depending on the value of IMODE. Current applications only use the DOT IV format - referred to as the VARSOR format in this document. Both the first collision source and uncollided fluence moment data are written in this format. The VARSOR format is defined in the following manner:

```

C                                                    -VSOR0010
C                                                    VSOR0020
C***** VSOR0030
C                REVISED 10 NOV 76                    -VSOR0040
C                                                    -VSOR0050
CF      VARSOR                                         -VSOR0060
CE      VARIABLE MESH SOURCE MOMENT DATA             -VSOR0070
C                                                    -VSOR0080
C***** VSOR0090
C                                                    VSOR0100
CD      ORDER OF GROUPS IS BY DECREASING ENERGY     VSOR0110
CD      I IS THE FIRST-DIMENSION INDEX                VSOR0120
CD      J IS THE SECOND-DIMENSION INDEX              VSOR0130
CD      JM=1 FOR 1-DIMENSIONAL GEOMETRY              VSOR0140
CD      IF ISOP.GT.0, SOURCE IS FIRST-COLLISION TYPE VSOR0150
C                                                    VSOR0160
C----- VSOR0170
CS      FILE STRUCTURE                                -VSOR0180
CS                                                    -VSOR0190
CS      RECORD TYPE                                  PRESENT IF    -VSOR0200
CS      -----
CS      FILE IDENTIFICATION                          ALWAYS        -VSOR0220
CS      FILE LABEL                                   ALWAYS        -VSOR0230
CS      FILE CONTROL                                 ALWAYS        -VSOR0240
CS      FILE INTEGER PARAMETERS                     ALWAYS        -VSOR0250
CS                                                    -VSOR0260
CS ***** (REPEAT OVER ALL GROUPS)                 -VSOR0270
CS *          SOURCE MOMENTS                          ALWAYS        -VSOR0280
CS *****
C                                                    -VSOR0300
CS ***** (REPEAT OVER ALL GROUPS)                 -VSOR0310
CS *          SCALAR UNCOLLIDED FLUX                 ISOP.GT.0     -VSOR0320
CS *****
C                                                    -VSOR0340
C----- VSOR0350
C                                                    VSOR0360
C                                                    VSOR0370
C----- VSOR0380
CR      FILE IDENTIFICATION                          -VSOR0390
C                                                    -VSOR0400
CL      HNAME,(HUSE(I),I=1,2),IVERS                 -VSOR0410
C                                                    -VSOR0420
CW      1+3*MULT=NUMBER OF WORDS                    -VSOR0430
C                                                    -VSOR0440
CD      HNAME      HOLLERITH FILE NAME - VARSOR     -(A6)        -VSOR0450
CD      HUSE(I)    HOLLERITH USER IDENTIFICATION    -(A6)        -VSOR0460

```

CD	IVERS	FILE VERSION NUMBER	-VSOR0470
CD	MULT	DOUBLE PRECISION PARAMETER	-VSOR0480
CD		1- A6 WORD IS SINGLE WORD	-VSOR0490
CD		2- A6 WORD IS DOUBLE PRECISION WORD	-VSOR0500
C			-VSOR0510
C			-VSOR0520
C			VSOR0530
C			VSOR0540
C			-VSOR0550
C			-VSOR0560
CR		FILE LABEL	-VSOR0570
C			-VSOR0580
CL		DATE,USER,CHARGE,CASE,TIME,(TTTL(I),I=1,12)	-VSOR0590
C			-VSOR0600
CW		17*MULT=NUMBER OF WORDS	-VSOR0610
C			-VSOR0620
CD	DATE	AS PROVIDED BY TIMER OPTION 4 - (A6)	-VSOR0630
CD	USER	AS PROVIDED BY TIMER OPTION 5 - (A6)	-VSOR0640
CD	CHARGE	AS PROVIDED BY TIMER OPTION 6 - (A6)	-VSOR0650
CD	CASE	AS PROVIDED BY TIMER OPTION 7 - (A6)	-VSOR0660
CD	TIME	AS PROVIDED BY TIMER OPTION 8 - (A6)	-VSOR0670
CD	TTTL(I)	TITLE PROVIDED BY USER - (A6)	-VSOR0680
C			-VSOR0690
C			-VSOR0700
C			VSOR0710
C			VSOR0720
C			-VSOR0730
CR		FILE CONTROL	VSOR0740
C			-VSOR0750
CD	IGM,NEUT,JM,LM,IMA,MMA,ISM,IMSISM,ISOP,(IDUM(N),N=1,16)		-VSOR0760
C			-VSOR0770
CW		25=NUMBER OF WORDS	-VSOR0780
C			-VSOR0790
CD	IGM	NUMBER OF ENERGY GROUPS	-VSOR0800
CD	NEUT	LAST NEUTRON GROUP	-VSOR0810
CD		(IGM IF ALL NEUTRONS, 0 IF ALL GAMMA)	-VSOR0820
CD	JM	NUMBER OF SECOND-DIMENSION (J) INTERVALS	-VSOR0830
CD	LM	MAXIMUM LENGTH OF MOMENT EXPANSION	-VSOR0840
CD	IMA	MAXIMUM NUMBER OF FIRST-DIMENSION INTERVALS	-VSOR0850
CD	MMA	NUMBER OF BOUNDARY DIRECTIONS	-VSOR0860
CD	ISM	NUMBER OF I-BOUNDARY SETS	-VSOR0870
CD	IMSISM	TOTAL NUMBER OF I-INTERVALS, ALL I-SETS	-VSOR0880
CD	ISOP	UNCOLLIDED FLUX FLAG	-VSOR0890
CD		0 - NO UNCOLLIDED FLUX RECORDS PRESENT	-VSOR0900
CD		1 - UNCOLLIDED FLUX RECORDS PRESENT	-VSOR0910
CD	IDUM(I)	ARRAY SET TO 0	-VSOR0920
C			-VSOR0930
C			-VSOR0940
C			VSOR0950
C			VSOR0960
C			-VSOR0970
CR		FILE INTEGER PARAMETERS	-VSOR0980
C			-VSOR0990

CL	(LMBIG(IG),IG=1,IGM),	-VSOR1000
CL	*(IMBIS(IS),IS=1,ISM),(ISET(J),J=1,JM)	-VSOR1010
C		-VSOR1020
CW	IGM+ISM+JM=NUMBER OF WORDS	-VSOR1030
C		-VSOR1040
CD	LMBIG(IG) LENGTH OF MOMENT EXPANSION FOR GROUP IG	-VSOR1050
CD	IMBIS(IS) NUMBER OF INTERVALS IN ISET IS	-VSOR1060
CD	ISET(J) I-SET ASSIGNED TO INTERVAL J	-VSOR1070
C		-VSOR1080
C		VSOR1090
C		VSOR1100
C		VSOR1110
C		VSOR1120
CR	SOURCE MOMENTS	VSOR1130
C		-VSOR1140
CL	((SORM(I,L),I=1,IMS),L=1,LMS)	-VSOR1150
C		-VSOR1160
CW	IMS*LMS=NUMBER OF WORDS	-VSOR1170
C		-VSOR1180
C	DO 1 J=1,JM	-VSOR1190
C 1	READ(N) *LIST AS ABOVE*	-VSOR1200
C		-VSOR1210
CD	SORM SOURCE BY INTERVAL AND MOMENT INDEX	-VSOR1220
CD	IMS IMBIS(IS) FOR IS CORRESPONDING TO J	-VSOR1230
CD	LMS LMBIG(IG)	-VSOR1240
C		-VSOR1250
C		VSOR1260
C		VSOR1270
C		VSOR1280
C		VSOR1290
CR	SCALAR UNCOLLIDED FLUX	-VSOR1300
C		-VSOR1310
CL	(FLUM(I),I=1,IMS)	-VSOR1320
C		-VSOR1330
CW	IMS=NUMBER OF WORDS	-VSOR1340
C		-VSOR1350
C	DO 1 J=1,JM	-VSOR1360
C 1	READ(N) *LIST AS ABOVE*	-VSOR1370
C		-VSOR1380
CD	FLUX UNCOLLIDED FLUX BY INTERVAL	-VSOR1390
C		-VSOR1400
C		VSOR1410
C		VSOR1420
C		VSOR1430
C		VSOR1440
C		VSOR1450
C	END	VSOR1460

3.6 LOGICAL UNIT REQUIREMENTS

Below is a listing of the files required to execute a GRTUNCL case along with the default values used in the code. In setting up a GRTUNCL case, efforts must be made for these units to be available.

- | | | |
|------------------|-------|---|
| 1. Logical Unit | 1 | - SCRATCH, (holds group independent cross sections from input if logical unit 4 is not a group-independent (GIP) tape |
| 2. Logical Unit | 2 | - SCRATCH, (holds GIP cross sections after mixing) |
| 3. Logical Unit | 4 | - ANISN/GIP formatted Cross-section Library
Input depending on value for IDAT1 (required if MTP>0) |
| 5. Logical Unit | NPSO | - First Collision Source Output |
| 6. Logical Unit | NFLSV | - Uncollided Flux Moments Output |
| 7. Logical Unit | NTNPR | - Large Scale Print Output |
| 8. Logical Unit | 91 | - SCRATCH |
| 9. Logical Unit | 92 | - SCRATCH |
| 10. Logical Unit | 6 | - Printed Output |
| 11. Logical Unit | 5 | - Card Input |

Many of these subroutines also call other subroutines. Many are entirely system dependent. Each configuration to be distributed contains an appropriate set of service subroutines, insofar as possible. The realities of computing environments may require local modification or substitution. The specifications given in Reference 4, together with extensive in-stream comments, provide guides for such modification.

3.7 REFERENCES

1. W. A. Rhoades and R. L. Childs, "The DORT Two-Dimensional Discrete Ordinates Transport Code," Nuclear Science & Engineering 99, 1, pp. 88-89, (May 1988).
2. R. A. Lillie, R. G. Alsmiller, Jr., and J. T. Mihalczko, "Design Calculations for a 14-MeV Neutron Collimator," Nuclear Technology Vol. 43, pp. 373-377, (May 1979).
3. W. W. Engle, Jr., "A USER'S MANUAL FOR ANISN, A One-Dimensional Discrete-Ordinates Transport Code with Anisotropic Scattering," K-1693, Oak Ridge National Laboratory, (March 1967).
4. W. A. Rhoades, "The ALC1 Program for Cross-Section Library Management," ORNL-TM-4015, Oak Ridge National Laboratory, (December 1972).
5. J. O. Johnson, J. D. Drischler, and J. M. Barnes, "Analysis of the Fall-1989 Two-Meter Box Test Bed Experiments Performed at the Army Pulse Radiation Facility (APRF)," ORNL/TM-11777, Oak Ridge National Laboratory, (May 1991).

6. R. T. Santoro et al., "DNA Radiation Environments Program Fall 1989 2-Meter Box Experiments and Analysis," ORNL/TM-11840, Oak Ridge National Laboratory, (May 1991).

3.8 SAMPLE PROBLEM

The sample problem demonstrates the calculation of the air-over-ground environment for the two-meter box experiments.^{5,6} Figure 3-1 shows a simple diagram of the geometry modeled in the GRTUNCL input. A complete listing of the input cards for the sample problem is given in Figure 3-2, and some selected output is shown in Figure 3-3.

In viewing Figure 3-2, the input illustrates; 8 material zones (IZM), 66 radial intervals (IM), 98 axial intervals (JM), 69 energy groups (IGM), a cross-section table length (IHM) of 72, no upscatter (IHT=3, and IHS=4), and a mixing table length (MS) of 0. No material data was read in from cards (MCR=0) and 54 materials (9 different mixtures, each with a P_0 through P_5 component) were read in from a GIP tape (MTP=54, and IDAT1=2). Thus, the total number of materials (MT) was 54, and no print was requested for the printed output (IPRTC=1). A DOT IV formatted first collision source file was output (IMODE=4) on logical unit 23 (NPSO=23) and the first two groups of uncollided fluence were printed (IPRTF=2). The input source was a point source located 16.143 meters above the $z=0.0$ plane (ZPT), at $r=0.0$ (RPT), and was entered as an angular/energy dependent source with 40 directions specified (IZ3=40). Eighteen materials (3 mixtures) were used in the calculation which correspond to the first eighteen materials output in the GIP sample problem shown in the last section (ground, borated concrete, and air). The three mixtures and eight material zones illustrates the multiple zone option per material eluded to in Section 3.3. All comments after the slash (/) are ignored in FIDO input and are only useful for quick identification of the input parameters. The GRTUNCL sample input in Figure 3-2 shows an angular and energy dependent source distribution with units 4π *particles/steradian per leaking neutron. The energy dependence (15* array) is already represented in the shape function (14* array) and is therefore entered as ones.

The selected GRTUNCL output shown in Figure 3-3 first illustrates the input parameters read in the first data block, followed by the blocking and memory requirements to run this particular GRTUNCL case with this order of blocking, and an indication that the second data block has been successfully read. The output then produces the zone number by interval map, the material number by interval map, and a table listing the input in the 2*, 3*, 4*, 6*, 7*, 9*, 10\$, 11\$, and 12* arrays. This output is useful for checking the input to make sure there are no errors. This table is followed by a listing of the fission spectrum (1* array), then the source distribution (13*, 14*, and 15* arrays). The output then shows some messages informing the user of the completion of the calculations (by block) and the time required to perform each block. After the calculation is complete (all blocks calculated), GRTUNCL prints the balance table. This table is useful for checking the source normalization, and leakages for the system. Errors in the model, cross sections, or mesh should make themselves evident in this table. Finally, the output lists the fission density by interval and the first collision source by interval (for the number of groups specified in the input).

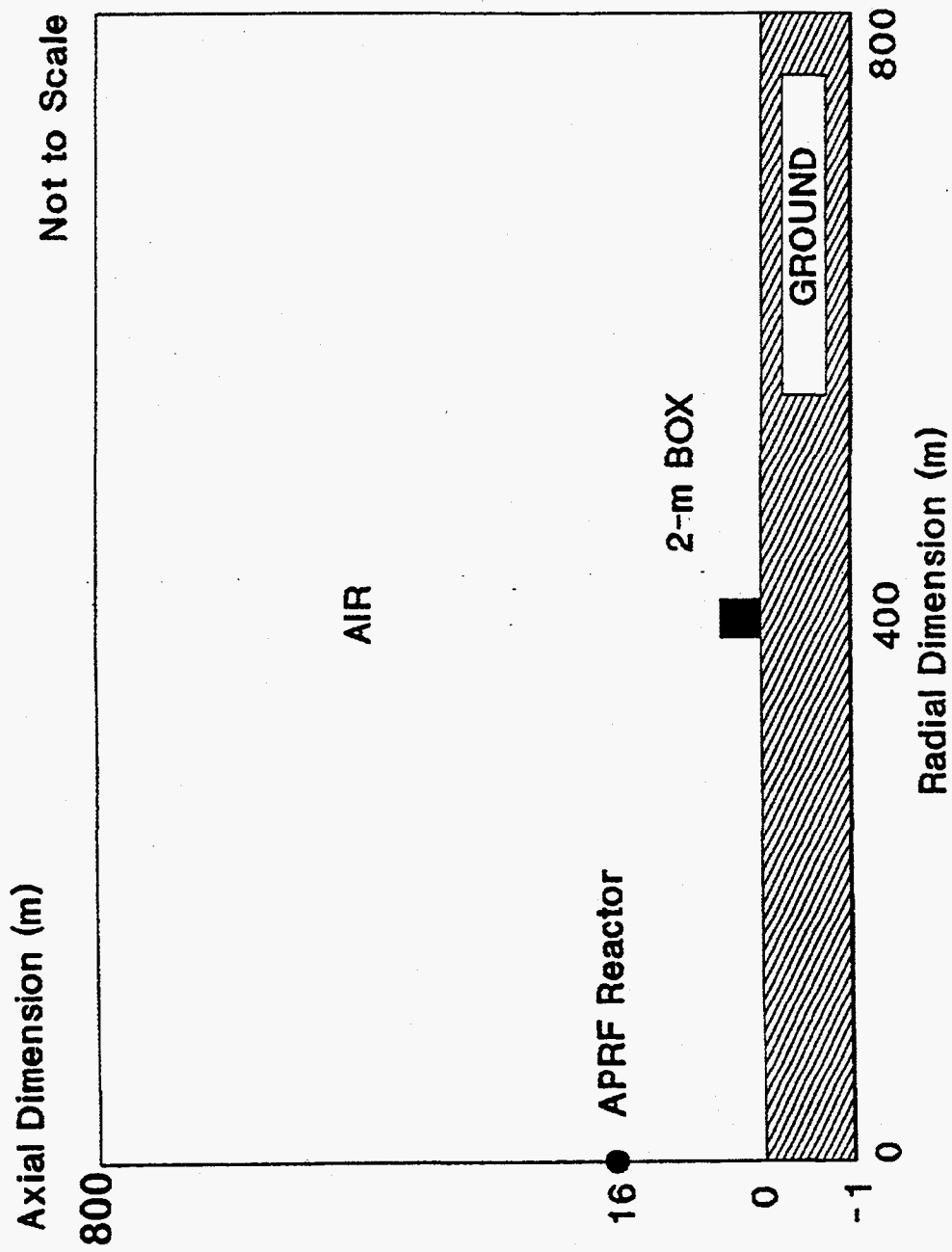


Figure 3-1. Schematic Diagram of the Air-Over-Ground Geometry Model Used in the GRTUNCL Analysis.

' aprf air-over-ground using new saic 1989 angle-energy leakage source
' 16.143m source height, simple topography out to 400m test site
' 34% ground moisture, 10/24/89(a) air parameters

1\$\$ 0 5 8 66 98 / ith,isct,izm,im,jm
69 3 4 72 0 / igm,iht,ihs,ihm,ms
0 54 54 2 0 / mcr,mtp,mt,idat1,noa
4 1 0 23 2 / imode,iprtc,nflsv,npso,iprtf
0 40 0 300 0 / iprts,iz3,idfac,nbuf,ntnpr

2** 0 1614.3 0 / xnf,zpt,rpt

t

1** f0 /fission spectrum

2** /axii (jm+1)

-80 -75 -70 -65 -60 -55 -50 -45 -40 -35 -30 -25 -20 -15 -10 -5 -2.5
-1 0 50 150 250 489 749 949 1102 1220 1311 1381 1435 1476 1508 1532
1551 1566 1577 1585 1592 1597 1601 1604 1607 1608.5 1610 1614.3 1619
1620.5 1622 1624 1627 1631 1636 1643 1651 1662 1677 1696 1720 1752
1793 1847 1917 2008 2126 2279 2479 2739 3076 3514 4085 4826 5789 7042
8670 10787 13000 16000 19000 22000 25000 28000 31000 34000 37000 40000
43000 46000 49000 52000 55000 58000 61000 64000 67000 70000 73000
76000 78000 80000

4** /radii (im+1)

0 4.6 6 7.8 10 13 17 22 29 37 48 63 82 106 138 179 233 303 394 512 665
865 1125 1462 1900 2471 3212 4175 5428 7056 9000 11000 13000 15000
16500 17500 19000 21000 23000 25000 27000 28500 29500 30500 31500
33000 35000 37000 38500 39500 40500 41500 43000 45000 47000 49000
51000 54000 57000 60000 63000 66000 69000 72000 75000 78000 80000

8\$\$ / zone numbers by interval

' zones 1, 2, & 3-aprf ground, 4 & 5-borated concrete, 6, 7, & 8-air
66r1 8q66 /j-ints 1-9
19r5 47r1 2q66 /j-ints 10-12
19r4 3r3 8r1 3r3 3r2 5r3 3r2 4r3 3r2 3 14r1 5q66 /j-ints 13-18
33r7 3r6 5r7 3r6 4r7 3r6 7 14r8 3q66 /j-ints 19-22
52r7 14r8 3q66 /j-ints 23-26
66r8 71q66 /j-ints 27-98

9\$\$ 3r-1 2r-7 3r-13 / mat by zone

Figure 3-2. Sample GRTUNCL Input for the
Two-Meter Box Air-Over-Ground Analysis.

13** / angular directions of source (-1. is down +1. is up)
-.99794 -.98973 -.97337 -.94900 -.91680 -.88117 -.84355 -.80122
-.75441 -.70316 -.64809 -.58978 -.52822 -.46383 -.39684 -.32761
-.25670 -.18443 -.11105 -.03705 +.03705 +.11105 +.18443 +.25670
+.32761 +.39684 +.46383 +.52822 +.58978 +.64809 +.70316 +.75441
+.80122 +.84355 +.88117 +.91680 +.94900 +.97337 +.98973 +.99794

14**
' aprf angular leakage source, s(angle,energy)/40 angles/dabl69/(3-1-90)
' units are 4*pi*particles/steradian per leaking neutron
1.41e-06 1.43e-06 1.65e-06 1.85e-06 2.02e-06 2.37e-06 2.49e-06 2.60e-06
2.67e-06 2.74e-06 2.70e-06 2.75e-06 2.81e-06 2.86e-06 2.91e-06 3.00e-06
3.03e-06 3.05e-06 3.07e-06 3.07e-06 3.07e-06 3.07e-06 3.07e-06 3.07e-06
3.05e-06 2.98e-06 2.98e-06 2.96e-06 2.96e-06 2.95e-06 3.00e-06 2.95e-06
2.79e-06 2.46e-06 2.07e-06 1.53e-06 1.60e-06 1.74e-06 1.92e-06 2.02e-06

[IZ3*IGM entries]

1.49e-07 1.90e-07 2.28e-07 2.62e-07 2.93e-07 3.19e-07 3.35e-07 3.47e-07
3.49e-07 3.38e-07 3.31e-07 3.43e-07 3.47e-07 3.36e-07 3.24e-07 3.16e-07
3.05e-07 2.88e-07 2.60e-07 2.21e-07 1.88e-07 1.88e-07 1.92e-07 1.94e-07
2.00e-07 1.99e-07 2.02e-07 2.04e-07 2.04e-07 2.02e-07 2.02e-07 2.09e-07
2.11e-07 2.11e-07 2.04e-07 1.34e-07 9.76e-08 8.75e-08 7.01e-08 6.14e-08

15** / source multiplier for each energy group
69r1.0
t

Figure 3-2. (continued)

```

* * * execution began on 8/12/96 (225) at time 15:10:28
***** grtunc1 (ornl 6 apr 92) *****
on cray, rbuf*1000 is initial memory objective.
*** ibm aix configuration compiled 03/18/93 11:21:22
* aprf air-over-ground using new saic 1989 angle-energy leakage source
* 16.143m source height, simple topography out to 400m test site
* 34% ground moisture, 10/24/89(a) air parameters
1$ array 25 entries read
2* array 3 entries read
0t

```

```
1$$ array(25 entries)
```

```

ith 0
lsct 5
izm 8
im 66
jm 98

igm 69
iht 3
ihs 4
ihm 72
ms 0

mcr 0
mtp 54
mt 54
idatl 2
noa 0

imode 4
iprtc 1
nflsv 0
npso 23
iprtf 2

iprts 0
iz3 40
idfac 0
rbuf 300
rtmpr 0

```

```

2** array(3 entries)
xnf 0.000000E+00
zpt 1.614300E+03
rpt 0.000000E+00

```

```

first data location 16368
the mesh is divided into 36 blocks
idatl= 2
words required = 293212
words available = 300000
1* array 69 entries read
2* array 99 entries read
4* array 67 entries read
* zones 1, 2, & 3-aprf ground, 4 & 5-borated concrete, 6, 7, & 8-air
8$ array 6468 entries read
9$ array 8 entries read

```

Figure 3-3. Sample GRTUNCL Output for the Two-Meter Box Air-Over-Ground Analysis.

92... dddddd
91... dddddd
90... dddddd
89... dddddd
88... dddddd
86... dddddd
84... dddddd
83... dddddd
81... dddddd
80... dddddd
79... dddddd
78... dddddd
77... dddddd
76... dddddd
75... dddddd
74... dddddd
73... dddddd
72... dddddd
71... dddddd
70... dddddd
69... dddddd
68... dddddd
67... dddddd
66... dddddd
65... dddddd
64... dddddd
63... dddddd
62... dddddd
61... dddddd
59... dddddd
58... dddddd
57... dddddd
56... dddddd
55... dddddd
54... dddddd
53... dddddd
52... dddddd
51... dddddd
50... dddddd
49... dddddd
48... dddddd
47... dddddd
46... dddddd
45... dddddd
44... dddddd
43... dddddd
42... dddddd
41... dddddd
40... dddddd
39... dddddd
38... dddddd
37... dddddd
36... dddddd
35... dddddd
34... dddddd
33... dddddd
32... dddddd

Figure 3-3. (continued)

24 7.49000E+02 1.46200E+03
 25 9.49000E+02 1.90000E+03
 26 1.10200E+03 2.47100E+03
 27 1.22000E+03 3.21200E+03
 28 1.31100E+03 4.17500E+03
 29 1.38100E+03 5.42800E+03
 30 1.43500E+03 7.05600E+03
 31 1.47600E+03 9.00000E+03
 32 1.50800E+03 1.10000E+04
 33 1.53200E+03 1.30000E+04
 34 1.55100E+03 1.50000E+04
 35 1.56600E+03 1.65000E+04
 36 1.57700E+03 1.75000E+04
 37 1.58500E+03 1.90000E+04
 38 1.59200E+03 2.10000E+04
 39 1.59700E+03 2.30000E+04
 40 1.60100E+03 2.50000E+04
 41 1.60400E+03 2.70000E+04
 42 1.60700E+03 2.85000E+04
 43 1.60850E+03 2.95000E+04
 44 1.61000E+03 3.05000E+04
 45 1.61430E+03 3.15000E+04
 46 1.61900E+03 3.30000E+04
 47 1.62050E+03 3.50000E+04
 48 1.62200E+03 3.70000E+04
 49 1.62400E+03 3.85000E+04
 50 1.62700E+03 3.95000E+04
 51 1.63100E+03 4.05000E+04
 52 1.63600E+03 4.15000E+04
 53 1.64300E+03 4.30000E+04
 54 1.65100E+03 4.50000E+04
 55 1.66200E+03 4.70000E+04
 56 1.67700E+03 4.90000E+04
 57 1.69600E+03 5.10000E+04
 58 1.72000E+03 5.40000E+04
 59 1.75200E+03 5.70000E+04
 60 1.79300E+03 6.00000E+04
 61 1.84700E+03 6.30000E+04
 62 1.91700E+03 6.60000E+04
 63 2.00800E+03 6.90000E+04
 64 2.12600E+03 7.20000E+04
 65 2.27900E+03 7.50000E+04
 66 2.47900E+03 7.80000E+04
 67 2.73900E+03 8.00000E+04
 68 3.07600E+03
 69 3.51400E+03
 70 4.08500E+03
 71 4.82600E+03
 72 5.78900E+03
 73 7.04200E+03
 74 8.67000E+03
 75 1.07870E+04
 76 1.30000E+04
 77 1.60000E+04
 78 1.90000E+04
 79 2.20000E+04
 80 2.50000E+04
 81 2.80000E+04
 82 3.10000E+04
 83 3.40000E+04
 84 3.70000E+04

85 4.000000E+04
86 4.300000E+04
87 4.600000E+04
88 4.900000E+04
89 5.200000E+04
90 5.500000E+04
91 5.800000E+04
92 6.100000E+04
93 6.400000E+04
94 6.700000E+04
95 7.000000E+04
96 7.300000E+04
97 7.600000E+04
98 7.800000E+04
99 8.000000E+04
chi
1 0.000000E+00
2 0.000000E+00
3 0.000000E+00
4 0.000000E+00
5 0.000000E+00
6 0.000000E+00
7 0.000000E+00
8 0.000000E+00
9 0.000000E+00
10 0.000000E+00
11 0.000000E+00
12 0.000000E+00
13 0.000000E+00
14 0.000000E+00
15 0.000000E+00
16 0.000000E+00
17 0.000000E+00
18 0.000000E+00
19 0.000000E+00
20 0.000000E+00
21 0.000000E+00
22 0.000000E+00
23 0.000000E+00
24 0.000000E+00
25 0.000000E+00
26 0.000000E+00
27 0.000000E+00
28 0.000000E+00
29 0.000000E+00
30 0.000000E+00
31 0.000000E+00
32 0.000000E+00
33 0.000000E+00
34 0.000000E+00
35 0.000000E+00
36 0.000000E+00
37 0.000000E+00
38 0.000000E+00
39 0.000000E+00
40 0.000000E+00
41 0.000000E+00
42 0.000000E+00
43 0.000000E+00
44 0.000000E+00
45 0.000000E+00

46 0.00000E+00
47 0.00000E+00
48 0.00000E+00
49 0.00000E+00
50 0.00000E+00
51 0.00000E+00
52 0.00000E+00
53 0.00000E+00
54 0.00000E+00
55 0.00000E+00
56 0.00000E+00
57 0.00000E+00
58 0.00000E+00
59 0.00000E+00
60 0.00000E+00
61 0.00000E+00
62 0.00000E+00
63 0.00000E+00
64 0.00000E+00
65 0.00000E+00
66 0.00000E+00
67 0.00000E+00
68 0.00000E+00
69 0.00000E+00

apr f air-over-ground using new saic 1989 angle-energy leakage source
spectrum eta f(eta)

1 1.00000E+00-9.97940E-01 1.41000E-06
2 1.00000E+00-9.89730E-01 1.43000E-06
3 1.00000E+00-9.73370E-01 1.65000E-06
4 1.00000E+00-9.49000E-01 1.85000E-06
5 1.00000E+00-9.16800E-01 2.02000E-06
6 1.00000E+00-8.81170E-01 2.37000E-06
7 1.00000E+00-8.43550E-01 2.49000E-06
8 1.00000E+00-8.01220E-01 2.60000E-06
9 1.00000E+00-7.54410E-01 2.67000E-06
10 1.00000E+00-7.03160E-01 2.74000E-06
11 1.00000E+00-6.48090E-01 2.70000E-06
12 1.00000E+00-5.89780E-01 2.75000E-06
13 1.00000E+00-5.28220E-01 2.81000E-06
14 1.00000E+00-4.63830E-01 2.86000E-06
15 1.00000E+00-3.96840E-01 2.91000E-06
16 1.00000E+00-3.27610E-01 3.00000E-06
17 1.00000E+00-2.56700E-01 3.03000E-06
18 1.00000E+00-1.84430E-01 3.05000E-06
19 1.00000E+00-1.11050E-01 3.07000E-06
20 1.00000E+00-3.70500E-02 3.07000E-06
21 1.00000E+00 3.70500E-02 3.07000E-06
22 1.00000E+00 1.11050E-01 3.07000E-06
23 1.00000E+00 1.84430E-01 3.07000E-06
24 1.00000E+00 2.56700E-01 3.07000E-06
25 1.00000E+00 3.27610E-01 3.05000E-06
26 1.00000E+00 3.96840E-01 2.98000E-06
27 1.00000E+00 4.63830E-01 2.98000E-06
28 1.00000E+00 5.28220E-01 2.96000E-06
29 1.00000E+00 5.89780E-01 2.96000E-06
30 1.00000E+00 6.48090E-01 2.95000E-06
31 1.00000E+00 7.03160E-01 3.00000E-06
32 1.00000E+00 7.54410E-01 2.95000E-06
33 1.00000E+00 8.01220E-01 2.79000E-06
34 1.00000E+00 8.43550E-01 2.46000E-06
35 1.00000E+00 8.81170E-01 2.07000E-06

Figure 3-3. (continued)

36 1.00000E+00 9.16800E-01 1.53000E-06
 37 1.00000E+00 9.49000E-01 1.60000E-06
 38 1.00000E+00 9.73370E-01 1.74000E-06
 39 1.00000E+00 9.89730E-01 1.92000E-06
 40 1.00000E+00 9.97940E-01 2.02000E-06
 41 1.00000E+00
 42 1.00000E+00
 43 1.00000E+00
 44 1.00000E+00
 45 1.00000E+00
 46 1.00000E+00
 47 1.00000E+00
 48 1.00000E+00
 49 1.00000E+00
 50 1.00000E+00
 51 1.00000E+00
 52 1.00000E+00
 53 1.00000E+00
 54 1.00000E+00
 55 1.00000E+00
 56 1.00000E+00
 57 1.00000E+00
 58 1.00000E+00
 59 1.00000E+00
 60 1.00000E+00
 61 1.00000E+00
 62 1.00000E+00
 63 1.00000E+00
 64 1.00000E+00
 65 1.00000E+00
 66 1.00000E+00
 67 1.00000E+00
 68 1.00000E+00
 69 1.00000E+00

unnormalized srcce = 6.90000E+01

block	calcs started at	.018min.
block	1 completed at	.101min.
block	2 completed at	.182min.
block	3 completed at	.263min.
block	4 completed at	.345min.
block	5 completed at	.428min.
block	6 completed at	.513min.
block	7 completed at	.598min.
block	8 completed at	.679min.
block	9 completed at	.763min.
block	10 completed at	.845min.
block	11 completed at	.929min.
block	12 completed at	1.011min.
block	13 completed at	1.094min.
block	14 completed at	1.176min.
block	15 completed at	1.259min.
block	16 completed at	1.341min.
block	17 completed at	1.423min.
block	18 completed at	1.505min.
block	19 completed at	1.588min.
block	20 completed at	1.670min.
block	21 completed at	1.753min.
block	22 completed at	1.835min.

Figure 3-3. (continued)

2 1.07591E-05-1.23753E-11 3.42216E-09 6.44414E-10 4.07895E-09
 3 1.24565E-05-1.73627E-11 4.26229E-09 8.29990E-10 5.10964E-09
 4 1.1532E-06-1.34794E-11 3.28316E-09 6.39556E-10 3.93620E-09
 5 7.04891E-05-9.85650E-11 2.62022E-08 5.08858E-09 3.13874E-08
 6 2.83191E-05-3.94955E-11 1.16444E-08 2.21998E-09 1.39039E-08
 7 2.13035E-04-1.50664E-10 1.17756E-07 2.30153E-08 1.40922E-07
 8 4.60803E-04-8.76166E-10 3.70026E-07 7.32468E-08 4.44149E-07
 9 8.91883E-04-1.99238E-09 1.18370E-06 2.39589E-07 1.42528E-06
 10 1.59968E-03-2.00267E-09 2.31856E-06 4.65638E-07 2.78620E-06
 11 2.63393E-03-7.73890E-09 1.98255E-06 3.77267E-07 2.36256E-06
 12 6.72393E-03-7.48710E-09 9.50816E-06 1.83583E-06 1.13515E-05
 13 2.09598E-02-3.31993E-09 1.69938E-05 3.06098E-06 2.00582E-05
 14 5.9402E-03-4.15460E-10 1.59011E-05 3.04676E-06 1.89483E-05
 15 2.19329E-02-2.17046E-10 2.82237E-06 4.41078E-07 3.26367E-06
 16 6.27034E-02-7.84719E-12 5.15899E-06 7.79804E-07 5.93880E-06
 17 6.56423E-02-9.32579E-10 5.69914E-05 9.85782E-06 6.68501E-05
 18 1.04967E-02-3.03411E-09 1.80896E-05 3.39414E-06 2.14867E-05
 19 7.68555E-02-2.20303E-11 2.17639E-05 3.63055E-06 2.53945E-05
 20 9.03129E-02-2.50887E-12 3.29074E-06 4.93965E-07 3.78471E-06
 21 9.61213E-02-5.35780E-15 1.46816E-06 2.18053E-07 1.68621E-06
 22 5.27601E-02-1.27450E-20 8.05274E-08 1.10281E-08 9.15555E-08
 23 5.82897E-02-9.89144E-17 5.21786E-06 8.72970E-07 6.09083E-06
 24 3.41645E-02-4.99962E-16 1.38525E-06 1.87136E-07 1.57239E-06
 25 5.22346E-02-1.20851E-15 5.46274E-07 7.96667E-08 6.25941E-07
 26 4.88532E-02-2.70115E-17 1.82622E-06 2.91076E-07 2.11730E-06
 27 1.01478E-01-1.36170E-25 2.47214E-09 2.58055E-10 2.73020E-09
 28 7.11288E-02-1.06922E-20 1.68580E-08 2.03424E-09 1.88923E-08
 29 4.63480E-02-1.09984E-23 2.45894E-09 2.38988E-10 2.69793E-09
 30 2.12024E-02-3.37558E-23 2.20942E-10 2.03914E-11 2.41334E-10
 31 1.80737E-02-1.21628E-26 1.26723E-11 1.01032E-12 1.36826E-11
 32 4.23493E-03-3.09829E-29 1.04171E-13 8.02113E-15 1.12192E-13
 33 1.49434E-03-5.06954E-31 5.71456E-15 3.14986E-16 6.02965E-15
 34 4.34480E-04-6.54652E-31 5.73575E-16 7.63378E-17 6.49913E-16
 35 9.05235E-04-1.10238E-31 2.70574E-16 2.15748E-17 2.92149E-16
 36 2.45922E-04-1.34847E-33 8.45354E-18 6.47688E-19 9.10123E-18
 37 3.72120E-05-5.03707E-35 1.40673E-19 1.58866E-20 1.56560E-19
 38 3.36068E-06-5.57123E-36 2.06729E-21 4.03580E-22 2.47087E-21
 39 4.76344E-07-5.36536E-37 9.92158E-23 2.55748E-23 1.24791E-22
 40 1.13398E-07-1.27659E-37 5.95114E-24 2.09104E-24 8.04218E-24
 41 1.88760E-08-1.57209E-38 3.89822E-25 1.62597E-25 5.52419E-25
 42 2.44621E-09-9.96138E-40 3.70676E-26 1.73316E-26 5.43991E-26
 43 4.61859E-10 0.00000E+00 5.50897E-27 2.47929E-27 7.98826E-27
 44 6.75769E-11 0.00000E+00 5.87626E-28 2.43023E-28 8.30649E-28
 45 1.17765E-11 0.00000E+00 5.88339E-29 2.18894E-29 7.77733E-29
 46 1.85923E-12 0.00000E+00 6.19833E-32 1.92715E-32 8.12549E-32
 47 1.62175E-08-1.00784E-10 9.43995E-10 3.52313E-10 1.39709E-09
 48 8.11090E-08-4.22772E-10 4.14318E-09 1.50732E-09 6.07327E-09
 49 3.73676E-06-1.70578E-08 1.68661E-07 4.94261E-08 2.35145E-07
 50 1.18880E-04-4.27079E-07 4.47361E-06 1.34231E-06 6.24301E-06
 51 1.74687E-04-4.21695E-07 5.87575E-06 1.52315E-06 7.82059E-06
 52 4.41183E-04-7.18547E-07 1.33670E-05 3.01218E-06 1.70977E-05
 53 1.72274E-03-1.87154E-06 4.28340E-05 8.99649E-06 5.37020E-05
 54 4.45535E-03-2.93805E-06 8.24115E-05 1.67041E-05 1.02054E-04
 55 1.44603E-02-4.65321E-06 1.71922E-04 3.36793E-05 2.10254E-04
 56 1.54080E-02-2.26712E-06 1.16225E-04 2.13096E-05 1.39801E-04
 57 2.60688E-02-1.79828E-06 1.25034E-04 2.19494E-05 1.48782E-04
 58 4.38189E-02-1.02020E-06 1.10233E-04 1.80700E-05 1.29323E-04
 59 7.95954E-03-3.55974E-07 7.52923E-05 1.11317E-05 8.67801E-05
 60 7.39111E-02-4.51912E-08 2.01774E-05 2.80565E-06 2.30283E-05
 61 6.70498E-02-3.75891E-09 4.54535E-06 5.29687E-07 5.07880E-06
 62 3.07221E-02-1.44062E-10 4.20441E-07 4.04300E-08 4.61015E-07

Figure 3-3. (continued)

group	1	2	3	4	5	6	7	8
63	2.47184E-02	4.84771E-12	3.21983E-08	4.15263E-09	3.63558E-08			
64	4.53559E-03	1.15044E-14	6.50443E-10	7.76091E-11	7.28063E-10			
65	5.48991E-04	1.18756E-17	1.43772E-11	1.53202E-12	1.59092E-11			
66	2.27423E-05	5.02749E-24	4.11464E-14	5.56658E-15	4.67130E-14			
67	5.95163E-07	0.00000E+00	1.46362E-18	1.77325E-19	1.64094E-18			
68	6.58337E-08	0.00000E+00	1.09848E-28	9.15849E-30	1.19007E-28			
69	2.44651E-07	0.00000E+00	0.00000E+00	0.00000E+00	0.00000E+00			
70	1.36329E+00	1.65618E-05	9.40107E-04	1.70541E-04	1.12721E-03			
1	1.46785E-18	2.60373E-18	4.61867E-18	8.19303E-18	1.45339E-17	2.57825E-17	4.57380E-17	8.11403E-17
2	1.46779E-18	2.60363E-18	4.61849E-18	8.19275E-18	1.45334E-17	2.57817E-17	4.57367E-17	8.11382E-17
3	1.46774E-18	2.60354E-18	4.61834E-18	8.19250E-18	1.45330E-17	2.57810E-17	4.57355E-17	8.11363E-17
4	1.46766E-18	2.60339E-18	4.61810E-18	8.19141E-18	1.45323E-17	2.57799E-17	4.57337E-17	8.11333E-17
5	1.46751E-18	2.60315E-18	4.61770E-18	8.19141E-18	1.45312E-17	2.57780E-17	4.57306E-17	8.11282E-17
6	1.46726E-18	2.60274E-18	4.61699E-18	8.19024E-18	1.45292E-17	2.57747E-17	4.57252E-17	8.11192E-17
7	1.46685E-18	2.60203E-18	4.61581E-18	8.18626E-18	1.45259E-17	2.57693E-17	4.57161E-17	8.11044E-17
8	1.46613E-18	2.60081E-18	4.61376E-18	8.18481E-18	1.45201E-17	2.57597E-17	4.57003E-17	8.10785E-17
9	1.46495E-18	2.59883E-18	4.61043E-18	8.17922E-18	1.45108E-17	2.57442E-17	4.56748E-17	8.10365E-17
10	1.46303E-18	2.59559E-18	4.60498E-18	8.17010E-18	1.44956E-17	2.57189E-17	4.56329E-17	8.09679E-17
11	1.45963E-18	2.58985E-18	4.59533E-18	8.15392E-18	1.44686E-17	2.56740E-17	4.55588E-17	8.08467E-17
12	1.45385E-18	2.58009E-18	4.57888E-18	8.12636E-18	1.44226E-17	2.55976E-17	4.54324E-17	8.06387E-17
13	1.44438E-18	2.56410E-18	4.55198E-18	8.00557E-18	1.42208E-17	2.54723E-17	4.52254E-17	8.02986E-17
14	1.42853E-18	2.53732E-18	4.50689E-18	8.00557E-18	1.42208E-17	2.54723E-17	4.52254E-17	8.02986E-17
15	1.40212E-18	2.49267E-18	4.43163E-18	7.87923E-18	1.40095E-17	2.49105E-17	4.48777E-17	7.97274E-17
16	1.35862E-18	2.41903E-18	4.30739E-18	7.67032E-18	1.36597E-17	2.43275E-17	4.33294E-17	7.71787E-17
17	1.30824E-18	2.33662E-18	4.17381E-18	7.45626E-18	1.33215E-17	2.38029E-17	4.25356E-17	7.60188E-17
18	1.26918E-18	2.27735E-18	4.08696E-18	7.33568E-18	1.31688E-17	2.36442E-17	4.24590E-17	7.62583E-17
19	1.16476E-18	2.10473E-18	3.80416E-18	6.87743E-18	1.24365E-17	2.24947E-17	4.06976E-17	7.36491E-17
20	3.66799E-18	6.70934E-18	1.22771E-17	2.24741E-17	4.11563E-17	7.53985E-17	1.38185E-16	2.53360E-16
21	2.67661E-18	5.00046E-18	9.34761E-18	1.74848E-17	3.27260E-17	6.12917E-17	1.14866E-16	2.15407E-16
22	1.60461E-18	3.09194E-18	5.96339E-18	1.15135E-17	2.22501E-17	4.30416E-17	8.33457E-17	1.61555E-16
23	6.06702E-19	1.23001E-18	2.49737E-18	5.07822E-18	1.03419E-17	2.10939E-17	4.30913E-17	8.81668E-17
24	1.31698E-19	2.89953E-19	6.35403E-19	1.40041E-18	3.09353E-18	6.84951E-18	1.51998E-17	3.37858E-17
25	1.32936E-20	3.28246E-20	8.13163E-20	2.02112E-19	5.04029E-19	1.26120E-18	3.16663E-18	7.97823E-18
26	5.46992E-22	1.60247E-21	4.71636E-21	1.39462E-20	4.14340E-20	1.23689E-19	3.71020E-19	1.11835E-18
27	6.91455E-24	2.57342E-23	9.63892E-23	3.63363E-22	1.37873E-21	5.26586E-21	2.02460E-20	7.83645E-20
28	2.00907E-26	1.03734E-25	5.40237E-25	2.83810E-24	1.50412E-23	8.04236E-23	4.33812E-22	2.36103E-21
29	8.86130E-30	7.09735E-29	5.75011E-28	4.71284E-27	3.90808E-26	3.27919E-25	2.78443E-24	2.39289E-23
30	5.81171E-34	8.11178E-33	1.14928E-31	1.65309E-30	2.41426E-29	3.58055E-28	5.39335E-27	8.25216E-26
31	1.39074E-38	3.60936E-37	9.54495E-36	2.57248E-34	7.06710E-33	1.97930E-31	5.65251E-30	1.64631E-28
32	2.90699E-43	1.41727E-41	7.08604E-40	3.62469E-38	1.89737E-36	1.01657E-34	5.57596E-33	3.13180E-31
33	0.00000E+00	0.00000E+00	5.32493E-44	5.23385E-42	5.23187E-38	5.37461E-38	5.67500E-36	6.16056E-34
34	0.00000E+00	0.00000E+00	0.00000E+00	0.00000E+00	4.09179E-43	7.44132E-41	1.39524E-38	6.69908E-36
35	0.00000E+00	0.00000E+00	0.00000E+00	0.00000E+00	2.80260E-45	6.82432E-43	1.92849E-40	5.63923E-38
36	0.00000E+00	0.00000E+00	0.00000E+00	0.00000E+00	0.00000E+00	5.60519E-45	2.68629E-42	1.18762E-39
37	0.00000E+00	0.00000E+00	0.00000E+00	0.00000E+00	0.00000E+00	0.00000E+00	7.00649E-45	5.40341E-42
38	0.00000E+00	0.00000E+00	0.00000E+00	0.00000E+00	0.00000E+00	0.00000E+00	0.00000E+00	1.12104E-44
39	0.00000E+00	0.00000E+00	0.00000E+00	0.00000E+00	0.00000E+00	0.00000E+00	0.00000E+00	0.00000E+00
40	through	66	same as above					

Y Z 97 Z 98
1 6.42204E-20 5.18375E-20
2 through 7 same as above
8 6.42203E-20 5.18375E-20
9 6.42203E-20 5.18374E-20

Figure 3-3. (continued)

10 through 10 same as above
 11 6.42201E-20 5.18373E-20

•
 •
 •

61 7.72899E-21 6.56007E-21
 62 6.39203E-21 5.48237E-21
 63 5.24005E-21 4.50965E-21
 64 4.27860E-21 3.89453E-21
 65 3.47792E-21 3.01535E-21
 66 2.89955E-21 2.53354E-21
 group 2

	Y	Z	1	Z	2	Z	3	Z	4	Z	5	Z	6	Z	7	Z	8
1	3.05221E-18	5.63974E-18	1.04210E-17	1.92562E-17	3.55828E-17	6.57531E-17	1.21507E-16	1.21507E-16	1.21507E-16	1.21507E-16	1.21507E-16	1.21507E-16	1.21507E-16	1.21507E-16	1.21507E-16	1.21507E-16	2.24539E-16
2	3.05206E-18	5.63948E-18	1.04206E-17	1.92555E-17	3.55814E-17	6.57506E-17	1.21502E-16	1.21502E-16	1.21502E-16	1.21502E-16	1.21502E-16	1.21502E-16	1.21502E-16	1.21502E-16	1.21502E-16	1.21502E-16	2.24532E-16
3	3.05193E-18	5.63926E-18	1.04202E-17	1.92548E-17	3.55802E-17	6.57486E-17	1.21499E-16	1.21499E-16	1.21499E-16	1.21499E-16	1.21499E-16	1.21499E-16	1.21499E-16	1.21499E-16	1.21499E-16	1.21499E-16	2.24525E-16
4	3.05173E-18	5.63890E-18	1.04196E-17	1.92537E-17	3.55783E-17	6.57452E-17	1.21493E-16	1.21493E-16	1.21493E-16	1.21493E-16	1.21493E-16	1.21493E-16	1.21493E-16	1.21493E-16	1.21493E-16	1.21493E-16	2.24515E-16
5	3.05139E-18	5.63830E-18	1.04185E-17	1.92518E-17	3.55750E-17	6.57395E-17	1.21483E-16	1.21483E-16	1.21483E-16	1.21483E-16	1.21483E-16	1.21483E-16	1.21483E-16	1.21483E-16	1.21483E-16	1.21483E-16	2.24498E-16

•
 •
 •

34	0.00000E+00	0.00000E+00	0.00000E+00	0.00000E+00	1.82169E-44	4.86110E-42	1.32862E-39	3.75512E-37
35	0.00000E+00	0.00000E+00	0.00000E+00	0.00000E+00	0.00000E+00	3.22299E-44	1.37005E-41	6.02983E-39
36	0.00000E+00	0.00000E+00	0.00000E+00	0.00000E+00	0.00000E+00	0.00000E+00	1.42932E-43	9.75808E-41
37	0.00000E+00	0.00000E+00	0.00000E+00	0.00000E+00	0.00000E+00	0.00000E+00	0.00000E+00	3.06884E-43
38	0.00000E+00	0.00000E+00	0.00000E+00	0.00000E+00	0.00000E+00	0.00000E+00	0.00000E+00	0.00000E+00
39	through	66	same as above					

•
 •
 •

	Y	Z	97	Z	98
1	2.04869E-19	1.64622E-19			
2	through	7	same as above		
8	2.04869E-19	1.64622E-19			
9	2.04869E-19	1.64622E-19			
10	through	10	same as above		
11	2.04868E-19	1.64621E-19			

•
 •
 •

62 1.98675E-20 1.69567E-20
 63 1.62545E-20 1.39209E-20
 64 1.32432E-20 1.13804E-20
 65 1.07373E-20 9.26696E-21
 66 8.91505E-21 7.76568E-21

*** accumulated charge = 3.1480 min. *** charge increment = 3.1480min.

Figure 3-3. (continued)

**4.0 GRTUNCL3D - A THREE DIMENSIONAL ANALYTIC
FIRST COLLISION SOURCE CODE**

[Section to be added in a later version of the MASH code system]

5.0 DORT: A TWO-DIMENSIONAL DISCRETE ORDINATES TRANSPORT CODE*

5.1 INTRODUCTION TO DORT

5.1.1 Background

A summary of the mathematical basis for the method of discrete ordinates as we use in DORT¹ today is given by Lathrop and Brinkley.² Mynatt et al.³ give a full mathematical development, applications information, and comparisons of results with experiments. Carlson and Lathrop⁴ give a full development of the method with emphasis on physical principles and evaluation techniques. They also give an annotated bibliography of early work in the field including a very early report by Carlson in 1953.⁵ A 1958 paper by Carlson and Bell⁶ may have been the first widely-distributed description of the "discrete S_n method" as they called it. In 1960, Carlson, Lee, and Worlton published a description of the DSN code, which used their method.⁷ Davison,⁸ in 1957, gave a thorough review of fundamental discrete-ordinates theory, and a review of Carlson's work in an Appendix. Davison acknowledges a 1953 book by Chandrasekhar⁹ as the origin of the method as he presents it, and a 1943 paper by Wick¹⁰ as the origin of the basic idea.

In this section, we follow the notation of Lathrop and Brinkley to some extent. Their TWOTRAN II code was useful to us in constructing DOT 4¹¹, and it may be worthwhile to comment on the relationship between TWOTRAN and DOT. The earlier versions of DOT actually descended from the LASL codes DTK and DDK, and from the LASL/UNC code DDF/2DF. A version of DOT was distributed informally in 1966, although formal publication was not made until the DOT III version in 1973.¹² Early versions of TWOTRAN were published in a 1968 GA report¹³ and elsewhere.

Descendants of both TWOTRAN and DOT remain in widespread use today, and their very different capabilities apparently justify this dual existence. Numerous other writings pertinent to DOT development appear in ANS Transactions and elsewhere. A reasonably complete bibliography of related material is given in Appendix C of Reference 14.

5.1.2 The Problem Solved

DORT is primarily intended to solve large neutron and photon transport problems on a wide variety of computer types using the method of discrete ordinates. Most DORT problems deal with the calculation of radiation resulting from a given extraneous source, i.e., "fixed-source" problems. If such a system has fissile material and is subcritical, the multiplication can be calculated. The code also has K_{eff} capability and various types of searches. A diffusion theory section is valuable for initiating such problems or as an alternative to the primary discrete ordinates section where applicable.

Special remeshing features allow the number of first-dimension (i) mesh intervals to vary with the second dimension (j) index. An arbitrary coarse mesh can be used for fluence

* W. A. Rhoades and R. L. Childs, "The DORT Two-Dimensional Discrete Ordinates Transport Code," *Nuclear Science & Engineering* 99, 1, pp. 88-89, (May 1988).

acceleration, saving memory and CPU time. The directional quadrature set can be chosen from an arbitrary number of input sets. The choice can vary with spatial option and with energy group. The flexibility has proven quite effective in concentrating CPU effort in areas needing attention, such as streaming gaps. Biased direction sets can be used when streaming is primarily in the upward/downward directions.

A variety of options allow sources to be specified at internal or external boundaries, distributed by space and energy, or determined from an input fluence guess. "First-collision-source" data, actually an analytical first-flight scattering source, can be accommodated. Output files for an "analytical-last-flight" integration can be obtained. These features provide increased accuracy when dealing with out-of-system or localized sources or detector locations.

A single output file contains both distributed fluence moments and boundary directional fluences, so that this file, plus the original input data, provide an "exact" restart. This allows a large problem to be solved in several computer runs without loss of efficiency.

Both 1-D and 2-D geometries can be treated. Discrete ordinates geometries include 1-D plane or slab and 2-D XZ, R Θ , or RZ. The diffusion-theory section has triangular-mesh capability as well. A powerful slab reflection/transmission feature is available. A variety of acceleration options are available. Extensive use of input options and output edits give the user very direct control over the iteration process. While this places a burden of decision-making on him, it is essential to the solution of large and difficult problems. Default and recommended values assist the uninitiated in solving problems without much prior use of the code.

Output source information to be used in coupling to other problems can be obtained. Typical applications include "bootstrapping," in which a very large problem is solved in several segments; core-vessel combinations, in which a core is solved in an eigenvalue calculation and then represented by internal boundary conditions in a fixed-source vessel calculation; coupled discrete-ordinates-Monte Carlo calculations; and RZ air-ground calculations coupled to 3-D discrete ordinates analysis of local features.

Portions of this section were extracted from Reference 14 for completeness. The interested user should consult that document for a full description of the DORT code. An extensive problem set and a tutorial description is available to demonstrate the various features and problem setup techniques.

5.1.3 Code Structure

This code and its predecessors have been adapted to a large variety of computers from the IBM 7090 to modern Crays. In order to maintain compatibility without undue confusion, a "unified source file" concept is used; only a single version of the basic code is kept, with final configuration details supplied when a file is prepared for compilation. Standard language and programming practices are used throughout the main body of the code. In-stream "language flags" make minor language adjustments as required when a specific configuration is tailored. Interchangeable interface packages provide coupling with system-dependent library features.

On all computers, direct (random) access scratch files are used as an extension of memory. Data are retrieved from the files into large buffers controlled by the I/O manager routine.

The working program then uses and updates the buffers before their return to the scratch files. Since communication with the buffers is processed entirely through the interface package, the buffers can be located in a large cache memory such as the LCM on the late CDC 7600 or, presumably, on a Cray SSD device. The code attempts to make the maximum use of available memory in order to minimize I/O costs and delays. Reversion to more extensive use of scratch-files is automatic when required.

The flexibility provided, together with the close control of the solution process, requires an extensive and complicated input data list. Most of these data can be ignored for most problems. A diverse set of sample problems serves as a guide to actual requirements for practical problems.

5.2 THEORETICAL BASIS

5.2.1 The Integro-Differential Transport Equation

The Boltzmann transport equation, as applied to static neutron and photon transport,² can be expressed:

$$\begin{aligned} \nabla \cdot \underline{\Omega} \psi(r, E, \underline{\Omega}) + \sigma^T(r, E, \underline{\Omega}) \psi(r, E, \underline{\Omega}) = \\ \int \int \sigma^s(r, E, E', \underline{\Omega}, \underline{\Omega}') \psi(r, E', \underline{\Omega}') d\underline{\Omega}' dE' \\ + \frac{1}{4\pi} \chi(r, E) \int \int v(r, E') \sigma^F(r, E') \psi(r, E', \underline{\Omega}') d\underline{\Omega}' dE' + Q(r, E, \underline{\Omega}) \end{aligned} \quad (5-1)$$

In this, $d\Omega$ is a differential solid angle about the direction vector Ω , dE is a differential energy about E , and r is a position vector with reference to an arbitrary origin. The directional fluence function, ψ , is defined such that the number of particles moving in volume dr about r with energies falling within dE and directions of motion within $d\Omega$ will be $\psi d\Omega dE dr$. Also, σ^T and σ^F are macroscopic cross sections for total interaction and fission, respectively, and σ^s is the cross section for scattering from energy E' and direction Ω' to energy E and direction Ω . The functions v and χ represent the total fission yield of secondary particles and the corresponding energy distribution. Q represents an extraneous source, if any.

Although the general Boltzmann equation includes time dependence, removal of that dependence in the static form presented here is an important simplification. Certain other simplifications will also be made later. As a practical matter, scattering is generally independent of initial direction, so that it can be expressed in terms of the single scattering angle:

$$\mu_0 = \underline{\Omega}' \cdot \underline{\Omega} \quad (5-2)$$

rather than as a function of two direction vectors. Although some applications exist for the dependence of σ^T on Ω , they are unusual, and this dependence is not allowed in DORT. A somewhat weaker justification exists for the removal of the dependence of χ on space. In fact, if more than one fissile species exists in the system, and if the species do not always fission in the same proportion, χ will depend on space. Nonetheless, the code does not presently allow such dependence.

5.2.2 The Finite Difference Formulation

The procedures for obtaining a finite-difference equation from Equation 5-1 are discussed thoroughly in References 3 and 4, although the form presented here follows Reference 2:

$$\begin{aligned}
 W_m \mu_m \left(A_{i+\frac{1}{2},j} N_{i+\frac{1}{2},j,m,g} - A_{i-\frac{1}{2},j} N_{i-\frac{1}{2},j,m,g} \right) \\
 + W_m \tau_m \left(B_{i,j+\frac{1}{2}} N_{i,j+\frac{1}{2},m,g} - B_{i,j-\frac{1}{2}} N_{i,j-\frac{1}{2},m,g} \right) \\
 + \left(A_{i+\frac{1}{2},j} - A_{i-\frac{1}{2},j} \right) \left(\alpha_{m+\frac{1}{2}} N_{i,j,m+\frac{1}{2},g} - \alpha_{m-\frac{1}{2}} N_{i,j,m-\frac{1}{2},g} \right) \\
 + \sigma_{i,j,g}^T W_m V_{i,j} N_{i,j,m,g} = W_m V_{i,j} S_{i,j,m,g}
 \end{aligned} \tag{5-3}$$

It can be shown that the formulation of Mynatt et al.³ is equivalent to this.

In this notation, subscripts i and j represent mesh intervals in the first and second space dimensions. The subscript m refers to the direction in a ordered set of directions along which fluence is to be evaluated. Subscripts such as $i + 1/2$ refer to the interval boundaries, e.g., boundary $i + 1/2$ is the boundary separating interval i from interval $i + 1$. In the case of m , this is somewhat artificial, since each m represents a discrete direction with no defined sector of solid angle associated. In fact, directions represented by successive m 's may not even be "adjacent" in direction space. Even so, the equation requires coupling between certain fluences having consecutive m values, and the coupling terms, α , will be defined in a consistent manner. Subscripts such as $m + 1/2$, then, merely denote artificial intermediate values. The subscript g refers to energy group.

It may be noted at this point that obvious subscripts are frequently omitted in discrete-ordinates writings, e.g., the first term of Equation 5-3 might later be written:

$$W \mu \left(A_{i+\frac{1}{2}} N_{i+\frac{1}{2}} - A_{i-\frac{1}{2}} N_{i-\frac{1}{2}} \right)$$

In practice, this approach is probably less confusing than the inclusion of long lists of redundant subscripts.

In certain discussions, I and J are understood to be the upper limits of i and j . It may also be noted that space mesh positions are discussed such that boundaries having $i = 1/2$, $i = I + 1/2$, $j = 1/2$, and $j = J + 1/2$ are spoken of as "left," "right," "bottom," and "top," boundaries, regardless of geometry.

The ordered set of directions of particle travel are characterized by their direction cosines, (μ_m, ξ_m, η_m) . In all geometries, μ_m is the cosine of the angle which the direction of travel makes with the first-dimension axis, i.e., X or R, while η_m is the cosine of the angle with the Z axis (Table 5-1). In each case, ξ_m is the cosine with the remaining direction vector, either along the Y axis, or in the azimuthal direction in the case of R Θ .

Due to symmetry, no flow is associated with one of the direction cosines, either η or ξ . Thus, τ is used to represent either ξ or η , as shown in Table 5-1. Also, ω is allowed to represent the remaining cosine. The parameters A and B are cell areas perpendicular to the axes from which μ and τ are measured.

Table 5-1. Directional Properties of the Geometries.

Geometry	1-D			2-D		
	XZ	RZ	R Θ	XZ	RZ	R Θ
Dimensions Solved	X	R	R	X,Z	R,Z	R, Θ
Dimension Corresponding to μ	X	R	R	X	R	R
Dimension Corresponding to η	Y	Θ	Θ	Y	Θ	Θ
Dimension Corresponding to ξ	Z	Z	Z	Z	Z	Z
Cosine Corresponding to τ	η	η	ξ	η	η	ξ
Cosine Corresponding to ω	ξ	ξ	η	ξ	ξ	η
Dimension Perpendicular to A	X	R	R	X	R	R
Dimension Perpendicular to B	Z	Z	Θ	Z	Z	Θ

Each direction has an associated weight, W_m . Quantities involving integrals over all directions are to be evaluated by sums with W_m as the weighting function. N represents the directional fluence, ψ , in direction, m , although it will be seen that N has different units. V and S are the volume and source in a given mesh cell, and σ^T is the macroscopic total cross section. It is assumed that S includes extraneous sources, scattering from other energy

groups, scattering at the given energy from other directions, fission, and any other particle sources, e.g., (n,2n).

As indicated in Table 5-1, the 1-D geometries evaluate fluence dependence in only the first dimension. In such cases, the usual evaluation procedures are used, but $B=0$.

It can be observed that, except for the terms in α , Equation 5-1 is simply a statement of particle balance for a given cell, and could have been written down directly. From this, it is evident that the discrete-ordinates equation conserves particles inherently, if the α terms are defined such as to conserve.

The terms in α are effective only in curved geometry, RZ or R Θ . Their physical meaning can be made apparent by considering a particle moving inward along a path which will take it closer to the axis of a cylinder. While η is a constant for such a path, μ constantly increases from negative, through zero, and ultimately toward $\mu = +1$ as the particle moves away from the centerline. Thus, the discrete-ordinates equation must show a comparable flow toward directions of larger μ for comparable particle paths.

In order to allow manageable evaluation of the terms in α , an ordering discipline is imposed upon the directions represented by m . Since the α terms must couple directions of like η , directions of like η are grouped contiguously, in order of increasing μ . The groups of directions with like η (" η levels") are ordered such that all directions with $\eta < 0$ precede all directions with $\eta > 0$. Thus, the α -flow, following an actual path inward and then outward, is always toward directions of increasing m within an η level. It can also be seen that there must be no flow between η levels in order to be consistent with the physical model.

The recursion relationship for the α 's can be obtained at this point by observing that Equation 5-3 must be valid in a source-free region where N is uniform. Since no constraint may be placed upon σ^T , A , B , or V , then it must follow that, for a given η level:

$$-W_m \mu_m = \alpha_{m+\frac{1}{2}} - \alpha_{m-\frac{1}{2}} \quad (5-4)$$

Since it is required that α coupling be only between directions within an η level, then $\alpha_{m-1/2} = 0$ for the first direction of the level. It is essential that, for each level:

$$\sum_m W_m \mu_m = 0, \quad (5-5)$$

so that $\alpha_{m+1/2}$ will be 0 for the last m of that level, and there will be no net flow into or out of the η level. This insures that particle conservation is rigorously met. Symmetrical

quadrature sets always obey this condition, and it is important that unsymmetrical sets obey this condition, also.

There is certain advantage to be gained by substituting a new variable, β for α :

$$\beta_m = \frac{1}{W_m} \left(\alpha_{m+\frac{1}{2}} + \alpha_{m-\frac{1}{2}} \right) . \quad (5-6)$$

The recursion relationship for the β_m can be obtained by applying its definition to the recursion relationship for α :

$$W_m \beta_m = \alpha_{m+\frac{1}{2}} + \alpha_{m-\frac{1}{2}} , \quad (5-7)$$

$$W_{m+1} \beta_{m+1} = \alpha_{m+\frac{3}{2}} + \alpha_{m+\frac{1}{2}} , \quad (5-8)$$

$$\alpha_{m+\frac{1}{2}} = \alpha_{m-\frac{1}{2}} - W_m \mu_m , \quad (5-9)$$

and

$$\alpha_{m+\frac{3}{2}} = \alpha_{m+\frac{1}{2}} - W_{m+1} \mu_{m+1} . \quad (5-10)$$

Therefore

$$W_{m+1} \beta_{m+1} = W_m \beta_m - (W_{m+1} \mu_{m+1} + W_m \mu_m) . \quad (5-11)$$

Recalling that $\alpha_{m-1/2} = 0$ for the first direction of each η level, then it follows that $\beta_m = -\mu_m$ for such levels; at least if $W_m \neq 0$. As will be discussed later, this relationship is assumed even when $W_m = 0$.

It is important, both in applying boundary conditions and in obtaining proper stability, to "follow the flow" in writing the recursion formulas; i.e., all directions with $\mu < 0$ must be evaluated from large X or R values toward small, and so with the other dimension. Similarly, positive μ values require evaluation from small X to large, etc. These procedures can be written in a single formula by use of subscript increments defined in terms of the signum function (Sg); which has value ± 1 according to the sign of its argument:

$$c = \frac{1}{2} Sg(\mu_m) ; d = \frac{1}{2} Sg(\tau_m) . \quad (5-12)$$

Written in terms of β , c , and d , Equation 5-3 can be simplified to:

$$|\mu|(A_{i+c}N_{i+c} - A_{i-c}N_{i-c}) + |\tau|B(N_{j+d} - N_{j-d}) + \frac{1}{2} \Delta A \left\{ (\beta_m - \mu_m)N_{m+\frac{1}{2}} - (\beta_m + \mu_m)N_{m-\frac{1}{2}} \right\} + V\sigma^T N = VS \quad , \quad (5-13)$$

where

$$\Delta A = A_{i+\frac{1}{2}} - A_{i-\frac{1}{2}} \quad (5-14)$$

and where N is simply a simplified representation of $N_{i,j,m,g}$, etc.

5.2.3 Fluence Evaluation Strategy

Evaluation "following the flow," as discussed above, is also evaluation "sweeping away from boundary conditions into the mesh." Since evaluation always begins with $m = 1$, the first sweep must be toward smaller values of i and j . Where I and J represent the largest values of i and j , then the boundary values $N_{I+1/2}$ and $N_{J+1/2}$ are decided *a priori* based on physical considerations at the outer boundaries of the system. No such physical considerations govern the boundary fluence at $m = 1/2$, however, as will be seen.

Before dealing with $N_{1/2}$, let us observe that, even with N_{i-c} and N_{j-d} known from boundary considerations and $N_{m-1/2}$ to be defined by a yet-unspecified process, Equation 5-3 would still involve 4 unknowns. The three advance boundary values, N_{i+c} , N_{j+d} , $N_{m+1/2}$ have been treated as completely independent, and are, therefore, not completely defined by Equation 5-3. In fact, all of the values of N represent values of a single continuous function ψ at adjacent locations, and cannot vary more freely than ψ does. If we suspect that ψ can be approximated adequately by straight-line segments between adjacent boundaries, then the following "linear" or "diamond" difference model results:

$$N = \frac{1}{2} (N_{i+c} - N_{i-c}) \quad , \quad (5-15a)$$

$$N = \frac{1}{2} (N_{j+d} - N_{j-d}) \quad , \quad (5-15b)$$

and

$$N = \frac{1}{2} \left(N_{m+\frac{1}{2}} - N_{m-\frac{1}{2}} \right) \quad , \quad (5-15c)$$

As previously discussed, $\beta_1 = -\mu_1$. Accordingly, Equations 5-13 and 5-15 cannot yield direct information as to an appropriate value of $N_{1/2}$, and the other results are independent

of this value. Accordingly, $N_{1/2}$ is arbitrary and unknown. If N is to be related to $N_{1/2}$ and $N_{3/2}$, the only acceptable assumption is :

$$N_{\frac{3}{2}} = N_{\frac{1}{2}} \quad (5-16)$$

Since each η level begins with a $\beta_m = -\mu_m$, each must start with an "Initiating direction" having:

$$N_{m+\frac{1}{2}} = N_m ; \beta = -\mu \quad (5-17)$$

If an initiating direction occurs for $m > 1$, and m' is the predecessor to m , then Equation 5-15 defines values for $m' + 1/2$ and $m - 1/2$ which do not agree. In fact, the fluence is not required to be continuous between directions on different η levels, and they do not, in general, describe adjacent directions. Thus, there is neither physical nor mathematical requirement for continuity of fluence between them.

It has been traditional in the early DOT codes to allow these initiating directions to have $W_m = 0$, i.e., "zero-weight directions," and to adjust their directions such that $\xi = 0$. Carlson and Lathrop describe this procedure.⁴ On the other hand, TWOTRAN II uses directions having small, finite weights and having W_m small, but not 0. Tomlinson et al.¹³ showed that, other factors being equal, this choice does not affect the results of test problems significantly. Both types of calculations are available in DORT, although the direction sets input to the code must always contain directions with $W_m = 0$ to signal the beginning of a new η level. When TWOTRAN-like calculations are done, or in XZ geometry, fluence is not calculated in directions having $W_m = 0$.

Having decided on boundary values for initiating the sweeps, Equations 5-15 and 5-17 define the remaining unknowns in terms of the single unknown, N , for the initial direction of each η level:

$$N_{i+c} = 2N - N_{i-c} \quad (5-18)$$

$$N_{j+d} = 2N - N_{j-d} \quad (5-19)$$

Defining, as a matter of convenience:

$$\bar{A} = \frac{1}{2} \left(A_{i+\frac{1}{2}} + A_{i-\frac{1}{2}} \right) \quad (5-20)$$

observing that:

$$2|\mu|A_{i+c} + \Delta A(\beta - \mu) = 2|\mu|\bar{A} + \Delta A\beta \quad (5-21)$$

and recalling that $\beta = -\mu$ for the initial direction of each η -level, the value of N can be written explicitly:

$$N = \frac{VS + 2|\mu|\bar{A}N_{i-c} + 2|\tau|BN_{j-d}}{V\sigma^T + 2|\mu|\bar{A} + 2|\tau|B}; \beta = -\mu . \quad (5-22)$$

This equation applies to the initiating directions, whether $W = 0$ for such directions or not. For all other directions, Equation 5-17 does not apply, and $N_{m-1/2}$ is obtained by applying Equation 5-15c to the preceding directions:

$$N_{\frac{m+1}{2}} = 2N - N_{\frac{m-1}{2}}; \beta \neq -\mu . \quad (5-23)$$

Since $\beta = -\mu$ for such directions, terms in β appear in the formulation for N :

$$N = \frac{VS + 2|\mu|\bar{A}N_{i-c} + 2|\tau|BN_{j-d} + \Delta A\beta N_{\frac{m-1}{2}}}{V\sigma^T + 2|\mu|\bar{A} + 2|\tau|B + \Delta A\beta}; \beta \neq -\mu . \quad (5-24)$$

At this point, an explicit sweep pattern has been found. Determining $N_{m=1/2}$, $N_{I+1/2}$, and $N_{J+1/2}$ as described, Equation 5-22 gives $N_{I,J,1}$ explicitly. Equation 5-18 gives $N_{I-1/2}$ explicitly, recalling that $\mu < 0$ for the first direction, and thus $c = -1/2$. This evaluation can proceed for all i 's down to the boundary value at $i = 1/2$. With these values in storage, values for $m = 1 1/2$ can be found using Equation 5-17. If that η -level contains additional directions with $\mu < 0$, values for $m = 2$ are evaluated from Equation 5-24, and extrapolated with Equation 5-23. This process continues for all m 's for which $\eta < 0$ and $\mu < 0$. Having these values, the values for directions having $\eta < 0$ and $\mu > 0$ at $i = 1/2$ can be determined from physical boundary conditions. The sweep proceeds as before, except, of course, that evaluation is from $i = 1/2$ to $i = I + 1/2$. From these values, Equation 5-19 determines $N_{I-1/2}$, and the process proceeds as before downward to $j = 1/2$. Boundary values at $j = 1/2$ for directions having $\eta > 0$ are determined from physical boundary conditions at the bottom boundary, and the sweep resumes, this time from $j = 1/2$ to $j = J + 1/2$.

5.2.4 Additional Theory Information

There is an excellent description of the detailed inner workings of the DORT code given in Reference 14. In this document, the interested user will find the detailed information on the various fluence weighting models, sweep strategies, source terms, boundary conditions, iteration strategies, rebalance and acceleration techniques, spatial and directional remeshing techniques, directional quadrature sets, and other information relevant to a full understanding of the DORT code. This information will not be repeated here.

5.3 DORT INPUT DATA SPECIFICATIONS

5.3.1 Card-Image Format

The card-image input data for a problem consist of a title card followed by a variable number of blocks of data separated by "T" delimiters. Within each block, a variable number of data arrays are specified, keyed according to an array number, and identified as to real or integer type.

A separator card must be placed between successive problem decks. If it contains the word "DIAG" in the first four columns, a non-fatal diagnostic will be given by ERRO. If the word "DUMP" appears, a fatal diagnostic is given. If the word "=END" appears, execution will stop. Otherwise, the next problem begins immediately. No data are retained in memory between problems. At the end of execution, all data files are closed. Control is then returned to the driver, if the code was invoked by a driver, or else to the operating system.

All of the card-image input except the title card and separator card are read by the FIDO input processor. The format required for FIDO data entries is described in Appendix A. The data arrays and blocks to be read are described in following sections. The first four blocks of data are permanent, and their "T" delimiter **must** be supplied whether array entries are required or not.

Blocks, after the first four, containing arrays numbered 91 and higher, are options supplied to allow certain simple problems to be solved without the labor of preparing formal fluence and source input files. The conditions under which these blocks are required are included in their description.

As each array of data is read, its length is compared with the required length, and an error message is given if appropriate. After each block of data, a call to subroutine ERRO is made if any of the arrays in the block were of improper length, or if the data were otherwise unsuitable. ERRO prints an explanation of the error and sets an error flag. Data are edited as soon as possible after each block is completed.

Processing of input continues for as long as possible, even after an error. In most cases, this allows the user to test all of his data blocks in spite of an early error. Execution is terminated at the end of input processing if a sufficiently severe error has been encountered.

It is possible that one error will cause subsequent data to be erroneously flagged as wrong. If data which appear correct are flagged by an error message, this possibility should be considered. An error can also cause subsequent system related failures, such as addressing or storage errors.

The first four blocks of data contain, in general terms:

1. control parameter input arrays (61-63) which set array lengths explicitly and control execution options.
2. primary input arrays (71-78) whose lengths depend upon arrays (61-63), and whose contents determine later array lengths. These arrays describe variable-mesh, variable quadrature, variable P_L , and super-mesh features.

3. secondary input arrays (81-87), whose length depend upon arrays (61-78), and whose contents determine later array lengths. These include the directional quadrature specification set, coarse mesh specification, assignment of direction sets to super-mesh cells, and assignment of material zones to edit regions.
4. general input arrays (1-30), which do not determine the lengths of other input arrays. These include space-mesh specifications, cross-section mixing instructions, specification of activity edits, and much more.

In the remainder of Section 5.3 of this report, the broad concepts required to understand the input data are discussed, followed by a detailed specification of the input data, and finally, clarification of several input-related topics.

5.3.2 Space Meshes

Five different subdivisions of the problem space are determined from the input data. Two sets of fine-mesh interval boundaries (2* and 4* arrays) are input, corresponding to the two spatial dimensions. The intersection of these boundaries forms the fine-mesh grid cells. (In R Θ geometry, the 2* array is entered in units of revolutions, not radians.)

A coarse mesh, specified by an additional 2 sets of intersecting boundaries (85* and 86* arrays), is used in the fluence acceleration routines. A good choice of coarse mesh can save both memory space and execution time without impairing the convergence of a problem. In some cases, proper application of the coarse mesh can help the convergence rate as well. A coarse mesh of one mean-free-path is ideal for many problems. Default options allow the coarse mesh to be identical to the fine mesh if the variable space mesh feature (described later) is not used. A coarse-mesh I-boundary must also be a boundary in each of the fine-mesh I-boundary sets. A coarse-mesh J-boundary must also be a fine-mesh J-boundary.

A super mesh is similarly specified (75* and 76* arrays) for use with the variable quadrature feature (described later), and with certain search options. A super-group representation (74\$ array) is also required when variable quadrature is used. The location of the super-mesh and super-group boundaries is chosen by the user as desired, except that the super-mesh boundaries must also be fine-mesh boundaries.

Material zones (8\$ array) are always specified. A material zone must contain only one cross section set, although many zones may share a single cross section set. In addition to cross section assignment, certain input and edit features depend upon material zones.

Edit regions (84\$ array) are groupings of material zones used for the purpose of condensing certain output tables. Certain input and edit features depend upon edit regions.

5.3.3 Variable Space Mesh

The fine mesh can be specified such that the I mesh depends upon J. To accomplish this, several "I-sets" are specified, with different numbers of intervals and different interval boundaries. The ISET(J) array then relates the proper set of boundaries to the J-level. Prudent use of this feature can save computation time and storage by concentrating work in areas requiring a fine mesh. I-direction coarse-mesh and super-mesh boundaries must be contained in all fine-mesh I-sets. Left and right boundaries of all I-sets must coincide. A "standard" I-set, which is as large as any of the I-sets, must be chosen. Boundary fluences and sources are kept in the standard I-set format.

5.3.4 Variable Directional Quadrature

The directional quadrature sets, "M-sets," are specified by super-zone and super-group. For example, this allows the user to specify a highly biased quadrature in the area of a streaming crack at high energy without wasting such detail elsewhere in the problem. A standard M-set must be chosen which:

1. has as many directions up and as many down as any set,
2. has exactly $|MM|$ directions, and
3. has as many η levels upward and as many downward as any set.

5.3.5 Variable Legendre Expansion

The order of moment expansion (P_l) may be specified by cross section set (78\$) and by energy group (77\$). The former option allows selective examination of anisotropic effects, while the group dependence can save computation time in lower energy groups, where anisotropy is less pronounced.

NOTE: These features have not been made operable in current versions of the code.

5.3.6 Adjoint Data

If an adjoint problem is to be solved, all data in the first four blocks are entered in the normal manner. All input files supplied by the user, and any arrays numbered 91 and higher, must be supplied in adjoint form, i.e., reversed with respect to energy. For files having directional information, the user should remember that an adjoint problem is solved as a function of $-\Omega$, rather than Ω where Ω is a direction specified by the quadrature set. In other words, if $\mu > 0$ and $\eta > 0$ for a given direction, the adjoint data calculated for that direction will be that appropriate to a particle moving in the $(-\mu, -\eta)$ direction. Directional input files must be similarly reversed, and directional output files will be. Output files have the energy groups in the order calculated, i.e., reversed from the usual order.

5.3.7 Card-Image Input Specifications

In the following section, the symbol "@" indicates that a detailed discussion is given elsewhere in this region. The symbol "#" denotes the word "number," and "RV" means "recommended value." After each array, the length is specified in parentheses. If an array or block is not always supplied, the conditional requirement is given in brackets. The symbol "*" denotes a feature not presently operable.

5.4 DORT INPUT REQUIREMENTS

The following input cards are required to execute DORT. Default values are specified in parentheses.

Title Card (72 alphanumeric character description)

INPUT DATA BLOCK 1

61\$ Array - Data Set Logical Unit Reference Numbers @ (length subject to change)

NOTE: Leaving a unit as 0 disables the corresponding feature.

NTFLX	fluence guess input unit
NTFOG	fluence output unit
NTSIG	cross-section unit (default = 8)
NTBSI	external boundary source input unit
NTDSI	distributed source input unit (must supply scratch unit if INPSRM > 0)

- 5 ---

NTFCI	reserved (enter 0)
NTIBI	internal boundary source input unit
NTIBO	internal boundary fluence output unit
NTNPR	large-scale print unit (all print goes on standard output unit if NTNPR = 0)
NTDIR	directional fluence output unit

- 10 ---

NTDSO	distributed source output unit
NTSCL	scalar flux output unit
NTZNF	zone flux output unit

E (terminate array with "E")

62\$ Array - Integer Control Parameters (length subject to change)

IADJ 0/1 = forward/adjoint calculation
ISCTM maximum order of scattering (L of P_L)
(negative indicates P_L calculation is specified by
energy group (77\$ array))*
IZM number of material zones
IM maximum number of 1st-dimensional (I) spatial intervals (radial) in any
I-set (negative indicates number of intervals varies with 2nd
dimension, i.e., variable mesh)
JM number of 2nd-dimension (J) spatial intervals (axial)

- 5 ---

IGM number of energy groups
IHT position of total cross section in cross-section table @
IHS position of self-scatter cross section in cross-section table @
IHM length of cross-section table for each energy group @
MIXL cross-section mixing table length @

- 10 ---

MMESH number of material zone bodies (0 = no effect)
MTP number of cross-section sets from NTSIG
(0 has the effect of MTP = MTM) @
MTM total number of materials, including mixtures @
IDFAC density factor input option
0 implies feature not used
1 implies DNIJ(I,J) input as 3*, used to modify cross sections
MM maximum number of directions in any M-set
(negative indicates variable quadrature is used)

- 15 ---

INGEOM geometry option @
0 X-Y slab
1 R-Z cylinder
2 R-Θ circle
3 180° - 360° triangular
4 60° triangular
5 90° triangular
6 120° triangular
IBL left boundary condition
0 void
1 reflected
2 periodic
3 cylindrical
4 fixed boundary source
5 albedo
IBR right boundary condition 0/1/2/3/4/5 (see IBL)
IBB bottom boundary condition 0/1/2/3/4/5 (see IBL)
IBT top boundary condition 0/1/2/3/4/5 (see IBL)

- 20 ---

ISRMX source (outer) iteration maximum (default = 1)
IFXMI initial fluence (inner) iteration maximum per group
(default = 20) @
(negative indicates maximum given by group (28\$ array))
IFXMF final fluence (inner) iteration maximum per group @
(no effect if 0)
MODE fluence extrapolation model (default = 4)
0 linear with negatives set to 0
1 linear with no fixup of negatives
2 scalar weighted
3 zero weighted
4 theta weighted
5 vector weighted
KTYPE calculation type @
0 fixed source
1 K (eigenvalue) search
2 DB² search
3 concentration search
4 dimension search

- 25 ---

IACC rebalance method in discrete ordinates section
(default = 2) @
0 single groupwise rebalance factor
1 diffusion acceleration
2 partial current acceleration
KALF rebalance stabilization @
0 standard acceleration method
1 alternate acceleration method
IGTYPE solution method @
0 discrete ordinates used always
N method selected by group (7\$ array) for first
N outers, then finishing with discrete ordinates
INPFXM fluence input option
0 fluence set to 0, or read from unit NTFLX
if NTFLX > 0
1 FIJ(I,J) read as 93* array for each group
2 FIJ(I,J)*FG(G), uses 93* and 95* arrays
3 FI(I)*FJ(J)*FG(G), uses 93*, 94*, and 95* arrays
INPSRM distributed source input options 0/1/2/3
(options are analogous to INPFXM; use 96*, 97*,
98* arrays) (NTDSI > 0 is required if INPSRM > 0)

- 30 ---

NJNTSR interior boundary source at NJNTSR J-boundaries will be
input from NTIBI (may be 0)
NINTSR interior boundary source at NINTSR I-boundaries will be
input from NTIBI (may be 0)

NJNTFX interior boundary fluence at NJNTFX J-boundaries will be written on NTIBO (may be 0)
 NINTFX interior boundary fluence at NINTFX I-boundaries will be written on NTIBO (may be 0)
 IACT number of region and pointwise activities calculated @ (negative indicates region activities only)
 0 no effect
 N calculate N activities

- 35 ---

IRED balance table output control
 In general, IRED is the largest number in the 84\$ array (IZNRT[IZ]), except that:
 IRED= -1 provides one region per zone, balance tables will be given for the entire system only
 IRED= 0 no balance table output, but one region for each zone
 IRED= 1 combines all zones into a single region
 IRED= IZM one region for each zone, balances for IZM regions
 IPDB2 punch J-direction DB² from balance table output
 0 no DB² produced
 1 single average DB²
 2 IGM groupwise DB² values
 3 IGM*NREG groupwise and regionwise DB² values
 (use negative entry to bypass balance table print)
 IFXPRT scalar fluence print option (default = 1)
 0 scalar fluence for all groups printed in output phase
 1 scalar fluence not printed
 2 scalar fluence printed as calculated
 (+10 to delete flux iteration print, i.e., 10, 11, 12)
 ICSPRT cross section print option (default = 1)
 0 cross sections printed
 1 cross sections not printed
 IDIRF directional fluence
 0 directional fluence not saved
 1 directional fluence saved and printed
 2 directional fluence saved but not printed
 (directional fluence will be written onto NTDIR if IDIRF > 0 and NTDIR > 0)

- 40 ---

JDIRF first J-interval (axial) for directional fluence output
 JDIRL last J-interval (axial) for directional fluence output
 NBUF not used
 IEPSBZ zone importance convergence (uses 24* array) @
 0 feature not used
 1 zone importance used
 11 as 1 & zone convergence printed after convergence
 21 as 1 & zone convergence printed after each iteration

MINBLK minimum J-blocking for fluence moment storage (RV=0) @
 0 1 space block per group, all groups in memory allowed
 1 1 space block per group, 1 group in memory allowed
 N at least N space blocks required, 1 group in memory

- 45 ---

MAXBLK maximum J-blocking @
 0 JM space blocks per group allowed
 1 only 1 space block per group allowed
 N maximum of N space blocks per group allowed
 ISBT standard I-set for boundary fluences (default = 1)
 MSBT standard M-set for boundary fluences (default = 1)
 MSDM standard M-set for dimensioning (default = 1)
 (MSDM = MSBT always in this version)
 IBFSCL number of fluence iterations before first rebalance
 in first source iteration (default = 1) @

- 50 ---

INTSCL minimum number of rebalance iterations (default = 4) @
 ITMSCL maximum number of rebalance iterations (default = 50) @
 NOFIS fission spectrum option (default = 1)
 0 fission calculated with χ normalized to 1.0
 1 fission calculated with input χ values (unnormalized)
 2 fission calculation bypassed, saving memory space
 (NOFIS will be set to 2 if the 1* array is 0)
 IFDB2Z DB² input option
 0 option not used
 1 DB2Z(IG,IZ) entered as 6* array by group, then by region
 ISWP type of diffusion theory sweep (RV=4 or 5)
 0 line inversion in direction of largest number of mesh intervals
 1 alternating direction (line-column) on consecutive outer iterations
 2 line inversion
 3 column inversion
 4 alternating direction (line-column) on consecutive
 inner iterations
 5 alternating direction (column-line) on consecutive
 inner iterations
 6 line inversion outward from center J interval

- 55 ---

KEYJN J-interval for key fluence print (ignored if 0)
 (default = 1) @
 KEYIN I-interval for key fluence print (ignored if 0)
 (default = 1) @
 NSIGTP reserved (used 0)
 NORPOS cross section table position for output normalization
 (option not used if NORPOS=0)

NORMAT cross-section material number for output normalization
(0 implies use macro cross section set in each zone; negative implies
do not use density factor in normalization)

- 60 ---

MSTMAX maximum number of M-sets (0 implies JM sets allowed)
NEGFIX negative scattering source fixup (default = -1) @
-1 economy fixup used
0 option not used
1 full source fixup used
2 initial fixup used
LOCOBJ initial memory allocation, words*1000 @
(0 implies use default)
LCMOBJ file segment size, words*1000 @
(0 implies unlimited segment length)
NKEYFX length of key fluence arrays (29\$, 30\$) @
(0 bypasses feature, negative causes print only at convergence or
iteration limit for each group)

- 65 ---

NCNDIN maximum user condition code allowed (default = 4)
NEUT last neutron group number (default = -1)
(use of default implies NEUT = IGM)
ITALLY initiate internal timing analysis routines
-1 internal timing turned on
0 no effect
NEUTAG groupwise activity multiplication control
0 no effect
N calculate activities (25\$ and 26\$) over first N groups only
ISCTC maximum order of Legendre expansion of the cross sections
0 no effect

E (terminate array with "E")

63* Array - Real Control Parameters (length subject to change)

TMAX maximum minutes of CPU time for this problem (0 ignored) @
XNF value to which source is normalized (0 ignored if
KTYPE = 0, otherwise 0 implies XNF = 1.0)
EPS eigenvalue convergence criterion (source iterations)
(default = 1.0E-4) @
EPP pointwise fluence convergence criterion
(fluence iterations) (negative: source iterations can
halt without meeting EPP) (default = 1.0E-3) @
EPV volumetric fluence convergence criterion
(fluence iterations) @

- 5 ---

EPF Pointwise fission convergence criterion
(default = 1.0E-3) @
EKOBJ k-effective sought in search (KTYPE > 1) or initial
k-effective (KTYPE = 1) (default = 1.0) @
EVTH k-effective convergence ratio (default = 0.2) @
EVCHM maximum EV change ratio per iteration (default = 1.5) @
EVMAX maximum EV change ratio, overall (default = 10.0) @

- 10 ---

EVKMX maximum allowed k-effective - EKOBJ (default = 1.0) @
EVI initial eigenvalue (default = 1.0) @
DEVDKI initial eigenvalue slope (default = -1.0) @
EVDELK initial eigenvalue increment (default = 0.3) @
SORMIN maximum source iteration acceleration (default = 10.0) @

- 15 ---

CONACC fluence acceleration acceptance criterion (default = 1.0)
CONSCL fluence acceleration convergence criterion
(default = 1.0E-4) @
CONEPS fluence acceleration convergence ratio (default = 0.01)
WSOLMN reserved (enter 0)
WSOLII fluence acceleration damping increment (default = -1.5)
(negative indicates use only as required)

- 20 ---

WSOLCN fluence acceleration damping constant (default = 1.5)
(negative indicates use only on first source iteration)
ORF diffusion theory fluence acceleration factor
(default = 0.6)
FSNACC reserved (enter 0)
FLXMIN minimum fluence for convergence tests
(default = 1.0E-30) @
SMOOTH reserved (enter 0)

- 25 ---

EPO source iteration fluence convergence criterion @
EXTRCV source iteration extrapolation convergence criterion @
(default = 0.2)
THETA theta-weighted extrapolation model parameter
(default = 0.9)
ESP1 reserved (enter 0)
ESP2 reserved (enter 0)

E (terminate array with "E")

T (terminate block with "T") [T always required]

INPUT DATA BLOCK 2

Primary Dimension-Setting Arrays (Omit arrays not needed)

71\$ Array	ISET(J)	(# = JM)	[IM < 0]
	Index of radial mesh set to use at each J level. (default = Set 1)		
72\$ Array	IMBIS(ISET)	(# = JM)	[IM < 0]
	Number of intervals in each I set; then fill array with 0's.		
73\$ Array	MMBMS(MSET)	(# = MSTMAX)	[MM < 0]
	Number of directions in each M set; then fill array with 0's.		
74\$ Array	ISZNG(IG)	(# = IGM)	[MM < 0]
	Super group number by group (default = a single supergroup)		
75* Array	SZNBZ(JSZ)	(# = JM)	[MM < 0 or KTYPE > 1]
	J super mesh boundaries Enter as many boundaries as desired. Then fill with 0. (default = a single superzone)		
76* Array	SZNBZ(ISZ)	(# = IIM)	[MM < 0 or KTYPE > 1]
	I super mesh boundaries Enter as in 75*		
77\$ Array	ISCTG(IG)	(# = IGM)	[ISCTM < 0]
	Order of Legendre expansion used in calculation		
78\$ Array	NSIG(MT)	(# = MTM)	[MCR < 0]
	Order of Legendre expansion of cross section sets		

T (terminate block with "T") [T always required]

From these, the following are determined:

MGSZN	= largest super group number [1 if MM > 0]
NJSZN	= number of J super zone boundaries [1 if MM > 0]
NISZN	= number of I super zone boundaries [1 if MM > 0]
ISM	= # non-zero entries in 72\$ [1 if IM > 0]
MSM	= # non-zero entries in 73\$ [1 if MM > 0]
IMSISM	= sum of IMBIS, all I sets [IM if IM > 0]
MMSMSM	= sum of MMBMS, all M sets [MM if MM > 0]
IMSJM	= sum of IMBIS(ISET(J)), all J [IM*JM if IM > 0]
IMA	= IIM
MMA	= IIM
MMSIMS	= MMA*IMA
MMSJM	= MMA*JM
IHP	= IHM + 1 if IHS > IHT + 1; otherwise = IHM

INPUT DATA BLOCK 3

Secondary Dimension-Setting Arrays (Omit arrays not needed)

- 81* Array** W(M,MSET) (# = MMSMSM)
Directional weights
- 82* Array** EMU(M,MSET) (# = MMSMSM)
 μ , cosine of angle with X or R direction
- 83* Array** ETA(M,MSET) (# = MMSMSM)
 τ , cosine of angle with Z or Θ direction
- 84\$ Array** IZNRG(IZ) (# = IZM) [IRED 0 or IACT 0]
Region number by zone (default controlled by value of
IRED, one region per zone if IRED=IZM, 0, or -1; one region if
IZM = 1; otherwise IZNRG must be specified in full)
- 85* Array** ZCMB(JC) (# = JM)
J coarse mesh boundaries
Enter as many boundaries as desired up to the limit, JM.
Then fill with any number at least as large as the last J fine-mesh
boundary. (default = 1 coarse mesh for each interval)
- 86* Array** RCMB(IC) (# = IMA)
I coarse mesh boundaries, as in 85*
- 87\$ Array** IJGSZ(ISZ,JSZ,IGSZ) (# = NISZN*NJSZN*NGSZN) [MM < 0]
M set by I super mesh,
then by J super mesh,
then by super group

T (terminate block with "T") [T always required]

From these, the following are determined:

JCM = # of coarse mesh boundaries entered in the ZCMB array
ICM = # of coarse mesh boundaries entered in the RCMB array
NREG = maximum of IZNRG(IZ) array
ICMJCM = ICM*JCM
ICPJCP = (ICM + 1)*(JCM + 1)

INPUT DATA BLOCK 4

General Input Arrays (Omit arrays not needed)

1* Array	CHI(IG) fission spectrum fractions, χ , by group (# = IGM)
2* Array	ZIN(J) Z or Θ fine-mesh boundaries (# = JM + 1)
3* Array	DNIJ(I,J) density factor (# = IMSJM) [IDFAC > 0] (default = 1.0)
4* Array	RIN(I, ISET) X or R fine-mesh boundaries (# = IMSISM + ISM)
5* Array	ENER(IG) top neutron energy group boundaries + bottom energy of last neutron group + top photon energy group boundaries + bottom energy of last group (# = IGM + 2) [NTFOG > 0] @
6* Array	DB2Z(IG, IZ) DB ² by group, then by region (# = IGM * NREG) [IFDB2Z > 0]
7\$ Array	ITHYG(IG) theory by group (# = IGM) [IGTYPE > 0] @
8\$ Array	IJZN(I, J) material zone by fine space mesh (# = IMSJM) @
9\$ Array	IZMT(IJZN) material number by material zone (# = IZM)
10\$ Array	MIXT(MIX) mixture ID (# = MIXL)
11\$ Array	NUCL(MIX) nuclide ID (# = MIXL)
12* Array	DENS(MIX) number density (# = MIXL)
13\$ Array	MATL(MT) ID number by material (# = MTM) (default MATL(MT) = MT)
14* Array	ZNTRSR(JNTRSR) Z or Θ boundary positions for J-boundary source input (# = NJNTRSR)
15* Array	RNTRSR(INTRSR) X or R boundary positions for I-boundary source input (# = NINTRSR)
16* Array	ZNTRFX(JNTRFX) Z or Θ boundary positions for J-boundary fluence output (# = NJNTRFX)
17* Array	RNTRFX(INTRFX) X or R boundary positions for I-boundary fluence output (# = NINTRFX)
18* Array	FJSRZ(JSZN) J-Super zone search fraction (# = NJSZN) @ [KTYPE = 4]

- 19* Array FISRZ(ISZN) I-Super zone search fraction (# = NISZN) @
[KTYPE = 4]
- 20* Array ABDOL(IG,J) left boundary albedo (# = IGM*JM) [IBL = 5]
- 21* Array ABDOR(IG,J) right boundary albedo (# = IGM*JM) [IBR = 5]
- 22* Array ABDOB(IG,I) bottom boundary albedo (# = IGM*IMA) [IBB = 5]
- 23* Array ABDOT(IG,I) top boundary albedo (# = IGM*IMA) [IBT = 5]
- 24* Array EPSBZ(IZ) fluence error importance by material zone (# = IZM) [if
IEPSBZ > 0] @
- 25\$ Array ICMAT(IAC) material to be used in activity calculations
(# = IIACTI) @
- 26\$ Array ICPOS(IAC) cross section table position for activity (# = IIACTI) @
- 27* Array ACMUL(IAC) activity multiplier (# = IIACTI) @
- 28\$ Array ITMBG(IG) initial iteration limit by group (# = IGM)
[IFXMI < 0] @
- 29\$ Array KEYAJ(NKEY) J positions of key fluences in ascending order
(# = INKEYFXI) @
- 30\$ Array KEYAI(NKEY) I positions of key fluences in ascending order for
like J (# = INKEYFXI) @

T (terminate block with "T") [T always required]

INPUT DATA BLOCK 5

External Boundary Source Input

[required if INGEOM < 20 and IBL, IBR, IBB, or IBT = 4]

- 91* Array SII(M,J) (# = MMA*JM) [IBL = 4 or IBR = 4]
I boundary source for a group
- 92* Array SJI(M,I) (# = MMA*IMA) [IBB = 4 or IBT = 4]
J boundary source for a group

T (terminate block with "T") [T required if any arrays are required]

Left and right sources are intermingled in the same array according to direction. If $\mu > 0$, the source applies to the left boundary; if $\mu < 0$, to the right. Likewise, if $\tau > 0$, a

J-boundary source applies to the bottom; if $\tau < 0$, the source applies to the top boundary. If any blocks of this type are required, IGM are required.

If IADJ > 0, the energy groups must be entered in reversed order. Omit block and delimiter if INGEOM = 20, or if no arrays are required.

INPUT DATA BLOCK 6

Fluence Guess Input [required if INPFXM > 0]

93* Array FIJ(I,J), FIJ(I,J) or FI(I) as INPFXM = 1, 2, or 3
(# = IMSJM, IMSJM, or IM) [INPFXM > 0]

94* Array FJ(J) (# = JM) [INPFXM = 3]

95* Array FG(IG) (# = IGM) [INPFXM > 1]

Note: Each array of this block must be followed by "T". If no arrays are required, no "T" is required. If IADJ > 0, energy groups must be specified in reversed order.

INPUT DATA BLOCK 7

Distributed Source Input [required if INPSRM > 0]

96* Array as 93* Array above

97* Array as 94* Array above

98* Array as 95* Array above

5.5 DORT INPUT DATA NOTES

5.5.1 Special Geometry Features

If INGEOM \geq 10, a one-dimensional problem will be solved with vertical flow suppressed. Use void boundary condition at top and bottom. RZ direction sets must be used with INGEOM = 11, while R θ sets must be used with INGEOM = 12. Solutions with INGEOM = 11 or 12 yield essentially the same result.

If INGEOM = 20, KTYPE = 0, and IBR = 4, a combined reflection/transmission problem in slab geometry is solved. Omit the 91* and 92* array blocks, and supply the input spectrum as CHI. The code will generate a boundary source in the leftmost direction of

non-zero weight of each downward q level. The value of JM must be the number of downward η levels. In this case, J corresponds to the incident η level, not to a Y-direction mesh. The 2* array should be filled with the values 0.0, 1.0, 2.0, ... JM. The first η level will correspond to the last J level. |CHI(IGM)| particles will enter each level in each group. If CHI(I) < 0, the emerging fluence is printed by direction, then by space interval.

If INGEOM = 30, the calculation proceeds as with INGEOM = 20, except that emerging fluence will be calculated for a source entering each group JDIRF \leq IGI \leq JDIRL in turn, and leaving in all groups IGI \leq IGO \leq IGM. The total source per group in each J-level is |CHI(IGD)|. If CHI < 0, the fluence from sources entering that group will be printed. The problem is "double differential," in that the fluence leaving each group resulting from a source in each individual input group is calculated.

If $3 \leq$ INGEOM ≤ 6 , and if all iterations are to be performed in diffusion theory, equilateral-triangular geometry is available. Geometry options, together with the required value of IM, are:

INGEOM	TRIANGULAR GEOMETRY OPTION	VALUE OF IM
3	180°-360° Symmetry	User's option
4	60° Symmetry	2*JM-1
5 (not operable)	90° Symmetry	2*JM+1
6	120° Symmetry	2*JM

The resulting geometry is illustrated in Figure 5-1.

The mesh input data involve certain unusual requirements. In most cases, the value of IM is a function of JM as shown above. Also, the radial dimensions used for input do not correspond directly to the actual dimensions of the mesh. For all but 90° symmetry, every mesh interval is an equilateral triangle with sides having a length S.

JM + 1 J-interval boundaries are entered, beginning with 0, and with spacing $\sqrt{3} S/2$. With 120°, 180°, or 360° symmetry, IM + 1 I-interval boundaries are entered, beginning with 0, and with spacing S/2. With 60° symmetry, the code will automatically set IM to negative, and require the entry of JM I-sets. The *j*th I-set has 2j boundaries with spacing S/2. The description applicable to 90° symmetry is not available.

For all cases, the (1,1) mesh interval is a triangle with vertex down. Example meshes are shown for the various triangular geometry options.

For 60° symmetry, the parameter ISBT should be set equal to JM, and the bottom boundary condition must be reflected. For 120° symmetry, the left and bottom boundaries must be periodic if periodic boundary conditions are selected.

5.5.2 Special Theory Options

If IGTYP E > 0, then the first IGTYP E outer iterations will be performed using alternate theory specified by group in the 7\$ array. If the *g*th entry is N_g then the first $|N_g|$ inner iterations of the first IGTYP E outer iterations on group, *g*, will be performed using diffusion theory if $N_g > 0$. If $|N_g|$ is less than the applicable maximum number of

iterations, the iterations will be completed in transport theory, even though the alternate theory may have achieved convergence.

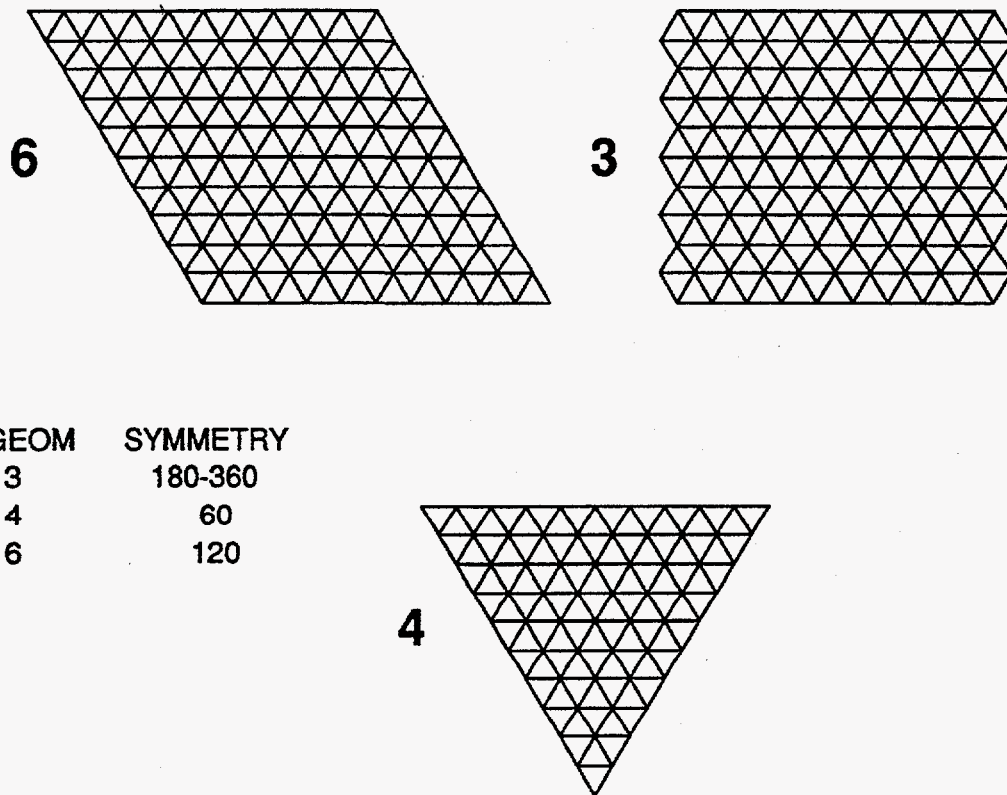


Figure 5-1. Triangular Geometry Options.

5.5.3 Cross Section Input and Mixing

The internal cross section storage comprises MTM sets of cross sections for each energy group. The first MTP sets are read from logical unit NTSIG, which is always required. The remainder are prepared using a "mixing table," described below. [It is intended that the first MTP "materials" will be microscopic nuclide data, and the remainder will be macroscopic mixtures, although other uses are possible.] The material numbers entered in the IZMT array (9\$) must be integers between 1 and MTM, corresponding to the appropriate data.

Each material consists of IHP cross sections as indicated in the description of the ORDOSW input file. If ISCTM > 0, then ISCTM sets of Legendre expansion data must follow each set designated in the IZMT array. If MCR < 0, then the required number of expansion sets is indicated in the NSIG array (78\$) (this feature is not presently operable).

If MIXL > 0, cross sections are to be modified by a mixing table, specified by the MIXT, NUCL, DENS, and MATL arrays (10\$, 11\$, 12*, and 13\$). The MATL array assigns an

arbitrary ID number to each material. If it is not entered, the ID's 1,2,....., MTM are assumed. Each integer entered in the MIXT and NUCL arrays must be one of these ID's, or 0. In the following:

m = number of the material having ID $|p|$ if $p \neq 0$; otherwise 0

n = number of the material having ID $|q|$ if $q \neq 0$; otherwise 0

and the interpretation of the table is as follows:

<u>MIXT</u>	<u>NUCL</u>	<u>DENS</u>
p	q	d

- (a) If $q = 0$, then the data of material m will be multiplied by d .
- (b) If $q > 0$, then the data of material n , multiplied by d , will be added to that of material m .
- (c) If $q = p$, the data of material m will be modified by the eigenvalue in concentration searches.
- (d) If $p < 0$, the appropriate Legendre expansion components will be treated as was the principal set.

Each set of entries is executed in sequence. In searches, the table may be executed repeatedly. As an example, with MIXL = 6, MTM = 11, and ISCTM = 3.

I	MIXT	NUCL	DENS	MATL
1	1000	0	0	10
2	1000	10	.1	20
3	1000	20	.2	30
4	1000	1000	0	40
5	-2000	0	0	50
6	-2000	30	.3	60
7				1000
8				2000
9				3000
10				4000
11				5000

Material 7 will consist of:

Material 1 * .1 + material 2 * .2

and will be modified by the eigenvalue.

Materials 8, 9, 10, 11 will be:

Materials 3, 4, 5, and 6 * .3.

Although the value of σ^A does not affect the fluence in a calculation directly, it must be used to obtain correct balance tables. It should meet the condition:

$$\sigma_g^T = \sigma_g^A + \sum_{g'} \sigma_{g \rightarrow g'}$$

If $\sigma^T(g)$ is replaced by a "transport cross section" in reactor core problems, a must be $\sigma_{g-g'}$ reduced such as to maintain σ^A constant.

It may be important to note that many standard cross section files such as ISOTXS and MATXS have Legendre expansion data which must be multiplied by $2l + 1$, where l is the expansion index, for use in DORT. It is intended that this be done in the code which prepares the ORDOSW (or optional GIP input file).

5.5.4 Activity Edits

A very general provision for obtaining energy-integrated reaction rates is provided. The arrays ICMAT, ICPOS, and ACMUL define an "activity table," interpreted as follows:

<u>ICMAT</u>	<u>ICPOS</u>	<u>ACMUL</u>
r	s	t

$$A_{i,j} = t d_{i,j} C_{i,j,r,s} \sum_g \phi_{g,j,i} \sigma_{g,r,s}$$

$$B_z = \sum_{i,j} X_{i,j,z} A_{i,j} V_{i,j}$$

where

- i,j = space mesh indices
- g = energy group index
- lr = material number
- lsl = cross section table position number
- t = arbitrary multiplier
- d = density factor if used, else 1
- Φ = fluence
- σ = cross section
- C = the "number density" of material lr in space cell i,j
- X = 1 if cell i,j is in edit region Z, else 0

The value of C is determined as follows:

- (a) If r is the macro material used in cell i,j, then C = 1,
- (b) If r is 0, then C = 1, and the cross sections for the macro material in material in cell i,j are used,
- (c) If r < 0, then C = 1,
- (d) If r > 0 and is not the macro, then C is the sum of all assignments of r to the macro according to the mixing table. Suppose IACT = 4 and the following table is entered, referring back to the mixing table illustrated above; and suppose material 7 is named as a macro in a portion of the problem:

I	ICMAT	ICPOS	ACMUL
1	7	3	1.
2	-7	3	1.
3	0	4	500.
4	1	5	1.
5	1	-5	1.

Activity 1 will use position 3 of material 7, but will be 0 where 7 is not the macro. Activity 2 will be similar, but will be calculated whether 7 is the macro or not. Activity 3 will use position 4 of the macro in each space cell, and will multiply the result by 500. Activity 4 will use position 5 of material 1 and a "number density" of .1 wherever 7 is the macro, since .1* material 1 was added to material 7 in the mixing table.

As a special feature, if $|s| > IHP$, then the value of CHI (1*) for the group will be used to replace σ , and c and d will be everywhere 1. This can be useful in adjoint problems.

If $s < 0$, the activity will be written on the punch data set. This can be used for fission density output, for example, as in Activity 5 of the illustration.

5.5.5 Negative Source Removal

Any problem using ISCTM > 0 may incur negative source generation. This is simply due to the failure of a truncated P_L expansion to describe the cross section adequately. If the problem has no areas of monodirectional flow or void, this effect will probably not be noticed, and will usually cause no harm. Voids or monodirectional flow, however, can result in severe distortions, or even negative scalar values for the fluence. The NEGFIX > 0 option will remove these distortions in most cases. The penalty in CPU time is usually in the range of 15-30%, although it can be higher if a major portion of the problem is so affected.

5.5.6 Problem Type Specification

Five major types of calculation are available, chosen by KTYPE:

- KTYPE = 0 M calculation - fixed source or subcritical multiplication
- = 1 K calculation - determines K_{eff}

- = 2 B search - modify DB^2 to produce specified K_{eff}
- = 3 C search - modify concentrations to produce specified K_{eff}
- = 4 D search - modify dimensions to produce specified K_{eff}

When $KTYPE = 0$ and $CHI = 0$ (1* array) or $NOFIS = 2$, a simple fixed-source problem is solved. Fluence from the input source is determined in one source iteration unless upscatter cross sections are used. Upscatter requires $ISRMX > 1$ and $EPO > 0$ for satisfactory results.

If some values of $CHI \neq 0$ and $NOFIS \neq 2$, fissions resulting from the fixed source and the input fluence guess, if any, are calculated in the first source iteration. These are added to the fixed source to begin the second iteration, and so on until subsequent fission generations have been accounted for. Since these subcritical multiplication problems tend to be slowly convergent, source iteration acceleration, discussed elsewhere, is used. If the system is, by itself, supercritical, this calculation will surely fail; a reflection of the fact that the fluence would be divergent in such a physical situation. The number of fission neutrons produced per source neutron is determined by iteration. Several source iterations are required. When $KTYPE = 1$, a calculation of K_{eff} is performed. Acceleration of the source iterations is discussed elsewhere.

K calculations can be improved somewhat by setting EVI equal to the best-available estimate of K . This is especially important in the case of restarts.

When $KTYPE > 1$, properties of the system configuration are changed in order to drive K_{eff} , calculated as described above, to a specified value, $EKOBJ$. For each configuration, the value of K_{eff} is partially converged, the configuration is changed, and the process continues until K_{eff} has stabilized and it is near the objective value. Additional details of this process are given in another section.

5.5.7 Iteration Limits and Convergence

In general, source iterations will be performed until the time $TMAX$ is exceeded ($IXX = 8$), the iterations limit $ISRMX$ is exceeded ($IXX = 1$), or convergence is reached. Source iteration convergence has not been reached if:

($IXX = 2$) the problem uses diffusion-theory source iterations followed by transport theory, and transport theory has not begun.

($IXX = 3$) the search has not converged; i.e., $KTYPE > 1$, $EPS > 0$, and:

$$\epsilon^s = \left| \frac{K^N - EKOBJ}{K^N} \right| > EPS$$

where: K^N is the value of K_{eff} for the latest (Nth) source.

($IXX = 4$) iteration fluence iterations for some group have not converged; i.e., $EPO > 0$ and:

$$\epsilon^F = \left| \frac{\phi_{i,j,g}^N - \phi_{i,j,g}^{N-1}}{\phi_{i,j,g}^N} \right| > EPO$$

(IXX = 5) fission density has not converged; i.e., EPF > 0 and:

$$\epsilon^D = \left| \frac{F_{i,j}^N - F_{i,j}^{N-1}}{F_{i,j}^N} \right| > EPF$$

(IXX = 6) K_{eff} has not converged; i.e., EPS > 0 and:

$$\epsilon^K = \left| \frac{K^N - K^{N-1}}{K^N} \right| > EPS$$

(IXX = 7) No source iterations have been completed.

The value of IXX is printed at each iteration, together with each of the above measures of convergence.

In general, problems with KTYPE > 0 require several outer iterations for convergence, while problems with KTYPE = 0 require only 1. In the latter case, performing several outer iterations can be very wasteful. Exceptional cases are fixed-source (KTYPE = 0) problems with non-zero fission or with upscatter. In these cases, several outer iterations are required.

The fluence iteration limit for each source iteration will be IFXMI or, if IFXMI < 0, the groupwise value from input array 28\$. After K^N and fission density have converged, the iteration limit is changed to IFXMF if IFXMF > 0. Fluence iterations proceed until the time TMAX is exceeded, the iteration limit is exceeded, or convergence is reached. Fluence convergence has not been reached if:

- Pointwise fluence convergence has not been reached; i.e., EPP > 0 and:

$$\epsilon^P = \left| \frac{\phi_{i,j,g}^n - \phi_{i,j,g}^{n-1}}{\phi_{i,j,g}^n} \right| W_{i,j} > EPO$$

n = fluence iteration index

Where W_{ij} is the value of the importance function (24* array) for the position i,j if IEPSBZ > 0, and otherwise 1.0. The largest ϵ^P for any group after the last fluence iteration is called "group convergence", ϵ^G .

- Volumetric fluence convergence has not been reached; i.e., $EPV > 0$ and:

$$\frac{\sum_{i,j} |\phi_{i,j,g}^n - \phi_{i,j,g}^{n-1}| W_{i,j} V_{i,j}}{\sum_{i,j} \phi_{i,j,g}^n W_{i,j} V_{i,j}} > EPV$$

Fluences less than FLXMIN are not considered in the tests. This prevents values near zero, which are badly affected by roundoff, from thwarting convergence. FLXMIN also is used as a minimum coarse-mesh fluence by the fluence acceleration routines, preventing similar degeneracy there.

5.5.8 Search Strategy

The searches proceed by successive adjustment of the eigenvalue, EV. EV is constrained to be positive, and extensive checks prevent oscillation and overextrapolation. Each search seeks a value of EV which adjusts K_{eff} to an input value, EKOBJ. EV is used to adjust the system parameters as follows:

$$\text{B search: } (DB^2)_{\text{eff}} = (DB^2)_{\text{input}} * EV$$

$$\text{C search: } (C)_{\text{eff}} = (C)_{\text{input}} * (1 + f(EV - 1))$$

To adjust material m in this way, an entry is made in the mixing table:

<u>10\$</u>	<u>11\$</u>	<u>12*</u>
m	m	f

$$\text{D search: } (\Delta d)_{\text{eff}} = (\Delta d)_{\text{input}} * (1 + f(EV - 1))$$

Here, d represents either dimension and f is the superzone search fraction input (18* or 19* array)

The initial estimate of EV is EVI. Defining search convergence as:

$$\text{CONVSR} = (K^N - EKOBJ)/K^N$$

and eigenvalue convergence as:

$$\text{CVK} = (K^N - K^{N-1})/K^N$$

the initial value of EV is used until:

$$CVK < EVTH * \max(EPS, \min(0.1, CONVSR))$$

The second value of EV is determined by linear extrapolation if EVDELK = 0, using the input value of eigenvalue dependence on K, DEVDKI. If EVDELK ≠ 0, the second EV is:

$$EVI \pm EVDELK$$

where the sign of DEVDKI is used to determine the correct step direction. Subsequent values of EV are obtained by nonlinear interpolation if possible, and linear when nonlinear fails.

Each new value of EV is constrained to the range between EV*EVCHM and EV/EVCHM. EV is always limited to the range between EVI*EVMAX and EVI/EVMAX. If EV moves to its limit and stays there, or if K exceeds the range between EKOBJ+EVKMAX and EKOBJ-EVKMAX, the search is stopped.

5.5.9 Upscatter Rebalance

If upscatter is present in a problem, upscatter rebalance is performed after source iteration 2 and successive iterations. All fluences within the upscatter energy range are multiplied by a factor DVUPS:

$$DVUPS = UPSS / (UPSS - (UPSP - UPS))$$

where: IGUPS = first group into which upscatter is non-zero
UPS = previous upscatter sum
UPSP = new upscatter sum
UPSS = sum of all scatter into groups ≥ IGUPS from groups < IGUPS

This factor is applied to fluences for all energy groups ≥ IGUPS, bringing the system into global balance. This procedure is usually helpful, and has not been observed to cause erratic behavior. The value of $\epsilon^u = DVUPS - 1$ is printed in the output data as upscatter convergence.

5.5.10 Fission Rescaling

An approach analogous to upscatter rebalance is used when a fixed source is used with a multiplying medium. In these cases, fluences for all energy groups are multiplied by FSNORM:

$$FSNORM = FXSUM / (FXSUM - (SRNEW - FSOLD))$$

where: FXSUM = total fixed source
 SRNEW = new fission source estimate
 FSOLD = previous fission source estimate

Since the upscatter rebalance is applied before fission sums are calculated, there is no conflict between these procedures, and one supplements the other.

5.5.11 Fission Extrapolation

After these rebalance and rescaling procedures, a feature is provided to use a fixed fission acceleration factor:

$$(\text{FSNIJ})_{\text{extrap}} = (\text{FSNIJ})_{\text{calc}} + f[(\text{FSNIJ})_{\text{calc}} - (\text{FSOIJ})_{\text{final}}]$$

where: FSNIJ = new fission distribution
 FSOIJ = previous fission distribution
 f = FSNACC, an input parameter, adjusted downward as necessary to insure that no fission value is changed more than 20%

No extrapolation of fluences is attempted with this procedure. Tests have shown that reasonably chosen values of FSNACC speed the convergence of certain problems, especially M calculations, and cause oscillation in others. Its use is not generally recommended. The option of FSNACC has been removed from DORT.

5.5.12 Error-Mode Extrapolation

To accomplish error-mode extrapolation, DORT accumulates the sum FERAH and the eigenvalue estimate λ :

$$\text{FERAH} = \Sigma[(\text{FSNIJ})_{\text{extrap}} - (\text{FSOIJ})_{\text{extrap}}]$$

$$\lambda = (\text{FERAH})_{\text{new}} / (\text{FERAH})_{\text{previous}}$$

and an error-mode removal parameter Θ :

$$\Theta = \lambda / (1 - \lambda)$$

When estimates of Θ in three successive iterations are in fractional agreement within EXTRCV, the fission is extrapolated according to:

$$(\text{FSNIJ})_{\text{final}} = (\text{FSNIJ})_{\text{extrap}} + \Theta[(\text{FSNIJ})_{\text{extrap}} - (\text{FSOIJ})_{\text{final}}]$$

where Θ' is Θ adjusted so that the fission density will change by no more than $|SORMIN|$, where SORMIN is a input value. The fluences are similarly extrapolated by the factor Θ' , with each fluence limited by the $|SORMIN|$ ratio.

Tests show this procedure to be safe and effective. It is compatible with upscatter rebalance and can be used together with fission rescaling.

If fission rescaling is not used, Θ , in certain cases, may be 100 or larger. In such cases, single-precision IBM calculations may not be sufficient to provide a stable value of Θ , and so the extrapolation is not effective. Rescaling may lower Θ in such cases to a manageable value, i.e., to 25 or less.

As a counter example, if a system is driven by a source at its periphery, the unmultiplied fluence due to the source is so different in shape from the final fluence solution that fission rescaling may slow or thwart convergence. A negative value of SORMIN must be used in such cases, so that fission rescaling is disabled.

5.5.13 Fluence Iteration Acceleration

Five types of fluence iteration acceleration can be selected:

IACC	KALF	Result
0	any	Groupwise rebalance
1	0	Diffusion acceleration, corner mesh
1	1	Diffusion acceleration, centered mesh
2	0	(Conventional) Partial current rebalance, J stabilized
2	1	(Conventional) Partial current rebalance, Φ stabilized

Corner-mesh diffusion acceleration (CNRDA) is usually best for "normal" problems. High-energy neutron groups in problems having complex geometry may be better solved by partial-current rebalance (PCR). The choices of stabilization with PCR are of roughly equal merit. In the case of problems having two facing reflected or periodic boundaries, such as cell or $R\Theta$ problems, it is often helpful to use the coarse-mesh feature to specify only one interval in the reflected (or periodic) direction, and to specify PCR. (In such a case, the code will arrange one interval as a default unless the 85*/86* array is entered explicitly.)

All of the fluence iteration acceleration schemes except the groupwise rebalance require the performance of a certain number of rebalance iterations after each fluence iteration. Default input parameters constrain this number between 4 and 50 (INTSCL and ITMSCL). In 1-D problems, or if the coarse mesh has only 1 interval in either direction, INTSCL = 1 is appropriate. In K calculations and searches, a lower value of ITMSCL (e.g., 8) can lower costs. Within the iteration limits, the iterations are terminated when:

$$\text{MAX}_{i,j} \left| \frac{\phi_{i,j}^K - \phi_{i,j}^{K-1}}{\phi_{i,j}^K} \right| < \text{CONSCL}$$

It is often effective to make CONSCL less than EPP by roughly a factor of 10, and to leave CONACC at its default value. Other combinations are often used, however.

If IBFSCL > 0, rebalance iterations are bypassed on the first fluence iteration of the first source iteration. This sometimes saves CPU time on very difficult problems, and sometimes prevents certain types of early iteration failure. On less difficult problems, especially those using diffusion acceleration, it may lower efficiency slightly.

If WSOLOI > 0, fluence acceleration will not be performed on those energy groups for which, for all materials of a problem:

$$\sigma^S / \sigma^T < \text{WSOLOI}$$

This can save unneeded CPU effort without impairing convergence rate.

5.5.14 Stabilization

The partial-current rebalance method requires choice of a "stabilization factor," F. The effect of this factor is to adjust the rebalance matrix in such a way as to insure positive factors if F > 1.0. The user inputs an initial value, WSOLCN, and an increment, WSOLII. If WSOLII > 0, F is increased by WSOLII after each rebalance. If WSOLII < 0, F is increased by |WSOLII| only when incipient oscillation is detected.

The choice of these factors has a very large effect on the running time of difficult problems. Some combinations are shown in Table 5-2. If diffusion acceleration can be used, this difficult choice is avoided.

Table 5-2. Typical Stabilization Values

WSOLCN	WSOLII	Comments
1.0	0	Satisfactory for many well-behaved core problems which are probably better solved by diffusion acceleration.
1.0	1.0	Satisfactory for many difficult fixed-source problems
4.0	1.0	One solver of very difficult problem uses this
1.0	-1.5	This may be a "best-buy" single choice.

5.5.15 Input Source and Fluence Specification

For K_{eff} and configuration search problems, the initial source is generated internally based on the fission cross sections and the fluence guess. For fixed-source problems, the user must supply an external source of particles. This can be done by supplying an external source file containing an internal or external boundary source, a distributed source, or a first-collision source. The external boundary source and distributed source can be generated internally by card-image input in a few simple cases. At least one non-zero source type must always be supplied.

An external boundary source is indicated by the appropriate choice of boundary condition. If input parameter $\text{NTBSI} > 0$, the logical unit NTBSI is to contain the information. Otherwise, it is to be found in the card-image input. Formats for these inputs are explained elsewhere in this region.

A distributed source is to be supplied on logical unit NTDSI if $\text{NTDSI} > 0$ and $\text{INPSRM} = 0$. If $\text{INPSRM} > 0$, NTDSI must point to a scratch device onto which a source generated from card images will be placed.

A first-collision source is to be supplied on NTFCI if $\text{NTFCI} > 0$. This source is simply a special type of distributed source, and is specified by a special type of distributed source file format. In such a case, the file also gives the "uncollided fluence" the scattering of which will lead to the source. This fluence is added to the fluence calculated by the code in some of the output results. (It is subtracted from a fluence guess on NTFLX , if any.)

Internal boundary sources are indicated by $\text{NJNTR} > 0$ and/or $\text{NINTSR} > 0$. In these cases, internal boundaries are specified in the 14* and 15* arrays at which sources input from logical unit NTIBI are located.

In principle, several types of sources can coexist. Little actual experience is available in these areas, however, and such results should be carefully checked.

If $\text{KTYPE} > 0$, a non-zero fluence guess is always required. If $\text{NTFLX} > 0$ and $\text{INPFXM} = 0$, the fluence is to be supplied on logical unit NTFLX . If $\text{INPFXM} > 0$, the fluence guess is to be generated from card images. Problems with $\text{KTYPE} = 0$ are usually started without a fluence guess, unless the problem has been partially solved in a previous execution.

5.5.16 Key Fluence Monitoring

In many cases, the convergence of all of the fluence data is of less interest than convergence of one or a few key fluences. If $\text{KEYJN} > 0$ and $\text{KEYIN} > 0$, the value of a single key fluence will be printed in the fluence-iteration monitor line. If not, the position of maximum fluence change at the second fluence iteration will be so monitored. In addition, an arbitrary array of key fluences can be specified by adjusting NKEYFX . If desired, these fluences can be printed only after the convergence of each energy group.

5.5.17 Energy Boundary Input

The energy boundaries are used only for transfer to the output files. They may be ignored for most applications. The ordering is:

Combined Neutron-Photon	Neutron Only	Photon Only
E_1^{MAX}	E_1^{MAX}	0
E_2^{MAX}	⋮	E_1^{MAX}
⋮	⋮	⋮
E_{NEUT}^{MAX} (last neutron group)	E_{IGM}^{MAX}	E_{IGM}^{MAX}
E_{NEUT}^{MIN}	0	E_{IGM}^{MIN}
E_{n+1}^{MAX} (first photon group)		
⋮		
E_{IGM}^{MAX}		
E_{IGM}^{MIN} (last photon group)		

5.5.18 Fluence Extrapolation Model

The choice of mode can have an important influence on both CPU time requirements and the accuracy of the solutions. In general, the Θ -weighted model gives reasonable results for a wide range of problems. The linear-zero model is similar to the tried-and-proven method used in TWOTRAN-II. It gives well-accepted and rapid solutions to problems such as a reactor core not containing severe heterogeneities. It will often fail to converge or give inaccurate results for difficult deep penetration problems, however. The ordinary weighted model almost always converges better than the other models. Its results are usually not suitable for K_{eff} calculations, but it is used exclusively by many deep-penetration analysts.

5.5.19 Alternate Zone Map Input

An alternate "combinatorial-geometry" option is available. Rather than the usual 8\$ description, supply the following:

-z ₁	i ₁	j ₁	I ₁	J ₁
-z ₂	i ₂	j ₂	I ₂	J ₂
etc.				
F 0				

Each set of five integers contains:

- z: The zone number, tagged with a negative
- i] Indices of lower, lefthand corner of zone in
j] zone map
- I] Indices of upper, righthand corner of zone in
J] zone map

As many descriptors as required to a limit of IMSJM are used, and the remainder of the array is filled with 0. Zones can be overlaid as desired. This type of 8\$ array must not be intermingled with the traditional type within a given problem. When used with variable mesh, the zones are understood to be cylindrical in space, although they may be discontinuous in the zone map printout.

5.5.20 Notes On DORT Mesh For An Air-Over-Ground Problem

When setting up an air-over-ground DORT problem, both radial and axial mesh near the source must be chosen to restrict $1/R^2$ attenuation between boundaries to about a factor of 2. In the sample problem given in below, a basic 100-cm exclusion radius is used, and only one interval is needed within that. Then, mesh is chosen such that:

$$R_i = R_o + d_{i-1} \quad (i=1, 2, \dots)$$

$$d_i = d_{i-1} + \Delta d$$

$$\Delta d = \gamma d_{i-1} \text{ or in other words, so that no } r_i \text{ is more than } 1+\gamma \text{ times } d_{i-1}. \quad 0 < \gamma < 1$$

(A γ of .3 is a good choice for all air-over-ground problems.)

Table 5-3 shows the radial mesh, where $R_0=0$, $d_0=100$, and $\gamma=0.3$. When the calculated Δd exceeds 3000, 3000 should be used. The same approach is used above the source, as shown in Table 5-4. The mesh downward from the source (Table 5-5) is begun the same way, but it will meet the mesh upward from the ground (Table 5-6).

The basic mesh upward from the ground uses a larger value of d_0 , and proceeds upward until the Δd it predicts is larger than Δd predicted by the downward mesh. The two sets are joined at 6500 in this illustration, a compromise between 6096 and 6943. In the actual problem, additional intervals are added below 550 to account for ground effects. A small interval near the vehicle may be desired, also. Meshes for other source heights can be deduced from this illustration.

Table 5-3. Radial mesh
away from source.

R	Δd	d
0	-	100
100	30	130
130	39	169
169	51	220
220	66	286
286	86	371
371	111	483
483	145	627
627	188	816
816	245	1,060
1,060	310	1,379
1,379	414	1,792
1,792	538	2,330
2,330	699	3,029
3,029	909	3,937
3,937	1,181	5,119
5,119	1,536	6,654
6,654	1,996	8,650
8,650	2,595	11,246
11,246	3,374	14,619

Table 5-4. Mesh upward
from source.

Z	Δd	d
12,750	-	100
12,850	30	130
12,880	39	169
12,919	51	220
12,970	66	286
13,036	86	371
13,121	111	483
13,233	145	627
13,377	188	816
13,566	245	1,060
13,810	310	1,379
14,129	414	1,792
14,542	538	2,330
15,080	699	3,029
15,779	909	3,937
16,687	1,181	5,119
17,869	1,536	6,654
19,404	1,996	8,650
21,400	2,595	11,246
23,996	3,374	14,619

Table 5-5. Mesh downward from source.

Z	Δd	d
12,750	-	-100
12,650	-30	-130
12,620	-39	-169
12,581	-51	-220
12,530	-66	-286
12,464	-86	-371
12,379	-111	-483
12,267	-145	-627
12,113	-188	-816
11,934	-245	-1,060
11,690	-318	-1,379
11,371	-414	-1,792
10,958	-538	-2,330
10,420	-699	-3,029
9,721	-909	-3,937
8,813	-1,181	-5,119
7,631	-1,536	-6,654
→6,096	-1,996	-8,650
4,100	-2,595	-11,426

Table 5-6. Mesh upward from ground.

Z	Δd	d
50	-	500
550	150	650
700	195	845
895	254	1,098
1,148	330	1,428
1,478	428	1,856
1,906	557	2,413
2,463	724	3,137
3,187	941	4,079
4,128	1,224	5,302
5,352	1,591	6,893
→6,943	2,068	8,961
9,011	2,688	11,649
11,699	3,495	15,144

5.6 DORT INPUT AND OUTPUT FILE FORMATS

The GIP file is defined exactly as the records labeled "CROSS SECTION DATA" in the ORDOSW file (of which only the cross-section portion is listed), and has no other record types. The "DOT III Angular Fluence Tape" is defined in the DOT III User's Manual,¹² and is simulated by DORT as accurately as possible. The user should consult Reference 14 for the full description of the ORDOSW file.

```

C                                     -VSOR0010
C                                     VSOR0020
C***** VSOR0030
C             REVISED 10 NOV 76      -VSOR0040
C                                     -VSOR0050
CF    VARSOR                          -VSOR0060
CE    VARIABLE MESH SOURCE MOMENT DATA -VSOR0070
C                                     -VSOR0080
C***** VSOR0090
C                                     VSOR0100
CD    ORDER OF GROUPS IS BY DECREASING ENERGY VSOR0110

```

CD	I IS THE FIRST-DIMENSION INDEX		VSOR0120
CD	J IS THE SECOND-DIMENSION INDEX		VSOR0130
CD	JM=1 FOR 1-DIMENSIONAL GEOMETRY		VSOR0140
CD	IF ISOP.GT.0, SOURCE IS FIRST-COLLISION TYPE		VSOR0150
C			VSOR0160
C			VSOR0170
CS	FILE STRUCTURE		-VSOR0180
CS			-VSOR0190
CS	RECORD TYPE	PRESENT IF	-VSOR0200
CS			-VSOR0210
CS	FILE IDENTIFICATION	ALWAYS	-VSOR0220
CS	FILE LABEL	ALWAYS	-VSOR0230
CS	FILE CONTROL	ALWAYS	-VSOR0240
CS	FILE INTEGER PARAMETERS	ALWAYS	-VSOR0250
CS			-VSOR0260
CS	***** (REPEAT OVER ALL GROUPS)		-VSOR0270
CS *	SOURCE MOMENTS	ALWAYS	-VSOR0280
CS	*****		-VSOR0290
C			-VSOR0300
CS	***** (REPEAT OVER ALL GROUPS)		-VSOR0310
CS *	SCALAR UNCOLLIDED FLUX	ISOP.GT.0	-VSOR0320
CS	*****		-VSOR0330
C			-VSOR0340
C			VSOR0350
C			VSOR0360
C			VSOR0370
C			VSOR0380
CR	FILE IDENTIFICATION		-VSOR0390
C			-VSOR0400
CL	HNAME,(HUSE(I),I=1,2),IVERS		-VSOR0410
C			-VSOR0420
CW	1+3*MULT=NUMBER OF WORDS		-VSOR0430
C			-VSOR0440
CD	HNAME	HOLLERITH FILE NAME - VARSOR - (A6)	-VSOR0450
CD	HUSE(I)	HOLLERITH USER IDENTIFICATION - (A6)	-VSOR0460
CD	IVERS	FILE VERSION NUMBER	-VSOR0470
CD	MULT	DOUBLE PRECISION PARAMETER	-VSOR0480
CD		1- A6 WORD IS SINGLE WORD	-VSOR0490
CD		2- A6 WORD IS DOUBLE PRECISION WORD	-VSOR0500
C			-VSOR0510
C			VSOR0520
C			VSOR0530
C			VSOR0540
C			VSOR0550
C			-VSOR0560
CR	FILE LABEL		-VSOR0570
C			-VSOR0580
CL	DATE,USER,CHARGE,CASE,TIME,(TITL(I),I=1,12)		-VSOR0590
C			-VSOR0600
CW	17*MULT=NUMBER OF WORDS		-VSOR0610
C			-VSOR0620
CD	DATE	AS PROVIDED BY TIMER OPTION 4 - (A6)	-VSOR0630
CD	USER	AS PROVIDED BY TIMER OPTION 5 - (A6)	-VSOR0640

CD	CHARGE	AS PROVIDED BY TIMER OPTION 6	-(A6)	-VSOR0650
CD	CASE	AS PROVIDED BY TIMER OPTION 7	-(A6)	-VSOR0660
CD	TIME	AS PROVIDED BY TIMER OPTION 8	-(A6)	-VSOR0670
CD	TITL(I)	TITLE PROVIDED BY USER	-(A6)	-VSOR0680
C				-VSOR0690
C				VSOR0700
C				VSOR0710
C				VSOR0720
C				VSOR0730
CR		FILE CONTROL		VSOR0740
C				-VSOR0750
CD	IGM,NEUT,JM,LM,IMA,MMA,ISM,IMSISM,ISOP,(IDUM(N),N=1,16)			-VSOR0760
C				-VSOR0770
CW	25=NUMBER OF WORDS			-VSOR0780
C				-VSOR0790
CD	IGM	NUMBER OF ENERGY GROUPS		-VSOR0800
CD	NEUT	LAST NEUTRON GROUP		-VSOR0810
CD		(IGM IF ALL NEUTRONS, 0 IF ALL GAMMA)		-VSOR0820
CD	JM	NUMBER OF SECOND-DIMENSION (J) INTERVALS		VSOR0830
CD	LM	MAXIMUM LENGTH OF MOMENT EXPANSION		VSOR0840
CD	IMA	MAXIMUM NUMBER OF FIRST-DIMENSION INTERVALS		-VSOR0850
CD	MMA	NUMBER OF BOUNDARY DIRECTIONS		-VSOR0860
CD	ISM	NUMBER OF I-BOUNDARY SETS		-VSOR0870
CD	IMSISM	TOTAL NUMBER OF I-INTERVALS, ALL I-SETS		-VSOR0880
CD	ISOP	UNCOLLIDED FLUX FLAG		-VSOR0890
CD		0 - NO UNCOLLIDED FLUX RECORDS PRESENT		-VSOR0900
CD		1 - UNCOLLIDED FLUX RECORDS PRESENT		-VSOR0910
CD	IDUM(I)	ARRAY SET TO 0		-VSOR0920
C				-VSOR0930
C				VSOR0940
C				VSOR0950
C				VSOR0960
C				VSOR0970
CR		FILE INTEGER PARAMETERS		-VSOR0980
C				-VSOR0990
CL	(LMBIG(IG),IG=1,IGM),			-VSOR1000
CL	*(IMBIS(IS),IS=1,ISM),(ISET(J),J=1,JM)			-VSOR1010
C				-VSOR1020
CW	IGM+ISM+JM=NUMBER OF WORDS			-VSOR1030
C				-VSOR1040
CD	LMBIG(IG)	LENGTH OF MOMENT EXPANSION FOR GROUP IG		-VSOR1050
CD	IMBIS(IS)	NUMBER OF INTERVALS IN ISET IS		-VSOR1060
CD	ISET(J)	I-SET ASSIGNED TO INTERVAL J		-VSOR1070
C				-VSOR1080
C				VSOR1090
C				VSOR1100
C				VSOR1110
C				VSOR1120
CR		SOURCE MOMENTS		VSOR1130
C				-VSOR1140
CL	((SORM(I,L),I=1,IMS),L=1,LMS)			-VSOR1150
C				-VSOR1160
CW	IMS*LMS=NUMBER OF WORDS			-VSOR1170

C			-VSOR1180
C	DO 1 J=1,JM		-VSOR1190
C	1 READ(N) *LIST AS ABOVE*		-VSOR1200
C			-VSOR1210
CD	SORM	SOURCE BY INTERVAL AND MOMENT INDEX	-VSOR1220
CD	IMS	IMBIS(IS) FOR IS CORRESPONDING TO J	-VSOR1230
CD	LMS	LMBIG(IG)	-VSOR1240
C			-VSOR1250
C	-----		VSOR1260
C			VSOR1270
C			VSOR1280
C	-----		VSOR1290
CR	SCALAR UNCOLLIDED FLUX		-VSOR1300
C			-VSOR1310
CL	(FLUM(I),I=1,IMS)		-VSOR1320
C			-VSOR1330
CW	IMS=NUMBER OF WORDS		-VSOR1340
C			-VSOR1350
C	DO 1 J=1,JM		-VSOR1360
C	1 READ(N) *LIST AS ABOVE*		-VSOR1370
C			-VSOR1380
CD	FLUX	UNCOLLIDED FLUX BY INTERVAL	-VSOR1390
C			-VSOR1400
C	-----		VSOR1410
C			VSOR1420
C			VSOR1430
C			VSOR1440
C			VSOR1450
C	END		VSOR1460
C			-VRFL0010
C			VRFL0020
C	*****		VRFL0030
C		REVISED 10 NOV 76	-VRFL0040
C			-VRFL0050
CF	VARFLM		-VRFL0060
CE	VARIABLE MESH FLUX MOMENT DATA WITH BOUNDARY FLUXES		-VRFL0070
C			-VRFL0080
C	*****		VRFL0090
C			VRFL0100
CD	ORDER OF GROUPS IS BY DECREASING ENERGY		VRFL0110
CD	I IS THE FIRST-DIMENSION INDEX		VRFL0120
CD	J IS THE SECOND-DIMENSION INDEX		VRFL0130
CD	JM=1 FOR 1-DIMENSIONAL GEOMETRY		VRFL0140
C			VRFL0150
C	-----		VRFL0160
CS	FILE STRUCTURE		-VRFL0170
CS			-VRFL0180
CS	RECORD TYPE	PRESENT IF	-VRFL0190
CS	-----	-----	VRFL0200
CS	FILE IDENTIFICATION	ALWAYS	-VRFL0210
CS	FILE LABEL	ALWAYS	-VRFL0220
CS	FILE CONTROL	ALWAYS	-VRFL0230
CS	FILE INTEGER PARAMETERS	ALWAYS	-VRFL0240

CS	FILE REAL	PARAMETERS	ALWAYS	-VRFL0250
CS				-VRFL0270
CS	***** (REPEAT OVER ALL GROUPS)			-VRFL0280
CS	*	FLUX MOMENTS	ALWAYS	-VRFL0290
CS	*	BOUNDARY DIRECTIONAL FLUX	ALWAYS	-VRFL0300
CS	*****			-VRFL0310
C				VRFL0320
C	-----			VRFL0330
C				VRFL0340
C				VRFL0350
C	-----			VRFL0360
CR	FILE IDENTIFICATION			-VRFL0370
C				-VRFL0380
CL	HNAME,(HUSE(I),I=1,2),IVERS			-VRFL0390
C				-VRFL0400
CW	1+3*MULT=NUMBER OF WORDS			-VRFL0410
C				-VRFL0420
CD	HNAME	HOLLERITH FILE NAME	VARFLM - (A6)	-VRFL0430
CD	HUSE(I)	HOLLERITH USER IDENTIFICATION	- (A6)	-VRFL0440
CD	IVERS	FILE VERSION NUMBER		-VRFL0450
CD	MULT	DOUBLE PRECISION PARAMETER		-VRFL0460
CD		1- A6 WORD IS SINGLE WORD		-VRFL0470
CD		2- A6 WORD IS DOUBLE PRECISION WORD		-VRFL0480
C				VRFL0490
C	-----			VRFL0500
C				VRFL0510
C				VRFL0520
C	-----			VRFL0530
C				-VRFL0540
CR	FILE LABEL			-VRFL0550
C				-VRFL0560
CL	DATE,USER,CHARGE,CASE,TIME,(TTTL(I),I=1,12)			-VRFL0570
C				-VRFL0580
CW	17*MULI=NUMBER OF WORDS			-VRFL0590
C				-VRFL0600
CD	DATE	AS PROVIDED BY TIMER OPTION 4	- (A6)	-VRFL0610
CD	USER	AS PROVIDED BY TIMER OPTION 5	- (A6)	-VRFL0620
CD	CHARGE	AS PROVIDED BY TIMER OPTION 6	- (A6)	-VRFL0630
CD	CASE	AS PROVIDED BY TIMER OPTION 7	- (A6)	-VRFL0640
CD	TIME	AS PROVIDED BY TIMER OPTION 8	- (A6)	-VRFL0650
CD	TTTL(I)	TITLE PROVIDED BY USER	- (A6)	-VRFL0660
C				-VRFL0670
C	-----			VRFL0680
C				VRFL0690
C				VRFL0700
C	-----			VRFL0710
CR	FILE CONTROL			-VRFL0720
C				-VRFL0730
CD	IGM,NEUT, JM,LM,IMA,MMA,ISM,IMSISM,ISBT,ITER,(IDUM(N),N=1,15)			-VRFL0740
C				-VRFL0750
CW	25=NUMBER OF WORDS			-VRFL0760
C				-VRFL0770
CD	IGM	NUMBER OF ENERGY GROUPS		-VRFL0780

CD	NEUT	LAST NEUTRON GROUP	-VRFL0790
CD		(IGM IF ALL NEUTRONS, 0 IF ALL GAMMAS)	-VRFL0800
CD	JM	NUMBER OF SECOND-DIMENSION (J) INTERVALS	-VRFL0810
CD	LM	MAXIMUM LENGTH OF MOMENT EXPANSION	-VRFL0820
CD	IMA	MAXIMUM NUMBER OF FIRST-DIMENSION INTERVALS	-VRFL0830
CD	MMA	NUMBER OF BOUNDARY DIRECTIONS	-VRFL0840
CD	ISM	NUMBER OF I-BOUNDARY SETS	-VRFL0850
CD	IMSISM	TOTAL NUMBER OF I-INTERVALS, ALL I-SETS	-VRFL0860
CD	ISBT	I-SET FOR SYSTEM BOUNDARIES	-VRFL0870
CD	ITER	OUTER ITERATION NUMBER AT WHICH FLUX WAS	-VRFL0880
CD		WRITTEN	-VRFL0890
CD	IDUM(I)	ARRAY SET TO 0	-VRFL0900
C			-VRFL0910
C			VRFL0920
C			VRFL0930
C			VRFL0940
C			VRFL0950
CR	FILE INTEGER PARAMETERS		-VRFL0960
C			-VRFL0970
CL	(LMBIG(IG),IG=1,IGM),		-VRFL0980
CL	*(IMBIS(IS),IS=1,ISM),(ISET(J),J=1,JM)		-VRFL0990
C			-VRFL1000
CW	IGM+ISM+JM=NUMBER OF WORDS		-VRFL1010
C			-VRFL1020
CD	LMBIG(IG)	LENGTH OF MOMENT EXPANSION FOR GROUP IG	-VRFL1030
CD	IMBIS(IS)	NUMBER OF INTERVALS IN ISET IS	-VRFL1040
CD	ISET(J)	I-SET ASSIGNED TO INTERVAL J	-VRFL1050
C			-VRFL1060
C			VRFL1070
C			VRFL1080
C			VRFL1090
C			VRFL1100
CR	FILE REAL PARAMETERS		-VRFL1110
C			-VRFL1120
CL	(Z(J),J=1,JM1),((R(I,IS),I=1,IM1),IS=1,ISM),		-VRFL1130
CL	*(ENER(IG),IG=1,IGM),EMIN,ENEUT,EV,DEVDK,EFFK,POWER,		-VRFL1140
CL	*(DUMRL(I),I=1,13)		-VRFL1150
C			-VRFL1160
CW	JM+IMSISM+ISM+IGM+20=NUMBER OF WORDS		-VRFL1170
C			-VRFL1180
CD	Z(J)	J-INTERVAL BOUNDARIES	-VRFL1190
CD	R(I,IS)	I-INTERVAL BOUNDARIES FOR I-SET I	-VRFL1200
CD	ENER(IG)	TOP ENERGY BOUNDARY OF GROUP IG	-VRFL1210
CD	EMIN	BOTTOM ENERGY BOUNDARY OF GROUP IGM	-VRFL1220
CD	ENEUT	BOTTOM ENERGY BOUNDARY OF GROUP NEUT	-VRFL1230
CD		0 IF NEUT=0*	-VRFL1240
CD	EV	EIGENVALUE	-VRFL1250
CD	DEVDK	DERIVATIVE OF EV VS. EFFK	-VRFL1260
CD	EFFK	EFFECTIVE MULTIPLICATION FACTOR	-VRFL1270
CD	POWER	POWER (WATTS) TO WHICH FLUX IS NORMALIZED	-VRFL1280
CD	DUMRL	ARRAY SET TO 0	-VRFL1290
CD	JM1	JM+1	-VRFL1300
CD	IM1	IMBIS(IS)+1	-VRFL1310

C		-VRFL1320	
C		VRFL1330	
C		VRFL1340	
C		VRFL1350	
C		VRFL1360	
C		VRFL1370	
C		VRFL1380	
CR	FLUX MOMENTS	-VRFL1390	
C		-VRFL1400	
CL	((FLUM(I,L),I=1,IMS),L=1,LMS)	-VRFL1410	
C		-VRFL1420	
CW	IMS*LMS=NUMBER OF WORDS	-VRFL1430	
C		-VRFL1440	
C	DO 1 J=1,JM	-VRFL1450	
C 1	READ(N) *LIST AS ABOVE*	-VRFL1460	
C		-VRFL1470	
CD	FLUM	FLUX BY INTERVAL AND MOMENT INDEX	-VRFL1480
CD	IMS	IMBIS(IS) FOR IS CORRESPONDING TO J	-VRFL1490
CD	LMS	LMBIG(IG)	-VRFL1500
C		-VRFL1510	
C		VRFL1520	
C		VRFL1530	
C		VRFL1540	
C		VRFL1550	
CR	BOUNDARY DIRECTIONAL FLUX	-VRFL1560	
C		-VRFL1570	
CL	((FIO(M,J),M=1,MMA),J=1,JM), ((FJO(M,I),M=1,MMA),I=1,IMB)	-VRFL1580	
C		-VRFL1590	
CW	MMA*(JM+IMB)=NUMBER OF WORDS	-VRFL1600	
C		-VRFL1610	
CD	FIO	DIRECTIONAL FLUX OUTGOING BY DIRECTION AND	-VRFL1620
CD		J-INTERVAL	-VRFL1630
CD	FJO	DIRECTIONAL FLUX OUTGOING BY DIRECTION AND	-VRFL1640
CD		I-INTERVAL. FJO=0 FOR A 1-D GEOMETRY	-VRFL1650
CD	IMB	IMBIS(IS) FOR IS CORRESPONDING TO ISBT	-VRFL1660
C		-VRFL1670	
C		VRFL1680	
C		VRFL1690	
C		VRFL1700	
C		VRFL1710	
C		VRFL1720	
C	END	VRFL1730	
C		-BNDS0010	
C		***** BNDS0020	
C		PROPOSED 8 OCT 76	-BNDS0030
C		-BNDS0040	
CF	BNDRYS	-BNDS0050	
CE	MULTIPLE BOUNDARY SOURCE DATA	-BNDS0060	
C		-BNDS0070	
C		***** BNDS0080	
C		BNDS0090	
CD	ORDER OF GROUPS IS BY DECREASING ENERGY	BNDS0100	
CD	I IS THE FIRST-DIMENSION INDEX	BNDS0110	

CD	J IS THE SECOND-DIMENSION INDEX		BNDS0120
CD	JM=1 FOR 1-DIMENSIONAL GEOMETRY		BNDS0130
CD	NINTSR=NJNTR=1 FOR EXTERNAL BOUNDARY DATA,		BNDS0140
CD	AND Z(1)=R(1)=0 IN THAT CASE		BNDS0150
C			BNDS0160
C			BNDS0170
CS	FILE STRUCTURE		-BNDS0180
CS			-BNDS0190
CS	RECORD TYPE	PRESENT IF	-BNDS0200
CS	-----	-----	-BNDS0210
CS	FILE IDENTIFICATION	ALWAYS	-BNDS0220
CS	FILE LABEL	ALWAYS	-BNDS0230
CS	FILE CONTROL	ALWAYS	-BNDS0240
CS	MESH DESCRIPTION	ALWAYS	-BNDS0250
CS			-BNDS0260
CS	***** (REPEAT OVER ALL GROUPS)		-BNDS0270
CS	* I-BOUNDARY DIRECTIONAL SOURCE	NINTSR.GT.0	-BNDS0280
CS	* J-BOUNDARY DIRECTIONAL SOURCE	NJNTR.GT.0	-BNDS0290
CS	*****		-BNDS0300
C			-BNDS0310
C			BNDS0320
C			BNDS0330
C			BNDS0340
C			BNDS0350
CR	FILE IDENTIFICATION		-BNDS0360
C			-BNDS0370
CL	HNAME,(HUSE(I),I=1,2),IVERS		-BNDS0380
C			-BNDS0390
CW	1+3*MULT=NUMBER OF WORDS		-BNDS0400
C			-BNDS0410
CD	HNAME HOLLERITH FILE NAME - BNDRYS - (A6)		-BNDS0420
CD	HUSE(I) HOLLERITH USER IDENTIFICATION - (A6)		-BNDS0430
CD	IVERS FILE VERSION NUMBER		-BNDS0440
CD	MULT DOUBLE PRECISION PARAMETER		-BNDS0450
CD	1- A6 WORD IS SINGLE WORD		-BNDS0460
CD	2- A6 WORD IS DOUBLE PRECISION WORD		-BNDS0470
C			-BNDS0480
C			BNDS0490
C			BNDS0500
C			BNDS0510
C			BNDS0520
CR	FILE LABEL		-BNDS0530
C			-BNDS0540
CL	DATE,USER,CHARGE,CASE,TIME,(TITL(I),I=1,12)		-BNDS0550
C			-BNDS0560
CW	17*MULT=NUMBER OF WORDS		-BNDS0570
C			-BNDS0580
CD	DATE AS PROVIDED BY TIMER OPTION 4 - (A6)		-BNDS0590
CD	USER AS PROVIDED BY TIMER OPTION 5 - (A6)		-BNDS0600
CD	CRARGE AS PROVIDED BY TIMER OPTION 6 - (A6)		-BNDS0610
CD	CASE AS PROVIDED BY TIMER OPTION 7 - (A6)		-BNDS0620
CD	TIME AS PROVIDED BY TIMER OPTION 8 - (A6)		-BNDS0630
CD	TITL(I) TITLE PROVIDED BY USER (A6)		-BNDS0640

C		-BNDS0650
C		BNDS0660
C		BNDS0670
C		BNDS0680
C		BNDS0690
CR	FILE CONTROL	-BNDS0700
C		-BNDS0710
CL	IGM,JM,IMA,MMA,NINTSR,NJNTSR,(IDUM(I),I=1,19)	-BNDS0720
C		-BNDS0730
CW	25=NUMBER OF WORDS	-BNDS0740
C		-BNDS0750
CD	IGM NUMBER OF ENERGY GROUPS	-BNDS0760
CD	JM NUMBER OF SECOND-DIMENSION (J) INTERVALS	-BNDS0770
CD	IMA NUMBER OF FIRST-DIMENSION INTERVALS	-BNDS0780
CD	MMA NUMBER OF BOUNDARY DIRECTIONS	-BNDS0790
CD	NINTSR NUMBER OF I-BOUNDARY SOURCES	-BNDS0800
CD	NJNTSR NUMBER OF J-BOUNDARY SOURCES	-BNDS0810
CD	IDUM(I) ARRAY SET TO 0	-BNDS0820
C		-BNDS0830
C		BNDS0840
C		BNDS0850
C		BNDS0860
C		BNDS0870
CR	MESH DESCRIPTION	-BNDS0880
C		-BNDS0890
CL	(Z(J),J=1,NJNTSR),(R(I),I=1,NINTSR)	-BNDS0900
C		-BNDS0910
CW	JM+IMA=NUMBER OF WORDS	-BNDS0920
C		-BNDS0930
CD	Z(J) POSITION FROM WHICH J-BOUNDARY SOURCES TAKEN	-BNDS0940
CD	R(I) POSITION FROM WHICH I-BOUNDARY SOURCES TAKEN	-BNDS0950
C		-BNDS0960
C		BNDS0970
C		BNDS0980
C		BNDS0990
C		BNDS1000
CR	I-BOUNDARY DIRECTIONAL SOURCES	-BNDS1010
C		-BNDS1020
CL	((BIJ(M,J,N),M=1,MMA),J=1,JM),N=1,NINTSR)	-BNDS1030
C		-BNDS1040
CW	MMA*JM*NINTSR=NUMBER OF WORDS	-BNDS1050
C		-BNDS1060
CD	BIJ(M,J,N) SOURCE IN DIRECTION M, INTERVAL J, SET N	-BNDS1070
C		-BNDS1080
C		BNDS1090
C		BNDS1100
C		BNDS1110
C		BNDS1120
CR	J-BOUNDARY DIRECTIONAL SOURCES	-BNDS1130
C		-BNDS1140
CL	((BJI(M,I,N),M=1,MMA),I=1,IMA),N=1,NJNTSR)	-BNDS1150
C		-BNDS1160
CW	MMA*IMA*NJNTSR=NUMBER OF WORDS	-BNDS1170

C		-BNDS1180
CD	BJI(M,I,N) SOURCE IN DIRECTION M, INTERVAL I, SET N	-BNDS1190
C		-BNDS1200
C	-----	BNDS1210
C		BNDS1220
C		BNDS1230
C		BNDS1240
C		BNDS1250
C	END	BNDS1260

NOTE: This is only the cross section portion of the ORDOSW file.

C	-----
C	
CR	PRINCIPAL CROSS SECTION DESCRIPTION
C	
CL	(PCSD(IH),IH=1,IHT)
C	
CW	NUMBER OF WORDS = MULT*IHT
C	
CD	PCSD(IH) PRINCIPAL CROSS SECTION LABELS - (A6)
C	
C	-----

C	-----
C	
CR	NUCLIDE IDENTIFICATION
C	
CL	(NUC(MT),MT=1,MTM)
C	
CW	NUMBER OF WORDS = MULT*MTM
C	
CD	NUC(MT) NUCLIDE LABELS - (A6)
C	
C	-----

C	-----
C	
CR	CROSS SECTION DATA
C	
CL	((SIG(IH,MT),IH=1,IHP),MT=1,MTM)
C	
CW	NUMBER OF WORDS = IHP*MTM
C	
CD	SIG(IH,MT) CROSS SECTION DATA BY TABLE POSITION, THEN BY
CD	NUCLIDE. TABLE POSITIONS CONTAIN --
CD	1 TO IHT-5 ARBITRARY DATA, SPECIFIED BY USER, OR ABSENT
CD	IHT-4 FISSION YIELD FRACTION (RECOMMENDED)
CD	IHT-3 FISSION CROSS SECTION (RECOMMENDED)
CD	IHT-2 ABSORPTION CROSS SECTION
CD	IHT-1 NEUTRON PRODUCTION CROSS SECTION

```

CD          IHT-0  TOTAL CROSS SECTION
CD          IHT+1  UPSCATTER FROM GROUP IG+(IHS-1-IHT) TO IG
CD          .....
CD          .....
CD          IHS-1  UPSCATTER FROM GROUP IG+1 TO IG
CD          IHS    SELF SCATTER FOR GROUP IG
CD          IHT+1  DOWNSCATTER FROM GROUP IG-1 TO IG
CD          .....
CD          .....
CD          IHM    DOWNSCATTER FROM GROUP IG+IHS-IHM TO IG
CD          IHM+1  TOTAL SCATTER FROM GROUP G TO ALL GROUPS
CD                   (PRESENT ONLY IF IHS IS GREATER THAN IHT+1)
CD
CD          IHS MAY BE IHT+1 IF UPSCATTER IS ABSENT.
CD          TRANSFERS FROM GROUPS LESS THAN 1 OR GREATER
CD                   THAN IGM ARE ZERO. POSITIONS LESS THAN OR
CD                   EQUAL TO IHT ARE ZERO FOR PL COMPONENTS
CD                   OTHER THAN THE 0TH.
CD          EACH COMPONENT OF A PL SET IS TREATED AS A
CD                   SEPERATE NUCLIDE.  THUS, M SETS WOULD
CD                   COMPRISE M*NQUAD+M NUCLIDES
CD          IHP    EQUALS IHM UNLESS IHS.GT.IHT+1, THEN IHM+1
C
C

```

5.7 LOGICAL UNIT REQUIREMENTS

5.7.1 Input and Output Data Files

The specifications of the user input and output data files are shown below. The GIP file is defined exactly as the records labeled "CROSS SECTION DATA" in the ORDOSW file, and has no other record types. The "DOT III Angular Fluence Tape" is defined in the DOT III User's Manual,¹² and is simulated by DORT as accurately as possible. An alternate format is used when the albedo generation option is used.

The correspondence of file type to use in the code is:

SYMBOL	FILE TYPE	USE
NTFLX	VARFLM	Fluence and moment input
NTFOG	VARFLM	Fluence and moment output
NTSIG	ORDOSW or GIP	Cross section input
NTBSI	BNDRYS	External boundary source input
NTDSI	VARSOR	Distributed source moment input
NTFCI	VARSOR	First collision source input
NTIBI	BNDRYS	Internal boundary source input
NTIBO	BNDRYS	Internal boundary fluence output
NTDIR	DOT III "Angular Fluence Tape"	Directional fluence output
NTDSO	VARSOR	Directional fluence moment output

Logical units 5 and 6 are also used by DORT as the standard card image input and printed output units respectively.

5.7.2 Scratch Data Sets

The following lists the scratch data sets, the length of each record, and the number of records:

Table 5-7. DORT Scratch Data Set Record Information

Logical Unit Number	Logical Unit Symbol	Description	Record Length (1 record)	Number of Records (nrec)	Required If:
81		Scalar Fluence Scratch	IMA*JM	IGM	Not used at this time
82	NDSIG	Cross-Section Scratch	IHM*MTM	IGM	Always
83	NDBTL	Balance Table Scratch	NREG*10+IZM+8	IGM	IRED ≠ 0
84	NDBSI	Boundary Source Scratch	(IMA+JM)*MMA (IMA*NJNTSR +JM*NINTSR)*MMA +ICMJCM+NREG	IGM	NTBSI > 0 (NINTSR > 0 or NJNTSR > 0)
91	NDFLX	Fluence Scratch	IMA*LM*JBLK1	NJBLK*IGM	NJBLK > 0
92	NDSOR	Total Source Scratch	IMA*LM*JBLK1	NJBLK	NJBLK > 0
93	NDSIN	IN-Source Scratch	IMA*LM*JBLK1	NJBLK	NJBLK > 0
94	NDBFX	Boundary Fluence Scratch	(IMA+JM)*MMA	IGM	Always
95	NDFIJ	Scalar Fluence Scratch	IMA*JM	IGM	Always

NOTE: The symbol "#" denotes the word "number."

- JBLK1 = #J levels per J block, $1 \leq JBLK1 \leq JM$
- NJBLK = #J blocks, $MINBLK \leq NJBLK \leq MAXBLK$ (NJBLK = 0 if fluences are stored in working memory)
- LM = maximum number of moments (including 0th) in spherical harmonic expansion, $LM = 1 + \lceil ISCT \rceil * ((\lceil ISCT \rceil + 3)) / 2$
- NREG = number of edit regions
- IZM = number of material zones

For unit 84, if $NTBSI > 0$ and $NINTSR > 0$, for example, this file will have IGM + IGM records.

The number of J blocks, NJBLK, is controlled by input data. When default values of MINBLK and MAXBLK are used, the code will attempt to hold all fluence and source data in fast memory, i.e., NJBLK = 0. Failing in this, it will attempt to allocate space for the entire mesh to be held as 1 block in the user-buffer area, i.e., NJBLK = 1. Failing in this, the space mesh is broken into as many blocks as required. NJBLK is restricted to limits specified by MINBLK and MAXBLK.

5.8 DETAILS OF DORT JOB REQUIREMENTS

5.8.1 CPU Time Usage

A reasonably accurate time limit should be calculated and entered as TMAX for all problems which run more than a few minutes. The maximum time given to the operator or operating system should be somewhat larger than TMAX. This allows DORT to complete its I/O and data summaries if the time is exceeded during the iteration phase. The CPU time required, C, can be estimated by the following formula:

$$C = A + \left[\frac{FW}{FR} \right] * \frac{150}{SF}$$

$$FW = \sum_P \sum_G \sum_F \sum_J \sum_I MM$$

where

- FW = fluence work
- MM = number of directions
- I,J = space-mesh indices
- F = inner (fluence) iteration index
- G = energy group
- P = outer (source) iteration index
- FR = fluence rate on the reference machine
- SF = the speed factor for the machine used
- A = overhead (I/O, problem setup, and summary activities)

The value of FR depends somewhat upon the class of problem solved. FR is about 1.0 million fluences per minute for large P_3 problems using the weighted difference model. The linear-zero model sometimes runs a bit faster, and a P_0 calculation runs as much as 40% faster.

5.8.2 Problem Printed Output

Each DORT job starts with a notice of the date and time, followed by a record of the particular version of the code being used, and messages from the programmer informing the user of warnings or special features. The title supplied by the user as input data is next. As each array of input data is read, a notice of the array number and length is made.

The first array edits are of the 61\$ (logical unit assignments), 62\$ (integer control parameters), and 63* (real control parameters). The initial allocation of fast memory and (CDC only) slow memory are listed, followed by primary dimension-setting arrays, mixing table information, material assignment, importance, fission spectrum, and search fractions.

The next section is a set of data describing the directional remesh process, $MM < 0$. These tables are largely for the benefit of programmers in diagnosing troublesome problems. The

quadrature set assignment by super-zone is an input array. The transition table indicates which transition set governs the transition from the row M-Set to the column M-Set.

The unpacking arrays follow; one for each M-Set. These integers simply indicate places in a full IMMI-direction array where data corresponding to a smaller M-Set can be kept without being overwritten.

The actual transition sets are given next. Each set consists of two columns of integers. Each position in each column corresponds to a direction in the corresponding M-Set. The remeshing routine decodes the integers in order to determine how to construct fluences in a new M-Set which correspond to a previous M-Set. Since the tables are given in unpacked form, as needed by the code, unused positions are filled with "-1."

The direction sets are listed, together with "BETA" (the μ -flow coupling term), μ -mates, τ -mates, and level-mates. The μ -mate of direction (μ, τ) is direction ($-\mu, \tau$). The τ -mate is direction ($\mu, -\tau$). The level-mate is the first direction in the η -level containing the τ -mate. Unsymmetric direction sets may not possess all of these mates. If a mate required for a boundary condition can not be found, an error flag is set.

The values of the coupling set C_{mj} are edited, followed by the J fine-mesh and I fine-mesh sets. The real values of super-mesh and coarse-mesh boundaries are interpreted into integer assignment tables edited at this point. The total size of these meshes, number of super groups, and of edit zones are given, together with related input array edits.

Maps of the zone and material assignments are given, together with the integral values of the unnormalized input sources by group, with the total as group IGM + 1. A table of storage usage gives data useful to the programmer, as well as items needed in adjusting the input data, as discussed elsewhere.

A source iteration monitor line ends each source iteration, and initial values are indicated in an "iteration 0" line. Entries on this line are:

ITN	Source iteration number
FLX	Number of fluence iterations completed for this source iteration
CUM	Cumulative number of source iterations
CNV	$10 * IXX + IFCONV$
	IXX as noted earlier in Section 5.5.7
	IFCONV = 0 Source iterations are to continue
	= 1 One more iteration is required
	= 2 Iterations are to stop at once
	= 3,4,5 As in 0,1,2, but configuration recalculation is required
ACC	$100 * ISR + 10 * NEWCFG + IACX$
	ISR = 0 No eigenvalue extrapolation was performed
	= 1 Linear eigenvalue extrapolation was performed
	= 2 Nonlinear eigenvalue extrapolation was performed (2-point)
	= 3 Nonlinear eigenvalue extrapolation was performed (3-point)
	NEWCFG = 0 Old configuration is to be used

	= 3	New configuration is to be used
IACX	= 0	Extrapolation of fluences was bypassed
	= 1	Extrapolation of fluences was performed
IFX		I-position of maximum fluence change between source iterations
JFX		J-position of maximum fluence change between source iterations
GFX		Group of maximum fluence change between source iterations
EV		Eigenvalue edit
K		K-effective edit
K-CNV		K convergence, ϵ^k
FSN-CNV		Fission convergence, ϵ^D
FLX-CNV		Fluence convergence, ϵ^F
GRP-CNV		Group-convergence, ϵ^G
SRH-CNV		Search convergence, ϵ^S
UPS-CNV		Upscatter convergence, ϵ^U
EXTRAP		Fission extrapolation factor
TIME		Time iteration was completed

The interpretations of EV and K are:

KTYPE	EV edit	Kedit
0	$\Sigma V \nu \sigma^F \Phi$ ($\Sigma \chi V \Phi$ for adjoint)	$\Sigma \chi V \nu \sigma^F \Phi$
1	"	"
2,3,4	search eigenvalue	"

If the χ 's do not sum to 1, K will differ from EV in a K-calculation by a ratio equal to the sum of χ . Even if χ is precisely normalized to 1 by selecting the input value NOFIS = 0, EV and K may be slightly different due to roundoff.

As each fluence iteration is performed on each energy group, another monitor line is printed. It contains:

GRP	Energy group number
ITN	Fluence iteration number
IMFD	I-position of maximum fluence change
JMFD	J-position of maximum fluence change

MX FX DV	Relative maximum fluence change
MX DV FX	Most rapidly changing fluence value
REBL	Number of rebalance iterations - a negative value means the rebalance factors were not used
REBL ERR	Maximum relative change in rebalance factors in the last iteration
MAX REBL	Largest amount by which any factor deviates from 1
GRP REBL	Amount by which groupwise rebalance factor (whether used or not) deviates from 1
VOLM ERR	Volumetric convergence, discussed earlier, except that absolute value is not used
KEY FLUX	Value of single key fluence requested by input data, after acceleration
NEGFIX	Maximum fraction of negative total source at any position, if NEGFIX = 1
SOURCE	Total of all sources into a group, including external boundary sources
TIME	The time at which group iteration is begun is given at the end of the heading column. Arbitrary diagnostic information is given below the time indication.

Iterations performed using diffusion theory will provide only the first six items. Edits of key fluence values and/or convergence by region may follow each iteration or the set of iterations for each group, according to the options chosen. The interpretation of fluence convergence also depends on options chosen, as discussed earlier.

If a dimension search has been performed, the final dimensions are edited. Fluence and fission source edits follow, together with activity edits by interval and region.

System balance tables follow by group and region. Group and system totals are given as IGM + 1 and NREG + 1. The columns are largely self-explanatory. One may note that an external boundary source is external to the system, and is, therefore, included in these tables as a flow at the corresponding boundary. Flow and leakage signs are such that a positive value is outward from the region. Fission source is source used to calculate the fluence, while fission rate is the fission which results from the fluences. They will tend to differ by K times the sum over g of the χ_g in a K-calculation. Inscatter and outscatter are scatter to and from the energy group. They should, in general, be equal in neutron-only problems. This will not be true in coupled n- γ problems. The outscatter is calculated from:

$$\text{outscatter} = \text{collisions} - \text{selfscatter} - \text{absorption}$$

and will be valid only if the absorption cross section meets the balance condition.

The edit of selfscatter per collision is valuable in judging the difficulty of converging fluences for a given energy group. In general, values larger than 0.85 may give the PCR fluence acceleration difficulty. The average density factor is collision weighted.

The value of OUT/IN approaches unity for well-converged problems. It is:

$$\frac{\text{Collision} + \text{DB}^2 \text{ Loss} + \text{Positive Boundary Outflow}}{\text{Fixed Source} + \text{Fission Source} + \text{Inscatter} + \text{Negative Boundary Outflow}}$$

Sources, flows, leakage, and OUT/IN may not be correct in the case of groups in which no iterations are performed.

The fluences, as well as balance table information which depend on them, are not divided by K_{eff} , and will, in general, tend to vary according to K_{eff} . Some users speak of this condition as "fluences normalized according to K."

Each problem ends with a summary of clock and CPU time binned according to major sections of the code. Depending on configuration, some bins may not have labels. These are for diagnostic information only.

Some output may not appear in certain problems, depending on the options chosen. The use of NTPRT can alter the order of printing on some systems, or can transfer some output items to alternate output devices.

5.9 REFERENCES

1. W. A. Rhoades and R. L. Childs, "The DORT Two-Dimensional Discrete Ordinates Transport Code," *Nuclear Science & Engineering* **99**, 1, pp. 88-89, (May 1988).
2. K. D. Lathrop and F. W. Brinkley, "TWOTRAN-II, An Interfaced, Exportable Version of the TWOTRAN Code for Two-Dimensional Transport," LA-4848-MS, (July 1973).
3. F. R. Mynatt, et al., "Development of Two-Dimensional Discrete Ordinates Transport Theory for Radiation Shielding," CTC-INF-952, (August 1969).
4. B. G. Carlson and K. D. Lathrop, "Transport-Theory - The Method of Discrete Ordinates," LA-3251-MS, (Rev. October 1965).
5. B. G. Carlson, "Solution of the Transport Equation by S_n Approximations," LA-1599, (October 1953).
6. B. G. Carlson and G. I. Bell, "Solution of the Transport Equation by the S_n Method," *Proc. U.N. Intern. Conf. Peaceful Uses At. Energy*, 2nd, Geneva P/2386, (1958).

7. B. Carlson, C. Lee, and J. Worlton, "The DSN and TDC Neutron Transport Codes," LAMS-2346, (February 1960).
8. B. Davison, *Neutron Transport Theory*, Oxford University Press, 174 (1957).
9. S. Chandrasekhar, *Radiative Transfer*, Oxford University Press, (1950).
10. G. C. Wick, "Uber Ebene Diffusionsprobleme," *Z. Phys.*, **121**, 702 (1943).
11. W. A. Rhoades, D. B. Simpson, R. L. Childs, and W. W. Engle, Jr., "The DOT-IV Two-Dimensional Discrete Ordinates Transport Code with Space-Dependent Mesh and Quadrature," ORNL/TM-6529, Oak Ridge National Laboratory, (January 1979).
12. W. A. Rhoades and F. R. Mynatt, "The DOT III Two-Dimensional Discrete Ordinates Transport Code," ORNL-TM-4280, Oak Ridge National Laboratory, (September 1973).
13. K. D. Lathrop, "TWOTRAN - A FORTRAN Program for Two-Dimensional Transport," GA-8747, (July 1968).
14. W. A. Rhoades and R. L. Childs, "An Updated Version of the DOT 4 One- and Two-Dimensional Neutron/Photon Transport Code," ORNL-5851, Oak Ridge National Laboratory, (January 1979).
15. J. O. Johnson, J. D. Drischler, and J. M. Barnes, "Analysis of the Fall-1989 Two-Meter Box Test Bed Experiments Performed at the Army Pulse Radiation Facility (APRF)," ORNL/TM-11777, Oak Ridge National Laboratory, (May 1991).
16. R. T. Santoro et al., "DNA Radiation Environments Program Fall 1989 2-Meter Box Experiments and Analysis," ORNL/TM-11840, Oak Ridge National Laboratory, (May 1991).

5.10 SAMPLE PROBLEM

The sample problem demonstrates the calculation of the air-over-ground environment for the two-meter box experiments.^{15, 16} Figure 5-2 shows a simple diagram of the geometry modeled in the DORT input. (It should be noted again that the DORT and GRTUNCL geometry models are equivalent for the analysis performed in MASH.) A complete listing of the input cards for the sample problem is given in Figure 5-3, and some selected output is shown in Figure 5-4.

The DORT input stream shown in Figure 5-3 includes a tremendous amount of control parameters in the first data block (61\$, 62\$, and 63* arrays). The user will note that most of these parameters are system or code defaults. Consequently, only those parameters of particular importance to the sample problem will be emphasized. The 61\$ array parameters indicate the input and output files utilized in this calculation. It should be noted that this particular DORT case utilized an input fluence guess (NTFLX). This was because this calculation was restarted from a previous one. If no input fluence guess is used, this unit

would be zero. The scalar fluences were written on unit 21 (NTFOG), the cross sections (from GIP) were input on unit 4 (NTSIG), the directional fluences were written on unit 22 (NTDIR), and the distributed source was read in from unit 23 (NTDSI). The distributed source represents the output file from the GRTUNCL sample problem discussed in Section 3.0, and the cross sections are from the GIP sample problem discussed in Section 2.0. The user should compare the parameters used in these two problems with the ones used in the DORT case to see how the different programs interact.

In viewing Figure 5-3, the input illustrates; 8 material zones (IZM), 66 radial intervals (IM), 98 axial intervals (JM), 69 energy groups (IGM), a cross-section table length (IHM) of 72, no upscatter (IHT=3, and IHS=4), and a mixing table length (MS) of 0. 54 materials (9 different mixtures, each with a P_0 through P_5 component) were read in from a GIP tape (MTP=54). The total number of materials (MTM) was 54, and no print was requested for the printed output (ICSPRT=1). The problem included; 240 directions in the quadrature set (MM=240), RZ geometry (INGEOM=1), group dependent fluence iteration (IFXMI=-20), theta weighted fluence extrapolation model (MODE=4), directional fluences saved (IDIRF=2), and 20 key fluences printed at the group convergence (NKEYYFX=-20). The group dependent fluence iteration scheme is given in the 24\$ array. The axial and radial intervals for the key fluences are given in the 29\$ and 30\$ arrays. The first directional fluence axial interval saved was 13 (JDIRF), and the last interval saved was 25 (JDIRL). The user should note these two parameters match parameters used in the VISTA sample problem given in the Section 5.0. A zone dependent convergence criterion was chosen (IEPSBZ=11) and the convergence parameters for each material zone are in the 24* array. This parameter is useful when performing a large air-over-ground problem, and the user does not want to converge the entire mesh to a fine convergence criteria when only a portion of the mesh is really important. In the sample problem, there was a tight convergence criteria used at the locations of importance in the mesh, a less strict criteria used around these areas, and then a minimal criteria used for the areas of least importance. The zone numbers by interval are entered in the 8\$ array, and the material by zone is entered in the 9\$ array. These arrays along with the axial intervals (2* array) and radial intervals (4* array) match the same arrays in the GRTUNCL sample problem, with the exception that GRTUNCL requires a negative entry in the 9\$ array for to indicate the higher order of cross section scattering.

A full description of the DORT printed output is given in Section 5.8.2 above. The user should consult this section for viewing the sample problem output. The selected DORT output shown in Figure 5-4 first illustrates the input parameters read in the first data block, followed by the initial memory requirements to run this particular DORT case. The output then produces the directional remesh arrays, followed by indicators that the second, third, and fourth data blocks have been successfully read. A listing of some of the parameters in the third data block (10\$, 11\$, 12*, 9\$, 24*, etc.) are next in tabular form. This table is followed by the quadrature information and Legendre coefficients for scattering integrals. This information is followed by the fine mesh sets, the zone number and material number by interval maps. This table is followed by a listing of storage information useful to the programmer. Next, the source iteration information followed by the key fluence array is printed for each group. This is an important table in that the problem convergence is illustrated here. Finally, the system balance tables, depending on the option chosen, (IRED) are printed. In this sample problem, a balance table was chosen for each zone in the problem along with a system table. The last line printed on the sample problem output is a summary of clock and CPU time used.

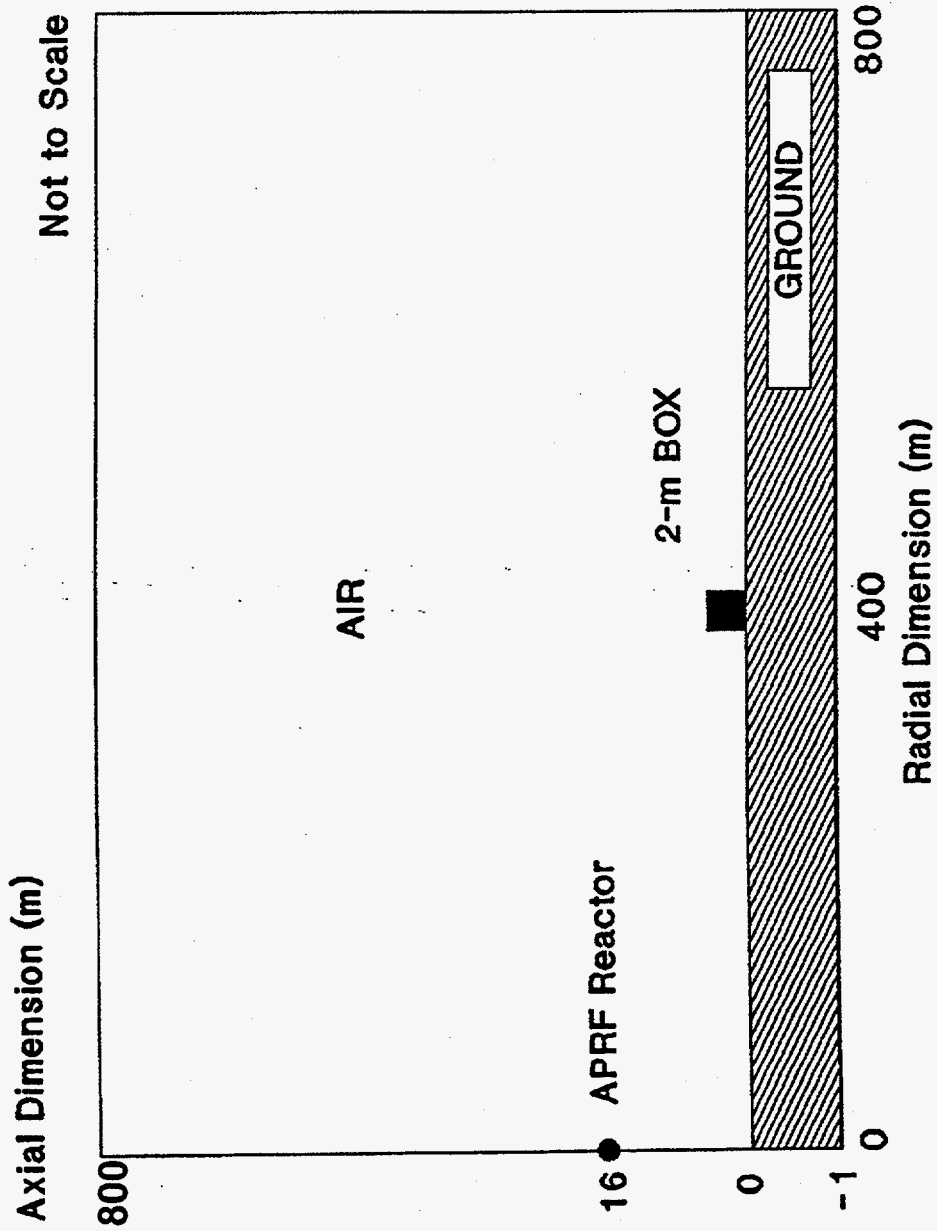


Figure 5-2. Schematic Diagram of the Air-Over-Ground Geometry Model Used in the DORT Analysis.

' dort - aprf aog using saic 1989 angle-energy leakage source, mm = 240
 ' 16.143m source height, simple topography out to 400m test site
 ' 34% ground moisture, 10/24/89(a) air parameters

```
61$$ 0 21 4 0 23 / ntflx,ntfog,ntsig,ntbsi,ntdsi
      0 0 0 0 22 / ntfci,ntibi,ntibo,ntnpr,ntdir
      0 e / ntdso
```

```
62$$ 0 5 8 66 98 / iadj,isctm,izm,im,jm
      69 3 4 72 0 / igm,iht,ihs,ihm,mixl
      0 54 54 0 240 / mcr,mtp,mtm,idfac,mm
      1 1 0 0 0 / ingeom,ibl,ibr,ibb,ibt
      1 -20 0 4 0 / isrmx,ifxmi,ifxmf,mode,ktype
      2 0 0 0 0 / iacc,kalf,igtype,inpfxm,inpsrm
      0 0 0 0 0 / njntsr,nintsr,njntfx,nintfx,iact
      8 0 1 1 2 / ired,ipdb2,ifxpvt,icsprt,idirf
      13 25 120 11 1 / jdirf,jdirl,nbuf,iepsbz,minblk
      1 1 1 1 1 / maxblk,isbt,msbt,msdm,ibfsc1
      4 50 2 0 0 / intsc1,itmscl,nofis,ifdb2z,iswp
      19 28 0 0 0 / keyjn,keyin,nsigtp,norpos,normal
      0 2 1000 0 -20 / mstmax,negfix,locobj,lcmobj,nkeyfx
      4 46 0 0 0 / ncnadin,neut,itally,isp1,isp2
      e
```

```
63** 240 0.0 1-4 1-2 0.0 / tmax,xnf,eps,epp,epv
      1-3 1.0 0.2 1.5 10.0 /epf,ekobj,evth,evchm,evmax
      1.0 1.0 -1.0 0.3 10.0 /evkmx,evi,devdki,evdelk,sormin
      1.0 1-4 1-2 0.3 -1.5 /conacc,conscl,coneps,wsoloi,wsolii
      1.5 0.6 0.0 1-60 0.0 /wsolcn,orf,fsnacc,flxmin,smooth
      1-2 0.2 0.9 / epo,extrcv,theta
      e t
      t
```

```
81** / wts mm240
      0 2r102900-8 0 2r307825-8 0 2r510200-8 0 2r708425-8 0
      2r901350-8 0 563869-8 316131-8 n2 0 641385-8 359590-8 n2 0
      714976-8 400849-8 n2 0 784547-8 439853-8 n2 0 857529-8
      480771-8 n2 0 642875-8 293289-8 479164-8 n3 0 681415-8
      310872-8 507890-8 n3 0 716550-8 326901-8 534077-8 n3 0
      745915-8 340298-8 555965-8 n3 0 775565-8 353825-8 578064-8
      n3 0 489468-8 386282-8 513536-8 364389-8 n4 0 500102-8
      394674-8 524693-8 372306-8 n4 0 508580-8 401365-8 533587-8
      378617-8 n4 0 515474-8 406806-8 540820-8 383750-8 n4 0
      517107-8 408094-8 542534-8 384965-8 n4 q120
```

Figure 5-3. Sample DORT Input for the Two-Meter Box Air-Over-Ground Analysis.

82** / mus mm240

-641230-7 -421582-7 m1 -142963-6 -939923-7 m1 -229252-6
-150724-6 m1 -315291-6 -207291-6 m1 -399349-6 -262555-6 m1
-472796-6 -411087-6 -143488-6 m2 -537046-6 -466952-6
-162988-6 m2 -598374-6 -520275-6 -181600-6 m2 -656401-6
-570729-6 -199211-6 m2 -711034-6 -618231-6 -215791-6 m2
-761567-6 -713133-6 -470428-6 -164201-6 m3 -807567-6
-756207-6 -498843-6 -174119-6 m3 -849108-6 -795106-6
-524503-6 -183075-6 m3 -885925-6 -829582-6 -547246-6
-191013-6 m3 -917890-6 -859514-6 -566991-6 -197905-6 m3
-944812-6 -922954-6 -765692-6 -505099-6 -176303-6 m4
-966490-6 -944130-6 -783260-6 -516688-6 -180348-6 m4
-982847-6 -960108-6 -796516-6 -525433-6 -183400-6 m4
-993815-6 -970823-6 -805405-6 -531297-6 -185447-6 m4
-999313-6 -976194-6 -809860-6 -534236-6 -186473-6 m4 ql20

83** / etas mm240

3r-.997942 3r-.989728 3r-.973367 3r-.948995 3r-.916799
5r-.881172 5r-.843553 5r-.801217 5r-.754412 5r-.703158
7r-.648086 7r-.589776 7r-.528222 7r-.463828 7r-.396835
9r-.327613 9r-.256704 9r-.184425 9r-.111045 9r-.037054 g120

84\$\$ 1 2 3 4 5 6 7 8 / reg nos by zone

t
1** f0 / fission spectrum

2** /axii (jm+1)

-80 -75 -70 -65 -60 -55 -50 -45 -40 -35 -30 -25 -20 -15 -10 -5 -2.5
-1 0 50 150 250 489 749 949 1102 1220 1311 1381 1435 1476 1508 1532
1551 1566 1577 1585 1592 1597 1601 1604 1607 1608.5 1610 1614.3 1619
1620.5 1622 1624 1627 1631 1636 1643 1651 1662 1677 1696 1720 1752
1793 1847 1917 2008 2126 2279 2479 2739 3076 3514 4085 4826 5789 7042
8670 10787 13000 16000 19000 22000 25000 28000 31000 34000 37000 40000
43000 46000 49000 52000 55000 58000 61000 64000 67000 70000 73000
76000 78000 80000

4** /radii (im+1)

0 4.6 6 7.8 10 13 17 22 29 37 48 63 82 106 138 179 233 303 394 512 665
865 1125 1462 1900 2471 3212 4175 5428 7056 9000 11000 13000 15000
16500 17500 19000 21000 23000 25000 27000 28500 29500 30500 31500
33000 35000 37000 38500 39500 40500 41500 43000 45000 47000 49000
51000 54000 57000 60000 63000 66000 69000 72000 75000 78000 80000

5** f1 / energy group boundaries

Figure 5-3. (continued)

8\$\$ / zone numbers by interval
' zones 1, 2, & 3-aprf ground, 4 & 5-borated concrete, 6, 7, & 8-air
66r1 8q66 /j-ints 1-9
19r5 47r1 2q66 /j-ints 10-12
19r4 3r3 8r1 3r3 3r2 5r3 3r2 4r3 3r2 3 14r1 5q66 /j-ints 13-18
33r7 3r6 5r7 3r6 4r7 3r6 7 14r8 3q66 /j-ints 19-22
52r7 14r8 3q66 /j-ints 23-26
66r8 71q66 /j-ints 27-98

9\$\$ 3r1 2r7 3r13 / mat by zone

24** 1.-10 1.0 1.-1 1.-2 1.-10 1.0 1.-1 1.-10 / importance by zone

28\$\$ 35r8 11r25 23r8 / inners by grp

29\$\$ 13r19 3r20 3r21 22 / key flx j-pos's

30\$\$ 31 34 35 36 39 42 43 44 49 50 51
53 56 35 43 50 1q3 50 / key flx i-pos's
t

Figure 5-3. (continued)

```

* * * execution began on 11/08/96 (313) at time 15:24:39
*** workstation configuration compiled 11/08/96 14:06:03 user=jdd process= 14404 case=
*** dort 3.2 31 oct 96 ornl
this is an experimental version. do not use it for ga work.
information files distributed with the source material must be read by all users.
the documents for this code are ornl 5851, updated by the information files supplied with the source material.
new definitions and/or defaults for certain items are indicated in the parameter edit.
one should especially note:
.mode 3 is traditional zero-weighted difference.
.mode 4 is theta-weighted difference; gives zero-weighted results when theta=0.
.both 3&4 use best routines for the computer used.
.mode 2 is scalar theta-weighted on all computers.
.mode 5 is vector theta-weighted on all computers.

```

ntdso output is now in varsor2d format. ntdso output no longer contains the volume element.

```

the db2z array is by zone, not by region.
key fluxes may now be in any order.
defaults have recently changed for nofis, keyjn, keyin, sormin, wsolcn, conacc, coneps, negfix.
coneps relaxes acceleration convergence in early iterations to reduce cost.
mmesh controls comgeom-like zone description.
lcmobj segments large direct access files for easier allocation and storage.
isctc.gt.0 allows 9$$ to refer to materials, i.e. 1, 2, etc., as in tort. not allowed with mixl.ne.0.

```

for the most difficult deep penetration problems, it may be helpful to double default values of ibfsc1, itm scl, wsolli, & wsolcn, while setting negfix=-1 or 2.

for the most difficult k-eff problems, user may wish to set ifxmi=2 or 4, mode=0, sormin=300., conacc=.1, and wsolcn=-3. for pointwise flux convergence after the last source iteration, e.g., reactor + shield, set ifxmf and epp. for pointwise flux convergence between successive source iterations, e.g., upscatter problems, set epo.

for large cray problems, set locobj to a large value, at least 3,000.

minblk=maxblk=1 may reduce memory charges on some systems.

' dort - aprf aog using saic 1989 angle-energy leakage source, mm = 240

' 16.143m source height, simple topography out to 400m test site

' 34% ground moisture, 10/24/89(a) air parameters

61\$ array 14 entries read

62\$ array 86 entries read

63\$ array 38 entries read

0t

```

61 $ $
ntflx = 0 flux guess input unit if.gt.0
ntfog = 21 flux output unit if.gt.0
ntsig = 4 cross section unit (default=8)
ntbsi = 0 boundary source input unit if.gt.0
ntdsi = 23 distributed source input unit if.gt.0 (must supply scratch if inpsrm.gt.0)
ntfci = 0 reserved (enter 0)
ntibi = 0 internal boundary source input if.gt.0
ntibo = 0 internal boundary flux output if.gt.0
ntnpr = 0 large-scale print unit if.gt.0
ntdir = 22 directional flux output unit if.gt.0
10
ntdso = 0 distributed source output unit if.gt.0
ntsc1 = 0 scalar flux output unit if.gt.0
ntznf = 0 zone flux output unit if.gt.0
62 $ $
ladj = 0 0=forward calculation; 1=adjoint

```

Figure 5-4. Sample DORT Output for the Two-Meter Box Air-Over-Ground Analysis.

```

isctm = 5 maximum order of pl scattering
izm = 8 number of material zones
im = 66 number of radial intervals (negative implies variable mesh is used)
jm = 98 number of axial intervals
jgm = 69 number of energy groups
iht = 3 position of total cross section
ihm = 4 position of self-scatter cross section
mixl = 72 cross section table length per group
10 mixing table length

mmesh = 0 number of material zone bodies (0=no effect)
mtp = 54 number of materials from ntsig (0 implies mtm)
mtm = 54 total number of materials
idfac = 0 0=no density factors; 1=input dens(i,j)
nm = 240 maximum number of directions in quadrature (negative indicates variable quadrature is used)
ngeom = 1 0=x-y geometry; 1=r-z; 2=r-theta; 3=180-360 triangle; 4=60 triangle; 5=90 triangle; 6=120 triangle
ibl = 1 (0=void
ibr = 0 1=reflected
ibb = 0 2=periodic
ibt = 0 3=cylindrical
20

isrnx = 1 source iteration maximum
ifxmi = -20 initial flux iteration maximum per group (if.ne.0) (negative indicates limit in itmbg) (default=1)
ifxmf = 0 final flux iteration maximum per group (if.ne.0) (negative indicates limit in itmbg) (default=20)
mode = 4 0=lin-zero; 1=linear; 2=scalar wtd; 3=0 wtd; 4=theta wtd; 5=vector wtd
ktype = 0 0=fixed source; 1=k search; 2=db2 search; 3=concentration search; 4=dimension search (default=4)
iacc = 2 0=groupwise rebalance; 1=diffusion acceleration; 2=partial current acceleration (default=2)
kalf = 0 0=standard acceleration procedure; 1=alternate
igtpe = 0 0=discrete ordinates; n=theory specified by group for n outers, then finish with discrete ordinates
inpfxm = 0 0=flux guess 0 or on nntfx; 1=fj(i,j) g times; 2=fj(i,j)*fg(g); 3=fi(i)*fj(j)*fg(g)
inpsrm = 0 distributed source input, same as inpfxm (requires ntdsi.gt.0)
30

njntsr = 0 0=no effect; n=interior boundary source at n j-boundaries input from ntibi
nintsr = 0 0=no effect; n=interior boundary source at n i-boundaries input from ntibi
njntfx = 0 0=no effect; n=interior boundary flux at n j-boundaries written on ntibo
nintfx = 0 0=no effect; n=interior boundary flux at n i-boundaries written on ntibo
iact = 0 0=no effect; n=calculate n activities (negative bypasses pointwise activity print)
ired = 8 -1=izm regions, system balances only; 0=no bal; 1=1 region; izm=izm regions (unless iznrg entered)
ipdb2 = 0 0=no effect; 1=punch average db2 value; 2=igm values; 3=igm*nrg values (neg=no balance table print)
ifxprt = 1 0=scalar flux printed; 1=not printed; 2= printed as calc (+10 to delete flux itn print) (default=1)
icsprt = 1 0=cross sections printed; 1=not printed
idifrf = 2 0=directional flux not saved; 1=saved and printed; 2=saved but not printed (default=1)
40

jdirf = 13 first axial interval for directional flux output (0=no effect)
jdirl = 25 last axial interval for directional flux output (0=no effect)
nbuf = 120 no effect
iepsbz = 11 0=no effect; 1=use zone impt convg; 11=use & print final convg; 21=use & print convg every itn
minblk = 1 minimum j-blocking (0=all groups stored in memory if possible; rv=0)
maxblk = 1 maximum j-blocking (0 implies jm)
isbt = 1 i set for boundaries (default=1)
msbt = 1 m set for boundaries (default=1)
msdm = 1 m set for dimensioning (default=1)
ibfscf = 1 no. flux itns before accel (default=1)
50

```

```

intscl = 4 min no. flux acceleration itns (default=4)
itmocl = 50 max no. flux acceleration itns (default=50)
nofis = 2 0-normalized fission; 1=unnormalized; 2=none (default=1)
ifdbz2 = 0 0=no effect; 1=db2 supplied by group, then by region
iswp = 0 type of diffusion theory sweep (rv=4 or 5)
keyjn = 19 j-interval for key flux output (default=1)
keyin = 28 i-interval for key flux output (default=1)
nsigtp = 0 reserved (use 0)
norpos = 0 c.s. position for normalization (0 ignored)
normat = 0 c.s. material for normalization (0 indicates macro in each zone; neg indicates do not apply dens factor)
60
mstmax = 0 maximum number of m-sets (0 implies mstm=jm)
negfix = 2 0=none; 1=full source fixup; 2=initial fixup; -1=economy fixup
locobj = 1000 initial memory allocation, words*1000 (0 implies use default)
lcmobj = 0 file segment size, words*1000 (0 implies unlimited segment length)
nkeyfx = -20 length of key flux array (negative prints array only at group convergence)
ncndin = 4 maximum user condition code (default=4)
neut = 46 last neutron group (default=-1; implies igm)
italy = 0 0: no effect; -1: internal timing analysis
neutac = 0 0: no effect; n=activities over first n groups only
isctc = 0 order of cross section expansion (if .gt.0)
63 **
tmax = 2.40000E+02 maximum cpu time for this prob (0.0=no effect)
xnf = 0.00000E+00 source normalization factor (0.0=no effect)
eps = 1.00000E-04 eigenvalue convergence criterion (default=1.0e-4)
epj = 1.00000E-02 pointwise flux convergence criterion (default=1.0e-3)
epv = 0.00000E+00 volumetric flux convergence criterion
epf = 1.00000E-03 fission convergence criterion (default=1.0e-3)
ekobj = 1.00000E+00 keff sought in b, c, d search; k estimate in k search
evth = 2.00000E-01 keff convergence ratio (default=0.2)
evchm = 1.50000E+00 maximum ev change ratio, each itn (default=1.5)
evmax = 1.00000E+01 maximum ev change ratio, overall (default=10.0)
10
evkmx = 1.00000E+00 maximum valid keff-ekobj (default=1.0)
evi = 1.00000E+00 initial eigenvalue (default=1.0)
devdki = -1.00000E+00 initial eigenvalue slope (default=-1.0)
evdelk = 3.00000E-01 initial eigenvalue increment (default=0.3)
sormin = 1.00000E+01 maximum source iteration acceleration (default=10.0)
conacc = 1.00000E+00 flux acceleration acceptance criterion (default=1.)
consc1 = 1.00000E-04 flux acceleration converg. criterion (default=1.0e-4)
coneps = 1.00000E-02 flux acceleration convergence ratio (default=0.01)
wsolm = 3.00000E-01 reserved (use 0)
wsolli = -1.50000E+00 flux acceleration damping increment (neg: use only as required, default=-1.5)
20
wsolcn = 1.50000E+00 flux acceleration damping constant (neg: use only on first source iteration, default= 1.5)
orf = 6.00000E-01 diffusion theory flux acceleration parameter (default=0.6)
fsnacc = 0.00000E+00 reserved (use 0)
flxmin = 0.00000E+00 minimum flux for convergence tests (default=1.0e-30, 1.0e-60 on tray)
smooth = 0.00000E+00 reserved (use 0)
epo = 1.00000E-02 source iteration flux convergence criterion
extrcv = 2.00000E-01 extrapolation convergence criterion (default=0.2)
theta = 9.00000E-01 theta-weighting parameter (default=0.9)
esp1 = 0.00000E+00 reserved (use 0)
esp2 = 0.00000E+00 reserved (use 0)

```

Figure 5-4. (continued)

```

initial memory objective = 1000000
0t
im by mm by
im set mm set
1 1 1 66
2 1 1 240
3 1 1
4 1 1
5 1 1

81* array 240 entries read
82* array 240 entries read
83* array 240 entries read
84$ array 8 entries read
0t
1* array 69 entries read
2* array 99 entries read
4* array 67 entries read
5* array 71 entries read
zones 1, 2, & 3-aprif ground, 4 & 5-borated concrete, 6, 7, & 8-air
8$ array 6468 entries read
9$ array 8 entries read
24* array 8 entries read
28$ array 69 entries read
29$ array 20 entries read
30$ array 20 entries read
0t
mixture id nuclide id density material id matl/zone err impt chi i srch frac j srch frac
1 1 1.00000E-10 0.00000E+00 0.00000E+00 0.00000E+00
2 1 1.00000E+00 0.00000E+00
3 1 1.00000E-01 0.00000E+00
4 7 1.00000E-02 0.00000E+00
5 7 1.00000E-10 0.00000E+00
6 13 1.00000E+00 0.00000E+00
7 13 1.00000E-01 0.00000E+00
8 13 1.00000E-10 0.00000E+00
9 0.00000E+00
10 0.00000E+00
11 0.00000E+00
12 0.00000E+00

1 of p(1) 1 of p(1)
by group by matl
i super zn j super zn super group
1.00000E+30 1.00000E+30 1

```

Figure 5-4. (continued)

0.00000E+00
 0.00000E+00
 0.00000E+00
 0.00000E+00
 0.00000E+00

65
 66
 67
 68
 69

sn	constants for direction set	1	tau	beta	mu-mate	tau-mate	level-mate
	weight	mu					
1	0.00000E+00	-6.41230E-02	-9.97942E-01	0.00000E+00	0	121	121
2	1.02900E-03	4.21582E-02	-9.97942E-01	4.21582E-02	3	122	121
3	1.02900E-03	4.21582E-02	-9.97942E-01	4.21582E-02	2	123	121
4	0.00000E+00	-1.42963E-01	-9.89728E-01	0.00000E+00	0	124	124
5	3.07825E-03	-9.39923E-02	-9.89728E-01	9.39923E-02	6	125	124
6	3.07825E-03	-9.39923E-02	-9.89728E-01	9.39923E-02	5	126	124
236	3.84965E-03	-1.86473E-01	3.70540E-02	6.03187E+00	237	116	112
237	3.84965E-03	1.86473E-01	3.70540E-02	6.03187E+00	236	117	112
238	5.42534E-03	5.34236E-01	3.70540E-02	3.61347E+00	235	118	112
239	4.08094E-03	8.09860E-01	3.70540E-02	3.28378E+00	234	119	112
240	5.17107E-03	9.76194E-01	3.70540E-02	9.76194E-01	233	120	112

mom.	dir. 1	dir. 2	dir. 3	dir. 4	dir. 5	dir. 6	dir. 7	dir. 8
1	-6.41230E-02	-4.21582E-02	4.21582E-02	-1.42963E-01	-9.39923E-02	9.39923E-02	-2.29252E-01	-1.50724E-01
2	-9.97942E-01	-9.97942E-01	-9.97942E-01	-9.89728E-01	-9.89728E-01	-9.89728E-01	-9.73367E-01	-9.73367E-01
3	-4.93832E-01	-4.97334E-01	-4.97334E-01	-4.69342E-01	-4.86748E-01	-4.86748E-01	-4.21165E-01	-4.65923E-01
4	1.10836E-01	7.28699E-02	7.28699E-02	2.45076E-01	1.61127E-01	1.61127E-01	3.86501E-01	2.54109E-01
5	8.62464E-01	8.60443E-01	8.60443E-01	8.48325E-01	8.38276E-01	8.38276E-01	8.20510E-01	7.94669E-01
6	9.55254E-02	6.30500E-02	6.30500E-02	2.07140E-01	1.38912E-01	1.38912E-01	3.13756E-01	2.17526E-01
7	5.98548E-01	6.05681E-01	6.05681E-01	5.44145E-01	5.79310E-01	5.79310E-01	4.39428E-01	5.28357E-01
8	-1.23663E-01	-8.11127E-02	8.11127E-02	-2.71188E-01	-1.76183E-01	-1.76183E-01	-4.20612E-01	-2.67826E-01
9	-7.85698E-01	-7.80173E-01	-7.80173E-01	-7.66456E-01	-7.39218E-01	-7.39218E-01	-7.29070E-01	-6.60186E-01
10	3.59655E-01	3.68349E-01	3.68349E-01	3.00184E-01	3.42212E-01	3.42212E-01	1.89998E-01	2.92066E-01
11	-1.50312E-01	-9.93674E-02	9.93674E-02	-3.19580E-01	-2.16084E-01	-2.16084E-01	-4.64337E-01	-3.29508E-01
12	-5.40695E-01	-5.48503E-01	-5.48503E-01	-4.69248E-01	-5.07642E-01	-5.07642E-01	-3.34786E-01	-4.31384E-01
13	1.33296E-01	8.70206E-02	-8.70206E-02	2.89908E-01	1.83829E-01	1.83829E-01	4.42213E-01	2.63268E-01
14	7.33441E-01	7.23129E-01	7.23129E-01	7.09589E-01	6.59254E-01	6.59254E-01	6.63819E-01	5.39040E-01
15	-1.17932E-01	-7.83921E-02	7.83921E-02	-2.42959E-01	-1.69028E-01	-1.69028E-01	-3.29408E-01	-2.53259E-01
16	-4.55487E-01	-4.71137E-01	-4.71137E-01	-3.46250E-01	-4.20672E-01	-4.20672E-01	-1.51837E-01	-3.26463E-01
17	1.61573E-01	1.06730E-01	-1.06730E-01	3.36752E-01	2.26891E-01	2.26891E-01	4.68688E-01	3.30154E-01
18	5.00459E-01	5.07782E-01	5.07782E-01	4.13709E-01	4.50070E-01	4.50070E-01	2.54134E-01	3.47390E-01
19	-1.41091E-01	-9.14575E-02	9.14575E-02	-3.04335E-01	-1.85895E-01	-1.85895E-01	-4.56546E-01	-2.43739E-01
20	-6.94371E-01	-6.78113E-01	-6.78113E-01	-6.66260E-01	-5.87803E-01	-5.87803E-01	-6.12981E-01	-4.22969E-01

Figure 5-4. (continued)

nom.	dir. 233	dir. 234	dir. 235	dir. 236	dir. 237	dir. 238	dir. 239	dir. 240	j smesh	j cmesh
1	-9.76194E-01	-8.09860E-01	-5.34236E-01	-1.86473E-01	1.86473E-01	5.34236E-01	8.09860E-01	9.76194E-01	1	1
2	3.70540E-02	3.70540E-02	3.70540E-02	3.70540E-02	3.70540E-02	3.70540E-02	3.70540E-02	3.70540E-02	2	2
3	9.29432E-01	4.83810E-01	-7.18878E-02	-4.47842E-01	-4.47842E-01	-7.18878E-02	4.83810E-01	9.29432E-01	3	3
4	-6.26515E-02	-5.19763E-02	-3.42869E-02	-1.19677E-02	1.19677E-02	-3.42869E-02	-5.19763E-02	-6.26515E-02	4	4
5	-3.83642E-02	-2.95644E-01	-6.16477E-01	-8.33534E-01	-8.33534E-01	-6.16477E-01	-2.95644E-01	-3.83642E-02	5	5
6	-8.61381E-01	-1.13124E-01	4.20166E-01	2.63499E-01	-2.63499E-01	-4.20166E-01	1.13124E-01	8.61381E-01	6	6
7	8.54259E-02	5.17207E-02	9.68991E-03	-1.87458E-02	-1.87458E-02	9.68991E-03	5.17207E-02	8.54259E-02	7	7
8	8.37435E-01	5.35383E-01	7.36436E-01	3.47555E-01	-3.47555E-01	-7.36436E-01	-5.35383E-01	-8.37435E-02	8	8
9	-3.97268E-03	-3.00814E-02	-6.26384E-02	-8.46646E-02	-8.46646E-02	-6.26384E-02	-3.00814E-02	-3.97268E-03	9	9
10	7.74457E-01	-2.02532E-01	-3.38903E-01	2.49894E-01	2.49894E-01	-3.38903E-01	-2.02532E-01	7.74457E-01	10	10
11	-1.04968E-01	-3.77473E-02	1.56833E-02	-1.50579E-02	-1.50579E-02	1.56833E-02	-3.77473E-02	-1.04968E-01	11	11
12	-1.40429E-01	-6.85319E-01	-3.97081E-01	4.07081E-01	4.07081E-01	-3.97081E-01	-6.85319E-01	-1.40429E-01	12	12
13	1.02639E-02	6.4451E-02	8.85366E-02	4.17702E-02	-4.17702E-02	-8.85366E-02	-6.4451E-02	-1.02639E-02	13	13
14	1.23696E-03	8.47908E-02	3.71831E-01	6.81146E-01	6.81146E-01	3.71831E-01	8.47908E-02	1.23696E-03	14	14
15	-6.71732E-01	3.85740E-01	-1.02355E-02	-2.94677E-01	2.94677E-01	-1.02355E-02	-3.85740E-01	6.71732E-01	15	15
16	1.20713E-01	1.52719E-02	-2.30530E-02	9.66143E-03	9.66143E-03	-2.30530E-02	1.52719E-02	1.20713E-01	16	16
17	2.05926E-01	6.85312E-01	-1.40068E-01	-4.11811E-01	4.11811E-01	1.40068E-01	-6.85312E-01	-2.05926E-01	17	17
18	-1.99151E-02	-9.75521E-02	-6.49923E-02	3.84751E-02	3.84751E-02	-6.49923E-02	-9.75521E-02	-1.99151E-02	18	18
19	-3.70834E-03	-2.06007E-01	-5.95937E-01	-3.81046E-01	3.81046E-01	5.95937E-01	-2.06007E-01	-3.70834E-03	19	19
20	2.15182E-04	1.51474E-02	6.58629E-02	1.20408E-01	1.20408E-01	6.58629E-02	1.51474E-02	2.15182E-04	20	20

Figure 5-4. (continued)

25	9.49000E+02	1.02550E+03	1.53000E+02
26	1.10200E+03	1.16100E+03	1.18000E+02
27	1.22000E+03	1.26550E+03	9.10000E+01
28	1.31100E+03	1.34600E+03	7.00000E+01
29	1.38100E+03	1.40800E+03	5.40000E+01
30	1.43500E+03	1.45550E+03	4.10000E+01
31	1.47600E+03	1.49200E+03	3.20000E+01
32	1.50800E+03	1.52000E+03	2.40000E+01
33	1.53200E+03	1.54150E+03	1.90000E+01
34	1.55100E+03	1.55850E+03	1.50000E+01
35	1.56600E+03	1.57150E+03	1.10000E+01
36	1.57700E+03	1.58100E+03	8.00000E+00
37	1.58500E+03	1.58850E+03	7.00000E+00
38	1.59200E+03	1.59450E+03	5.00000E+00
39	1.59700E+03	1.59900E+03	4.00000E+00
40	1.60100E+03	1.60250E+03	3.00000E+00
41	1.60400E+03	1.60550E+03	3.00000E+00
42	1.60700E+03	1.60775E+03	1.50000E+00
43	1.60850E+03	1.60925E+03	1.50000E+00
44	1.61000E+03	1.61215E+03	4.30005E+00
45	1.61430E+03	1.61665E+03	4.69995E+00
46	1.61900E+03	1.61975E+03	1.50000E+00
47	1.62050E+03	1.62125E+03	1.50000E+00
48	1.62200E+03	1.62300E+03	2.00000E+00
49	1.62400E+03	1.62550E+03	3.00000E+00
50	1.62700E+03	1.62900E+03	4.00000E+00
51	1.63100E+03	1.63350E+03	5.00000E+00
52	1.63600E+03	1.63950E+03	7.00000E+00
53	1.64300E+03	1.64700E+03	8.00000E+00
54	1.65100E+03	1.65650E+03	1.10000E+01
55	1.66200E+03	1.66950E+03	1.50000E+01
56	1.67700E+03	1.68650E+03	1.90000E+01
57	1.69600E+03	1.70800E+03	2.40000E+01
58	1.72000E+03	1.73600E+03	3.20000E+01
59	1.75200E+03	1.77250E+03	4.10000E+01
60	1.79300E+03	1.82000E+03	5.40000E+01
61	1.84700E+03	1.88200E+03	7.00000E+01
62	1.91700E+03	1.96250E+03	9.10000E+01
63	2.00800E+03	2.06700E+03	1.18000E+02
64	2.12600E+03	2.20250E+03	1.53000E+02
65	2.27900E+03	2.37900E+03	2.00000E+02
66	2.47900E+03	2.60900E+03	2.60000E+02
67	2.73900E+03	2.90750E+03	3.37000E+02
68	3.07600E+03	3.29500E+03	4.38000E+02
69	3.51400E+03	3.79950E+03	5.71000E+02
70	4.08500E+03	4.45550E+03	7.41000E+02
71	4.82600E+03	5.30750E+03	9.63000E+02
72	5.78900E+03	6.41550E+03	1.25300E+03
73	7.04200E+03	7.85600E+03	1.62800E+03
74	8.67000E+03	9.72850E+03	2.11700E+03
75	1.07870E+04	1.18935E+04	2.21300E+03
76	1.30000E+04	1.45000E+04	3.00000E+03
77	1.60000E+04	1.75000E+04	3.00000E+03
78	1.90000E+04	2.05000E+04	3.00000E+03
79	2.20000E+04	2.35000E+04	3.00000E+03

Figure 5-4. (continued)

initial i-mesh set	radius	midpoint	delta r	ah	av	vr	i smesh	i cmesh
80	2.50000E+04	2.65000E+04	3.00000E+03	6.64761E+01	0.00000E+00	6.64761E+01	1	1
81	2.80000E+04	2.95000E+04	3.00000E+03	4.66212E+01	2.89027E+01	4.66212E+01	2	2
82	3.10000E+04	3.25000E+04	3.00000E+03	7.80372E+01	3.76991E+01	7.80372E+01	3	3
83	3.40000E+04	3.55000E+04	3.00000E+03	1.23025E+02	4.90088E+01	1.23025E+02	4	4
84	3.70000E+04	3.85000E+04	3.00000E+03	2.16770E+02	6.28319E+01	2.16770E+02	5	5
85	4.00000E+04	4.15000E+04	3.00000E+03	3.76991E+02	8.16814E+01	3.76991E+02	6	6
86	4.30000E+04	4.45000E+04	3.00000E+03	6.12611E+02	1.06814E+02	6.12611E+02	7	7
87	4.60000E+04	4.75000E+04	3.00000E+03	1.12155E+03	1.38230E+02	1.12155E+03	8	8
88	4.90000E+04	5.05000E+04	3.00000E+03	1.65876E+03	1.82212E+02	1.65876E+03	9	9
89	5.20000E+04	5.35000E+04	3.00000E+03	2.93739E+03	2.32478E+02	2.93739E+03	10	10
90	5.50000E+04	5.65000E+04	3.00000E+03	5.23075E+03	3.01593E+02	5.23075E+03	11	11
91	5.80000E+04	5.95000E+04	3.00000E+03	8.65509E+03	3.95884E+02	8.65509E+03	12	12
92	6.10000E+04	6.25000E+04	3.00000E+03	1.41749E+04	5.15221E+02	1.41749E+04	13	13
93	6.40000E+04	6.55000E+04	3.00000E+03	2.45296E+04	6.66018E+02	2.45296E+04	14	14
94	6.70000E+04	6.85000E+04	3.00000E+03	4.08313E+04	8.67080E+02	4.08313E+04	15	15
95	7.00000E+04	7.15000E+04	3.00000E+03	6.98942E+04	1.12469E+03	6.98942E+04	16	16
96	7.30000E+04	7.45000E+04	3.00000E+03	1.17873E+05	1.46398E+03	1.17873E+05	17	17
97	7.60000E+04	7.70000E+04	2.00000E+03	1.99262E+05	1.90381E+03	1.99262E+05	18	18
98	7.80000E+04	7.90000E+04	2.00000E+03	3.35861E+05	2.47558E+03	3.35861E+05	19	19
99	8.00000E+04	8.02800E+03	1.94400E+03	5.65741E+05	3.21699E+03	5.65741E+05	20	20
				9.61327E+05	4.17832E+03	9.61327E+05	21	21
				1.62546E+06	5.43498E+03	1.62546E+06	22	22
				2.73890E+06	7.06858E+03	2.73890E+06	23	23
				4.62617E+06	9.18602E+03	4.62617E+06	24	24
				7.84092E+06	1.19381E+04	7.84092E+06	25	25
				1.32296E+07	1.55258E+04	1.32296E+07	26	26
				2.23483E+07	2.01816E+04	2.23483E+07	27	27
				3.78014E+07	2.62323E+04	3.78014E+07	28	28
				6.38496E+07	3.41051E+04	6.38496E+07	29	29
				9.80581E+07	4.43342E+04	9.80581E+07	30	30

initial i-mesh set 1
radius midpoint delta r
ah av vr
i smesh i cmesh

initial i-mesh set	radius	midpoint	delta r	ah	av	vr	i smesh	i cmesh
1	0.00000E+00	2.30000E+00	4.60000E+00	6.64761E+01	0.00000E+00	6.64761E+01	1	1
2	4.60000E+00	5.30000E+00	1.40000E+00	4.66212E+01	2.89027E+01	4.66212E+01	2	2
3	6.00000E+00	6.90000E+00	1.80000E+00	7.80372E+01	3.76991E+01	7.80372E+01	3	3
4	7.80000E+00	8.90000E+00	2.20000E+00	1.23025E+02	4.90088E+01	1.23025E+02	4	4
5	1.00000E+01	1.15000E+01	3.00000E+00	2.16770E+02	6.28319E+01	2.16770E+02	5	5
6	1.30000E+01	1.50000E+01	4.00000E+00	3.76991E+02	8.16814E+01	3.76991E+02	6	6
7	1.70000E+01	1.95000E+01	5.00000E+00	6.12611E+02	1.06814E+02	6.12611E+02	7	7
8	2.20000E+01	2.55000E+01	7.00000E+00	1.12155E+03	1.38230E+02	1.12155E+03	8	8
9	2.90000E+01	3.30000E+01	8.00000E+00	1.65876E+03	1.82212E+02	1.65876E+03	9	9
10	3.70000E+01	4.25000E+01	1.10000E+01	2.93739E+03	2.32478E+02	2.93739E+03	10	10
11	4.80000E+01	5.55000E+01	1.50000E+01	5.23075E+03	3.01593E+02	5.23075E+03	11	11
12	6.30000E+01	7.25000E+01	1.90000E+01	8.65509E+03	3.95884E+02	8.65509E+03	12	12
13	8.20000E+01	9.40000E+01	2.40000E+01	1.41749E+04	5.15221E+02	1.41749E+04	13	13
14	1.06000E+02	1.22000E+02	3.20000E+01	2.45296E+04	6.66018E+02	2.45296E+04	14	14
15	1.38000E+02	1.58500E+02	4.10000E+01	4.08313E+04	8.67080E+02	4.08313E+04	15	15
16	1.79000E+02	2.06000E+02	5.40000E+01	6.98942E+04	1.12469E+03	6.98942E+04	16	16
17	2.33000E+02	2.68000E+02	7.00000E+01	1.17873E+05	1.46398E+03	1.17873E+05	17	17
18	3.03000E+02	3.48500E+02	9.10000E+01	1.99262E+05	1.90381E+03	1.99262E+05	18	18
19	3.94000E+02	4.53000E+02	1.18000E+02	3.35861E+05	2.47558E+03	3.35861E+05	19	19
20	5.12000E+02	5.88500E+02	1.53000E+02	5.65741E+05	3.21699E+03	5.65741E+05	20	20
21	6.65000E+02	7.65000E+02	2.00000E+02	9.61327E+05	4.17832E+03	9.61327E+05	21	21
22	8.65000E+02	9.95000E+02	2.60000E+02	1.62546E+06	5.43498E+03	1.62546E+06	22	22
23	1.12500E+03	1.29350E+03	3.37000E+02	2.73890E+06	7.06858E+03	2.73890E+06	23	23
24	1.46200E+03	1.68100E+03	4.38000E+02	4.62617E+06	9.18602E+03	4.62617E+06	24	24
25	1.90000E+03	2.18550E+03	5.71000E+02	7.84092E+06	1.19381E+04	7.84092E+06	25	25
26	2.47100E+03	2.84150E+03	7.41000E+02	1.32296E+07	1.55258E+04	1.32296E+07	26	26
27	3.21200E+03	3.69350E+03	9.63000E+02	2.23483E+07	2.01816E+04	2.23483E+07	27	27
28	4.17500E+03	4.80150E+03	1.25300E+03	3.78014E+07	2.62323E+04	3.78014E+07	28	28
29	5.42800E+03	6.24200E+03	1.62800E+03	6.38496E+07	3.41051E+04	6.38496E+07	29	29
30	7.05600E+03	8.02800E+03	1.94400E+03	9.80581E+07	4.43342E+04	9.80581E+07	30	30

Figure 5-4. (continued)

edit	reg/zn	i	cm	bandry	j	cm	bandry	key flux i	key flux j	theory	type	itn	limit
1	1							31	19			8	
2	2							34	19			8	
3	3							35	19			8	
4	4							36	19			8	
5	5							39	19			8	
6	6							42	19			8	
7	7							43	19			8	
8	8							44	19			8	
9								49	19			8	
10								50	19			8	
11								51	19			8	
12								53	19			8	
13								56	19			8	
14								35	20			8	
15								43	20			8	
16								50	20			8	
17								35	21			8	
31	9.00000E+03	1.00000E+04	2.00000E+03					1.25664E+08	5.65487E+04	1.25664E+08		31	
32	1.10000E+04	1.20000E+04	2.00000E+03					1.50796E+08	6.91150E+04	1.50796E+08		32	
33	1.30000E+04	1.40000E+04	2.00000E+03					1.75929E+08	8.16814E+04	1.75929E+08		33	
34	1.50000E+04	1.57500E+04	1.50000E+03					1.48440E+08	9.42478E+04	1.48440E+08		34	
35	1.65000E+04	1.70000E+04	1.00000E+03					1.06814E+08	1.03673E+05	1.06814E+08		35	
36	1.75000E+04	1.82500E+04	1.50000E+03					1.72002E+08	1.09956E+05	1.72002E+08		36	
37	1.90000E+04	2.00000E+04	2.00000E+03					2.51327E+08	1.19381E+05	2.51327E+08		37	
38	2.10000E+04	2.20000E+04	2.00000E+03					2.76460E+08	1.31947E+05	2.76460E+08		38	
39	2.30000E+04	2.40000E+04	2.00000E+03					3.01593E+08	1.44513E+05	3.01593E+08		39	
40	2.50000E+04	2.60000E+04	2.00000E+03					3.26726E+08	1.57080E+05	3.26726E+08		40	
41	2.70000E+04	2.77500E+04	1.50000E+03					2.61538E+08	1.69646E+05	2.61538E+08		41	
42	2.85000E+04	2.90000E+04	1.00000E+03					1.82212E+08	1.79071E+05	1.82212E+08		42	
43	2.95000E+04	3.00000E+04	1.00000E+03					1.88496E+08	1.85354E+05	1.88496E+08		43	
44	3.05000E+04	3.10000E+04	1.00000E+03					1.94779E+08	1.91637E+05	1.94779E+08		44	
45	3.15000E+04	3.22500E+04	1.50000E+03					3.03949E+08	1.97920E+05	3.03949E+08		45	
46	3.30000E+04	3.40000E+04	2.00000E+03					4.27257E+08	2.07345E+05	4.27257E+08		46	
47	3.50000E+04	3.60000E+04	2.00000E+03					4.52389E+08	2.19911E+05	4.52389E+08		47	
48	3.70000E+04	3.77500E+04	1.50000E+03					3.55785E+08	2.32478E+05	3.55785E+08		48	
49	3.85000E+04	3.90000E+04	1.00000E+03					2.45044E+08	2.41903E+05	2.45044E+08		49	
50	3.95000E+04	4.00000E+04	1.00000E+03					2.51327E+08	2.48186E+05	2.51327E+08		50	
51	4.05000E+04	4.10000E+04	1.00000E+03					2.57611E+08	2.54469E+05	2.57611E+08		51	
52	4.15000E+04	4.22500E+04	1.50000E+03					3.98197E+08	2.60752E+05	3.98197E+08		52	
53	4.30000E+04	4.40000E+04	2.00000E+03					5.52920E+08	2.70177E+05	5.52920E+08		53	
54	4.50000E+04	4.60000E+04	2.00000E+03					5.78053E+08	2.82743E+05	5.78053E+08		54	
55	4.70000E+04	4.80000E+04	2.00000E+03					6.03186E+08	2.95310E+05	6.03186E+08		55	
56	4.90000E+04	5.00000E+04	2.00000E+03					6.28319E+08	3.07876E+05	6.28319E+08		56	
57	5.10000E+04	5.25000E+04	3.00000E+03					9.89602E+08	3.20442E+05	9.89602E+08		57	
58	5.40000E+04	5.55000E+04	3.00000E+03					1.04615E+09	3.39292E+05	1.04615E+09		58	
59	5.70000E+04	5.85000E+04	3.00000E+03					1.10270E+09	3.58142E+05	1.10270E+09		59	
60	6.00000E+04	6.15000E+04	3.00000E+03					1.15925E+09	3.76991E+05	1.15925E+09		60	
61	6.30000E+04	6.45000E+04	3.00000E+03					1.21580E+09	3.95841E+05	1.21580E+09		61	
62	6.60000E+04	6.75000E+04	3.00000E+03					1.27235E+09	4.14690E+05	1.27235E+09		62	
63	6.90000E+04	7.05000E+04	3.00000E+03					1.32889E+09	4.33540E+05	1.32889E+09		63	
64	7.20000E+04	7.35000E+04	3.00000E+03					1.38544E+09	4.52389E+05	1.38544E+09		64	
65	7.50000E+04	7.65000E+04	3.00000E+03					1.44199E+09	4.71239E+05	1.44199E+09		65	
66	7.80000E+04	7.90000E+04	2.00000E+03					9.92743E+08	4.90088E+05	9.92743E+08		66	
67	8.00000E+04							5.02655E+05					

Figure 5-4. (continued)

94... dddddd
93... dddddd
92... dddddd
91... dddddd
90... dddddd
89... dddddd
88... dddddd
87... dddddd
86... dddddd
85... dddddd
84... dddddd
83... dddddd
82... dddddd
81... dddddd
80... dddddd
79... dddddd
78... dddddd
77... dddddd
76... dddddd
75... dddddd
74... dddddd
73... dddddd
72... dddddd
71... dddddd
70... dddddd
69... dddddd
68... dddddd
67... dddddd
66... dddddd
65... dddddd
64... dddddd
63... dddddd
62... dddddd
61... dddddd
60... dddddd
59... dddddd
58... dddddd
57... dddddd
56... dddddd
55... dddddd
54... dddddd
53... dddddd
52... dddddd
51... dddddd
50... dddddd
49... dddddd
48... dddddd
47... dddddd
46... dddddd
45... dddddd
44... dddddd
43... dddddd
42... dddddd
41... dddddd
40... dddddd

Figure 5-4. (continued)


```

end of geometric arrays = 24013
end of fast memory arrays = 9794675
end of user buffers = 9794675
groups in memory= 69, blocks per group= 1
end of primary input arrays = 105
end of secondary input arrays = 1000
end of general input arrays = 7909
end of indexing arrays = 8137
end of geometric arrays = 24013
end of fast memory arrays = 160127
end of user buffers = 567611
groups in memory= 1, blocks per group= 1
final memory requirement = 567611
*** accumulated charge = .1255 min. *** charge increment = .1255min.
unnorm fission rate= 0.00000E+00
unnorm distributed source
1 * 1.24E-06 2.24E-06 5.67E-06 3.86E-06 3.30E-05 * 8.56E-06 7.91E-05 1.68E-04 3.32E-04 6.32E-04
11 * 1.11E-03 3.17E-03 1.20E-02 3.69E-03 1.41E-02 * 4.25E-02 4.44E-02 7.63E-03 6.04E-02 8.00E-02
21 * 9.05E-02 4.98E-02 5.38E-02 3.80E-02 4.97E-02 * 4.96E-02 1.12E-01 8.43E-02 6.30E-02 3.19E-02
31 * 3.24E-02 1.00E-02 4.45E-03 1.25E-03 4.26E-03 * 2.27E-03 6.61E-04 1.93E-04 8.86E-05 4.98E-05
41 * 2.06E-05 5.24E-06 2.17E-06 5.52E-07 * 9.26E-08 7.13E-07 2.89E-06 3.75E-06 1.06E-05
51 * 9.44E-05 3.71E-04 4.70E-04 7.92E-04 * 2.34E-03 * 3.05E-03 8.45E-03 1.66E-02 3.63E-02 4.90E-02
61 * 8.22E-02 7.83E-02 1.04E-01 1.34E-02 2.54E-03 * 2.19E-04 2.22E-05 1.19E-05 1.56E-05 1.35E+00
itn-flx-cum-cnv-acc-ix-jfx-gfx-----k-cnv-fsn cnv-grp cnv-flx cv-ups cv---extr-----Charge %%
0 0 0 71 0 0 0 0 0.000000E+00 0.000000E+00 0.0E+00 0.0E+00 0.0E+00 1.1E+00 0.0E+00 .2877 %%
grp itn imfd jmfid*mx fx dv*mx dv fx*rebl*rebl err*max rebl*rb dv fx*grp rebl*key flux* neg fix* source* charge= .4235
1 1 51 22 1.00E+00 5.82E-18 22 6.03E-03 3.19E+01 1.18E+01 1.83E-15 1.00E+00 1.24E-06 1.5110 0 1.5 .95 %
1 2 51 13 6.52E-01 9.40E-20 8-2.73E-03 4.82E+00 4.74E-01-1.25E-04 1.70E-15 1.52E-01 1.24E-06 1.5110 0 1.5 1.51 %
1 3 51 13 2.29E-01 1.80E-19 7 1.60E-03 9.63E-01 8.63E-02-2.71E-04 1.72E-15 1.52E-01 1.24E-06 1.5110 0 1.5 2.07 %
1 4 51 13 4.07E-02 2.03E-19 7 2.30E-04 2.78E-01 1.26E-02 1.07E-04 1.72E-15 1.52E-01 1.24E-06 1.5110 0 1.5 2.63 %
1 5 44 14-3.00E-03 1.04E-18 5-9.69E-05 7.85E-02-1.29E-03 3.77E-05 1.72E-15 1.52E-01 1.24E-06 1.5110 0 1.5 3.19 %
1 6 35 13-1.24E-03 2.84E-18 4 8.70E-05 1.75E-02-6.44E-04 2.03E-05 1.72E-15 1.52E-01 1.24E-06 1.5110 0 1.5 3.75 %
convergence by region
1 * 1.30E-12 -1.24E-03 2.28E-04 -5.93E-05 1.05E-13 *-2.73E-04 9.07E-04 -4.70E-13
keyflx 5.59751E-16 2.47926E-16 1.63222E-16 1.60827E-16 6.70290E-17 4.05892E-17 3.52694E-17 3.62052E-17 1.56113E-17 1.43520E-17
keyflx 1.29557E-17 9.73172E-18 5.57250E-18 1.98160E-16 3.90875E-17 1.44040E-17 2.05118E-16 4.14108E-17 1.42091E-17 1.43202E-17
grp itn imfd jmfid*mx fx dv*mx dv fx*rebl*rebl err*max rebl*rb dv fx*grp rebl*key flux* neg fix* source* charge= 3.7622
2 1 51 12 1.00E+00 1.18E-17 12 9.28E-03 6.85E-01 3.18E-01 2.16E-01 2.90E-15 2.93E-01 2.49E-06 1.5610 0 1.5 4.29 %
2 2 34 14 2.18E-01 4.22E-18 7 1.29E-03 7.29E-02 2.65E-02 1.97E-04 2.80E-15 2.93E-01 2.49E-06 1.5610 0 1.5 4.81 %
2 3 34 13 5.56E-02 1.91E-18 6-3.89E-04 2.01E-02 6.34E-03-9.95E-06 2.81E-15 2.93E-01 2.49E-06 1.5610 0 1.5 5.33 %
2 4 34 13 7.91E-03 1.94E-18 5 8.53E-05 7.32E-03 8.89E-04-2.62E-05 2.81E-15 2.93E-01 2.49E-06 1.5610 0 1.5 5.86 %
2 5 42 14-1.48E-03 8.79E-19 4 5.38E-05 2.07E-03-2.55E-04 3.58E-07 2.81E-15 2.93E-01 2.49E-06 1.5610 0 1.5 6.38 %
convergence by region
1 * 5.66E-13 -1.48E-03 4.36E-04 -2.78E-05 -1.28E-13 *-1.47E-04 -4.21E-05 2.08E-13
keyflx 9.05431E-16 4.00094E-16 2.45928E-16 2.44714E-16 9.42318E-17 5.51173E-17 4.84455E-17 4.94381E-17 1.99848E-17 1.82608E-17
keyflx 1.62507E-17 1.17194E-17 6.17441E-18 3.04360E-16 5.37335E-17 1.81317E-17 3.15251E-16 5.77238E-17 1.77573E-17 1.76394E-17
grp itn imfd jmfid*mx fx dv*mx dv fx*rebl*rebl err*max rebl*rb dv fx*grp rebl*key flux* neg fix* source* charge= 6.3890
3 1 51 22 1.00E+00 3.09E-17 13 9.94E-03 1.43E+00 4.95E-01 3.18E-01 7.97E-15 1.26E-01 6.41E-06 1.6110 0 1.5 6.90 %

```

Figure 5-4. (continued)

```

3 2 34 13 2.67E-01 4.90E-18 8-2.21E-03 1.93E-01 5.55E-02-3.13E-04 7.65E-15 1.26E-01 6.41E-06 1.6110 0 1.5 7.43 %
3 3 34 13 6.10E-02 5.50E-18 7 5.44E-04 6.21E-02 9.98E-03-3.78E-05 7.67E-15 1.26E-01 6.41E-06 1.6110 0 1.5 7.95 %
3 4 43 13 6.77E-03 8.72E-19 6-8.87E-05 1.42E-02 1.10E-03 8.11E-06 7.67E-15 1.26E-01 6.41E-06 1.6110 0 1.5 8.47 %
3 5 43 13 1.58E-03 8.74E-19 4-7.14E-05 3.32E-03 3.45E-04-1.01E-05 7.67E-15 1.26E-01 6.41E-06 1.6110 0 1.5 9.00 %
convergence by region
1 * 7.72E-13 1.58E-03 2.67E-04 2.72E-05 6.41E-14 * 8.18E-05 -1.98E-04 -2.30E-13

keyflx 2.40136E-15 1.03099E-15 6.61657E-16 6.60072E-16 2.63206E-16 1.55654E-16 1.32675E-16 1.39607E-16 5.69379E-17 5.236661E-17
keyflx 4.67616E-17 3.42989E-17 1.86578E-17 8.18493E-16 1.51100E-16 5.23058E-17 8.46579E-16 1.60550E-16 5.13558E-17 5.14554E-17

grp itn imfd jmfid*mx fx dv*mx dv fx*rebl*rebl err*max rebl*rb dv fx*grp rebl*key flux* neg fix* source* charge= 9.0088
4 1 51 22 1.00E+00 2.58E-17 12-7.63E-03 1.14E+00 4.18E-01 2.76E-01 5.48E-15 1.29E-01 4.98E-06 1.6510 0 1.5 9.55 %
4 2 35 13 1.83E-01 4.50E-18 9 1.52E-03 1.44E-01 3.59E-02-2.69E-04 5.31E-15 1.23E-01 4.98E-06 1.6510 0 1.5 10.11 %
4 3 36 13 3.25E-02 3.89E-18 8-2.74E-04 3.47E-02 4.90E-03-2.00E-05 5.33E-15 1.22E-01 4.98E-06 1.6510 0 1.5 10.66 %
4 4 44 13 4.12E-03 8.16E-19 6-8.34E-05 8.01E-03 6.31E-04-3.40E-06 5.33E-15 1.22E-01 4.98E-06 1.6510 0 1.5 11.22 %
4 5 34 15 1.03E-03 4.82E-17 4-6.60E-05 1.99E-03 3.82E-05 4.77E-07 5.33E-15 1.22E-01 4.98E-06 1.6510 0 1.5 11.78 %
convergence by region
1 * 4.66E-13 1.03E-03 -2.15E-04 -3.02E-05 2.92E-14 * -8.55E-05 2.45E-04 -2.95E-13

keyflx 1.70593E-15 7.42489E-16 4.86350E-16 4.79770E-16 1.96220E-16 1.16952E-16 1.00969E-16 1.04327E-16 4.40428E-17 4.04042E-17
keyflx 3.63553E-17 2.69283E-17 1.49699E-17 5.93060E-16 1.13153E-16 4.05114E-17 6.13225E-16 1.19851E-16 3.99402E-17 4.01319E-17

grp itn imfd jmfid*mx fx dv*mx dv fx*rebl*rebl err*max rebl*rb dv fx*grp rebl*key flux* neg fix* source* charge= 117.2502
67 1 51 22 1.00E+00 3.76E-13 6-6.70E-03 1.64E+00 1.17E+00 1.03E+00 3.28E-11 0.00E+00 3.03E-01 1.4610 0 1.5 117.53 %
67 2 50 19 1.18E-01 8.04E-13 7 6.34E-04 1.09E-01 3.29E-02-2.66E-03 3.56E-11 0.00E+00 3.03E-01 1.4610 0 1.5 117.80 %
67 3 36 18-1.11E-02 4.50E-12 8 1.02E-04 1.10E-02-1.58E-03 2.46E-04 3.52E-11 0.00E+00 3.03E-01 1.4610 0 1.5 118.08 %
67 4 34 18 1.22E-03 5.95E-12 6-5.65E-05 2.57E-03-2.47E-04-2.54E-05 3.52E-11 0.00E+00 3.03E-01 1.4610 5 3.0 118.36 %
67 5 42 22 4.83E-04 2.55E-12 4-3.59E-05 3.92E-04 2.50E-04-1.01E-06 3.52E-11 0.00E+00 3.03E-01 1.4610 1 4.5 118.64 %
convergence by region
1 * 3.81E-14 1.82E-04 1.84E-05 -2.18E-06 1.17E-15 * 4.83E-04 5.90E-05 1.43E-13

keyflx 1.67766E-11 8.58305E-12 7.46720E-12 6.52526E-12 3.62822E-12 2.23216E-12 2.03126E-12 1.84758E-12 9.01212E-13 8.24606E-13
keyflx 7.56914E-13 5.86198E-13 3.56174E-13 7.73950E-12 2.10507E-12 8.55456E-13 8.05236E-12 2.19185E-12 8.90896E-13 9.41716E-13

grp itn imfd jmfid*mx fx dv*mx dv fx*rebl*rebl err*max rebl*rb dv fx*grp rebl*key flux* neg fix* source* charge= 118.7045
68 1 51 22 1.00E+00 3.51E-14 5 9.63E-03 5.86E-01 4.40E-01 4.68E-01 1.68E-12 0.00E+00 5.23E-02 1.4610 0 1.5 118.98 %
68 2 51 19 8.32E-02 4.00E-14 4-7.61E-04 2.09E-02 1.03E-02 9.28E-04 1.80E-12 0.00E+00 5.23E-02 1.4610 0 1.5 119.26 %
68 3 50 19 1.27E-03 4.41E-14 4 2.61E-05 1.07E-03 1.49E-04 1.67E-05 1.80E-12 0.00E+00 5.23E-02 1.4610 0 1.5 119.54 %
68 4 51 19 7.45E-05 4.04E-14 4 3.58E-06-1.23E-04 1.07E-05-2.38E-07 1.80E-12 0.00E+00 5.23E-02 1.4610 1 3.0 119.82 %
convergence by region
1 * -2.05E-14 -3.89E-05 4.20E-06 8.24E-07 -2.62E-16 * 7.45E-05 1.80E-05 9.91E-14

keyflx 8.84121E-13 4.55679E-13 3.96764E-13 3.47131E-13 1.93499E-13 1.19209E-13 1.08451E-13 9.86920E-14 4.81721E-14 4.40963E-14
keyflx 4.04502E-14 3.13447E-14 1.90428E-14 4.28611E-13 1.17221E-13 4.77076E-14 4.63652E-13 1.26905E-13 5.16656E-14 5.70643E-14

```

Figure 5-4. (continued)

37 4.02663E-04 0.00000E+00 0.00000E+00 2.16294E-01 4.64315E-01 2.14149E-01 3.27504E-05 0.00000E+00 9.99999E-01 3.80977E-01
38 1.24001E-04 0.00000E+00 0.00000E+00 1.80591E-01 3.93893E-01 1.78859E-01 4.87907E-05 0.00000E+00 9.99987E-01 2.81952E-01
39 5.85842E-05 0.00000E+00 0.00000E+00 1.79632E-01 3.95475E-01 1.77864E-01 5.70831E-05 0.00000E+00 9.99985E-01 2.79642E-01
40 3.31540E-05 0.00000E+00 0.00000E+00 2.12502E-01 4.59413E-01 2.10118E-01 8.78551E-05 0.00000E+00 1.00002E+00 3.69893E-01
41 1.37673E-05 0.00000E+00 0.00000E+00 2.37130E-01 5.13684E-01 2.34284E-01 1.77354E-04 0.00000E+00 1.00007E+00 4.58388E-01
42 3.49454E-06 0.00000E+00 0.00000E+00 2.09148E-01 4.59011E-01 2.45713E-04 2.45713E-04 0.00000E+00 1.00002E+00 3.63751E-01
43 1.45115E-06 0.00000E+00 0.00000E+00 2.33387E-01 5.13167E-01 2.30039E-01 5.36656E-04 0.00000E+00 9.99963E-01 4.49958E-01
44 3.68261E-07 0.00000E+00 0.00000E+00 2.05490E-01 4.99327E-01 2.01848E-01 7.95714E-04 0.00000E+00 1.00005E+00 3.82108E-01
45 1.34164E-07 0.00000E+00 0.00000E+00 2.10139E-01 5.90366E-01 2.04957E-01 4.42968E-03 0.00000E+00 9.99956E-01 4.20209E-01
46 6.09354E-08 0.00000E+00 0.00000E+00 3.11873E-01 9.20959E-01 4.15340E-04 2.27143E-01 0.00000E+00 1.00002E+00 1.46793E+01
47 6.10596E-08 0.00000E+00 0.00000E+00 4.83905E-08 3.75205E-02 3.32449E-07 6.94510E-12 0.00000E+00 9.99983E-01 9.79752E-06
48 1.65622E-07 0.00000E+00 0.00000E+00 2.30298E-07 1.32448E-02 1.86553E-06 4.86774E-11 0.00000E+00 9.99992E-01 5.17131E-05
49 6.74113E-07 0.00000E+00 0.00000E+00 6.48747E-05 2.83712E-02 3.95277E-04 2.00528E-08 0.00000E+00 9.99986E-01 1.05967E-02
50 5.31978E-06 0.00000E+00 0.00000E+00 1.14335E-03 3.95105E-02 1.15841E-03 4.20942E-08 0.00000E+00 9.99987E-01 2.95956E-02
51 2.16745E-04 0.00000E+00 0.00000E+00 1.08735E-02 2.96937E-02 6.11562E-03 4.03434E-07 0.00000E+00 9.99999E-01 2.30213E-01
52 1.64772E-04 0.00000E+00 0.00000E+00 6.28784E-02 3.36900E-02 1.14755E-01 5.49305E-02 2.17684E-02 2.03882E-06 9.99928E-01 4.43841E-01
53 5.65614E-05 0.00000E+00 0.00000E+00 6.35172E-03 4.33717E-02 7.58944E-03 4.1182E-07 0.00000E+00 9.99979E-01 1.61609E-01
54 1.85979E-04 0.00000E+00 0.00000E+00 1.92945E-02 5.82230E-02 1.79215E-02 1.16061E-06 0.00000E+00 9.99972E-01 3.53803E-01
55 7.29800E-04 0.00000E+00 0.00000E+00 2.58438E-02 8.31050E-02 2.47684E-02 2.03882E-06 0.00000E+00 9.99928E-01 4.43841E-01
56 9.38931E-04 0.00000E+00 0.00000E+00 9.34928E-03 6.31106E-02 1.01244E-02 1.00113E-06 0.00000E+00 9.99775E-01 1.57837E-01
57 1.95893E-03 0.00000E+00 0.00000E+00 1.99167E-01 8.36486E-02 1.14755E-01 5.49305E-02 2.16968E-05 0.00000E+00 9.99898E-01 9.23210E-01
58 5.34497E-03 0.00000E+00 0.00000E+00 5.05965E-02 1.14755E-01 8.04399E-01 7.86961E-02 2.16968E-05 0.00000E+00 9.99898E-01 9.23210E-01
59 9.81074E-03 0.00000E+00 0.00000E+00 6.83971E-02 1.91326E-01 8.59265E-02 4.2672E-05 0.00000E+00 9.99982E-01 8.53398E-01
60 1.26971E-02 0.00000E+00 0.00000E+00 7.22668E-02 1.91326E-01 8.59265E-02 4.2672E-05 0.00000E+00 9.99982E-01 8.53398E-01
61 2.06866E-02 0.00000E+00 0.00000E+00 1.34767E-01 2.69855E-01 1.57534E-01 1.97622E-04 0.00000E+00 1.00001E+00 1.43589E+00
62 1.82833E-02 0.00000E+00 0.00000E+00 1.64075E-01 3.13818E-01 1.83785E-01 6.45169E-04 0.00000E+00 9.99979E-01 1.50282E+00
63 2.39173E-02 0.00000E+00 0.00000E+00 3.78285E-01 5.70520E-01 3.51231E-01 5.8964E-03 0.00000E+00 9.99996E-01 3.82976E+00
64 2.62855E-02 0.00000E+00 0.00000E+00 3.50995E-01 5.25628E-01 3.18310E-01 4.2034E-02 0.00000E+00 9.99996E-01 2.78129E+00
65 4.47174E-04 0.00000E+00 0.00000E+00 3.26401E-01 5.43524E-01 2.33977E-02 1.93177E-02 0.00000E+00 9.99999E-01 2.23372E+00
66 3.68820E-05 0.00000E+00 0.00000E+00 2.34635E-01 5.38988E-01 6.47121E-02 1.75247E-01 0.00000E+00 9.99998E-01 1.14830E+00
67 1.16395E-05 0.00000E+00 0.00000E+00 6.78822E-02 3.18174E-01 4.65706E-03 6.55469E-02 0.00000E+00 1.00000E+00 1.17485E-01
68 7.40996E-06 0.00000E+00 0.00000E+00 5.96550E-03 1.32955E-01 8.33733E-05 6.04213E-03 0.00000E+00 1.00000E+00 3.08363E-03
69 1.00870E-05 0.00000E+00 0.00000E+00 1.41234E-03 3.02810E-02 9.36579E-07 1.42141E-03 0.00000E+00 1.00000E+00 1.32034E-04
70 2.94378E-01 0.00000E+00 0.00000E+00 5.78418E+00 8.44673E-01 5.48332E+00 6.17853E-01 0.00000E+00 1.00002E+00 4.27000E+01
grp. lift outflow rgt outflow bot outflow top outflow lift netflow rgt netflow bot netflow top netflow tot leakage collisions
1 4.77864E-11 1.32674E-10 2.94290E-10 1.72755E-08 6.29137E-10 1.31626E-10 2.94290E-10 1.15845E-07 1.16049E-07 6.19424E-07
2 2.69040E-11 2.04306E-10 1.21779E-10 1.33118E-08 1.01977E-09 2.03764E-10 1.21779E-10 1.97860E-07 1.98554E-07 9.11497E-07
3 1.03842E-10 5.25501E-10 4.23637E-10 5.26987E-08 2.66188E-09 5.24201E-10 4.23637E-10 5.05465E-07 5.07179E-07 2.44773E-06
4 1.10034E-10 3.74775E-10 3.94206E-10 4.60725E-08 1.80361E-09 3.72452E-10 3.94206E-10 3.56144E-07 3.57181E-07 1.76531E-06
5 1.93243E-09 3.23638E-09 4.37594E-09 6.69155E-07 1.47010E-08 3.18299E-09 4.37594E-09 2.97525E-06 2.98240E-06 1.64086E-05
6 6.93969E-10 1.18865E-10 6.15954E-10 2.01349E-07 3.31003E-09 7.02637E-10 6.15954E-10 7.08524E-07 7.10516E-07 3.95094E-06
7 3.78399E-09 6.58872E-09 3.88969E-09 1.33633E-06 3.05225E-08 6.39493E-09 3.88969E-09 6.82797E-06 6.84820E-06 3.46785E-05
8 9.91510E-09 1.45686E-08 1.15785E-08 3.41084E-06 6.03570E-08 1.40259E-08 1.15785E-08 1.42179E-05 1.42527E-05 7.03275E-05
9 2.36602E-08 2.70221E-08 2.11154E-08 7.87398E-06 1.00241E-07 2.56003E-08 2.11154E-08 2.71948E-05 2.72483E-05 1.33097E-04
10 4.73656E-08 4.78290E-08 3.78112E-08 1.58592E-05 1.64653E-07 4.46348E-08 3.78112E-08 5.23474E-05 5.24420E-05 2.47864E-04
11 9.22413E-08 7.70723E-08 3.78112E-08 3.10265E-05 2.66333E-07 7.06188E-08 3.78112E-08 9.23384E-05 9.23963E-05 4.41509E-04
12 3.10177E-07 2.20807E-07 1.09393E-07 1.03442E-04 6.71262E-07 1.96079E-07 1.09393E-07 2.75499E-04 2.75864E-04 1.31292E-03
13 1.33654E-06 7.76394E-07 2.38455E-07 4.77723E-04 2.46227E-06 6.50638E-07 2.38455E-07 1.02674E-03 1.02831E-03 6.08418E-03
14 4.58204E-07 2.36257E-07 5.94738E-08 1.71777E-04 7.14175E-07 5.76546E-07 1.71777E-04 2.21070E-04 2.21535E-04 2.10721E-03
15 1.71748E-06 7.68730E-07 1.33087E-07 6.68799E-04 2.1920E-06 5.1920E-06 6.68799E-04 2.20367E-03 2.2217E-03 8.42869E-03
16 6.00326E-06 2.53707E-06 1.73725E-07 2.58764E-03 5.95614E-06 1.39121E-06 1.73725E-07 3.87173E-03 3.87612E-03 3.25740E-02
17 8.65918E-06 2.76209E-06 2.23950E-07 3.62755E-04 1.4024E-06 3.62755E-06 2.23950E-07 4.61959E-03 4.61959E-03 3.36320E-02
18 1.47491E-06 5.61164E-07 6.42783E-08 5.58843E-04 1.29319E-06 3.55229E-07 6.42783E-08 9.36885E-04 9.37759E-04 5.37090E-03
19 7.23762E-06 2.98703E-06 1.49268E-07 3.16133E-03 6.99365E-06 1.90214E-06 1.49268E-07 7.70768E-03 7.71262E-03 4.25589E-02
20 1.13989E-05 3.65771E-06 1.32533E-07 5.70036E-03 5.69519E-06 2.00650E-06 1.32533E-07 4.93333E-03 4.93333E-03 6.47071E-02

Figure 5-4. (continued)

21 1.35988E-05 3.79433E-06 9.97690E-08 7.54010E-03-3.83695E-06 1.76763E-06 9.97690E-08-1.23297E-02-1.23297E-02 9.34978E-02
22 5.89801E-06 1.52388E-06 3.40688E-08 3.75948E-03-2.74710E-06 6.11853E-07 3.40688E-08-7.41810E-03-7.42020E-03 5.72409E-02
23 9.8819E-06 2.39930E-06 4.59202E-08 6.60857E-03-4.52936E-07 8.44973E-07 4.59202E-08-8.39969E-03-8.39925E-03 7.20021E-02
24 8.29719E-05 1.70727E-06 3.19167E-08 5.83165E-03 3.99073E-07 3.19167E-08-4.60324E-03-4.60166E-03 5.29900E-02
25 1.00436E-05 2.32981E-06 4.38265E-08 1.14123E-07 6.66888E-07 4.38265E-08-6.92533E-03-6.92450E-03 7.01409E-02
26 9.21204E-06 2.31635E-06 3.85562E-08 5.82546E-03-2.76278E-07 7.11335E-07 3.85562E-08-9.03017E-03-9.02969E-03 7.64052E-02
27 1.87650E-05 3.52205E-06 6.18718E-08 1.32508E-02-2.19584E-06 3.77002E-06 6.18718E-08-1.72176E-02-1.72194E-02 2.24117E-01
28 2.23700E-05 3.86070E-06 5.95176E-08 1.67609E-02 4.72498E-06-3.77002E-06 5.95176E-08-1.67343E-02-1.67343E-02 2.11665E-01
29 2.06693E-05 3.41614E-06 5.06741E-08 1.57182E-02 5.15636E-06-4.16930E-07 5.06741E-08-1.44569E-02-1.44521E-02 2.35503E-01
30 1.38453E-05 2.42109E-06 3.58481E-08 1.01365E-02 3.19175E-06-2.51125E-07 3.58481E-08-1.49500E-03-1.49203E-03 1.60629E-01
31 2.14864E-05 4.55507E-06 6.90958E-08 1.75930E-02 4.64636E-06-2.33472E-07 6.90958E-08-7.36035E-07-7.35575E-07 3.23905E-01
32 1.23834E-05 2.64557E-06 3.03262E-08 8.94683E-03 2.27931E-06 1.26171E-07 3.03262E-08-2.06239E-03-2.05995E-03 1.81175E-01
33 8.99407E-06 1.67177E-06 1.89109E-08 6.43458E-03 2.35086E-06-1.93915E-07 1.89109E-08-6.66736E-04-6.64558E-04 1.37927E-01
34 3.33493E-06 6.91814E-07 7.77134E-09 2.36185E-03 7.70028E-07-7.70028E-07 2.36185E-03-1.53271E-04-1.52500E-04 5.16463E-02
35 1.93187E-05 4.85882E-06 4.15685E-08 1.34511E-02 3.47536E-06 7.14131E-07 4.15685E-08-2.02813E-04-2.07044E-04 3.09836E-01
36 2.69465E-05 8.23082E-06 6.31678E-08 1.80824E-02 2.14164E-06 2.24663E-06 6.31678E-08-2.59625E-03-2.60070E-03 4.53716E-01
37 2.29339E-05 8.19644E-06 5.58736E-08 1.47864E-02 2.77811E-07 2.91937E-06 5.58736E-08-2.49834E-03-2.50159E-03 3.99828E-01
38 1.68446E-05 6.69615E-06 3.95797E-08 1.05147E-02-6.74067E-07 7.23478E-06 3.95797E-08-1.80149E-03-1.80358E-03 2.95175E-01
39 1.65901E-05 6.98116E-06 4.05672E-08 1.00836E-02-1.39793E-06 2.98959E-06 4.05672E-08-1.76381E-03-1.76545E-03 2.94316E-01
40 2.17701E-05 1.03635E-05 4.68606E-08 1.28339E-02-3.23280E-06 5.01436E-06 4.68606E-08-2.33493E-03-2.33676E-03 3.88847E-01
41 2.67214E-05 1.39128E-05 5.42822E-08 1.51871E-02-6.96031E-06 7.18598E-06 5.42822E-08-2.71807E-03-2.71835E-03 4.82117E-01
42 2.10511E-05 1.15757E-05 5.04211E-08 1.15876E-02-8.23660E-06 6.16754E-06 5.04211E-08-2.12043E-03-2.11841E-03 3.82714E-01
43 2.59063E-05 1.48499E-05 8.06125E-08 1.37805E-02-1.52897E-05 8.07624E-06 8.06125E-08-2.80168E-03-2.79455E-03 4.73623E-01
44 2.19494E-05 1.27396E-05 4.97531E-08 1.12418E-02-1.73167E-05 6.93172E-06 4.97531E-08-2.87965E-03-2.86932E-03 4.04742E-01
45 2.42128E-05 1.42775E-05 8.10414E-08 1.17945E-02-2.19639E-05 7.82521E-06 8.10414E-08-3.73077E-03-3.71671E-03 5.03741E-01
46 1.02833E-03 4.90104E-04 1.69698E-06 1.61782E-01-4.70768E-04 2.58705E-04 1.69698E-06-8.51915E-02-8.49811E-02 2.87855E-01
47 1.99500E-10 2.04462E-10 9.66203E-09 1.58892E-08-1.64161E-10 1.74899E-10 9.66203E-09-2.32685E-07-2.23012E-07 3.45416E-07
48 7.71257E-10 1.11926E-09 4.86262E-08 1.26474E-07-8.39546E-10 9.32970E-10 4.86262E-08-1.51841E-06-1.46969E-06 1.90623E-06
49 1.31917E-07 1.94794E-07 9.80336E-06 1.72810E-05-5.23207E-08 1.19529E-07 9.80336E-06-3.39614E-04-3.29744E-04 4.06831E-04
50 1.33486E-06 3.44631E-07 1.92244E-05 2.90688E-04 2.09508E-08 4.60684E-08 2.90688E-04-6.0684E-08-6.0684E-08 1.90623E-06
51 1.20788E-05 2.58322E-06 1.09001E-04 2.68014E-03 3.26834E-07 4.08579E-08 1.09001E-04-1.04502E-03-1.15439E-03 9.97190E-03
52 6.71111E-06 1.55285E-06 7.62866E-05 1.48424E-03 1.14816E-07 1.08569E-07 7.62866E-05-2.11849E-04-2.88358E-04 6.32914E-03
53 6.51361E-06 2.12136E-06 9.23210E-05 1.36910E-03-5.93031E-08 5.19830E-07 9.23210E-05-1.27451E-03-1.18173E-03 7.93396E-03
54 1.83901E-05 4.23036E-06 1.44685E-04 4.13490E-03-9.55406E-08 3.10233E-07 1.44685E-04-1.41229E-03-1.55719E-03 7.90307E-02
55 2.25673E-05 5.36490E-06 1.76777E-04 5.10104E-03-9.37243E-07 5.57212E-07 1.76777E-04-1.62472E-03-1.80112E-03 2.70155E-02
56 6.53224E-06 1.52688E-06 9.38748E-05 1.42721E-03-8.90352E-07 1.54918E-07 9.38748E-05-6.72226E-05-1.60362E-04 1.08074E-02
57 1.54319E-04 4.10115E-05 2.83516E-04 3.67362E-02-1.18575E-05 8.14976E-06 2.83516E-04-2.01402E-02-2.04200E-02 1.97197E-01
58 3.11043E-05 6.69411E-06 2.63008E-04 7.10719E-03-5.30289E-06 5.99023E-07 2.63008E-04-7.36002E-04-9.94306E-04 6.20616E-02
59 3.49301E-05 9.17499E-06 3.33308E-04 8.02913E-03-1.53631E-05 2.23689E-06 3.33308E-04-8.40475E-04-5.20293E-04 9.60494E-02
60 2.96669E-05 9.05464E-06 2.57522E-04 7.53557E-03-2.14206E-05 3.43808E-06 2.57522E-04-1.91445E-03-1.67491E-03 1.07134E-01
61 5.33473E-05 1.01231E-05 3.12362E-04 1.47062E-02-3.47083E-06 6.11613E-07 3.12362E-04-2.56483E-03-2.25532E-03 2.16000E-01
62 6.25502E-05 1.36806E-05 2.34461E-04 1.76567E-02-1.25729E-05 3.65166E-06 2.34461E-04-1.75757E-03-1.53203E-03 2.68777E-01
63 1.78573E-04 4.41563E-05 4.02172E-04 5.05226E-02 7.14934E-06 1.19394E-05 4.02172E-04-4.98161E-04-4.98161E-04 8.40133E-01
64 1.18172E-04 4.21262E-05 2.61083E-04 3.47646E-02-1.63584E-05 1.85765E-05 2.61083E-04-8.43015E-04-1.10632E-03 7.43117E-01
65 9.13289E-05 3.57741E-05 1.71522E-04 2.68540E-02-2.18843E-05 1.59650E-05 1.71522E-04-8.14108E-04-6.48506E-04 7.17442E-01
66 4.52072E-05 2.03343E-05 6.53285E-05 1.43202E-02-1.45847E-05 9.47845E-06 6.53285E-05-5.34707E-03-5.28685E-03 5.20504E-01
67 4.66827E-06 2.41627E-06 4.32177E-06 1.77961E-03-1.82554E-06 1.19769E-06 4.32177E-06-2.31328E-03-2.30959E-03 1.02965E-01
68 1.40659E-07 7.82780E-08 1.60498E-07 6.56500E-05-6.09304E-08 4.13777E-08 1.60498E-07-1.52736E-04-1.52595E-04 7.06481E-03
69 9.07158E-09 4.59863E-09 3.15837E-10 1.59566E-06-3.15525E-09 2.56151E-09 3.15837E-10-8.02498E-08-7.99719E-08 1.46676E-03
70 2.37117E-03 9.06395E-04 3.31512E-03 6.86063E-01-6.76296E-04 4.02687E-04 3.31512E-03-2.56555E-02-2.26137E-02 3.92834E-01

Figure 5-4. (continued)

balance for region 9, volume = 1.61010E+15, average density factor = 1.0000

grp.	fix source	fsn source	fsn rate	insscatter	silfscat/col	outscatter	absorption	db2 loss	out/in	flux*volume
1	1.23725E-06	0.00000E+00	0.00000E+00	0.00000E+00	4.45159E-01	1.05920E-06	1.54981E-07	0.00000E+00	9.99410E-01	1.65640E+02
2	2.24093E-06	0.00000E+00	0.00000E+00	2.44393E-07	1.77906E-01	2.12950E-06	3.43825E-07	0.00000E+00	1.00055E+00	2.14349E-02
3	5.67008E-06	0.00000E+00	0.00000E+00	7.40765E-07	2.19466E-01	5.31588E-06	1.04198E-06	0.00000E+00	9.99708E-01	6.17104E-02
4	3.86187E-06	0.00000E+00	0.00000E+00	1.11588E-06	2.17559E-01	4.10498E-06	8.20837E-07	0.00000E+00	9.99319E-01	4.74912E-02
5	3.30240E-05	0.00000E+00	0.00000E+00	2.61826E-06	4.01312E-01	2.73273E-05	7.78794E-06	0.00000E+00	9.99558E-01	4.41619E-01
6	5.5889E-06	0.00000E+00	0.00000E+00	2.21033E-06	2.00426E-01	8.96308E-06	1.73443E-06	0.00000E+00	9.99852E-01	9.81881E-02
7	7.90955E-05	0.00000E+00	0.00000E+00	8.54229E-06	3.02807E-01	6.97022E-05	1.68444E-05	0.00000E+00	9.99242E-01	9.87523E-01
8	1.68411E-04	0.00000E+00	0.00000E+00	2.17380E-05	2.80375E-01	1.52582E-04	3.47087E-05	0.00000E+00	9.99279E-01	2.23355E+00
9	3.37333E-04	0.00000E+00	0.00000E+00	5.36457E-05	2.61897E-01	3.15845E-04	6.20802E-05	0.00000E+00	9.99252E-01	4.84574E+00
10	6.32488E-04	0.00000E+00	0.00000E+00	1.26267E-04	2.52946E-01	6.37640E-04	1.05841E-04	0.00000E+00	9.99296E-01	9.69863E+00
11	1.10553E-03	0.00000E+00	0.00000E+00	2.65936E-04	3.48143E-01	1.17975E-03	1.73352E-04	0.00000E+00	9.99314E-01	1.15780E+01
12	3.17243E-03	0.00000E+00	0.00000E+00	7.32651E-04	3.28285E-01	3.29570E-03	5.30040E-04	0.00000E+00	9.99460E-01	5.35765E+01
13	1.19696E-02	0.00000E+00	0.00000E+00	2.38466E-03	4.20289E-01	1.20829E-02	2.01022E-03	0.00000E+00	9.99629E-01	2.08909E+02
14	3.68689E-03	0.00000E+00	0.00000E+00	2.49741E-03	3.43624E-01	5.05817E-03	9.1794E-04	0.00000E+00	9.99668E-01	8.11124E+01
15	1.40728E-02	0.00000E+00	0.00000E+00	7.61358E-03	3.43434E-01	1.77094E-02	3.82864E-03	0.00000E+00	9.99766E-01	2.13321E+02
16	4.24809E-02	0.00000E+00	0.00000E+00	1.64068E-02	4.88079E-01	4.90250E-02	9.60530E-03	0.00000E+00	9.99858E-01	6.54460E+02
17	4.44206E-02	0.00000E+00	0.00000E+00	3.49796E-02	3.61281E-01	7.13371E-02	7.38100E-03	0.00000E+00	9.99929E-01	9.83535E+02
18	7.62656E-03	0.00000E+00	0.00000E+00	1.19793E-02	8.49243E-02	1.86373E-02	7.91847E-04	0.00000E+00	9.99947E-01	1.98435E+02
19	6.03732E-02	0.00000E+00	0.00000E+00	5.45344E-02	3.84512E-01	1.08973E-01	5.12044E-03	0.00000E+00	9.99934E-01	1.36955E+03
20	8.00460E-02	0.00000E+00	0.00000E+00	9.21855E-02	4.34103E-01	1.65381E-01	6.10209E-03	0.00000E+00	9.99962E-01	1.80719E+03
21	9.04905E-02	0.00000E+00	0.00000E+00	1.38592E-01	4.72778E-01	2.21791E-01	6.44968E-03	0.00000E+00	9.99966E-01	2.32819E+03
22	4.97560E-02	0.00000E+00	0.00000E+00	1.38290E-01	3.40708E-01	1.87232E-01	4.79032E-04	0.00000E+00	9.99972E-01	1.19743E+03
23	5.37793E-02	0.00000E+00	0.00000E+00	1.67724E-01	2.91613E-01	2.19991E-01	7.07800E-04	0.00000E+00	9.99990E-01	1.94366E+03
24	3.80490E-02	0.00000E+00	0.00000E+00	1.57916E-01	1.81494E-01	1.94401E-01	1.04833E-03	0.00000E+00	9.99980E-01	1.38260E+03
25	4.97456E-02	0.00000E+00	0.00000E+00	2.04934E-01	2.57498E-01	2.47260E-01	6.82016E-03	0.00000E+00	9.9992E-01	1.79307E+03
26	4.95609E-02	0.00000E+00	0.00000E+00	2.17122E-01	2.83262E-01	2.61348E-01	4.40888E-03	0.00000E+00	9.9990E-01	2.18276E+03
27	1.11854E-01	0.00000E+00	0.00000E+00	3.29462E-01	5.93507E-01	4.37414E-01	2.97007E-03	0.00000E+00	9.99988E-01	3.56807E+03
28	8.43217E-02	0.00000E+00	0.00000E+00	4.10278E-01	5.43800E-01	4.93261E-01	2.94182E-04	0.00000E+00	9.99997E-01	4.25062E+03
29	6.30480E-02	0.00000E+00	0.00000E+00	4.52875E-01	5.8420E-01	5.14511E-01	3.26792E-04	0.00000E+00	9.99998E-01	4.42050E+03
30	3.18592E-02	0.00000E+00	0.00000E+00	4.37545E-01	4.96329E-01	4.68420E-01	2.18530E-04	0.00000E+00	9.99999E-01	3.12929E+03
31	3.24106E-02	0.00000E+00	0.00000E+00	5.64425E-01	6.75930E-01	5.95137E-01	4.07611E-04	0.00000E+00	1.00000E+00	5.26622E+03
32	1.00056E-02	0.00000E+00	0.00000E+00	4.67961E-01	5.48587E-01	4.77137E-01	2.19075E-04	0.00000E+00	1.00000E+00	2.61790E+03
33	4.47968E-03	0.00000E+00	0.00000E+00	4.23472E-01	4.71635E-01	4.73255E-01	1.72599E-04	0.00000E+00	1.00000E+00	1.84689E+03
34	1.25252E-03	0.00000E+00	0.00000E+00	2.46693E-01	1.96646E-01	2.47723E-01	6.77675E-05	0.00000E+00	1.00000E+00	6.83769E+02
35	4.26044E-03	0.00000E+00	0.00000E+00	5.73067E-01	7.00457E-01	5.75859E-01	4.91004E-04	0.00000E+00	9.99976E-01	4.07592E+03
36	2.27007E-03	0.00000E+00	0.00000E+00	6.62640E-01	7.50960E-01	6.62767E-01	1.02876E-03	0.00000E+00	1.00002E+00	5.09410E+03
37	6.60660E-04	0.00000E+00	0.00000E+00	6.35059E-01	7.27855E-01	6.33424E-01	1.34021E-03	0.00000E+00	9.99990E-01	4.12800E+03
38	1.92604E-04	0.00000E+00	0.00000E+00	5.67086E-01	6.76936E-01	5.65104E-01	1.50201E-03	0.00000E+00	9.99993E-01	2.96344E+03
39	8.85917E-05	0.00000E+00	0.00000E+00	5.65499E-01	6.76864E-01	5.62888E-01	2.05715E-03	0.00000E+00	9.9992E-01	2.85792E+03
40	4.98109E-05	0.00000E+00	0.00000E+00	6.29603E-01	7.26966E-01	6.24897E-01	3.95795E-03	0.00000E+00	1.00000E+00	3.62105E+03
41	2.06471E-05	0.00000E+00	0.00000E+00	6.77104E-01	7.62347E-01	6.68009E-01	8.19098E-03	0.00000E+00	1.00002E+00	4.34746E+03
42	5.23748E-06	0.00000E+00	0.00000E+00	6.17649E-01	7.21436E-01	6.06127E-01	1.07762E-02	0.00000E+00	1.00001E+00	3.32443E+03
43	2.17410E-06	0.00000E+00	0.00000E+00	6.58032E-01	7.48857E-01	6.35630E-01	2.14720E-02	0.00000E+00	9.99985E-01	3.80572E+03
44	5.51670E-07	0.00000E+00	0.00000E+00	5.86896E-01	7.09295E-01	5.59420E-01	2.68203E-02	0.00000E+00	9.99988E-01	2.74279E+03
45	2.01157E-07	0.00000E+00	0.00000E+00	5.76601E-01	7.17526E-01	5.38014E-01	3.80181E-02	0.00000E+00	9.9992E-01	2.34960E+03
46	9.26385E-08	0.00000E+00	0.00000E+00	7.48832E-01	9.86241E-01	7.69977E-04	7.48016E-01	0.00000E+00	1.00001E+00	5.10748E+03
47	1.72727E-07	0.00000E+00	0.00000E+00	8.54726E-07	3.99410E-02	1.38851E-06	1.60277E-11	0.00000E+00	1.00000E+00	4.15119E-02
48	2.88594E-06	0.00000E+00	0.00000E+00	7.40927E-06	2.25052E-02	9.21377E-06	1.22446E-10	0.00000E+00	1.00000E+00	2.70375E-01
49	3.74544E-06	0.00000E+00	0.00000E+00	2.46315E-02	3.94171E-02	2.20366E-02	3.22683E-08	0.00000E+00	9.99993E-01	6.28013E+01
50	1.05979E-05	0.00000E+00	0.00000E+00	3.24092E-03	4.04268E-02	3.04688E-03	7.72649E-08	0.00000E+00	9.99974E-01	4.89771E+01
51	9.44495E-05	0.00000E+00	0.00000E+00	2.13597E-02	2.72977E-02	2.07489E-02	6.82649E-07	0.00000E+00	9.99990E-01	2.11378E+02

Figure 5-4. (continued)

52 3.70708E-04 0.00000E+00 0.00000E+00 0.00000E+00 1.50685E-02 3.41422E-02 1.47876E-02 5.12554E-07 0.00000E+00 9.99963E-01 1.83080E+02
53 4.70194E-04 0.00000E+00 0.00000E+00 0.00000E+00 2.65328E-02 4.40269E-02 2.55833E-02 8.47495E-07 0.00000E+00 9.99958E-01 4.24627E+02
54 7.92362E-04 0.00000E+00 0.00000E+00 0.00000E+00 4.02401E-02 5.85836E-02 3.98661E-02 2.01883E-06 0.00000E+00 9.99924E-01 3.52561E+02
55 2.34128E-03 0.00000E+00 0.00000E+00 0.00000E+00 5.48699E-02 8.34239E-02 5.57148E-02 3.57540E-06 0.00000E+00 9.99849E-01 4.59987E+02
56 3.04634E-03 0.00000E+00 0.00000E+00 0.00000E+00 2.14583E-02 6.32695E-02 3.68772E-02 1.76817E-06 0.00000E+00 9.99734E-01 1.99410E+02
57 8.44820E-03 0.00000E+00 0.00000E+00 0.00000E+00 3.65452E-01 8.37180E-02 3.71531E-01 3.81814E-05 0.00000E+00 9.99957E-01 1.67425E+03
58 1.65855E-02 0.00000E+00 0.00000E+00 0.00000E+00 1.10912E-01 1.14813E-01 1.25186E-01 1.56456E-05 0.00000E+00 9.99717E-01 8.61328E+03
59 3.62709E-02 0.00000E+00 0.00000E+00 0.00000E+00 1.47007E-01 1.80455E-01 1.80237E-01 3.74178E-05 0.00000E+00 9.99815E-01 1.16306E+03
60 4.89721E-02 0.00000E+00 0.00000E+00 0.00000E+00 1.58311E-01 1.91345E-01 2.04772E-01 5.83551E-05 0.00000E+00 9.99981E-01 1.17984E+03
61 8.21703E-02 0.00000E+00 0.00000E+00 0.00000E+00 3.07709E-01 2.69900E-01 3.86420E-01 3.96719E-04 0.00000E+00 1.00002E+00 2.05842E+03
62 7.83336E-02 0.00000E+00 0.00000E+00 0.00000E+00 3.83395E-01 3.14010E-01 4.58135E-01 1.19747E-03 0.00000E+00 9.99974E-01 2.26470E+03
63 1.04088E-01 0.00000E+00 0.00000E+00 0.00000E+00 8.21272E-01 5.72318E-01 9.03380E-01 1.78767E-02 0.00000E+00 1.00001E+00 6.11027E+03
64 1.33837E-02 0.00000E+00 0.00000E+00 0.00000E+00 9.01911E-01 5.33290E-01 8.49579E-01 6.27827E-02 0.00000E+00 9.99999E-01 4.81610E+03
65 2.53643E-03 0.00000E+00 0.00000E+00 0.00000E+00 6.69769E-01 5.71192E-01 6.95117E-01 1.74604E-01 0.00000E+00 1.00000E+00 4.81433E+03
66 2.18620E-04 0.00000E+00 0.00000E+00 0.00000E+00 6.96332E-01 6.49680E-01 2.96805E-01 3.97189E-01 0.00000E+00 1.00000E+00 5.12885E+03
67 2.21792E-05 0.00000E+00 0.00000E+00 0.00000E+00 3.02616E-01 5.37733E-01 2.26954E-03 5.00147E-02 0.00000E+00 1.00000E+00 1.57279E+03
68 1.19278E-05 0.00000E+00 0.00000E+00 0.00000E+00 5.23002E-02 3.28190E-01 2.26954E-03 5.00147E-02 0.00000E+00 1.00000E+00 1.15520E+02
69 1.56127E-05 0.00000E+00 0.00000E+00 0.00000E+00 4.67068E-03 6.28329E-02 6.55553E-06 4.67960E-03 0.00000E+00 1.00000E+00 1.02465E+00
70 1.34653E+00 0.00000E+00 0.00000E+00 0.00000E+00 1.73861E+01 8.15628E-01 1.67889E+01 1.88605E+00 0.00000E+00 1.00000E+00 1.20333E+05
grp. lift outflow rgt outflow bot outflow top outflow left outflow rgt netflow bot netflow top netflow tot leakage collisions
1 0.00000E+00 1.57426E-08 2.94290E-10 5.72945E-09 0.00000E+00 1.57426E-08 2.94290E-10 5.72945E-09 2.17663E-08 2.18834E-06
2 0.00000E+00 1.02965E-08 1.21779E-10 3.23003E-09 0.00000E+00 1.02965E-08 1.21779E-10 3.23003E-09 1.36487E-08 3.00857E-06
3 0.00000E+00 3.78478E-08 4.23637E-10 1.22570E-08 0.00000E+00 3.78478E-08 4.23637E-10 1.22570E-08 5.05284E-08 8.38707E-06
4 0.00000E+00 5.2872E-08 3.94206E-10 1.19839E-08 0.00000E+00 5.2872E-08 3.94206E-10 1.19839E-08 4.76652E-08 6.29538E-06
5 0.00000E+00 3.62128E-07 4.37594E-09 1.34339E-07 0.00000E+00 3.62128E-07 4.37594E-09 1.34339E-07 5.00843E-07 5.86537E-05
6 0.00000E+00 5.11446E-08 6.15954E-10 1.79881E-08 0.00000E+00 5.11446E-08 6.15954E-10 1.79881E-08 6.97487E-08 1.33790E-05
7 0.00000E+00 7.37518E-07 3.88969E-09 2.54860E-07 0.00000E+00 7.37518E-07 3.88969E-09 2.54860E-07 9.6267E-07 1.24136E-04
8 0.00000E+00 1.96973E-06 1.15785E-08 6.88042E-07 0.00000E+00 1.96973E-06 1.15785E-08 6.88042E-07 2.66935E-06 2.60261E-04
9 0.00000E+00 2.11154E-08 2.11154E-08 1.85276E-06 0.00000E+00 2.11154E-08 1.85276E-06 0.00000E+00 7.06518E-06 5.11884E-04
10 0.00000E+00 1.06461E-05 5.4884E-08 3.89116E-06 0.00000E+00 1.06461E-05 5.4884E-08 3.89116E-06 1.45627E-05 9.95217E-04
11 0.00000E+00 1.24723E-05 3.78112E-08 4.60697E-06 0.00000E+00 1.24723E-05 3.78112E-08 4.60697E-06 1.71170E-05 1.79968E-03
12 0.00000E+00 5.1562E-05 1.09393E-07 2.10644E-05 0.00000E+00 5.1562E-05 1.09393E-07 2.10644E-05 7.63300E-05 5.48324E-03
13 0.00000E+00 1.80655E-04 2.38455E-07 7.20063E-05 0.00000E+00 1.80655E-04 2.38455E-07 7.20063E-05 2.52900E-04 2.43091E-02
14 0.00000E+00 1.08191E-04 5.94738E-08 4.33878E-05 0.00000E+00 1.08191E-04 5.94738E-08 4.33878E-05 1.51638E-04 7.97217E-03
15 0.00000E+00 9.98789E-05 1.33087E-07 4.05415E-05 0.00000E+00 9.98789E-05 1.33087E-07 4.05415E-05 1.40553E-04 3.28041E-02
16 0.00000E+00 1.68907E-04 1.73725E-07 7.19892E-05 0.00000E+00 1.68907E-04 1.73725E-07 7.19892E-05 2.41070E-04 1.14530E-01
17 0.00000E+00 4.69676E-04 2.3950E-07 2.03382E-04 0.00000E+00 4.69676E-04 2.3950E-07 2.03382E-04 6.73281E-04 1.23244E-01
18 0.00000E+00 1.21818E-04 6.42783E-08 5.36401E-05 0.00000E+00 1.21818E-04 6.42783E-08 5.36401E-05 1.75522E-04 2.12333E-02
19 0.00000E+00 5.50599E-04 1.49268E-07 2.50829E-04 0.00000E+00 5.50599E-04 1.49268E-07 2.50829E-04 8.01578E-04 1.85371E-01
20 0.00000E+00 4.98767E-04 1.32533E-07 2.37978E-04 0.00000E+00 4.98767E-04 1.32533E-07 2.37978E-04 7.36877E-04 3.03029E-01
21 0.00000E+00 5.52496E-04 9.97690E-08 2.74831E-04 0.00000E+00 5.52496E-04 9.97690E-08 2.74831E-04 8.27427E-04 4.32912E-01
22 0.00000E+00 2.16622E-04 3.40688E-08 1.10238E-04 0.00000E+00 2.16622E-04 3.40688E-08 1.10238E-04 3.26894E-04 2.69975E-01
23 0.00000E+00 5.29071E-04 4.59202E-08 2.72233E-04 0.00000E+00 5.29071E-04 4.59202E-08 2.72233E-04 8.01350E-04 3.11551E-01
24 0.00000E+00 3.29534E-04 3.19167E-08 1.72183E-04 0.00000E+00 3.29534E-04 3.19167E-08 1.72183E-04 5.01749E-04 2.38788E-01
25 0.00000E+00 3.89387E-04 4.38265E-08 2.06957E-04 0.00000E+00 3.89387E-04 4.38265E-08 2.06957E-04 5.96388E-04 3.42195E-01
26 0.00000E+00 6.01551E-04 3.85562E-08 3.22869E-04 0.00000E+00 6.01551E-04 3.85562E-08 3.22869E-04 9.28459E-04 3.70783E-01
27 0.00000E+00 5.91922E-04 6.18718E-08 3.27856E-04 0.00000E+00 5.91922E-04 6.18718E-08 3.27856E-04 9.19840E-04 1.08133E+00
28 0.00000E+00 6.66074E-04 5.95176E-08 3.75140E-04 0.00000E+00 6.66074E-04 5.95176E-08 3.75140E-04 1.04127E-03 1.08188E+00
29 0.00000E+00 6.87004E-04 5.06741E-08 3.94874E-04 0.00000E+00 6.87004E-04 5.06741E-08 3.94874E-04 1.08193E-03 1.23884E+00
30 0.00000E+00 4.82113E-04 3.58481E-08 2.81392E-04 0.00000E+00 4.82113E-04 3.58481E-08 2.81392E-04 7.63541E-04 9.30448E-01
31 0.00000E+00 8.11635E-04 6.90958E-08 4.84536E-04 0.00000E+00 8.11635E-04 6.90958E-08 4.84536E-04 1.29624E-03 1.83770E+00
32 0.00000E+00 3.80646E-04 3.03262E-08 2.29933E-04 0.00000E+00 3.80646E-04 3.03262E-08 2.29933E-04 6.10609E-04 1.05747E+00
33 0.00000E+00 2.61936E-04 1.89109E-08 1.59362E-04 0.00000E+00 2.61936E-04 1.89109E-08 1.59362E-04 4.21317E-04 8.09096E-01
34 0.00000E+00 9.61419E-05 7.77134E-09 5.86788E-05 0.00000E+00 9.61419E-05 7.77134E-09 5.86788E-05 1.54828E-04 3.08446E-01
35 0.00000E+00 5.75857E-04 4.15685E-08 3.56016E-04 0.00000E+00 5.75857E-04 4.15685E-08 3.56016E-04 9.31914E-04 1.92410E+00

Figure 5-4. (continued)

```

36 0.00000E+00 7.14641E-04 6.31678E-08 4.48106E-04 0.00000E+00 7.14641E-04 6.31678E-08 4.48106E-04 1.16281E-03 2.66542E+00
37 0.00000E+00 5.70628E-04 5.58736E-08 3.60870E-04 0.00000E+00 5.70628E-04 5.58736E-08 3.60870E-04 3.15554E-04 2.33245E+00
38 0.00000E+00 4.03385E-04 3.95797E-08 2.55791E-04 0.00000E+00 4.03385E-04 3.95797E-08 2.55791E-04 6.59215E-04 1.75385E+00
39 0.00000E+00 3.88434E-04 4.05672E-08 2.45384E-04 0.00000E+00 3.88434E-04 4.05672E-08 2.45384E-04 6.33859E-04 1.74830E+00
40 0.00000E+00 4.92660E-04 4.68606E-08 3.10264E-04 0.00000E+00 4.92660E-04 4.68606E-08 3.10264E-04 8.02971E-04 2.30321E+00
41 0.00000E+00 6.00327E-04 5.42822E-08 3.78308E-04 0.00000E+00 6.00327E-04 5.42822E-08 3.78308E-04 9.78690E-04 2.84532E+00
42 0.00000E+00 4.68478E-04 5.04211E-08 2.95663E-04 0.00000E+00 4.68478E-04 5.04211E-08 2.95663E-04 7.64191E-04 2.14588E+00
43 0.00000E+00 5.49560E-04 8.06125E-08 3.47565E-04 0.00000E+00 5.49560E-04 8.06125E-08 3.47565E-04 8.97206E-04 2.61644E+00
44 0.00000E+00 3.98933E-04 4.97531E-08 2.52959E-04 0.00000E+00 3.98933E-04 4.97531E-08 2.52959E-04 6.52902E-04 2.01662E+00
45 0.00000E+00 3.38914E-04 2.13728E-04 8.10414E-08 3.38914E-04 8.10414E-08 2.13728E-04 8.10414E-08 5.2723E-04 2.03924E+00
46 0.00000E+00 4.07014E-04 1.69698E-06 2.14502E-04 0.00000E+00 4.07014E-04 1.69698E-06 2.14502E-04 6.23213E-04 5.44231E+01
47 0.00000E+00 1.13490E-07 9.66203E-09 5.57783E-08 0.00000E+00 1.13490E-07 9.66203E-09 5.57783E-08 1.78930E-07 1.44629E-06
48 0.00000E+00 6.93044E-07 4.86262E-08 3.39642E-07 0.00000E+00 6.93044E-07 4.86262E-08 3.39642E-07 1.08131E-06 9.42603E-06
49 0.00000E+00 1.70578E-04 9.80336E-06 8.27819E-05 0.00000E+00 1.70578E-04 9.80336E-06 8.27819E-05 2.63163E-04 2.27127E-03
50 0.00000E+00 2.19548E-04 1.92244E-05 6.32931E-05 0.00000E+00 2.19548E-04 1.92244E-05 6.32931E-05 2.04471E-04 3.17532E-03
51 0.00000E+00 3.76938E-04 1.09001E-04 2.18360E-04 0.00000E+00 3.76938E-04 1.09001E-04 2.18360E-04 7.04299E-04 2.13319E-02
52 0.00000E+00 3.72203E-04 7.62866E-05 2.01970E-04 0.00000E+00 3.72203E-04 7.62866E-05 2.01970E-04 6.50460E-04 1.53109E-02
53 0.00000E+00 8.75939E-04 9.23210E-05 4.48932E-04 0.00000E+00 8.75939E-04 9.23210E-05 4.48932E-04 1.41719E-03 2.67629E-02
54 0.00000E+00 6.61476E-04 1.44685E-04 3.54847E-04 0.00000E+00 6.61476E-04 1.44685E-04 3.54847E-04 1.16101E-03 4.23490E-02
55 0.00000E+00 8.61406E-04 1.76777E-04 4.45223E-04 0.00000E+00 8.61406E-04 1.76777E-04 4.45223E-04 1.48341E-03 6.07897E-02
56 0.00000E+00 4.81708E-04 9.38748E-05 2.33153E-04 0.00000E+00 4.81708E-04 9.38748E-05 2.33153E-04 8.08736E-04 5.58990E-02
57 0.00000E+00 1.35407E-03 2.83516E-04 6.76241E-04 0.00000E+00 1.35407E-03 2.83516E-04 6.76241E-04 2.31383E-03 4.05518E-01
58 0.00000E+00 1.33946E-03 2.63008E-04 6.59761E-04 0.00000E+00 1.33946E-03 2.63008E-04 6.59761E-04 1.41441E-01
59 0.00000E+00 1.78909E-03 3.33308E-04 8.40528E-04 0.00000E+00 1.78909E-03 3.33308E-04 8.40528E-04 2.96293E-03 2.19968E-01
60 0.00000E+00 1.49070E-03 2.57522E-04 6.82410E-04 0.00000E+00 1.49070E-03 2.57522E-04 6.82410E-04 2.43063E-03 2.53319E-01
61 0.00000E+00 1.89545E-03 3.12362E-04 8.65088E-04 0.00000E+00 1.89545E-03 3.12362E-04 8.65088E-04 3.07290E-03 5.29814E-01
62 0.00000E+00 1.47409E-03 2.34461E-04 6.69315E-04 0.00000E+00 1.47409E-03 2.34461E-04 6.69315E-04 2.37787E-03 6.69592E-01
63 0.00000E+00 2.54668E-03 4.02172E-04 1.17786E-03 0.00000E+00 2.54668E-03 4.02172E-04 1.17786E-03 4.12671E-03 2.15407E+00
64 0.00000E+00 1.82128E-03 2.61083E-04 8.49530E-04 0.00000E+00 1.82128E-03 2.61083E-04 8.49530E-04 2.93189E-03 1.95488E+00
65 0.00000E+00 1.64268E-03 1.71522E-04 7.74912E-04 0.00000E+00 1.64268E-03 1.71522E-04 7.74912E-04 2.58911E-03 2.02833E+00
66 0.00000E+00 1.61357E-03 6.53285E-05 7.78416E-04 0.00000E+00 1.61357E-03 6.53285E-05 7.78416E-04 2.45731E-03 1.98131E+00
67 0.00000E+00 3.87290E-04 4.32177E-06 1.89186E-04 0.00000E+00 3.87290E-04 4.32177E-06 1.89186E-04 5.80798E-04 6.53427E-01
68 0.00000E+00 1.86114E-05 1.60498E-07 9.18758E-06 0.00000E+00 1.86114E-05 1.60498E-07 9.18758E-06 2.79595E-05 7.78259E-02
69 0.00000E+00 9.47925E-08 3.15837E-10 4.75800E-08 0.00000E+00 9.47925E-08 3.15837E-10 4.75800E-08 1.42688E-07 5.00035E-03
70 0.00000E+00 3.60872E-02 3.31512E-03 1.85780E-02 0.00000E+00 3.60872E-02 3.31512E-03 1.85780E-02 5.79803E-02 1.01290E+02

```

```

*** accumulated charge = 121.3182 min. *** charge increment = .2688min.
problem real time = 127.4218
cpu time = 120.0023
cumulative real time = 127.4218
*** accumulated charge = 121.3230 min. *** charge increment = .0048min.
charge analysis - - - -

```

	cpu	sys	tot
minutes	120.0023	1.3207	121.3230
seconds	7200.14	79.24	7279.38
percent	98.91	1.09	100.00

Figure 5-4. (continued)

**6.0 TORT: 3-DIMENSIONAL DISCRETE ORDINATES NEUTRON-PHOTON
TRANSPORT CODE**

[Section to be added in a later version of the MASH code system]

7.0 VISTA: A VARIABLE INPUT SOURCE TRANSFORMATION AND ASSEMBLY CODE FOR DORT FLUX DATA*

7.1 INTRODUCTION TO VISTA

7.1.1 Background

The Variable Inter Source Transformation and Assembly (VISTA) code processes directional fluences from a two-dimensional directional fluence file produced by DORT¹. These fluences in the DORT fluence file are modified and reformatted for use in the forward-adjoint folding process of the DRC module in MASH or for use in DOTTOR² to produce a boundary source for TORT³.

VISTA was developed by W. A. Rhoades to replace the VISA module of the Vehicle Code System (VCS)^{4,5} as the code for processing the scalar and angular fluences from DORT and the uncollided fluence file from GRTUNCL. An additional incentive for the development of VISTA was to have a code capable of processing the DORT directional flux files for eventual use in the TORT code. VISTA represents an improvement to VISA through increased generalization, and the addition of several new output options. In particular, VISTA can produce a file formatted for use in the DRC module of MASH, or a file formatted for use in DOTTOR (a code which transforms 2-D fluence information into a 3-D boundary source at or near the coupling surface for use in TORT). Furthermore, VISTA can copy old MASH or DOTTOR formatted files to new files, convert MASH formatted output files to DOTTOR formatted output files, and combine two MASH or DOTTOR formatted files into new DRC or DOTTOR formatted files.

The basic approach in VISTA is similar to that of an unpublished code from the 1960's named LIMBO. The exact authors of LIMBO are unknown, but they may have included R. D. Rodgers, F. R. Mynatt, and/or M. L. Gritzner. Credit for the preservation and availability of LIMBO belongs to J. V. Pace, III.

7.1.2 Method Used

Because of the large volume of data, it is not practical to produce properly-normalized directional fluence files from DORT. Further, when the GRTUNCL code is used to produce a first-collision source for DORT, the uncollided fluence, i.e., the fluence resulting from the particle flight before the first collision, is not included in the DORT output.

VISTA repairs the normalization problem by calculating the scalar fluence for each mesh cell, comparing this with the scalar fluence file produced by DORT, and normalizing the directional fluence such that it corresponds exactly to the DORT result. Then, the uncollided fluence from GRTUNCL is added to the directional fluence in the direction

*VISTA is an updated and undocumented version of the VISA program found in the following reference: W. A. Rhoades, M. B. Emmett, G. W. Morrison, J. V. Pace, III, and L. M. Petrie, "Vehicle Code System (VCS) User's Manual," ORNL-TM-4648, Oak Ridge National Laboratory, (August 1974).

applicable at each mesh cell. The processing can be restricted to a subset of the space mesh, reducing the volume of the output file.

As the new data are calculated, they are dumped to a random-access scratch file. Then, the data are retrieved in the order required by the requested output format and transferred to the output file. On some computer systems, reading and writing in the sorting step can proceed concurrently. For convenience, limited ability to transform between formats is included. Certain input and output files can be either formatted or unformatted as a convenience in using data shipped between computers through a network.

7.2 VISTA INPUT REQUIREMENTS

The following input cards are required to execute VISTA. Default values are in brackets ([]).

Title Card (72 alphanumeric character description)

INPUT DATA BLOCK 1

1\$ Array - Integer Control Parameters

NIP	number of radial intervals output
JPL	first axial interval output
JPU	last axial interval output
NED	print edit control parameter = 0 implies no effect > 0 implies print NED source groups
NORM	scalar fluence normalization control flag 0/1 = normalize/do not normalize to scalar fluence

- 5 ---

ISGRP	number of groups on uncollided fluence file = 0 implies use collided fluence only < 0 implies use uncollided fluence only
NFLSV	logical unit number of scalar fluence input, [1]
NAFT	logical unit number of angular fluence input, [2]
NUNCL	logical unit number of uncollided fluence input, [3]
NDATA	logical unit number of source output, [4]

- 10 ---

N5	logical unit number for card input, [5]
N6	logical unit number for printed output, [6]
NJ1	first axial interval input control flag = 0 implies set NJ1 = 1 > 0 implies first axial interval input
NJM	last axial interval input control flag

= 0 implies set NJM = JM
 > 0 implies last axial interval input
NAFTI NAFT missing groups control flag
 < 0 implies first NAFTI groups = 1.0, all others = 0.0
 = 0 implies no effect
 > 0 implies number of groups missing at beginning of NAFT

- 15 ---

NTYPE fluence file output option control flag
 = 0 implies process DORT files on NFLSV, NAFT, NUNCL into MASH output on NDATA
 = 1 implies process DORT files on NFLSV, NAFT, NUNCL into DOTTOR output on NDATA
 = 10 implies copy MASH output file on NFLSV to a new MASH output file on NDATA
 = 11 implies copy DOTTOR output file on NFLSV to a new DOTTOR output file on NDATA
 = 21 implies convert MASH output file on NFLSV to a DOTTOR output file on NDATA
 = 30 implies combine MASH output files on NUNCL and NFLSV to a new MASH output file on NDATA
 = 31 implies combine DOTTOR output files on NUNCL and NFLSV to a new DOTTOR output file on NDATA

NEUI last neutron group control flag
 (required if NGAMX > 0 and NTYPE = 0 or 1)
 < 0 implies gamma output only

NGAMX initial missing gamma group control flag
 = 0 implies no effect
 > 0 implies NGAMX initial gamma groups missing on all input files (NFLSV, NAFT, and NUNCL)

= 0 implies no effect
 > 0 implies NGAMX initial gamma groups missing on all input files (NFLSV, NAFT, and NUNCL)

= 0 implies no effect
 > 0 implies NGAMX initial gamma groups missing on input file NUNCL

] — NTYPE=0 or 1

] — NTYPE=30 or 31

E (terminate array with "E")

T (terminate block with "T") [T always required]

INPUT DATA BLOCK 2 [omit data block if NTYPE 10]

2* Array

SH height of point source
HSA cosine of angle with z axis into which source is emitted

XNEUT NFLSV fluence file multiplier (if NTYPE = 30 or 31) [1.0]
XGAM NUNCL fluence file multiplier (if NTYPE = 30 or 31) [1.0]

E (terminate array with "E")

4\$ Array

IVAL values of radial intervals to be output (NIP entries)

T (terminate block with "T") [T always required]

7.3 VISTA INPUT DATA NOTES

Except for the title card, all data are read using the FIDO input system. A detailed description of the FIDO input system is given in Appendix A. Data arrays are entered in blocks, each terminated by a "T". Unused data arrays (e.g., 2* and 4\$ if NTYPE = 10) are not entered, but a "T" must still be entered to signal the termination of each block.

NIP The number of radial intervals output should encompass the TORT geometry for a DOTTOR formatted source file. At present, the DRC module in MASH only uses one radial interval for the source. Therefore, the value for NIP is usually set to one, although it is not required to be just one. It should be noted that a new version of DRC is in the testing stage that will allow interpolation in the DORT radial mesh and then NIP will have the same meaning for MASH as it does for DOTTOR.

NFLSV, NAFT, and NUNCL Logical unit numbers for these input fluence files specified less than zero (i.e., negative entries) imply FORMATTED or BCD files instead of binary files.

JPL and JPU The output axial intervals must be equal to, or a subset of, the input axial intervals (NJ1 and NJM) from the DORT file. These intervals should also encompass the TORT or MASH geometry in the Z direction.

NED This parameter controls the print of the output source file by group. Care should be taken in using this control flag because it could produce large amounts of output.

NJ1 and NJM These parameters **must** correspond to the parameters JDIRF and JDIRL in the 62\$ array of DORT. These parameters in DORT give the axial intervals that are written out on the directional fluence file. Consequently, the same NJ1 and NJM values **must** be read as input into VISTA.

NAFTI This parameter is primarily used to tell the number of initial groups on NAFT which had a zero source. For instance, if the initial source distribution used in GRTUNCL and DORT did not have any values in the first eight groups, then NAFTI would equal eight (assuming no upscatter).

NEUI This parameter is used to output a gamma only file from a coupled neutron-gamma file if input negative.

NOTE: If you execute a coupled neutron-gamma DORT problem with all neutron source groups zero and with or without gamma source groups zero, you must output a full neutron-gamma coupled source file. You cannot output a gamma only source file.

NGAMX This parameter is only used to indicate missing (or deleted) gamma groups from the input fluence files.

SH The source height entered here must correspond to the source height used in GRTUNCL and/or DORT.

IVAL This parameter should correspond to the NIP interval(s) of the DORT mesh required to encompass the TORT geometry, or the radial distance for the source for MASH required by the DRC module.

7.4 VISTA INPUT FLUENCE FILE FORMAT

As stated earlier, VISTA's primary function is to process, modify, and reformat directional fluence files from the DORT code into a suitable format for use in either MASH or DOTTOR. Also, VISTA can perform a number of utility functions (i.e., copy, convert, and combine) on previously processed VISTA files. Consequently, VISTA will read several different types of input file formats depending on the value of NTYPE. For this section, only the primary function of VISTA will be addressed. The MASH formatted source file will be addressed in the next section, and the interested reader should consult the DOTTOR manual (Ref. 2) for information on the DOTTOR formatted source file.

To accomplish its primary function, VISTA reads a DOT IV formatted file - referred to as the VARSOR format in this document. Both the uncollided fluence on unit NUNCL and the scalar and directional fluence files on NFLSV and NAFT, respectively, are written in this format. The VARSOR format is defined in the following manner:

```

C                                                    -VSOR0010
C                                                    VSOR0020
C***** VSOR0030
C          REVISED 10 NOV 76                        -VSOR0040
C                                                    -VSOR0050
CF      VARSOR                                     -VSOR0060
CE      VARIABLE MESH SOURCE MOMENT DATA          -VSOR0070
C                                                    -VSOR0080
C***** VSOR0090
C                                                    VSOR0100
CD      ORDER OF GROUPS IS BY DECREASING ENERGY  VSOR0110
CD      I IS THE FIRST-DIMENSION INDEX             VSOR0120
CD      J IS THE SECOND-DIMENSION INDEX            VSOR0130
CD      JM=1 FOR 1-DIMENSIONAL GEOMETRY            VSOR0140
CD      IF ISOP.GT.0, SOURCE IS FIRST-COLLISION TYPE VSOR0150
C                                                    VSOR0160
C----- VSOR0170
CS      FILE STRUCTURE                             -VSOR0180
CS                                                    -VSOR0190

```


CS	RECORD TYPE	PRESENT IF	-VSOR0200
CS	-----	-----	-VSOR0210
CS	FILE IDENTIFICATION	ALWAYS	-VSOR0220
CS	FILE LABEL	ALWAYS	-VSOR0230
CS	FILE CONTROL	ALWAYS	-VSOR0240
CS	FILE INTEGER PARAMETERS	ALWAYS	-VSOR0250
CS			-VSOR0260
CS	***** (REPEAT OVER ALL GROUPS)		-VSOR0270
CS *	SOURCE MOMENTS	ALWAYS	-VSOR0280
CS	*****		-VSOR0290
C			-VSOR0300
CS	***** (REPEAT OVER ALL GROUPS)		-VSOR0310
CS *	SCALAR UNCOLLIDED FLUX	ISOP.GT.0	-VSOR0320
CS	*****		-VSOR0330
C			-VSOR0340
C			VSOR0350
C			VSOR0360
C			VSOR0370
C			VSOR0380
CR	FILE IDENTIFICATION		-VSOR0390
C			-VSOR0400
CL	HNAME,(HUSE(I),I=1,2),IVERS		-VSOR0410
C			-VSOR0420
CW	1+3*MULT=NUMBER OF WORDS		-VSOR0430
C			-VSOR0440
CD	HNAME	HOLLERITH FILE NAME - VARSOR - (A6)	-VSOR0450
CD	HUSE(I)	HOLLERITH USER IDENTIFICATION - (A6)	-VSOR0460
CD	IVERS	FILE VERSION NUMBER	-VSOR0470
CD	MULT	DOUBLE PRECISION PARAMETER	-VSOR0480
CD		1- A6 WORD IS SINGLE WORD	-VSOR0490
CD		2- A6 WORD IS DOUBLE PRECISION WORD	-VSOR0500
C			-VSOR0510
C			VSOR0520
C			VSOR0530
C			VSOR0540
C			VSOR0550
C			-VSOR0560
CR	FILE LABEL		-VSOR0570
C			-VSOR0580
CL	DATE,USER,CHARGE,CASE,TIME,(TTTL(I),I=1,12)		-VSOR0590
C			-VSOR0600
CW	17*MULT=NUMBER OF WORDS		-VSOR0610
C			-VSOR0620
CD	DATE	AS PROVIDED BY TIMER OPTION 4 - (A6)	-VSOR0630
CD	USER	AS PROVIDED BY TIMER OPTION 5 - (A6)	-VSOR0640
CD	CHARGE	AS PROVIDED BY TIMER OPTION 6 - (A6)	-VSOR0650
CD	CASE	AS PROVIDED BY TIMER OPTION 7 - (A6)	-VSOR0660
CD	TIME	AS PROVIDED BY TIMER OPTION 8 - (A6)	-VSOR0670
CD	TTTL(I)	TITLE PROVIDED BY USER - (A6)	-VSOR0680
C			-VSOR0690
C			VSOR0700
C			VSOR0710
C			VSOR0720

C		VSOR0730
CR	FILE CONTROL	VSOR0740
C		-VSOR0750
CD	IGM, NEUT, JM, LM, IMA, MMA, ISM, IMSISM, ISOP, (IDUM(N), N=1, 16)	-VSOR0760
C		-VSOR0770
CW	25=NUMBER OF WORDS	-VSOR0780
C		-VSOR0790
CD	IGM NUMBER OF ENERGY GROUPS	-VSOR0800
CD	NEUT LAST NEUTRON GROUP	-VSOR0810
CD	(IGM IF ALL NEUTRONS, 0 IF ALL GAMMA)	-VSOR0820
CD	JM NUMBER OF SECOND-DIMENSION (J) INTERVALS	-VSOR0830
CD	LM MAXIMUM LENGTH OF MOMENT EXPANSION	-VSOR0840
CD	IMA MAXIMUM NUMBER OF FIRST-DIMENSION INTERVALS	-VSOR0850
CD	MMA NUMBER OF BOUNDARY DIRECTIONS	-VSOR0860
CD	ISM NUMBER OF I-BOUNDARY SETS	-VSOR0870
CD	IMSISM TOTAL NUMBER OF I-INTERVALS, ALL I-SETS	-VSOR0880
CD	ISOPUN COLLIDED FLUX FLAG	-VSOR0890
CD	0 - NO UNCOLLIDED FLUX RECORDS PRESENT	-VSOR0900
CD	1 - UNCOLLIDED FLUX RECORDS PRESENT	-VSOR0910
CD	IDUM(I) ARRAY SET TO 0	-VSOR0920
C		-VSOR0930
C		VSOR0940
C		VSOR0950
C		VSOR0960
C		VSOR0970
CR	FILE INTEGER PARAMETERS	-VSOR0980
C		-VSOR0990
CL	(LMBIG(IG), IG=1, IGM),	-VSOR1000
CL	*(IMBIS(IS), IS=1, ISM), (ISET(J), J=1, JM)	-VSOR1010
C		-VSOR1020
CW	IGM+ISM+JM=NUMBER OF WORDS	-VSOR1030
C		-VSOR1040
CD	LMBIG(IG) LENGTH OF MOMENT EXPANSION FOR GROUP IG	-VSOR1050
CD	IMBIS(IS) NUMBER OF INTERVALS IN ISET IS	-VSOR1060
CD	ISET(J) I-SET ASSIGNED TO INTERVAL J	-VSOR1070
C		-VSOR1080
C		VSOR1090
C		VSOR1100
C		VSOR1110
C		VSOR1120
CR	SOURCE MOMENTS	VSOR1130
C		-VSOR1140
CL	((SORM(I, L), I=1, IMS), L=1, LMS)	-VSOR1150
C		-VSOR1160
CW	IMS*LMS=NUMBER OF WORDS	-VSOR1170
C		-VSOR1180
C	DO 1 J=1, JM	-VSOR1190
C	1 READ(N) *LIST AS ABOVE*	-VSOR1200
C		-VSOR1210
CD	SORM SOURCE BY INTERVAL AND MOMENT INDEX	-VSOR1220
CD	IMS IMBIS(IS) FOR IS CORRESPONDING TO J	-VSOR1230
CD	LMS LMBIG(IG)	-VSOR1240
C		-VSOR1250

C	-----	VSOR1260
C		VSOR1270
C		VSOR1280
C	-----	VSOR1290
CR	SCALAR UNCOLLIDED FLUX	-VSOR1300
C		-VSOR1310
CL	(FLUM(I),I=1,IMS)	-VSOR1320
C		-VSOR1330
CW	IMS=NUMBER OF WORDS	-VSOR1340
C		-VSOR1350
C	DO 1 J=1,JM	-VSOR1360
C 1	READ(N) *LIST AS ABOVE*	-VSOR1370
C		-VSOR1380
CD	FLUX UNCOLLIDED FLUX BY INTERVAL	-VSOR1390
C		-VSOR1400
C	-----	VSOR1410
C		VSOR1420
C		VSOR1430
C		VSOR1440
C		VSOR1450
C	END	VSOR1460

7.5 VISTA OUTPUT FILES

The VISTA code produces two types of output file - a DOTTOR formatted source file and a MASH formatted source file. The DOTTOR formatted source file will not be addressed in this manual, and the interested reader should consult Reference 2. The MASH formatted source file is as follows:

Record 1: TITLE, TDOT - 144 Alphanumeric Characters

Record 2:

MM	-	Number of quadrature directions
IM	-	Number of radial intervals
JM	-	Number of axial intervals
IGM	-	Number of energy groups
IGP	-	Number of energy groups plus 1
MMDN	-	Number of directions downward
NJP	-	Number of axial fluences
ISH	-	Height of source point
ISHA	-	Cosine of source angle (with Z-axis)
NIP	-	Number of radial fluences
JPL	-	Index of first J interval on file
JPU	-	Index of last J interval on file

11 additional VISTA input values not used in MASH

Record 3: IVAL - Array of radial interval numbers being output

Record 4: [MM values per array; 3*MM total values]

WT - Weights from DORT quadrature
 AMU - Mu's from DORT quadrature
 ETA - Eta's from DORT quadrature

Record 5: [NIP + NJP values]

R - Midpoints of radial bins
 Z - Midpoints of axial bins

Record 6 to END: [NANG*NJFLX values per record]
 [IGM records per radius, and NIFLX radii]

FLUX - Directional fluences

It should be noted that much of the information on the DOTTOR formatted source file is similar to the information given above in the MASH formatted source file.

7.6 LOGICAL UNIT REQUIREMENTS

Below is a listing of the files required to execute a VISTA case along with the default values used in the code. In setting up a VISTA case, efforts must be made for these units to be available.

1. Logical Unit NFLSV - DORT Scalar fluence input file
2. Logical Unit NAFT - DORT directional fluence input file
3. Logical Unit NUNCL - GRTUNCL uncollided fluence input file
4. Logical Unit NDATA - MASH or DOTTOR formatted output source file
5. Logical Unit 91 - SCRATCH
6. Logical Unit 6 - Printed Output
7. Logical Unit 5 - Card Input

Default logical unit assignments for the first four data files are 1, 2, 3, and 4.

NOTE: Logical unit numbers for the input fluence files (NFLSV, NAFT, NUNCL) specified less than zero (i.e., negative entries) imply FORMATTED or BCD files instead of binary files.

7.7 REFERENCES

1. W. A. Rhoades and R. L. Childs, "The DORT Two-Dimensional Discrete Ordinates Transport Code," Nuclear Science & Engineering 99, 1, pp. 88-89, (May 1988).
2. J. L. Thompson, M. B. Emmett, and H. L. Dodds, Jr., "Development and Evaluation of DOTTOR, A Computer Code to Couple Two-Dimensional to Three-Dimensional Discrete Ordinates Calculations," ORNL/TM-9919, Oak Ridge National Laboratory, (April 1986).
3. W. A. Rhoades and R. L. Childs, "The TORT Three-Dimensional Neutron/Photon Transport Code," ORNL-6268, Oak Ridge National Laboratory, (November 1987).
4. W. A. Rhoades, "Development of a Code System for Determining Radiation Protection of Armored Vehicles (The VCS Code)," ORNL-TM-4664, Oak Ridge National Laboratory, (October 1974).
5. W. A. Rhoades, M. B. Emmett, G. W. Morrison, J. V. Pace, III, and L. M. Petrie, "Vehicle Code System (VCS) User's Manual," ORNL-TM-4648, Oak Ridge National Laboratory, (August 1974).
6. J. O. Johnson, J. D. Drischler, and J. M. Barnes, "Analysis of the Fall-1989 Two-Meter Box Test Bed Experiments Performed at the Army Pulse Radiation Facility (APRF)," ORNL/TM-11777, Oak Ridge National Laboratory, (May 1991).

7.8 SAMPLE PROBLEM

The sample problem demonstrates the processing of the DORT and GRTUNCL fluence files from the calculation of the air-over-ground environment for the two-meter box experiments at 400 meters.⁶ Figure 7-1 depicts a simple diagram of which portion of the DORT geometry is being processed for output from VISTA. A complete listing of the input cards for the sample problem is given in Figure 7-2, and some selected output is shown in Figure 7-3.

In viewing Figure 7-2, the input illustrates; 1 radial interval output (NIP), DORT interval 13 as the first axial interval output (JPL), and DORT interval 25 as the last axial interval output (JPU). No source groups were printed (NED) and the output fluences were to be normalized to the scalar fluence (NORM). There were 69 energy groups (IGM), DORT interval 13 was the first axial interval input (NJ1), and DORT axial interval 25 was the last axial interval input (NJM). There were no groups missing in the input directional fluence file (NAFTI), 46 neutron energy groups (NEUI), and no initial gamma groups missing (NGAMX). A MASH formatted output source file was requested (NTYPE=0). All comments after the slash (/) are ignored in FIDO input and are only useful for quick identification of the input parameters. Finally, the VISTA sample input in Figure 7-2 shows a source height (from GRTUNCL) of 16.143 meters (SH) and a value of 50 for the DORT radial interval (IVAL).

The selected VISTA output shown in Figure 7-3 first illustrates the input parameters read in the first two data blocks along with some of the parameters obtained from the DORT input directional fluence files. The memory requirements are also given in this output. This

output is followed by an "angle number by DORT interval" array which represents the particular direction in the DORT quadrature of the uncollided component of the fluence. This array is followed by more information from the DORT directional fluence file, i.e., quadrature information, radial position of the interval IVAL (400 meters), and the axial positions corresponding to the axial intervals input (NJ1 and NJM) and output (JPL and JPU). Finally, the output illustrates the progress of the source output reformatting (and normalization if selected) by group. The source is written to the SCRATCH unit (91) and after completion written to the output unit NDATA. If source group edits (NED>0) had been requested, they would appear at this point. One check for proper execution of VISTA is by examining the scaling adjustment factors printed by group. These factors should be on the order of 10^{-2} or less if correct information (input) has been given and there is a reasonable degree of convergence in the DORT directional fluence files.

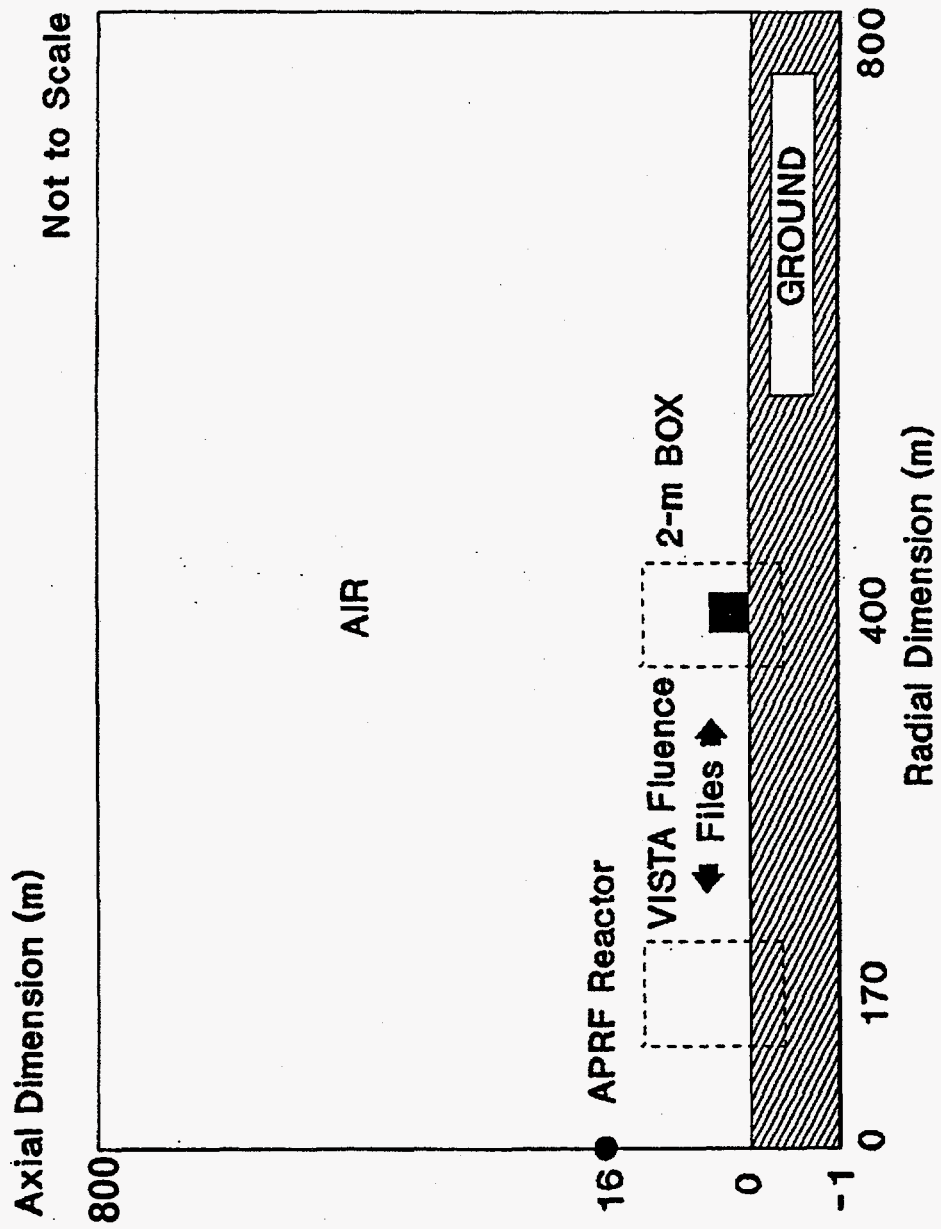


Figure 7-1. Schematic Diagram of the Air-Over-Ground Geometry Model Used in the VISTA Analysis

aprf aog/400m/simple topo/16.14m sh/34% ground moisture/10-24-89(a) air

1\$\$ 1 13 25 0 0 /nip,jpl,jpu,ned,norm
69 21 22 23 24 /isgrp,nflsv,naft,nuncl,ndata
5 6 13 25 0 /n5,n6,nj1,njm,naftm
0 46 0 /ntype,neui,ngamx
e t

2** 1614.3 0 e /sh,hsa

4\$\$ 50 e /ival
t

Figure 7-2. Sample VISTA Input for the
Two-Meter Box Air-Over-Ground Analysis.


```

* * * execution began on 11/11/96 (316) at time 10:21:00
***** visa 2.8.4 12 mar 93  ornl
*** workstation configuration compiled 11/08/96 14:06:03 user=jdd process= 17216 case=
'apr f aog/400m/simple topo/16.14m sh/34% ground moisture/10-24-89(a) air
1$ array 20 entries read
0t
parameter input .....
nlp = 1 no. radial intervals output
jpl = 13 first axial interval output
jpu = 25 last axial interval output
ned = 0 edit ned source groups
norm = 0 0: normalize to scalar flux; 1: do not
isgri = 69 no. of groups on nunci (0: use collided flux only) (negative: use uncollided only --- for testing)
nflsv = 21 logical no. scalar flux input default=1 (old visa output if ntype.ge.10)
naft = 22 logical no. directional flux input default=2 (may be 0 if ntype.ge.10)
nunci = 23 logical no. uncollided flux input default=3 (may be 0)
ndata = 24 logical no. source output default=4
10 ----
n5 = 5 logical no. standard input default=5
n6 = 6 logical no. standard output default=6
nj1 = 13 first axial interval input; 0 implies=1
njm = 25 last axial interval input; 0 implies=jm
nafti = 0 no. groups missing at beginning of naft (negative: first n groups=1, others 0 -- for testing)
ntype = 0 0/1: create vcs/torsed file; 10/11: copy vcs/torsed on nflsv; 21: vcs to torsed; 30/31: nunci+nflsv
neu1 = 46 last neutron group (rqd if ngamx.gt.0 and ntype=0,1) (negative: delete neutron output groups)
ngamx = 0 no. gamma groups added to group structure (ntype=0,1); initial groups missing on nunci (ntype=30,31)
---data processed from dort job: ' dort - apr f aog using saic 1989 angle-energy leakage source, mm = 240
parameters from old file .....
mm = 240 no. of directions
lm = 66 no. of radial intervals
jm = 98 no. of axial intervals
igm = 69 no. of energy groups maximum
derived parameters .....
lqi = 69 no. of energy groups input

lgo = 69 no. of energy groups output
*** 39738 data locations required vs. available 150000
2* array 6 entries read
4$ array 1 entries read
0t
sh = 1.61430E+03 height of point source (ntype.lt.10)
hsa = 0.00000E+00 not used (enter 0)
xneut= 1.00000E+00 nflsv multiplier (ntype=30or31, dflt=1)
xgam = 1.00000E+00 nunci multiplier (ntype=30or31, dflt=1)
weight emu eta ivalue r z
1 0.00000E+00 -6.41230E-02 -9.97942E-01 4.000000E+04 -1.75000E+01
2 1.02900E-03 -4.21582E-02 -9.97942E-01 -1.25000E+01
3 1.02900E-03 4.21582E-02 -9.97942E-01 -7.50000E+00
4 0.00000E+00 -1.42963E-01 -9.89728E-01 -3.75000E+00
5 3.07825E-03 -9.39923E-02 -9.89728E-01 -1.75000E+00
6 3.07825E-03 9.39923E-02 -9.89728E-01 -5.00000E-01
7 0.00000E+00 -2.29252E-01 -9.73367E-01 2.50000E+01
8 5.10200E-03 -1.50724E-01 -9.73367E-01 1.00000E+02
9 5.10200E-03 1.50724E-01 -9.73367E-01 2.00000E+02
10 0.00000E+00 -3.15291E-01 -9.48995E-01 3.69500E+02

```

Figure 7-3. Sample VISTA Output for the Two-Meter Box Air-Over-Ground Analysis.

6.19000E+02
8.49000E+02
1.02550E+03

11 7.08425E-03-2.07291E-01-9.48995E-01
12 7.08425E-03 2.07291E-01-9.48995E-01
13 0.00000E+00-3.99349E-01-9.16799E-01
14 9.01350E-03-2.62555E-01-9.16799E-01
15 9.01350E-03 2.62555E-01-9.16799E-01
16 0.00000E+00-4.72796E-01-8.81172E-01
17 5.63869E-03-4.11087E-01-8.81172E-01
18 3.16131E-03-1.43488E-01-8.81172E-01
19 3.16131E-03 1.43488E-01-8.81172E-01
20 5.63869E-03 4.11087E-01-8.81172E-01
21 0.00000E+00-5.37046E-01-8.43553E-01
22 6.41385E-03-4.66952E-01-8.43553E-01
23 3.59590E-03-1.62988E-01-8.43553E-01
24 3.59590E-03 1.62988E-01-8.43553E-01
25 6.41385E-03 4.66952E-01-8.43553E-01
26 0.00000E+00-5.98374E-01-8.01217E-01
27 7.14976E-03-5.20275E-01-8.01217E-01
28 4.00849E-03-1.81600E-01-8.01217E-01
29 4.00849E-03 1.81600E-01-8.01217E-01
30 7.14976E-03 5.20275E-01-8.01217E-01
31 0.00000E+00-6.56401E-01-7.54412E-01
32 7.84547E-03-5.70729E-01-7.54412E-01
33 4.39853E-03-1.99211E-01-7.54412E-01
34 4.39853E-03 1.99211E-01-7.54412E-01
35 7.84547E-03 5.70729E-01-7.54412E-01

228 3.83750E-03 1.85447E-01 1.11045E-01
229 5.40820E-03 5.31297E-01 1.11045E-01
230 4.06806E-03 8.05405E-01 1.11045E-01
231 5.15474E-03 9.70823E-01 1.11045E-01
232 0.00000E+00-9.99313E-01 3.70540E-02
233 5.17107E-03-9.76194E-01 3.70540E-02
234 4.06806E-03-8.09860E-01 3.70540E-02
235 5.42534E-03-5.34236E-01 3.70540E-02
236 3.84965E-03-1.86473E-01 3.70540E-02
237 3.84965E-03 1.86473E-01 3.70540E-02
238 5.42534E-03 5.34236E-01 3.70540E-02
239 4.06806E-03 8.09860E-01 3.70540E-02
240 5.17107E-03 9.76194E-01 3.70540E-02

*** accumulated charge = .0142 min. *** charge increment = .0140min.
total source for group 1 onto 91 with maximum scaling adjustment = .56928E-03
total source for group 2 onto 91 with maximum scaling adjustment = .67949E-04
total source for group 3 onto 91 with maximum scaling adjustment = .28193E-04
total source for group 4 onto 91 with maximum scaling adjustment = .34451E-04
total source for group 5 onto 91 with maximum scaling adjustment = .23651E-03
total source for group 6 onto 91 with maximum scaling adjustment = .19372E-04
total source for group 7 onto 91 with maximum scaling adjustment = .27144E-03
total source for group 8 onto 91 with maximum scaling adjustment = .39339E-04
total source for group 9 onto 91 with maximum scaling adjustment = .49651E-04
total source for group 10 onto 91 with maximum scaling adjustment = .14132E-03

Figure 7-3. (continued)

total source for group	11	onto	91	with	maximum	scaling	adjustment=	.59408E-03
total source for group	12	onto	91	with	maximum	scaling	adjustment=	.10741E-03
total source for group	13	onto	91	with	maximum	scaling	adjustment=	.51379E-04
total source for group	14	onto	91	with	maximum	scaling	adjustment=	.47356E-03
total source for group	15	onto	91	with	maximum	scaling	adjustment=	.35131E-03
total source for group	16	onto	91	with	maximum	scaling	adjustment=	.15110E-03
total source for group	17	onto	91	with	maximum	scaling	adjustment=	.25630E-04
total source for group	18	onto	91	with	maximum	scaling	adjustment=	.73910E-05
total source for group	19	onto	91	with	maximum	scaling	adjustment=	.41127E-04
total source for group	20	onto	91	with	maximum	scaling	adjustment=	.11218E-03
total source for group	21	onto	91	with	maximum	scaling	adjustment=	.57209E-03
total source for group	22	onto	91	with	maximum	scaling	adjustment=	.61786E-03
total source for group	23	onto	91	with	maximum	scaling	adjustment=	.11325E-03
total source for group	24	onto	91	with	maximum	scaling	adjustment=	.96202E-04
total source for group	25	onto	91	with	maximum	scaling	adjustment=	.13971E-03
total source for group	26	onto	91	with	maximum	scaling	adjustment=	.28884E-03
total source for group	27	onto	91	with	maximum	scaling	adjustment=	.45806E-03
total source for group	28	onto	91	with	maximum	scaling	adjustment=	.20999E-03
total source for group	29	onto	91	with	maximum	scaling	adjustment=	.17977E-03
total source for group	30	onto	91	with	maximum	scaling	adjustment=	.20760E-03
total source for group	31	onto	91	with	maximum	scaling	adjustment=	.20093E-03
total source for group	32	onto	91	with	maximum	scaling	adjustment=	.46849E-04
total source for group	33	onto	91	with	maximum	scaling	adjustment=	.14520E-03
total source for group	34	onto	91	with	maximum	scaling	adjustment=	.68426E-04
total source for group	35	onto	91	with	maximum	scaling	adjustment=	.25725E-03
total source for group	36	onto	91	with	maximum	scaling	adjustment=	.18382E-03
total source for group	37	onto	91	with	maximum	scaling	adjustment=	.10979E-03
total source for group	38	onto	91	with	maximum	scaling	adjustment=	.34451E-04
total source for group	39	onto	91	with	maximum	scaling	adjustment=	.33617E-04
total source for group	40	onto	91	with	maximum	scaling	adjustment=	.18096E-03
total source for group	41	onto	91	with	maximum	scaling	adjustment=	.12290E-02
total source for group	42	onto	91	with	maximum	scaling	adjustment=	.39923E-03
total source for group	43	onto	91	with	maximum	scaling	adjustment=	.12296E-02
total source for group	44	onto	91	with	maximum	scaling	adjustment=	.26330E-02
total source for group	45	onto	91	with	maximum	scaling	adjustment=	.42627E-02
total source for group	46	onto	91	with	maximum	scaling	adjustment=	.27406E-01
total source for group	47	onto	91	with	maximum	scaling	adjustment=	.95367E-06
total source for group	48	onto	91	with	maximum	scaling	adjustment=	.59605E-06
total source for group	49	onto	91	with	maximum	scaling	adjustment=	.71526E-06
total source for group	50	onto	91	with	maximum	scaling	adjustment=	.47684E-06
total source for group	51	onto	91	with	maximum	scaling	adjustment=	.11921E-05
total source for group	52	onto	91	with	maximum	scaling	adjustment=	.26226E-05
total source for group	53	onto	91	with	maximum	scaling	adjustment=	.59605E-06
total source for group	54	onto	91	with	maximum	scaling	adjustment=	.88215E-05
total source for group	55	onto	91	with	maximum	scaling	adjustment=	.27776E-04
total source for group	56	onto	91	with	maximum	scaling	adjustment=	.10729E-05
total source for group	57	onto	91	with	maximum	scaling	adjustment=	.23842E-05
total source for group	58	onto	91	with	maximum	scaling	adjustment=	.71526E-05
total source for group	59	onto	91	with	maximum	scaling	adjustment=	.32067E-04
total source for group	60	onto	91	with	maximum	scaling	adjustment=	.30637E-04
total source for group	61	onto	91	with	maximum	scaling	adjustment=	.13751E-03
total source for group	62	onto	91	with	maximum	scaling	adjustment=	.19246E-03
total source for group	63	onto	91	with	maximum	scaling	adjustment=	.35721E-03
total source for group	64	onto	91	with	maximum	scaling	adjustment=	.96762E-03
total source for group	65	onto	91	with	maximum	scaling	adjustment=	.63086E-03
total source for group	66	onto	91	with	maximum	scaling	adjustment=	.81182E-03
total source for group	67	onto	91	with	maximum	scaling	adjustment=	.22745E-03

Figure 7-3. (continued)

total source for group 68 onto 91 with maximum scaling adjustment= .13709E-04
total source for group 69 onto 91 with maximum scaling adjustment= .35763E-06
*** accumulated charge = .2872 min. *** charge increment = .2730min.

charge analysis	cpu	sys	tot
minutes	.0968	.1905	.2873
seconds	5.81	11.43	17.24
percent	33.70	66.30	100.00

**8.0 VISTA3D - A VARIABLE INPUT SOURCE TRANSFORMATION
AND ASSEMBLY CODE FOR TORT FLUX DATA**

[Section to be added in a later version of the MASH code system]

9.0 MORSE: A MULTIGROUP OAK RIDGE STOCHASTIC EXPERIMENT CODE*

9.1 INTRODUCTION TO MORSE

The Multigroup Oak Ridge Stochastic Experiment code (MORSE)¹ is a multipurpose neutron and gamma-ray transport Monte Carlo code. Some of its features include the ability to treat the transport of either neutrons or gamma rays or a coupled neutron and secondary gamma-ray problem. The MORSE code also incorporates multigroup cross sections, an option of solving either the forward or adjoint problem, and modular input-output, cross section, analysis, and geometry modules. MORSE contains time dependence for both shielding and criticality problems, an albedo option at any material boundary, a three-dimensional combinatorial geometry package, and several types of optional importance sampling. Finally, MORSE includes a set of debugging routines accessible from anywhere in the program.

Traditionally, Monte Carlo codes for solving neutron and gamma-ray transport problems have been separate codes. This has been due to the physics of the interaction processes and the corresponding cross-section information required. However, when multigroup cross sections are employed, the energy group to energy group transfers contain the cross sections for all processes. Also, for anisotropic scattering each group-to-group transfer has an associated angular distribution which is a weighted average over the various cross sections involved in the energy transfer process. Thus, these multigroup cross sections have the same format for both neutrons and gamma rays. In addition, the generation of secondary gamma rays may be considered as just another group-to-group transfer. Therefore, using multigroup cross sections, the logic of the random walk process (the process of being transported from one collision to another) is identical for both neutrons and gamma rays.

The use of multigroup cross sections in a Monte Carlo code means that the effort required to produce cross-section libraries is reduced. Coupled neutron gamma-ray cross-section libraries are available from the Radiation Shielding Information Center at Oak Ridge National Laboratory.

Cross sections may be read in either the DTF-IV² format or ANISN³ and DOT^{4,6} format. The ANISN/DOT formatted cross-section file may be in either fixed or free form. The auxiliary information giving the number of groups, elements, Legendre coefficients, etc., is used to produce the necessary probability tables needed by the random walk module. The possible transport cases that can be treated are neutron only, gamma ray only, coupled neutron-gamma ray, gamma ray from a coupled set, and fission, with all of the above options for either a forward or adjoint case and for isotropic or anisotropic scattering up to a P_{16} expansion of the angular distribution. The option of storing the Legendre coefficients for use in a next-event estimator is also provided.

While the capabilities and versatility of MORSE are well documented for applications to a wide variety of problems in both the forward and adjoint mode of operation, **in the MASH code system, MORSE is only used in adjoint mode for the analysis**

* M. B. Emmett, "The MORSE Monte Carlo Radiation Transport Code System," ORNL-4972 (1975), ORNL-4972/R1 (1983), ORNL-4972/R2 (1984), Oak Ridge National Laboratory

of the complex target description (vehicle) and to create the leakage tape for input to DRC2.

9.1.1 Theoretical Basis

Monte Carlo like discrete ordinates solves the Boltzmann transport equation to obtain the estimates of the neutron or gamma-ray fluence. The general time-dependent integro-differential form of the Boltzmann transport equation, the derivation of which can be regarded as a bookkeeping process that sets the net storage of particles within a differential element of phase space ($drdEd\Omega$) equal to the particle gains minus the particle losses in ($drdEd\Omega$) and leads to the following useful form:

$$\begin{aligned} \frac{1}{v} \frac{\partial}{\partial t} \Phi(r, E, \Omega, t) + \Omega \cdot \nabla \Phi(r, E, \Omega, t) + \Sigma_t(r, E) \Phi(r, E, \Omega, t) \\ = S(r, E, \Omega, t) + \int \int dE' d\Omega' \Sigma_s(r, E' \rightarrow E, \Omega' \rightarrow \Omega) \Phi(r, E', \Omega', t) \end{aligned} \quad (9-1)$$

where

(r, E, Ω, t) denotes the general seven-dimensional phase space,

r = position variable,

E = the particle's kinetic energy,

v = the particle's speed corresponding to its kinetic energy E ,

Ω = a unit vector which describes the particle's direction of motion,

t = time variable,

$$\Phi(r, E, \Omega, t) =$$

the time dependent angular fluence,

$$\Phi(r, E, \Omega, t) dEd\Omega =$$

the number of particles that cross a unit area normal to the Ω direction per unit time at the space point r and time t with energies in dE about E and with directions that lie within the differential solid angle $d\Omega$ about the unit vector Ω ,

$$\frac{1}{v} \frac{\partial}{\partial t} \Phi(r, E, \Omega, t) dEd\Omega =$$

net storage (gains minus losses) per unit volume and time at the space point r and time t of particles with energies in dE about E and with directions which lie in $d\Omega$ about Ω ,

$$\Omega \cdot \nabla \Phi(r, E, \Omega, t) dE d\Omega =$$

net convective loss per unit volume and time at the space point r and time t of particles with energies in dE about E and directions which lie in $d\Omega$ about Ω ,

$$\Sigma_t(r, E) =$$

the total cross section at the space point r for particles of energy E ,

$$\Sigma_t(r, E) \Phi(r, E, \Omega, t) dE d\Omega =$$

collision loss per unit volume and time at the space point r and time t of particles with energies in dE about E and directions which lie in $d\Omega$ about Ω ,

$$\Sigma_s(r, E' \rightarrow E, \Omega' \rightarrow \Omega) dE d\Omega =$$

the differential scattering cross section which describes the probability per unit path that a particle with energy E' and an initial direction Ω' undergoes a scattering collision at the space point r which places it into a new direction that lies in $d\Omega$ about Ω with a new energy in dE about E ,

$$\left[\iint \Sigma_s(r, E' \rightarrow E, \Omega' \rightarrow \Omega) \Phi(r, E, \Omega, t) dE' d\Omega' \right] dE d\Omega =$$

in-scattering gain per unit volume and time at the space point r and time t of particles with energies in dE about E and directions which lie in $d\Omega$ about Ω ,

$$S(r, E, \Omega, t) dE d\Omega =$$

source particles emitted per unit volume and time at the space point r and time t of particles with energies in dE about E and directions which lie in $d\Omega$ about Ω .

An effect of interest such as biological dose, energy deposition, or particle fluence (denoted by λ) for a given problem can be expressed in terms of the fluence field $\Phi(r, E, \Omega, t)$ and an appropriate response function $P^\Phi(r, E, \Omega, t)$ due to a unit angular fluence and is given by:

$$\lambda = \iiint P^\Phi(r, E, \Omega, t) \Phi(r, E, \Omega, t) dr dE d\Omega dt. \quad (9-2)$$

Consistent with the MORSE code, the energy dependence of Equation (9-1) is represented in terms of energy groups. A "group" form of Equation (9-1) is obtained by integrating each term with respect to the energy variable over the energy interval ΔE_g . MORSE solves the integral form of the Boltzmann transport equation. Section 4.10 of Reference 1 details the derivation of many integral forms of the Boltzmann transport equation and its adjoint. In this report only a summary of the two particular equations used for the forward and adjoint analysis will be given, and the interested user should consult Reference 1 for further details.

The solution of the forward integral transport equation by Monte Carlo generally involves a solution for $\chi_g(r, \Omega, t)$, referred to as the integral emergent particle density, i.e., the density of particles with phase space coordinates (r, Ω, t) leaving collisions. Quantities of interest are then obtained by summing the contributions over all collisions, and frequently over most of phase space. The "Integral Emergent Particle Density Equation" is written (in operator notation) as:

$$\chi_g(r, \Omega, t) = S_g(r, \Omega, t) + C_{g'-g}(r, \Omega' \rightarrow \Omega) T_{g'}(r' \rightarrow r, \Omega') \chi_{g'}(r', \Omega', t') \quad (9-3)$$

where

$T_{g'}(r' \rightarrow r, \Omega')$ = the transport integral operator, and

$C_{g'-g}(r, \Omega' \rightarrow \Omega)$ = the collision integral operator.

The "Integral Emergent Particle Density Equation" was selected as the basis for the forward random walk since the source particles would be introduced according to the natural distribution.

The random walk based on the above Equation (9-3) would introduce a particle into the system according to the source function. The particle travels to the site of its first collision as determined by the transport kernel (operator). Its weight is modified by the non-absorption probability and a new energy group and flight direction are selected from the

collision kernel (operator). The transport and collision kernels are applied successively determining the particle's emergent phase space coordinates corresponding to the second, third, etc., collision sites until the random walk is terminated due to the reduction of the particle's weight below some cut-off value or because the particle escapes from that portion of phase space associated with a particular problem (for example, escape from the system, slowing down below and energy cut-off, or exceeding some arbitrarily specified age cut-off).

In some cases, particularly in MASH, it is of interest to solve the adjoint problem. This involves solving the "Adjoint Integro-Differential Boltzmann Equation" given below.

$$\begin{aligned}
 & -\frac{1}{v} \frac{\partial}{\partial t} \Phi^*(r, E, \Omega, t) - \Omega \cdot \nabla \Phi^*(r, E, \Omega, t) + \Sigma_t(r, E) \Phi^*(r, E, \Omega, t) \\
 & = S^*(r, E, \Omega, t) + \iint \Sigma_s(r, E \rightarrow E', \Omega \rightarrow \Omega') \Phi^*(r, E', \Omega', t) dE' d\Omega'
 \end{aligned} \tag{9-4}$$

where

$$\Phi^*(r, E, \Omega, t) =$$

the time dependent angular adjoint fluence,

and the other terms defined for the forward transport equation have equivalent meaning for the adjoint equation. The adjoint fluence is sometimes referred to as the particle's importance.

The solution of the adjoint integral transport equation by Monte Carlo generally involves a solution for $G_g(r, \Omega, t)$, referred to as the integral emergent adjunton density, i.e., the density of adjuntons with phase space coordinates (r, Ω, t) leaving collisions. Quantities of interest are then obtained by summing the contributions over all collisions, and frequently over most of phase space. The "Integral Emergent Adjuncton Density Equation" is written (in operator notation) as:

$$G_g(r, \Omega, t) = P_g^\Phi(r, \Omega, t) + C_{g'-g}(r, \Omega' \rightarrow \Omega) T_{g'}(r' \rightarrow r, \Omega') G_{g'}(r', \Omega', t) \tag{9-5}$$

where

$$T_{g'}(r' \rightarrow r, \Omega) = \text{the transport integral operator,}$$

$$C_{g'-g}(r, \Omega' \rightarrow \Omega) = \text{the collision integral operator, and}$$

$$P_g^\Phi(r, \Omega, t) = \text{the source of adjuntons.}$$

Equation (9-5) is almost identical to the forward equation given in Equation (9-3) which defines the forward emergent particle density and serves as the formal basis of the random walk in MORSE. Consequently, the same logic in MORSE can be used for both the forward and adjoint mode of solution. The Monte Carlo solution of Equation (9-5) will generate data from which the adjointon fluence $\chi_g^*(r,\Omega,t)$ and other quantities of interest can be determined. The general use of $\chi_g^*(r,\Omega,t)$ must take into account the reversal of directions between adjointons and real particles, i.e., Ω (adjoint) = - Ω (forward). Further, if outward boundary crossings would be scored in the forward problem, the corresponding source adjointons would be introduced in the inward direction. Likewise, adjointons would be scored for entering a volume from which the source particles in the forward problem would be emitted. It should be noted that many sources and response functions are isotropic, and the problem of directional reversal need not be considered. The various relationships between the adjoint and forward quantities are derived in Section 4.10 of Reference 1.

9.1.2 In-Group Energy Biasing

One feature of MORSE alluded to in the introduction was that several types of optional importance sampling techniques are available to the user. In standard MORSE, these include splitting, Russian roulette, exponential transform, and source energy biasing to name a few. In the MASH version of MORSE, there is an additional biasing scheme referred to as in-group energy biasing. In-group energy biasing is a methodology developed by W. Scott of SAIC¹⁶⁻¹⁸ to adjust for irregularities observed in adjoint Monte Carlo analyses in thick media where the weights of adjoint particles could, in undergoing multiple scattering events, become very large, i.e., "the fat particle" problem. Such particles may be scored with a wide variety of weight values. This results in a very inefficient calculation with poor statistical precision, which is not improved by longer run times. The procedure was first implemented in the MIFT2¹⁹ version of the VCS^{20,21} MORSE code by SAIC. After testing by both SAIC and ORNL, the procedure was installed into this version of MASH. A detailed description of the theoretical basis for in-group biasing is presented in Appendix B. The user should examine this section to understand the physics of the biasing technique. Here only a cursory explanation of how in-group biasing works is given.

In-group energy biasing is easy to use. Unlike other Monte Carlo biasing methods, in-group biasing does not require that the user set up and input, based on his judgment, arrays of data to improve the efficiency of the Monte Carlo calculation. This means that a person less skilled in adjoint Monte Carlo can often successfully use MASH or adjoint MORSE, since use of in-group bias requires only the setting of a switch in MASH. Success in the use of the other biasing methods generally requires considerable adjoint Monte Carlo experience.

The major objective of the in-group biasing scheme is to eliminate the instability in the variance for random walks. This is equivalent to eliminating the problem in which the weight of an adjoint particle can grow unbounded by many repeated in-group scatterings.

The defining feature of in-group energy biasing is that for all but the last group, a particle's weight only changes when it scatters to a new group. If the particle stays in the same group, its weight does not change. Thus, when an adjoint particle has a probability of non-

absorption (PNAB) greater than 1.0, its weight will not increase so long as it scatters in the same group. When it finally upscatters to a new group, its weight will be increased by a fixed amount that is a function only of the cross sections and not of how many times the particle scattered in the same group. With standard adjoint MORSE, such a particle would have its weight increased by PNAB each time that it scattered so that its final weight upon upscatter would depend upon how many in-group scatterings that it had.

9.2 MORSE CODE STRUCTURE

Input to MORSE is read in five separate modules: (1) random walk; (2) cross section; (3) user; (4) source; and (5) geometry. The random walk input is read in subroutines INPUT1 and INPUT2 and includes all variables needed for the random walk process. The cross-section input is read in cross-section module subroutines XSEC, JINPUT, and READSG. The parameters needed to set aside storage are read in XSEC, the mixing parameters are read in JINPUT, and the actual cross sections are read by READSG. Cross sections may be either on card or on tape. Input information required for analysis of the histories is read by subroutine SCORIN of the analysis package which is called from INPUT2. Since the source varies from problem to problem, input may also be read in by subroutine SORIN for the definition of the source. The geometry input is read by subroutine JOMIN. Any additional input required by the user may be read in by subroutine INSCOR which is called from SCORIN.

In general, output of input parameters occurs in the same routine in which the input was read. In addition, there are two routines (OUTPT and OUTPT2) for the output of results of the random walk process. Output of analysis results is generally performed in subroutine NRUN, but may also be done in a user-written routine ENDRUN which is called by NRUN.

The input section takes care of setting up all variables needed in the transport process. It should be noted that initial calculations by the cross-section module stem from subroutine calls in XSEC. The analysis portion of the code is interfaced with MORSE through BANKR with several uses made of cross-section routines in making estimates of the quantity of interest. With the exception of output from the random walk process, the rest of the code consists of subroutine calls by MORSE. The geometry module is interfaced through GOMST, and the source is interfaced through MSOUR. The diagnostic module is independent and any part of it may be executed from any routine.

The diagnostic module provides an easy means of printing out, in useful form, the information in the various labelled commons and any part of blank common. The IBM-360 version also has the following features: a special routine is provided for printing out the particle bank; by loading parts of core with a junk word, the diagnostic package can determine which variables have been used; a "repeating line" feature is also included.

The usual geometry module for MORSE is the combinatorial geometry package (CG).⁷ However, the MORSE code in MASH contains the GIFT5 geometry package developed at BRL.⁸⁻¹¹ The GIFT5 geometry package is similar to CG; however, it contains a significant increase in the number of primitive bodies or "solids" and some added advantages relative to Monte Carlo tracking in complex geometries. The GIFT5 geometry package was first installed into the MIFT2¹⁹ code by SAIC. After considerable testing, the package was installed into this version of MORSE for the MASH code system.

An albedo scattering may be forced to occur at every entry into a specified medium. A sample subroutine is provided for specular reflection and a subroutine call is provided (ALBIN, called from XSEC) for reading and storing albedo data of any degree of complexity. Thus transport of particles may be carried out in parts of the problem and an albedo scattering treated for other parts of the problem.

Time dependence is included by keeping track of the chronological age of the particle. For neutrons the age is incremented by the time needed to travel the distance between collisions if it traveled at a velocity corresponding to the average energy of the group. Provision is made for inputting a thermal group velocity separately. Nonrelativistic mechanics are assumed. The age of secondary gamma rays is determined from the neutron age at the collision site and is incremented by determining the time required to travel between collisions at the speed of light. For fission problems the age of the parent is given to the daughters at birth.

There are several types of importance sampling techniques included in the code. The Russian roulette and splitting logic of O5R¹² is an option in MORSE. Also, the exponential transform is provided with parameters allowed as a function of energy and importance region. Source energy biasing is an option as well as energy biasing at each collision. In fission problems the fission weights may be renormalized as a function of an estimate of K_{eff} so that the number of histories per generation remain approximately constant. If desired, all importance sampling may be turned off.

Some other general features include the ability to run problems without the use of magnetic tapes, the ability to terminate a job internally after a set elapsed CPU time and obtain the output based on the number of histories treated up to that time, batch processing for the purpose of determining statistics for groups of particles, and a repeat run feature so that results for a time-dependent fission problem may be obtained with statistical estimates. The output of numerous counters permits one to obtain an insight into the physics of the problem.

9.2.1 Random Walk Module

The basic random walk process of choosing a source particle and then following it through its history of events is governed by the routines in this module of MORSE. A given problem is performed by following a number of batches of particles which then constitute a run. Multiple runs are also permitted. The batch process feature is used so that statistical variations between groups of particles can be determined. Thus, a batch of source particles is generated and stored in the bank. The random walk for this batch of particles is determined by picking one particle out of the bank and transporting it from collision to collision, splitting it into two particles, killing by Russian roulette, and generating secondary particles (either gamma rays or fission neutrons) and storing them in the bank for future processing. Termination of a history occurs when a particle leaks from the system, reaches an energy cutoff, reaches an age limit, or is killed by Russian roulette.

The random walk module performs the necessary bookkeeping for the bank and the transportation and generation of new particles and relays this information to the analysis module for estimation of the desired quantities. Use is made of the cross-section module and the geometry module during the random walk process and the input-output routines for the reading and printing of pertinent information about the problem.

In this module the main program is used to set aside the storage required in blank common and to pass this information to subroutine MORSE which is the executive routine for the random walk process. After performing the necessary input operations and setting up storage requirements, the walk process consists of three nested loops: one for runs, one for batches, and the inner-most is for particles. After each termination of the batch loop, some bookkeeping is required before the generation of a new batch of source particles. After the termination of a run, a summary of the particle terminations, scattering counters, and secondary production counters are output, as well as the results of Russian roulette and splitting for each group and importance region.

There are only two main labelled commons (APOLLO and NUTRON) in the random walk routines. Tables 4.4 and 4.5 in Reference 1 list the definitions of the variables in these two commons. The parameters stored in these commons are labelled by "current" and "previous" descriptors which refer to values of parameters leaving the current and previous event sites, respectively (WTBC is the exception, being the weight entering the current event site). Also note that "event" includes boundary crossings, albedo collisions, etc., as well as real collisions. The user is afforded access to these parameters through several different calls to subroutine BANKR throughout the random walk. The calling routine and location in the random walk where BANKR is called is given in Table 9-1. The user can then interact with the random walk through additional programming only in subroutine BANKR and not need to work with the random walk routines themselves. The user also has an input option to write a collision tape for further analysis.

Table 9-1. BANKR Arguments.

BANKR Argument	Called From	Location of BANKR Call in Random Walk
-1	MORSE	After call to INPUT - to set parameters for new problem.
-2	MORSE	At the beginning of each batch of NSTRT particles.
-3	MORSE	At the end of each batch of NSTRT particles.
-4	MORSE	At the end of each set of NITS batches a new problem is about to begin.
1	MSOUR	At a source event.
2	TESTW	After a splitting has occurred.
3	FPROB	After a fission has occurred,
4	GSTORE	After a secondary particle has been generated.
5	MORSE	After a real collision has occurred post-collision parameters are available.
6	MORSE	After an albedo collision has occurred - post-collision parameters are available.
7	NXTCOL	After a boundary crossing occurs (the track has encountered a new geometry medium other than the albedo or void media).
8	NXTCOL	After an escape occurs (the geometry has encountered medium zero).
9	MORSE	After the post-collision energy group exceeds the maximum desired.
10	MORSE	After the maximum chronological age has been exceeded.
11	TESTW	After a Russian roulette kill occurs.
12	TESTW	After a Russian roulette survival occurs.
13	GSTORE	After a secondary particle has been generated but no room in the bank is available.

The input allows the user to specify which of the thirteen positive BANKR Arguments to put on the tape as well as which of the 36 parameters listed in Table 9-2. These features of MORSE prove useful in applying the code to new and different problems.

Table 9-2. Variables That May be Written on Collision Tape (NBIND).

Variable Number	Variable Name	Variable Number	Variable Name
1	NCOLL	19	WTBC
2	NAME	20	ETAUSD
3	IG	21	ETA
4	U	22	AGEC
5	V	23	OLDAGE
6	W	24	NREG
7	X	25	NMED
8	Y	26	NAMEX
9	Z	27	WATEF
10	WATE	28	BLZNT
11	IGO	29	BLZON
12	UOLD	30	VEL(IG)
13	VOLD	31	VEL(IGO)
14	WOLD	32	TSIG
15	XOLD	33	PNAB
16	YOLD	34	NXTRA
17	ZOLD	35	EXTRA1
18	OLDWT	36	EXTRA2

9.2.2 Multigroup Cross-Section Module

The function of this module in the multigroup Monte Carlo code is to read ANISN-type³ cross sections for media or elements, mix several elements together to obtain media cross sections, determine group-to-group transfer probabilities and determine the probabilities and angles of scattering for each group-to-group transfer. All variables are flexibly dimensioned and are part of blank common.

Various types of cross sections can be processed by the cross-section module. Neutron only, gamma ray only, neutron gamma-ray coupled, or gamma rays from coupled neutron gamma-ray cross sections can be processed for either a forward or an adjoint problem with or without fission. The Legendre coefficients are stored if a next-event estimator is to be used. Table 9-3 indicates the relationship between the various input parameters in the random walk module and the cross section module. The user must be careful that these particular parameters match.

The cross sections are read for one coefficient and one element into a buffer area. Then these cross sections are decomposed into total, fission, and downscatter matrix and stored in temporary arrays so that they may be mixed to form media cross sections. The total and fission cross sections are stored only once for an element, but the downscatter matrix is stored for each coefficient.

The cross sections are transposed as stored if an adjoint problem is being solved. Two major reordering steps are carried out to produce an adjoint cross-section library:

1. The inscatter matrix is transposed, i.e., the table position associated with group g describing scattering from g' to g is changed to describe scattering from g to g' .
2. The ordering of the groups is reversed, i.e., data for group IGM appear first in the output file, followed by IGM-1, etc.

After all cross sections are stored, the contribution of each element to the cross section for the media is determined. Also at this time the sum of the downscatter vector for each group is determined for the future calculation of the nonabsorption probability; the gamma-production cross section is also determined by summing the transfers to the gamma groups. After the cross sections for the medium have been determined, the nonabsorption probability, fission probability, and gamma-production probabilities are formed by dividing by the total cross section. The downscatter matrix is converted to a probability table by dividing by the scattering cross section.

Table 9-3. Examples of the Relationship Between Random Walk and Cross Section Module Group Input Parameters.

Case A - Neutron Only Cross Sections (22 groups)
 Case B - Gamma-Ray Only Cross Sections (18 groups)
 Case C - Neutron Gamma-Ray Coupled Cross Sections (22-18 groups)

Problem Type						
Input Variable	Case A Top 14 Groups	Case B Top 17 Groups	Case C n Only Top 14 gps	Case C γ Only Top 17 gps	Case C n + γ 14n + 17 γ	
MORSE Input						
NGPQTN	14	0	14	0	14] CARD B Variables
NGPQTG	0	17	0	17	17	
NMGP	22	18	22	18	40	
NMTG	22	18	22	18	40	
NGP	22	18	22	0	22 ^a] CARD XB Variables
NGG	0	0	0	18	18	
INGP	22	18	40	40	40	

^aMust be equal to total number of neutron groups in the data; otherwise it picks up the gammas from the wrong location.

Note: For Cross sections with full downscatter, NDS = NGP, NDSG = NGG, INDS = INGP, and ITBL = number of downscatters + number of upscatters + 3. Usually, ISGG = number of upscatters + 4; i.e., NUS + 4.

A simple three group example showing the relationship between a forward and adjoint cross-section set is shown below. In this example, there is no upscatter, one activation cross section, and the cross-section input parameters (defined in Section 9.3.3) are IHT = 4, ISGG = 5, and ITBL = 7.

<u>Direct</u>	<u>Adjoint</u>
$\sigma^F(1)$	$\sigma^F(3)$
$\sigma^A(1)$	$\sigma^A(3)$
$v\sigma^F(1)$	$v\sigma^F(3)$
$\sigma^T(1)$	$\sigma^T(3)$
$\sigma(1 \rightarrow 1)$	$\sigma(3 \rightarrow 3)$
0	0
0	0
$\sigma^F(2)$	$\sigma^F(2)$
$\sigma^A(2)$	$\sigma^A(2)$
$v\sigma^F(2)$	$v\sigma^F(2)$
$\sigma^T(2)$	$\sigma^T(2)$
$\sigma(2 \rightarrow 2)$	$\sigma(2 \rightarrow 2)$
$\sigma(1 \rightarrow 2)$	$\sigma(2 \rightarrow 3)$
0	0
$\sigma^F(3)$	$\sigma^F(1)$
$\sigma^A(3)$	$\sigma^A(1)$
$v\sigma^F(3)$	$v\sigma^F(1)$
$\sigma^T(3)$	$\sigma^T(1)$
$\sigma(3 \rightarrow 3)$	$\sigma(1 \rightarrow 1)$
$\sigma(2 \rightarrow 3)$	$\sigma(1 \rightarrow 2)$
$\sigma(1 \rightarrow 3)$	$\sigma(1 \rightarrow 3)$

The Legendre coefficients for each group-to-group transfer are converted to angles and probabilities of scattering at those angles by the use of a generalized Gaussian quadrature using the angular distribution as a weight function. That is,

$$\int_{-1}^{+1} f(\mu)\omega(\mu)d\mu = \sum_{i=1}^n f(\mu_i)\omega_i$$

where

$f(\mu)$ is any polynomial of order $2n-1$ or less,

$\omega(\mu)$ is the angular distribution for μ , the cosine of the scattering angle,

μ_i is a set of discrete cosines, and

ω_i is the probability of the corresponding cosine.

Thus, a set of μ_i 's and ω_i 's that satisfy the equation must be found. To do this, a set of polynomials, Q_i , which is orthogonal with respect to the angular distribution, is defined such that

$$\int_{-1}^{+1} Q_i(\mu)Q_j(\mu)\omega(\mu)d\mu = \delta_{ij}N_i ,$$

where N_i is a normalization constant.

The moments of the angular distribution M_i , $i=1,2n-1$, determine the orthogonal polynomials, Q_i , $i=1,n$. The desired cosines, μ_i , are given by the roots of Q_n ,

$$Q_n(\mu_i) = 0,$$

and the corresponding probabilities are

$$\omega_i = \left(\sum_{k=1}^{n-1} \frac{Q_k^2(\mu_i)}{N_k} \right)^{-1}$$

In the process of deriving the orthogonal polynomials, some restrictions on the moments of the angular distribution are obtained. These restrictions arise if both the original distribution and the derived point distribution are to be everywhere non-negative. The restrictions are:

1) $N_i > 0$ for $i=1,n$.

This restriction may be written in terms of the determinant of the moments:

$$\begin{vmatrix}
 1 & M_1 & M_2 & \cdot & \cdot & \cdot & M_i \\
 M_1 & M_2 & M_3 & \cdot & \cdot & \cdot & M_{i+1} \\
 \cdot & \cdot & \cdot & \cdot & \cdot & \cdot & \cdot \\
 \cdot & \cdot & \cdot & \cdot & \cdot & \cdot & \cdot \\
 \cdot & \cdot & \cdot & \cdot & \cdot & \cdot & \cdot \\
 M_i & M_{i+1} & M_{i+2} & \cdot & \cdot & \cdot & M_{2i}
 \end{vmatrix} > 0$$

2) The roots of $Q_i(\mu)$ must all lie in the interval

$$-1 \leq \mu_j \leq 1.$$

It must be emphasized that the restriction arising from the original distribution being everywhere positive (or zero) does not restrict the truncated expansion of the distribution to be everywhere positive. That is, moments from a truncated distribution that is not necessarily everywhere positive are used to derive a discrete distribution with positive probabilities.

Other characteristics of this representation are that the information is compact, the angles are clustered where the angular distribution is peaked, and because of the restrictions, cross sections that have blunders in them are rejected because they produce angles outside the range of -1 to +1.

An option on input makes it possible to write a tape containing the processed cross sections and all variables from Common LOCSIG needed during the random walk process. In starting a new case, the normal cross-section input, except for the cross sections and the mixing cards, is required. Both the information from input and from tape are printed for compatibility checks. Note that if an adjoint problem is being solved, the input information and the information for tape will not be identical.

One of the more important options provided for in this package is the ability to treat upscattering. Thus, multigroup cross sections with many thermal groups may be utilized. (In a crude way photoneutron production may be treated as an upscatter process from a gamma-ray group to a neutron group.) Also, the capability of using cross sections with partial downscatter is present.

The downscatter array made it possible to have a feature that is helpful in reducing cross-section storage requirements for neutron problems involving materials other than hydrogen when a cross-section tape is used. For non-hydrogenous media there is very seldom complete downscatter to thermal energy, so a routine was added to search the P_0 array to

determine the minimum downscattered energy group for any element and for each group. The zero cross sections for downscatters below this energy group are not stored, and thus the storage requirements are reduced.

Another important feature of this module is the ability to use a point cross-section representation for the total, scattering, and fission cross sections. Either an O5R¹² or an O6R^{13,14} (variable supergroup boundaries) format tape (CODE7) may be used over a specified energy range. The energy of a particle is chosen uniformly within an energy group for the purpose of selecting the particle track lengths or calculating a nonabsorption probability. For gamma rays or for neutron energies outside the specified range, the total cross section from the multigroup cross sections is used. (Point, total, and scattering cross sections for the adjoint case can also be used.) For some applications, detailed nonabsorption probabilities and fission probabilities may also be required. The logic was included in the new module for the cross-section manipulation required for the use of the point cross sections. Up to 16 point cross-section media with up to 100 supergroups are allowed.

One major change in philosophy has been made for the case in which point cross sections are used. The modular framework of MORSE is broken in this case in that Subroutine GTSC uses the energies corresponding to the multigroup boundaries in order to set up an array of indices. It is assumed by GTSC that the energies exist in the first NTG cells of Blank Common.

An executive program XCHEKR¹⁵ may be used in conjunction with this cross-section module independent of MORSE for the purpose of checking and editing multigroup cross sections. Also, this executive program may be used to generate a processed cross-section tape independent of a MORSE calculation.

9.2.3 The GIFT5 Geometry Package

GIFT5 geometry is similar to the older MORSE combinatorial geometry in that specified geometric shapes (spheres, cylinders, parallelepipeds, etc.) may be combined to describe complex geometry configurations. As with MORSE combinatorial geometry, a GIFT5 geometry file is comprised largely of a "body" or "solids" table followed by a "zone" or "region" table in which the bodies are combined by (+), (-), or (OR) operators. In GIFT5 geometry, however, "bodies" (MORSE terminology) are called "solids" and "zones" (MORSE terminology) are called "regions". In the GIFT5 graphics code there is no equivalent to the "regions" as used in MORSE. In MASH, where the term "region" could have a double meaning, the MORSE equivalent of "region" is called "importance region" to minimize any confusion. In this section the GIFT terminology, i.e., solids and regions, equivalent to bodies and zones in MORSE, will be used.

Installation of the GIFT5 geometry in MASH was greatly facilitated by BRL's initial installation of GIFT into MORSE to derive MIFT, in which they (BRL) had developed the necessary interfaces between MORSE and the GIFT geometry, and SAIC's installation of GIFT5 into MIFT2. SAIC's installation of GIFT5 in MIFT2 consisted largely of replacing GIFT geometry routines with GIFT5 routines. The subsequent installation of GIFT5 into the MORSE code in MASH involved mainly a transfer of the MIFT2 logic into the MORSE logic with a few changes necessary to accommodate the minor differences in the two codes.

MASH interfaces with the GIFT5 geometry routines in four major locations: INPUT1 for processing of the input geometry data, LOOKZ to identify the region (zone) for starting

particles, and GOMST and NXTCOL to track particles during the random walk. INPUT1 calls GIFTM, which sets a few switches and calls GENI.

GENI calls SOLIN, which processes the solids (bodies) table, REGIN, which processes the regions (zones) table, IDIN, which processes the identification table, and RPPIN which processes any boundary RPP information. SOLIN calls ALBERT, which processes ARB input data, and ARIN, which processes ARS input data. Several other routines, including DOT, CROSS, EQUIV, UNITV, UN2, ARANG2, CPOINT, and PLANE, are called by these routines to perform miscellaneous operations such as vector dot products, cross products and sorts. GENI and routines called by GENI analyze the geometry for obvious errors, such as XMAX smaller than XMIN for an RPP or non-coplanar points on an ARB, and print error messages when such errors are found. GENI then stores the geometry data with XMAX, XMIN, YMAX, YMIN, ZMAX, and ZMIN bounding values for each region (zone) for use in subsequent analyses.

LOOKZ calls RAY to identify the starting region location for starting particles. RAY calculates the region numbers and intercept distances for all regions on a line-of-sight from the particle start point to exit from the defined geometry.

GOMST and NXTCOL determine the particle coordinates at the next collision site by calculating the expected flight path distance in mean free paths, then tracking the particle through the different regions and materials of the geometry until the mean free path is "expended" or until the particle escapes from the geometry.

First, in NXTCOL, the mean free path for the particle path is calculated with a call to GETETA, a flag, MARK, is set to 1, and the call to GOMST is made. In GOMST the distance DISTO for the particle mean free path in the current medium is calculated. Then the particle starting coordinates and direction cosines, XB and WB are stored. A call to the GIFT5 REGION subroutine is made to determine the distance along the particle line-of-sight to exit from the current region, and a test is made to determine whether the particle does, in fact, exit the region. If it does exit the region, a call to GIFT5 subroutine RAY is made to calculate intercepts of the particle line-of-sight, MARK is set to 0 (indicating a region boundary crossing) and the distance traveled is cumulated. A test on MARK is then made. If MARK is equal to 1, the collision site is in the same region as before and GOMST and NXTCOL are exited. If MARK is zero, a boundary crossing occurred and tests are made first for the extended path scoring option (if "Yes", a score is made), then for particle escape (if "Yes", an escape is scored). If there is no escape, the flight distance in the new medium is calculated.

As seen in the foregoing paragraph, particle tracking uses calls to GIFT5 subroutines RAY and REGION. Given a particle line-of-sight defined by a starting point and a direction, REGION calculates the distance along the ray to all entry and exit points for a specified region. Because a region can have complicated shapes, it is possible for a ray to have several entry and exit points. While REGION calculates entry and exit points for only one specified region, RAY does so for all regions on the line-of-sight.

The particle tracking logic with GIFT5 routines is considerably different from the tracking logic in combinatorial geometry MORSE-CG. In MORSE, each time a particle exits a region, MORSE-CG searches an "experience" table to determine candidate neighboring regions which the particle might be entering. If analysis shows that the particle is not entering any of the regions in the experience table, or if there are no candidate regions in the table, all regions are checked sequentially until the new region is found. When the new region is found, it is added to the experience table.

MASH, during the processing of the input geometry data, performs three steps which facilitate later particle tracking. First, bounding X, Y, and Z values are found for each region, and the resulting XMIN, XMAX, YMIN, YMAX, ZMIN, ZMAX are stored in the MASTER/ASTER array (the Region RPP Table discussed in Appendix C). Second, these XMIN, XMAX, YMIN, YMAX, etc., data sets are each sorted, high value first, carrying along the region number, and stored in the MASTER/ASTER array. Third, the bounding RPP for the entire problem geometry is defined and stored.

During particle tracking, MASH first derives the RPP which bounds the particle flight path line-of-sight (ray) from its starting point to escape from the defined geometry. Next it compares the XMIN, XMAX, ..., ZMAX data for this bounding RPP to the region min-max table to derive the shortest list of candidate regions that the ray might intercept. Then for each region on the list, it compares the region min/max values with the ray RPP, eliminating any region RPP that doesn't intersect the ray RPP. Next a "fly by" test is performed, then a check of whether the ray actually penetrates the region bounding RPP. Last, if all of the above tests are passed, a check is made, via a call to REGION, to determine whether the ray penetrates the region.

The above procedure is performed in RAY for all candidate regions. When it is found that the ray does penetrate a region, the RIN and ROUT distances (distances along the ray to region entry and exit, respectively) are added to a list (RAYIN and RAYOUT), in common RAYINT, along with the region number, IREGON, and a count of the number of entries on the list, NINT. Last, the RAYIN/RAYOUT list is checked for overlapping regions. If overlapping regions are found, an error message is written.

In initial testing of MIFT2 after installation of the GIFT5 geometry routines, SAIC found that particle tracking resulted in undetected errors whenever there were undefined regions in the geometry. While vehicle geometries for VCS analysis have not intentionally been developed with undefined regions, undefined regions could result from errors in developing the complex vehicle geometry. The result of undefined regions in MIFT, before corrections were implemented, was that particles got lost in the sense that their X,Y,Z coordinates did not correspond to the regions. In the analysis of a test case vehicle, for example, in which the interior air region was intentionally left undefined, the effect was to fill the interior with the steel boundary material.

In MORSE-CG, entry of particles into an undefined region also results in the particle getting lost. MORSE-CG, however, kills the particles by setting the weight (WATE) to zero and picks up a new particle after writing a message.

The error in the treatment of undefined regions was corrected (by SAIC) in MIFT2 by the addition of subroutine RAYCHK, which is called by NXTCOL immediately after the call to subroutine RAY. Fortunately the RAYIN and RAYOUT arrays from RAY contain all the information necessary to reconstruct the ray penetration parameters for the undefined region. When a particle encounters an undefined region, RAYCHK reconstructs the ray parameters and assigns a region number of -99 and a material number of 1000 (void) to the undefined region. RAYCHK then prints a message for each of the first 25 undefined region encounters, giving the region numbers of adjacent regions to help locate the problem area. The RAYCHK subroutine was included in the installation of GIFT5 into the MASH version of MORSE.

There is, of course, a danger of analyzing an erroneous geometry with a code that treats geometric undefined regions or overlapping regions or both. The best solution appears to

have the code print a limited number (e.g., 20) of messages indicating that it has found undefined or overlapping regions and then to continue the calculation. Users could alter the logic to terminate after the message, if they wish. In any event, the user must be responsible to generate the correct code input.

The bulk of the data used in GIFT5 is stored in a single large array in COMMON GIFTCM. This array has various names in different routines, but usually appears as MASTER or ASTER. MASTER and ASTER are equivalenced for storage of both real and integer data. This array is currently dimensioned to 5,000 in the GIFT5 geometry routines and subroutine GOMST of the MORSE random walk interface routines. The value of 5,000 defines the storage used throughout the code, and a user who wishes to redimension this value either upward or downward needs to change this common size throughout the code. This size is sufficient for a medium size problem. SAIC used a MASTER/ASTER array size of 15,000 for the analysis of some very large problems. It was, for example, sufficient for the analysis of the MPGS (Mobile Position Gun System) test case, which consists of 281 solids and 233 regions, and the Long Island Barracks, which consisted of 308 solids and 311 regions.

There are 12 sets of data stored in the MASTER/ASTER array as follows:

1. Solid pointers, one word per solid plus 1, integer data. Two values are packed in each word, ITYPE in the right 15 bits and LOCDA in the next 16 bits. ITYPE is the solid type, and LOCDA is the beginning location at which specific data for the solid are stored.
2. Solid data, as required to describe the solids, real.
3. Region pointers, integer, one word for each region. Two values are packed in each word, NUMDES in the right 15 bits and LOCDES in the next 16 bits. NUMDES is the number of solids in the region description and LOCDES is the beginning location at which the region descriptors for the specific region are stored.
4. Region descriptors, integer, one word per descriptor, NUMDES descriptors per region. Two numbers are packed in each word, the solid number in the right 15 bits and an operator code number in the left 16 bits. The operator code is 1 for OR+, 2 for OR-, 3 for RG+, 4 for RG-, 5 for + and 6 for -.
5. Region circumscribing RPP data (XMIN, XMAX, YMIN, YMAX, ZMIN, ZMAX limits for each region). Six words of real data are stored for each region (zone).
6. Ordered region numbers, integer, sorted into the order large to small, first based on XMIN values for circumscribing RPP, then an XMAX, on YMIN, on YMAX, on ZMIN, and last on ZMAX. The total size of this part of the MASTER/ASTER array is six times the number of regions, beginning at storage location LREGION.
7. XMIN, XMAX, YMIN, YMAX, ZMIN, and ZMAX for RPP that circumscribes the overall defined geometry. Six words, real, beginning at storage location LENRPP.
8. Identification table, integer, one word for each region. Two values are packed in each word, ISPACE in the right 15 bits and ITEM in the next 16 bits. ISPACE is the space code number (columns 11-15 of the input identification table) and ITEM is the component code number (columns 6-10 of the input identification table).

9. Region ray table, integer, one word per region. Three values are packed in each word. The right 15 bits stores the ray number, the next 10 bits stores the location where the ray end is stored and the next 10 bits stores the location where the ray start is stored.
10. Ray intersection table storing distance (RIN) from start of ray to first intersection of solid. Real, not packed. One word per solid.
11. Ray intersection table storing distance (ROUT) from start of ray to last intersection of solid. Real, not packed. One word per solid.
12. Surfaces and ray count, one word per solid. Three integers packed per word, the ray number is the right 14 bits, the surface number at ray exit in the next 9 bits, and the surface number at ray entry in the next 9 bits.

9.2.4 Modifications to MORSE for In-Group Biasing

Several routines in the MORSE module of MASH were modified to incorporate the changes to add the in-group biasing option. Subroutines COLISN, GPROB, GSTORE, GTIOUT, and INPUT1 were modified, and a new subroutine GETLOC was added. Also, invoking the in-group bias option changes the definition of the quantity GWLO from the probability of secondary particle production to the fraction of the probability of secondary particle production specified by the cross sections (natural probability).

Subroutine INPUT1 was modified to read the in-group biasing switch INGB as the eighth parameter on CARD I. Variable INGB turns on the in-group when equal to 1; otherwise, the option is off. INGB is in COMMON/IGBABS/. Subroutine COLISN handles scattering probabilities P_{ij} which give the probability of scattering to group j when a scattering has occurred in group i . Originally the particle weight WATE was multiplied by $PNAB_i$, the non-absorption probability for group i where i was the group coming into the collision; and then a random number was compared with the probabilities P_{ij} to select the outgoing group. This sampling scheme was modified for in-group biasing. The same coding is used except that the random number is compared to $F \cdot P_{ij}$, where F is a bias factor as follows:

$$\text{if } i = j = 1, \text{ then } F = 1.0$$

$$\text{if } i = j \neq 1, \text{ then } F = PNAB_i$$

$$\text{if } i \neq j, \quad \text{then } F = \frac{1 - P_{ii} PNAB_i}{1 - P_{ii}}$$

After the outgoing group has been sampled, the weight is corrected by

$$WATE = WATE * PNAB/F.$$

The method implemented correctly treats in-group biasing with or without energy biasing and includes logic for splitting when WATE exceeds WTMAX. The splitting game actually resamples the upscatter distribution for each splitting secondary particle. In this way each secondary is independent of the others so that the probability transition is more completely represented than in the original scheme where all splitting secondaries had the same energy group and the same direction cosines.

9.2.5 Modifications to MORSE-CG for the MASH Code System

The current version of MASH contains the newest MORSE-CG routines. The main differences between this and the previous VCS have been explained elsewhere in this report. The routines that are peculiar to MASH have been rewritten with the following characteristics:

1. All arrays are now variably dimensioned. This required the addition of several arrays of data to blank common. Table 9-4 defines these variables.
2. All tape unit numbers are variables.
3. Common structure is revised, having fewer commons with more variables in each. A labelled common IVCS was added for this purpose, and it is defined in Table 9-5.
4. Subroutine structure is slightly different. One of the changes was to split subroutine BANKR into two routines, BANKR and NBANKR.
5. Problems terminate in an orderly manner. If a job fails because the particle name exceeds the maximum storage allowed (IMAXN), data generated for all but the last batch is copied from the scratch unit to the user's save unit. A message is printed by the new routine EREND to notify the user of this and of how many batches were actually completed.
6. A new MORSE leakage tape format is used in order to provide more definitive information on the case that was run.

9.3 MORSE INPUT REQUIREMENTS

This section describes the input data for the MORSE program. The data is free-form. Most of the rules governing FIDO free-form input in Appendix A are appropriate. MORSE free-form input requires that the "\$\$" and the "***" **not** begin in column 1. Error messages will be printed in this case, but users often misinterpret them. Therefore, begin the "\$\$" and "***" parameters in column 2. MORSE input also **does not** require data block terminators "T". Standard MORSE includes the SAMBO input (after the cross-section module input). The MORSE component in MASH does not include the SAMBO routines since the analysis of the adjoint leakage tape is performed in DRC. Consequently, the additional input data after the cross-section input are special data required by MASH. This data replaces the usual SAMBO analysis input.

Table 9-4. Location of MASH Arrays in BLANK COMMON.

Mnemonic variable name	Location in blank common BC(I) or NC(I)	Purpose
ILEAK(NB)	$I = NLAST + NB - 1$	Number of particles/batch that leak from system
ILEAK(NITS+1)	$I = NLAST + NITS$	Number of records of leakage parameters
ASORC(NB)	$I = LOCLK + NB - 1$	Total source weight for batch NB
BUF(IPOS)	$I = LOCASC + IPOS - 1$	Temporary storage of leakage parameters
IGRUP(IN)	$I = LOCBUF + IN - 1$	Group number of source energy in forward mode
IDET(IN)	$I = LOCIGP + IN - 1$	Detector number where response for escaping particle IN will be stored
IVEH(IN)	$I = LOCIDT + IN - 1$	Signal indicating where (γ, n) conversion occurred
RDEN(NR)	$I = LOCIVH + NR - 1$	Density factor for altering total cross section for importance region NR

Table 9-5. Definition of Variables in Common IVCS.

Variable	Definition
SWATE	Total source weight for current batch
TOTS	Total particle weight for the entire run (i.e., the summation from 1 to NITS batches of SWATE)
IMAXN	The size of arrays IVEH, IGRUP, IDET - defined as 5*NMOST
MAXSZ	The size of the buffer for the leakage parameters (set at 1000)
IGRND	Media number of ground
IAIR	Media number of air
NREC	Number of records written to scratch unit ISCU
NAME1	The name of the particle that split
ISCU	Logical unit number of scratch unit for leakage parameter storage (set to 23)
ICTU	Logical unit number of MORSE leakage tape (set to 24)
IPOS	Counter for number of leakage parameters in buffer
LOCLK	Starting location in blank common of ILEAK array
LOCASC	Starting location in blank common of ASORC array
LOCBUF	Starting location in blank common of BUF array
LOCIGP	Starting location in blank common of IGRUP array
LOCIDT	Starting location in blank common of IDET array
LOCIVH	Starting location in blank common of IVEH array
LOCRDN	Starting location in blank common of RDEN array
TTL(10)	Title of problem (will be written to leakage tape)

9.3.1 Random Walk Input Instructions

This input is read by subroutine INPUT1.

CARD A Job Title Card [20A4]

TITLE 80 alphanumeric character description

[NOTE: Any character other than a blank or alphanumeric in column one will terminate the job.]

CARD B Job Control Parameters [Begin array with "\$\$"]

\$\$

NSTRT	number of particles per batch
NMOST	maximum number of particles allowed for in the bank(s); may equal NSTRT if no splitting, fission, and secondary generation
NITS	number of batches
NQUIT	number of sets of NITS batches to be run without calling subroutine INPUT
NGPQTN	number of neutron groups being analyzed

- 5 ---

NGPQTG	number of gamma-ray groups being analyzed
NMGP	number of primary particle groups for which cross sections are stored; should be same as NGP (or the same as NGG when NGP = 0) on Card XB read by subroutine XSEC
NMTG	total number of groups for which cross sections are stored; should be same as NGP+NGG as read on Card XB read by subroutine XSEC
NCOLTP	set greater than zero if a collision tape is desired; the collision tape is written by the user routine BANKR
IADJM	set greater than zero for an adjoint problem

[NOTE: For MASH analysis, IADJM is always set > 0]

- 10 ---

MAXTIM	maximum clock time in minutes allowed for the problem to be on the computer
MEDIA	number of cross-section media; should agree with NMED on Card XB read by subroutine XSEC
MEDALB	albedo scattering medium is absolute value of MEDALB; MEDALB = 0, no albedo information to be read in, MEDALB < 0, albedo only problem - no cross sections are to be read, MEDALB > 0, coupled albedo and transport problem.

[NOTE: For MASH analysis, MEDALB is always set = 0]

[NOTE: See Table 9-3 in Section 9.2.2 for examples on parameters NGPQTN, NGPQTG, NMGP, and NMTG.]

CARD C Source Control Parameters [Use "\$\$" and "***" as indicated]

\$\$

ISOUR source energy group if > 0
[if ISOUR < 0 or if ISOUR = 0 and NGPFS ≠ 0,
SORIN is called for input of Cards E1 and E2.]

NGPFS number of groups for which the source spectrum is
to be defined. [If ISOUR < 0, NGPFS ≥ 2]

ISBIAS no source energy biasing if set equal to zero;
otherwise the source energy is to be biased,
and Cards E2 are required.

NOTUSD an unused variable. Must specify a "0".

**

WTSTRT weight assigned to each source particle

EBOTN lower energy limit of lowest neutron group (eV) (group NMGP)

EBOTG lower energy limit of lowest gamma-ray group (eV)
(group NMTG)

TCUT age in sec at which particles are retired;
if TCUT = 0, no time kill is performed

VELTH velocity of group NMGP when NGPQTN > 0;
i.e., thermal-neutron velocity (cm/sec)

CARD D Source Control Parameters [Begin with "***".]

**

XSTRT
YSTRT } X, Y, Z coordinates for source particles
ZSTRT }

AGSTRT starting age for source particles.

UINP
VINP } source particle direction cosines;
WINP } if all are equal to zero,
isotropic directions are chosen in MORSE

[NOTE: Source data on Cards C and D will be overridden by any changes in subroutine SOURCE.]

CARDS E1 Input Source Distribution [Begin with "***"]

[NOTE: Omit if ISOUR on Card C > 0 or if ISOUR = NGPFS = 0]

**

FS NGPFS values of FS, where FS equals the unnormalized fraction of source particles in each group

CARDS E2 Relative Importance of Group Source [Begin with "***"]

[NOTE: Omit if ISOUR > 0 or if ISOUR ≤ 0 and ISBIAS = 0]

**

BFS NGPFS values of BFS, the relative importance of a source in group I. (If ISBIAS > 0)

CARDS F Energy Group Boundaries [Begin with "***"]

**

ENER NMTG values of ENER, the energies (in eV) at the upper edge of the energy group boundaries

[NOTE: The lower energies of groups NMGP and NMTG were read on Card C.]

CARD G Collision Tape Control Parameters [2I5,5X,36I1,5X,13I1]

[NOTE: Omit if NCOLTP on Card B ≤ 0]

NHISTR logical tape number for the first collision tape.
NHISMX the highest logical number that a collision tape may be assigned.
NBIND(J),J=1,36 an index to indicate the collision parameters to be written on tape.
NCOLLS(J),J=1,13 an index to indicate the types of collisions to be put on tape.

CARD H Random Number [5X,3Z4]

RANDOM starting random number.

CARD I Biasing Control Parameters [Begin with "\$\$"]

\$\$

NSPLT index indicating that splitting is allowed (if > 0)

NKILL index indicating that Russian roulette is allowed (if > 0)
 NPAST index indicating that exponential transform is invoked (if > 0)
 (Subroutine DIREC required)
 NOLEAK index indicating that non-leakage is invoked (if > 0)
 IEBIAS index indicating that energy biasing is allowed (if > 0)

- 5 ---

MXREG number of importance regions described by geometry input
 (will be set to one if ≤ 0)
 MAXGP group number of last group for which Russian roulette or
 splitting or exponential transform is to be performed.

[Note: For adjoint, set MAXGP = NMTG or oversteoring results.]

INGB in-group bias switch (**INGB = 1 recommended**)
 = 1 implies use in-group biasing
 = 0 implies do not use in-group biasing

CARD J Biasing Parameters [use "\$\$" and "***" as indicated]

[NOTE: Omit if NSPLT + NKILL + NPAST = 0]

\$\$

NGP1
 NDG
 NGP2
 NRG1
 NDRG
 NRG2



The following weight standards and path-stretching parameters are assigned from energy group NGP1 to energy group NGP2, inclusive, in steps of NDG and from importance region NRG1 to importance region NRG2, inclusive, in steps of NDRG. If NGP1 = 0, groups 1 to MAXGP will be used; if NRG1 = 0, importance regions 1 to MXREG will be used (both in steps of one). Usually, NDG = 1 and NDRG = 1.

**

WTHIH1 weight above which splitting will occur.
 WTLOW1 weight below which Russian roulette is played.
 WTAVE1 weight given those particles surviving Russian roulette.
 PATH path-length stretching parameters for use in
 exponential transform (usually $0 \leq \text{PATH} \leq 1$).

[NOTE: The above information is repeated until data for all groups and importance regions are input.]

[NOTE: End Card(s) J with a negative value of NGP1, i.e., NGP1= -1
 example \$\$ -1 0 0 0 0 0 ** 0.0 0.0 0.0 0.0]

CARDS K Energy Biasing Parameters [Begin with "***"]

[NOTE: Omit if IEBIAS on Card I ≤ 0]

**

((EPROB(IG,NREG), IG = 1, NMTG), NREG = 1, MXREG)

Values of the relative energy importance of particles leaving a collision in importance region NREG. Input for each region must start on a new card.

CARD L Problem Identification [Begin with "\$\$"]

\$\$

NSOUR	set ≤ 0 for a fixed source problem; otherwise the source is from fissions generated in a previous batch
MFISTP	index for fission problem, if ≤ 0 no fissions are allowed
NKCALC	the number of the first batch to be included in the estimate of K_{eff} ; if ≤ 0 no estimate of K_{eff} is made
NORMF	the weight standards and fission weights are unchanged if ≤ 0 ; otherwise fission weights will be multiplied, at the end of each batch, by the latest estimate of K_{eff} and the weight standards are multiplied by the ratio of fission weights produced in previous batch to the average starting weight for the previous batch. For time-dependent decaying systems, NORMF should be > 0 .

CARDS M Fission Neutron Weights [Begin with "***"]

[NOTE: Omit if MFISTP on Card L ≤ 0]

**

(FWLO(I), I = 1, MXREG)

values of the weight to be assigned to fission neutrons.

CARDS N Fission Induced Source Particle Fractions [Begin with "***"]

[NOTE: Omit if MFISTP on Card L ≤ 0]

**

(FSE(IG,IMED), IG = 1, NMGP), IMED = 1, MEDIA)

the fraction of fission-induced source particles in group IG and medium IMED.

[NOTE: Input for each medium must start on a new card.]

CARDS O Secondary Particle Production Probability [Begin with "***"]

[NOTE: Omit if $NGPQTN = 0$ or $NGPQTG = 0$, i.e., include if coupled neutron gamma-ray problem]

**

((GWLO(IG,NREG) IG = 1, NMGP or NMTG - NMGP), NREG = 1, MXREG)

values of the probability of generating a secondary particle. The secondary particle will be a gamma ray in the forward problem and a neutron in the adjoint problem. NMGP groups are read for each importance region in a forward problem and NMTG-NMGP for an adjoint problem.

[NOTE: The definition of GWLO depends on whether or not in-group biasing is specified (Card I, variable INGB), as follows:

INGB=1 (in-group biasing invoked) GWLO is the fraction of the natural production probability as specified by the cross sections and may be assigned values greater than, equal to, or less than one.

INGB=0 (no in-group biasing) GWLO is the probability of generating a gamma ray (adjoint neutron).]

[NOTE: Input for each importance region must start on a new card.]

CARD GA GIFT5 Program Control Card [10I1, 2F10.0, 3I5 format]

This input card is read in subroutine GIFTM.

[NOTE: Option is not set if = 0; otherwise the option is set]

IPRNT	print MASTER-ASTER array of processed geometry
ITEMPR	print identification table by item
IMNMAX	print ordered region rpp equivalents
ISOLEQ	print solid rpp equivalents
NOPRNT	suppress GENI printing

- 5 ---

IWSOL	print solid table
IWREG	print region table
IWRPP	print region rpp table
IWID	print region identification table
IWSUM	print summary table

- 10 ---

TOL	geometry tolerance
TOLLOS	line-of-sight tolerance

IVOID	void space code
IFANTM	phantom item code
IEND	signal end of components along ray

The control specifications card consists of first, a series of ten print control switches on 10I1 format, for which a 0 usually means "do not print" and a 1 means "print". "0000100000" appears useful for this card. Next are tolerances, for which 0.001 appears adequate. The last inputs on the card are void, phantom and ray end codes, 1, 0, and 0, respectively.

9.3.2 Cross-Section Module Input Instructions

This input is read by subroutine XSEC.

CARD XA Cross Section Title Card [20A4]

[NOTE: This title is also written on tape if a processed tape is written; therefore, it is suggested that the title be definitive.]

CARD XB Cross Section Control Parameters [Begin with "\$\$"]

\$\$

NGP	the number of primary groups for which there are cross sections to be stored. Should be same as NMGP input in MORSE.
NDS	number of primary downscatters for NGP (usually NGP).
NGG	number of secondary groups for which there are cross sections to be stored.
NDSG	number of secondary downscatters for NGG (Usually NGG).
INGP	total number of groups for which cross sections are to be input.

- 5 ---

ITBL	table length, i.e., the number of cross sections for each group; (usually equal to number of downscatters + number of upscatters + IHT).
ISGG	location of within-group scattering cross sections; (usually equal to number of upscatters plus IHT+1).
NMED	number of media for which cross sections are to be stored; should be same as MEDIA input in MORSE.
NELEM	number of elements for which cross sections are to be read.
NMIX	number of mixing operations (elements times density operations) to be performed (must be ≥ 1).

- 10 ---

NCOEF	number of coefficients for each element, including P_0 .
NSCT	number of discrete angles (usually the integer value of NCOEF/2).

ISTAT flag to store Legendre coefficients if greater than zero.
IHT location of total cross section in the table.

[NOTE: See Table 9-3 in Section 9.2.2 for examples on parameters NGP, NGG, and INGP.]

CARD XC Cross Section I/O parameters [Begin with "\$\$"]

\$\$

IRDSG switch to print the cross sections as they are read (if > 0).
ISTR switch to print cross sections as they are stored (if > 0).
IFMU switch to print intermediate results of μ 's calculation (if > 0).
(Ignored if IXTAPE < 0)
IMOM switch to print moments of angular distribution (if > 0). (Ignored if IXTAPE < 0)
IPRIN switch to print angles and probabilities (if > 0). (Ignored if IXTAPE < 0)

- 5 ---

IPUN switch to print results of bad Legendre coefficients (if > 0).
IDTF switch to signal that input format is DTF-IV format (if > 0); otherwise, ANISN format is assumed. (Ignored if IXTAPE < 0)
IXTAPE logical tape unit if binary cross section tape; set equal to 0 if cross sections are from cards. If negative, then the processed cross sections and other necessary data from a previous run will be read; in this case (IXTAPE < 0) no cross sections from cards and no mixing cards may be input. The absolute value of IXTAPE is the logical tape unit.
JXTAPE logical tape unit of a processed cross-section tape to be written. This processed tape will contain the title card, the variables from common LOCSIG and the pertinent cross sections from blank common.
IO6RT logical tape unit of a point cross-section tape in O6R format.

- 10 ---

IGQPT last group (MORSE multigroup structure) for which the O6R point cross sections are to be used (\leq NMGP).

CARD XD Element Identifiers [Begin with "\$\$"]

[NOTE: Omit if IXTAPE \leq 0]

Element identifiers for cross-section tape. If element identifiers are in same order as elements on tape, the efficiency of the code is increased due to fewer tape rewinds.

CARDS XE Cross Sections from Cards [Begin with "***" if free-form]

[NOTE: Omit if IXTAPE \neq 0]

If cross sections are in free-form, a card with "***" in columns 2 and 3 must precede the actual data. ANISN format if IDTF \leq 0; otherwise, DTF-IV format. Cross sections for INGP groups with a table length ITBL for NELEM elements each with NCOEF coefficients.

CARDS XF Cross-Section Mixing Table [Use "\$\$" and "***" as indicated]

[NOTE: Omit if IXTAPE $<$ 0]

\$\$

KM medium number.

KE element number occurring in medium KM (negative value indicates last mixing operation for that medium). Failure to have a negative value causes code not to generate angular probabilities for that media, i.e. (LEGEND and ANGLE not called).

**

RHO density of element KE in medium KM in units of atoms/(barn cm).

Example Card XF: \$\$ KM KE ** RHO

[NOTE: NMIX (see Card XB) cards are required.]

CARDS XG O6R Tape Control Parameter [Begin with "\$\$"]

[NOTE: Omit if IO6RT \leq 0]

\$\$

NXPM number of point cross-section sets per medium found on an O6R tape.
= 1, total cross section only,
= 2, total + scattering cross section,
= 3, total, scattering, and v *fission cross section.

9.3.3 Special MASH Input Instructions

In addition to the MORSE input described above, the following input data is required for a MASH run. These parameters are either included on the leakage tape read by DRC, or are used to determine parameters used on the leakage tape.

CARD AA Leakage Tape Title [10A4]

TTL Title to be placed on leakage tape

CARD BB Region Density Factors [Begin with "***"]

**

RDEN(I), I = 1, MXREG

Density factor for each importance region

CARD CC Air/Ground Media Indicators [Begin with "\$\$"]

\$\$

IGRND Media number of the ground
IAIR Media number of air

Two media numbers must be specified wherein a flag is placed on the product of secondary particle (neutron) generation. The variable names assigned to these numbers indicate that the conventional application of this input is to flag neutrons generated in the ground (IGRND) and the air (IAIR). Any media may be specified, with the understanding that the contribution of the flagged particles will be labeled GROUND and AIR, regardless of their true source.

9.3.4 GIFT5 Geometry Input Instructions

The GIFT5 input geometry consists of five parts as follows:

1. Title Card
2. Target Specification Card
3. Solids Table
4. Regions Table
5. Region Identification Table

Detailed descriptions of all these sections of input are given in Appendix C. Here, only the input instructions will be presented.

NOTE: The next six sections of input (Cards GB through Cards GG) for MASH are read from LOGICAL UNIT 8 (as currently configured). This is noted because the rest of the input is read from LOGICAL UNIT 5.

CARD GB GIFT5 Title Card [A2, 3X, A60 format]

TGTUN target unit specification [(cm) only for MASH]
ITITLE target geometry description title

This input card is read in subroutine GENI.

CARD GC GIFT5 Target Specification Card [2I5 format]

NSOLID number of geometry solids in Solids Table
NRMAX number of geometry regions in Regions Table

This input card is read in subroutine GENI.

CARD GD GIFT5 Solids Table [A5, A3, A1, 1X, 6F10.0, A10 format]

These input cards are read in subroutine SOLIN.

The solids table defines the basic geometric shapes. Table 9-6 summarizes the input for the different solid types. The basic format for all cards in the solids table is (A5, A3, A1, 1X, 6F10.0, A10) with the first field (A5) in the format normally used for the sequence number of the solid in the solid table, the second field (A3) used to designate solid type (e.g., RPP for rectangular parallelepiped or SPH for sphere) or blank if a continuation card for the solid, the third (A1) field used to designate a variant of the solid type (e.g., a 6 for a six-vertex arbitrary polyhedron or ARB6), the fourth field (6F10.0) used for the solid parameters, and the final (A10) field reserved for user notes or comments.

The parameters required to define the various solids are different from one type of solid to another. Usually, however, the parameters can be classified as being one of three types, a "vertex point", a "vector" or a "scalar". The vertex point is specified by its X,Y,Z coordinates, a vector is specified by its components in the X, Y, and Z directions, and a scalar is a single numeric value, for example the radius of a sphere.

The summary of the solids table input data given by Table 9-6 will be useful for persons familiar with combinatorial geometry, but a more detailed description of the geometry solid types and their input is necessary for new users and for users using new and more exotic solid types. Therefore a more detailed description of the various geometry solid types, including pictures, has been included. Because of its bulk, this description has been placed in Appendix C.

CARD GE GIFT5 Regions Table [I5, 1X, 9(A2, I5) 1X, A10 format]

These input cards are read in subroutine REGIN.

The GIFT5 geometry regions table is very similar to the zones table in MORSE combinatorial geometry. Via the regions table, the shape and space of several solids can be "combined" to define a component of the system being described. Three operators, a "+", a "-" and an "OR", and combinations thereof, are used to define the "intersection", "subtraction" or "union" of solids to form a more complex shape. A detailed description of how to use these operators, along with several examples, is given in Appendix B. The uninitiated user of combinatorial geometry should refer to these examples before attempting to model a complex geometry.

The general format for the regions table is I5, 1X, 9(A2,I5) 1X, A10. The first (I5) field is the region sequence number. Each line has provisions for nine pairs of OR operator fields and solid numbers with + or - sign, followed by 10 spaces for comment. (The 1X means an unused column on the card). Continuation cards can be used for regions described by the combination of more than nine bodies. For continuation cards, the region (first I5) entry is left blank.

[NOTE: The cards of the above format defining the various regions in the configuration are followed by a card with a -1 in columns 4 and 5. This "-1 CARD", as it is called, is the flag that marks the end of the region table.]

CARD GF GIFT5 Region Identification Table [5I5, 5X, A40 format]

These input cards are read in subroutine IDIN

The identification table is used to assign identification code numbers and additional information to the regions defined in the region table. Entries in the identification tables, in format (5I5, 5X, A40), are as follows:

Columns	Parameter
1 - 5	Region number
6 - 10	Component code number (1-9999)
11 - 15	MORSE importance region assignment (1, NRMAX)
16 - 20	Material code (1, NOMED)
21 - 25	Percent density (In percent)
31 - 70	Alphanumeric region description

NOTE: In MASH v1.0, only the region number (columns 1-5) was needed in the input. All the other columns could have been left blank (material numbers and importance region assignments were assigned in other input [Cards GH and GI] to MORSE). In MASH v1.5, all of the parameters specified for the Region Identification Table input are the same as those in MASH v1.0 except the Space code number. This has been replaced with the MORSE importance region assignment. For this input parameter, the importance region number for each geometry region is read in this array. In MASH v1.5, all of these arrays are now used and have to be input.

CARD GG GIFT5 Region RPP Table

[NOTE: The Region RPP Table discussed in Appendix C is optional and typically is not input in MASH. The GIFT5 program will automatically produce a Region RPP Table. Consequently, the user does not have to enter any data here.]

Table 9-6. Summary Description of Input for Solids Table.

1-5	6-8	9-10	11-20	21-30	31-40	41-50	51-60	61-70	71-80
NO.	RPP		XMIN	XMAX	YMIN	YMAX	ZMIN	ZMAX	COMMENTS
NO.	BOX		VX	VY	VZ	HX	HY	HZ	COMMENTS
NO.			WX	WY	WZ	DX	DY	DZ	COMMENTS
NO.	RAW		VX	VY	VZ	HX	HY	HZ	COMMENTS
NO.			WX	WY	WZ	DX	DY	DZ	COMMENTS
NO.	SPH		VX	VY	VZ	R			COMMENTS
NO.	ELL		VX	VY	VZ	AX	AY	AZ	COMMENTS
NO.			B						COMMENTS
NO.	ELL	G	VX	VY	VZ	AX	AY	AZ	COMMENTS
			BX	BY	BZ	CX	CY	AZ	COMMENTS
NO.	TOR		VX	VY	VZ	NX	NY	NZ	COMMENTS
			R1	R2					
NO.	RCC		VX	VY	VZ	HX	HY	HZ	COMMENTS
NO.			R						COMMENTS
NO.	REC		VX	VY	VZ	HX	HY	HZ	COMMENTS
NO.			AX	AY	AZ	BX	BY	BZ	COMMENTS
NO.	TRC		VX	VY	VZ	HX	HY	HZ	COMMENTS
NO.			R1	R2					
NO.	TEC		VX	VY	VZ	HX	HY	HZ	COMMENTS
NO.			AX	AY	AZ	BX	BY	BZ	COMMENTS
NO.			RATIO						COMMENTS
NO.	TGC		VX	VY	VZ	HX	HY	HZ	COMMENTS
NO.			AX	AY	AZ	BX	BY	BZ	COMMENTS
NO.			T(A)	T(B)					COMMENTS
NO.	HAF		A	B	C	D			COMMENTS
NO.	ARS		NC	NP	NR				COMMENTS
NO.			X1	Y1	Z1	X2	Y2	Z2	COMMENTS
NO.			X3	Y3	Z3	ETC.			COMMENTS

(START NEW CARD WITH EACH CURVE)
 CONVEX ARS HAS SAME INPUT EXCEPT COLS 9-10 NOT BLANK

Table 9-6. Summary Description of Input for Solids Table (Continued).

1-5	6-8	9-10	11-20	21-30	31-40	41-50	51-80	61-70	71-80
NO.	ARB	4	X1	Y1	Z1	X2	Y2	Z2	COMMENTS
NO.			X3	Y3	Z3	X4	Y4	Z4	COMMENTS
			FACES GENERATED 123 412 423 431						
NO.	ARB	5	X1	Y1	Z1	X2	X2	Z2	COMMENTS
NO.			X3	Y3	Z3	X4	Y4	Z4	COMMENTS
NO.			X5	Y5	Z5				COMMENTS
			FACES GENERATED 1234 512 523 534 541						
NO.	ARB	6	X1	Y1	Z1	X2	Y2	Z2	COMMENTS
NO.			X3	Y3	Z3	X4	Y4	Z4	COMMENTS
NO.			X5	Y5	Z5	X6	Y6	Z6	COMMENTS
			FACES GENERATED 1234 2365 1564 512 634						
NO.	ARB	7	X1	Y1	Z1	X2	Y2	Z2	COMMENTS
NO.			X3	Y3	Z3	X4	Y4	Z4	COMMENTS
NO.			X5	Y5	Z5	X6	Y6	Z6	COMMENTS
NO.			X7	Y7	Z7				COMMENTS
			FACES GENERATED 1234 587 145 2376 1265 4375						
NO.	ARB	8	X1	Y1	Z1	X2	Y2	Z2	COMMENTS
NO.			X3	Y3	Z3	X4	Y4	Z4	COMMENTS
NO.			X5	Y5	Z5	X6	Y6	Z6	COMMENTS
NO.			X7	Y7	Z7	X8	Y8	Z8	COMMENTS
			FACES GENERATED 1234 5678 1584 2376 1265 4378						
NO.	ARB	N	NPT	NPE	NEQ	NAE			COMMENTS
NO.			X1	Y1	Z1	ETC.			COMMENTS
			NPE.NE.0 [6(I4,2I30)] (NEG.=-Y)						
NO.			FACE1	FACE2	FACE3	ETC.			COMMENTS
			NEQ.NE.0						
NO.			A1	B1	C1	D1			COMMENTS
NO.			A2	B2	C2	D2			COMMENTS
NO.			ETC.						
			NAE.NE.0 [2(F10.4,I10)]						
NO.			AZ1	EL1	PN1	AZ2	EL2	PN2	COMMENTS
NO.			AZ3	EL3	PN3	ETC.			COMMENTS

Table 9-6. Summary Description of Input for Solids Table (Continued).

SOLID TABLE SYMBOLS (A5,A3,A2,6F10.0,A10)

V - VERTEX
H - HEIGHT VECTOR
W - WIDTH
D - DEPTH
N - NORMAL
A - SEMI-MAJOR AXIS
B - SEMI-MINOR AXIS
C - SEMI-MINOR AXIS OF ELLIPSE OF XSECT (ELLG)
R - RADIUS
T - LENGTH OF TOP AXIS WITH SAME DIRECTION AS BOTTOM AXIS
NC - NUMBER OF CURVES
NP - NUMBER OF POINTS PER CURVE
NR - NUMBER OF POINTS READ DIRECTLY

ARBN AND HAF SYMBOLS

NPT - NUMBER OF POINTS
NPE - NUMBER OF FACES DEFINED BY 3 POINTS
NEQ - NUMBER OF FACES DEFINED BY EQUATION
NAE - NUMBER OF FACES DEFINED BY AZ, EL AND POINT
A,B,C,D - PLANE EQUATION COEFFECIENTS $AX + BY + CZ = D$
AZ - AZIMUTH ANGLE
EL - ELEVATION ANGLE
PN - POINT NUMBER

9.4 ANISN NUCLIDE FORMAT CROSS-SECTION FILE

In a MORSE problem, cross sections are read from card input and/or from an external data set in nuclide-organized format, i.e., all the cross sections for one group of one nuclide, followed by other groups for that nuclide, and finally followed by data for other nuclides. Within a group, MORSE expects the ordering of data in the cross section table in the following format:

Table Position	Entry	Cross Section Type
1	$\sigma^1(g)$	First activation cross section (if any)
.	.	
.	.	
IHT-3	$\sigma^L(g)$	Last activation cross section (if any)
IHT-2	$\sigma^A(g)$	Absorption
IHT-1	$\nu\sigma^F(g)$	Neutron Production
IHT	$\sigma^T(g)$	Total removal
IHT+1	$\sigma^{TUS}(g)$	Total upscatter cross section from group g (omit this entry if NUS=0)
IHS-NUS	$\sigma(g+NUS \rightarrow g)$	Scattering from group g+NUS to g
.	.	
.	.	
.	.	
IHS-1	$\sigma(g+1 \rightarrow g)$	Scattering from group g+1 to g
IHS	$\sigma(g \rightarrow g)$	Scattering from group g to g
IHS+1	$\sigma(g-1 \rightarrow g)$	Scattering from group g-1 to g
.	.	
.	.	
.	.	
IHM	$\sigma(g-NDS \rightarrow g)$	Scattering from group g-NDS to g

From this, it can be seen that:

$$NUS = IHS - IHT - 2 = \text{number of upscatter groups, if greater than 0,}$$

$NDS = IHM - IHS =$ number of downscatter groups,

$L = IHT - 3 =$ number of activation cross sections.

Special illustrations of interest are:

$$IHM = IGM + 3$$

$$IHS = 4$$

$$IHT = 3$$



Full downscatter; no upscatter; no activation cross section

and,

$$IHM = IGM + 5 + NUS$$

$$IHS = 6 + NUS$$

$$IHT = 4$$



Full downscatter; NUS upscatter; room for an activation cross section in position 1.

Thus the parameters IHT, IHS, and IHM completely describe the format of the cross sections. If there are no activity cross sections, $IHT=3$. If there is no upscatter $IHS = IHT + 1$. If there is no downscatter $IHM = IHS$ (i.e. a one group problem). If there is upscatter, MORSE will compute a total upscatter cross section for each group of each material and place that cross section in position $IHM + 1$. The activity cross sections are not used in the MORSE code.

9.5 MORSE LEAKAGE TAPE OUTPUT FILE FOR DRC2

Because of the large amount of core storage required for the VISTA free-field fluences, the forward-adjoint coupling could not be accomplished as the Monte Carlo calculation was performed. The coupling involved the calculation of the integral

$$R = \int \Phi(P)\Phi^*(P)(\Omega \cdot n)dP$$

over the coupling surface S.

We define

$\Phi(P)$ = VISTA free-field fluences in phase space P.

$\Phi^*(P)$ = MORSE adjoint fluence in phase space P.

$\Omega \cdot n$ = cosine of angle between particle direction and inward normal.

The adjoint fluence at the r_s , the position of the surface S, is written on a leakage tape along with other variables necessary for coupling the MORSE results with the VISTA results in DRC2. The variables written on tape for each adjoint leakage are as follows:

1. IG - group number,
2. IGS - source group number,
3. WTBC - weight of the adjoint particle at leakage,
4. U - X direction cosine,
5. V - Y direction cosine,
6. W - Z direction cosine,
7. X - X location of leakage point
8. Y - Y location of leakage point
9. Z - Z location of leakage point
10. NBOD - body of leakage point
11. NSURF - surface of leakage point
12. NZONE - zone of leakage point
13. IDET - detector type in which particle is to be scored.

An output buffer was blocked to transfer the data from core to tape efficiently at the end of each batch. This permitted batch statistics to be calculated in the DRC code which reads the MORSE leakage tape and the VISTA fluence tape and performs the coupling. The leakage tape generated by MORSE contains the following data:

-
- Record 1 - Title and date of MORSE run
 - Record 2 - Initial Data Record - 24 words
 - Record 3 - Energy Group Structure, Velocities, Source Spectra and Biasing Function - 4*NMTG words
 - Record 4 - A Block of Leakage Information for 125 Adjoint Particles - 1625 words
 -
 -
 -

Record N -

A detailed description of the contents of the above records is given below:

- I. Record 1 - A 40 character title plus a 32 character date of run
- II. Record 2 - The USER labeled common (plus parameter INGB) is written in Record 2. The total number of groups, number of batches, etc., are contained in this record, as defined in Table 9-7.
- III. Record 3 - The multigroup energy structure and group velocities are contained in Record 3. The data are:

E(1) - Upper energy limit of Group 1.

E(NMTG) - Upper energy limit of Group NMTG.
 VEL(1) - Velocity of Group 1.

VEL(NMTG) - Velocity of Group NMTG.
 F(1) - Fraction of Source in Group 1

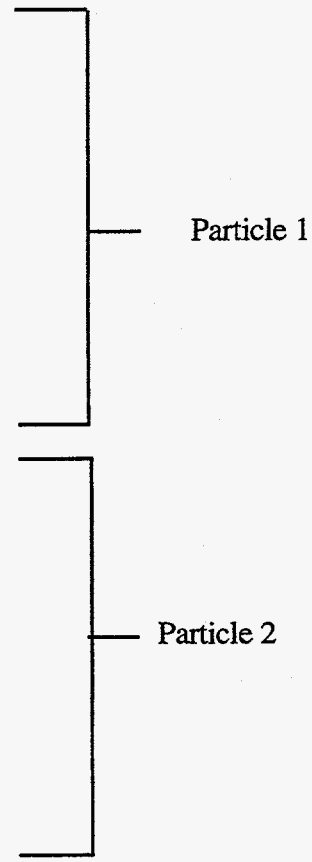
F(NMTG) - Fraction of Source in Group NMTG
 B(1) - Biased Fraction in Group 1

B(NMTG) - Biased Fraction of Source in Group NMTG

IV. Record 4 - The adjoint leakage fluence blocked in groups of 125 particles.

- B(1) - IG Energy Group
- B(2) - IGS Source Group
- B(3) - WTBC Weight at leakage
- B(4) - U direction
- B(5) - V cosines
- B(6) - W at leakage
- B(7) - X Radial distance at leakage
- B(8) - Y Radial distance at leakage
- B(9) - Z Height at leakage
- B(10) - Region number
- B(11) - Solid number
- B(12) - Solid surface number
- B(13) - IDET detector type

- . " " "
- . " " "
- . " " "
- . " " "
- . " " "
- . " " "
- . " " "
- . " " "



B(1625) - IDET Detector Type

- V. Additional records in the format of Record 4 to a total of $L(NITS+1)$ leakage records.
-

9.6 LOGICAL UNIT REQUIREMENTS

Below is a listing of the files required to execute a MORSE case along with the default values used in the code. In setting up a MORSE case, efforts must be made for these units to be available.

1. Logical Unit IXTAPE - Cross Section Input File [Default=10]
2. Logical Unit JXTAPE - Cross Section Output File [Default=2]
3. Logical Unit ISCU - MORSE Adjoint Leakage Scratch File [Default=23]
4. Logical Unit ICTU - MORSE Adjoint Leakage File [Default=24]
5. Logical Unit IO - Printed Output [Default=6]
6. Logical Unit I1 - MORSE Card Input File [Default=5]
7. Logical Unit IO8 - GIFT5 Card Input File [Default=8]
8. Logical Unit IO9 - GIFT5 Geometry Scratch Unit [Default=9]

Table 9-7. Definitions of Variables in USER COMMON.

Number	Variable	Definition
1	AGSTRT	Initial chronological age to be assigned to source particles
2	WTSTRT	Initial weight to be assigned to source particles
3	XSTRT	Initial x position to be assigned to source particles
4	YSTRT	Initial y position to be assigned to source particles
5	ZSTRT	Initial z position to be assigned to source particles
6	DFF	Normalization for adjoint problems
7	EBOTN	Lower energy boundary (eV) of last neutron group (group NMGP)
8	EBOTG	Lower energy boundary (eV) of last gamma-ray group (group NMTG)
9	TCUT	Chronological age limit
10	I0	Logical unit for output
11	I1	Logical unit for input
12	IADJM	Adjoint switch (> 0 for adjoint problem)
13	NGPQT1	Problem-dependent energy group limit
14	NGPQT2	Problem-dependent energy group limit
15	NGPQT3	Problem-dependent energy group limit
16	NGPQTG	Group number of lowest energy gamma-ray group to be treated
17	NGPQTN	Group number of lowest energy neutron group to be treated
18	NITS	Number of batches to be run
19	NLAST	Last cell in BLANK COMMON used by random walk package
20	NLEFT	Number of cells in BLANK COMMON available to user
21	NMGP	Number of primary energy groups
22	NMTG	Total number of energy groups
23	NSTRT	Number of source particles for each batch

9.7 REFERENCES

1. M. B. Emmett, "The MORSE Monte Carlo Radiation Transport Code System," ORNL-4972 (1975), ORNL-4972/R1 (1983), ORNL-4972/R2 (1984), Oak Ridge National Laboratory.
2. K. D. Lathrop, "DTF-IV, A FORTRAN-IV Program for Solving the Multigroup Transport Equation with Anisotropic Scattering," LA-3373, Los Alamos National Laboratory, (1965).
3. W. W. Engle, Jr., "A USER'S MANUAL FOR ANISN, A One-Dimensional Discrete-Ordinates Transport Code with Anisotropic Scattering," K-1693, Oak Ridge National Laboratory, (March 1967).

4. W. A. Rhoades and F. R. Mynatt, "The DOT III Two-Dimensional Discrete Ordinates Transport Code," ORNL-TM-4280, Oak Ridge National Laboratory, (September 1973).
5. W. A. Rhoades, D. B. Simpson, R. L. Childs, and W. W. Engle, Jr. "The DOT IV Two-Dimensional Discrete Ordinates Transport Code with Space-Dependent Mesh and Quadrature," ORNL/TM-6529, Oak Ridge National Laboratory (January 1979).
6. W. A. Rhoades and R. L. Childs, "An Updated Version of the DOT 4 One- and Two-Dimensional Neutron/Photon Transport Code," ORNL-5851, Oak Ridge National Laboratory (1982).
7. E. A. Straker, W. H. Scott, Jr., and N. R. Byrn, "The MORSE Code with Combinatorial Geometry," Defense Nuclear Agency DNA 2860T, SAI-72-511-LJ, Science Applications International Corporation, (May 1972).
8. Lawrence W. Bain, Jr. and Mathew J. Reisinger, "The GIFT Code User Manual; Volume I. Introduction and Input Requirements," BRL 1802, Ballistic Research Laboratory, (July 1975).
9. Gary G. Kuehl, Lawrence W. Bain, Jr. and Mathew J. Reisinger, "The GIFT Code User Manual; Volume II. The Output Options," ARBRL-TR-02189, Ballistic Research Laboratory, (September 1979).
10. A. E. Rainis and Ralph E. Rexroad, "MIFT: GIFT Combinatorial Geometry Input to VCS Code," BRL Report No. 1967, Ballistic Research Laboratory, (March 1977).
11. "The GIFT5 Geometry Package", Ballistic Research Laboratory, (No formal documentation exist for GIFT5.)
12. D. C. Irving, R. M. Freestone, Jr. and F. B. K. Kam, "O5R, A General Purpose Monte Carlo Neutron Transport Code," ORNL-3622, Oak Ridge National Laboratory, (1965).
13. C. L. Thompson and E. A. Straker, "O6R-ACTIFK, Monte Carlo Neutron Transport Code," ORNL-CF-69-8-36, Oak Ridge National Laboratory, (1969).
14. D. C. Irving, "Description of the CDC-1604 Version of the O6R Neutron Monte Carlo Transport Code," ORNL-TM-3518, Oak Ridge National Laboratory, (1971).
15. C. E. Burgart and E. A. Straker, "XCHEKR - A Multigroup Cross Section Editing and Checking Code," ORNL-TM-3518, Oak Ridge National Laboratory, (1971).
16. W. H. Scott, Jr., "Vehicle Code System (VCS) Documentation and Uncertainty Analysis," SAI Report SAI-133-79-977-LJ, Science Applications International Corporation, (December 1979).
17. W. H. Scott, Jr., and V. E. Staggs, "Adjoint Energy Biasing and Thermal Neutron Diffusion in the MORSE and VCS Codes," SAI-133-81-384-LJ Science Applications International Corporation, (November 1981).

18. W. H. Scott, Jr., et al., "Predictive Algorithm for Radiation Protection," Volume 1, "VCS In-Group Energy Bias, The DACM Code and DOT Calculations," SAIC-85/1710, Science Applications International Corporation, (May 1985).
19. J. A. Stoddard, S. D. Egbert, and W. H. Scott, Jr., "The Vehicle Code System with In-Group Energy Bias and GIFT5 Geometry," DNA-TR-87-23, Science Applications International Corporation, (January 1987).
20. W. A. Rhoades and M. B. Emmett et al., "Vehicle Code System (VCS User's Manual)," ORNL/TM-4648, Oak Ridge National Laboratory (August 1974).
21. W. A. Rhoades et al., "Development of a Code System for Determining Radiation Protection of Armored Vehicles (The VCS Code)," ORNL/TM-4664, Oak Ridge National Laboratory, (October 1974).
22. J. O. Johnson, J. D. Drischler, and J. M. Barnes, "Analysis of the Fall-1989 Two-Meter Box Test Bed Experiments Performed at the Army Pulse Radiation Facility (APRF)," ORNL/TM-11777, Oak Ridge National Laboratory, (May 1991).
23. R. T. Santoro et al., "DNA Radiation Environments Program Fall 1989 2-Meter Box Experiments and Analysis," ORNL/TM-11840, Oak Ridge National Laboratory, (May 1991).

9.8 SAMPLE PROBLEM

The sample problem demonstrates the adjoint Monte Carlo analysis of the two-meter box experiments.^{22,23} The two-meter box, i.e., "NATO standard test bed" is a large cubical steel walled box with a layer of 5.08-cm-thick steel plates mounted on the top, bottom, and all four sides. The exterior set of plates yield overall outside dimensions for the box of 220.32 cm x 220.32 cm x 220.32 cm, and are removable. The interior steel box has outside dimensions 210.16 cm x 210.16 cm x 210.16 cm with each wall having a thickness of 5.08 cm. This yields an interior air space with dimensions of 200 cm x 200 cm x 200 cm and thus gives the test bed the common name - "the two-meter box." The box also contains lift tabs (for movement by crane), drainage holes at the base, a cable access hole at the base on the back side of the box, and two hatches. The hatches are located in the center of the top and back faces of the box and the hatch diameters in the interior box and outside plates are staggered to mitigate radiation streaming paths into the box. The hatches are included for loading and unloading experimental equipment, e.g., detectors, phantoms, etc., and for simulating open-hatch vehicle experiments. An isometric view of the two-meter box test bed is shown in Figure 9-1.

A complete listing of the input cards for the sample problem is given in Figure 9-2, and Figure 9-3, and some selected output is shown in Figure 9-4. Figure 9-2 represents the input on logical unit 5 which contains the random walk input, the GIFT5 geometry card GA, the cross-section input, and the special MASH input for output to DRC2. Figure 9-3 illustrates the GIFT5 geometry input read on logical unit 8 for the Two-Meter Box for geometry Cards GB, GC, GD, GE, and GF). In viewing Figure 9-2, the input illustrates; the descriptive title for the MORSE case, 1000 particle per batch (NSTRT), 50 batches (NITS), and a maximum number of particles to be stored in the banks of 1500 (NMOST). Only one set of 50 batches was to be run (NQUIT). The energy group numbers being analyzed include 46 neutron groups (NGPQTN), 23 gamma groups (NGPQTG), 46

primary particle groups (NMGP), and 69 total groups (NMTG). The adjoint mode switch was set to one (IADJM=1 always), 120 minutes of CPU time was allowed (MAXTIM), and there were nine cross section media for the problem (MEDIA).

The source was sampled from the distribution on Cards E1 (ISOUR=0, and NGPFS=69). Also, the input source energy spectrum was biased (ISBIAS=1) and the biasing parameters were read from Cards E2. Each starting particle had an initial weight of 1.0 (WTSTRT), and was initiated from the X, Y, Z position corresponding to (0.0, 0.0, 110.16 cm) in the geometry. Since UINP, VINP, and WINP were all zero, the source was assumed to be isotropic. The energy group boundaries are read from Cards F1. Card G was omitted because no collision tape was requested (NCOLTP = 0 on Card B). After the energy group boundaries, the starting random number seed is input (Card H).

The next input card (Card I) indicates the splitting and Russian roulette are to be used (NSPLT and NKILL = 1) on one importance region (MXREG=1) for all 69 energy groups (MAXGP=69). Furthermore, in-group energy biasing is turned on (INGB=1).

One Card J is input for each importance region, to give the weight standards for the splitting and Russian roulette. This input is terminated by the -1 for NGP1 on the last Card J.

Card K is omitted because IEBIAS was equal to zero. All parameters on Card L are zero for this problem and consequently, Card M and Card N are not required. Card O is input one time for each importance region (MXREG on Card I). In this example, a GWLO parameter was set to 1.0 for all regions and all groups. This has proven to be the most efficient use of this parameter with in-group biasing turned on.

The GIFT5 program control card (Card GA) is next in the input stream, with the first 10 control parameters set to zero, the tolerances set to 0.001 and the final three parameters set to zero. If the last three parameters are set to zero, GIFT5 will use the defaults.

This input is followed by the GIFT5 geometry input. The GIFT5 geometry input is read from logical unit 8 and is presented in Figure 9-3.

The next section of input is the cross section Cards XA through XG. The energy group parameters (on Card XB) match the parameters read in Card B. There are nine cross section media (NMED), 24 elements (NELEM) to be read in from logical unit 2 (IXTAPE) and 67 mixing operations (NMIX) to be performed. The cross section set was P₅, (NCOEF=6), and the number of discrete angles was 3 (NSCAT=NCOEF/2). All of the cross-section print triggers on Card XC are turned off. The element identifiers (all P_i components) are entered on the Cards XD. There are 144 entries on these cards (NCOEF times NELEM). Card XE is omitted since the input ANISN library is on unit IXTAPE. The next 67 cards correspond to the mixing table on Card XF. The nine different materials are constructed on these cards.

Finally, the input in Figure 9-2 shows the special MASH input for use with DRC2. This includes the short title card (40 characters) on Card AA, the importance region density factors (all 1.0 in this problem) on Card BB, and the air and ground identifiers (2 and 1, respectively) on Card CC.

Figure 9-3 illustrates the five GIFT5 geometry input Cards GB through GF read in on logical unit 8. The title card indicates units of centimeters and the target. The second card indicates 49 solids in the solid table, and 24 regions in the region table. The 49 solids

follow (Cards GD) and then the 24 regions (Cards GE) Note the "-1" card to end the region table. Finally, the input shows the region identification table (24 cards, one for each region) The only information used from this card is the first column.

The coupling surface used in the MORSE sample calculation to tabulate the adjoint leakage current was a RPP centered about the box (solid 1 in the solid table). Other coupling surfaces such as a sphere, right circular cylinder, etc., could be used also. The only assumption is that the VISTA free-field fluence at a given height does not vary between X-Y positions in the vehicle coordinate system. In order to include the particle leakage from the top and bottom of the vehicle, the RPP extended from below the air-ground interface to several centimeters above the top surface of the vehicle. The coupling surface is always the exterior boundary of the Monte Carlo geometry, i.e. where the particle enters the external void. Adjoint particles that cross this surface are terminated and recorded on the history data set.

The selected MORSE output shown in Figure 9-4 first illustrates the input parameters read in the first four input data cards from logical unit 5, followed by tables of the input source spectrum and biasing parameters (Cards E1 and E2 and the input energy group boundaries (Cards F) This is followed by the splitting and Russian roulette parameters for the different importance regions (Cards I and J) and the secondary production parameters by energy group for the importance regions (Cards O). The next sections of input are from the GIFT5 geometry package and give detailed edits of the geometry input data on logical unit 8. This print can be suppressed by setting the NOPRNT switch on Card GA to one. The geometry input array edits are followed by a storage summary for the geometry data, and then edits of the material region and importance region information.

The output in Figure 9-4 then edits the processing of the cross section input on Cards XA through XG. On this sample problem, this information is suppressed. Large amounts of printout can be generated if the user is not careful with the print triggers on Card XC. The input in Figure 9-2 illustrates the input the first time the sample problem was executed and illustrates what is required for an initial case. Once that case is run, and the cross-section set is saved for future use, only Cards XA, XB, and XC are required for the cross section input.

The cross section edits are followed by a statement informing the user of the last location used in blank common. This is an indication of how much core space the problem required based on the input received from the user. The normalized CDF for the adjoint source sampling is printed next, followed by the adjoint group structure. The next section of printout illustrates the actual random walk (by batch). Each batch will give the starting random number for the batch, the average source particles starting parameters, the time required to execute the batch, and a sequence of counters for the batch which correspond to the 13 positive arguments for subroutine BANKR illustrated in Table 9-1 of Section 9.2.1 of this report. This information is useful in determining how well the user has set the problem up. Unfortunately, the best teacher in properly interpreting these counters is experience. The output also indicates several calls to subroutine RAYCHK, indicating an undefined region(s) in the geometry. This sequence of output is ended by the total time required to process all NITS batches.

The last section of output comes from the analysis routines which summarize the events that occurred in the random walk process for the entire run. The first table is a summary table of the particle deaths, labeled "neutron deaths" followed by a table of scatterings by medium. The next several pages of output are different counters (by importance region and group) for the entire random walk. These tables include the real scattering counters, track

length counters, secondary production counters, number of splittings, number of upscatter splittings, number of Russian roulette kills, and the number of Russian roulette survivals. Unfortunately, like the batch summary counters, only experience will increase the users full understanding and interpretation of all these arrays. The last output line informs the user of the total amount of CPU required to run the problem.

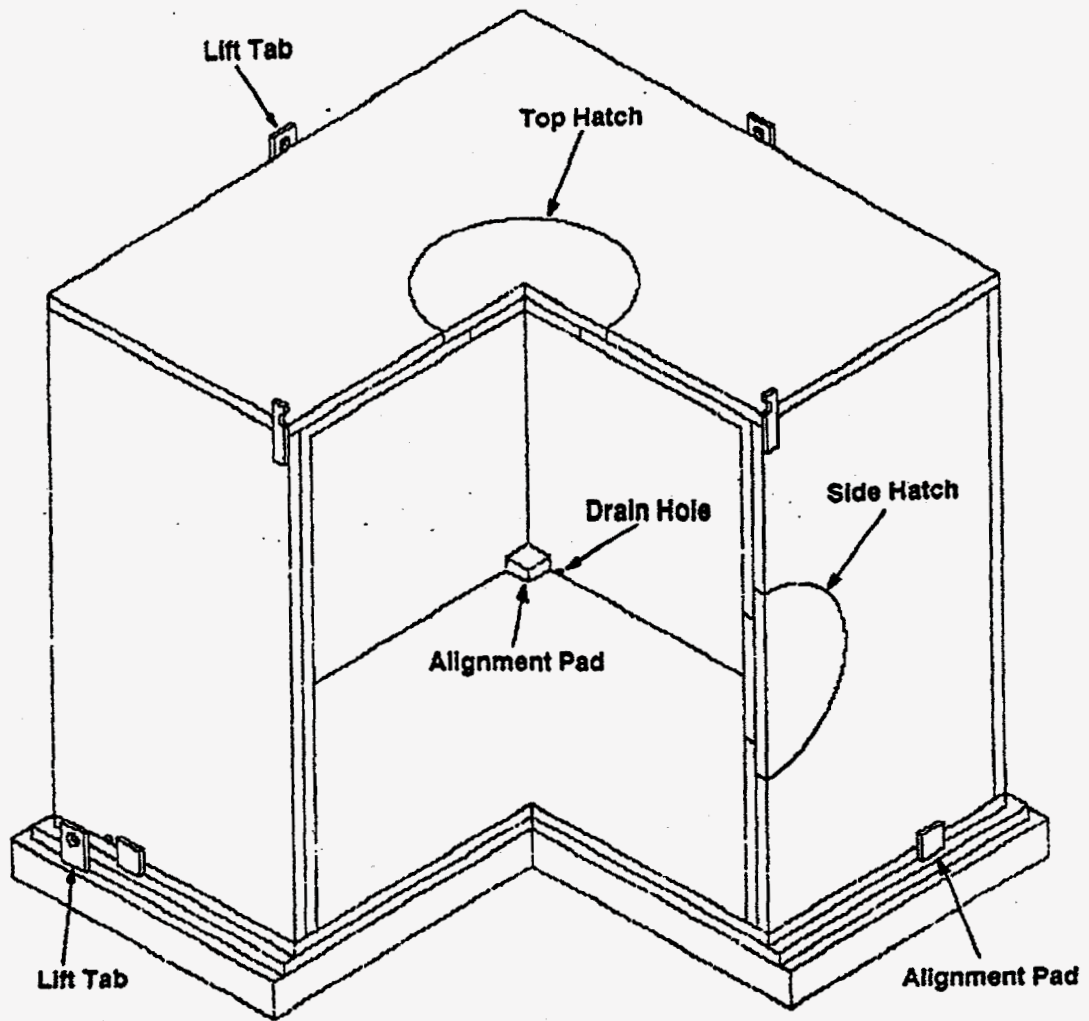


Figure 9-1. Schematic Diagram of the Two-Meter Box Geometry Model Used in the MORSE Analysis.


```

aprf two meter box calc/4in steel/dabl 46n-23g/detailed geometry model
$$ 1000 1500 50 1 46 23 46 69 0 1 120 9 0
$$ 0 69 1 0
** 1.0 1.0-05 1.0+04 0.0 2.2+05
** 0.0 0.0 110.16 0.0 0.0 0.0 0.0
** 69r1.0
** 8r1.0 11r2.0 8r4.0 3r2.0 16r1.0 3r3.0 12r6.0 8r3.0
** 1.9640+7 1.6905+7 1.4918+7 1.4191+7 1.3840+7 1.2523+7 1.2214+7
1.1052+7 1.0000+7 9.0484+6 8.1873+6 7.4082+6 6.3763+6 4.9658+6
4.7237+6 4.0657+6 3.0119+6 2.3852+6 2.3069+6 1.8268+6 1.4227+6
1.1080+6 9.6164+5 8.2085+5 7.4274+5 6.3927+5 5.5023+5 3.6883+5
2.4724+5 1.5764+5 1.1109+5 5.2475+4 3.4307+4 2.4788+4 2.1875+4
1.0595+4 3.3546+3 1.2341+3 5.8295+2 2.7536+2 1.0130+2 2.9023+1
1.0677+1 3.0590+0 1.12535+0 4.1399-1 2.0000+7 1.4000+7 1.2000+7
1.0000+7 8.0000+6 7.0000+6 6.0000+6 5.0000+6 4.0000+6 3.0000+6
2.5000+6 2.0000+6 1.5000+6 1.0000+6 7.0000+5 4.5500+5 3.0000+5
1.5000+5 1.0000+5 7.0000+4 4.5000+4 3.0000+4 2.0000+4
0000343276244615
$$ 1 1 0 0 0 1 69 1
$$ 1 1 69 1 1 1 ** 5.0+00 5.0-02 2.0-01 0.0
$$ -1 9r0
$$ 0 0 0 0
** 23r1.0
0000000000 0.001 0.001 0 0 0
2m box exp/aprf aog. 5/90 exp. ss90-130-39 s90e5, 1020 steel + phantom n.d.
$$ 46 46 23 23 69 72 4 9 24 67 6 3 0 3
$$ 0 0 0 0 0 0 0 2 0 0 0
$$ 1 2 3 4 5 6 43 44 45 46 47 48 49 50
51 52 53 54 55 56 57 58 59 60 61 62 63 64
65 66 67 68 69 70 71 72 79 80 81 82 83 84
85 86 87 88 89 90 91 92 93 94 95 96 97 98
99 100 101 102 103 104 105 106 107 108 109 110 111 112
113 114 115 116 117 118 119 120 121 122 123 124 125 126
127 128 129 130 131 132 133 134 135 136 137 138 157 158
159 160 161 162 163 164 165 166 167 168 169 170 171 172
173 174 175 176 177 178 179 180 181 182 183 184 185 186
199 200 201 202 203 204 205 206 207 208 209 210 223 224
225 226 227 228
$$ 1 1 ** 4.8016-2
$$ 1 2 ** 8.8600-9
$$ 1 3 ** 3.2435-8
$$ 1 4 ** 3.4889-4
$$ 1 5 ** 4.3922-5
$$ 1 6 ** 4.3043-2
$$ 1 7 ** 1.3186-4
$$ 1 8 ** 8.4348-5
$$ 1 9 ** 1.2722-3
$$ 1 10 ** 8.7935-3
$$ 1 12 ** 3.3368-6
$$ 1 13 ** 3.2693-6
$$ 1 15 ** 1.8926-4
$$ 1 16 ** 2.4025-5
$$ 1 17 ** 6.6540-6

```

Figure 9-2. Sample MORSE Input for the Two-Meter Box Analysis.

\$\$	1	18	**	2.9695-4
\$\$	1	19	**	2.5719-7
\$\$	1	20	**	2.5817-7
\$\$	1	21	**	4.4903-7
\$\$	1	-24	**	6.7608-8
\$\$	2	1	**	7.0106-7
\$\$	2	5	**	3.8326-5
\$\$	2	6	**	1.0632-5
\$\$	2	-14	**	2.2922-7
\$\$	3	4	**	8.0783-4
\$\$	3	10	**	4.2132-4
\$\$	3	11	**	6.1126-5
\$\$	3	12	**	7.3810-5
\$\$	3	17	**	3.8771-4
\$\$	3	-18	**	8.3911-2
\$\$	4	1	**	1.6543-2
\$\$	4	4	**	1.1849-2
\$\$	4	5	**	1.0228-3
\$\$	4	6	**	3.8166-3
\$\$	4	7	**	1.7367-9
\$\$	4	9	**	1.3057-9
\$\$	4	-13	**	7.1279-8
\$\$	5	1	**	5.8845-2
\$\$	5	4	**	3.3642-2
\$\$	5	5	**	1.9850-3
\$\$	5	6	**	7.7235-3
\$\$	5	7	**	2.3220-7
\$\$	5	9	**	2.2899-9
\$\$	5	-13	**	2.3527-8
\$\$	6	1	**	6.1368-2
\$\$	6	4	**	1.7881-2
\$\$	6	5	**	1.8400-3
\$\$	6	6	**	2.5237-2
\$\$	6	7	**	1.1955-4
\$\$	6	8	**	3.8839-5
\$\$	6	10	**	6.0036-7
\$\$	6	11	**	1.3868-3
\$\$	6	12	**	4.5488-5
\$\$	6	13	**	3.4006-5
\$\$	6	15	**	3.2988-5
\$\$	6	16	**	2.1435-3
\$\$	6	-18	**	1.2077-6
\$\$	7	1	**	6.6854-2
\$\$	7	-6	**	3.3427-2
\$\$	8	1	**	3.9800-2
\$\$	8	4	**	4.5400-2
\$\$	8	-6	**	8.5200-3
\$\$	9	1	**	7.1300-2
\$\$	9	2	**	4.8700-4
\$\$	9	3	**	1.9700-3
\$\$	9	4	**	3.4100-2
\$\$	9	-6	**	3.6400-3

two meter box/detailed geometry/46n-23g

** 1.0

\$\$ 1 2

Figure 9-2. (continued)

cm 2.0 meter cubic box geometry (4 inches of steel)

49 24

1rpp	-120.0000	120.0000	-120.0000	120.0000	-15.0000	230.0000
2rpp	-115.2398	115.2398	-115.2398	115.2398	0.0000	5.0800
3rpp	-110.1598	110.1598	-110.1598	110.1598	5.0800	10.1600
4rpp	-99.9998	-89.8398	-99.9998	-89.8398	10.1600	15.2400
5rpp	89.8398	99.9998	-99.9998	-89.8398	10.1600	15.2400
6rpp	89.8398	99.9998	89.8398	99.9998	10.1600	15.2400
7rpp	-99.9998	-89.8398	89.8398	99.9998	10.1600	15.2400
8rpp	-105.0798	105.0798	-105.0798	105.0798	10.1600	215.2396
9rpp	-99.9998	99.9998	-99.9998	99.9998	10.1600	210.1596
10rpp	-79.6798	-69.5198	-112.0598	-110.1598	5.0800	15.2400
11rpp	69.5198	79.6798	-112.0598	-110.1598	5.0800	15.2400
12rpp	110.1598	112.0598	-79.6798	-69.5298	5.0800	15.2400
13rpp	110.1598	112.0598	69.5298	79.6798	5.0800	15.2400
14rpp	69.5198	79.6798	110.1598	112.0598	5.0800	15.2400
15rpp	-79.6798	-69.5198	110.1598	112.0598	5.0800	15.2400
16rpp	-112.0598	-110.1598	69.5198	79.6798	5.0800	15.2400
17rpp	-112.0598	-110.1598	-79.6798	-69.5198	5.0800	15.2400
18rpp	-99.9998	-89.8398	-117.1398	-115.2398	0.0000	15.2400
19rpp	89.8398	99.9998	-117.1398	-115.2398	0.0000	15.2400
20rpp	89.8398	99.9998	115.2398	117.1398	0.0000	15.2400
21rpp	-99.9998	-89.8398	115.2398	117.1398	0.0000	15.2400
22rcc	-94.9198	-117.1398	10.1600	0.0000	1.9000	0.0000
	2.5400					
23rcc	94.9198	-117.1398	10.1600	0.0000	1.9000	0.0000
	2.5400					
24rcc	94.9198	115.2398	10.1600	0.0000	1.9000	0.0000
	2.5400					
25rcc	-94.9198	115.2398	10.1600	0.0000	1.9000	0.0000
	2.5400					
26rcc	0.0000	0.0000	210.1596	0.0000	0.0000	5.0800
	25.4000					
27rcc	99.9998	0.0000	110.1598	5.0800	0.0000	0.0000
	25.4000					
28rcc	99.9998	-49.1998	10.1600	10.1600	0.0000	0.0000
	5.0800					
29rpp	-110.1598	110.1598	-110.1598	-105.0798	10.1600	215.2396
30rpp	105.0798	110.1598	-105.0798	105.0798	10.1600	215.2396
31rpp	-110.1598	110.1598	105.0798	110.1598	10.1600	215.2396
32rpp	-110.1598	-105.0798	-105.0798	105.0798	10.1600	215.2396
33rpp	-110.1598	110.1598	-110.1598	110.1598	215.2396	220.3196
34rcc	0.0000	0.0000	215.2396	0.0000	0.0000	5.0800
	37.4650					
35rcc	105.0798	0.0000	110.1598	5.0800	0.0000	0.0000
	37.4650					
36rpp	-5.0800	5.0800	-112.0598	-110.1598	205.1596	228.0196
37rpp	110.1598	112.0598	-5.0800	5.0800	205.1596	228.0196
38rpp	-5.0800	5.0800	110.1598	112.0598	205.1596	228.0196
39rpp	-112.0598	-110.1598	-5.0800	5.0800	205.1596	228.0196

Figure 9-3. Sample GIFT5 Input for the Two-Meter Box Analysis

40rcc	0.0000	-112.0598	222.9396	0.0000	1.9000	0.0000				
	2.5400									
41rcc	110.1598	0.0000	222.9396	1.9000	0.0000	0.0000				
	2.5400									
42rcc	0.0000	110.1598	222.9396	0.0000	1.9000	0.0000				
	2.5400									
43rcc	-112.0598	0.0000	222.9396	1.9000	0.0000	0.0000				
	2.5400									
44rcc	-85.0000	-110.1598	11.4300	0.0000	10.1600	0.0000				
	1.2700									
45rcc	85.0000	-110.1598	11.4300	0.0000	10.1600	0.0000				
	1.2700									
46rcc	85.0000	99.9998	11.4300	0.0000	10.1600	0.0000				
	1.2700									
47rcc	-85.0000	99.9998	11.4300	0.0000	10.1600	0.0000				
	1.2700									
48rpp	-120.0000	120.0000	-120.0000	120.0000	-15.0000	0.0000				
49rpp	-125.0	125.0000	-125.0	125.0000	-16.00	235.0000				
1	1	-2	-3	-8	-10	-11	-12	-13	-14	z1001
	-15	-16	-17	-18	-19	-20	-21	-22	-23	air
	-24	-25	-28	-29	-30	-31	-32	-33	-34	
	-35	-36	-37	-38	-39	-40	-41	-42	-43	
	-44	-45	-46	-47	-48					
2	2	-3	-10	-11	-12	-13	-14	-15	-16	z1002
	-17	-18	-19	-20	-21					base
3	3	-4	-5	-6	-7	-8	-9	-10	-11	z1003
	-12	-13	-14	-15	-16	-17	-29	-30	-31	base
	-32									
4 or	4or	5or	6or	7						z1004
5	8	-9	-26	-27	-28	-44	-45	-46	-47	z1005
6	9	-4	-5	-6	-7	-26	-27	-28	-44	z1006
	-45	-46	-47							air
7 or	10or	11or	12or	13or	14or	15or	16or	17		z1007
8 or	18	-22or	19	-23or	20	-24or	21	-25		z1008
9 or	22or	23or	24or	25						z1009
10	26									z1010
11	27									z1011
12	28	-3								z1012
13	29	-8	-30	-32	-33	-36	-44	-45		z1013
14	30	-8	-33	-35	-37	-28				z1014
15	31	-8	-30	-32	-33	-38	-46	-47		z1015
16	32	-8	-33	-39						z1016
17	33	-8	-34	-36	-37	-38	-39			z1017
18 or	36	-40or	37	-41or	38	-42or	39	-43		z1018
19 or	40or	41or	42or	43						z1019
20 or	44or	45or	46or	47						z1020
21	34	-26								z1021
22	35	-27								z1022
23	48	-2								z1023
24	49	-1								z1024
-1										
1	1	1	2	100	/box/z1001/surrounding/air					
2	1	1	3	100	/box/z1002/bottom/base/pad					

Figure 9-3. (continued)

3	1	1	3	100	/box/z1003/upper/base/pad
4	1	1	3	100	/box/z1004/inner/alignment/pad
5	1	1	3	100	/box/z1005/inner/box
6	1	1	2	100	/box/z1006/inner/box/air-void
7	1	1	3	100	/box/z1007/outer/wall/alignment/pad
8	1	1	3	100	/box/z1008/base/pad/lift/eyelets
9	1	1	2	100	/box/z1009/eyelets/voids-air
10	1	1	3	100	/box/z1010/inner/box/top/hatch
11	1	1	3	100	/box/z1011/inner/box/side/hatch
12	1	1	2	100	/box/z1012/inner/outer/cable/run/void-air
13	1	1	3	100	/box/z1013/outer/wall/negative/y-axis
14	1	1	3	100	/box/z1014/outer/wall/positive/x-axis
15	1	1	3	100	/box/z1015/outer/wall/positive/y-axis
16	1	1	3	100	/box/z1016/outer/wall/negative/x-axis
17	1	1	3	100	/box/z1017/outer/top
18	1	1	3	100	/box/z1018/outer/wall/lift/eyelets
19	1	1	2	100	/box/z1019/outer/wall/lift/eyelets/void-air
20	1	1	2	100	/box/z1020/inner/outer/drain/holes
21	1	1	3	100	/box/z1021/outer/top/hatch
22	1	1	3	100	/box/z1022/outer/wall/side/hatch
23	1	1	1	100	/box/z1023/ground
24	1	1	0	100	/box/z1024/external/void

Figure 9-3. (continued)

*** mash version 1.5 *** fortran and compilation frozen 01-01-96 ***

*** This problem started: Thu Jun 25 21:03:51 1998

aprf two meter box calc/4in steel/dabl 46n-23g/detailed geometry model

nstr	nmost	nits	nquit	ngpqt	ngpqtg	nmgp	nmgt	ncoltp	iadjm	maxtim	media	medalb
1000	1500	50	1	46	23	46	69	0	1	120	9	0
isour	ngpfs	isbias	1	1.0000E+00	1.0000E-05	1.0000E+04	0.0000E+00	0.0000E+00	2.2000E+05			
0	69											

xstr	ystr	zstr	agstr	uinp	vimp	wimp
0.000E+00	0.000E+00	1.102E+02	0.000E+00	.000000	.000000	.000000

adjoint case - nrun will modify output by dff= 6.90000E+01

group	source data unnormalized fraction	normalized fraction	relative importance	normalized biased fraction
1	1.0000E+00	.014493	1.0000E+00	.005291
2	1.0000E+00	.014493	1.0000E+00	.005291
3	1.0000E+00	.014493	1.0000E+00	.005291
4	1.0000E+00	.014493	1.0000E+00	.005291
5	1.0000E+00	.014493	1.0000E+00	.005291
6	1.0000E+00	.014493	1.0000E+00	.005291
7	1.0000E+00	.014493	1.0000E+00	.005291
8	1.0000E+00	.014493	1.0000E+00	.005291
9	1.0000E+00	.014493	2.0000E+00	.010582
10	1.0000E+00	.014493	2.0000E+00	.010582
60	1.0000E+00	.014493	6.0000E+00	.031746
61	1.0000E+00	.014493	6.0000E+00	.031746
62	1.0000E+00	.014493	3.0000E+00	.015873
63	1.0000E+00	.014493	3.0000E+00	.015873
64	1.0000E+00	.014493	3.0000E+00	.015873
65	1.0000E+00	.014493	3.0000E+00	.015873
66	1.0000E+00	.014493	3.0000E+00	.015873
67	1.0000E+00	.014493	3.0000E+00	.015873
68	1.0000E+00	.014493	3.0000E+00	.015873
69	1.0000E+00	.014493	3.0000E+00	.015873
total	6.9000E+01			

group parameters, group numbers greater than 46 correspond to secondary particles

group	upper edge (ev)	velocity (cm/sec)
1	1.9640E+07	5.9118E+09
2	1.6905E+07	5.5167E+09
3	1.4918E+07	5.2762E+09
4	1.4191E+07	5.1776E+09
5	1.3840E+07	5.0212E+09
6	1.2523E+07	4.8639E+09
7	1.2214E+07	4.7170E+09
8	1.1052E+07	4.4870E+09
9	1.0000E+07	4.2681E+09
10	9.0484E+06	4.0600E+09
60	1.0000E+06	2.9979E+10
61	7.0000E+05	2.9979E+10

Figure 9-4. Sample MORSE Output for the Two-Meter Box Analysis

```

62 4.5500E+05 2.9979E+10
63 3.0000E+05 2.9979E+10
64 1.5000E+05 2.9979E+10
65 1.0000E+05 2.9979E+10
66 7.0000E+04 2.9979E+10
67 4.5000E+04 2.9979E+10
68 3.0000E+04 2.9979E+10
69 2.0000E+04 2.9979E+10

initial random number = 000343276244

nsp1= 1 nkill= 1 npast= 0 nleak= 0 iebias= 0 mxreg= 1 maxgp= 69 ingb= 1
weight standards for splitting and russian roulette and pathlength stretching parameters
ngp1 ndg npp2 nrg1 ndig nrg2 wthihl wtlowl wtlavel xnu
1 1 69 1 1 1 5.0000E+00 5.0000E-02 2.0000E-01 .0000E+00

```

this is an adjoint problem. the adjoint group structure (ia) is related to the forward group structure (i) by (ia=mtg+1-i).

the above arrays are given in the forward group structure.

in-group adjoint energy biasing used.

```

nsour= 0 mfistp= 0 nkcalc= 0 normf= 0
gwlw(ig,nreg)
group region 1
1 1.0000E+00
2 1.0000E+00
3 1.0000E+00
4 1.0000E+00
5 1.0000E+00
6 1.0000E+00
7 1.0000E+00
8 1.0000E+00
9 1.0000E+00
10 1.0000E+00
11 1.0000E+00
12 1.0000E+00
13 1.0000E+00
14 1.0000E+00
15 1.0000E+00
16 1.0000E+00
17 1.0000E+00
18 1.0000E+00
19 1.0000E+00
20 1.0000E+00
21 1.0000E+00
22 1.0000E+00
23 1.0000E+00

```

```

gift program - cdc fortran v version
program set 1982 november 1
execution date time
begin execution

enter geni

title - 2.0 meter cubic box geometry (4 inches of steel)
target units (cm)

no. of solids 49
max no. of regions 24

```

Figure 9-4. (continued)

				description of solids				
1	1	rpp	-120.0000	120.0000	-120.0000	120.0000	-15.0000	230.0000
2	2	rpp	-115.2398	115.2398	-115.2398	115.2398	.0000	5.0800
3	3	rpp	-110.1598	110.1598	-110.1598	110.1598	5.0800	10.1600
4	4	rpp	-99.9998	99.9998	-99.9998	99.9998	10.1600	15.2400
5	5	rpp	89.8398	99.9998	-89.8398	89.8398	10.1600	15.2400
6	6	rpp	89.8398	99.9998	-89.8398	89.8398	10.1600	15.2400
7	7	rpp	-99.9998	99.9998	-99.9998	99.9998	10.1600	15.2400
8	8	rpp	-105.0798	105.0798	-105.0798	105.0798	10.1600	215.2396
9	9	rpp	-99.9998	99.9998	-99.9998	99.9998	10.1600	210.1596
10	10	rpp	-79.6798	-69.5198	-112.0598	-110.1598	5.0800	15.2400
11	11	rpp	69.5198	79.6798	-112.0598	-110.1598	5.0800	15.2400
12	12	rpp	110.1598	112.0598	-79.6798	-69.5198	5.0800	15.2400
13	13	rpp	110.1598	112.0598	69.5298	79.6798	5.0800	15.2400
14	14	rpp	69.5198	79.6798	110.1598	112.0598	5.0800	15.2400
15	15	rpp	-79.6798	-69.5198	110.1598	112.0598	5.0800	15.2400
16	16	rpp	-112.0598	-110.1598	69.5198	79.6798	5.0800	15.2400
17	17	rpp	-112.0598	-110.1598	-79.6798	-69.5198	5.0800	15.2400
18	18	rpp	-99.9998	99.9998	-89.8398	-117.1398	.0000	15.2400
19	19	rpp	89.8398	99.9998	-117.1398	-115.2398	.0000	15.2400
20	20	rpp	89.8398	99.9998	115.2398	117.1398	.0000	15.2400
21	21	rpp	-99.9998	99.9998	115.2398	117.1398	.0000	15.2400
22	22	rcc	-94.9198	-117.1398	10.1600	.0000	1.9000	.0000
23	23	rcc	94.9198	-117.1398	10.1600	.0000	1.9000	.0000
24	24	rcc	94.9198	115.2398	10.1600	.0000	1.9000	.0000
25	25	rcc	-94.9198	115.2398	10.1600	.0000	1.9000	.0000
26	26	rcc	.0000	.0000	210.1596	.0000	.0000	5.0800
27	27	rcc	99.9998	.0000	110.1598	5.0800	.0000	.0000
28	28	rcc	99.9998	-49.1998	10.1600	10.1600	.0000	.0000
29	29	rpp	-110.1598	110.1598	-105.0798	-105.0798	10.1600	215.2396
30	30	rpp	105.0798	110.1598	-105.0798	-105.0798	10.1600	215.2396
31	31	rpp	-110.1598	110.1598	105.0798	110.1598	10.1600	215.2396
32	32	rpp	-110.1598	-105.0798	-105.0798	-105.0798	10.1600	215.2396
33	33	rpp	-110.1598	110.1598	110.1598	110.1598	215.2396	220.3196
34	34	rcc	.0000	.0000	215.2396	.0000	.0000	5.0800
35	35	rcc	37.4650	.0000	110.1598	5.0800	.0000	.0000
36	36	rpp	37.4650	-5.0800	-112.0598	-110.1598	205.1596	228.0196
37	37	rpp	-5.0800	110.1598	-5.0800	-5.0800	205.1596	228.0196
38	38	rpp	-5.0800	5.0800	110.1598	112.0598	205.1596	228.0196
39	39	rpp	-112.0598	-110.1598	-5.0800	-5.0800	205.1596	228.0196
40	40	rcc	.0000	.0000	222.9396	.0000	1.9000	.0000
41	41	rcc	110.1598	.0000	222.9396	1.9000	.0000	.0000
42	42	rcc	.0000	110.1598	222.9396	.0000	1.9000	.0000
43	43	rcc	2.5400	.0000	222.9396	1.9000	.0000	.0000
44	44	rcc	-85.0000	-110.1598	11.4300	.0000	10.1600	.0000
45	45	rcc	85.0000	-110.1598	11.4300	.0000	10.1600	.0000
46	46	rcc	85.0000	99.9998	11.4300	.0000	10.1600	.0000
47	47	rcc	-85.0000	99.9998	11.4300	.0000	10.1600	.0000

Figure 9-4. (continued)


```

48 48 rpp 1.2700 -120.0000 120.0000 -120.0000 120.0000 -15.0000 .0000
49 49 rpp -120.0000 125.0000 -125.0000 -125.0000 125.0000 -16.0000 235.0000
location of solid pointers lbody = 1
location of solid data lsolid = 51
number rpp box sph rcc rec trc ell raw arb tec tgc haf tor ars
storage 32 0 0 17 0 0 0 0 0 0 0 0 0 0 0 0 0 0 0 0 0 0
192 0 0 119 0 0 0 0 0 0 0 0 0 0 0 0 0 0 0 0 0 0 0
storage for solid data 326
storage for solid pointers 49
total storage for solids 375
region combination data
1 1 1 -8 -10 -11 -12 -13 -14 -14
-15 -16 -17 -18 -19 -20 -21 -22 -23
-24 -25 -26 -27 -28 -29 -30 -31 -32 -33 -34
-35 -36 -37 -38 -39 -40 -41 -42 -43
-44 -45 -46 -47 -48 0 0 -14 -15 -16
-17 -18 -19 -20 -21 0 0 -9 -10 -11
-12 -13 -14 -15 -16 -17 -18 -19 -20 -21 -22 -23
-24 -25 -26 -27 -28 -29 -30 -31 -32 -33 -34
-35 -36 -37 -38 -39 -40 -41 -42 -43 -44 -45 -46 -47 -48
4 4 or 5 or 6 or 7 or 8 or 9 or 10 or 11 or 12 or 13 or 14 or 15 or 16 or 17 or 18 or 19 or 20 or 21 or 22 or 23 or 24 or 25 or 26 or 27 or 28 or 29 or 30 or 31 or 32 or 33 or 34 or 35 or 36 or 37 or 38 or 39 or 40 or 41 or 42 or 43 or 44 or 45 or 46 or 47 or 48 or 49
location of region pointers lregd = 377
location of region list lregl = 401
number of descriptors 180
storage for region pointers 24
total storage for regions 204
region rpp equivalents
1 -120.0000 120.0000 -120.0000 120.0000 -15.0000 230.0000
2 -115.2398 115.2398 -115.2398 115.2398 .0000 5.0800
3 -110.1598 110.1598 -110.1598 110.1598 5.0800 10.1600
4 -99.9998 99.9998 -99.9998 99.9998 10.1600 15.2400
5 -105.0798 105.0798 -105.0798 105.0798 10.1600 215.2396

```

Figure 9-4. (continued)

```

6 -99.9998 99.9998 -99.9998 99.9998 10.1600 210.1596
7 -112.0598 112.0598 -112.0598 112.0598 5.0800 15.2400
8 -99.9998 99.9998 -117.1398 117.1398 .0000 15.2400
9 -97.4598 97.4598 -117.1398 117.1398 7.6200 12.7000
10 -25.4000 25.4000 -25.4000 25.4000 210.1596 215.2396
11 99.9998 105.0798 -25.4000 25.4000 84.7598 135.5598
12 99.9998 110.1598 -54.2798 -44.1198 5.0800 15.2400
13 -110.1598 110.1598 -110.1598 105.0798 10.1600 215.2396
14 105.0798 110.1598 -105.0798 105.0798 10.1600 215.2396
15 -110.1598 110.1598 105.0798 105.0798 10.1600 215.2396
16 -110.1598 -105.0798 -105.0798 105.0798 10.1600 215.2396
17 -110.1598 110.1598 -110.1598 110.1598 215.2396 220.3196
18 -112.0598 112.0598 -112.0598 112.0598 205.1596 228.0196
19 -112.0598 112.0598 -112.0598 112.0598 220.3996 225.4796
20 -86.2700 86.2700 -110.1598 110.1598 10.1600 12.7000
21 -37.4650 37.4650 -37.4650 37.4650 215.2396 220.3196
22 105.0798 110.1598 -37.4650 37.4650 72.6948 147.6248
23 -120.0000 120.0000 -120.0000 120.0000 -15.0000 .0000
24 -125.0000 125.0000 -125.0000 125.0000 -16.0000 235.0000

location of region rpp equiv lregmm = 581
location of region list lregion = 725
index for middle of list middle = 16
total storage for region min and max = 288

location of enclosing rpp lenrpp = 869

xmin xmax ymin ymax zmin zmax
-125.0000 125.0000 -125.0000 125.000000 -16.00000 235.00000

```

This option is no longer valid * * * * * - ignore this error message and continue problem.

```

storage summary
number of solids 49
location of solid pointers lbody = 1
location of solid data lsolid = 51
number of regions 24
location of region pointers lregd = 377
location of region list lregl = 401

number of descriptors 180
storage for region pointers 24
total storage for regions 204

location of region rpp equiv lregmm = 581
location of region list lregion = 725
index for middle of list middle = 16
total storage for region min and max = 288

location of enclosing rpp lenrpp = 869

location of ident table lirfo = 875
storage for ident table 24
location of region ray storage lrry = 899
location of rin storage lrin = 923
location of rout storage lrout = 972
location of surfaces/ray num lro = 1021
loc next available storage lrogeom = 1070
total storage for geometry data 922
total working storage 171

```

Figure 9-4. (continued)

total storage in master-aster 1069
 time for input processing .000 seconds
 leave geni

tolerance for overlap tol = .0010
 tolerance for line of sight tollos = .0010

identification table
 region item imprtnc material percent description

1	1	1	2	100	box/
2	1	1	3	100	box/
3	1	1	3	100	box/
4	1	1	3	100	box/
5	1	1	3	100	box/
6	1	1	2	100	box/
7	1	1	3	100	box/
8	1	1	3	100	box/
9	1	1	2	100	box/
10	1	1	3	100	box/
11	1	1	3	100	box/
12	1	1	2	100	box/
13	1	1	3	100	box/
14	1	1	3	100	box/
15	1	1	3	100	box/
16	1	1	3	100	box/
17	1	1	3	100	box/
18	1	1	3	100	box/
19	1	1	2	100	box/
20	1	1	2	100	box/
21	1	1	3	100	box/
22	1	1	3	100	box/
23	1	1	1	100	box/
24	1	1	0	100	box/

location of ident table lirfo = 875
 storage for ident table 24

material/importance numbers by zone

1	2	3	3	3	2	3	3	3	3	3	3	2	3	3	3	2	2
1	1	1	1	1	1	1	1	1	1	1	1	1	1	1	1	1	1
21	3	3	1	0													
	1	1	1	1													

nggeom= 3945, nglast= 3945

- 2m box exp/aprf aog. 5/90 exp. ss90-130-39 s90e5, 1020 steel + phantom n.d.
- number of primary groups (ngp) 46
- number of primary downscatters (nds) 46
- number of secondary groups (ngg) 23
- number of secondary downscatters (nds) 23
- number of prim+sec groups (ingp) 69
- table length (itbl) 72
- loc of total (sig t) (iht) 3
- loc of within group (sig gg) (isgg) 4
- number of media (nmed) 9
- number of input elements (nelem) 24
- number of mixing entries (nmix) 67
- number of coefficients (ncoef) 6
- number of angles (nsct) 3
- restore coeff (lstat) 0
- adjoin switch (from morse) 1

Figure 9-4. (continued)

```

input/output options
irdsg (as read)      0
istr (as store)     0
ifmu (mus)          0
incom (moments)     0
iprin (angles,prob) 0
ipun (impossible coef) 0
card format (idtf)  0
input tape (ixtape) 2
morsac tape (ixtape) 0
o6r tape (io6rt)   0

```

```

elements from library tape
identifiers  1  2  3  4  5  6  43  44  45  46  47  48  49  50
51  52  53  54  55  56  57  58  59  60  61  62  63  64
65  66  67  68  69  70  71  72  79  80  81  82  83  84
85  86  87  88  89  90  91  92  93  94  95  96  97  98
99 100 101 102 103 104 105 106 107 108 109 110 111 112
113 114 115 116 117 118 119 120 121 122 123 124 125 126
127 128 129 130 131 132 133 134 135 136 137 138 157 158
159 160 161 162 163 164 165 166 167 168 169 170 171 172
173 174 175 176 177 178 179 180 181 182 183 184 185 186
199 200 201 202 203 204 205 206 207 208 209 210 223 224
225 226 227 228

```

```

*** element 1 id= 1 p0 h- 1 minx (130 1/1)
*** element 2 id= 43 p0 h- 10 sta ndar
*** element 3 id= 49 p0 b- 11 sta ndar
*** element 4 id= 55 p0 c 1306 sta ndar
*** element 5 id= 61 p0 n- 14 sta ndar
*** element 6 id= 67 p0 0- 16 sta ndar
*** element 7 id= 79 p0 na- 23 sta ndar
*** element 8 id= 85 p0 mg 27 sta ndar
*** element 9 id= 91 p0 al- 27 sta ndar
*** element 10 id= 97 p0 si 31 sta ndar
*** element 11 id= 103 p0 p- 31 sta ndar
*** element 12 id= 109 p0 s 1347 sta ndar
*** element 13 id= 115 p0 cl 1149 sta ndar
*** element 14 id= 121 p0 ar 8824 sta ndar
*** element 15 id= 127 p0 k 1150 sta ndar
*** element 16 id= 133 p0 ca 1320 sta ndar
*** element 17 id= 157 p0 mn- 55 sta ndar
*** element 18 id= 163 p0 fe 9326 sta ndar
*** element 19 id= 169 p0 co- 59 sta ndar
*** element 20 id= 175 p0 ni 1327 sta ndar
*** element 21 id= 181 p0 cu 1328 sta ndar
*** element 22 id= 199 p0 zr 8841 sta ndar
*** element 23 id= 205 p0 nb- 93 sta ndar
*** element 24 id= 223 p0 sn 8850 sta ndar

```

```

storage allocations
cross sections start at 3946
last location used (perm) 102754
temp locations used 519584 to 800000
excess storage (temp) 416830

```

```

*** element 1 id= 1 p0 h- 1 minx (130 1/1)
*** element 2 id= 2 p1 h- 1 minx (130 1/1)
*** element 3 id= 3 p2 h- 1 minx (130 1/1)
*** element 4 id= 4 p3 h- 1 minx (130 1/1)
*** element 5 id= 5 p4 h- 1 minx (130 1/1)
*** element 6 id= 6 p5 h- 1 minx (130 1/1)
*** element 2 id= 43 p0 b- 10 sta ndar
*** element 2 id= 44 p1 b- 10 sta ndar

```

Figure 9-4. (continued)

*** element	2	id=	45	p2	b-	10	1305	sta	ndar
*** element	2	id=	46	p3	b-	10	1305	sta	ndar
*** element	2	id=	47	p4	b-	10	1305	sta	ndar
*** element	2	id=	48	p5	b-	10	1305	sta	ndar

. . .

*** element	23	id=	205	p0	nb-	93	1189	sta	ndar
*** element	23	id=	206	p1	nb-	93	1189	sta	ndar
*** element	23	id=	207	p2	nb-	93	1189	sta	ndar
*** element	23	id=	208	p3	nb-	93	1189	sta	ndar
*** element	23	id=	209	p4	nb-	93	1189	sta	ndar
*** element	23	id=	210	p5	nb-	93	1189	sta	ndar
*** element	24	id=	223	p0	sn	8850	8850	sta	ndar
*** element	24	id=	224	p1	sn	8850	8850	sta	ndar
*** element	24	id=	225	p2	sn	8850	8850	sta	ndar
*** element	24	id=	226	p3	sn	8850	8850	sta	ndar
*** element	24	id=	227	p4	sn	8850	8850	sta	ndar
*** element	24	id=	228	p5	sn	8850	8850	sta	ndar

mixing table

media	1	contains element	1	with density	4.8016E-02
media	1	contains element	2	with density	8.8600E-09
media	1	contains element	3	with density	3.2435E-08
media	1	contains element	4	with density	3.4889E-04
media	1	contains element	5	with density	4.3922E-05
media	1	contains element	6	with density	4.3043E-02
media	1	contains element	7	with density	1.3186E-04
media	1	contains element	8	with density	8.4348E-05
media	1	contains element	9	with density	1.2722E-03
media	1	contains element	10	with density	8.7935E-03
media	1	contains element	12	with density	3.3368E-06
media	1	contains element	13	with density	3.2693E-06
media	1	contains element	15	with density	1.8926E-04
media	1	contains element	16	with density	2.4025E-05
media	1	contains element	17	with density	6.6540E-06
media	1	contains element	18	with density	2.9695E-04
media	1	contains element	19	with density	2.5719E-07
media	1	contains element	20	with density	2.5817E-07
media	1	contains element	21	with density	4.4903E-07
media	1	contains element	24	with density	6.7608E-08
media	2	contains element	1	with density	7.0106E-07
media	2	contains element	5	with density	3.8326E-05
media	2	contains element	6	with density	1.0632E-05
media	2	contains element	14	with density	2.2922E-07
media	3	contains element	4	with density	8.0783E-04
media	3	contains element	10	with density	4.2132E-04
media	3	contains element	11	with density	6.1126E-05
media	3	contains element	12	with density	7.3810E-05
media	3	contains element	17	with density	3.8771E-04
media	3	contains element	18	with density	8.3911E-02
media	4	contains element	1	with density	1.6543E-02
media	4	contains element	4	with density	1.1849E-02
media	4	contains element	5	with density	1.0228E-03
media	4	contains element	6	with density	3.8166E-03
media	4	contains element	7	with density	1.7367E-09
media	4	contains element	9	with density	1.3057E-09
media	4	contains element	13	with density	7.1279E-08
media	5	contains element	4	with density	5.8845E-02
media	5	contains element	1	with density	3.3642E-02
media	5	contains element	5	with density	1.9850E-03
media	5	contains element	6	with density	7.7235E-03
media	5	contains element	7	with density	2.3220E-07

Figure 9-4. (continued)

media	5	contains element	9	with density	2.2899E-09
media	5	contains element	13	with density	2.3527E-08
media	6	contains element	1	with density	6.1368E-02
media	6	contains element	4	with density	1.7881E-02
media	6	contains element	5	with density	1.8400E-03
media	6	contains element	6	with density	2.5237E-02
media	6	contains element	7	with density	1.1955E-04
media	6	contains element	8	with density	3.8839E-05
media	6	contains element	10	with density	6.0036E-07
media	6	contains element	11	with density	1.3868E-03
media	6	contains element	12	with density	4.5488E-05
media	6	contains element	13	with density	3.4006E-05
media	6	contains element	15	with density	3.2988E-05
media	6	contains element	16	with density	2.1435E-03
media	6	contains element	18	with density	1.2077E-06
media	7	contains element	1	with density	6.6854E-02
media	7	contains element	6	with density	3.3427E-02
media	8	contains element	1	with density	3.9800E-02
media	8	contains element	4	with density	4.5400E-02
media	8	contains element	6	with density	8.5200E-03
media	9	contains element	1	with density	7.1300E-02
media	9	contains element	2	with density	4.8700E-04
media	9	contains element	3	with density	1.9700E-03
media	9	contains element	4	with density	3.4100E-02
media	9	contains element	6	with density	3.6400E-03

banks start at 102755
last location used 123754
last location used in blank common is 147984

adjoint group parameters
normalized spectrum adjoint-group probabilities

1	1.4493E-02				
2	2.8986E-02				
3	4.3478E-02				
4	5.7971E-02				
5	7.2464E-02				
	.				
	.				
	.				
61	8.8406E-01				
62	8.9855E-01				
63	9.1304E-01				
64	9.2754E-01				
65	9.4203E-01				
66	9.5652E-01				
67	9.7101E-01				
68	9.8551E-01				
69	1.0000E+00				

group	upper edge	velocity
	(ev)	(cm/sec)
1	2.0000E+04	2.9979E+10
2	3.0000E+04	2.9979E+10
3	4.5000E+04	2.9979E+10
4	7.0000E+04	2.9979E+10
5	1.0000E+05	2.9979E+10
6	1.5000E+05	2.9979E+10
7	3.0000E+05	2.9979E+10
8	4.5000E+05	2.9979E+10
9	7.0000E+05	2.9979E+10
10	1.0000E+06	2.9979E+10

Figure 9-4. (continued)

```

60 9.0484E+06 4.0600E+09
61 1.0000E+07 4.2681E+09
62 1.1052E+07 4.4870E+09
63 1.2214E+07 4.7170E+09
64 1.2523E+07 4.8639E+09
65 1.3840E+07 5.0212E+09
66 1.4191E+07 5.1776E+09
67 1.4918E+07 5.2762E+09
68 1.6905E+07 5.5167E+09
69 1.9640E+07 5.9118E+09

```

time required for input was 74

***start batch 1 random=3FE952629C6FD8C0

source data
you are using the default version of source which sets wate to ddf and provides an energy ig.
wwave iave uave wave xave wave zave wave ageave
1.000E+03 35.06 -.0073 -.0032 .0111 0.000E+00 0.000E+00 1.102E+02 0.000E+00
you are using the default version of gmed which assumes geometry and xsect media are identical.
***undefined region detected by subroutine raychk.
undefined region is next to region 6

number of collisions of type ncoll	albedo	bdryx	escape	e-cut	timekill	r	kill	r	sury	gamlost
source split(d)	fishn	gngen	realcoll	0	7690	834	0	1592	201	0
1000	421	0	1005	23776	0	7690	834	0	1592	201

time required for the preceding batch was 24

***start batch 2 random=3FE14626DF6A33E0

source data
wwave iave uave wave wave xave wave zave wave ageave
1.023E+03 34.04 .0099 -.0181 -.0047 0.000E+00 0.000E+00 1.102E+02 0.000E+00
***undefined region detected by subroutine raychk.
undefined region is next to region 6

number of collisions of type ncoll	albedo	bdryx	escape	e-cut	timekill	r	kill	r	sury	gamlost
source split(d)	fishn	gngen	realcoll	0	7710	817	0	1547	187	0
1000	386	0	978	24157	0	7710	817	0	1547	187

time required for the preceding batch was 24

***start batch 3 random=3FD2E93031F94980

source data
wwave iave uave wave wave xave wave zave wave ageave
9.717E+02 35.09 -.0141 -.0155 .0658 0.000E+00 0.000E+00 1.102E+02 0.000E+00
***undefined region detected by subroutine raychk.
undefined region is next to region 15
***undefined region detected by subroutine raychk.
undefined region is next to region 6

number of collisions of type ncoll	albedo	bdryx	escape	e-cut	timekill	r	kill	r	sury	gamlost
source split(d)	fishn	gngen	realcoll	0	7073	756	0	1511	207	0
1000	165	0	1102	20593	0	7073	756	0	1511	207

time required for the preceding batch was 21

Figure 9-4. (continued)

```

:
:
:
***start batch 48          random=3FED9D759A06C9A0
source data
wwave 1.007E+03 35.45 iave .0133 wave -.0052 xave 0.000E+00 yave 1.102E+02 zave 0.000E+00
number of collisions of type ncoll
source split(d) 1000 231 0 1014 22821 fishn gamgen realcoll albedo 0 7426 706 0 0 0 0 0 0 0 0 0 0 0 0 0 0 0 0
time required for the preceding batch was 23

***start batch 49          random=3FD7CDEBE283F940
source data
wwave 1.003E+03 33.71 iave -.0028 wave -.0164 xave 0.000E+00 yave 1.102E+02 zave 0.000E+00
number of collisions of type ncoll
source split(d) 1000 224 0 981 22065 fishn gamgen realcoll albedo 0 6902 730 0 0 0 0 0 0 0 0 0 0 0 0 0 0 0 0 0
time required for the preceding batch was 22

***start batch 50          random=3FE35EE3BCA31160
source data
wwave 9.852E+02 36.21 iave -.0037 wave -.0506 xave 0.000E+00 yave 1.102E+02 zave 0.000E+00
number of collisions of type ncoll
source split(d) 1000 244 0 979 23306 fishn gamgen realcoll albedo 0 7560 744 0 0 0 0 0 0 0 0 0 0 0 0 0 0 0 0 0
time required for the preceding batch was 23
time required for the preceding 50 batches was 1180

neutron deaths
killed by russian roulette number weight
escaped 77927 .16692E+04
reached energy cutoff 38656 .38572E+05
reached time cutoff 0 .00000E+00
absorbed 0 .00000E+00
4.43577E+04

number of scatterings
medium number
1 33523
2 3076
3 1112141
4 0
5 0
6 0
7 0
8 0
9 0
total 1148740

real scattering counters

```

Figure 9-4. (continued)

energy group	region 1 number	weight
1	840	7.67E+02
2	834	7.57E+02
3	858	7.46E+02
4	948	8.30E+02
5	1182	9.42E+02
6	2302	1.18E+03
7	3396	1.93E+03
8	2355	2.34E+03
9	3333	2.43E+03
10	2811	2.50E+03
11	3150	2.29E+03
12	3155	2.15E+03
13	3416	2.17E+03
14	3838	2.15E+03
15	4152	2.11E+03
16	4204	2.11E+03
17	4396	2.21E+03
18	4349	2.12E+03
19	4543	2.10E+03
20	4472	2.31E+03
21	3379	2.26E+03
22	3303	2.35E+03
23	3452	2.45E+03
24	28636	1.82E+04
25	55508	2.36E+04
26	50413	2.74E+04
27	65613	3.75E+04
28	62649	4.33E+04
29	64425	4.85E+04
30	54028	5.65E+04

9-68

61	17779	1.68E+04
62	17586	1.60E+04
63	17904	1.56E+04
64	20048	1.58E+04
65	15833	1.54E+04
66	17391	1.60E+04
67	20127	1.57E+04
68	22540	1.56E+04
69	30064	1.52E+04

track length counters

energy group	region 1 number	weight
1	1472	8.11E+04
2	1612	8.80E+04
3	1666	8.75E+04
4	1820	9.25E+04
5	2169	9.43E+04
6	3815	9.77E+04
7	5093	1.13E+05
8	3558	1.16E+05
9	5388	1.17E+05
10	4813	1.19E+05
11	5403	1.13E+05
12	5581	1.10E+05
13	6181	1.12E+05
14	7009	1.19E+05

Figure 9-4. (continued)

15	7794	1.24E+05
16	8108	1.27E+05
17	8619	1.28E+05
18	8597	1.24E+05
19	8947	1.25E+05
20	8954	1.46E+05
21	6353	1.26E+05
22	6135	1.35E+05
23	6461	1.52E+05
24	32476	2.31E+05
25	63730	2.89E+05
26	58053	3.45E+05
27	75834	4.27E+05
28	72383	4.52E+05
29	74264	4.70E+05
30	62342	5.32E+05
61	28564	4.00E+05
62	28329	3.87E+05
63	29600	4.05E+05
64	33254	4.06E+05
65	26797	4.37E+05
66	29715	4.51E+05
67	34072	4.15E+05
68	39009	4.41E+05
69	53141	4.42E+05

secondary production counters (both the groups causing production and resulting from production)

energy group	region 1 number	weight
1	0	0.00E+00
2	0	0.00E+00
3	1	9.13E-01
4	3	2.03E+00
5	3	2.74E+00
6	56	2.85E+01
7	166	9.65E+01
8	305	2.99E+02
9	415	3.14E+02
10	9913	8.82E+03
11	7130	5.18E+03
12	3813	2.60E+03
13	3922	2.48E+03
14	4098	2.30E+03
15	7317	3.73E+03
16	3531	1.78E+03
17	2883	1.45E+03
18	2366	1.17E+03
19	4502	2.08E+03
20	1164	6.00E+02
21	39	2.65E+01
22	0	0.00E+00
23	0	0.00E+00
24	4614	2.40E+03
25	1042	5.57E+02
26	626	3.27E+02
27	341	1.74E+02
28	214	9.44E+01
29	121	5.66E+01
30	67	3.59E+01

61	3338	2.18E+03
62	3514	2.20E+03
63	3772	2.31E+03
64	3594	2.21E+03
65	2815	1.76E+03
66	2577	1.62E+03
67	2427	1.54E+03
68	2163	1.31E+03
69	1784	1.13E+03

number of splittings

energy group	region 1 number	weight
1	0	0.00E+00
2	0	0.00E+00
3	0	0.00E+00
4	0	0.00E+00
5	0	0.00E+00
6	0	0.00E+00
7	0	0.00E+00
8	0	0.00E+00
9	0	0.00E+00
10	0	0.00E+00
11	0	0.00E+00
12	0	0.00E+00
13	0	0.00E+00
14	0	0.00E+00
15	0	0.00E+00
16	0	0.00E+00
17	0	0.00E+00
18	0	0.00E+00
19	0	0.00E+00
20	0	0.00E+00
21	0	0.00E+00
22	0	0.00E+00
23	0	0.00E+00
24	2	5.40E+00
25	0	0.00E+00
26	1	2.60E+00
27	0	0.00E+00
28	0	0.00E+00
29	0	0.00E+00
30	0	0.00E+00

61	15	4.21E+01
62	5	1.49E+01
63	5	1.42E+01
64	5	1.48E+01
65	6	1.77E+01
66	10	2.74E+01
67	3	9.20E+00
68	3	8.50E+00
69	5	1.35E+01

number of upscattering splits

energy group	region 1 number	weight
1	0	0.00E+00

Figure 9-4. (continued)

2	0	0.00E+00
3	0	0.00E+00
4	0	0.00E+00
5	0	0.00E+00
6	0	0.00E+00
7	0	0.00E+00
8	0	0.00E+00
9	0	0.00E+00
10	55	2.25E+02
11	23	1.09E+02
12	22	9.33E+01
13	25	9.80E+01
14	26	1.07E+02
15	35	1.45E+02
16	41	1.56E+02
17	47	1.90E+02
18	45	1.78E+02
19	48	1.87E+02
20	62	2.45E+02
21	78	3.07E+02
22	79	3.06E+02
23	106	4.14E+02
24	0	0.00E+00
25	27	1.16E+02
26	11	3.73E+01
27	13	4.74E+01
28	16	5.00E+01
29	2	7.88E+00
30	6	1.67E+01

61	395	1.57E+03
62	426	1.67E+03
63	407	1.62E+03
64	417	1.67E+03
65	491	1.93E+03
66	505	2.03E+03
67	529	2.09E+03
68	562	2.24E+03
69	573	2.28E+03

number of russian roulette kills

energy group	region 1 number	weight
1	0	0.00E+00
2	809	1.55E+00
3	765	1.01E+00
4	782	4.56E+00
5	688	2.54E+01
6	132	3.82E+00
7	604	2.27E+01
8	26	9.78E-01
9	0	0.00E+00
10	0	0.00E+00
11	0	0.00E+00
12	0	0.00E+00
13	0	0.00E+00
14	1	3.28E-02
15	37	1.42E+00
16	99	3.62E+00
17	284	8.64E+00
18	632	1.74E+01

19	1118	2.48E+01
20	2278	4.77E+01
21	3058	7.02E+01
22	3946	8.11E+01
23	8583	1.04E+02
24	0	0.00E+00
25	1496	3.54E+01
26	1736	6.21E+01
27	540	1.90E+01
28	82	3.79E+00
29	558	2.57E+01
30	1	4.71E-02
	*	*
	*	*
61	693	2.08E+01
62	1043	2.92E+01
63	1512	3.95E+01
64	2101	5.86E+01
65	5235	6.67E+01
66	3375	6.61E+01
67	4991	1.13E+02
68	7073	1.73E+02
69	22557	5.00E+02

number of russian roulette survivals

energy group	region 1 number	weight
1	0	0.00E+00
2	6	4.86E-02
3	8	1.06E-02
4	24	1.43E-01
5	158	6.06E+00
6	24	6.92E-01
7	149	5.62E+00
8	9	3.39E-01
9	0	0.00E+00
10	0	0.00E+00
11	0	0.00E+00
12	0	0.00E+00
13	0	0.00E+00
14	0	0.00E+00
15	5	1.74E-01
16	12	4.24E-01
17	59	2.14E+00
18	103	3.36E+00
19	145	3.91E+00
20	296	8.29E+00
21	411	1.34E+01
22	446	1.41E+01
23	559	1.49E+01
24	0	0.00E+00
25	202	6.28E+00
26	397	1.47E+01
27	130	4.80E+00
28	32	1.49E+00
29	143	6.64E+00
30	0	0.00E+00
	*	*
	*	*
61	140	4.80E+00
62	187	6.15E+00

Figure 9-4. (continued)

```
63      220  7.22E+00
64      335  1.08E+01
65      377  8.27E+00
66      335  1.07E+01
67      636  1.83E+01
68      1036 3.37E+01
69      2976 9.75E+01
```

```
** next random number is 3FD81E91FFF5C340
```

```
total cpu time for this problem was 19.67 minutes.
```

```
*** This problem finished: Thu Jun 25 21:23:32 1998
```

```
*** * mash version 1.5 * * * * * fortran and compilation frozen 01-01-96 * * * * *
```

```
# # # A TOTAL NUMBER OF UNDEFINED BODIES ENCOUNTERED WAS 96 # # #
```

10.0 DRC2: A CODE WITH SPECIALIZED APPLICATIONS FOR COUPLING LOCALIZED MONTE CARLO ADJOINT CALCULATIONS WITH FLUENCES FROM TWO-DIMENSIONAL R-Z DORT DISCRETE ORDINATES AIR-OVER-GROUND CALCULATIONS

10.1 INTRODUCTION TO DRC2

The Detector Response Code (DRC) has been written and used to couple DORT¹ forward fluences with adjoint leakages from a special version of the MORSE² Monte Carlo computer code called MASH to compute the estimates of the fluences and doses within a structure or vehicle interior. Furthermore, DRC utilizes the free-field fluences and estimates from the in-vehicle fluences (and doses) to calculate neutron protection factors and reduction factors for the vehicle. DRC has always had specialized applications because of the limited use of MORSE features, limitations on input parameters, and the manner in which the detectors are used.

10.1.1 History

The Detector Response Code (DRC and DRC2) code in MASH has undergone several modifications from its early predecessor in the Vehicle Code System (VCS)^{3,4}. For MASH v1.0⁵, DRC was modified to contain the newest SAMBO² analysis routines from the MORSE code system. The main difference between these and previous SAMBO versions was that input data was now free-form and subroutine ENRGYS defines an array, IARR, which was key to the correspondence between the DRC analysis group number and the MORSE random walk group number for use by subroutine FLUXST when scoring group-dependent data. This eliminated the requirement in the old VCS-DRC of having the DORT free-field fluences and MORSE adjoint leakages calculated in the same group structure. Furthermore, with the development of the new 69 group (46n-23 γ) cross section set, it was advantageous to have DRC couple MORSE adjoint leakage calculations in 69 energy groups with previously calculated DORT free-field data in the old 58 group (37n-21 γ) group structure.

10.1.2 Background

The DRC2 code is an extensive modification of the DRC⁵ code, which has been used in the past for coupling. With DRC, the spatial dependence of the fluence was limited to axial variation. Linear interpolation was used to obtain the fluence at axial locations falling between the DORT fluence locations. However, since radial variation of the DORT fluences could be important for large vehicle systems or other large structures, the DRC2 code was developed to incorporate coupling with axially and radially varying DORT forward fluence fields. An option was included for specifying either linear or logarithmic interpolation or extrapolation of the fluences. In either case, linear is used when negatives are encountered.

DRC2 is set up to use the MASH file either with or without X-Y dependence or the MASH file with its fewer collision file parameters (8 vs. 10 or 13 defined parameters). In addition, DRC2 can calculate results for several range/orientations in a single pass through the code. Titles written to unit 11 are constructed from the input range and orientation data and the first 56 characters of the case title. The format is the expected one for an unpublished text-formatting and transmission-factor-calculating code (TFX).

The inclusion of X-Y dependent fluence fields in the DRC2 calculation and the calculation of results for several ranges and orientations in one pass through the code results in considerably more data in core than was the case with the DRC code. Therefore, if the allocated memory is not large enough to store all data in core, the code will perform the calculation "ex-core" with group blocking (i.e., the calculation is performed for a portion of the groups at a time until all group calculations are finished), provided data for at least one group will fit in core. There is probably little CPU charge penalty when the calculation is performed ex-core. The largest charge differences should be for IO (ex-core larger) and memory (in-core larger). For example, for a 69-group calculation performed ex-core with three blocks (29 groups each for the first two blocks) and then in-core, charge ratios (in-core to ex-core) were 1.02, 4.49, 0.23, and 1.51 for CPU, IO, memory, and total charges, respectively. A significant charge improvement was achieved for the ex-core calculation by reading the sequentially-processed forward fluence file with direct access rather than sequential. With sequential access and rewinding, the respective charge ratios were 9.37, 13.9, 2.36, and 8.18. Since the in-core calculation is likely to give the smallest total charge, whenever possible, one should allocate enough core to store fluence data for all groups. For the case cited, about 1.9 million words were required to store all data in core.

10.1.3 Method Used

The general structure of the MASH code system illustrated in Section 1.0 of this report shows all data relevant to the calculation of the vehicle protection and reduction factors as input to the DRC2 module. In particular, the GRTUNCL/DORT air-over-ground analysis of the radiation environment is passed through VISTA for renormalization and reformatting for use in DRC2 in calculating the free-field fluences and doses and for folding with the adjoint leakage information from MORSE to calculate the in-vehicle fluences and doses along with the vehicle protection and reduction factors as a function of range and vehicle orientation relative to the source. A special feature of MASH is that the MORSE adjoint leakage information contains both the leaking particle's starting energy (source energy) and final energy (leaking energy). This allows DRC2 to calculate an energy fluence inside of the vehicle which can then be folded with any input dose response function such as a detector response function or a tissue dose response function. Consequently, one MORSE calculation can be used to analyze several different possible dose responses and/or several different radiation environments (GRTUNCL/DORT calculations). The basic equation used by MASH to calculate the dose inside of a vehicle is given in Equation 10-1.⁵

$$\lambda = \int_A d\vec{x} \int_{4\pi} d\vec{\Omega} \sum_{IG} \Phi_{IG}(\vec{x}, \vec{\Omega}) \Phi_{IG}^*(\vec{x}, \vec{\Omega}) \vec{\Omega} \cdot \vec{n} \quad (10-1)$$

where λ is the dose,
 x is the space variable which is integrated over a closed surface A,
 Ω is the angle variable which is integrated over 4π steradians,
 IG is an energy group index summed over all the energy groups in the transport problem,

- Φ is the forward fluence calculated by the GRTUNCL/DORT codes,
- Φ^* is the adjoint fluence calculated by the MORSE code, and
- n is the unit vector normal to the area element A .

To derive the actual equations used by DRC2, it is necessary to consider that the adjoint fluence as calculated by adjoint Monte Carlo is approximated by Equation 10-2.

$$\Phi_{IG}^*(\bar{x}, \bar{\Omega}) \approx \frac{1}{N} \sum_{i=1}^{N_{IG}} \frac{W_{IG,i}^*}{\bar{\Omega}_i \cdot \bar{n}_i} \delta(\bar{x} - \bar{x}_i) \delta(\bar{\Omega} - \bar{\Omega}_i) \quad (10-2)$$

- where N is the total number of particles in the adjoint calculation,
- N_{IG} is the total number of particles that leak out of the calculation with energy group IG,
- i indicates a leaking particle,
- $W_{IG,i}^*$ is the weight of the i^{th} adjoint particle that leaks with energy group IG,
- x_i is the position of the i^{th} particle when it leaks,
- Ω_i is the direction of the i^{th} particle when it leaks, and
- δ is the Dirac delta function.

Therefore, Equation 10-2 approximates the adjoint fluence as a summation of Dirac delta functions (δ) over the weights. The factor of $1/(\Omega_i \cdot n_i)$ converts a leakage current into a leakage fluence. Equation 10-2 can be substituted into Equation 10-1, resulting in Equation 10-3.

$$\lambda = \frac{1}{N} \sum_{i=1}^N \Phi_{IG,i}(\bar{x}_i, \bar{\Omega}_i) W_{IG,i}^* \quad (10-3)$$

Here, the dose is calculated by a sum over the products of the weights of leakage particles and the angular fluences at the location and direction of the leaking particles. One of the advantages of DRC2 is the simplicity of Equation 10-3. In this equation, the DORT angular fluence is differential in angle as calculated in DORT per unit weight and the W^* is the actual particle leakage weight calculated by MORSE. In reality, DRC2 uses a slightly more complicated form of this equation as shown in Equation 10-4.

$$\Phi_{IGS}^V = \frac{1}{N \cdot S_{IGS}^*} \sum_{i=1}^N \Phi_{IG,i}(\bar{x}_i, \bar{\Omega}_i) W_{IG,IGS,i}^* \quad (10-4)$$

where IGS corresponds to the source energy of an adjoint particle which is also scored on the MORSE particle leakage tape,

Φ_{IGS}^V is the energy spectrum calculated by DRC2 inside the vehicle, and
 S_{IGS}^* is the energy spectrum sampled when performing the MORSE adjoint calculation.

Equation 10-4 then uses the particle leaking group, IG, and source energy, IGS, to transform Equation 10-3 into an equation for the energy spectrum inside of the vehicle. The dose inside of the vehicle is then calculated by Equation 10-5 which folds the internal energy spectrum with a response function of interest.

$$\lambda = \sum_{IGS} \Phi_{IGS}^V R_{IGS} \quad (10-5)$$

The solutions of Equations 10-4 and 10-5 can be seen in the FOLD and FLUXST subroutines within the programming of DRC2.

An additional quantity that is calculated by DRC2 is the free-field dose which is used to calculate the vehicle protection factors and reduction factors. The free-field dose is calculated from the DORT angular fluences by a different equation as shown in Equation 10-6.

$$\lambda_{ff}(\vec{x}) = \sum_{IG} R_{IG} \int_{4\pi} d\Omega \Phi_{IG}(\vec{x}, \vec{\Omega}) \quad (10-6)$$

where $\lambda_{ff}(x)$ is the free field dose at a point x which is calculated by summing a dose response over the scalar fluence at that point.

This is implemented in the code as shown in Equation 10-7 where the angular integration is replaced by a summation over all the DORT angle points.

$$\lambda_{ff}(\vec{x}) = \sum_{IG} R_{IG} \sum_K^{NANG} \Phi_{IG,K}(\vec{x}) W_K \quad (10-7)$$

where W_K is the angular quadrature weight,
K indicates an angle direction, and
NANG is the number of directions.

Equation 10-7 is performed in Subroutine FREDOS in the DRC2 code and is subsequently used to calculate protection and reduction factors.

The radiation transport coupling method employed in DRC2 allows for any complicated Monte Carlo geometry inside the coupling surface to be modeled in three dimensional detail. The two-dimensional GRTUNCL/DORT discrete ordinates air-over-ground environment is defined by an r-z coordinate system, where the radial axis r coincides with the x axis and is perpendicular to the y axis. The three dimensional Monte Carlo geometry system is completely contained within a cylindrical volume element defined by the maximum and minimum values chosen from the radial and axial mesh in VISTA. The coupling between the two systems occurs at the outer leakage surface of the Monte Carlo geometry within the cylindrical volume element. This coupling requires the Monte Carlo coordinate system to be rotated to align the x,y,z axes parallel to and in the same sense of the x,y,z axes of the GRTUNCL/DORT discrete ordinates system. When the adjoint Monte Carlo particle escapes its geometry system at a given point and in a given direction defined by its coordinate system, the coordinates, direction, and energy group can be converted to the discrete ordinates system so that the appropriate forward fluence can be determined in the evaluation of Equation 10-1. A full Eulerian rotation matrix is incorporated in DRC2 to allow for the alignment/rotation of the Monte Carlo geometry system within the discrete ordinates system. As presently configured, MASH allows for the rotation of the Monte Carlo geometry system in the x-y plane, i.e., rotation about the z axis. Future versions of MASH may allow full rotational capability. For additional information, a detailed derivation and description of radiation transport coupling methods can be found in Reference 6.

In order to calculate the protection and reduction factors, the MORSE adjoint leakage tape includes a parameter, IDET, which identifies the detector type in DRC2 in which a leaking particle is to be scored. Table 10-1 identifies the seven detector types utilized in DRC. The first four detector types are utilized on the MORSE adjoint leakage tape for scoring purposes. The last three detector types in Table 10-1, along with the free-field neutron, gamma ray, and total fluences and/or doses, are used in DRC2 to calculate the protection and reduction factors defined in Table 10-2.

In Table 10-2, the difference between the "protection factors" and "reduction factors" is the scoring of the vehicle produced secondary gamma dose (IDET=2 in MORSE or Detector 2 in Table 10-1). The neutron and gamma "protection factors" are a measure of how much the vehicle shielding reduces the dose from free-field neutrons and gammas, respectively, and is a useful parameter in engagement analysis. The "reductions factors," however, are a measure of how much the vehicle shielding alters the neutron or gamma dose as measured by a neutron or gamma sensitive detector. While the "protection factors" are most useful for engagement analyses, the "reduction factors" are most useful for comparing calculated results with experimental measurements.

Table 10-1. Detector Response Definitions in DRC2.

Detector	Response Definition
1	Direct neutron - a neutron entering the vehicle and contributing a neutron dose.
2	Capture gamma rays from vehicle - a gamma ray resulting from a neutron entering the vehicle and contributing a secondary gamma-ray dose.
3	Capture gamma rays from ground - a gamma ray resulting from a neutron entering the ground without passing through the vehicle and generating a secondary gamma-ray dose from a ground interaction. (This dose is already included in the upward-directed gamma rays that enter the vehicle. This generally is negligible.)
4	Direct gamma rays - a gamma ray entering the vehicle and contributing a gamma-ray dose. This source of gamma rays includes both gamma rays originating from the source, and capture gamma rays from the air.
5	Total gamma-ray dose - Sum of detectors 2, 3, and 4.
6	Gamma-ray dose from gamma rays entering the vehicle (usually dominated by direct gamma rays) - Sum of detectors 3 and 4.
7	Neutron and gamma-ray dose from neutrons incident on the vehicle - Sum of detectors 1 and 2.

Table 10-2. Definitions of Parameters and Protection Factors used to Characterize the Effectiveness of Shields.

Parameter	Response Definition
FFN	Free-Field Neutron Response
FFG	Free-Field Gamma Response
NPF	Neutron Protection Factor $NPF = FFN / Det. 7$
GPF	Gamma Protection Factor $GPF = FFG / Det. 6$
TPF	Total Protection Factor $TPF = (FFN+FFG)/(Det. 7 + Det. 6)$
NRF	Neutron Reduction Factor $NRF = FFN / Det. 1$
GRF	Gamma Reduction Factor $GRF = FFG / Det. 5$
TRF	Total Reduction Factor $TRF = (FFN+FFG)/(Det. 1 + Det. 5)$

10.2 DRC2 INPUT INSTRUCTIONS

In the input instructions, the term "vehicle" is used to refer to the object(s) or structure(s) perturbing the air-over-ground radiation field. It is modeled in the localized MASH calculation. A "vehicle system" includes the object(s) and the air and ground modeled in the MASH calculation.

Card A Title for this problem. [20A4]

Card B Job Control Parameters [Begin with "***" in columns 2 and 3.]

**

XD	x-location (cm) of the detector in MORSE geometry
YD	y-location (cm) of the detector in MORSE geometry
ZD	z-location (cm) of the detector in MORSE geometry
ZBOT	bottom of coupling surface relative to MORSE geometry (cm)
ZTOP	top of coupling surface relative to MORSE geometry (cm)

- 5 ---

IPRT	printout options
	0 = print VISTA file control data and vehicle doses
	1 = print VISTA file control data and free-field spectra
	2 = print VISTA file control data, free-field spectra, vehicle doses and dose spectra, and protection factors
	3 = print VISTA file control data, vehicle doses, and protection factors.

[NOTE: IPRT must be 2 for Unit 10 Output]

WATMX	maximum adjoint particle weight accepted
NDET	number of vehicle range/orientations
IDIF	0/>0 = same/different group structures for MORSE and VISTA data
KSIZ	k-words of storage to be allocated (0 uses the default size of 500k words or the value used in a previous case. One should use 0 in follow-on cases if the same core allocation is desired.)

- 10 ---

IBUFSZ	MASH collision file record length in words 1000 for MASH v1.0 1625 for MASH v1.5
NPARAM	number of parameters written on MASH collision file 8 for MASH v1.0 13 for MASH v1.5
IDXY	0 = no x-y data on collision file (valid for MASH v1.0 only) 1 = x-y data on collision file but no x-y dependence in the coupling calculation

2 = x-y data on collision file and x-y dependence in the
coupling calculation
IWW number of responses desired (less than or equal to 10.)

[NOTE: IWW = 0 implies 2 responses and IWW must be > 0 for unit 11 to be written.]

XQ x-location (cm) of the vehicle system rotation point relative to MORSE geometry

- 15 ---

YQ y-location (cm) of the vehicle system rotation point relative to MORSE geometry

INTERP 1/2 = linear/log flux interpolation
XNORM response function multiplier [Default = 1.0]

[NOTE: All the above parameters are read as real numbers and are converted to integers where required.]

Card C Ranges, MORSE-DORT Z offsets, and Orientation arrays
[Begin with "***" in columns 2 and 3.]

**

Ranges (XO(i),i=1,NDET) (cm) – DORT radii to the vehicle system rotation point for each case

MORSE-DORT Z offsets (ZO(i),i=1,NDET) – DORT ground-air interface z-location (cm) minus MORSE ground-air interface z-location (cm). For simplicity, the MORSE ground-air interface should be placed at z = 0.0. Then one need only specify the locations of the DORT ground-air interface.

Orientation array (ALPHA(i),i=1,NDET) – orientation angles (degrees counterclockwise) of the vehicle system with respect to the positive portion of the DORT system x-axis.

Card D NNEUT, NGAM [Begin with "\$\$" in columns 2 and 3.]

[NOTE: Omit if IDIF > 0]

\$\$

NNEUT group number of lowest energy neutron group in VISTA

NGAM group number of lowest energy gamma-ray group in VISTA

Card E VISTA energy group boundaries (NOG+2 entries)*
[Begin with "***" in columns 2 and 3.]

[NOTE: Omit if IDIF > 0]

**

Enter neutron upper energy boundaries in descending order followed by gamma-ray upper energy boundaries in descending order followed by the lower energy boundaries of the "NNEUT" neutron group and the "NGAM" gamma-ray group.

*[NOTE: NOG is read from the VISTA file and is equal to the number of groups for which data is provided on the file.]

- Card F Alphanumeric Title Information [20A4]
Card G Title or units for total responses for all detectors [20A4]
Card H Title or units for each total response [20A4]
Card I Response Function [Begin with "***" in columns 2 and 3.]

**

(RESP(i),i=1,NMTG) – enter values in order of decreasing energy

[NOTE: Repeat Cards H and I for each response function.]

- Card J Title of units for energy dependent fluence [20A4]

**NOTE: To run additional cases, re-specify all cards.
In these follow-on cases, set KSIZ on Card B
to zero to maintain the same core allocation.**

10.3 DRC2 INPUT DATA NOTES

Except for the title cards, all data are read using the MORSE FIDO input system. A detailed description of the FIDO input system (in general) is given in Appendix A. In MORSE FIDO, the array indicators "***" or "\$\$" must be entered in columns 2 and 3. In MORSE FIDO, data arrays are still entered in blocks, but the blocks are not terminated by a "T". Unused data arrays are not entered and careful attention must be paid to the order of each array, the size of each array, and the requirements for entering (or not entering the array). Multiple cases can be executed by re-specifying all cards and setting the KSIZ parameter on Card B to zero to maintain the same core allocation.

ZBOT and ZTOP These two parameters must be within the VISTA axial boundaries read by DRC2. The ZBOT and ZTOP boundaries represent the minimum and maximum values a leaking particle from the adjoint MORSE calculation will have. To fold these particles with the forward DORT fluences, the DORT axial mesh must encompass the MORSE axial mesh. In other words, the maximum z boundary written on the VISTA file must be greater than ZTOP and the minimum z boundary on the VISTA file must be less than ZBOT.

IPRT This parameter controls the amount of print from a DRC2 case. If IPRT=0, only information on the VISTA file control data and vehicle fluences and doses are printed. If IPRT=1, VISTA file control data and the free field fluences and doses are printed. For single DRC2 cases, IPRT=2 is recommended because the user will obtain VISTA file control data and both free-field and target fluence and dose information. If IPRT is set to 3, VISTA file control data and vehicle doses and protection factors are printed (no spectra). IPRT must equal 2 to obtain unit 10 output.

WATMX This parameter was used to set the maximum weight allowed for an adjoint leaking particle. With the use of in-group biasing, this parameter is obsolete and a value of zero will set the default value of 50.

NDET This parameter allows the user to specify several ranges and/or orientations in the same run. This input parameter governs the input in on Card C, (Ranges, Z Offsets, and Orientations).

IBUFSZ and **NPARM** are parameters designed to allow DRC2 to process MASH leakage files from the previously released version (MASH v1.0), and the current version (MASH v1.5).

IWW This parameter will allow the user multiple response functions (up to 10) on the same run. IWW equal to zero will require 2 responses, and IWW must be greater than zero to obtain unit 11 output.

XQ and **YQ** These parameters define the location within the MORSE geometry about which the target will be rotated. This is typically the origin (with respect to x- and y-directions) in the MORSE geometry.

XO(I) This parameter (Card C) defines the DORT ranges to the vehicle system rotation point defined by XQ and YQ. XO(I) must be entered by the number of vehicle range/orientations identified.

ZO(I) This parameter (Card C) allows for the case when the air-ground interface in the DORT calculation does not match the air-ground interface in the MORSE calculation. Typically, the DORT calculation will place the air-ground interface at z=0. The vehicle geometries analyzed, typically place the turret-track interface at z=0 and the air-ground interface at some value less than zero. Consequently, the user can make the two air-ground interfaces match through the parameter ZO(I). ZO(I) must be entered by the number of vehicle range/orientations identified.

ALPHA(I) This parameter (Card C) allows for different vehicle (or target) orientations relative to the source. The parameter is given in units of degrees and is specified for the rotation of the MORSE positive x-axis counterclockwise (as viewed from above) from the DORT positive r-axis. For example, a typical vehicle geometry in MORSE has the positive x-axis facing forward on the vehicle i.e., in the direction of the gun barrel for a tank. If the user wished to determine the protection factor for the tank facing the source, ALPHA(I) would have to be set to 180, the degrees rotation of the positive x-axis in MORSE with the positive r-axis in DORT. A value of 0 for ALPHA(I) would orient the tank with the rear facing the source. Care must be taken when determining the target rotation. ALPHA(I) must be entered by the number of vehicle range/orientations identified.

Cards D and E These cards are input if the VISTA and MORSE energy group structures do not coincide, i.e. IDIF>0 on Card B. This option is only valid for cases where the VISTA energy group structure is a subset of the MORSE energy group structure. This option was included in DRC2 to allow for coupling of new MORSE adjoint leakage tapes in 69 energy

groups (46n-23γ) and old DORT free-field fluence files in 58 energy groups (37n-21γ). Coupling of arbitrary group structures in DRC2 is now operational.

RESP The response functions are entered in order of decreasing energy and with the neutron response preceding the gamma-ray response.

10.3.1 Common Block Information

The input information for DRC2 is processed into several common block areas for use throughout the code. The common block structure was revised for the current version of DRC resulting in fewer commons with more variables in each. The three main commons used in DRC are BLANK COMMON, common TDT1, and common IDRC. The variables and structures of these three common blocks are defined in Tables 10-3, 10-4, and 10-5.

Table 10-3. Location of DRC2 arrays in BLANK COMMON.

Mnemonic name	Location in BLANK COMMON	Array Purpose
ENER(IG)	$I = 1 + IG - 1$	Upper limit of MORSE energy group IG in eV
VEL(IG)	$I = NMTG + IG - 1$	Velocity of MORSE energy group IG
FS(IG)	$I = 2 * NMTG + IG - 1$	Unnormalized fraction of source particles in MORSE energy group IG
BFS(IG)	$I = 3 * NMTG + IG - 1$	Relative importance of MORSE energy group IG
DELE(IG)	$I = 4 * NMTG + IG - 1$	Bin width of energy bin IG
ASORC(NB)	$I = LOCASC + NB - 1$	Total source weight for batch NB
BUF(IPOS)	$I = LOCBUF + IPOS - 1$	Temporary storage for MORSE collision tape data
IVAL(IF)	$I = IVL + IF - 1$	Index of radial fluence for fluence point IF
DWT(IANG)	$I = IWT + IANG - 1$	Weight for direction IANG from VISTA quadrature
AMU(IANG)	$I = IMU + IANG - 1$	Azimuthal angle corresponding to direction IANG
ETA(IANG)	$I = IET + IANG - 1$	Polar angle corresponding to direction IANG
R(IN)	$I = IR + IN - 1$	Radial mesh point corresponding to radial bin IN
Z(IN)	$I = IZ + IN - 1$	Axial mesh point corresponding to height bin IN
A(IA)	$I = IROT + IA - 1$	3 x 3 rotation matrix for rotating the vehicle
FDOS(IG)	$I = IFD + IG - 1$	Free-field dose for group IG
DELU(IG)	$I = IDU + IG - 1$	Logarithm of upper energy bound/lower energy bound for group IG
ICA(IG)	$I = ICE + IG - 1$	Correspondence of energy group numbers in VISTA with those in MORSE
VE(IGG)	$I = INV + IGG - 1$	VISTA energy group boundaries followed by NNEUT (number of neutron groups) and NGAM (number of gamma groups)
DELVE(IGG)	$I = INV + IGG - 1$	Delta E for VISTA energy group boundaries

Table 10-4. Definitions of variables in TDT1 COMMON.

Variable	Definition
NANG	Number of directions in quadrature from VISTA file
NRADI	Number of radii from VISTA file
NAXI	Number of axii from VISTA file
NOG	Number of energy groups from VISTA file
NOGPI	NOG + 1
NDWN	Number of downward directions from VISTA
NJFLX	Number of axial fluences on VISTA file
NIFLX	Number of radial fluences on VISTA file
JSTRT	Index of first J fluence
JLST	Index of last J fluence
IWT	Location of weights from VISTA quadrature
IMU	Location of mu's (azimuthal cosines) from VISTA quadrature
IET	Location of eta's (polar cosines) from VISTA quadrature
IR	Location of radii from VISTA file
IZ	Location of Z or axial points from VISTA file
IXO	Location of X centers of rotation
IZO	Location of Z centers of rotation
IALPHA	Location of rotation angles
ILDN	Location for re-normalized spectra
IROT	Location of rotation matrix A
IFD	Location of FDOS array in blank common
IDU	Location of DELU array in blank common
ICE	Location of ICA array in blank common
INV	Location for VISTA 'nneut', 'ngam', and energy boundary input (IDIF>0)
INVD	Location of VISTA group structure delta-E values
IZNEW	Location of Z midpoints for fluences selected from VISTA file
LPHI	Location of the PHI (azimuthal angle boundaries for quadrature) array
LNPHI	Location of the number of PHI angles per polar level (NPHI)
LNCMP	Location of the cumulative number of PHI angles by polar level (NCMP)
LPOL	Location of the POL (polar level boundaries for quadrature) array IGCX(2,NMTG)
LIANG	Location of the selected angles correspondences to the quadrature set (IANG)
LIGCX	Location of first and last VISTA group spanning each MORSE group (IDIF>0)
LGFRAC	Location of VISTA group fractions allocated to MORSE groups (IDIF>0)
LFRFLX	Location of free-field flux GFRAC(NMTG,NOG)
LFLUXI	Temporary location for regrouped VISTA fluences
ILST	Location after last permanent storage location. [Locations ILST to MAXSZ are used to fit into core fluences for as many groups as possible
NP	Calculated number of polar (eta) levels in quadrature set.
MANG	Number of non-zero weight directions in quadrature set.
NOD	Number of DRC detectors [=7; n, p, ... tot]
NZBOT	Index of bottom coupling surface ZBOT in array of VISTA axial boundaries
NZTOP	Index of top coupling surface ZTOP in array of VISTA axial boundaries
NZPTS	Number of axial points being processed
IDIF	Signal indicating whether the number of VISTA and MORSE energy boundaries are the same (0), or MORSE has more (1), or VISTA has more (2)
INTERP	Interpolation option (1/2 linear/logarithmic or exponential)

Table 10-5. Definition of variables in IDRC COMMON.

Variable	Definition
LEAK	Leakage value for current batch from MORSE
IBUFSZ	The size of the buffer for the collision parameters (Set at 1000)
NGPQTT	Not used
NMCTP	Logical unit number of MORSE collision tape
NSTAP	Logical unit number of VISTA fluence file
NIN	Logical unit number of standard input unit
NOU	Logical unit number of standard output unit
NSCR1	Logical unit number for scratch data set
NSCR2	Logical unit number for scratch data set
NSCR3	Logical unit number for scratch data set
NSCR4	Logical unit number for scratch data set
IRC	Counter for record number
NBTCH	Counter for batch number currently being processed
XD	Detector X location in MORSE geometry
YD	Detector Y location in MORSE geometry
ZD	Detector Z location in MORSE geometry
ZBOT	Bottom of coupling surface relative to MORSE geometry
ZTOP	Top of coupling surface relative to MORSE geometry
IPRT	Signal to print detector output only (0), free-field only (1), both of the above plus protection factors and energy-dependent arrays (2).
WATMX	Maximum weight accepted for processing
NDET	Number of range/orientations
MAXSZ	Size of blank common (500000)
TNDOS	Free-field neutron dose
TGDOS	Free-field gamma dose
TNFLX	Free-field neutron flux
TGFLX	Free-field gamma flux
TDOS	Total dose
TFLX	Total flux
TTTLM(18)	Alphanumeric title from MORSE collision tape
LOCDE	Location of DELE array, the delta energy for MORSE energy groups
LOCLK	Location in blank common of ILEAK array from MORSE collision tape
LOCASC	Location in blank common of ASORC array from MORSE collision tape
LOCBUF	Location in blank common of buffer array for collision parameters from MORSE
NPARAM	Number of parameters written on MORSE leakage file
NPREC	Number of particles/record on MORSE leakage file
IDXY	Trigger to indicate presence of X-Y data
XQ	X-location of MORSE rotation point in MORSE geometry
YQ	Y-location of MORSE rotation point in MORSE geometry

10.4 DRC2 INPUT FILE FORMATS

As stated earlier, DRC2's primary function is to couple the MORSE Monte Carlo adjoint leakage information with the DORT free-field fluences to compute the estimates of the fluences and doses within the vehicle interior. Furthermore, DRC2 utilizes the free-field fluences and estimates from the in-vehicle fluences (and doses) to calculate neutron protection factors and reduction factors for the vehicle.

To accomplish its primary function, DRC2 reads a VISTA formatted file to obtain the DORT free field fluence data, and a MORSE adjoint leakage tape to obtain the parameters necessary for it to estimate the fluences and doses within the vehicle interior. The format of the VISTA input source file is as follows:

Record 1: TITLE, TDOT - 144 Alphanumeric Characters

Record 2:

MM	-	Number of quadrature directions
IM	-	Number of radial intervals
JM	-	Number of axial intervals
IGM	-	Number of energy groups
IGP	-	Number of energy groups plus 1
MMDN	-	Number of directions downward
NJP	-	Number of axial fluences
ISH	-	Height of source point
ISHA	-	Cosine of source angle (with Z-axis)
NIP	-	Number of radial fluences
JPL	-	Index of first J interval on file
JPU	-	Index of last J interval on file
11 additional VISTA input values not used in MASH		

Record 3: IVAL - Array of radial interval numbers being output

Record 4: [MM values per array; 3*MM total values]

WT	-	Weights from DORT quadrature
AMU	-	Mu's from DORT quadrature
ETA	-	Eta's from DORT quadrature

Record 5: [NIP + NJP values]

R	-	Midpoints of radial bins
Z	-	Midpoints of axial bins

Record 6 to END: [NANG*NJFLX values per record
[IGM records per radius, and NIFLX radii]

FLUX	-	Directional fluences
------	---	----------------------

Because of the large amount of core storage required for the VISTA free-field fluences, the forward-adjoint coupling could not be accomplished as the Monte Carlo calculation was performed. The coupling involved the calculation of the integral

$$R = \int \Phi(P)\Phi^*(P)(\Omega \cdot n)dP$$

over the coupling surface S.

We define

$\Phi(P)$ = VISTA free-field fluences in phase space P.

$\Phi^*(P)$ = MORSE adjoint fluence in phase space P.

$\Omega \cdot n$ = cosine of angle between particle direction and inward normal.

The adjoint fluence at the r_s , the position of the surface S, was written on a leakage tape along with other variables necessary for coupling the MORSE results with the VISTA results. The variables written on tape for each adjoint leakage were as follows:

- | | | |
|-----|-------|--|
| 1. | IG | - the group number, |
| 2. | IGS | - the source group, |
| 3. | WTBC | - the weight of the adjoint particle at leakage, |
| 4. | U | - X direction cosine, |
| 5. | V | - Y direction cosine, |
| 6. | W | - Z direction cosine, |
| 7. | X | - X location of leakage point |
| 8. | Y | - Y location of leakage point |
| 9. | Z | - Z Location height of leakage point |
| 10. | NBOD | - Body of leakage point |
| 11. | NSURF | - Surf of leakage point |
| 12. | NZONE | - zone of leakage point |
| 13. | IDET | - detector type in which particle is to be scored. |

An output buffer was blocked to transfer the data from core to tape efficiently at the end of each batch. This permitted batch statistics to be calculated in the DRC2 code which reads the MORSE leakage tape and the VISTA fluence tape and performs the coupling. The leakage tape generated by MORSE contains the following data:

-
- Record 1 - Title and date of MORSE run
 - Record 2 - Initial Data Record - 24 words
 - Record 3 - Energy Group Structure, Velocities, Source Spectra and Biasing Function - 4*NMTG words
 - Record 4 - A Block of Leakage Information for 125 Adjoint Particles - 1625 words

.....

Record N -

A detailed description of the contents of the above records is given below:

- I. Record 1 - A 40 character title plus a 32 character date of run
- II. Record 2 - The USER labeled common (plus parameter INGB) is written in Record 2. The total number of groups, number of batches, etc., are contained in this record, as defined in Table 10-6.
- III. Record 3 - The multigroup energy structure and group velocities are contained in Record 3. The data are:

E(1) - Upper energy limit of Group 1.

.
.
.

E(NMTG) - Upper energy limit of Group NMTG.

VEL(1) - Velocity of Group 1.

.
.
.

VEL(NMTG) - Velocity of Group NMTG.

F(1) - Fraction of Source in Group 1

.
.
.

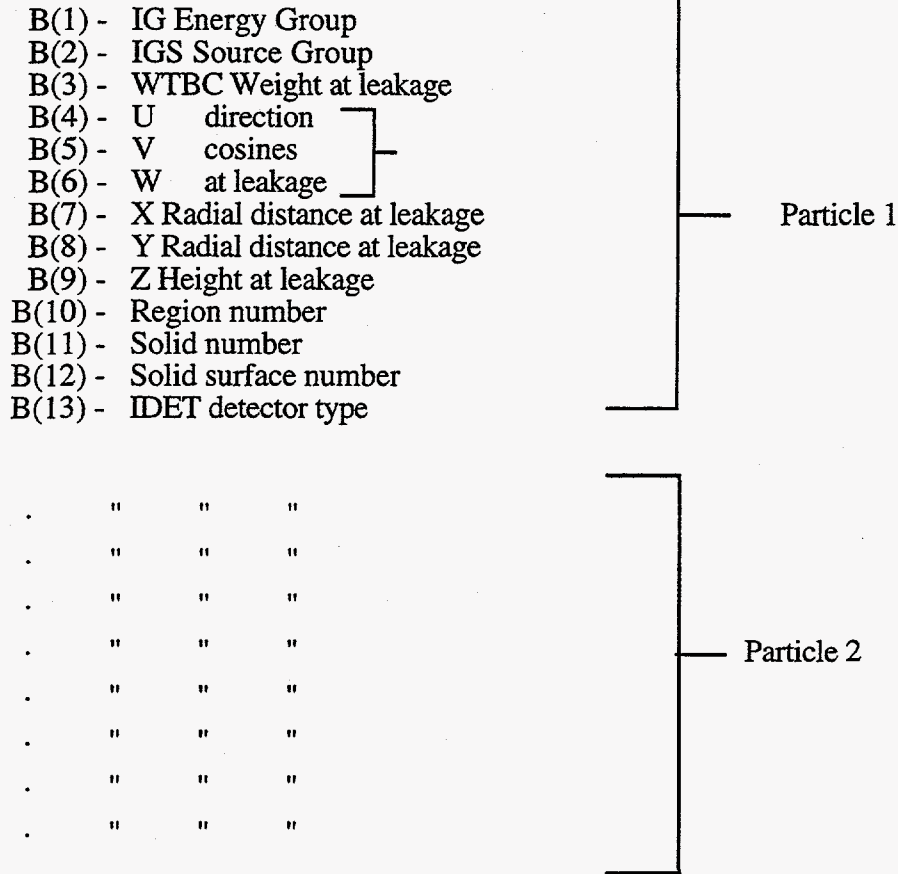
F(NMTG) - Fraction of Source in Group NMTG

B(1) - Biased Fraction in Group 1

.
.
.

B(NMTG) - Biased Fraction of Source in Group NMTG

IV. Record 4 - The adjoint leakage fluence blocked in groups of 125 particles.



B(1625) - IDET Detector Type

V. Additional records in the format of Record 4 to a total of L(NITS+1) leakage records.

10.5 DRC2 OUTPUT FILES AND LOGICAL UNIT REQUIREMENTS

DRC2 uses and creates several files. The files are assigned unit numbers 5, 6, 10, 11, 15, and 24. The respective default file names are ft05drc, ft06drc, ft10drc, ft11drc, ft15drc, and ft24msh. The names may be changed by specifying alternate names on the execute line as follows:

drc2 f5=a,f6=b,f10=c,f11=d,f15=e,f24=f

where the letters to the right of the equal signs represent the alternate names for the files. By unit numbers, the files are defined as follows:

Table 10-6. Definitions of Variables in USER COMMON.

Number	Variable	Definition
1	AGSTRT	Initial chronological age to be assigned to source particles
2	WTSTRT	Initial weight to be assigned to source particles
3	XSTRT	Initial x position to be assigned to source particles
4	YSTRT	Initial y position to be assigned to source particles
5	ZSTRT	Initial z position to be assigned to source particles
6	DFF	Normalization for adjoint problems
7	EBOTN	Lower energy boundary (eV) of last neutron group (group NMGP)
8	EBOTG	Lower energy boundary (eV) of last gamma-ray group (group NMTG)
9	TCUT	Chronological age limit
10	I0	Logical unit for output
11	I1	Logical unit for input
12	IADJM	Adjoint switch (> 0 for adjoint problem)
13	NGPQT1	Problem-dependent energy group limit
14	NGPQT2	Problem-dependent energy group limit
15	NGPQT3	Problem-dependent energy group limit
16	NGPQTG	Group number of lowest energy gamma-ray group to be treated
17	NGPQTN	Group number of lowest energy neutron group to be treated
18	NITS	Number of batches to be run
19	NLAST	Last cell in BLANK COMMON used by random walk package
20	NLEFT	Number of cells in BLANK COMMON available to user
21	NMGP	Number of primary energy groups
22	NMTG	Total number of energy groups
23	NSTRT	Number of source particles for each batch

DESCRIPTION OF DRC2 INPUT AND OUTPUT FILES

Unit Number	File Description
5	input file for DRC2
6	printed output file for DRC2
10	special output text file
11	special output text file
15	VISTA fluence file
24	MASH collision file

The special output text files contain formatted summary data for generating tabular output. Scratch files may be created and used, but their names are formed by the code and cannot be named by the user.

10.6 CODE SYSTEM

Several codes are executed to produce the final DRC2 results. Files produced by one code may be used by one or more of the other codes executed in the calculational sequence. The production of the forward fluence file generally involves a calculational sequence executing the GIP, GRTUNCL, DORT, and VISTA codes. The VISTA code creates the fluence file that is used by DRC2. The MASH code produces the collision file, and DRC2 couples the VISTA and MASH output files to produce the quantities of interest (fluence, dose, etc.). The sharing of files is outlined below, where "I" and "O" superscripts respectively indicate input and output for the codes. A code to the right uses data from a code to the left whenever the leftmost file on a line has a superscript "O" and a file to the right has a superscript "I". The underlined file names are default Cray file names that are used if alternative names are not assigned on the execute line. File names in quotes (") are generic names for the ANISN- ("ansxs") and GIP-formatted ("gipxs") cross-section files. The other names refer to the code internal variable names for the files.

Sharing of Files by Codes

GIP	GRTUNCL	DORT	VISTA	MASH	DRC2
"ansxs" ^I				<u>ft08msh</u> ^I	
"gipxs" ^{O*}	"gipxs" ^I npso ^O	"gipxs" ^I ntdsi ^I nflsv ^O ntdir ^O	nunci ^I nflsv ^I naft ^I ndata ^O	<u>ft24msh</u> ^O	<u>ft15drc</u> ^I <u>ft24msh</u> ^I

*GRTUNCL reads cross sections from unit 4; therefore in a calculational sequence, GIP should write cross sections to unit 4 and DORT, like GRTUNCL, should read cross sections from unit 4.

10.7 TEST PROBLEMS

Several test problems (see Appendix D) were run to verify the correct operation of the code features. These include:

1. a problem designed to reproduce free-field fluences calculated by DORT,
2. a calculation of detector responses in a relatively small system called the "metric doghouse" (the reference DRC test case),
3. calculations of detector responses in two relatively large systems to examine the effects of including x-y dependence in the coupling calculation, and
4. a problem solvable by DORT involving the calculation of detector responses in a shielded, large-radius, annular, cylindrical tunnel in an air-over-ground radiation field.

For the latter calculation, the deterministic results from the DORT calculation can serve as a basis for checking the accuracy of the results from the coupled method.

10.8 CONCLUSIONS

The DRC2 code has been written and tested and appears to be performing the coupling operation correctly. Results have been compared with some from the DRC code and some simulated DRC results (obtained with DRC2 by coupling without x-y dependence). Those results indicated that there were some significant effects (greater than 10%) of including x-y dependence in the coupling operation, but small effects were observed in small systems and even one reasonably large system. In addition, the good agreement for a test case solvable directly with DORT gave added assurance of the correctness of the coupling procedure.

Although the code allows for calculations with very large fluence data requirements to be solved "ex-core", one may incur a large IO cost penalty when data has to be stored ex-core. It is therefore recommended that, whenever possible, enough core be allocated so that all fluence data can be stored in core.

10.9 REFERENCES

1. Rhoades and R. L. Childs, "The DORT Two-Dimensional Discrete Ordinates Transport Code," Nucl. Sci. & Eng. 99, 1, 88-89 (May 1988).
2. M. B. Emmett, "The MORSE Monte Carlo Radiation Transport Code System," ORNL-4972 (1975), ORNL-4972/R1 (1983), ORNL-4972/R2 (1984), Union Carbide Corporation, Nuclear Division, Oak Ridge National Laboratory.
3. W. A. Rhoades, "Development of a Code System for Determining Radiation Protection of Armored Vehicles (The VCS Code)," ORNL-TM-4664, Oak Ridge National Laboratory, (October 1974).

4. W. A. Rhoades, M. B. Emmett, G. W. Morrison, J. V. Pace, III, and L. M. Petrie, "Vehicle Code System (VCS) User's Manual," ORNL/TM-4648 (August 1974).
5. J. O. Johnson, editor, "A User's Manual for MASH 1.0 - A Monte Carlo Adjoint Shielding Code," ORNL/TM-11778, Oak Ridge National Laboratory, (March 1992).
6. J. O. Johnson, J. D. Drischler, and J. M. Barnes, "Analysis of the Fall-1989 Two-Meter Box Test Bed Experiments Performed at the Army Pulse Radiation Facility (APRF)," ORNL/TM-11777, Oak Ridge National Laboratory, (May 1991).
7. R. T. Santoro et al., "DNA Radiation Environments Program Fall 1989 2-Meter Box Experiments and Analysis," ORNL/TM-11840, Oak Ridge National Laboratory, (May 1991).

10.10 SAMPLE PROBLEM

A complete listing of the input cards for the sample problem is given in Figure 10-1, and some selected output is shown in Figure 10-2. The sample problem demonstrates the processing of the VISTA fluence file for the air-over-ground free-field environment at 400 meters from the source and the MORSE adjoint calculation of the two-meter box experiments at 400 meters.^{6,7} In viewing Figure 10-1, the input illustrates; four range/orientations to be analyzed (NDET=4), a range of 400 meters (Card C, XO(I)=40000.0 cm), the DORT and MORSE air-ground interfaces were equivalent (Card C, ZO(I)=0.0), and four rotations of the box (ALPHA=0.0, 90.0 180.0, and 270.0). The minimum (ZBOT) and maximum (ZTOP) z boundaries in the MORSE geometry were -15.0 cm and 230.0 cm, respectively, and the detector height in the MORSE adjoint calculation was 110.16 cm. The print control flag (IPRT) was set to 2 to obtain both free-field and in-vehicle fluence and dose data, and the maximum weight allowed would default to the value pre-set in the code (WATMX=50.0). The VISTA and MORSE group structures were equivalent, so consequently, Cards D and E were omitted from the input. The next three title cards are for Cards F, G, and H. The response functions utilized in the DRC2 analysis are the flat response (which yields fluence) and the free-in-air tissue kerma response in units of $\text{gy}\cdot\text{cm}^2/\text{n},\gamma$. The last card is the input for Card J. This particular input deck did not exercise the option of stacking cases for different target orientations. **Notice** that the "***" values are in columns 2 and 3. DRC will not correctly identify the input if these FIDO control parameters are not in the proper columns.

The selected DRC2 output (from ft06drc) shown in Figure 10-2 first illustrates the input parameters read from Cards A and B, the rotation matrix for the parameter alpha, and a series of titles identifying the MORSE calculation, the VISTA calculation file, and the DORT calculation used to create the input files for this DRC case. The titles are followed by parameters relevant to the VISTA fluence file including some control parameters, the specific quadrature information, and radial and axial mesh points on the VISTA file. The output then contains some arrays used internal to DRC2 that may not be useful to the user. A title from the MORSE adjoint history file is then printed indicating whether the in-group biasing option in MORSE was invoked. The MORSE input source spectrum and bias function are then printed indicating the source sampling utilized in the adjoint calculation. Next, the output lists the response function title, the values of the response function to be folded with the free-field and in-vehicle fluences, and arrays relevant to the energy bins used in the DRC2 case, followed by an indication of the storage used in the DRC2 case. Much of this last set of output is similar to the output of the SAMBO routines in MORSE since DRC2 contains a modified version of SAMBO. The output lists the number of

MORSE leakages by batch, the total number of leakages, and the total number of MORSE leakage records read. This information can be cross referenced with the MORSE output.

The next output is the results of the calculations in subroutine FREDOS and represents the GRTUNCL/DORT free field fluence and dose at the detector location in the MORSE geometry. The following sequence of output is repeated for each response function and range/orientation. There can be a substantial amount if there are many responses (NRESP) and range/orientations (NDET). Both the spectra and integral totals are printed. This output is then followed by the DRC2 detector responses (Table 10-1) along with their fractional standard deviations and protection factors and reduction factors (Table 10-2) for the response function given in the input (Card I). These values are what the entire MASH analysis is geared to determine. Finally, the DRC output gives the energy dependent fluence and dose arrays for the first six detector types listed in Table 10-1 along with the normalized total neutron and photon fluence and dose arrays. The format of these arrays is quite cumbersome, however, useful information can be obtained from them. Future efforts will hopefully improve these output arrays into a more useful format.

The DRC2 output (from ft10drc) shown in Figure 10-3 is a more condensed version of the output described in the last paragraph. Only the total neutron and gamma fluence and dose spectra arrays are printed here, however. The different detector types and normalized spectra information is not output on this unit. The DRC2 output (from ft11drc) shown in Figure 10-4 only gives the integral values for the free-field neutron and gamma responses and the seven DRC2 detectors defined in Table 10-1 along with their fractional standard deviations. This data is repeated for each response function and range/orientation.

```

2m box exp/4in steel/dabl 46n-23g lib/aprf sh=16.143m/10-24-89(a) air
** 0.0      0.0    110.16   -15.0   230.0
    2.0      50.0    4.0      0.0    0.0
    1625.0   13.0    1.0      2.0    0.0
    0.0      1.0      1.0
** 4r40000.0
** 4r0.0
** 0.0 90.0 180.0 270.0
46 neutron - 23 gamma flat and free-in-air tissue kerma response input
-- 1=neut 2=veh n-g 3=grd n-g 4=photons
mash 46n/23g group flat response (fluence)
**
69r1.000
mash 46n/23g group free-in-air tissue kerma response (gy.cm2/n,g)
**
736532-16 704584-16 685894-16 674499-16 661555-16 638136-16 633529-16
598822-16 57632-15 551514-16 546431-16 512651-16 470858-16 457805-16
44359-15 419381-16 357307-16 332494-16 321126-16 291193-16 263438-16
252468-16 222507-16 205934-16 193682-16 179065-16 163746-16 130075-16
102563-16 806538-17 563405-17 359169-17 25917-16 213032-17 147572-17
628401-18 219938-18 925902-19 448136-19 20734-18 103718-19 932428-20
135874-19 228494-19 372646-19 129126-18 401109-16 317559-16 27612-15
23517-15 205102-16 185083-16 164356-16 143343-16 121273-16 1036-14
902669-17 755621-17 585321-17 42722-16 296381-17 192968-17 105409-17
529629-18 348187-18 313231-18 484629-18 10497-16 339599-17
energy group totals

```

Figure 10-1. Sample DRC2 Input for the Two-Meter Box Protection Factor Analysis.

This case began on Friday, June 26, 1998 at 10:55:09.

detector response code V2: aprf source with 2m box located at the 400m test site rotated 0 degrees

xd = x-loc. (cm) of det. in MORSE geom 0.00000E+00
yd = y-loc. (cm) of det. in MORSE geom 0.00000E+00
zd = z-loc. (cm) of det. in MORSE geom 1.10160E+02
zbot = bottom of coupling surface (cm) -1.50000E+01
ztop = top of coupling surface (cm) 2.30000E+02
iprt = 0 print vehicle doses only 2

1 print VISTA data+free field spectra
2 print VISTA data+ff spec+veh doses+spec+prot
3 print VISTA data+veh doses+prot facs
watmx = maximum weight accepted 5.00000E+01
ndet = no. of vehicle range/orientations 4
idif = 0/>0 same/different group structure 0
ksiz = k-words of storage to be allocated 0
ibufsz = MORSE collision file record length 1625
nparm = no. of parameters written on coll. file 13
idxy = 0 no x-y data 1

1 x-y data but no x-y dependence
2 x-y data and x-y dependence 2
iww = no. of responses desired (.le.10)
note: 0 implies 2 responses
xq = x-loc. (cm) of veh. sys. rot.point 0.00000E+00
yq = y-loc. (cm) of veh. sys. rot.point 0.00000E+00
interp= 1/2 -- linear/log flux interpolation 1
xnorm = normalization factor (default=1.0) 1.00000E+00

vehicle range/orientation parameters

loc. of morse origin rotation
i x z angle
1 4.00000E+04 0.00000E+00 0.00000E+00
2 4.00000E+04 0.00000E+00 9.00000E+01
3 4.00000E+04 0.00000E+00 1.80000E+02
4 4.00000E+04 0.00000E+00 2.70000E+02
rotation matrix for range/orientation no. 1
1.00000E+00 0.00000E+00 0.00000E+00
0.00000E+00 1.00000E+00 0.00000E+00
0.00000E+00 0.00000E+00 1.00000E+00
rotation matrix for range/orientation no. 2
1.94707E-07 -1.00000E+00 0.00000E+00
1.00000E+00 1.94707E-07 0.00000E+00
0.00000E+00 0.00000E+00 1.00000E+00
rotation matrix for range/orientation no. 3

Figure 10-2. Sample DRC2 Output (Unit ft06) For the Two-Miter Box Protection Factor Analysis

-1.00000E+00 -3.89414E-07 0.00000E+00
 3.89414E-07 -1.00000E+00 0.00000E+00
 0.00000E+00 0.00000E+00 1.00000E+00
 rotation matrix for range/orientation no. 4

-4.64912E-07 1.00000E+00 0.00000E+00
 -1.00000E+00 -4.64912E-07 0.00000E+00
 0.00000E+00 0.00000E+00 1.00000E+00

vehicle escape histories from: two meter box/detailed geometry/46n-23g
 fluence file from: 'aprf aog/2m box/16.14m sh/32% g.m./ss89-219 air/400m test site
 dot title (' aprf aog, two meter box experiments, saic 1990 leakage source.)

nang = no. of quadrature angles 240
 nradi = no. of radial points 123
 naxii = no. of axial points 146
 nog = no. of energy groups 69
 nogp1 = no. of energy groups plus 1 70
 ndwn = no. of angles down 120
 njflx = no. of axial fluxes 22
 niflx = no. of radial fluxes 1
 jstrt = index of first j flux 6
 jlst = index of last j flux 27

quadrature weights and angles

mu	eta	wgt
1-6.41230E-02	-9.97942E-01	0.00000E+00
2-4.21582E-02	-9.97942E-01	1.02900E-03
3 4.21582E-02	-9.97942E-01	1.02900E-03
4-1.42963E-01	-9.89728E-01	0.00000E+00
5-9.39923E-02	-9.89728E-01	3.07825E-03
6 9.39923E-02	-9.89728E-01	3.07825E-03
7-2.29252E-01	-9.73367E-01	0.00000E+00
8-1.50724E-01	-9.73367E-01	5.10200E-03
9 1.50724E-01	-9.73367E-01	5.10200E-03
10-3.15291E-01	-9.48995E-01	0.00000E+00

230 8.05405E-01	1.11045E-01	4.06806E-03
231 9.70823E-01	1.11045E-01	5.15474E-03
232-9.99313E-01	3.70540E-02	0.00000E+00
233-9.76194E-01	3.70540E-02	5.17107E-03
234-8.09860E-01	3.70540E-02	4.08094E-03
235-5.34236E-01	3.70540E-02	5.42534E-03
236-1.86473E-01	3.70540E-02	3.84965E-03
237 1.86473E-01	3.70540E-02	3.84965E-03
238 5.34236E-01	3.70540E-02	5.42534E-03
239 8.09860E-01	3.70540E-02	4.08094E-03
240 9.76194E-01	3.70540E-02	5.17107E-03

index of each radial flux

i flux index
 1 50

Figure 10-2. (continued)

radial and axial mesh points

i	radius	height	ncmp	phi	nphi	pol	znew	iang
1	4.00000E+04	-5.25000E+01	0	1-1.57080E+00	2	-9.95884E-01	-1.75000E+01	2
2	-4.75000E+01		2	2 0.00000E+00	2	-9.83571E-01	-1.25000E+01	3
3	-4.25000E+01		4	3-1.57080E+00	2	-9.63163E-01	-7.50000E+00	5
4	-3.75000E+01		6	4 0.00000E+00	2	-9.34826E-01	-3.75000E+00	6
5	-3.25000E+01		8	5-1.57080E+00	2	-8.98772E-01	-1.75000E+00	8
6	-2.75000E+01		10	6 0.00000E+00	4	-8.63572E-01	-5.00000E-01	9
7	-2.25000E+01		14	7-1.57080E+00	4	-8.23533E-01	2.50000E+01	11
8	-1.75000E+01		18	8 0.00000E+00	4	-7.78900E-01	1.00000E+02	12
9	-1.25000E+01		22	9-1.57080E+00	4	-7.29924E-01	2.00000E+02	14
10	-7.50000E+00		26	10 0.00000E+00	4	-6.76392E-01	3.00000E+02	15
11	-3.75000E+00							
12	-1.75000E+00							
13	-5.00000E-01							
14	2.50000E+01							
15	1.00000E+02							
16	2.00000E+02							
17	3.00000E+02							
18	4.00000E+02							
19	5.00000E+02							
20	6.25000E+02							
21	8.25000E+02							
22	1.02500E+03							
190	-7.84424E-01							229
191	-4.38425E-01							230
192	0.00000E+00							231
193	-2.70317E+00							233
194	-2.35717E+00							234
195	-1.89719E+00							235
196	-1.57080E+00							236
197	-1.24441E+00							237
198	-7.84424E-01							238
199	-4.38425E-01							239
200	0.00000E+00							240

the morse case was run with ingb = 1

Figure 10-2. (continued)

group	energy	group structure and source spectrum unnormalized source spectrum	bias function
1	1.9640E+07	1.0000E+00	5.2910E-03
2	1.6905E+07	1.0000E+00	5.2910E-03
3	1.4918E+07	1.0000E+00	5.2910E-03
4	1.4191E+07	1.0000E+00	5.2910E-03
5	1.3840E+07	1.0000E+00	5.2910E-03
6	1.2523E+07	1.0000E+00	5.2910E-03
7	1.2214E+07	1.0000E+00	5.2910E-03
8	1.1052E+07	1.0000E+00	5.2910E-03
9	1.0000E+07	1.0000E+00	1.0582E-02
10	9.0484E+06	1.0000E+00	1.0582E-02
60	1.0000E+06	1.0000E+00	3.1746E-02
61	7.0000E+05	1.0000E+00	3.1746E-02
62	4.5000E+05	1.0000E+00	1.5873E-02
63	3.0000E+05	1.0000E+00	1.5873E-02
64	1.5000E+05	1.0000E+00	1.5873E-02
65	1.0000E+05	1.0000E+00	1.5873E-02
66	7.0000E+04	1.0000E+00	1.5873E-02
67	4.5000E+04	1.0000E+00	1.5873E-02
68	3.0000E+04	1.0000E+00	1.5873E-02
69	2.0000E+04	1.0000E+00	1.5873E-02

46 neutron - 23 gamma kerma responses input
nd= 28, nne= 46, ne= 69, nt= 0, na= 0, nresp= 2, nex= 0, nexnd= 1

group	resp(1)	resp(2)
1	1.0000E+00	7.3653E-11
2	1.0000E+00	7.0458E-11
3	1.0000E+00	6.8589E-11
4	1.0000E+00	6.7450E-11
5	1.0000E+00	6.6155E-11
6	1.0000E+00	6.3814E-11
7	1.0000E+00	6.3353E-11
8	1.0000E+00	5.9882E-11
9	1.0000E+00	5.7632E-11
10	1.0000E+00	5.5151E-11
60	1.0000E+00	4.2722E-12
61	1.0000E+00	2.9638E-12
62	1.0000E+00	1.9297E-12
63	1.0000E+00	1.0541E-12
64	1.0000E+00	5.2963E-13
65	1.0000E+00	3.4819E-13
66	1.0000E+00	3.1323E-13
67	1.0000E+00	4.8463E-13
68	1.0000E+00	1.0497E-12
69	1.0000E+00	3.3960E-12

number of primary energy bins	46
-------------------------------	----

Figure 10-2. (continued)

total number of energy bins 69

bin no.	lower limit group	lower energy limit	delta e
1	1	1.964E+07	
2	1	1.690E+07	2.735E+06
3	2	1.492E+07	1.987E+06
4	3	1.419E+07	7.270E+05
5	4	1.384E+07	3.510E+05
6	5	1.252E+07	1.317E+06
7	6	1.221E+07	3.090E+05
	7	1.105E+07	1.162E+06
40	40	1.013E+02	1.741E+02
41	41	2.902E+01	7.228E+01
42	42	1.068E+01	1.835E+01
43	43	3.059E+00	7.618E+00
44	44	1.125E+00	1.934E+00
45	45	4.140E-01	7.114E-01
46	46	1.000E-05	4.140E-01
		2.000E+07	
47	47	1.400E+07	6.000E+06
48	48	1.200E+07	2.000E+06
49	49	1.000E+07	2.000E+06
50	50	8.000E+06	2.000E+06
51	51	7.000E+06	1.000E+06
52	52	6.000E+06	1.000E+06

63	63	1.500E+05	1.500E+05
64	64	1.000E+05	5.000E+04
65	65	7.000E+04	3.000E+04
66	66	4.500E+04	2.500E+04
67	67	3.000E+04	1.500E+04
68	68	2.000E+04	1.000E+04
69	69	1.000E+04	1.000E+04

number of time bins 0
 number of angle bins 0
 upper limits of cosine bins

16820 cells used by analysis, 473913 cells remain unused.
 first storage location used for fluxes is 22224
 last storage location used for fluxes is 160223
 calculation performed in 1 blocks with 69 groups per block

morse leakage by batch and total

834	817	756	782	711	724	836	744	790	819
866	789	717	773	774	819	757	694	752	823
801	734	793	677	695	710	794	723	791	764
754	862	791	764	844	770	889	787	749	774

Figure 10-2. (continued)

38656 The number of leakage data records in the file is 335

group structure and free field spectra for response no. 1
 energy case no. 1 orientation angle= .000 deg.
 flux = 4.0000E+04 zo= 0.0000E+00 free field dose

1	1.9640E+07	2.0816D-17
2	1.6905E+07	3.9818D-17
3	1.4918E+07	7.8459D-17
4	1.4191E+07	6.0482D-17
5	1.3840E+07	5.2644D-16
6	1.2523E+07	1.4442D-16
7	1.2214E+07	1.4021D-15
8	1.1052E+07	3.3927D-15
9	1.0000E+07	7.8346D-15
10	9.0484E+06	1.5103D-14

60	1.0000E+06	1.2007D-12
61	7.0000E+05	1.8856D-12
62	4.5000E+05	1.9414D-12
63	3.0000E+05	5.0504D-12
64	1.5000E+05	4.0326D-12
65	1.0000E+05	3.9536D-12
66	7.0000E+04	3.5901D-12
67	4.5000E+04	8.4369D-13
68	3.0000E+04	4.7151D-14
69	2.0000E+04	3.8029D-16

free field neutron flux = 5.7369D-11 free field photon flux = 2.9759D-11 free field total flux = 8.7128D-11
 free field neutron dose = 5.7369D-11 free field photon dose = 2.9759D-11 free field total dose = 8.7128D-11
 group structure and free field spectra for response no. 2 orientation angle= .000 deg.
 flux = 4.0000E+04 zo= 0.0000E+00 free field dose

1	1.9640E+07	2.0816D-17
2	1.6905E+07	3.9818D-17
3	1.4918E+07	7.8459D-17
4	1.4191E+07	6.0482D-17
5	1.3840E+07	5.2644D-16
6	1.2523E+07	1.4442D-16
7	1.2214E+07	1.4021D-15
8	1.1052E+07	3.3927D-15
9	1.0000E+07	7.8346D-15
10	9.0484E+06	1.5103D-14

60	1.0000E+06	5.1298D-24
61	7.0000E+05	5.5885D-24
62	4.5000E+05	3.7463D-24
63	3.0000E+05	5.3236D-24

Figure 10-2. (continued)

64 1.5000E+05 4.0326D-12 2.1358D-24
 65 1.0000E+05 3.9536D-12 1.3766D-24
 66 7.0000E+04 3.5901D-12 1.1245D-24
 67 4.5000E+04 8.4369D-13 4.0888D-25
 68 3.0000E+04 4.7151D-14 4.9494D-26
 69 2.0000E+04 3.8029D-16 1.2915D-27
 free field neutron flux = 5.7369D-11 free field photon flux = 2.9759D-11 free field total flux = 8.7128D-11
 free field neutron dose = 3.8556D-22 free field photon dose = 9.8921D-23 free field total dose = 4.8449D-22
 mash 46n/23g group flat response
 responses(detector) -- 1=neut 2=veh n-g 3=grd n-g 4=photons
 for case no. 1 orientation angle=.000 deg.

detector	uncoll	response	fsd	total	fsd	total
1	0.0000D+00	0.0000D+00	3.0277D-11	0.03087	3.0277D-11	0.03087
2	0.0000D+00	0.0000	3.6881D-12	0.06788	3.6881D-12	0.06788
3	0.0000D+00	0.0000	8.9955D-17	0.68508	8.9955D-17	0.68508
4	0.0000D+00	0.0000	9.4548D-13	0.11340	9.4548D-13	0.11340
5	0.0000D+00	0.0000	4.6337D-12	0.05816	4.6337D-12	0.05816
6	0.0000D+00	0.0000	9.4557D-13	0.11341	9.4557D-13	0.11341
7	0.0000D+00	0.0000	3.3965D-11	0.02898	3.3965D-11	0.02898

protection factor (neutrons) = 1.6891D+00
 protection factor (photons) = 3.1472D+01
 protection factor (total) = 2.4958D+00
 reduction factor (neutrons) = 1.8948D+00
 reduction factor (photons) = 6.4224D+00
 reduction factor (total) = 2.4958D+00
 mash 46n/23g group free-in-air tissue kerma response (gy.cm²/n.g)
 responses(detector) -- 1=neut 2=veh n-g 3=grd n-g 4=photons
 for case no. 1 orientation angle=.000 deg.

detector	uncoll	response	fsd	total	fsd	total
1	0.0000D+00	0.0000	2.6028D-22	0.04348	2.6028D-22	0.04348
2	0.0000D+00	0.0000	2.3177D-23	0.04989	2.3177D-23	0.04989
3	0.0000D+00	0.0000	4.6916D-28	0.56818	4.6916D-28	0.56818
4	0.0000D+00	0.0000	6.1605D-24	0.10011	6.1605D-24	0.10011
5	0.0000D+00	0.0000	2.9338D-23	0.04274	2.9338D-23	0.04274
6	0.0000D+00	0.0000	6.1610D-24	0.10010	6.1610D-24	0.10010
7	0.0000D+00	0.0000	2.8346D-22	0.04005	2.8346D-22	0.04005

protection factor (neutrons) = 1.3602D+00
 protection factor (photons) = 1.6056D+01
 protection factor (total) = 1.6728D+00
 reduction factor (neutrons) = 1.4813D+00
 reduction factor (photons) = 3.3718D+00
 reduction factor (total) = 1.6728D+00
 fluence(energy,detector) energy group totals
 for case no. 1 orientation angle=.000 deg.

energies	direct neutron	capture photons from vehicle	capture photon source from ground	direct photons	sum of all photons	photon source entering vehicle
1.964E+07	3.190D-18	0.0000D+00	0.0000D+00	0.0000D+00	0.0000D+00	0.0000D+00

Figure 10-2. (continued)

4.500E+04	0.000D+00 .000	2.400D-15 .657	0.000D+00 .000	4.774D-17 .934	2.448D-15 .644	4.774D-17 .934
3.000E+04	0.000D+00 .000	0.000D+00 .000	0.000D+00 .000	0.000D+00 .000	0.000D+00 .000	0.000D+00 .000
2.000E+04	0.000D+00 .000	0.000D+00 .000	0.000D+00 .000	0.000D+00 .000	0.000D+00 .000	0.000D+00 .000
1.000E+04	0.000D+00 .000	0.000D+00 .000	0.000D+00 .000	0.000D+00 .000	0.000D+00 .000	0.000D+00 .000

normalized fluence spectra per unit lethargy
for case no. 1 orientation angle = .000 deg.

neutrons photons

energies 1.964E+07	7.02558D-07 .555	0.00000D+00 .000	0.00000D+00 .000	0.00000D+00 .000	0.00000D+00 .000	0.00000D+00 .000
1.690E+07	2.41560D-07 .543	0.00000D+00 .000	0.00000D+00 .000	0.00000D+00 .000	0.00000D+00 .000	0.00000D+00 .000
1.492E+07	5.45148D-05 .575	0.00000D+00 .000	0.00000D+00 .000	0.00000D+00 .000	0.00000D+00 .000	0.00000D+00 .000
1.419E+07	3.37670D-05 .405	0.00000D+00 .000	0.00000D+00 .000	0.00000D+00 .000	0.00000D+00 .000	0.00000D+00 .000
1.384E+07	1.06538D-05 .480	0.00000D+00 .000	0.00000D+00 .000	0.00000D+00 .000	0.00000D+00 .000	0.00000D+00 .000
2.902E+01	2.48979D-02 .092	0.00000D+00 .000	0.00000D+00 .000	0.00000D+00 .000	0.00000D+00 .000	0.00000D+00 .000
1.068E+01	2.23524D-02 .074	0.00000D+00 .000	0.00000D+00 .000	0.00000D+00 .000	0.00000D+00 .000	0.00000D+00 .000
3.059E+00	1.51568D-02 .119	0.00000D+00 .000	0.00000D+00 .000	0.00000D+00 .000	0.00000D+00 .000	0.00000D+00 .000
1.125E+00	8.46207D-03 .113	0.00000D+00 .000	0.00000D+00 .000	0.00000D+00 .000	0.00000D+00 .000	0.00000D+00 .000
4.140E-01	1.21874D-04 .106	0.00000D+00 .000	0.00000D+00 .000	0.00000D+00 .000	0.00000D+00 .000	0.00000D+00 .000
1.000E-05 energies 2.000E+07	0.00000D+00 .000	1.97701D-06 .374	0.00000D+00 .000	0.00000D+00 .000	0.00000D+00 .000	0.00000D+00 .000
1.400E+07						

energies	for response no. 1 direct neutron	dose spectra (energy, detector) for case no. 2 capture photons from vehicle	capture photon source from ground	orientation angle = direct photons	sum of all photons	photon source entering vehicle
1.200E+07	0.00000D+00 .000	4.15165D-05 .570				
1.000E+07	0.00000D+00 .000	4.86983D-03 .296				
8.000E+06	0.00000D+00 .000	2.23900D-02 .179				
.	0.00000D+00 .000	5.37824D-01 .103				
.						
1.000E+05	0.00000D+00 .000	3.52151D-02 .303				
7.000E+04	0.00000D+00 .000	1.19565D-03 .644				
4.500E+04	0.00000D+00 .000	0.00000D+00 .000				
3.000E+04	0.00000D+00 .000	0.00000D+00 .000				
2.000E+04	0.00000D+00 .000	0.00000D+00 .000				
1.000E+04	0.00000D+00 .000	0.00000D+00 .000				
energies						
1.964E+07	2.349D-28 .555	0.000D+00 .000	0.000D+00 .000	0.000D+00 .000	0.000D+00 .000	0.000D+00 .000
1.690E+07	6.443D-29 .543	0.000D+00 .000	0.000D+00 .000	0.000D+00 .000	0.000D+00 .000	0.000D+00 .000
1.492E+07	5.656D-27 .575	0.000D+00 .000	0.000D+00 .000	0.000D+00 .000	0.000D+00 .000	0.000D+00 .000
1.419E+07	1.727D-27 .405	0.000D+00 .000	0.000D+00 .000	0.000D+00 .000	0.000D+00 .000	0.000D+00 .000
1.384E+07	2.134D-27 .480	0.000D+00 .000	0.000D+00 .000	0.000D+00 .000	0.000D+00 .000	0.000D+00 .000
.						
.						
.						

Figure 10-2. (continued)

2.902E+01	7.029D-27	0.000D+00	0.000D+00	0.000D+00	0.000D+00	0.000D+00	0.000D+00	0.000D+00	0.000D+00
	.092	.000	.000	.000	.000	.000	.000	.000	.000
1.068E+01	1.149D-26	0.000D+00	0.000D+00	0.000D+00	0.000D+00	0.000D+00	0.000D+00	0.000D+00	0.000D+00
	.074	.000	.000	.000	.000	.000	.000	.000	.000
3.059E+00	1.049D-26	0.000D+00	0.000D+00	0.000D+00	0.000D+00	0.000D+00	0.000D+00	0.000D+00	0.000D+00
	.119	.000	.000	.000	.000	.000	.000	.000	.000
1.125E+00	9.547D-27	0.000D+00	0.000D+00	0.000D+00	0.000D+00	0.000D+00	0.000D+00	0.000D+00	0.000D+00
	.113	.000	.000	.000	.000	.000	.000	.000	.000
4.140E-01	5.065D-27	0.000D+00	0.000D+00	0.000D+00	0.000D+00	0.000D+00	0.000D+00	0.000D+00	0.000D+00
	.106	.000	.000	.000	.000	.000	.000	.000	.000
1.000E-05	0.000D+00	0.000D+00	0.000D+00	0.000D+00	0.000D+00	0.000D+00	0.000D+00	0.000D+00	0.000D+00
energies	.000	.000	.000	.000	.000	.000	.000	.000	.000
2.000E+07	0.000D+00	0.000D+00	0.000D+00	0.000D+00	0.000D+00	0.000D+00	0.000D+00	0.000D+00	0.000D+00
	.000	.000	.000	.000	.000	.000	.000	.000	.000
1.400E+07	0.000D+00	0.000D+00	0.000D+00	0.000D+00	0.000D+00	0.000D+00	0.000D+00	0.000D+00	0.000D+00
	.000	.000	.000	.000	.000	.000	.000	.000	.000
1.200E+07	0.000D+00	0.000D+00	0.000D+00	0.000D+00	0.000D+00	0.000D+00	0.000D+00	0.000D+00	0.000D+00
	.000	.000	.000	.000	.000	.000	.000	.000	.000
1.000E+07	0.000D+00	0.000D+00	0.000D+00	0.000D+00	0.000D+00	0.000D+00	0.000D+00	0.000D+00	0.000D+00
	.000	.000	.000	.000	.000	.000	.000	.000	.000
8.000E+06	0.000D+00	0.000D+00	0.000D+00	0.000D+00	0.000D+00	0.000D+00	0.000D+00	0.000D+00	0.000D+00
	.000	.000	.000	.000	.000	.000	.000	.000	.000
.									
.									
1.000E+05	0.000D+00	0.000D+00	0.000D+00	0.000D+00	0.000D+00	0.000D+00	0.000D+00	0.000D+00	0.000D+00
	.000	.000	.000	.000	.000	.000	.000	.000	.000
7.000E+04	0.000D+00	0.000D+00	0.000D+00	0.000D+00	0.000D+00	0.000D+00	0.000D+00	0.000D+00	0.000D+00
	.000	.000	.000	.000	.000	.000	.000	.000	.000
4.500E+04	0.000D+00	0.000D+00	0.000D+00	0.000D+00	0.000D+00	0.000D+00	0.000D+00	0.000D+00	0.000D+00
	.000	.000	.000	.000	.000	.000	.000	.000	.000
3.000E+04	0.000D+00	0.000D+00	0.000D+00	0.000D+00	0.000D+00	0.000D+00	0.000D+00	0.000D+00	0.000D+00
	.000	.000	.000	.000	.000	.000	.000	.000	.000
2.000E+04	0.000D+00	0.000D+00	0.000D+00	0.000D+00	0.000D+00	0.000D+00	0.000D+00	0.000D+00	0.000D+00
	.000	.000	.000	.000	.000	.000	.000	.000	.000
1.000E+04	0.000D+00	0.000D+00	0.000D+00	0.000D+00	0.000D+00	0.000D+00	0.000D+00	0.000D+00	0.000D+00
	.000	.000	.000	.000	.000	.000	.000	.000	.000

Figure 10-2. (continued)

normalized dose spectra per unit lethargy for response 2
 for case no. 1 orientation angle= .000 deg.

energies	neutrons	photons
1.964E+07	6.01922D-06	0.00000D+00
	.555	.000
1.690E+07	1.97981D-06	0.00000D+00
	.543	.000
1.492E+07	4.34949D-04	0.00000D+00
	.575	.000
1.419E+07	2.64936D-04	0.00000D+00
	.405	.000
1.384E+07	8.19855D-05	0.00000D+00
	.480	.000
.		
.		
.		
2.902E+01	2.70051D-05	0.00000D+00
	.092	.000
1.068E+01	3.53287D-05	0.00000D+00
	.074	.000
3.059E+00	4.02856D-05	0.00000D+00
	.119	.000
1.125E+00	3.66809D-05	0.00000D+00
	.113	.000
4.140E-01	1.83059D-06	0.00000D+00
	.106	.000
1.000E-05		
energies		
2.000E+07	0.00000D+00	1.25247D-05
	.000	.374
1.400E+07	0.00000D+00	2.08228D-04
	.000	.570
1.200E+07	0.00000D+00	2.12377D-02
	.000	.296
1.000E+07	0.00000D+00	8.31631D-02
	.000	.179
8.000E+06	0.00000D+00	1.74223D+00
	.000	.103

Figure 10-2. (continued)

```

.
.
.
1.000E+05      1.93659D-03
.000
7.000E+04      5.91515D-05
.000
4.500E+04      0.00000D+00
.000
3.000E+04      0.00000D+00
.000
2.000E+04      0.00000D+00
.000
1.000E+04      0.00000D+00
.000
extra arrays of length nod= 7
19082      14871      91      4612      19574      4703      33953
group structure and free field spectra for response no. 1
xo= 4.0000E+04      zo= 0.0000E+00      case no. 2      orientation angle= 90.000 deg.
.
.
.
xo= 4.0000E+04      zo= 0.0000E+00      case no. 2      orientation angle= 90.000 deg.
.
.
.
mash 46n/23g group flat response
.
.
.
mash 46n/23g group free-in-air tissue kerma response (gy.cm2/n.g)
.
.
.
fluence(energy,detector) energy group totals
for case no. 2      orientation angle= 90.000 deg.
.
.
.
dose spectra(energy,detector)
for response no. 2      for case no. 2      orientation angle= 90.000 deg.
.
.
.
extra arrays of length nod= 7
19082      14871      91      4612      19574      4703      33953

```

Figure 10-2. (continued)

```

group structure and free field spectra for response no. 1
xo= 4.0000E+04  zo= 0.0000E+00  case no. 3  orientation angle= 180.000 deg.
.
.
group structure and free field spectra for response no. 2
xo= 4.0000E+04  zo= 0.0000E+00  case no. 3  orientation angle= 180.000 deg.
.
.
mash 46n/23g group flat response
.
.
mash 46n/23g group free-in-air tissue kerma response (gy.cm2/n.g)
.
.
fluence(energy,detector) energy group totals
for case no. 3  orientation angle= 180.000 deg.
.
.
dose spectra(energy,detector)
for response no. 2  for case no. 3  orientation angle= 180.000 deg.
.
.
extra arrays of length nod= 7
19082  14871  91  4612  19574  4703  33953
.
.
group structure and free field spectra for response no. 1
xo= 4.0000E+04  zo= 0.0000E+00  case no. 4  orientation angle= 270.000 deg.
.
.
group structure and free field spectra for response no. 2
xo= 4.0000E+04  zo= 0.0000E+00  case no. 4  orientation angle= 270.000 deg.
.
.
mash 46n/23g group flat response
.
.
mash 46n/23g group free-in-air tissue kerma response (gy.cm2/n.g)
.
.
fluence(energy,detector) energy group totals
for case no. 4  orientation angle= 270.000 deg.
.
.

```

Figure 10-2. (continued)

dose spectra (energy, detector)
for response no. 2 for case no. 4 orientation angle= 270.000 deg.
extra arrays of length ncd= 7

19082	14871	91	4612	19574	4703	33953
-------	-------	----	------	-------	------	-------

Elapsed time= .2137 minutes

This case ended on Friday, June 26, 1998 at 10:55:25.

Figure 10-2. (continued)

drc2 case: aprf source with 2m box located at the 400m test site rotated 0 degrees *

mesh case: two meter box/detailed geometry/46n-23g

aog fluence file from: 'aprf aog/2m box/16.14m sh/32% g.m./ss89-219 air/400m test site

dort case: 'aprf aog, two meter box experiments, saic 1990 leakage source
normalization factor is 1.00000E+00

dort free field neutron fluence and dose spectra for response function 2
for case no. 1 orientation angle= .000 deg. range= 4.0000E+04

neutron group	upper energy	free field neutron fluence	free field neutron dose
1	1.964E+07	2.082E-17	1.533E-27
2	1.690E+07	3.982E-17	2.806E-27
3	1.492E+07	7.846E-17	5.381E-27
4	1.419E+07	6.048E-17	4.079E-27
5	1.384E+07	5.264E-16	3.483E-26
6	1.252E+07	1.444E-16	9.216E-27
7	1.221E+07	1.402E-15	8.883E-26

40	2.754E+02	1.959E-12	4.063E-26
41	1.013E+02	2.426E-12	2.516E-26
42	2.902E+01	1.913E-12	1.784E-26
43	1.068E+01	2.310E-12	3.139E-26
44	3.059E+00	1.832E-12	4.185E-26
45	1.125E+00	1.838E-12	6.848E-26
46	4.140E-01	1.456E-11	1.879E-24
total	1.000E-05	5.737E-11	3.856E-22

dort free field gamma fluence and dose spectra for response function 2
for case no. 1 orientation angle= .000 deg. range= 4.0000E+04

gamma group	upper energy	free field gamma fluence	free field gamma dose
1	2.000E+07	4.012E-17	1.609E-27
2	1.400E+07	2.558E-16	8.124E-27
3	1.200E+07	6.863E-14	1.895E-24
4	1.000E+07	5.240E-14	1.232E-24
5	8.000E+06	2.140E-13	4.389E-24
6	7.000E+06	1.929E-13	3.571E-24

Figure 10-3. Sample DRC2 Output (Unit ft10) For the Two-Meter Box Protection Factor Analysis

18	1.500E+05	4.033E-12	2.136E-24
19	1.000E+05	3.954E-12	1.377E-24
20	7.000E+04	3.590E-12	1.125E-24
21	4.500E+04	8.437E-13	4.089E-25
22	3.000E+04	4.715E-14	4.949E-26
23	2.000E+04	3.803E-16	1.291E-27
total	1.000E+04	2.976E-11	9.892E-23

detector responses, protection factors, and reduction factors for response function 1

mash 46n/23g group flat response

parameter	value	fsd
detector 1	3.028E-11	.031
detector 2	3.688E-12	.068
detector 3	8.995E-17	.685
detector 4	9.455E-13	.113
detector 5	4.634E-12	.058
detector 6	9.456E-13	.113
detector 7	3.396E-11	.029
ff n flux	5.737D-11	
ff g flux	2.976D-11	
ff t flux	8.713D-11	
ff n dose	5.737D-11	
ff g dose	2.976D-11	
ff t dose	8.713D-11	

npf 1.689D+00

gpf 3.147D+01

tpf 2.496D+00

nrf 1.895D+00

grf 6.422D+00

trf 2.496D+00

detector responses, protection factors, and reduction factors for response function 2

mash 46n/23g group free-in-air tissue kerma response (gy.cm2/n.g)

parameter	value	fsd
detector 1	2.603E-22	.043
detector 2	2.318E-23	.050

detector 3 4.692E-28 .568
 detector 4 6.161E-24 .100
 detector 5 2.934E-23 .043
 detector 6 6.161E-24 .100
 detector 7 2.835E-22 .040

ff n flux 5.737D-11
 ff g flux 2.976D-11
 ff t flux 8.713D-11
 ff n dose 3.856D-22
 ff g dose 9.892D-23
 ff t dose 4.845D-22

npf 1.360D+00
 gpf 1.606D+01
 tpf 1.673D+00
 nrf 1.481D+00
 grf 3.372D+00

trf 1.673D+00
 neutron fluence spectrum at the detector location
 for case no. 1 orientation angle= .000 deg. range= 4.0000E+04

neutron group	upper energy	neutron fluence	fsd
1	1.964E+07	3.190D-18	.555
2	1.690E+07	9.145D-19	.543
3	1.492E+07	8.246D-17	.575
4	1.419E+07	2.560D-17	.405
5	1.384E+07	3.225D-17	.480
6	1.252E+07	7.591D-17	.881
7	1.221E+07	7.570D-17	.582

40	2.754E+02	8.959D-13	.105
41	1.013E+02	1.018D-12	.094
42	2.902E+01	7.538D-13	.092
43	1.068E+01	8.459D-13	.074
44	3.059E+00	4.589D-13	.119
45	1.125E+00	2.562D-13	.113
46	4.140E-01	3.923D-14	.106
total	1.000E-05	3.028D-11	

gamma fluence spectrum at the detector location
 for case no. 1 orientation angle= .000 deg. range= 4.0000E+04

gamma group	upper energy	gamma fluence	fsd
-------------	--------------	---------------	-----

Figure 10-3. (continued)

1 2.00E+07 3.267D-18 .374
 2 1.40E+07 2.965D-17 .570
 3 1.200E+07 4.114D-15 .296
 4 1.000E+07 2.315D-14 .179
 5 8.000E+06 3.328D-13 .103
 6 7.000E+06 8.937D-14 .139

18 1.500E+05 1.883D-13 .246
 19 1.000E+05 5.820D-14 .303
 20 7.000E+04 2.448D-15 .644
 21 4.500E+04 0.000D+00 .000
 22 3.000E+04 0.000D+00 .000
 23 2.000E+04 0.000D+00 .000
 total 1.000E+04 4.634D-12

neutron dose spectrum at the detector location for response function 2
 for case no. 1 orientation angle= .000 deg. range= 4.0000E+04

neutron group	upper energy	neutron dose	fsd
1	1.964E+07	2.349D-28	.555
2	1.690E+07	6.443D-29	.543
3	1.492E+07	5.656D-27	.575
4	1.419E+07	1.727D-27	.405
5	1.384E+07	2.134D-27	.480
6	1.252E+07	4.844D-27	.881
7	1.221E+07	4.796D-27	.582

gamma group	upper energy	gamma dose	fsd
40	2.754E+02	1.858D-26	.105
41	1.013E+02	1.056D-26	.094
42	2.902E+01	7.029D-27	.092
43	1.068E+01	1.149D-26	.074
44	3.059E+00	1.049D-26	.119
45	1.125E+00	9.547D-27	.113
46	4.140E-01	5.065D-27	.106
total	1.000E-05	2.603D-22	

gamma dose spectrum at the detector location for response function 2
 for case no. 1 orientation angle= .000 deg. range= 4.0000E+04

gamma group	upper energy	gamma dose	fsd
1	2.000E+07	1.311D-28	.374
2	1.400E+07	9.417D-28	.570
3	1.200E+07	1.136D-25	.296
4	1.000E+07	5.444D-25	.179
5	8.000E+06	6.825D-24	.103
6	7.000E+06	1.654D-24	.139

18	1.500E+05	9.974D-26	.246
19	1.000E+05	2.026D-26	.303
20	7.000E+04	7.667D-28	.644
21	4.500E+04	0.000D+00	.000


```

22 3.000E+04 0.000D+00 .000
23 2.000E+04 0.000D+00 .000
total 1.000E+04 2.934D-23
dort free field neutron fluence and dose spectra for response function 2
for case no. 2 orientation angle= 90.000 deg. range= 4.0000E+04

```

```

***** Case no. 1 sequence of data repeated for Case no. 2

```

```

dort free field neutron fluence and dose spectra for response function 2
for case no. 3 orientation angle= 180.000 deg. range= 4.0000E+04

```

```

***** Case no. 1 sequence of data repeated for Case no. 3

```

```

dort free field neutron fluence and dose spectra for response function 2
for case no. 4 orientation angle= 270.000 deg. range= 4.0000E+04

```

```

***** Case no. 1 sequence of data repeated for Case no. 4

```

**11.0 DRC3 - A CODE WITH SPECIALIZED APPLICATIONS FOR COUPLING
LOCALIZED MONTE CARLO ADJOINT CALCULATIONS WITH FLUENCES
FROM THREE-DIMENSIONAL X-Y-Z TORT DISCRETE ORDINATES
AIR-OVER-GROUND CALCULATIONS**

[Section to be added in a later version of the MASH code system]

APPENDIX A

FIDO INPUT

FIDO INPUT

The FIDO input method is especially devised to allow the entering or modifying of large data arrays with minimum effort. Special advantage is taken of patterns of repetition or symmetry wherever possible. The FIDO system was patterned after the input method used with the FLOCO coding system at Los Alamos and was first applied by Atomics International to the DTF-II¹ code. Since that time, numerous features requested by users have been added, a free-field option has been developed, and the application of FIDO has spread to innumerable codes.

The data are entered in units called "arrays". An array comprises a group of contiguous storage locations which are to be filled with data at one time. These arrays usually correspond on a one-to-one basis with FORTRAN arrays used in the program. A group of one or more arrays read with a single call to the FIDO package comprises a "block". A special delimiter is required to signify the end of each block. Arrays within a block may be read in any order with respect to each other, but an array belonging to one block must not be shifted to another. The same array can be entered repeatedly within the same block. For example, an array can be filled with zero using a special option, and then a few scattered locations could be changed by reading in a new set of data for that array. Some arrays can be omitted if no entries to that array are required. If no entries to any of the arrays in a block are required, but the condition requiring the block is met, the delimiter alone satisfies the input requirement. Three major types of input are available: free-field input, fixed-field input, and user-field input. Each field includes up to three subfields. Each array is identified by an "*array originator field*" having two subfields:

- Subfield 1: An integer *array identifier* signals the identity of the array to follow.
- Subfield 2: An *array type indicator*, used as follows:
 - "\$\$" free-field integer array
 - "**" free-field real array
 - "\$" fixed-field integer array
 - "*" fixed-field real array
 - "U" user-field, format to be read in
 - "V" user-field, previous format to be used

These subfields are written together, without blanks. Data are then placed in successive *data fields* until the required number of entries has been accounted for.

In entering data, it is convenient to think of an "index" or "pointer" which is under control of the user, and which specifies the position in the array into which the next data entry is to go. The pointer is always positioned at the first array location by entering the array originator field. The pointer subsequently moves according to the data operator chosen.

Free-field input allows an arbitrary number of fields to be entered in columns 1-72, with fields separated by one or more blanks. A field must begin and end in the same record. In general, a data field has up to three fields:

- Subfield 1: The *data numerator*, N_1 , an integer.
- Subfield 2: The *data operator*, N_2 , a character.
- Subfield 3: The *data entry*, N_3 , an integer or real number.

If subfields 1 and 2 are both used in a field, they must not be separated by blanks. Blanks may precede subfield 3, however. All entries following a "/" in a given record are ignored.

Single data entries use only N_3 , which may be entered with or without a decimal point. The type (integer/real) will be determined by the previous array identifier:

```
1$$ 1 2 3 /enter integers 1,2,3
2** 1. 1.1 2 /enter reals 1.0,1.1,2.0
```

An exponent field may be added, with or without the "E" identifier. No imbedded blanks within the subfield are allowed. The subfield must have no more than nine columns, including the decimal but not including the exponent field. The pointer is advanced by one for each entry:

```
                2** 1.E0 .11+1 200-2 /same entries as above
                3** 1234.5678E-3 /8 columns + decimal
BUT NOT        3** 1.23456789 /too many columns
AND NOT        3** 0.0E6 /produces wrong results
```

Multiple data entries use N_2 and (except the "F" operator) N_1 together with N_3 to enter several items with a single field. The type of operation is indicated by N_2 .

"R" indicates that data entry N_3 is to be repeated N_1 times. The pointer is advanced by N_1 .

"I" indicates linear interpolation. The data numerator, N_1 , indicates the number of interpolated points to be supplied. The data entry N_3 is entered, followed by N_1 interpolated entries equally spaced between that value and the value in the third subfield of the next field. The next field may be a single- or multiple-data entry. The pointer is advanced by $N_1 + 1$. The field following an "I" entry is then processed normally, according to its own data operator. The "I" entry is especially valuable for specifying a spatial mesh. In integer arrays, interpolated values will be rounded to the nearest integer.

"L" indicates logarithmic interpolation. The effect is the same as that of "I" except that the resulting data are evenly separated in log-space. This is obviously limited to positive real numbers.

"F" fills the remainder of the array with N_3 . N_1 is not used. For example, the following are equivalent ways of filling an 8-entry array:

```
2$$ 1 2 3 4 6 6 8 8
2$$ 2I1 4 2R6 F8 /same as above
```

Sequence data entries allow entries to be patterned after data entered by previous fields or previously existing in storage. Fields N_1 , N_2 , and N_3 are used, except that if N_1 is omitted, it is taken to be one.

"Q" is used to repeat sequences of numbers without modification. The length of the sequence is given by the third subfield, N_3 . The sequence of N_3 previous entries is to be repeated N_1 times. The pointer is advanced by $N_1 * N_3$. This feature is especially valuable in specifying matrices with repeated or symmetrical columns or rows.

"G" has the same effect as "Q" except that the sign of each entry of the sequence is changed each time it is entered.

"N" has the same effect as "Q," except that the order of the sequence is reversed each time it is entered.

"M" has the same effect as "Q," except that both the sign and the order of the sequence are reversed each time it is entered.

Options Q, G, and M are valuable in entering directional quadrature sets. As examples:

81**	1 2 3 1Q3	/1,2,3,1,2,3
82**	-3 -2 -1 M3	/-3,-2,-1,1,2,3
83**	3R-2 G3	/-2,-2,-2,2,2,2

Zero data entries use subfields N_1 and N_2 .

"Z" sets the next N_1 entries to zero. The pointer is advanced by N_1 . As an example:

1\$\$ 3Z 1 2 /0,0,0,1,2

Pointer-movement data entries move the pointer without changing the data array. Subfields N_1 , N_3 , or neither may be required.

"S" indicates that the pointer is to skip forward over N_1 positions, leaving those array positions unchanged.

"B" moves the pointer backward N_1 positions.

"A" moves the pointer to the position N_3 .

"E" skips over the remainder of the array. The array length criterion is satisfied by an "E," unless too many entries have been specified. No more entries to an array may be given following an "E," except that data entry may be restarted with an "A."

For example, given the following sequence of entries, comments indicate the result of reading an array of length 8:

1\$\$	1 2 3 4 5 6 E	/E terminates the array, leaving items 7 and 8 unchanged
1\$\$	2 1S 4 A7 7 8	/now we have 2,2,4,4,5,6,7,8
1\$\$	2I 1 4 1B F8	/now we have 1,2,3,8,8,8,8,8

Edit fields control printing within the FIDO subroutines.

"C" causes the position of the last array item entered to be printed. This is the position of the pointer, less 1. The pointer is not moved.

"O" causes the print trigger to be turned on. The trigger is originally off. When the trigger is on, each card image is listed as it is read.

"P" causes the print trigger to be turned off.

"/" occurring in column 1 causes the entire record to be ignored as input, but to be printed as a comment in the output stream.

A *block termination field* consists of a field having only "T" in the second subfield.

The *reading of data to an array* is terminated when a new array originator field is supplied, or when the block is terminated by a block termination field. If an incorrect number of positions has been filled, an error edit is given, and a flag is set which will later abort execution of the problem. FIDO then continues with the next array if an array originator was read. The new array originator need not begin a new record. Otherwise, FIDO returns control to the calling program. For example:

```
1$$ 1 2 3  2** FO T
```

User-field input allows the user to specify the input format. If "U" is specified as the array-type indicator, the FORTRAN format to be used must be supplied in columns 1-72 of the next record. The format must be enclosed by parentheses. The data for the entire array must follow on successive records. The rules of ordinary FORTRAN input as to exponents, blanks, etc., apply. If the array data do not fill the last record, the remainder of the record must be left blank. The user must insure that his format specifies the correct type of data, i.e., real or integer.

"V" has the same effect as "U" except that the format read in the last preceding "U" array is used.

For example, for an array of 4 entries:

```
10U  
(6I2)  
1 2 3 4  
11V  
4 3 2 1
```

would enter integers 1,2,3,4 into the 10th array and 4,3,2,1 into the 11th.

Fixed-field input uses 1 to 6 fields per input record, with fixed, 12-column fields. It is thoroughly described in the DOT IV document.² Because it has been almost entirely replaced by the free-field format, its description is not repeated here.

REFERENCES

1. W. W. Engle, Jr., M. A. Boling, and B. W. Colston, "DTF-II, A One-Dimensional, Multigroup Neutron Transport Program," NAA-SR-10951 (March 1966).
2. W. A. Rhoades, D. B. Simpson, R. L. Childs, and W. W. Engle, Jr., "The DOT-IV Two-Dimensional Discrete Ordinates Transport Code with Space-Dependent Mesh and Quadrature," ORNL/TM-6529 (January 1979).

APPENDIX B
IN-GROUP ENERGY BIASING

IN-GROUP ENERGY BIASING*

INTRODUCTION

This appendix describes the in-group energy biasing methodology¹ developed for the adjoint MORSE² calculation utilized in MASH. In-group energy biasing is a methodology developed by W. Scott of SAIC to adjust for irregularities observed in adjoint Monte Carlo analyses in thick media where the weights of adjoint particles could, in undergoing multiple scattering events, become very large. Further development of the methodology, discussed herein, suggests that in-group energy bias might have more-general use than initially expected. The in-group biasing procedure was first implemented in the MIFT2¹ version of the VCS^{3,4} MORSE code. The in-group biasing procedure has since been implemented in the MASH version of the MORSE code. The bulk of this appendix was extracted from the MIFT2 document¹ and has been included in this manual for completeness.

In-group energy biasing (or simply in-group biasing or in-group bias) is easy to use. Unlike other Monte Carlo biasing methods, in-group biasing does not require that the user set up and input, based on his judgment, arrays of data to improve the efficiency of the Monte Carlo calculation. This means that a person less skilled in adjoint Monte Carlo can often successfully use MASH or adjoint MORSE, since use of in-group bias requires only the setting of a switch in MASH. Success in the use of the other biasing methods generally requires considerable adjoint Monte Carlo experience.

Based on results obtained with the MIFT2 and MASH MORSE codes, in-group energy bias appears to generally improve both the answer and the statistics of the calculation. Based on theory, it may be expected that the largest gains from the use of in-group bias occur for fairly thick problems. However, improvements for thinner problems have been seen as well. Based on both the theory and the results of sample cases reported herein, it might be suggested that in-group bias always be used for adjoint Monte Carlo. However, in recognition that users may at times prefer not to use in-group bias or may wish to compare results obtained with and without the use of in-group bias, the methodology has been implemented with a switch so that its use is optional.

This appendix is divided into 6 subsections. Following this introduction section is a background section which traces the short history of the development of the in-group biasing methodology. The next section gives a theoretical basis for in-group bias, followed by a section describing the implementation of the in-group bias methodology into the MASH MORSE code. A section which discusses some comparisons of the results of analyses performed with and without in-group bias with each other and with experimental data, where available, follows. Finally, a list of references pertaining to the discussion given in this appendix is presented.

* J. A. Stoddard, S. D. Egbert, and W. D. Scott, Jr., "The Vehicle Code System with In-Group Energy Bias and GIFT5 Geometry," DNA-TR-87-23, Science Applications International Corporation, (January 1987).

BACKGROUND

It has long been recognized that for certain problems adjoint MORSE and MASH are very inefficient at obtaining adequate statistical variances in reasonable run times especially when compared to the efficiency of forward MORSE calculations. In a 1979 SAIC study⁵ for the BRL it was recognized that the problem stemmed from a poorly biased energy random walk that occurred in adjoint MORSE whenever the non-absorption probability (PNAB) was much greater than 1.0. At that time it was suggested that a modified adjoint scattering technique, referred to as "in-group energy biasing", would be significantly more efficient. The defining feature of in-group energy biasing is that for all but the last group, a particle's weight only changes when it scatters to a new group. If the particle stays in the same group (in-group scattering), its weight does not change. Thus, when an adjoint particle has a non-absorption probability greater than 1.0, its weight will not increase so long as it scatters in the same group. When it finally upscatters to a new group, its weight will be increased by a fixed amount that is a function only of the cross sections and not of how many times the particle scattered in the same group. With standard adjoint MORSE, such a particle would have its weight increased by PNAB each time that it scattered so that its final weight upon upscatter would depend upon how many in-group scatterings that it had.

In a 1981 study⁶ for the Wehrwissenschaftliche Dienststelle der Bundeswehr für ABC-Schutz (WWD) Laboratory in the Federal Republic of Germany, SAIC implemented the in-group energy biasing scheme into adjoint MORSE and demonstrated an increase in efficiency of factors of 4 to 5 over standard adjoint MORSE for a 10-cm-thick steel sphere. In that study in-group energy biasing was used for all energy groups.

In a recent effort for the U. S. Army Ballistic Research Laboratory (BRL), the in-group bias scheme was implemented in the BRL version of VCS, and some comparisons of its efficiency were made for other steel and polyethylene configurations. Also, theoretical derivations were made which indicated that in-group energy biasing should always be preferable to the standard MORSE scattering treatment in either forward or adjoint MORSE regardless of the value of the non-absorption probability PNAB.

In this effort a number of modifications were made to the in-group bias coding to improve its efficiency and clarity. More important, some additional test cases were run which further demonstrated the advantages of using in-group bias.

THEORETICAL BASIS FOR IN-GROUP ENERGY BIASING

The theoretical basis for in-group energy biasing is derived by comparing the analytic sample variance of the three-group infinite medium random walk under a variety of possible biasing schemes. Similar conclusions can be reached in two groups with considerably less algebra but with less generality. The procedure is to examine the Markov chains of all possible combinations and permutations of scatterings in three groups and to show that the scattering estimator scores in the random walk sum to the theoretical solution. The corresponding sample variance is then derived, and comparisons are made between the in-group and standard sampling schemes.

Two very important concepts which are stressed in this paper are the "fair game rule" and "particle weightings". The "fair game rule" is descriptive of the Monte Carlo treatment of

collisions. If a "fair game" is played in simulating the collision, forward or adjoint, a valid result should be obtained. Particle weightings offer some latitude in playing this "fair game", since tradeoffs can be made between probabilities and particle worth.

A historical example is appropriate here. Original Monte Carlo codes treated absorption events by halting the random walk for a particle whenever sampling indicated that an absorption event had occurred. Later it was recognized that it was more efficient to carry a particle weight and to treat absorption by reducing the weight by the non-absorption probability at each scatter. Particle histories were then terminated by Russian roulette whenever weights dropped below predetermined cutoffs. This non-absorption treatment avoided losing important histories just before they were about to score. In this example, a "fair game" was played by offsetting the probability of what happened at a scattering event with an appropriate change of particle weight. This concept of adjusting particle weights, within the fair game rule, to improve Monte Carlo statistics is the basis of Monte Carlo biasing schemes. More will be said about the fair game rule in the infinite medium problem described below.

Markov Chain Analysis of the Forward Three-Group Infinite Medium Problem

Consider the total dose deposited in an infinite medium due to a source of particles in three energy groups. The source is described by three probabilities S_1 , S_2 , and S_3 of beginning particles in the three groups. When the flux in each group is known, the dose is the inner product with the response function (or flux to dose conversion factor) R_1 , R_2 , and R_3 . The scattering properties of the medium are described by total cross sections in each group σ_1 , σ_2 , and σ_3 , and the downscatter cross section matrix,

$$\begin{pmatrix} \sigma_{11} & 0 & 0 \\ \sigma_{12} & \sigma_{22} & 0 \\ \sigma_{13} & \sigma_{23} & \sigma_{33} \end{pmatrix}$$

where σ_{ij} is the cross section for scattering from group i to group j . All upscatter cross sections are assumed to be zero. This problem can be solved directly without reference to Monte Carlo or Markov chains by equating the collision density in each group (the product of the flux Φ_i and the total cross section σ_i to the source in group i) from the original source S_i plus the scattering source as shown in Equation (1).

$$\begin{pmatrix} \sigma_1 \phi_1 \\ \sigma_2 \phi_2 \\ \sigma_3 \phi_3 \end{pmatrix} = \begin{pmatrix} S_1 \\ S_2 \\ S_3 \end{pmatrix} + \begin{pmatrix} \sigma_{11} & 0 & 0 \\ \sigma_{12} & \sigma_{22} & 0 \\ \sigma_{13} & \sigma_{23} & \sigma_{33} \end{pmatrix} \begin{pmatrix} \phi_1 \\ \phi_2 \\ \phi_3 \end{pmatrix} \quad (1)$$

Collision Density Original Source

This equation can be solved directly for the flux in each group, and the dose can be obtained by an inner product with the response,

$$\lambda = \sum_i R_i \phi_i \quad (2)$$

so that

$$\lambda = (R_1, R_2, R_3) \begin{pmatrix} \sigma_1 - \sigma_{11} & 0 & 0 \\ -\sigma_{12} & \sigma_2 - \sigma_{22} & 0 \\ -\sigma_{13} & -\sigma_{23} & \sigma_3 - \sigma_{33} \end{pmatrix}^{-1} \begin{pmatrix} S_1 \\ S_2 \\ S_3 \end{pmatrix} \quad (3)$$

The solution of the above equation is

$$\begin{aligned} \lambda = & \frac{R_1 S_1}{\sigma_1 - \sigma_{11}} + \frac{S_1 R_2 \sigma_{12}}{(\sigma_1 - \sigma_{11})(\sigma_2 - \sigma_{22})} \\ & + \frac{S_1 R_3 \sigma_{13}}{(\sigma_1 - \sigma_{11})(\sigma_3 - \sigma_{33})} + \frac{S_1 R_3 \sigma_{12} \sigma_{23}}{(\sigma_1 - \sigma_{11})(\sigma_2 - \sigma_{22})(\sigma_3 - \sigma_{33})} \\ & + \frac{S_2 R_2}{\sigma_2 - \sigma_{22}} + \frac{S_2 R_3 \sigma_{23}}{(\sigma_2 - \sigma_{22})(\sigma_3 - \sigma_{33})} + \frac{(S_3 R_3)}{\sigma_3 - \sigma_{33}} \end{aligned} \quad (4)$$

Notice that the solution for the dose contains seven terms which represent the seven possible means of scattering from a source group to a response group. The first, fifth, and seventh terms result from particles that began and scored in the same group. Each of these particles may have had zero to an infinite number of in-group scatterings. The second, third and sixth terms are the doses from particles that began in one group, had zero to many in-group scatterings, had one transition scattering to a new group and finally had zero to many in-group scatterings in the final group. The fourth term is the dose for particles that began in group one, scattered to group two, and then scattered to group three with any number of in-group scatterings between.

This same result can be derived by Monte Carlo theory considering the probabilities and weight changes of all possible scatterings. In standard forward MORSE the random walk is set up as follows: First, a source group is sampled and the particle weight is set to 1.0. The collision site (which does not matter in the infinite medium problem) is determined by sampling an exponential. The probability of absorption is treated by reducing the particle weight (multiplying the previous weight by the non-absorption probability). Then the probability of scatter to each group is sampled, and the next track proceeds in the new group. At each scattering a score is made equal to the particle weight before the collision times the response function divided by the total cross section.

When this score is made for each scatter, it is called a real scattering estimator. The non-absorption probability (PNAB in MORSE but called W here) is equal to the scattering cross section divided by the total cross section. For group one this is

$$W_1 = \frac{\sigma_{11} + \sigma_{12} + \sigma_{13}}{\sigma_1} = \frac{\sigma_{1s}}{\sigma_1} \quad (5)$$

Likewise, the group transfer probability is

$$P_{ij} = \frac{\sigma_{ij}}{\sum_j \sigma_{ij}} = \frac{\sigma_{ij}}{\sigma_{is}} \quad (6)$$

Thus, if a particle starts and continues to scatter in group one, its contribution to the dose is

$$\begin{aligned} \lambda_{11} &= \frac{S_1 R_1}{\sigma_1} \sum_{n=0}^{\infty} (W_1 P_{11})^n = \frac{S_1 R_1}{\sigma_1} \sum_{n=0}^{\infty} \left(\frac{\sigma_{1s}}{\sigma_1} \frac{\sigma_{11}}{\sigma_{1s}} \right)^n \\ &= \frac{S_1 R_1}{\sigma_1} \frac{1}{1 - \frac{\sigma_{11}}{\sigma_1}} = \frac{S_1 R_1}{\sigma_1 - \sigma_{11}} \end{aligned} \quad (7)$$

Notice that this term is identical to the first term in Equation (4). In a similar manner all combinations of possible sources and scatters can be shown to be equivalent to terms of Equation (4). As another example, particles that begin in group 1, transition to group 2 and finally scatter to group 3 correspond to the fourth term of Equation (4) as follows:

$$\begin{aligned} \lambda_{123} &= \frac{S_1 R_3}{\sigma_3} \left[\sum_{n=0}^{\infty} (W_1 P_{11})^n \right] W_1 P_{12} \left[\sum_{n=0}^{\infty} (W_2 P_{22})^n \right] W_2 P_{23} \left[\sum_{n=0}^{\infty} (W_3 P_{33})^n \right] \\ &= \frac{S_1 R_3 \sigma_{12} \sigma_{23}}{(\sigma_1 - \sigma_{11})(\sigma_2 - \sigma_{22})(\sigma_3 - \sigma_{33})} \end{aligned} \quad (8)$$

Thus, as expected, the Markov chain analysis of the MORSE random walk for three groups agrees identically with the analytic three-group solution given in Equation (4).

In addition to deriving the dose, the three-group problem can be analyzed for the sample variance of real scattering estimator procedure. The sample variance V is derived by summing the squares of all scores times the probability of making each score. Thus, the

sample variance of particles that begin in group one and score in group one, as in Equation (7) for the standard MORSE scattering scheme, is

$$V_{11} = \frac{S_1 R_1^2}{\sigma_1^2} \sum_{n=0}^{\infty} \left(\frac{\sigma_{1s}^2 \sigma_{11}}{\sigma_1^2 \sigma_{1s}} \right)^n = \frac{S_1 R_1^2}{\sigma_1^2 \left(1 - \frac{\sigma_{11} \sigma_{1s}}{\sigma_1^2} \right)} \quad (9)$$

$$= \frac{S_1 R_1^2}{\sigma_1^2 - \sigma_{11} \sigma_{1s}}$$

Notice that all factors that represent either scores or particle weights are squared while factors representing probabilities are not squared. In this manner all seven terms of the forward MORSE sample variance may be written:

$$V_{11} = \frac{S_1 R_1^2}{\sigma_1^2 - \sigma_{11} \sigma_{1s}} \quad V_{12} = \frac{S_1 R_2^2 \sigma_{12} \sigma_{1s}}{(\sigma_1^2 - \sigma_{11} \sigma_{1s})(\sigma_2^2 - \sigma_{22} \sigma_{2s})}$$

$$V_{13} = \frac{S_1 R_3^2 \sigma_{13} \sigma_{1s}}{(\sigma_1^2 - \sigma_{11} \sigma_{1s})(\sigma_3^2 - \sigma_{33} \sigma_{3s})}$$

$$V_{123} = \frac{S_1 R_3^2 \sigma_{12} \sigma_{1s} \sigma_{23} \sigma_{2s}}{(\sigma_1^2 - \sigma_{11} \sigma_{1s})(\sigma_2^2 - \sigma_{22} \sigma_{2s})(\sigma_3^2 - \sigma_{33}^2)} \quad (10)$$

$$V_{22} = \frac{S_2 R_2^2}{\sigma_2^2 - \sigma_{22} \sigma_{2s}} \quad V_{23} = \frac{S_2 R_3^2 \sigma_{23} \sigma_{2s}}{(\sigma_2^2 - \sigma_{22} \sigma_{2s})(\sigma_3^2 - \sigma_{33}^2)}$$

$$V_{33} = \frac{S_3 R_3^2}{(\sigma_3^2 - \sigma_{33}^2)}$$

All terms have the same form for each combination of transitions, and the denominator terms of $\sigma_i^2 - \sigma_{ii} \sigma_{is}$ appear in each case. In group 3 it reduces to $\sigma_{23} - \sigma_{33}^*$ because the scattering cross section is equivalent to the in-group cross section. Sometimes in forward MORSE the scattering cross section is greater than the total cross section. This can occur when multiplicity is included as a pseudo-scattering process such as with (n,2n) reactions or in gamma ray pair production. If the scattering cross section is sufficiently larger than the total cross section so that $\sigma_i^2 - \sigma_{ii} \sigma_{is}$ is near-zero, these terms of the variance become large and the calculation may not converge. When this occurs, longer run times may fail to improve MORSE statistics. Also, answers may vary widely, with results for cases with the best statistics tending to be deceptively low.

It is important to note that the non-absorption probability and group transfer probabilities in the problem solution, λ , always occur in product form, i.e., $W_i P_{ij}$. This suggests that the particle weights and transfer probabilities can each be adjusted in biasing schemes provided that the product remains unchanged. Since the answer λ depends only on the product, the

It is important to note that the non-absorption probability and group transfer probabilities in the problem solution, λ , always occur in product form, i.e., $W_i P_{ij}$. This suggests that the particle weights and transfer probabilities can each be adjusted in biasing schemes provided that the product remains unchanged. Since the answer λ depends only on the product, the answer will not be changed. The variance, however, is dependent on the separate W_i and P_{ij} terms; thus there is a potential in biasing to improve the variance.

Biasing in forward Monte Carlo calculations by modification of the W_i and P_{ij} terms, while retaining a constant product, is a powerful tool in improving Monte Carlo statistics, but that is not the only use of the concept. As will be seen, the concept carries over into adjoint random walks. First the product sufficiency, which is one part of the "fair game" rule, justifies the current treatment of group transfers in adjoint Monte Carlo simulations. Second, it can be used for biasing adjoint Monte Carlo analyses as well as forward calculations.

Adjoint Three-Group Analysis

An especially interesting feature of the MORSE Monte Carlo code is that the same scattering routines are used to track both forward and adjoint particles by using the transpose of the scattering cross section matrix for adjoint transport. In the adjoint, the non-absorption factor (PNAB) involves a sum of the scattering cross sections for those groups from which scattering could have come. In MORSE, the adjoint energy group indexes are reversed so that the highest energy particles have the highest group numbers. However, the same forward cross section notation is kept here to facilitate comparison with the forward walk. Keeping the same forward cross section group number notation, the adjoint scattering cross section for group three becomes

$$\sigma_{3s}^* = \sigma_{33} + \sigma_{23} + \sigma_{13} \quad (11)$$

Since σ_{23} and σ_{13} are not a part of the group three total cross section σ_3 , this adjoint scattering sum can be much different from the total cross section. For broad neutron groups in the inelastic level regime where there can be many higher energy groups that scatter into it, the adjoint scattering sum can be much greater than the total cross section. The adjoint non-absorption factor and the scattering probabilities then become

$$W_j = \frac{\sum_i \sigma_{ij}}{\sigma_j} = \frac{\sigma_{js}^*}{\sigma_j} \quad (12)$$

and

$$P_{ij} = \frac{\sigma_{ij}}{\sum_i \sigma_{ij}} = \frac{\sigma_{ij}}{\sigma_{js}^*} \quad (13)$$

where the asterisk indicates the adjoint summation of the scattering cross section rather than the forward summation. Note that unlike the forward scattering cross section, the adjoint

scattering cross section is not a physical quantity. In fact it depends more upon the energy group structure than the physical scattering process.

Clearly there is no direct physical basis, as with forward Monte Carlo Equations (5) and (6), for using the above weight changes and transfer probabilities for adjoint Monte Carlo. However, the product of the $W_j P_{ij}$ in Equations (12) and (13) is equivalent to that for the forward, and the adjoint random walk gets the same answer as the forward walk. In this case, the σ_{js}^* has no physical meaning, but it has the advantages of giving transfer probabilities P_{ij} which automatically sum to 1.0 and of following the adjoint calculation format in which the transpose of the cross section matrix is used. However, as will be seen below, the non-physical nature of the adjoint scattering cross section (Equation 11) can cause accuracy problems in adjoint Monte Carlo.

Consider the three-group infinite medium Markov chain. As mentioned above, the adjoint random walk will get the same dose as the forward walk. However, the sample variance of the standard MORSE adjoint walk, although similar in form to the forward sample variance, is quite different. When the particle weights are squared and the probabilities are not squared, the non-physical adjoint scattering cross section σ_{js}^* does not cancel

$$W_j^2 P_{ij} = \frac{\sigma_{js}^2}{\sigma_j^2} \frac{\sigma_{ij}}{\sigma_{js}^*} = \frac{\sigma_{ij} \sigma_{js}^*}{\sigma_j^2} \quad (14)$$

and the seven terms of the standard adjoint sample variance become

$$\begin{aligned} V_{11} &= \frac{R_1 S_1^2}{\sigma_1^2 - \sigma_{11}^2} & V_{22} &= \frac{R_2 S_2^2}{\sigma_2^2 - \sigma_{22} \sigma_{2s}^*} & V_{33} &= \frac{R_3 S_3^2}{\sigma_3^2 - \sigma_{33} \sigma_{3s}^*} \\ V_{21} &= \frac{R_2 S_1^2 \sigma_{12} \sigma_{2s}^*}{(\sigma_2^2 - \sigma_{22} \sigma_{2s}^*)(\sigma_1^2 - \sigma_{11}^2)} & V_{31} &= \frac{R_3 S_1^2 \sigma_{13} \sigma_{3s}^*}{(\sigma_3^2 - \sigma_{33} \sigma_{3s}^*)(\sigma_1^2 - \sigma_{11}^2)} \\ V_{32} &= \frac{R_3 S_2^2 \sigma_{23} \sigma_{3s}^*}{(\sigma_3^2 - \sigma_{33} \sigma_{3s}^*)(\sigma_2^2 - \sigma_{22} \sigma_{2s}^*)} \\ V_{321} &= \frac{R_3 S_1^2 \sigma_{23} \sigma_{3s}^* \sigma_{12} \sigma_{2s}^*}{(\sigma_3^2 - \sigma_{33} \sigma_{3s}^*)(\sigma_2^2 - \sigma_{22} \sigma_{2s}^*)(\sigma_1^2 - \sigma_{11}^2)} \end{aligned} \quad (15)$$

The form of these terms is very similar to the forward sample variance in Equation (10) including terms like $\sigma_i^2 - \sigma_{ii} \sigma_{is}^*$ in the denominators. Because of the physical nature of the forward scattering cross section, the forward MORSE random walk is nearly always well behaved. However, since the adjoint scattering cross section σ_{js}^* is often much greater than the total cross section σ_j , these terms can prevent the random walk from converging. In fact in the DLC-31 Data Library Collection⁷, adjoint iron cross sections have four groups (all in the vicinity of 1 MeV neutrons) where

$$\sigma_{ii}\sigma_{is}^* \geq \sigma_i^2 \quad (16)$$

Thus, infinite medium adjoint random walk for the iron with the DLC-31 cross sections will not converge. More generally, this occurs in adjoint MORSE whenever

$$P_{ii}PNAB_i \geq 1.0 \quad (17)$$

It is perhaps fortunate that the seriousness of this problem is not always observed. For realistic problems not involving deep penetration in thick media, reasonable answers are usually obtained, although with reduced efficiency.

In-Group Energy Bias Analysis

The major objective of the in-group biasing scheme is to eliminate the instability in the variance for random walks, i.e., to eliminate the $\sigma_i^2 - \sigma_{ii}\sigma_{is}^*$ terms which could be zero or negative for physically realistic cross section sets. Although not obvious from the foregoing, this is equivalent to eliminating the problem in which the weight of an adjoint particle can grow unbounded by many repeated in-group scatterings.

The approach is to utilize the fair game constraint in which the product $W_i P_{ij}$ is forced to remain constant while adjustments to certain W_i are made. Specifically, as mentioned in the background section, the weight of a particle undergoing in-group scattering is forced to remain unchanged. This "starting condition", along with the constant $W_i P_{ij}$ "fair game rule" and a couple of other physical requirements form a recursion-relation-like formulation which redefines all the W_i and P_{ij} . The result is the in-group bias formulation, the derivation and analysis of which are described below.

In the standard (not in-group biased) formulation, the weight change W_i was always equal to PNAB for group i . For in-group bias, this parameter is generalized to also have j dependence. Thus the fair game product rule becomes, utilizing Equations (12) and (13) (for the standard adjoint MORSE),

$$P_{ij}W_{ij} = \frac{\sigma_{ij}}{\sigma_j} \quad (18)$$

For in-group scattering for groups other than group 1, it was specified that there would be no weight change ($W = 1$); hence from Equation (18),

$$W_{jj} = 1.0 \quad \text{and} \quad P_{jj} = \frac{\sigma_{jj}}{\sigma_j} \quad (19)$$

for in-group scattering other than group 1. An exception is made for group 1, which, being the highest energy group, has no outscattering so that P_{11} must be 1.0. Thus from Equation (18) for group 1,

$$P_{11} = 1.0 \text{ and } W_{11} = \frac{\sigma_{11}}{\sigma_1} \quad (20)$$

The above expressions specify the P and W for in-group scattering. The out-of-group scattering P_{ij} and W_{ij} are specified by the physical requirement that the scattering probabilities must sum to 1.0 and by the desirability of having the other transfer probabilities be proportional to σ_{ij} . The result is

$$i \neq j, P_{ij} = \frac{\sigma_{ij}(\sigma_j - \sigma_{jj})}{\sigma_j(\sigma_{js}^* - \sigma_{jj})} \text{ and } W_{ij} = \frac{\sigma_{js}^* - \sigma_{jj}}{\sigma_j - \sigma_{jj}} \quad (21)$$

Thus, in three groups the adjoint in-group scattering and weight factors are specified as

$$P = \begin{pmatrix} \frac{\sigma_{33}}{\sigma_3} & 0 & 0 \\ \frac{\sigma_{23}(\sigma_3 - \sigma_{33})}{\sigma_3(\sigma_{23} + \sigma_{13})} & \frac{\sigma_{22}}{\sigma_2} & 0 \\ \frac{\sigma_{13}(\sigma_3 - \sigma_{33})}{\sigma_3(\sigma_{23} + \sigma_{13})} & \frac{\sigma_2 - \sigma_{22}}{\sigma_2} & 1 \end{pmatrix} \quad (22)$$

and

$$W = \begin{pmatrix} 1 & 0 & 0 \\ \frac{\sigma_{23} + \sigma_{13}}{\sigma_3 - \sigma_{33}} & 1 & 0 \\ \frac{\sigma_{23} + \sigma_{13}}{\sigma_3 - \sigma_{33}} & \frac{\sigma_{12}}{\sigma_2 - \sigma_{22}} & \frac{\sigma_{11}}{\sigma_1} \end{pmatrix} \quad (23)$$

From the probability and weight table the total dose can be derived just as in the standard adjoint case. As expected because the product of weight and probability is the same for both in-group and standard MORSE, the dose is the same (Equation 4). But the weight squared times the probability is different, making the in-group biased sample variance terms, given below, very different from the standard adjoint sample variance of Equation (15).

$$\begin{aligned}
 V_{11} &= \frac{R_1 S_1^2}{\sigma_1^2 - \sigma_{11}^2} & V_{22} &= \frac{R_2 S_2^2}{\sigma_2^2 - \sigma_{22} \sigma_2} & V_{33} &= \frac{R_3 S_3^2}{\sigma_3^2 - \sigma_{33} \sigma_3} \\
 V_{21} &= \frac{R_2 S_1^2 \sigma_{12}^2}{(\sigma_2 - \sigma_{22})^2 (\sigma_1^2 - \sigma_{11}^2)} & V_{31} &= \frac{R_3 S_1^2 \sigma_{13} (\sigma_{23} + \sigma_{13})}{(\sigma_3 - \sigma_{33})^2 (\sigma_1^2 - \sigma_{11}^2)} \\
 V_{32} &= \frac{R_3 S_2^2 \sigma_{23} (\sigma_{23} + \sigma_{13})}{(\sigma_3 - \sigma_{33})^2 (\sigma_2^2 - \sigma_{22} \sigma_2)} \\
 V_{321} &= \frac{R_3 S_1^2 \sigma_{23} (\sigma_{23} + \sigma_{13}) \sigma_{12}^2}{(\sigma_3 - \sigma_{33})^2 (\sigma_2 - \sigma_{22})^2 (\sigma_1^2 - \sigma_{11}^2)}
 \end{aligned} \tag{24}$$

In the above terms, all the denominators are positive, non-zero, and well behaved for physical cross sections. The possible infinite variance terms of the standard adjoint MORSE have been eliminated.

At this point the choice of no weight change on in-group scattering may seem somewhat arbitrary. In fact, this choice can be shown to be the optimum. When the in-group weight changes of 1.0 in the weight and probability tables (Equations 22 and 23) are set to variables, new tables are

$$W(x, y) = \begin{pmatrix} x & 0 & 0 \\ \frac{x(\sigma_{23} + \sigma_{13})}{x\sigma_3 - \sigma_{33}} & y & 0 \\ \frac{x(\sigma_{23} + \sigma_{13})}{x\sigma_3 - \sigma_{33}} & \frac{y\sigma_{12}}{y\sigma_2 - \sigma_{22}} & \frac{\sigma_{11}}{\sigma_1} \end{pmatrix} \tag{25}$$

and

$$P(x, y) = \begin{pmatrix} \frac{\sigma_{33}}{x\sigma_3} & 0 & 0 \\ \frac{\sigma_{23}(x\sigma_3 - \sigma_{33})}{x\sigma_3(\sigma_{23} + \sigma_{13})} & y & 0 \\ \frac{\sigma_{13}(x\sigma_{33} - \sigma_{33})}{x\sigma_3(\sigma_{23} + \sigma_{13})} & \frac{y\sigma_2 - \sigma_{22}}{y\sigma_2} & 1.0 \end{pmatrix} \quad (26)$$

When these probabilities are summed and multiplied by the weights squared over all seven transition possibilities, the terms all have the form of

$$\frac{x}{(x\sigma_3 - \sigma_{33})(\sigma_3 - x\sigma_{33})} \quad \text{or} \quad \frac{y}{(y\sigma_2 - \sigma_{22})(\sigma_2 - y\sigma_{22})} \quad (27)$$

The general features of the above functions are shown in Figure B-1. For the region $\sigma_{ii}/\sigma_i \leq x \leq \sigma_i/\sigma_{ii}$ of interest, the terms are minimized by a value of $x = 1.0$ regardless of the value of σ_i or σ_{ii} .

$$\frac{1}{(\sigma_3 - \sigma_{33})^2} \quad \text{or} \quad \frac{1}{(\sigma_2 - \sigma_{22})^2} \quad (28)$$

Thus, setting the in-group weight change factor to 1.0 appears to be an optimum in-group biasing scheme.

Having concluded that a weight change factor of 1.0 is optimum for the in-group biasing scheme, equivalent sample variance terms from standard adjoint and in-group adjoint MORSE (Equations 15 and 24) are now compared.

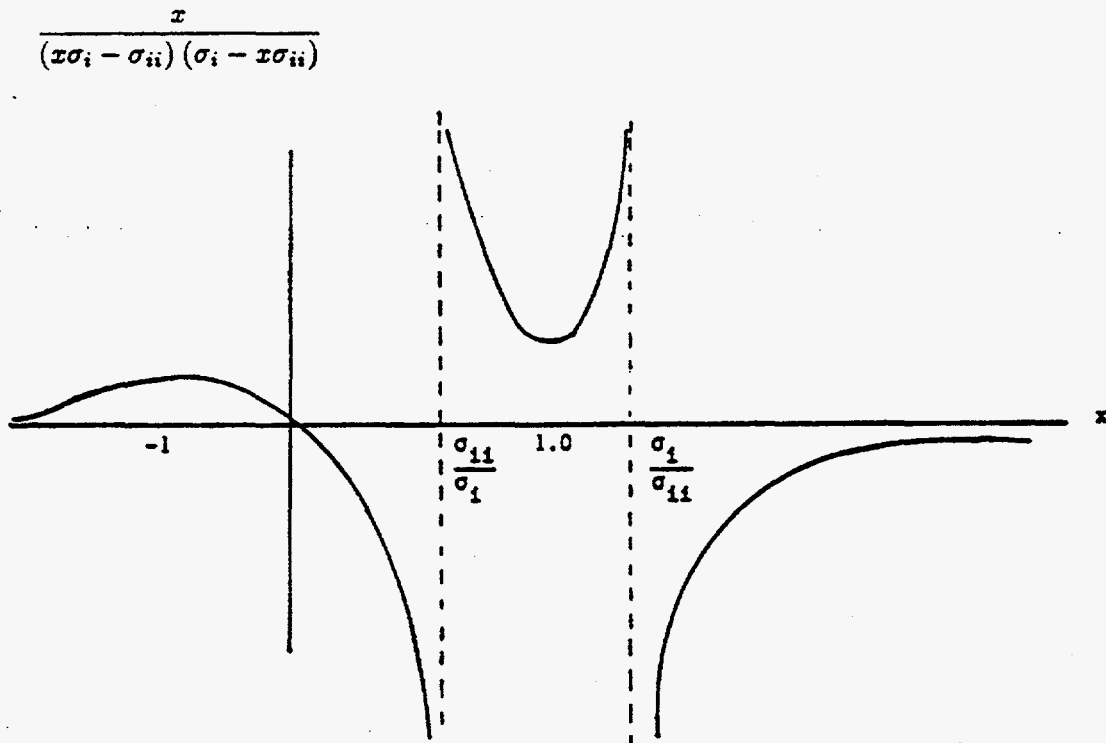


Figure B-1. Characteristics of functions in Equation (27).

Standard Adjoint

$$\frac{\sigma_{2s}^*}{\sigma_2^2 - \sigma_{22}\sigma_{2s}^*}$$

In-group Adjoint

$$\frac{\sigma_{12}}{(\sigma_2 - \sigma_{22})^2} = \frac{\sigma_{2s}^* - \sigma_{22}}{(\sigma_2 - \sigma_{22})^2} \quad (29)$$

or

$$\frac{\sigma_{3s}^*}{\sigma_3^2 - \sigma_{33}\sigma_{3s}^*}$$

$$\frac{\sigma_{23} + \sigma_{13}}{(\sigma_3 - \sigma_{33})^2} = \frac{\sigma_{3s}^* - \sigma_{33}}{(\sigma_3 - \sigma_{33})^2} \quad (30)$$

Analysis of the above terms indicates that the in-group adjoint variance is always less than the standard adjoint variance except at $\sigma_i = \sigma_{is}^*$, where the variances are equal. Also, the in-group variances are better behaved for physically valid cross section values, i.e., $\sigma_{is}^* \geq \sigma_{ii}$, $\sigma_i \geq \sigma_{ii}$, and no negative cross sections. This suggests that the in-group biasing technique

is generally superior to the standard methodology for MORSE adjoint analyses with no upscattering. Although in-group bias has not been exercised with forward MORSE, it appears from this analysis that in-group bias would be superior to the standard treatment in forward Monte Carlo as well as adjoint Monte Carlo.

IN-GROUP BIASING CODE MODIFICATIONS FOR MORSE

MORSE is easily modified to incorporate in-group energy bias. Scattering in MORSE is handled in subroutine COLISN using data in the form of the non-absorption factor $PNAB_i$ and the normalized scattering probabilities P_{ij} which give the probability of scattering to group j provided that a scattering has occurred in group i . The original coding is very simple in that the particle weight WATE is multiplied by $PNAB_i$, where i is the group coming into the collision, and then a random number is compared with the probabilities P_{ij} to select the outgoing group. This sampling scheme is easily modified to use in-group scattering. Define a bias factor F as follows:

$$\begin{aligned} i = j = 1 & & F = 1.0 \\ i = j \neq 1 & & F = PNAB_i \\ i \neq j & & F = \frac{1 - P_{ii}PNAB_i}{1 - P_{ii}} \end{aligned}$$

The same sampling coding is used except that the random number is compared to $F \cdot P_{ij}$ instead of simply P_{ij} as before. After the outgoing group has been sampled, the weight is corrected by

$$WATE = WATE \cdot PNAB/F$$

the above modifications have been implemented in MASH with a switch which permits in-group biasing to be used on option. The implementation correctly treats in-group biasing with or without E biasing, and includes logic for splitting whenever WATE exceeds WTMAX. Splitting in MORSE is normally performed in subroutine TESTW when a particle's weight is above an importance region- and energy-dependent maximum weight. The particle's weight is split into halves and an identical particle is written to the secondary bank. When the weight increase occurs at upscatter, the excessive weight is not identified until entering subroutine TESTW. Thus, all the splitting secondaries will have the same energy group and the same direction cosines. They will be essentially the same particle. This has been significantly improved by playing the splitting game in subroutine COLISN and actually resampling the upscatter distribution for each splitting secondary particle. In this manner each secondary is independent of the others so that this important probability transition is much more completely represented.

DEMONSTRATION CALCULATIONS

A number of demonstration calculations have been performed to compare VCS or MORSE results using in-group energy bias with results using the standard methodology. Reference 8 describes some results obtained by Siegfried Stuker of Wehrwissenschaftliche Dienststelle der Bundeswehr für ABC-Schutz (WWD), who tested the treatment in a series of 10 cm iron sphere calculations. Stuker determined that in-group biasing made a significant improvement when it was applied to energy groups with PNAB greater than 2.0^8 . He also discovered further improvement when in-group biasing was used for all energy groups including groups with PNAB less than one.

In addition to the calculations performed by Stuker, SAIC has performed calculations on several different test geometries including an iron sphere, a cubical box, and a steel shell resembling a van-like vehicle. These results are discussed in Reference 1. The results for the iron sphere were calculated in a previous effort and are taken from Reference 6. The results for the van-like vehicle have been described in Reference 5.

REFERENCES

1. J. A. Stoddard, S. D. Egbert, and W. D. Scott, Jr., "The Vehicle Code System with In-Group Energy Bias and GIFT5 Geometry," DNA-TR-87-23, Science Applications International Corporation, (January 1987).
2. M. B. Emmett, "The MORSE Monte Carlo Radiation Transport Code System." ORNL-4972 (February 1975); ORNL-4972/R1 (February 1983); ORNL 4972/R2, Oak Ridge National Laboratory, (July 1984).
3. W. A. Rhoades, "Development of a Code System for Determining Radiation Protection of Armored Vehicles (The VCS Code)," ORNL-TM-4664, Oak Ridge National Laboratory, (October 1974).
4. W. A. Rhoades, et.al., "Vehicle Code System (VCS) User's Manual," ORNL-TM-4648, Oak Ridge National Laboratory, (August 1974).
5. W. H. Scott, Jr., "Vehicle Code System (VCS) Documentation and Uncertainty Analysis," SAI Report SAI-133-79-977-LJ, Science Applications International Corporation, (December 1979).
6. W. H. Scott, Jr., and V. E. Staggs, "Adjoint Energy Biasing and Thermal Neutron Diffusion in the MORSE and VCS Codes," SAI Report SAI-133-81-384-LJ, Science Applications International Corporation, (November 1981).
7. D. E. Bartine, et.al., "Production and Testing of the DNA Few-Group Coupled Neutron-Gamma Cross-Section Library," ORNL/TM-4840, Oak Ridge National Laboratory, (1977).
8. S. Stuker and L. Schanzler, Wehrwissenschaftliche Dienststelle der Bundeswehr für ABC-Schutz (WWD), Letter to W.Scott of Science Applications International Corporation, April 28, 1981.

APPENDIX C
THE GIFT5 GEOMETRY PACKAGE

THE GIFTS GEOMETRY PACKAGE*

BACKGROUND

One of the major objectives of earlier efforts in the development of the Vehicle Code System (VCS)^{1,2} was to create a version of VCS which could treat vehicle models developed by the Ballistic Research Laboratory (BRL). BRL, a major user of VCS, has developed detailed combinatorial geometry models of a number of armored vehicles. In order to facilitate the vehicle modeling effort, which often takes a significant fraction of a person year per vehicle, BRL has developed a number of hardware and software tools and has extended the combinatorial geometry models of their codes (other than VCS) to treat a number of new solid "body" types. The result is that BRL has a number of vehicle models which could not be analyzed by VCS unless modified, at considerable time and dollar costs, for use by VCS.

In 1976-1977 BRL removed some of the geometry incompatibilities by installing the geometry package from the BRL GIFT graphics code^{3,4} into the VCS MORSE code. BRL named the result "MIFT" for MORSE with GIFT⁵. A review of the MIFT, VCS, GIFT, and GIFTS codes was performed by Science Applications International Corporation (SAIC) to evaluate and compare the geometry models and to determine the best way to upgrade the geometry treatment in VCS. The GIFTS geometry treatment was found to be superior to the VCS combinatorial geometry and older GIFT treatment in several ways, including the number of solid "body" types, diagnostics and checks of input data, and a tracking method which could correctly treat overlapping or undefined regions in the geometry. Drawbacks relative to the older VCS combinatorial geometry logic were a slightly larger computer run time for similar problems and increased size and complexity of the resulting VCS code. The GIFTS geometry package was first implemented in the MIFT version of the VCS MORSE code and called MIFT2⁶. The GIFTS geometry package has since been implemented in the current MASH version of the MORSE code. The bulk of this appendix was extracted from the GIFT document³ to give some background information on the GIFTS geometry package and has been included in this manual for completeness.

* Lawrence W. Bain, Jr. and Mathew J. Reisinger, "The GIFT Code User Manual; Volume I. Introduction and Input Requirements," BRL 1802, Ballistic Research Laboratory, (July 1975).

INTRODUCTION

GIFT5 geometry is similar to the older MORSE combinatorial geometry in that specified geometric shapes (spheres, cylinders, parallelepipeds, etc.) may be combined to describe complex geometry configurations. As with MORSE combinatorial geometry, a GIFT5 geometry file is comprised largely of a "body" or "solids" table followed by a "zones" or "region" table in which the bodies are combined by (+), (-), or (OR) operators. In GIFT5 geometry, however, "bodies" (MORSE terminology) are called "solids" and "zones" (MORSE terminology) are called "regions". In the GIFT5 graphics code there is no equivalent to the "regions" as used in MORSE. In MASH, where the term "region" could have a double meaning, the MORSE equivalent of "region" is called "importance region" to minimize any confusion. In this appendix the GIFT5 terminology, i.e., solids and regions, equivalent to bodies and zones in MORSE, will be used.

TARGET DESCRIPTION DATA

Target description data defines or models the three-dimensional shape and space of a simple or complex physical structure - the target. The GIFT5 geometry package uses a "combinatorial geometry" or "COM-GEOM" target description technique. This technique defines the shape and space of the components of the target as a single geometric "solid" (a box, a sphere, a cylinder, etc.), or the "combination" of several geometric solids. The parameters which define the spatial locations of the geometric solids used to model the components of the target are recorded in the "Solid Table." Each component (region) of the target is defined as a single solid or a "combination" of solids in the "Region Table."

The Solid and the Region Tables, and the other input data required to create the target description data for the GIFT5 geometry package are defined in the following sections of this appendix.

PRELIMINARY STEPS

The first step to model a target by any three-dimensional target description technique is to obtain engineering drawings, reports, or any other data which exhibit the physical dimensions of the target. The next step is to define a reference point on the target: the origin point (0) of an X,Y,Z right-handed coordinate system. For example, for tanks, the intersection of the turret datum line and the center lines of the turret is usually selected as the origin point. The parameters within the target description data may be recorded in inches or centimeters or any other unit of measure. For example, the X,Y,Z coordinate values for a point "P" can be given as (X = 1.4, Y = 1.0, Z = -1.0) inches or (X = 3.5, Y = 2.5, Z = -2.5) centimeters from the origin point (X,Y,Z = 0). Every parameter recorded in the target description data must be measured in the same unit of measure.

SOLIDS

Table C-1 lists the twenty geometric solids used by the GIFT5 geometry package. The letters under the "Symbol", column are the alphanumeric designation used in this report and on the input cards for the solid. The "Figure" column lists the figure(s) where the input data for the solid is described.

Each solid in a target description is identified by a unique number, 1, 2, 3, etc. This permits the space of any solid to be distinguished from the space of any other solid. The parameters required to define the twenty solids are different. The parameters can, however, be classified as being either a "vertex point," a "vector," or a "scalar."

A vertex point is a point defined by its X, Y and Z measurements (coordinate values) from the target reference or origin (0) point. For each of the twenty types of solids, at least one vertex point is used to locate the position of the solid in the referenced X,Y,Z space. For example, "V" is the vertex point for a box, while the centerpoint "C" is the vertex point for the sphere solid. Within this report, the dash (-) mark over a letter (V, C, H, etc.) will be used to indicate an X, Y and Z measurement.)

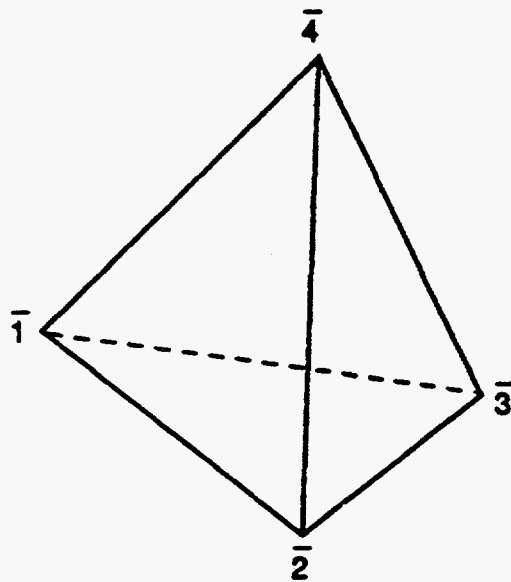
Certain solids require vector parameters to define the three-dimensional shape and space that they occupy. The BOX requires three vectors, H, W, D, which respectively represent the height, width, and depth of the BOX. Vectors also have an X, Y and Z measurement; however, the measurements of vectors are taken from the vertex point of the solid rather than the target reference or origin point. The X,Y,Z measurements of H, W and D vectors are taken from V, not the origin (0) point.

Some solids require scalar parameters to define their shape and space. Scalars are single numeric values. An example of a scalar is the radius parameter used to define the SPH solid.

Figures C-1 to C-20 illustrate and define the parameters and card input formats for each of the 20 solid types used by the GIFT5 geometry package. The comments on these figures must be given careful attention because the difference between certain solids is slight.

Table C-1. List of 20 Geometric Solids
used by the GIFT5 Geometry Package.

	Solid Name	Symbol	Figure
1.	Arbitrary Convex Polyhedron, 4 vertex	ARB4	C-1
2.	Arbitrary Convex Polyhedron, 5 vertex	ARB5	C-2
3.	Arbitrary Convex Polyhedron, 6 vertex	ARB6	C-3
4.	Arbitrary Convex Polyhedron, 7 vertex	ARB7	C-4
5.	Arbitrary Convex Polyhedron, 8 vertex	ARB8	C-5
6.	Arbitrary Convex Polyhedron, N vertex	ARBN	C-6
7.	Triangular Surfaced Polyhedrons	ARS	C-7
8.	Box	BOX	C-8
9.	Ellipsoid of Revolution	ELL	C-9
10.	Ellipsoid with Elliptical Cross Section	ELL G	C-10
11.	Half Space	HAF	C-11
12.	Right Angle Wedge	RAW	C-12
13.	Right Circular Cylinder	RCC	C-13
14.	Right Elliptical Cylinder	REC	C-14
15.	Rectangular Parallelepiped	RPP	C-15
16.	Sphere	SPH	C-16
17.	Truncated Elliptical Cone	TEC	C-17
18.	Truncated General Cone	TGC	C-18
19.	Torus	TOR	C-19
20.	Truncated Right Angle Cone	TRC	C-20



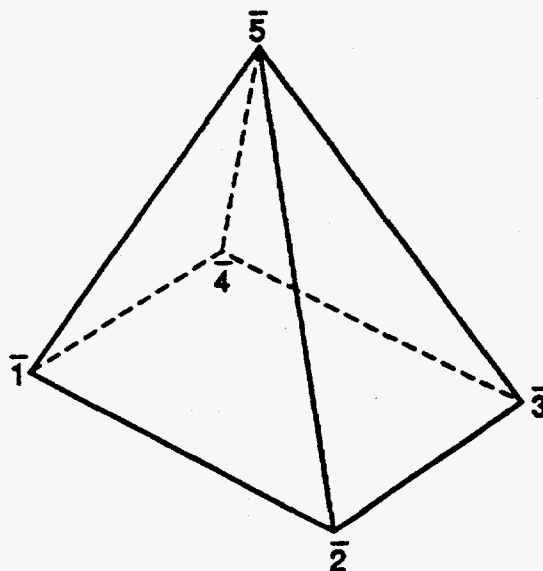
SPECIFY: The X, Y, Z coordinates of the four vertices of the Polyhedron. Vertices are the ordinal numbers 1 to 4 on the figure.

NOTES: This form of the ARB has four ("4" in card column 9) vertices and four faces each defined by three vertices. The GIFT code generates the four faces as: 123, 412, 423, 431.
 Card Columns 71-80 may be used for comments.
 Card Format: (I5, A3, A1, 1X, 6F10.0, A10)

CARD COLUMNS

1-5	6-8	9	11-20	21-30	31-40	41-50	51-60	61-70	Number of Cards
Solid Number	ARB	4	X1	Y1	Z1	X2	Y2	Z2	1 of 2
Solid Number			X3	Y3	Z3	X4	Y4	Z4	2 of 2

Figure C-1. Four-faced, four vertices, convex polyhedron (ARB4) input.



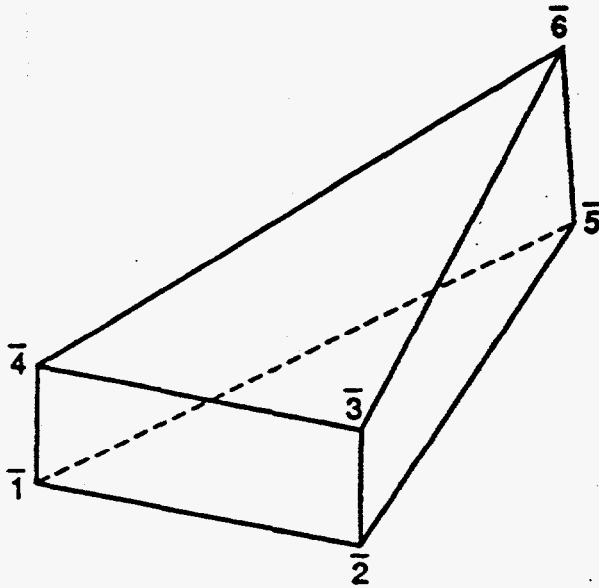
SPECIFY: The X, Y, Z coordinates of the five vertices of the polyhedron. Vertices are the ordinal numbers 1 to 5 on the figure.

NOTES: This form of the ARB has five ("5" in card column 9) vertices and five faces - one defined by four vertices, four faces defined by three vertices. The GIFT code generates the five faces as: 1234, 512, 523, 534, 541
 Card Columns 71-80 may be used for comments.
 Card Format: (I5, A3, A1, 1X, 6F10.0, A10)

CARD COLUMNS

1-5	6-8	9	11-20	21-30	31-40	41-50	51-60	61-70	Number of Cards
Solid Number	ARB	5	X1	Y1	Z1	X2	Y2	Z2	1 of 3
Solid Number			X3	Y3	Z3	X4	Y4	Z4	2 of 3
Solid Number			X5	Y5	Z5				3 of 3

Figure C-2. Five-faced, five vertices, convex polyhedron (ARB5) input.



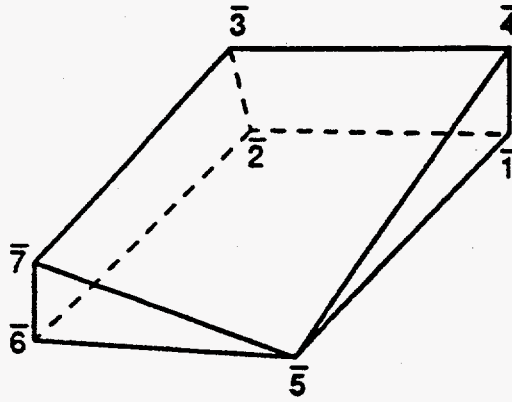
SPECIFY: The X, Y, Z coordinates of the six vertices of the polyhedron. Vertices are the ordinal numbers 1 to 6 on the figure.

NOTES: This form of the ARB has six ("6" in card column 9) vertices and five faces - three faces are defined by four vertices, two faces defined by three vertices. The GIFT code generates the six faces as: 1234, 2365, 1564, 512, 634. Columns 71-80 may be used for comments. Card Format: (I5, A3, A1, 1X, 6F10.0, A10)

CARD COLUMNS

1-5	6-8	9	11-20	21-30	31-40	41-50	51-60	61-70	Number of Cards
Solid Number	ARB	6	X1	Y1	Z1	X2	Y2	Z2	1 of 3
Solid Number			X3	Y3	Z3	X4	Y4	Z4	2 of 3
Solid Number			X5	Y5	Z5	X6	Y6	Z6	3 of 3

Figure C-3. Five-faced, six vertices, convex polyhedron (ARB6) input.



SPECIFY: The X, Y, Z coordinates of the seven vertices of the polyhedron. Vertices are the ordinal number 1 to 7 on the figure.

NOTES: This form of the ARB has seven ("7" in card column 9) vertices and six faces - four faces defined by four vertices, two faces defined by three vertices (triangular faces).

The GIFT code generates the six faces as:
1234, 567, 145, 2376, 1265, 4375.

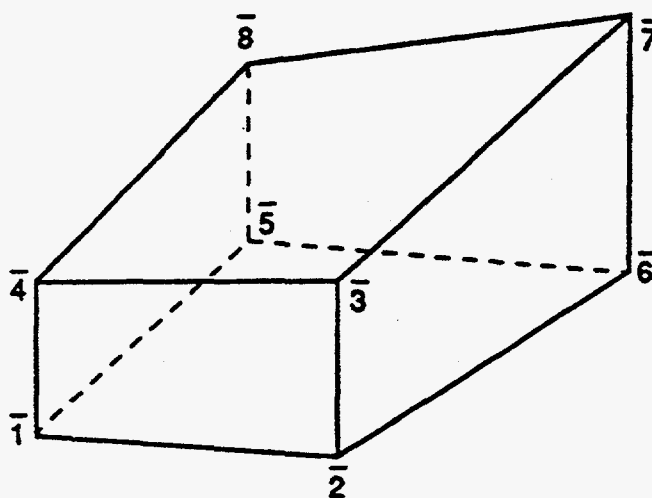
Card Columns 71-80 may be used for comments.

Card Format: (I5, A3, A1, 1X, 6F10.0, A10)

CARD COLUMNS

1-5	6-8	9	11-20	21-30	31-40	41-50	51-60	61-70	Number of Cards
Solid Number	ARB	7	X1	Y1	Z1	X2	Y2	Z2	1 of 4
Solid Number			X3	Y3	Z3	X4	Y4	Z4	2 of 4
Solid Number			X5	Y5	Z5	X6	Y6	Z6	3 of 4
Solid Number			X7	Y7	Z7				4 of 4

Figure C-4. Six-faced, seven vertices, convex polyhedron (ARB7) input.



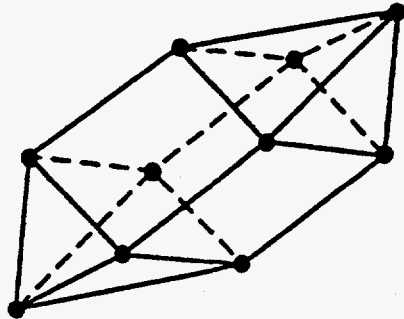
SPECIFY: The X, Y, Z coordinates of the eight vertices of the Polyhedron. Vertices are the ordinal numbers 1 to 8 on the figure.

NOTES: This form of the ARB has eight ("8" in card column 9) vertices and six faces each defined by four vertices.
 The GIFT code generates the six faces as:
 1234, 5678, 1584, 2376, 1265, and 4378.
 Card Columns 71-80 may be used for comments.
 Card Format: (I5, A3, A1, 1X, 6F10.0, A10)

CARD COLUMNS

1-5	6-8	9	11-20	21-30	31-40	41-50	51-60	61-70	Number of Cards
Solid Number	ARB	8	X1	Y1	Z1	X2	Y2	Z2	1 of 4
Solid Number			X3	Y3	Z3	X4	Y4	Z4	2 of 4
Solid Number			X5	Y5	Z5	X6	Y6	Z6	3 of 4
Solid Number			X7	Y7	Z7	X8	Y8	Z8	4 of 4

Figure C-5. Six-faces, eight vertices, convex polyhedron (ARB8) input.



SPECIFY: Bounding planes by any or all of three ways: points, equations, or point and vector normal to the plane.

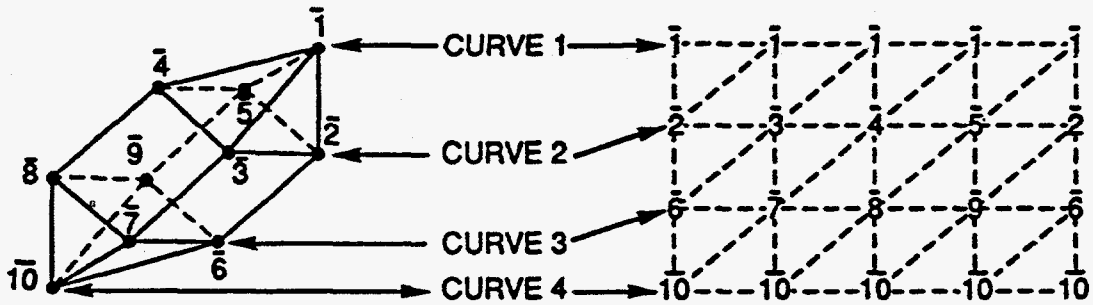
DEFINITIONS: NPT = number of points
 NPE = number of faces defined by 3 points
 NEQ = number of faces defined by equation
 NAE = number of faces defined by point and azimuth and elevation of vector normal to plane
 A,B,C,D = plane equation coefficients, $AX + BY + CZ = D$
 AZ = azimuthal angle, degrees
 EL = elevation angle, degrees
 PN = point number

NOTES: The defined faces must form a totally enclosed region.
 This ARB has the letter "N" in column 9.
 Columns 71-80 may be used for comments.
 Card Format: (I5, A3, A1, 1X, 6F10.0, A10) except faces input on [10X,6 (I4, 2I3), A10] format.

CARD COLUMNS

1-5	6-8	9	11-20	21-30	31-40	41-50	51-60	61-70	Number of Cards	
Solid Number	ARB	N	NPT	NPE	NEQ	NAE			1 of N	
Solid Number			X1	Y1	Z1	X2	Y2	etc.	2 of N	
Solid Number			FACE1, FACE2, FACE3, etc. on 10X, 6(I4, 2I3) format							as needed for NPE>0
Solid Number			A1	B1	C1	D1	(blank)	(blank)	as needed for NEQ>0	
Solid Number			AZ1	EL1	PN1	AZ2	EL2	PN2	as needed for NAE>0	

Figure C-6. N-faces, convex polyhedron (ARB N) input.



SPECIFY: The X, Y, Z coordinate values of the vertices of the concave or convex polyhedron. Order and record of the vertices by the number of curves (M) and number of points per curve (N) system.

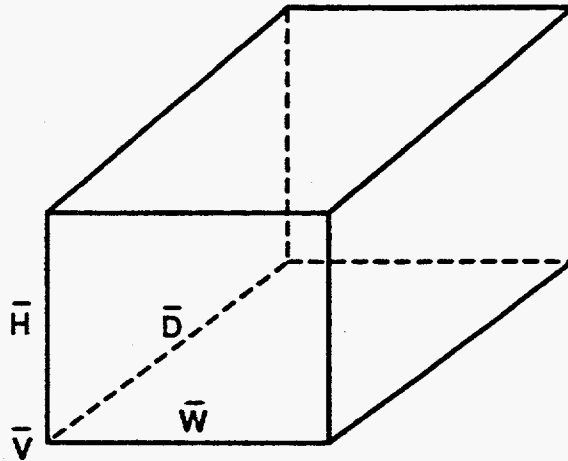
NOTES: The purpose of this solid type is to permit the easy conversion and use of target description data from other BRL codes. BRL recommends that polyhedrons be modeled as a "combination" of ARB's 4, 5, 6, 7, and 8's. The sample polyhedron has 10 unique vertices (1, 2, 3 ... 10); however, M=4, N=5, and 4x5 or 20 vertices are required and recorded to generate the triangular faces of this polyhedron. The order is illustrated by the M,N matrix above in which the vertices of the generated triangle faces are connected by dashes (- -). Each new curve begins on a new card: When N is odd, the card containing the last recorded point of a curve is followed by blanks in card columns 41-70.

Figure C-7. Triangular surfaced (ARS) polyhedron input.

CARD COLUMNS

1-5	6-8	11-20	21-30	31-40	41-50	51-60	61-70	Number of Cards
Solid Number	ARS	M	N					1 of n
Solid Number		X(1,1)	Y(1,1)	Z(1,1)	X(1,2)	Y(1,2)	Z(1,2)	2 of n
.		.						.
.		.						.
Solid Number		X(1,N)	Y(1,N)	Z(1,N)				$1 + \frac{(N+1)}{2}$ of n
Solid Number		X(2,1)	Y(2,1)	Z(2,1)	X(2,2)	Y(2,2)	Z(2,2)	
.		.						.
.		.						.
.		.						.
Solid Number		X(M,1)	Y(M,1)	Z(M,1)	X(M,2)	Y(M,2)	Z(M,2)	
.		.						.
.		.						.
.		.						.
Solid Number		X(M,N)	Y(M,N)	Z(M,N)				$n = 1 + M \frac{(N+1)}{2}$

Figure C-7. Triangular surfaces (ARS) polyhedron input (Continued).



SPECIFY: The vertex (V) at one of the corners by giving the X, Y, Z coordinates. The X, Y, Z components of the three mutually perpendicular vectors (H, W, D) from the vertex point V, representing the height, width, and depth of the box.

NOTES: The box may be arbitrarily oriented while the RPP must be parallel to the reference coordinate axes. The vectors H, W, and D may be interchanged on the card input.

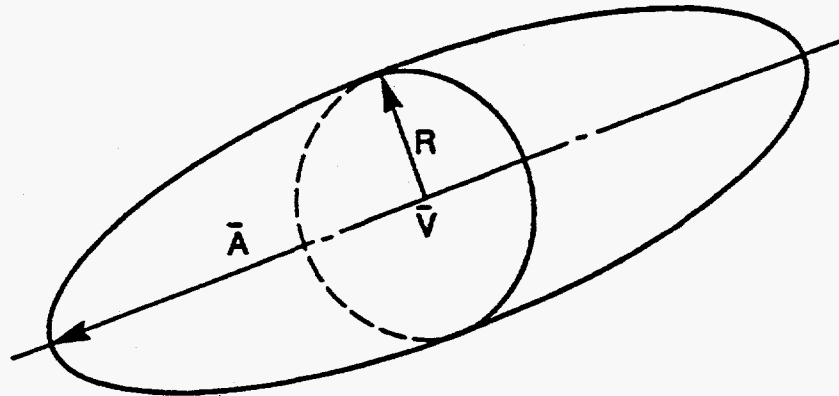
Card Columns 71-80 may be used for comments.

Card Format: (I5, A3, 2X, 6F10.0, A10)

CARD COLUMNS

1-5	6-8	11-20	21-30	31-40	41-50	51-60	61-70	Number of Cards
Solid Number	BOX	Vx	Vy	Vz	Hx	Hy	H _z	1 of 2
Solid Number							D _z	2 of 2

Figure C-8. Box (BOX) input.



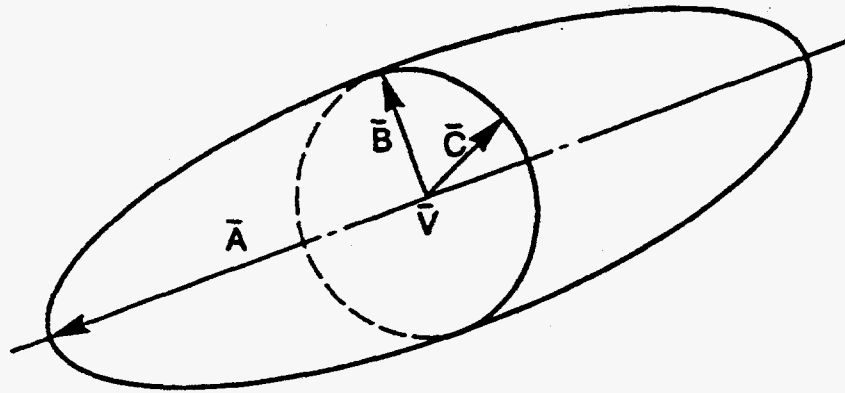
SPECIFY: The X, Y, Z coordinates of the vertex V at the center of the major axis, the vector A defining the semi-major axis, and the scalar R denoting the radius of the circular section taken at the center point V.

NOTES: Card Columns 71-80 may be used for comments.
Card Format: (I5, A3, 2X, 6F10.0, A10)

CARD COLUMNS

1-5	6-8	11-20	21-30	31-40	41-50	51-60	61-70	Number of Cards
Solid Number	ELL	Vx	Vy	Vz	Ax	Ay	Az	1 of 2
Solid Number		R						2 of 2

Figure C-9. Ellipsoid of revolution (ELL) input.



SPECIFY: The X, Y, Z coordinates of the vertex V at the center of the major axis, the vector A defining the semi-major axis, and vectors B and C defining semi-minor axes.

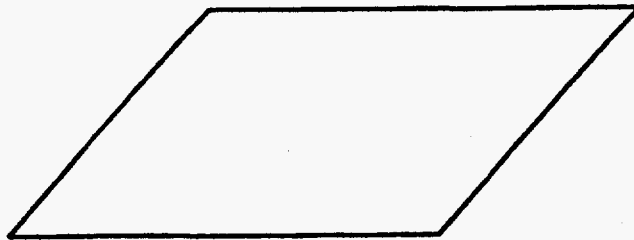
NOTES: The letter "G" in card column "9" denotes the second ELL input option. Vectors A, B, and C must be perpendicular. Card Columns 71-80 may be used for comments. Card Format: (I5, A3, A1, 1X, 6F10.0, A10)

CARD COLUMNS

1-5	6-8	9	11-20	21-30	31-40	41-50	51-60	61-70	Number of Cards
Solid Number	ELL	G	Vx	Vy	Vz	Ax	Ay	Az	1 of 2
Solid Number			Bx	By	Bz	Cx	Cy	Cz	2 of 2

Figure C-10. Input for ellipsoid with elliptical cross section (ELL G).

ORNL-DWG 90M-11865



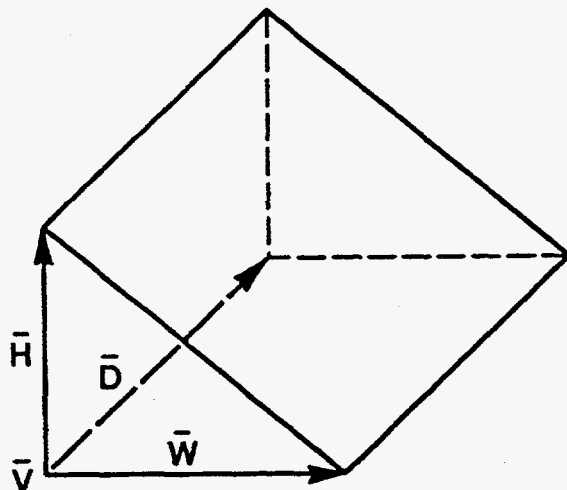
SPECIFY: Coefficients A, B, C and D of plane defined by the equation
 $AX + BY + CZ = D$.

NOTES: A, B, C can be viewed as vectors which point away from the desired space.
Example: for $A=B=D=0$ and $C=1$, plane is $Z=0$. $C=1$ points away from
desired space; hence desired space is $Z \leq 0$.
Card Columns 71-80 may be used for comments.
Card Format: (I5, A3, 2X, 6F10.0, A10)

CARD COLUMNS

1-5	6-8	11-20	21-30	31-40	41-50	51-60	61-70	Number of Cards
Solid Number	HAF	A	B	C	D			1 of 1

Figure C-11. Half space (HAF) input.



SPECIFY: The vertex (V) at one of the right-angled corners by giving the X, Y, and Z coordinate. The components of the three mutually perpendicular vectors (H, W, D), of which two (H, W) are the legs of the right triangle formed while the third (D) is the depth of the wedge.

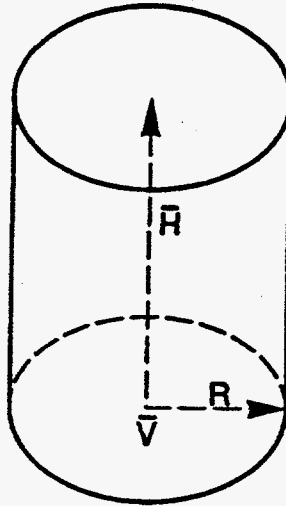
NOTES: The two legs H, W may be interchanged on card input, but the D vector must remain in position shown.
 Card Columns 71-80 may be used for comments.
 Card Format: (I5, A3, 2X, 6F10.0, A10)

CARD COLUMNS

1-5	6-8	11-20	21-30	31-40	41-50	51-60	61-70	Number of Cards
Solid Number	RAW	Vx	Vy	Vz	Hx	Hy	H _z	1 of 2
Solid Number		Wx	Wy	Wz	Dx	Dy	Dz	2 of 2

Figure C-12. Right angle wedge (RAW) input.

ORNL-DWG 90M-11873



SPECIFY: The vertex point V at the center of one base, height vector H and scalar R denoting the base radius.

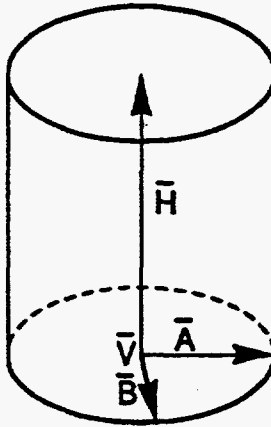
NOTES: Card Columns 71-80 may be used for comments.
Card Format: (I5, A3, 2X, 6F10.0, A10)

CARD COLUMNS

1-5	6-8	11-20	21-30	31-40	41-50	51-60	61-70	Number of Cards
Solid Number	RCC	V_x	V_y	V_z	H_x	H_y	H_z	1 of 2
Solid Number		R						2 of 2

Figure C-13. Right circular cylinder (RCC) input.

ORNL-DWG 90M-11867



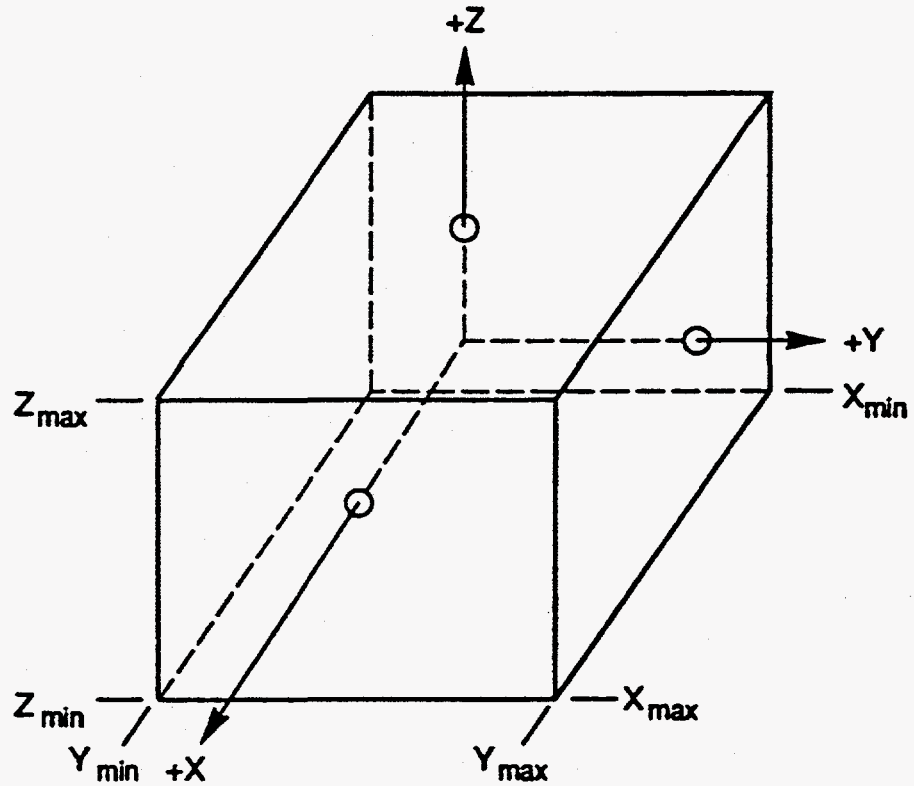
SPECIFY: The X, Y, Z coordinates of the center of the base ellipse V, height vector H, and vectors A and B in the base plane defining the semi-major and semi-minor axes, respectively.

NOTES: Card Columns 71-80 may be used for comments.
Card Format: (I5, A3, 2X, 6F10.0, A10)

CARD COLUMNS

1-5	6-8	11-20	21-30	31-40	41-50	51-60	61-70	Number of Cards
Solid Number	REC	Vx	Vy	Vz	Hx	Hy	H _z	1 of 2
Solid Number		Ax	Ay	Az	Bx	By	Bz	2 of 2

Figure C-14. Right elliptical cylinder (REC) input.



SPECIFY: The maximum (max) and the minimum (min) values of the X, Y, Z coordinates which bound the parallelepiped.

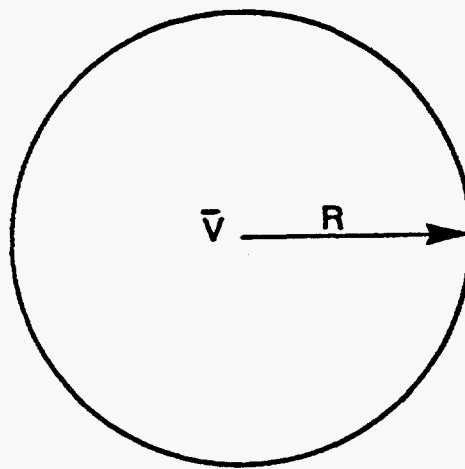
NOTES: The bounding planes must be parallel to the coordinate axes of the target.
 Card Columns 71-80 may-be used for comments.
 Card Format: (I5, A3, 2X, 6F10.0, A10)

CARD COLUMNS

1-5	6-8	11-20	21-30	31-40	41-50	51-60	61-70	Number of Cards
Solid Number	RPP	Xmin	Ymin	Zmin	Xmax	Ymax	Zmax	1 of 1

Figure C-15. Rectangular parallelepiped (RPP) input.

ORNL-DWG 90M-11871



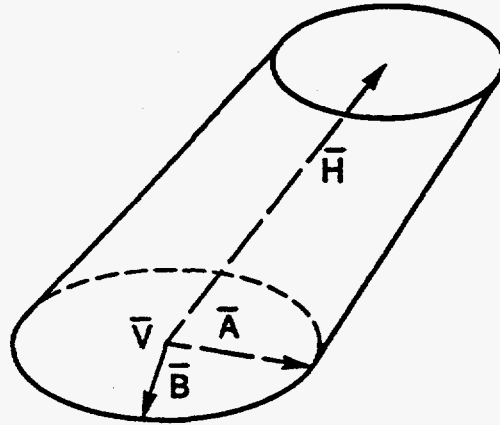
SPECIFY: The center point, V , and scalar R denoting the radius.

NOTES: Card Columns 71-80 may be used for comments.
Card Format: (I5, A3, 2X, 6F10.0, A10)

CARD COLUMNS

1-5	6-8	11-20	21-30	31-40	41-50	51-60	61-70	Number of Cards
Solid Number	SPH	Vx	Vy	Vz	R			1 of 1

Figure C-16. Sphere (SPH) input.



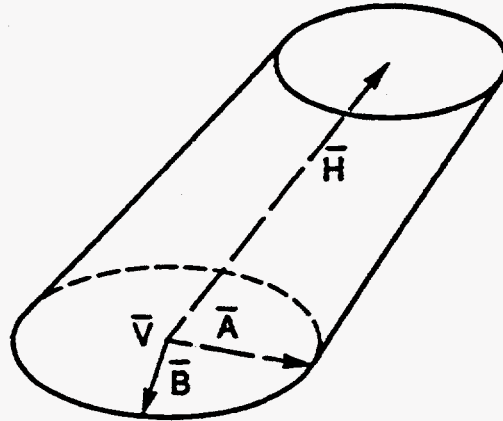
SPECIFY: The coordinates of vertex V at the center of the larger ellipse, and the X, Y, Z components of the height vector H and vectors A and B describing the semi-major and semi-minor axes. The ratio P of the larger to smaller ellipse.

NOTES: The height vector H does not have to be perpendicular to the plane containing vectors A and B . The ratio P may be determined by the magnitude (length) of semi-major vector A of the base ellipse divided by the length of semi-major axis of the upper ellipse: $P > 1$.
 Card Columns 71-80 may be used for comments.
 Card Format: (I5, A3, 2X, 6F10.0, A10)

CARD COLUMNS

1-5	6-8	11-20	21-30	31-40	41-50	51-60	61-70	Number of Cards
Solid Number	TEC	Vx	Vy	Vz	Hx	Hy	Hz	1 of 3
Solid Number		Ax	Ay	Az	Bx	By	Bz	2 of 3
Solid Number		P						3 of 3

Figure C-17. Truncated elliptic cone (TEC) input.



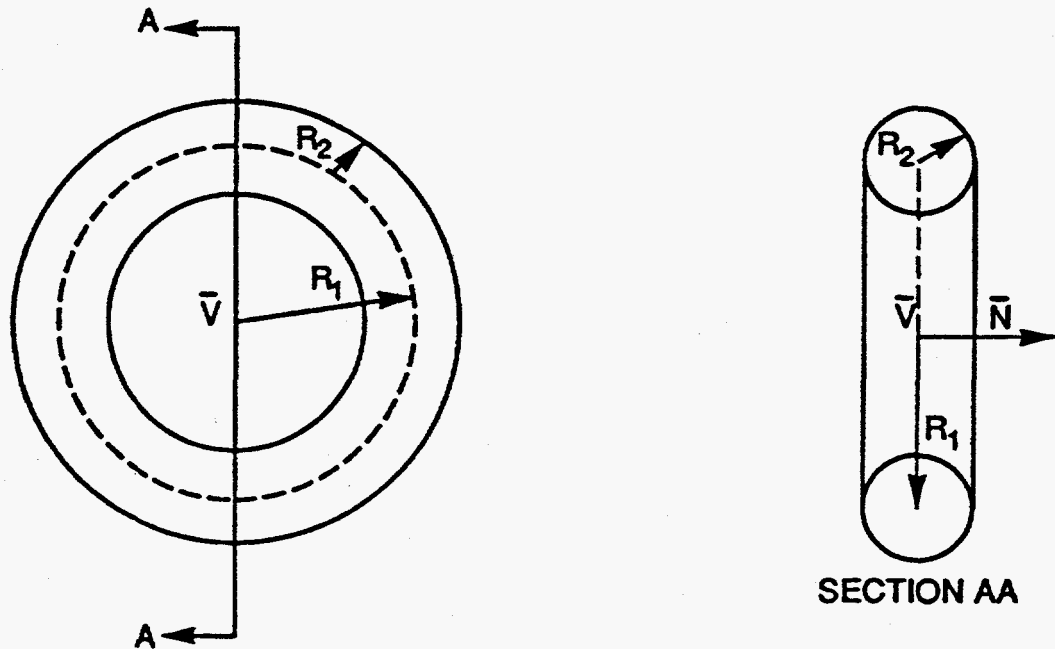
SPECIFY: The coordinates of vertex V at the center of the larger ellipse, and the X, Y, Z components of the height vector H and vectors A and B describing the semi-major and semi-minor axes. The ratios $T(A)$ and $T(B)$ of the semi-major and semi-minor axes for the smaller ellipse.

NOTES: The height vector H does not have to be perpendicular to the plane containing vectors A and B . The semi-major and semi-minor axes of the smaller ellipse, $T(A) \cdot A$ and $T(B) \cdot B$, respectively, must be parallel to the semi-major and semi-minor axes, respectively, of the larger ellipse.
 Card Columns 71-80 may be used for comments.
 Card Format: (I5, A3, 2X, 6F10.0, A10)

CARD COLUMNS

1-5	6-8	11-20	21-30	31-40	41-50	51-60	61-70	Number of Cards
Solid Number	TGC	V_x	V_y	V_z	H_x	H_y	H_z	1 of 3
Solid Number		A_x	A_y	A_z	B_x	B_y	B_z	2 of 3
Solid Number		TA	TB					3 of 3

Figure C-18. Truncated general cone (TGC) input.



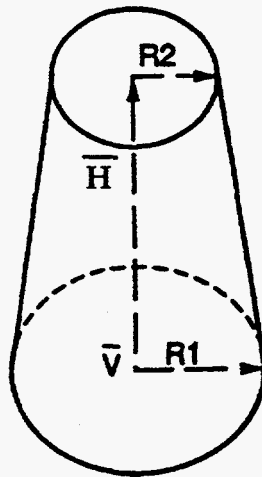
SPECIFY: The vertex V at the center of the torus, a normal vector N to the plane in which the locus of the mid-points of the circular cross sections lies, and the scalars $R1$, the distance from the center V to the mid-point of the circular cross section, and $R2$, the radius of the circular cross section.

NOTES: Card Columns 71-80 may be used for comments.
Card Format: (I5, A3, 2X, 6F10.0, A10)

CARD COLUMNS

1-5	6-8	11-20	21-30	31-40	41-50	51-60	61-70	Number of Cards
Solid Number	TOR	Vx	Vy	Vz	Nx	Ny	Nz	1 of 2
Solid Number		R1	R2					2 of 2

Figure C-19. Torus (TOR) input.



SPECIFY: The vertex V at the center of the larger base, height vector H and scalars $R1$ and $R2$ denoting the radii of the larger and smaller bases, respectively.

NOTES: Card Columns 71-80 may be used for comments.
Card Format: (I5, A3, 2X, 6F10.0, A10)

CARD COLUMNS

1-5	6-8	11-20	21-30	31-40	41-50	51-60	61-70	Number of Cards
Solid Number	TRC	Vx	Vy	Vz	Hx	Hy	Hz	1 of 2
Solid Number		R1	R2					2 of 2

Figure C-20. Truncated right angle cone (TRC) input.

SOLID TABLE

A Solid Table contains the input cards for every solid used to describe the target. Table C-2 is the Solid Table for a sample target. Twenty solids are used to describe the sample target.

Every solid within a Solid Table must have a unique number. The numbering of the solids in the Solid Table begins with the number "1" and is consecutive (1, 2, 3 ...). No hierarchy exists between the solids; any solid type can be numbered "1, or 2, or 3,..."

"COMBINATION" OF SOLIDS

The three-dimensional shape and space of several solids can be "combined" to define a component of a target. Figure C-21 illustrates the concepts of "intersection," "subtraction," and "union" which are used to "combine" the space of several solids.

Section A of Figure C-21 exhibits an RPP and SPH which overlap. For discussion, suppose that the RPP is the first solid in a Solid Table; it is therefore numbered "1". If the SPH is the second solid in the Solid Table, it is therefore numbered "2". The "intersection" (+) of the RPP (1) and the SPH (2) solid is represented as "1 + 2". The "1 + 2" symbolization may be interpreted as the space of the first (1) solid in the Solid Table that overlaps or "intersects" (+) the space of the second (2) solid in the Solid Table. The dashed (/) area in section B of Figure C-21 represents the space of "1 + 2", the space of the RPP (1) that overlaps the space of the SPH (2).

The "Subtraction" (-) of the space of the SPH (2) from the space of the RPP (1) is represented by "1 - 2". The "1 - 2" symbolization may be interpreted as the space of the first (1) solid removing or "subtracting" the space of the second solid in the Solid Table. The dashed area in section C of the Figure C-21 represents the space of "1 - 2" the space of the RPP removing the space of the SPH. Note that the space resulting from "1 + 2" and "2 + 1" (intersect relationship) would be the same; however, "1 - 2" results in a space different from "2 - 1", the space of the SPH removing the space of the RPP.

The "union" (OR) of the space of the RPP (1) and the SPH (2) is represented by "1 OR 2". The "1 OR 2" symbolization is the space of the first (1) solid "and" or "union" (OR) of the space of the second solid (2) in the Solid Table. The dashed area in section E on Figure C-21 represents "1 OR 2", the space of the RPP "and" the space of the SPH. As the intersect relationship, the union relationship of "1 OR 2" and "2 OR 1" results in the same space.

To model irregular shaped components of a target may require the intersection, subtraction, and union of many different solids. In section A on Figure C-22 a third solid (numbered "3") has been added to the RPP and SPH configuration used in Figure C-21. The third (3) solid may be a BOX or another RPP.

The dashed area in section B of Figure C-22 represents the space resulting from the intersection of solids 1, 2, and 3 (1 + 2 + 3). A process to arrive at the results of "1 + 2 + 3" is to visualize the area resulting from "1 + 2" (shown in Figure C-21) and then find the intersect (+) of the third (3) solid with the area from "1 + 2".

Table C-2. Solid Table for the Sample Target.

1	TOR	21.5	0.0	37.0	1.0	0.0	0.0	STEERING
1		8.0	1.0					WHEEL
2	ARB4	21.5	-6.0	33.5	21.5	6.0	33.5	CENTER
2		21.5	0.0	44.0	40.0	0.0	37.0	STEERING
3	ARB5	75.0	-36.0	12.0	75.0	36.0	12.0	FRONT
3		75.0	36.0	48.0	75.0	-36.0	48.0	3-2
3		100.0	0.0	12.0				3-3
4	ARB8	-75.0	-36.0	12.0	-75.0	36.0	12.0	REAR
4		-75.0	36.0	48.0	-75.0	-36.0	48.0	4-2
4		-100.0	-24.0	12.0	-100.0	24.0	12.0	4-3
4		-100.0	24.0	20.0	-100.0	-24.0	20.0	4-4
5	ELL	20.0	0.0	48.0	-20.0	0.0	48.0	BUBBLE
5		50.0						
6	RPP	-75.0	75.0	-36.0	36.0	12.0	48.0	BODY
7	RCC	60.0	-36.0	12.0	0.0	8.0	0.0	WHEEL
7		12.0						
8	RCC	60.0	36.0	12.0	0.0	-8.0	0.0	WHEEL
8		12.0						
9	RCC	-60.0	-36.0	12.0	0.0	8.0	0.0	WHEEL
9		12.0						
10	RCC	-60.0	36.0	12.0	0.0	-8.0	0.0	WHEEL
10		12.0						
11	ARS	6.0	5.0					ENGINE
11		-30.0	-10.0	15.0	-30.0	-10.0	15.0	11-2
11		-30.0	-10.0	15.0	-30.0	-10.0	15.0	11-3
11		-30.0	-10.0	15.0				11-4
11		-30.0	-10.0	15.0	-70.0	-10.0	15.0	11-5
11		-70.0	10.0	15.0	-30.0	10.0	15.0	11-6
11		-30.0	-10.0	15.0				11-7
11		-30.0	-10.0	25.0	-70.0	-10.0	25.0	11-8
11		-70.0	10.0	25.0	-30.0	10.0	25.0	11-9
11		-30.0	-10.0	25.0				11-10
11		-30.0	-20.0	35.0	-70.0	-20.0	35.0	11-11
11		-70.0	20.0	35.0	-30.0	20.0	35.0	11-12
11		-30.0	-20.0	35.0				11-13
11		-30.0	-10.0	45.0	-70.0	-10.0	45.0	11-14
11		-70.0	10.0	45.0	-30.0	10.0	45.0	11-15
11		-30.0	-10.0	45.0				11-16
11		-30.0	-10.0	45.0	-30.0	-10.0	45.0	11-17
11		-30.0	-10.0	45.0	-30.0	-10.0	45.0	11-18
11		-30.0	-10.0	45.0				11-19
12	RAW	-70.0	0.0	35.0	0.0	-11.0	11.0	ENGINE
12		0.0	11.0	11.0	40.0	0.0	0.0	
13	REC	0.0	0.0	24.0	0.0	0.0	28.0	TRUNK
13		0.0	7.5	0.0	0.0	0.0	0.0	
14	SPH	0.0	0.0	52.0	5.0			HEAD
15	TEC	0.0	-7.5	49.0	20.0	0.0	-12.0	ARM
15		0.0	0.0	3.0	0.0	2.0	0.0	15-2
15		2.0						15-3
16	TEC	0.0	7.5	49.0	20.0	0.0	-12.0	ARM
16		0.0	0.0	3.0	0.0	2.0	0.0	16-2
16		2.0						16-3
17	TRC	-2.0	-4.5	27.0	32.0	0.0	-12.0	LEG
17		3.0	2.0					
18	TRC	-2.0	4.5	27.0	32.0	0.0	-12.0	LEG
18		3.0	2.0					
19	ELL	0.0	0.0	48.0	24.0	0.0	0.0	(1.0)
19		14.0						
20	BOX	-74.0	-35.0	13.0	148.0	0.0	0.0	(1.0)
20		0.0	70.0	0.0	0.0	0.0	34.0	

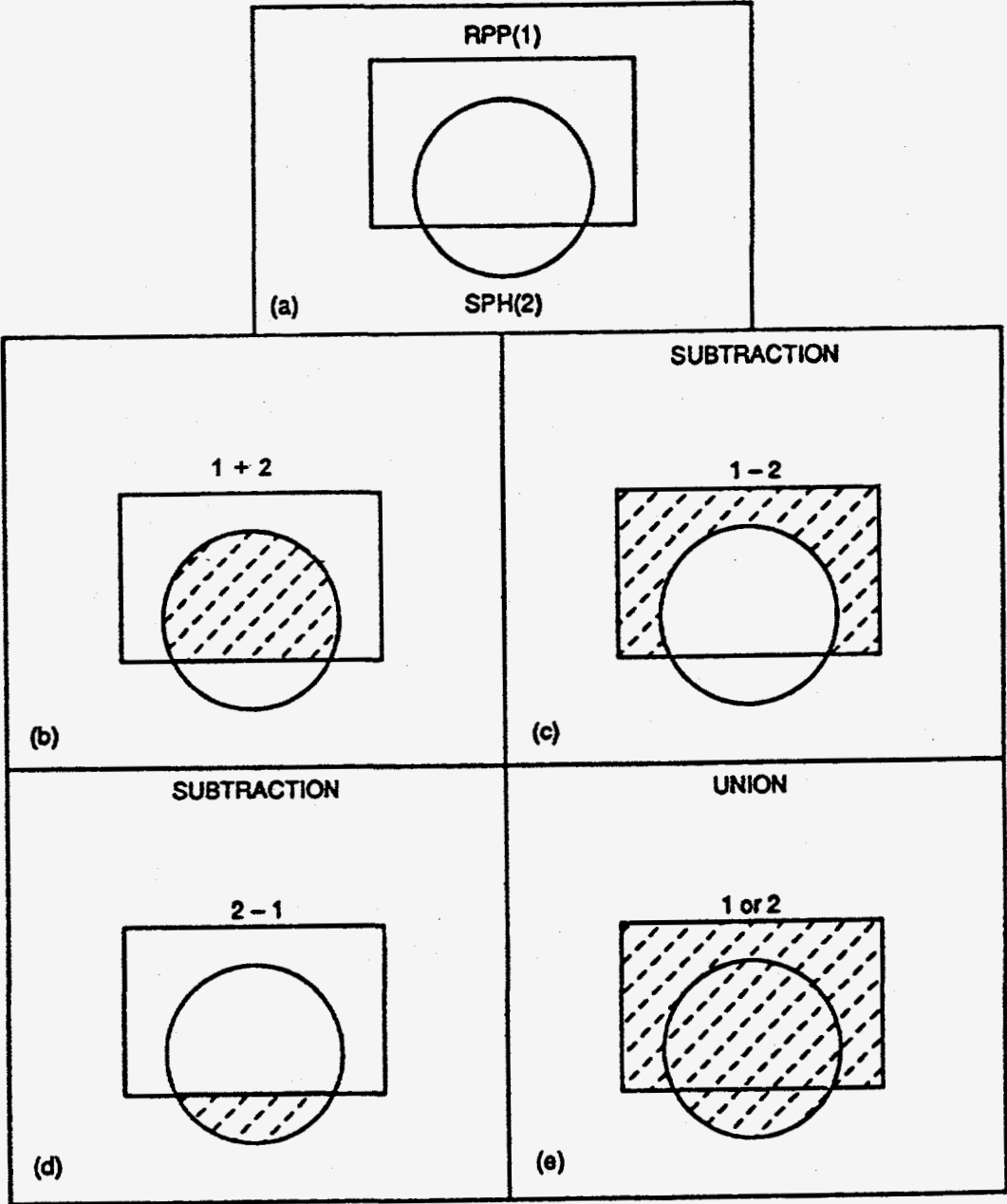


Figure C-21. Intersection, Subtraction, and Union Between Two Solids.

The dashed area in section C of Figure C-22 represents the space resulting from the relationship "3 - 1", the space of the third (3) solid removing or subtracting the space of the first (1) solid.

The dashed area in section D represents the space resulting from "1 + 2 - 3". Again analyzing the final space by steps: first, visualize the "1 + 2" relationship, then remove or subtract the space of solid "3".

The dashed area in section E represents the space resulting from "1 OR 2 OR 3".

The dashed area in section F represents the space of "1 + 2 - 3 OR 3 - 1". Note that the space of "1 + 2 - 3 OR 3 - 1" shown in section F is the union of the spaces represented in sections D and C. In section F, the OR symbol separates the "1 + 2 - 3" portion from the "3 - 1" portion. The solids and relationships of the first portion (1 + 2 - 3) do not influence the solids and relationships of the second portion (3 - 1).

REGION TABLE

For every component of the target which is being modeled, a region card(s) defines the shape and space of the component as a single solid or combination of several solids. On the region cards, the solids are referred to by their unique solid number and the combination symbols "+, -, OR" are used. The set of region cards which defines the components of the target is called the "Region Table." Figure C-23 displays the input format for the region card(s); a printout of the input cards required for a sample region (111); and a printout of the region cards that comprise the Region Table for the sample target.

The regions in the Region Table, as the solids within the Solid Table, are numbered consecutively; the first region is numbered "1", the second number "2", the third numbered "3", etc.

On Figure C-23, the sample region is numbered "111", implying that it is the one hundred and eleventh region in some Region Table. Two region cards are required to define our sample region "1 + 2 - 3 OR 4 OR 5 + 6 - 7 - 8 OR 9 - 10 + 11 + 12 OR 13". Any number of region cards may be required to define a region; however, only the first card contains the region number. Note that the region number "111" appears in card columns 3, 4, 5 only on the first card.

Card columns 70-80 (comments) on the region card may include any comments, but including an identification of the card is recommended when more than one card is required to define a region. For example, the comments "111-1" and "111-2" in columns 70-80 on the sample region cards mean "111" first (1) and second (2) card, respectively.

When the "OR" relationship is used in the definition of a region, "OR" must be punched in card columns 7-8 on the first region card. Note the "OR" after "111" on the first region card for the sample region. The sample region reads: "OR 1 + 2 - 3 OR 4 ... " which is the same as "1 + 2 - 3 OR 4 ... "; the introductory "OR" indicates to the GIFT5 geometry package that the "OR" relationship will be used in the description of the region.

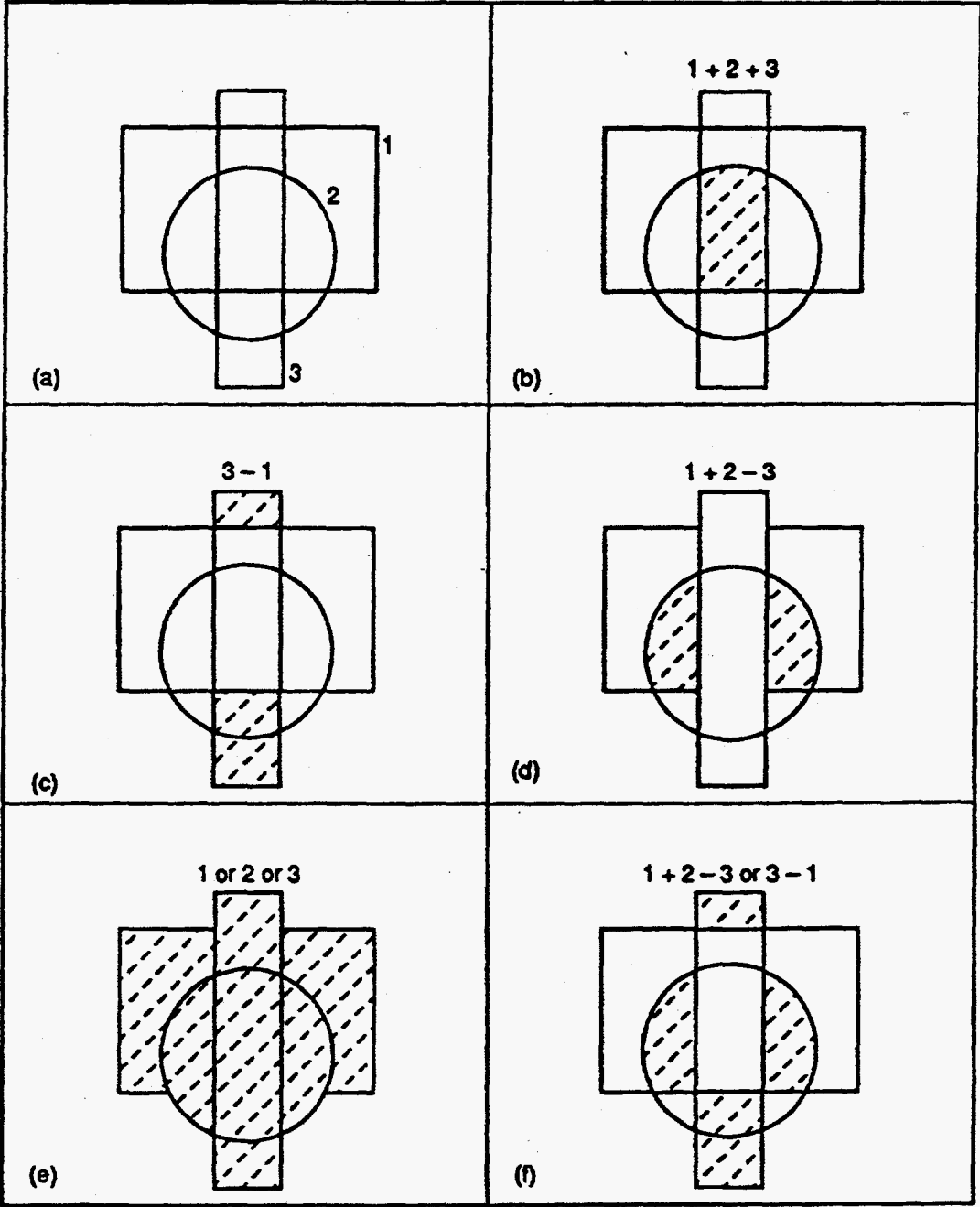


Figure C-22. Intersection, Subtraction, and Union Between Three Solids.

CARD COLUMNS

1-5	7-8	9-13	14-20	21-27	28-34	35-41	42-48	49-55	56-62	63-64	65-69	70-80
Region Number	OR	(±) Solid Number	(±) Solid Number	Comments

Card Format: (I5, 1X, 9(A2, I5), A1, 2A5)

Note: The first two card columns are reserved for OR if necessary, while the remaining five card columns are used for (±) Solid Numbers. For example: card columns 14 and 15 are for OR if needed while columns 16-20 are used for (±) Solid Numbers.

SAMPLE REGION INPUT FOR 1+2-3 OR 4 OR 5+6-7-8 OR 9-10+11+12 OR 13

```

111 OR      1      2      -3OR   4OR   5      6      -7      -8OR   9      111-1
              -10     11     12OR   13
    
```

REGION TABLE FOR THE SAMPLE TARGET

```

1          1      -2
2          2
3          3
4          4
5          5      -6      -19
6          6      -20     -19     -7      -8      -9      -10
7          7
8          8
9          9
10         10
11         11     -12
12
13         13     -15     -16     -17     -18
14         14     -13
15         15
16         16
17         17
18         18
19         19
20         20
-1
    
```

Figure C-23. Card Input for the Region Cards and the Region Table for the Sample Target.

On the region cards, the "+" symbol need not be punched. Reviewing the region cards for region 111 and the Region Table for the sample target, note that no "+" symbols are used. A non-punch or blank before a solid number implies the intersection (+) relationship.

There are twenty regions in the Region Table for the sample target, and the region numbers in the table are numbered consecutively (1 to 20). The last card (after region number "20" card) in the Region Table contains "-1" in card columns 4 and 5. The "-1 CARD", as it is called, is the flag or mark that indicates the end of the Region Table and must follow the Region Table.

RECOMMENDED PROCEDURES FOR THE REGION TABLE

The Solid Table for the sample target (Table C-2) contains twenty solids and the Region Table contains twenty regions (Figure C-23). The number of solids and the number of regions may be different; however, experience gained from modeling targets containing many solids has proven the usefulness of the following scheme. Note that region number "1" in the Region Table for the sample target begins with the solid number "1"; region number "2" begins with solid number "2"; region "3" with solid "3" ... region "20" with solid "20". Only region number "12" does not follow the pattern. In fact, region "12" sans any solid numbers is called a "dummy region" because no space is defined by the region. In a Region Table any number of "dummy regions" like region "12" may be used. A "dummy region" is a region card containing only a region number. Because the regions must be numbered consecutively, the purpose of region "12" is to maintain the pattern of region "13, 14, 15 ... 20" beginning with solid number "13, 14, 15 ... 20". When the region number is equal to the first solid number, it is easy to locate the components of the modeled target, to correct errors, and to modify the Solid and Region Tables. Using "dummy regions" and having the first solid and region number for non-dummy regions equal is recommended.

The Region Table for the sample target does not contain any "OR" or union relationships. The OR relationship between solids may be used but its usage is not recommended. (A later section of this appendix presents a technique which is logically equivalent to the "OR" relationship).

REGION IDENTIFICATION TABLE

The Region Identification Table assigns an identification (code) number to each region in the Region Table. Table C-3 exhibits a grouping of identification numbers from 1 to 998 used to identify the components of military vehicles - tanks, trucks, etc. Numbers from 1 to 99 are assigned to the regions in the Region Table which represent "personnel and miscellaneous interior components"; numbers from 100 to 199 are assigned to the regions in the Region Table which represent "armor and vehicle structure components";...; numbers from 900 to 998 are used to identify the regions in the Region Table which represent components that are "ammunition."

Table C-3. Identification Numbers Used for Vehicles and Air Regions within the Vehicles in the GIFT5 Geometry Package.

Identification Number	Components of the Target Vehicle
1 To 99	Personnel And Miscellaneous Interior Components
100 To 199	Armor And Vehicle Structure Components
200 To 299	Fuel Storage And Supply System Components
300 To 399	Miscellaneous Exterior Components
400 To 499	Armament (Not Ammo) Systems Components
500 To 599	Track Suspension System Components
600 To 699	Wheel Suspension System Components
700 To 799	Engine, Transmission, And Their Power Components
800 To 899	Environment And Safety Components
900 To 998	Ammunition
*501	Use For Track Only. Gift5 Generates 502 For Track Edge
*111	Use For Dummy Regions
*999	Never Use. Special Number For Gift5 Geometry Package

Identification Number	Components Of The Air Regions In Vehicles
01	Air In General. Gift5 Assigns "01" In Description Gaps
02	Crew Compartment Air For Vehicles
03	Passenger Compartment Air For Vehicles
05	Engine Compartment Air For Vehicles
10 To 98	May Use. No Special Usage Defined By Gift5
*09	Never Use. Special Number For Gift5 Geometry Package

* SPECIAL USAGE IDENTIFICATION NUMBERS

CARD COLUMNS

1-10	6-10	11-15	16-20	21-25	26-30	31-78
Region Number	Item Code Number	Air Space Code Number	Material Code	Percent Density		Alphanumeric Description of the Region

Card Format: (5I5, 5X, A48)

REGION	IDENTIFICATION	TABLE FOR THE	SAMPLE	TARGET	
1	40		STEERING WHEEL	1-2	TOR
2	41		STEERING SHAFT	2	ARB4
3	100		BODY FRONT	3	ARB5
4	100		BODY REAR	4	ARB8
5	101		BUBBLE	5-6-19	ELL
6	100		BODY CENTER	6-20-19-7-8-9-10	RPP
7	651		WHEEL RIGHT FRONT	7	RCC
8	652		WHEEL LEFT FRONT	8	RCC
9	653		WHEEL RIGHT REAR	9	RCC
10	654		WHEEL LEFT REAR	10	RCC
11	701		ENGINE	11-12	ARS
12	111		DUMMY REGION	0	RAW
13	31		MAN-TORSO	13-15-16-17-18	REC
14	31		MAN-HEAD	14-13	SPH
15	31		MAN-ARM	15	TEC
16	31		MAN-ARM	16	TEC
17	31		MAN-LEG	17	TRC
18	31		MAN-LEG	18	TRC
19		02	INSIDE AIR (BUBBLE)	19	ELL
20		02	INSIDE AIR (BODY)	20	BOX

Figure C-24. Card Input for the Region Identification Table and a Region Identification Table for the Sample Target.

Regions in the Region Table may also define spaces which represent air within and around a target or vehicle. For example, regions may define the air space where the crew members of a vehicle are (crew compartment air), the air space where the passengers are, and the air space surrounding the engine of the vehicle. Respectively, the identification numbers "02", "03" and "05" (shown in Table C-3) are assigned to these air spaces.

Figure C-24 presents the card input format and a printout of the Region Identification Table for the sample target. On the input cards, the region number is followed by either a component (item) or an air space identification (code) number; a region either models an item or it models an air space. In the Region Identification Table, regions 19 and 20 are identified as "02" air spaces, while region numbers 1 to 18 have item numbers. For example, Region 1 has been identified by component number "40", and represents the "steering wheel" as the comments on the region identification card indicate. The "1-2", also contained in the comment section of this card, is the Region Table description of region 1 where solid 1 is a "TOR". (The verbal and region description, and the solid type are contained in the comment section of the region identification cards for the other regions.) Comments should verbally describe and define the component or air space that the region models.

The user is not required to define any air spaces in the Region and Region Identification Tables. Air spaces are defined if the user wants to identify special air spaces within and

around the target such as the crew and engine compartment air. Regions 19 and 20 of the sample target identify the air space (02) inside of the sample target (a car). Regions 19 and 20 were included to illustrate air space usage; otherwise, regions 19 and 20 may have been omitted from the Region and the Region Identification Tables.

SPECIAL REGION IDENTIFICATION NUMBERS

In Table C-3 certain identification numbers are preceded by an asterisk (*); these identification numbers have specific meanings. **Never** use number "999" to identify a component and never use "09" to identify an air space.

The number "111" is used to identify the "dummy regions" in the Region Table. For example, for the sample target, region 12 is a dummy region; thus, it is identified by the special number "111". The last special identification number is "501"; this number is only used to identify regions that model the tracks of tracked vehicles. The "501" number is sometimes converted by the GIFT5 geometry package into "502", which indicates the edge of the track.

Users of the GIFT5 geometry package may use the identification system shown in Table C-3 or develop an original grouping scheme, but the usage of the special numbers (501, 111, 999 and 09 air) cannot change.

USING IDENTIFICATION NUMBERS TO "COMBINE" REGIONS

In Figure C-24, note that regions 13 to 18 have a common identification number (31), while regions 3, 4 and 6 have a common identification number (100). Regions with a common identification number are "combined" as the "OR" relationship combines solids. For example, because regions 13 to 18 are identified by the same code number (31), these regions are equivalent to the following single region: "13 - 15 - 16 - 17 - 18 OR 14 - 13 OR 15 OR 16 OR 17 OR 18".

It is recommended that the user not use the "OR" relationship, but use common identification numbers to combine regions. There are several reasons why it is more desirable to use the same identification numbers for several simple regions rather than use the OR relationship to create one large region. The computer run-time is increased when the OR relationship is used. It is easier to locate the parts of a component when they are defined by several regions with the same identification number. For example, regions 13 to 18 define the different parts of the man or the driver of the sample vehicle. If a user wanted to place a helmet on the man's head, the man's head is quickly identified to be region "14". If regions 13 to 18 were grouped into a single region by using the OR relationship, it would be harder to locate the head of the man. A user may be required to identify the different parts of the man such as his head, legs, arms, and torso. The users would only have to assign unique identification numbers to regions 13 to 18. If the man was a single region using the OR relationship, the user would be required to identify the parts of the man and then create new regions and region identification cards. The problems associated with the use of the OR relationship expand as the complexity of the target increases; therefore, it is recommended that the OR relationship not be used.

RULES FOR REGIONS

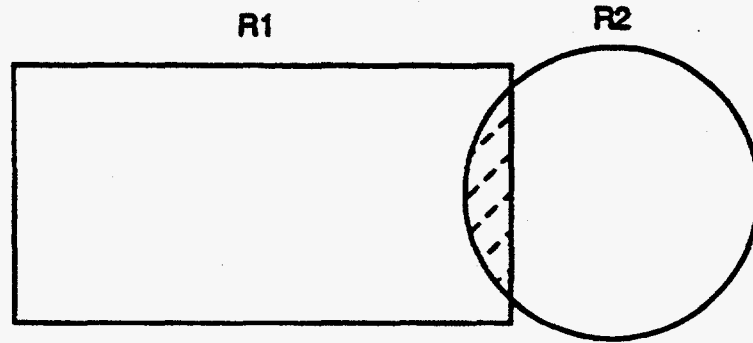
The Region Identification Table defines each region in the Region Table as either a component or an air space. Rules exist for regions that model components or items, while different rules apply for regions that define air spaces. Figure C-25 provides illustrations for the rules of the regions.

Section A of Figure C-25 exhibits two regions: R1 is a BOX and R2 is a SPH. The SPH and BOX are shown to overlap: the area of overlap contains dashed (/) lines. The three-dimensional SPH and BOX solids are represented on a two-dimensional plane; thus it is assumed that in depth they also overlap. If R1 is defined to be the space of the BOX, while R2 is the space of the SPH in a Region Table, and if R1 and R2 were identified in the Region Identification Table as components or items, then the only rule for regions that model components is violated - **REGIONS THAT MODEL COMPONENTS CANNOT OVERLAP**. In the physical world components cannot overlap or share a common space; thus, R1 and R2 cannot overlap if they model physical components. Regions that model components and overlap indicate errors either in the Solid Table data or in the Region Table data.

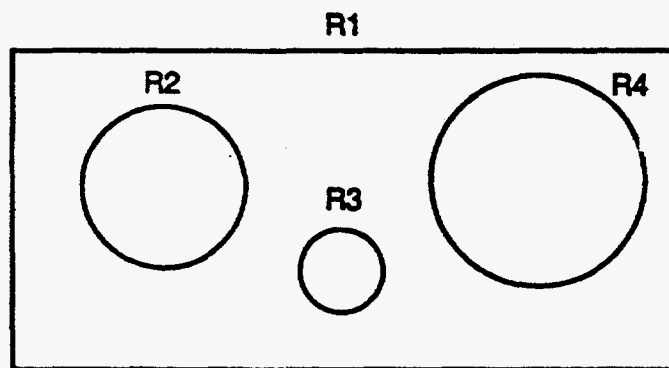
If R1 is the space of the BOX while R2 is the space of the SPH, and if R1 and R2 are identified as items, then they must be correctly defined in the Solid Table to assure that they do not overlap. It may be impossible to measure and record the BOX, SPH, or any solid parameters accurately enough to assure that the solids do not overlap. If the overlap is small, the user can modify the model of the regions: R1 can be redefined to be the BOX minus (subtract or less) (-) the space of the SPH, removing the space of the SPH that overlaps the BOX from the model of the BOX; or R2 can be modified in a similar manner to remove the overlap space of the BOX from the SPH. Solids can overlap, but regions identified as components cannot. In the next section of this appendix, it will be explained how the user can specify the amount of overlap between solids to be ignored by the GIFT5 geometry package.

Section B of Figure C-25, displays four regions: R1 is a BOX while R2, R3 and R4 are SPH's. The rules for regions identified in the Region Identification Table as air spaces are different from the rules of the regions identified as components. If R1 is identified in the Region Identification Table as an air space while R2, R3 and R4 are identified as components, then region R1 can be defined as the space of the BOX. **REGIONS IDENTIFIED AS AIR SPACES CAN OVERLAP ANY REGIONS IDENTIFIED AS COMPONENTS**. Imagine R1 as a BOX that defines the air in a rectangular room, while R2, R3, R4 are components within the room. The BOX or R1 would define the space of the air in the room and R2, R3, R4, would be components within the air space (R1) of the room. If R1, R2, R3, and R4 were all identified in the Region Identification Table as components, then to avoid overlap, R1 would have to be defined as the space of the BOX less or subtracting (-) the solids that define the space occupied by regions R2, R3, and R4.

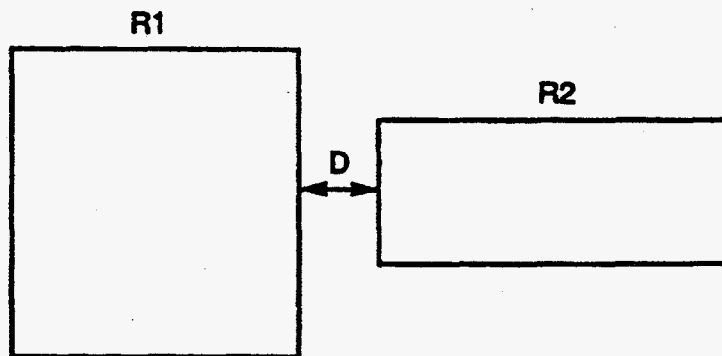
Examining the Solid Table, the Region Table and the Region Identification Table for the sample target, note that both regions 19 and 20 are identified as 02 air space and the spaces defined by regions 19 and 20 overlap each other. **REGIONS IDENTIFIED AS AIR SPACES CAN OVERLAP REGIONS WITH THE SAME AIRSPACE IDENTIFICATION CODE NUMBER.**



SECTION A



SECTION B



SECTION C

Figure C-25. Illustrations for Region Rules.

REGIONS WITH AIRSPACE CODE NUMBERS CANNOT OVERLAP REGIONS WITH DIFFERENT AIR SPACE CODE NUMBERS. If region 19 of the sample target was identified in the Region Identification Table with any air space code number other than 02, and region 20 retained its 02 code number, then regions 19 and 20 could not overlap.

GIFT5 GEOMETRY PACKAGE MEMORY REQUIREMENTS AND REGION TOLERANCES

The GIFT5 geometry package is not flexibly dimensioned. As such, changes have to be made to the main program to accommodate large target descriptions or different tolerance values for the target description. There are two specific lines within the GIFT5 geometry package that specify the memory size, and two specific lines that give the default values for region tolerances for the target description data.

Lines "COMMON ASTER (5000)" and "NDQ=5000" specify the amount (5000) of words of memory storage reserved for the target description data: Solid, Region, Region Identification Tables, and other geometric data that are stored in the computer's core memory. The memory size required for a given target description is difficult to compute because a large number of factors must be considered. A crude estimate of the amount of memory words of storage required is 45 times the number of solids in the target description data.

The "5000" memory words indicated on the printout is large enough for the sample target; however, the "5000" words would not be large enough for a target description containing hundred of solids and regions. If a target description has 1000 solids, then 45 times the number of solids (1000), or 45,000 words, is a crude estimate of memory requirements. To run the 1000 solid target description, the user must change the "COMMON ASTER (5000)" line to "COMMON ASTER (45000)" and the "NDQ=5000" line to "ND=45000". If 45,000 words is insufficient, then one of the following statements will be outputted depending upon what data was being stored when the memory was exceeded: 1) NO MORE ROOM FOR SOLID DATA, 2) NO MORE ROOM FOR REGION DATA, 3) NO ROOM FOR IDENTIFICATION TABLE, 4) NO ROOM FOR WORKING STORAGE. Working storage is the memory required to perform the calculations of the GIFT5 geometry package. If one of the above statements is output, then the numeric value of the "COMMON ASTER" and "NDQ=" lines must be enlarged to store the target description data.

Section C of Figure C-25 illustrates two regions, R1 and R2, and a distance "D" between the two regions. Suppose that D is a small distance between R1 and R2 that occurred because the input parameters for the solids which define R1 and R2 could not be measured and recorded accurately enough. The GIFT5 geometry package allows the users to specify the gap distance "D" between item and air regions to be ignored or tolerated. TOL is the overlap tolerance, while TOLLOS is the gap tolerance. The value of 0.0001 is one ten-thousandth of the unit of measurement (inches, centimeters, etc.) used in the target description model. For most target descriptions, the "TOL=0.0001" and "TOLLOS=0.0001" lines are replaced by "TOL=0.01" and "TOLLOS=0.01" or one hundredth of the unit of measure is the tolerance used. The user can decide and set the numeric values of TOL and TOLLOS to be used with his target description data.

REGION RPP TABLE

An RPP solid (see Figure C-15) can be defined to enclose or contain the space or volume of any region. The minimum and maximum X, Y, and Z coordinate values (XMIN, XMAX, YMIN, YMAX, ZMIN and ZMAX) of the RPP solid that encloses a region may be interpreted as follows: The region is located between XMIN and XMAX, is between YMIN and YMAX, and is between ZMIN and ZMAX. Figure C-26 presents the card input format and a printout of the Region RPP Table for the sample target.

The first card of the Region RPP Table for the sample target states that region number "1" is enclosed by an RPP with XMIN=20.0, XMAX=23.0, YMIN=-10.0, YMAX=10.0, ZMIN=28.0, and ZMAX=46.0. Note that the sample table does not include a card input for region "12" because region "12" is a "dummy region." Region "2" modeling the steering shaft or any region may be omitted from the Region RPP Table. In fact, no Region RPP Table is required because the GIFT5 geometry package computes a set of enclosing RPP values (XMIN, XMAX, YMIN ... ZMAX) for any region in the Region Table not included in the Region RPP Table.

The option to input enclosing RPP values for some or every region is provided because the GIFT5 geometry package may not compute a "desirable" set of RPP values. For example, an RPP with XMIN, YMIN, and ZMIN values of -200.0 and XMAX, YMAX, ZMAX values of 200.0 would enclose every region of the sample target; however, the region RPP values on Figure C-26 define smaller volumes or spaces and are "better fitting" enclosing RPP's and thus more desirable RPP values. For most regions, the GIFT5 geometry package computes a good enclosing RPP; however, the computed enclosing RPP values for a few regions can be improved. The smaller the volume or the better fit of the RPP that encloses a region, the shorter the computer run time for the GIFT5 geometry package.

THE TITLE AND TARGET SPECIFICATION CARDS

To complete the target description, two additional cards are required - the Title Card and the Target Specification Card. Figure C-27 exhibits the card input for these cards.

The Title Card contains the name of the target, the date the model was prepared, the units of measure used in the model, and any other important information on the modeled target. Only the first 65 card columns of the Title Card are read by the GIFT5 geometry package; however, card columns 66 to 80 may contain additional information on the target.

The Target Specification Card contains the number of solids and the number of regions used to model the target.

CARD COLUMNS

1-10	11-20	21-30	31-40	41-50	51-60	61-70	Number of Cards
Solid Number	Xmin	Ymin	Zmin	Xmax	Ymax	Zmax	1 of 1

Card Format: (I10, 6F10.0)

REGION RPP TABLE FOR THE SAMPLE TARGET

1	20.0	23.0	-10.0	10.0	28.0	46.0
2	21.0	40.0	-6.0	6.0	33.0	44.0
3	74.0	101.0	-36.0	36.0	12.0	48.0
4	-101.0	-74.0	-36.0	36.0	12.0	48.0
5	-25.5	25.5	-15.5	15.5	45.0	63.0
6	-75.0	75.0	-36.0	36.0	12.0	48.0
7	47.0	72.5	-36.0	-28.0	0.0	24.0
8	47.0	72.5	28.0	36.0	0.0	24.0
9	-72.5	-47.0	-36.0	-28.0	0.0	24.0
10	-72.5	-47.0	28.0	36.0	0.0	24.0
11	-70.0	-30.0	-20.0	20.0	15.0	45.0
13	-5.0	5.0	-7.5	7.5	24.0	52.0
14	-5.5	5.5	-5.5	5.5	52.0	57.0
15	0.0	20.0	-10.0	-5.5	35.0	52.5
16	0.0	20.0	5.0	10.0	35.0	52.5
17	-3.5	31.0	-8.0	-1.0	12.0	30.0
18	-3.5	31.0	1.0	8.0	12.0	30.0
19	-24.5	24.5	-15.0	15.0	34.0	62.0
20	-75.0	75.0	-35.0	35.0	13.0	47.0

Figure C-26. Card Input for the Region RPP Table and the Region RPP Table for the Sample Target.

TITLE CARD

CARD COLUMNS

1-2	3-5	6-65
Target Units		Alphanumeric Description of the target: including title, date prepared, etc.

Card Format: (A2, 3X, A60)

TARGET SPECIFICATION CARD

CARD COLUMNS

1-5	6-10
Number of Solids in the Solid Table	Number of Regions in the Region Table

Card Format: (2I5)

Figure C-27. Card Input for the Title Card
and Target Specification Card.

CARD ORDER FOR THE TARGET DESCRIPTION INPUT

The order of the card input for the target description data is as follows. The first card is the Title card, followed by the Target Specification card. Next comes the Solid Table - as required by the target description. Be sure the number of solids on the Target Specification card match the number of solids in the Solid Table. Next comes the Region Table - as required by the target description. Again, make sure the number of regions on the Target Specification card match the number of regions in the Region Table. The Region Table is followed by the Region RPP Table. This Table is not required and usually not input. Finally, the Region RPP Table (or Region Table if the Region RPP Table is omitted) is followed by the Region Identification Table. Note that the Region Table is followed by the "-1 Card" while a blank card follows both the Region RPP and the Region Identification Tables. If no Region RPP cards are used, the blank card indicating the end of the Region RPP Table will follow the "-1 Card".

REFERENCES

1. W. A. Rhoades, "Development of a Code System for Determining Radiation Protection of Armored Vehicles (The VCS Code)," ORNL-TM-4664, Oak Ridge National Laboratory, (October 1974).
2. W. A. Rhoades, et.al., "Vehicle Code System (VCS) User's Manual," ORNL-TM-4648, Oak Ridge National Laboratory, (August 1974).
3. Lawrence W. Bain, Jr. and Mathew J. Reisinger, "The GIFT Code User Manual; Volume I. Introduction and Input Requirements," BRL 1802, Ballistic Research Laboratory, (July 1975).
4. Gary G. Kuehl, Lawrence W. Bain, Jr. and Mathew J. Reisinger, "The GIFT Code User Manual; Volume II. The Output Options," ARBRL-TR-02189, Ballistic Research Laboratory, (September 1979).
5. A. E. Rainis and Ralph E. Rexroad, "MIFT: GIFT Combinatorial Geometry Input to VCS Code," BRL 1967, Ballistic Research Laboratory, (March 1977).
6. J. A. Stoddard, S. D. Egbert, and W. D. Scott, Jr., "The Vehicle Code System with In-Group Energy Bias and GIFT5 Geometry," DNA-TR-87-23, Science Applications International Corporation, (January 1987).

APPENDIX D
DRC2 VERIFICATION AND VALIDATION TEST PROBLEM SUITE

DRC2 VERIFICATION AND VALIDATION TEST PROBLEM SUITE*

Test Problem 1: Free-Field Fluence Calculation

For this test problem, a 2-group DORT¹ calculation is performed for a point source in air 300m above a purely absorbing medium. Then an adjoint MASH² calculation is performed for a 1 cm × 1 cm × 50.5 cm air box over a purely absorbing medium ("ground") with the detector located at the x-y center of the box 50 cm above "ground" [i.e., at the coordinate location (100.0,0.0,50.0)]. Coupling of the forward fluences with the adjoint leakages is performed with DRC2 and the results are compared with the free-field fluences also calculated by DRC2. Logarithmic interpolation of the VISTA fluences is used.

This problem is intended to demonstrate whether the coupled calculation reproduces the free-field fluences calculated by DORT. The DORT calculation file, MASH calculation file, and DRC2 calculation file can be found in the DRC2 documentation.

The DORT and DRC2 fluences are compared in Table 1 for 25,000 and 105,000 MASH histories. For the two cases, the last six range/orientation combinations shown in Table 1 correspond to VISTA R-mesh locations and the detector is at a VISTA Z-mesh location. Hence, the free-field fluences should be calculated almost exactly at these range/orientations. The results show that the free-field fluences are reproduced within about 4%. Also, since the system is very small in its x and y dimensions, the inclusion of x-y fluence dependence in the coupling did not significantly influence the results. There is only the slightest variation due to the small distance of the escape surface from the detector point.

The agreement of the coupled results with the DORT free-field results did not improve with the increased number of histories. However, as noted in Table 1, the fractional standard deviations (fsd's) of the results were cut in half in most cases from the range 0.018-0.035 to the range 0.010-0.014. The DRC2 results generally fall within three fsd's about the DORT results.

There were only two scatterings in the air in the small box for the 25,000 history case and only one for the 105,000 history case. The scatterings were undersampled, but those few scatterings should not have contributed much to the fluence, since scatterings below the detector point must direct the neutron upward for it to contribute significantly (the upward-directed angular fluence in the air from 0 to 50 cm above the purely absorbing medium should be much smaller than the downward-directed angular fluence).

Test Problem 2: Metric Doghouse

The second test case is a two-group calculation of detector responses within a 3 m × 1 m × 1 m building with 5-cm-thick side walls and a 10-cm-thick roof all composed of purely absorbing material and a 1 m-wide doorway along and at one end of the 3 m wall (X dimension). A drawing of the building is shown in Figure 1. The detector is centered on the doorway and at the Y center of the room. This problem was calculated mainly to compare

*C. O. Slater, "DRC2: A Code with Specialized Applications for Coupling Localized Monte Carlo Adjoint Calculations with Fluences from Two-Dimensional R-Z Discrete Ordinates Air-Over-Ground Calculations," ORNL/TM-11873, Oak Ridge National Laboratory, (January 1992).

results with those obtained with DRC for this same test problem. The DORT calculation file, MASH calculation file*, and DRC2 calculation file can be found in the DRC2 documentation. The DORT calculation used a 30 direction quadrature set (S_6) and a P_3 cross-section Legendre expansion. For this problem, the coupling surface is at the outside of the building. Rigorous calculations using forward and adjoint coupling require that the coupling surface be located at such a distance from the object (building, vehicle, etc.) that there is no significant perturbation of the free-field fluence by the object. In practice, if the object is small, the coupling surface may be located very close to the object. The effect the metric doghouse, with its purely absorbing walls, has on the inward-directed free-field fluences at the house outer surface is not known. Certainly, fluences incident on surfaces hidden from direct view of the source will be perturbed. The contributions of those fluences to the calculated response may be small, however, because the fluences are basically forward peaked.

Protection factors calculated by DRC2 are compared in Table 2 for coupling with and without x-y dependent forward fluences and both without and with in-group biasing (INGB=0 or 1, respectively). It is noted that for this small system, x-y dependent coupling influenced the answers very little. A greater difference is shown between results without in-group biasing and those with in-group biasing. Also note that DRC gave essentially the same result as the no X-Y dependence DRC2 at the one point indicated in Table 2, differing by only 0.05% for both INGB=0 and INGB=1. Fractional standard deviations ranged from 0.015 to 0.029.

Test Problem 3: Large (30m × 6m × 3m) Steel-Topped Concrete Building

The third test case is a 69-group (46 neutron and 23 gamma-ray) calculation of detector responses in a large (30 m long by 6 m wide by 3 m high) steel-topped concrete building. The side walls of the building are 20 cm thick and are composed of ordinary concrete. The floor is a 10-cm-thick slab of borated concrete and the roof is a 10-cm-thick steel slab. There are two doorways, two windows, an interior partial concrete wall, and an opening in the roof. Drawings of the building are shown in Figures 2 and 3. Figure 3, with the roof removed, shows the interior of the building. The detector position is near a window and the interior partial wall so that it may be shielded by the wall or exposed by the window or the roof opening, depending on the orientation. The system rotation point is at $x=1500$ cm and $y=300$ cm.

This problem is intended to test the effects on calculated responses of including x-y dependence in the coupling calculation. While the building may occupy only one DORT radial mesh interval or portions of two, the variation of the fluence across the expanse of the building could be significant.

The source for the calculation is a point source at zero radius and 300 m above the ground. It consists of prompt neutron and gamma-ray fission sources obtained by extrapolating and regrouping data from Ref. 3 and combining without regard to normalization except that all values were multiplied by 10^{15} . The tissue dose response function was obtained from the DABL69⁴ response function set. A 240 direction quadrature set and the DABL69 cross section library with a P_5 Legendre expansion were used.

*This file also contains input for an air-over-ground free-field fluence calculation using a larger air box than that used in Test Problem 1. Results from this calculation were superseded by those reported in Test Problem 1.

Table 3 is a comparison of neutron and gamma-ray tissue dose protection factors calculated with DRC2 using x-y dependent coupling with those calculated by DRC2 using no x-y dependent coupling. At close range (26.73 m) and an orientation (172.5 deg.) where the detector position is partially exposed due to the roof opening, the neutron and gamma-ray protection factors calculated with x-y dependent coupling show a greater than 10% difference from the result with no x-y dependent coupling. At distant ranges, the 180 deg. orientation gives the largest differences in the protection factors, probably because of the exposure provided by the roof opening. Although the neutron protection factors differ by less than 5%, the gamma-ray protection factors at two range/orientations differ by greater than 10%.

Even though differences in neutron protection factors were less than 5% at distant ranges, Table 4 shows that the calculated neutron doses can differ by greater amounts. The protection factors tend to differ less than the fluences or doses because the division of the free-field quantities by the shielded quantities cancels errors in both quantities, particularly when there is not much spectral shift in the important energy regions. Fractional standard deviations of the cited results are in the range 0.027 to 0.059 with x-y dependent coupling and 0.027 to 0.049 without x-y dependent coupling.

Test Problem 4: BREN Six-House Cluster

The fourth test case involves the calculation of neutron and gamma-ray dose rates and protection factors at a detector location within a BREN six-house cluster. A picture of the cluster (from Ref. 5) is shown in Figure 4. A plan view of the cluster is shown in Figure 5. The detector locations identified on the figure have no meaning for this test problem. The box enclosing the local system geometry is about 25.4 m \times 25.3 m \times 10.2 m. Overall, this system is larger than that for test problem 3. However, because VISTA fluences were available for only four radial locations and these were 300 to 500 m apart, the entire system can fit within one interval between the VISTA fluence points (The fluences were obtained from a file created by W. A. Rhoades). The ranges were chosen at the VISTA fluence locations; hence for a given range, the calculated fluences incident on the system may involve up to three of the VISTA fluence radial points in the interpolation of the fluences. Logarithmic interpolation of the fluences was used.

For a rotation point at the center of the system, the surface points are removed from the VISTA fluence points by at most about 6% of the distance between adjacent points. Thus, the x-y dependent fluence values should be 94 to 100% of the VISTA fluence values when linear interpolation is used and one could expect little difference between results obtained with x-y dependent coupling and those obtained with no x-y dependent coupling. For the fluence differences over the given ranges, logarithmic interpolation should also show small differences between the x-y dependent and the no x-y dependent results.

Table 5 compares soft tissue kerma total protection factors calculated by DRC2 using x-y dependence in the coupling operation to those calculated by DRC2 without using x-y dependence in the coupling operation. All differences are essentially 3% or less. Table 6 compares DRC and DRC2 calculated soft tissue kerma total protection factors. Differences less than 3% are observed here also. Finally, Table 7 compares DRC and DRC2 calculated soft tissue kerma values. The differences are generally larger than those observed for the protection factors, but they fall within the 6% variation in the incident fluence over the surface of the system mentioned above. With no x-y dependent coupling, DRC2 gives the same results as DRC. Fractional standard deviations of total quantities ranged from about 0.01 to 0.06. The uncertainties associated with the dose due to capture gamma rays in the houses were generally greater than 30%.

A computation charge comparison between DRC and DRC2 was also made for this test problem. A separate DRC calculation was performed for each range, but results for all four orientations were obtained from a single calculation. The DRC2 calculation was performed for all ranges and orientations in a single pass through the code. In addition, the core allocation was large enough that fluence data for all groups could be stored in core during coupling (430,000 words were allocated versus slightly more than 423,000 required). The DRC core allocation was fixed at 150,000 words. Both the DRC and DRC2 calculations were performed for two source conditions, and DRC2 performed the calculations with and without x-y dependence of the forward fluence during coupling. For these calculational conditions, the DRC to DRC2 charge ratios for the case of no x-y dependence in the DRC2 coupling were 1.90, 2.34, 0.65, and 1.79 for CPU, IO, memory, and total charges, respectively. The respective ratios for the case with x-y dependence in DRC2 were 1.91, 3.23, 0.76, and 1.88. IO and memory charges for a DRC2 calculation having no x-y dependence in the coupling with one of the sources appeared to be anomalous. The IO charge was 75% higher than that for the x-y dependent coupling case with the same source and 80% higher than that for both no x-y and x-y dependent coupling with the other source. Smaller differences were noted for the memory charges. The memory charge was 37% higher than that for the x-y dependent coupling case with the same source and 25% higher than that for both no x-y and x-y dependent coupling with the other source.

From the above time comparisons, it would appear that DRC2 has a distinct advantage in all categories except memory, for which DRC has a slight advantage. The larger memory charge for DRC2 may be attributed to the greater amount of storage allocated (280,000 more words than DRC). Also, it can be noted from the above data that the IO and memory charges can fluctuate significantly between similar calculations (compare the no x-y dependent versus the x-y dependent cases). While the CPU charges are about the same for the two DRC2 cases, IO charges differ by about 38% and memory charges differ by about 17%.

Test Problem 5: Large Radius, Air-Filled, Annular, Cylindrical Concrete Tunnel

The fifth test case involves the calculation of neutron and gamma-ray fluences and doses within a large-radius, 9.8 m wide, air-filled, annular, cylindrical concrete tunnel. The concrete walls surrounding the tunnel are 20 cm thick, and the tunnel is centered at a radius of 3.45×10^4 cm. A sketch of the problem geometry is shown in Figure 6. The geometry for the calculation is such that DORT should be able to calculate the desired quantities.

Therefore, the DRC2-calculated results can be compared against reasonably well-known quantities and the accuracy of the DRC2 coupling process can be established.

Again, the DABL69 group structure that was used in test problem 3 is used here. The source and cross-section library are the same. An S_{12} quadrature (96 directions) was used initially rather than the 240-direction quadrature. However, the 240-direction quadrature is used in the final analysis, mainly to aid in the transport down range of secondary gamma rays produced near the source. In addition, two air-layer thicknesses are used in the MASH calculations (10.8 m and 50 m). A mean-free-path in the air mixture ranges from 19 to 171 m for neutrons and 4.3 to 460 m for gamma rays. The optical thickness of the thicker air layer is several mean-free-paths for several neutron and gamma-ray groups. Hopefully, this layer is thick enough that the presence of the concrete tunnel would not perturb the free-field fluence at the system boundaries.

The DRC2 results obtained by folding adjoint leakages and forward fluences are compared to the DORT-calculated results in Table 8. Fractional standard deviations of the results are also given. With the 10.8-m-thick air layer, both the x-y dependent and no x-y dependent DRC2 results are reasonably close to the DORT results. The results without x-y dependence are slightly lower. An analysis of the DRC2 results showed a significant contribution to the gamma-ray fluence and dose from the production of secondary gamma rays in the regions around the tunnel. As shown in the Table 8, all fractional standard deviations are less than 0.07 for the 10.8-m-thick air layer.

When one compares the results for the 50-m-thick air layer to those for the 10.8-m-thick air layer, one finds that overall agreement for the 50-m-thick air layer results improves for the x-y dependent coupling case. In particular, excellent agreement is achieved for the neutron and gamma-ray fluences, but the agreement for the doses worsens slightly. Perhaps, the better agreement for the fluences may be attributed to the adjoint source being a fluence response function. The results obtained with no x-y dependence in the coupling operation are lower than the DORT results by 14 to 25%. Fractional standard deviations range from 0.034 to 0.085. The good agreement between the DRC2 x-y dependent results and the DORT results give added confidence in the correctness of the DRC2 coupling procedure.

As mentioned above, (Section 6.2) the air layer around the object should be thick enough that the fluence at the boundary of the air layer is not perturbed by the presence of the object. Since the 50-m-thick air layer led to better overall agreement with DORT than did the 10.8-m-thick air layer, perturbations to fluences at system boundaries with those air layer thicknesses were examined. Table 9 shows the maximum percent differences between the above-ground perturbed and unperturbed neutron and gamma-ray total fluences as a function of leakage surface. The six surfaces shown represent the leakage surfaces used in the MASH calculations (i.e., a top and inner and outer radial surfaces bounding either a 10.8-m-thick or a 50-m-thick air layer surrounding the concrete tunnel). One can see that there is much more perturbation for the 10.8-m-thick air layer surfaces. The outer radial surface shows greater differences because the tunnel partially shields some points on that surface.

For the top surface, the perturbation is significant for the 10.8-m-thick air layer but is much less for the 50-m-thick air layer. There is probably less perturbation of the inward-directed fluences than that shown in Table 9.

It should be noted that the results for the MASH calculations were quite sensitive to the GWLO values input. In addition, the value of NMOST had to be increased for some changes in GWLO due to "imaxn" being exceeded. Therefore, to eliminate the requirement for having to input these values and to guard against inappropriate selections of the parameters, the calculations were performed as if they were neutron only and a modified version of the MASH code (called MASHY) sorted the various collision or pseudo-collision events. This required an additional input card following the last MASH input card (the air and ground media identifiers). The input is free form; hence, the data should be preceded by '\$\$' in columns 2 and 3. The two entries on the card are:

jptyp	a signal to indicate no effect if 0 or a coupled problem run as neutron-only if 1, and
jprigp	the number of neutron groups.

The code calculates the gamma-to-neutron transfer probabilities through the cross-section scattering matrix. MASHY uses the above parameters along with old and new group numbers to determine when a gamma-to-neutron transfer has occurred at real scattering events.

Finally, the change to a 240-direction quadrature and the inclusion of the thicker air layer in the MASH calculation led to a very large data storage requirement in DRC2. Nearly six million words would be required to store all data in core (i.e., data for 69 groups, 200 nonzero weight directions, 10 i mesh, and 42 j mesh). The DRC2 calculation was performed with a core allocation of three million words. While a CPU charge of about two minutes was required for the four calculations (for two coupling surfaces with and without x-y dependence during coupling), large memory and IO charges resulted in a total charge of about 30 minutes. For the DRC2 calculation of the perturbed fluence by integration of the perturbed DORT-VISTA angular fluences, the total charge was only about three seconds.

REFERENCES

1. Rhoades and R. L. Childs, "The DORT Two-Dimensional Discrete Ordinates Transport Code," *Nucl. Sci. & Eng.* **99**, 1, 88-89 (May 1988).
2. J. O. Johnson, editor, "A User's Manual for MASH 1.0 - A Monte Carlo Adjoint Shielding Code," ORNL/TM-11778 (in publication).
3. D. E. Bartine, J. R. Knight, J. V. Pace, III, and R. Roussin, "Production and Testing of the DNA Few-Group Coupled Neutron-Gamma Cross-Section Library," ORNL/TM-4840, (1977).
4. D. T. Ingersoll, R. W. Roussin, C. Y. Fu, and J. E. White, "DABL69: A Broad-Group Neutron/Photon Cross-Section Library for Defense Nuclear Applications," ORNL/TM-10568 (1989).
5. W. C. Roesch, ed., "US-Japan Joint Reassessment of Atomic Bomb Radiation Dosimetry in Hiroshima and Nagasaki," Vol. 1, Radiation Effects Research Foundation, Hiroshima, Japan, 1987.

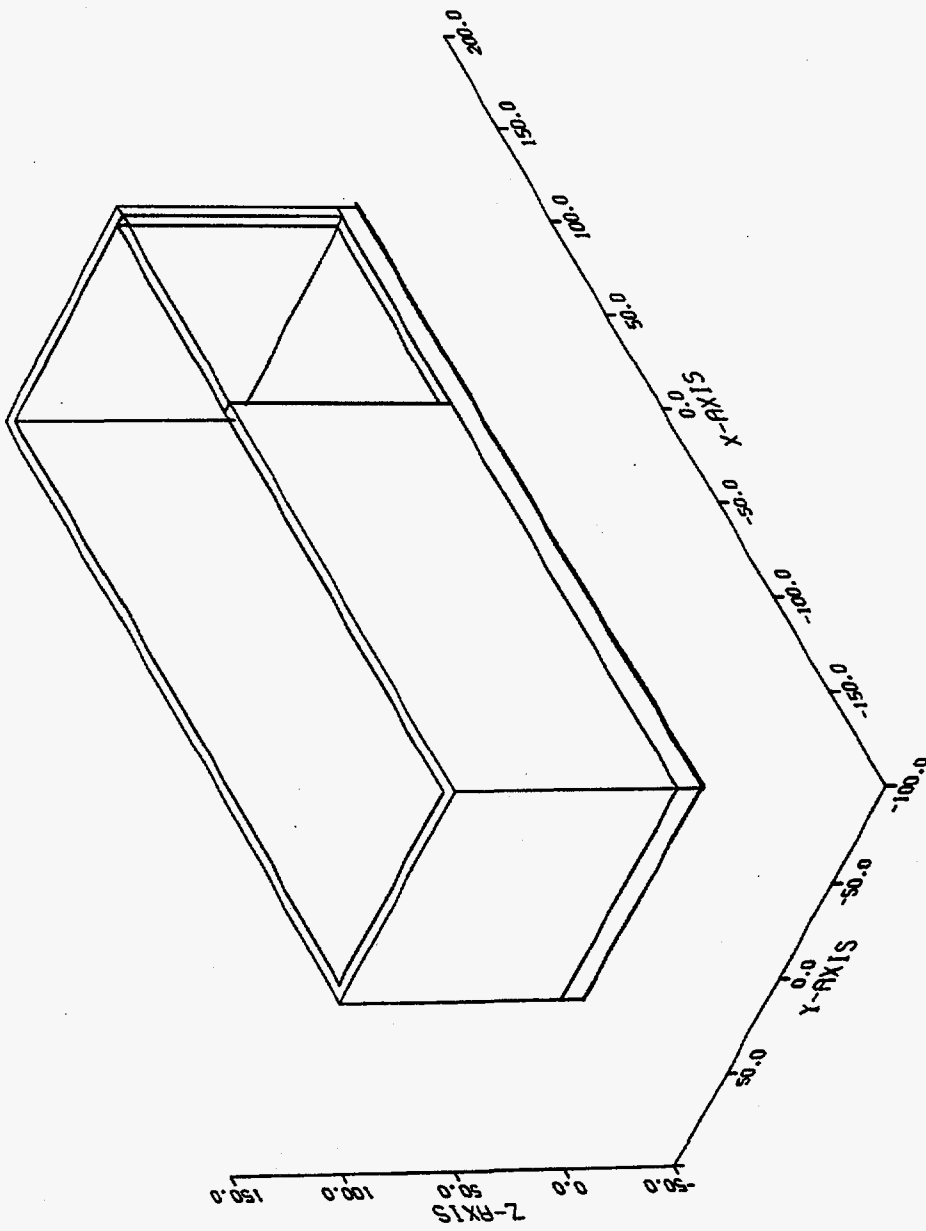


Figure D-1. Geometry for Test Problem 2: Metric Doghouse

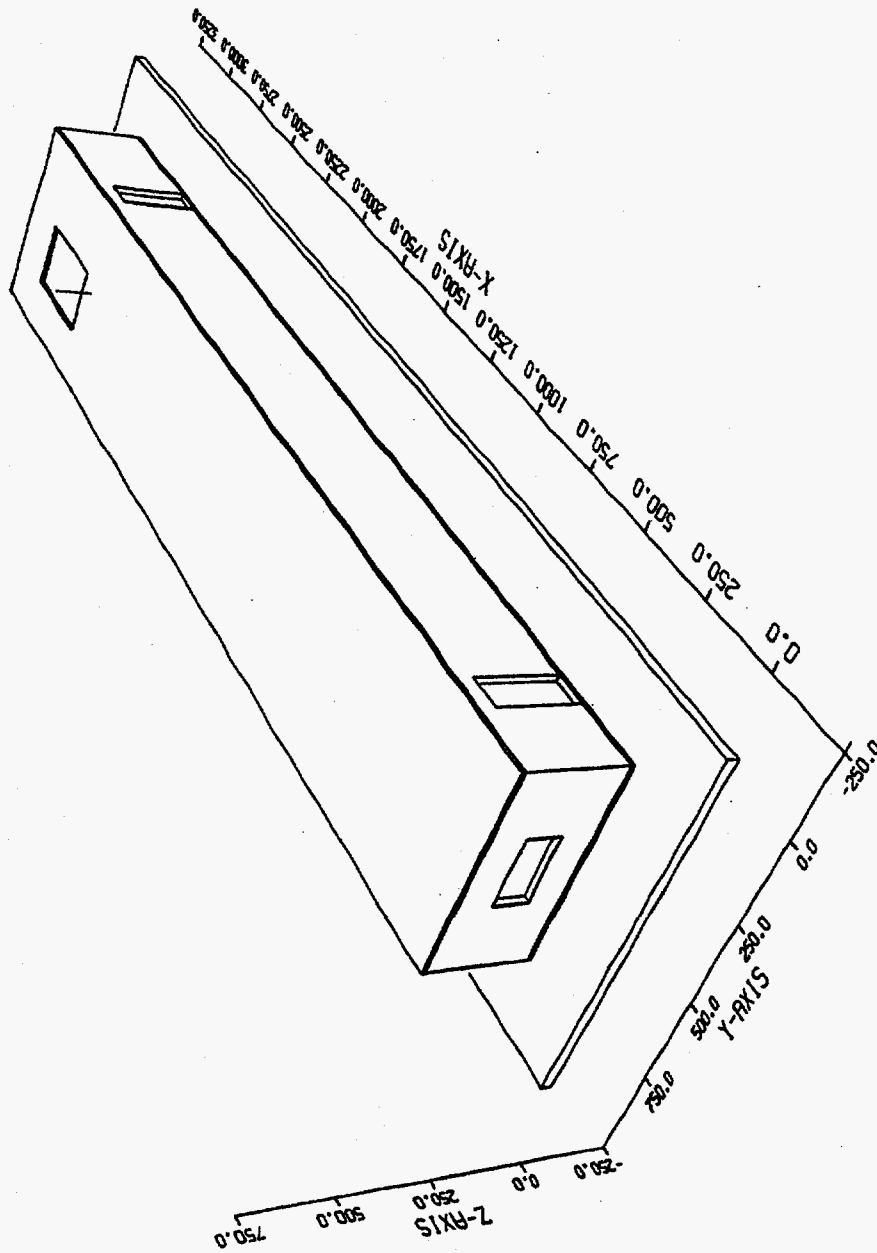


Figure D-2. Exterior View of the Geometry for Test Problem 3: Large, Steel-Topped Concrete Building

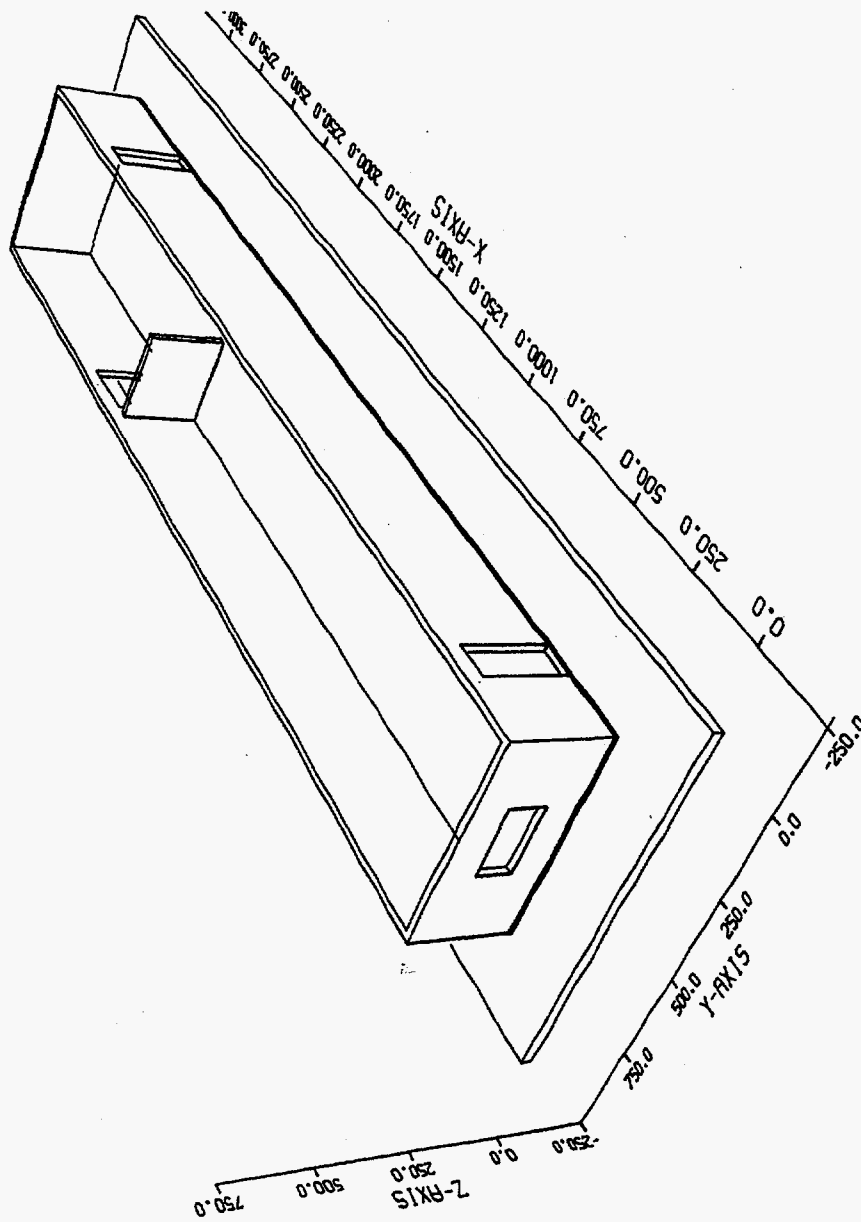
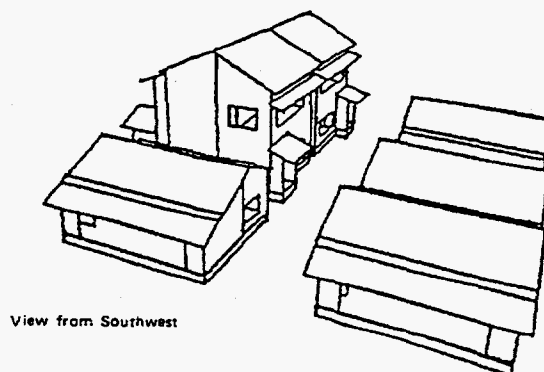
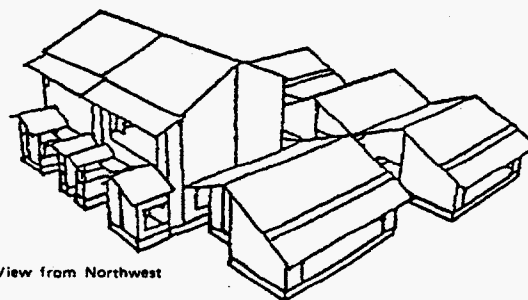


Figure D-3. Interior View of the Geometry for Test Problem 3: Large, Steel-Topped Concrete Building.



View from Southwest



View from Northwest

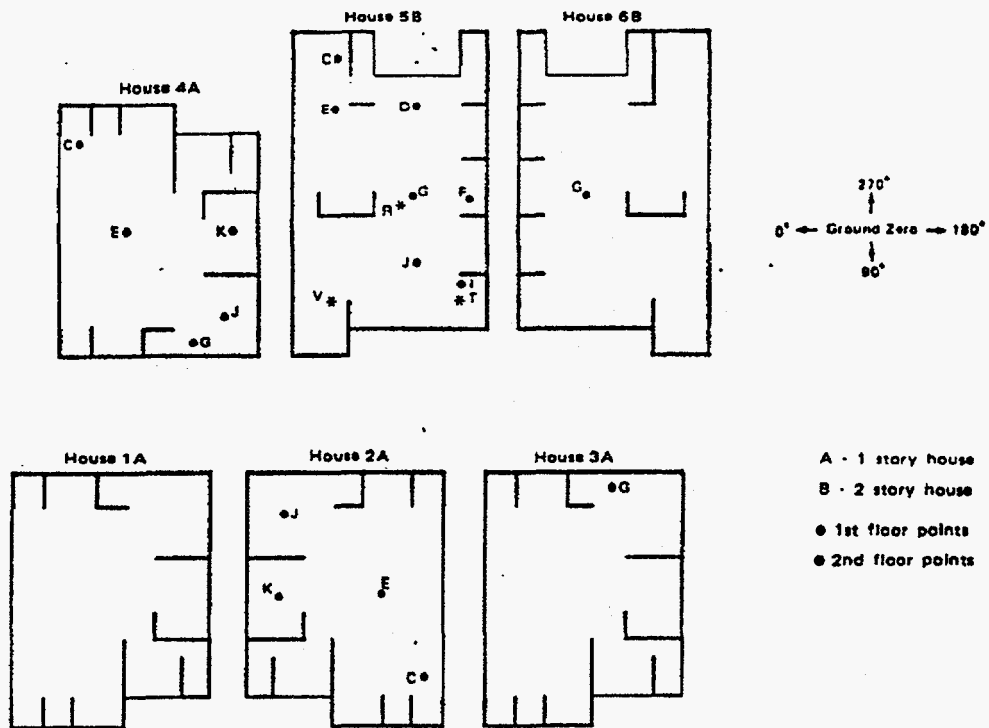
Combinatorial geometry of the six-house cluster model

Dimensions of Model Japanese Houses (cm)

House Type	Roof Peak	Length	Width	Second Story Floor Height	Partition Height
Single story house A	475	872	700	-	270
Two story house B	915	858 ^a	675	400	315
Tenement (one unit)	860	700 ^a	500	360	300

^aMain portion of house

Figure D-4. Geometry for Test Problem 4: BREN Six-House Cluster.



Plan of the six-house cluster showing location of detectors

Figure D-5. View of the Geometry for Test Problem 4: BREN Six-House Cluster.

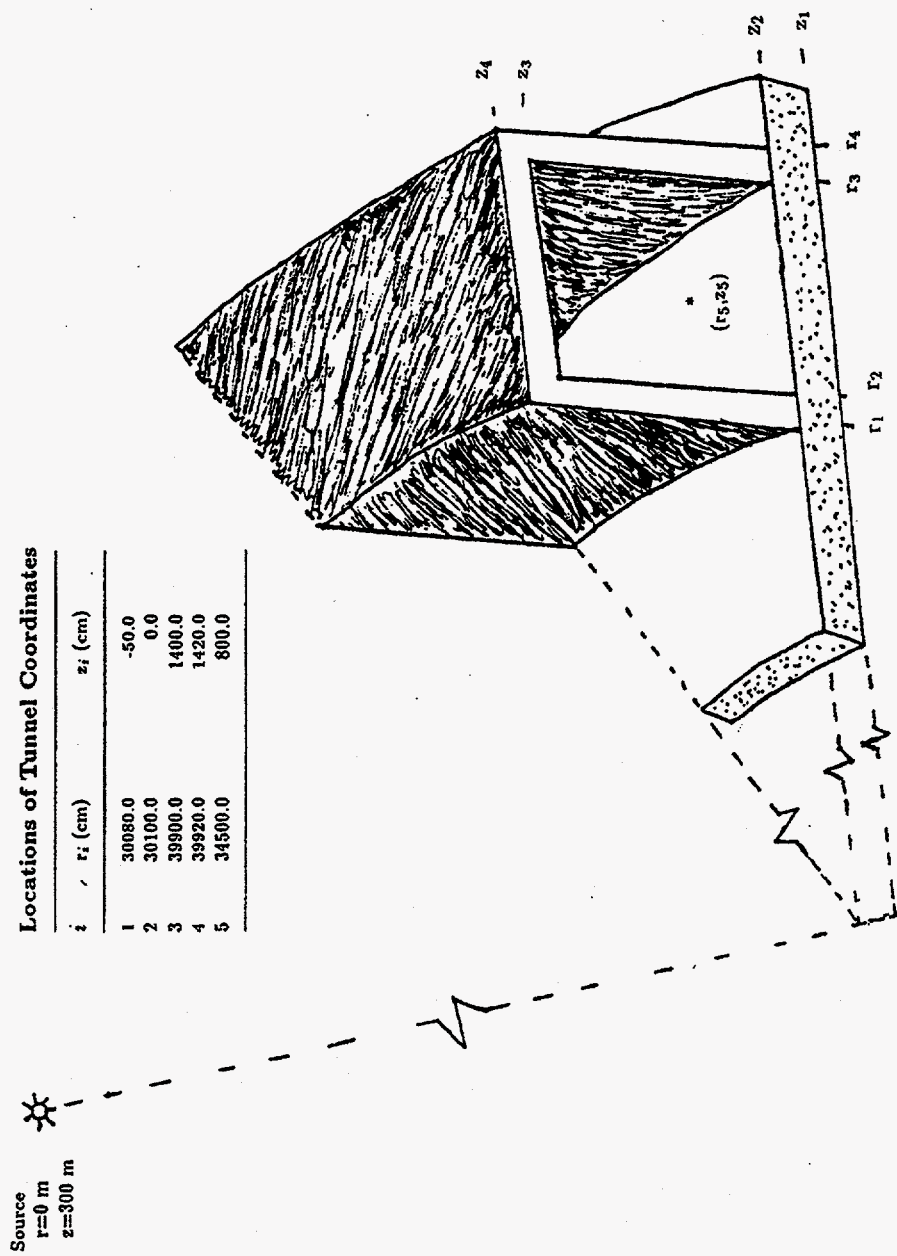


Figure D-6. Sketch of the Geometry for Test Problem 5: Large-Radius, Air-Filled, Annular, Cylindrical Concrete Tunnel.

Table D-1. Comparison of DORT and DRC2 Calculated Fluxes for Test Problem 1: Free-Field Fluence Calculation

Range (cm)	Orientation (degrees)	DORT Fluence/DRC2 Fluence	
		With No X-Y Dependence	With X-Y Dependence
Case 1 (240 Directions: 25,000 Histories)			
24556	45	0.999(.030)*	0.999(.030)
24556	270	1.009(.027)	1.009(.027)
33000	60	1.008(.035)	1.008(.035)
33000	210	1.036(.029)	1.036(.029)
42500	150	0.994(.021)	0.994(.021)
42500	330	1.040(.018)	1.040(.018)
24500	45	0.999(.030)	0.999(.030)
24500	270	1.009(.027)	1.009(.027)
34500	60	1.004(.034)	1.004(.034)
34500	210	1.032(.029)	1.032(.029)
44417	150	0.960(.024)	0.960(.024)
44417	330	1.008(.020)	1.008(.020)
Case 2 (240 Directions: 105,000 Histories)			
24556	45	1.001(.014)	1.001(.014)
24556	270	1.021(.013)	1.021(.013)
33000	60	1.003(.012)	1.003(.012)
33000	210	1.011(.013)	1.011(.013)
42500	150	1.037(.011)	1.037(.011)
42500	330	1.020(.010)	1.020(.010)
24500	45	1.000(.014)	1.000(.014)
24500	270	1.021(.013)	1.021(.013)
34500	60	0.998(.012)	0.998(.012)
34500	210	1.007(.013)	1.007(.013)
44417	150	1.010(.011)	1.010(.011)
44417	330	0.993(.011)	0.993(.011)

*Fractional standard deviations are shown in parentheses.

Table D-2. Comparison of DRC2 Calculated Protection Factors
for Test Problem 2: Metric Doghouse

Range (cm)	Orientation (degrees)	DRC2 Protection Factors		% Difference
		With No X-Y Dependence	With X-Y Dependence	
Case 1 (INGB=0)				
24556	45	2.715	2.718	0.11
24556	270	1.912**	1.908	-0.21
33000	60	2.576	2.574	-0.08
33000	210	2.104	2.104	-
42500	150	2.261	2.258	-0.13
42500	330	2.373	2.368	-0.21
Case 2 (INGB=1)				
24556	45	2.798	2.797	-0.04
24556	270	1.883**	1.880	-0.16
33000	60	2.643	2.642	-0.04
33000	210	2.062	2.060	-0.10
42500	150	2.302	2.298	-0.17
42500	330	2.375	2.371	-0.17

$$* \left(\frac{x - y \text{ dep}}{\text{no } x - y \text{ dep}} - 1 \right) \times 100.$$

**DRC calculated a protection factor of 1.913.

***DRC calculated a protection factor of 1.884.

Table D-3. Comparison of DRC2 Calculated Neutron and Gamma-Ray Tissue Dose Protection Factors for Test Problem 3: Large Steel-Topped Concrete Building

Range (m)	Orientation (degrees)	Protection Factors (tissue dose)		
		With No X-Y Dependence	With X-Y Dependence	% Difference*
Neutron				
26.73	0	2.997	2.774	-7.44
26.73	172.5	2.700	2.986	10.6
150	0	4.077	4.131	1.32
150	90	2.769	2.792	0.83
150	180	3.194	3.127	-2.1
150	270	3.797	3.821	0.63
300	0	4.026	4.090	1.59
300	90	2.422	2.399	-0.95
300	180	3.088	2.939	-4.83
300	270	3.624	3.588	-0.99
Gamma Ray				
26.73	0	39.41	39.88	1.19
26.73	172.5	21.33	26.48	24.1
150	0	36.53	37.46	2.55
150	90	12.60	13.39	6.27
150	180	16.27	18.30	12.5
150	270	25.79	25.90	0.43
300	0	33.33	34.07	2.22
300	90	6.630	6.742	1.69
300	180	13.45	12.04	-10.5
300	270	16.04	15.56	-2.99

$$* \left(\frac{\text{x - y dep}}{\text{no x - y dep}} - 1 \right) \times 100.$$

Table D-4. Comparison of DRC2 Calculated Neutron Tissue Dose Protection Factors for Test Problem 3: Large Steel-Topped Concrete Building

	Orientation (degrees)	Neutron Tissue Dose*		% Difference**
		With No X-Y Dependence	With X-Y Dependence	
26.73	0	4.035-2***	4.157-2	3.02
26.73	172.5	4.475-2	4.215-2	-5.81
150	0	5.297-3	4.822-3	8.97
150	90	8.123-3	8.081-3	-0.52
150	180	6.966-3	7.702-3	10.6
150	270	5.757-3	5.673-3	-1.46
300	0	8.580-4	7.918-4	-7.72
300	90	1.517-3	1.539-3	1.45
300	180	1.164-3	1.308-3	12.4
300	270	9.742-4	9.790-4	0.49

*The free-field doses are 1.323-1, 2.499-2, and 4.079-3 at 26.73m, 150m, and 300m, respectively. With the detector located about 550 cm from the vehicle system rotation point, the x-y dependent free-field dose varies from 7.6% below to 8.2% above the reference values, the largest variations being for 0- and 180-degree rotations.

$$** \left(\frac{\text{x-y dep}}{\text{no x-y dep}} - 1 \right) \times 100.$$

***Read as 4.035×10^{-2} .

Table D-5. Comparison of DRC2 Calculated
Soft Tissue Kerma Total Protection Factors
for Test Problem 4: BREN Six-House Cluster

Range (m)	Orientation (degrees)	Soft Tissue Kerma Total Protection Factor		% Difference*
		With No X-Y Dependence	With X-Y Dependence	
700	0	1.509	1.481	-1.86
700	90	1.682	1.632	-2.97
700	180	3.378	3.349	-0.86
700	270	1.825	1.780	-2.47
1000	0	1.341	1.352	0.82
1000	90	1.836	1.817	-1.03
1000	180	4.514	4.472	-0.93
1000	270	2.244	2.191	-2.36
1500	0	1.098	1.095	-0.27
1500	90	1.846	1.826	-1.08
1500	180	5.824	5.682	-2.44
1500	270	3.009	2.922	-2.89
2000	0	0.945	0.939	-0.63
2000	90	1.824	1.804	-1.10
2000	180	6.596	6.393	-3.08
2000	270	3.654	3.597	-1.56

$$* \left(\frac{\text{x - y dep}}{\text{no x - y dep}} - 1 \right) \times 100.$$

Table D-6. Comparison of DRC and DRC2 Calculated
Soft Tissue Kerma Protection Factors for
Test Problem 4: BREN Six-House Cluster

Range (m)	Orientation (degrees)	Soft Tissue Kerma Total Protection Factor		
		DRC	DRC2	% Difference*
700	0	1.506	1.481	-1.66
700	90	1.680	1.632	-2.86
700	180	3.372	3.349	-0.68
700	270	1.822	1.780	-2.31
1000	0	1.339	1.352	0.97
1000	90	1.832	1.817	-0.82
1000	180	4.506	4.472	-0.75
1000	270	2.241	2.191	-2.23
1500	0	1.096	1.095	-0.09
1500	90	1.843	1.826	-0.92
1500	180	5.813	5.682	-2.25
1500	270	3.003	2.922	-2.70
2000	0	0.943	0.939	-0.42
2000	90	1.821	1.804	-0.93
2000	180	6.584	6.393	-2.90
2000	270	3.647	3.597	-1.37

$$* \left(\frac{\text{DRC2}}{\text{DRC}} - 1 \right) \times 100.$$

Table D-7. Comparison of DRC and DRC2 Calculated Soft Tissue Kerma for Test Problem 4: BREN Six-House Cluster

Soft Tissue Kerma*				
Range (m)	(degrees)	DRC	DRC2 (X-Y dep)	% Difference**
700	0	9.23+2***	9.73+2	5.42
700	90	8.28+2	8.72+2	5.31
700	180	4.12+2	4.01+2	-2.67
700	270	7.63+2	7.65+2	0.26
1000	0	2.78+2	2.86+2	2.88
1000	90	2.03+2	2.10+2	3.45
1000	180	8.26+1	8.07+1	-2.30
1000	270	1.66+2	1.67+2	0.60
1500	0	4.44+1	4.59+1	3.38
1500	90	2.64+1	2.72+1	3.03
1500	180	8.36+0	8.32+0	-0.48
1500	270	1.62+1	1.64+1	1.23
2000	0	8.29+0	8.58+0	3.50
2000	90	4.29+0	4.42+0	3.03
2000	180	1.19+0	1.19+0	—
2000	270	2.14+0	2.14+0	—

*The DRC2-calculated free-field kerma values are 1393, 372.9, 48.7, and 7.831 at 700m, 1000m, 1500m, and 2000m, respectively. They differ slightly from the DRC values because of logarithmic versus linear interpolation in the Z direction. The x-y dependent values vary from about 2% below to 3.5% above the reference values.

** $\left(\frac{\text{DRC2}}{\text{DRC}} - 1 \right) \times 100.$

***Read as 9.23×10^2 .

Table D-8. Comparison of DRC2 and DORT Calculated Fluences and Doses for Test Problem 5: Large-Radius, Air-Filled, Cylindrical Concrete Tunnel

DORT Calculation		
Calculated Quantity	Perturbed	Unperturbed
Neutron Fluence	4.225+3 ^a	7.263+4
Gamma-Ray Fluence	3.960+3	3.881+4
Neutron dose	7.335-5	1.361-3
Gamma-Ray Dose	4.387-5	4.243-4

DRC2 with 10.8-m-Thick Air Layer		
Calculated Quantity	With No X-Y Dependence	With X-Y Dependence
Neutron Fluence	3.911+3[0.026](0.93) ^b	4.035+3[0.027](0.96)
Gamma-Ray Fluence	4.010+3[0.066](1.04)	4.209+3[0.067](1.06)
Neutron Dose	6.761-5[0.035](0.92)	6.975-5[0.034](0.95)
Gamma-Ray Dose	4.295-5[0.066](0.98)	4.408-5[0.066](1.00)

DRC2 with 50.0-m-Thick Air Layer		
Calculated Quantity	With No X-Y Dependence	With X-Y Dependence
Neutron Fluence	3.650+3[0.042](0.86)	4.228+3[0.044](1.00)
Gamma-Ray Fluence	3.342+3[0.062](0.84)	3.971+3[0.068](1.00)
Neutron Dose	5.490-5[0.034](0.75)	6.903-5[0.060](0.94)
Gamma-Ray Dose	3.730-5[0.078](0.85)	4.506-5[0.085](1.03)

^aRead as 4.225 x 10³.

^bFractional standard deviations are in brackets and ratios of DRC2 to DORT quantities are in parentheses.

Table D-9. Maximum Percent Differences Between the Above-Ground Perturbed and Unperturbed Neutron and Gamma-Ray Total Fluences as a Function of a Leakage Surface for Test Problem 5: Large-Radius, Air-Filled, Cylindrical Concrete Tunnel.

Leakage Surface	Maximum Percent Difference in Fluences*	
	Neutron	Gamma-Ray
Inner Radial		
10.8-m Air Layer	10.5	3.3
50.0-m Air Layer	0.4	1.2
Outer Radial		
10.8-m Air Layer	39.0	47.6
50.0-m Air Layer	9.3	14.2
Top		
10.8-m Air Layer	8.8	15.2
50.0-m Air Layer	-1.4	6.7

$$* \left(\frac{\text{Unperturbed Fluence}}{\text{Perturbed Fluence}} - 1 \right) \times 100.$$

APPENDIX E
MASH 1.5 CODE SYSTEM ABSTRACT

MASH 1.5 CODE SYSTEM ABSTRACT

1. NAME AND TITLE

MASH 1.5 - A Monte Carlo Adjoint Shielding Code System

2. COMPUTER FOR WHICH PROGRAM IS DESIGNED

MASH was originally developed on a Cray computer (Cray X-MP, Cray Y-MP, and Cray 2). MASH 1.5 has been developed and tested on an IBM RISC 6000 Workstation. Since it can operate with minimal machine-dependent coding or explicit subroutine library calls, (e.g., random number package for MORSE, date and time routines for MORSE and DRC2), it should be portable and operable on other UNIX based workstations with sufficient memory and disk storage.

3. NATURE OF PROBLEM SOLVED

MASH calculates neutron and gamma-ray environments and radiation protection factors for armored military vehicles, structures, trenches, and other shielding configurations. The principal application is to determine the radiation shielding characteristics of armored vehicles from prompt radiation due to a nuclear weapon detonation. MASH 1.5, however, can be used to analyze the effects of fallout fields and radiological warfare threats for uniformly distributed sources. The shielding effectiveness can be characterized for both personnel and electronic equipment as a function of weapon detonation height, source/target ground range, and vehicle orientation and configuration.

4. METHOD OF SOLUTION

The discrete ordinates calculation determines the fluence on a coupling surface surrounding the shielding geometry due to an external neutron/gamma-ray source. The Monte Carlo calculation determines the effectiveness of the fluence at that surface in causing a response in a detector within the shielding geometry, i.e., the "dose importance" of the coupling surface fluence. A coupling code folds the fluence together with the dose importance, giving the desired dose response. The coupling code can determine the dose response as a function of the shielding geometry orientation relative to the source, distance from the source, and energy response of the detector.

The code system includes the GRTUNCL and DORT codes for air-over-ground transport calculations, the MORSE code with the GIFT5 combinatorial geometry package for adjoint shielding calculations, and several peripheral codes that perform the required data preparations, transformations, and coupling functions. MASH 1.5 is an improved and enhanced version of the previously released MASH 1.0 code system developed at Oak Ridge National Laboratory (ORNL).

5. RESTRICTIONS OR LIMITATIONS

MASH is a modular code system made up of several codes, each with their own set of restrictions and limitations. System requirements include a FORTRAN and C compiler, a VGA graphics board and monitor, and a large (>500 Mbytes) disk storage area. Most of the modules utilize dynamic dimensioning, however, MORSE and DRC2 use a large

container array in Blank Common to accommodate this. Typically, machine size and disk storage space will provide the overall limit.

6. TYPICAL RUNNING TIME

Since a typical MASH problem involves running a sequence of codes, quantifying total running time is difficult. The running time varies depending on the complexity of the problem. The two modules in MASH requiring the bulk of the running time are DORT and MORSE. Typical DORT run times for a 800 meter by 800 meter air-over-ground calculation with 240 angles and 69 energy groups is approximately 2.0 hours CPU on an IBM RISC 6000 590H Workstation. A typical adjoint MORSE analysis of a vehicle with approximately 300 bodies and 300 regions requires approximately 2 hours of CPU time to obtain adequate statistics on the integral results.

7. RELATED AND AUXILIARY PROGRAMS

MASH is a modular code system made up of a collection of programs. These codes include:

GIP	Cross-section input preparation
GRTUNCL	Analytic first collision source code
DORT	Two dimensional discrete ordinates transport code
VISTA	Vehicle input source transformation and assembly code
MORSE	A general purpose Monte Carlo multigroup neutron and gamma-ray transport code system with the GIFT combinatorial geometry package
DRC2	A detector response code

8. STATUS

MASH Version 1.5 available on IBM RISC 6000 Workstation - June 1996

9. REFERENCES

1. J. O. Johnson, editor, "A User's Manual for MASH 1.0 - A Monte Carlo Adjoint Shielding Code System," ORNL/TM-11778, Oak Ridge National Laboratory, (March 1992).
2. J. O. Johnson, editor, "A User's Manual for MASH 1.5 - A Monte Carlo Adjoint Shielding Code System," ORNL/TM-11778/R1, Oak Ridge National Laboratory, (June 1997).
3. W. A. Rhoades and R. L. Childs, "The DORT Two-Dimensional Discrete- Ordinates Transport Code," Nuclear Science & Engineering 99, 1, pp. 88-89, (May 1988).
4. M. B. Emmett, "The MORSE Monte Carlo Radiation Transport Code System." ORNL-4972 (February 1975); ORNL-4972/R1 (February 1983); ORNL 4972/R2, Oak Ridge National Laboratory, (July 1984).
5. Lawrence W. Bain, Jr. and Mathew J. Reisinger, "The GIFT Code User Manual; Volume I. Introduction and Input Requirements," BRL 1802, Ballistic Research Laboratory, (July 1975).

10. COMPUTER HARDWARE REQUIREMENTS

MASH is a modular code system made up of several codes, each with their own set of computer hardware requirements. All of the modules are designed to be applicable to most full-scale computers that support direct (random) access disk storage or the equivalent. Machine-dependent features such as calls to system-dependent subroutines are restricted to interchangeable interface packages. The code originators maintain a configuration for the IBM RISC 6000 Workstation only.

11. COMPUTER SOFTWARE REQUIREMENTS

MASH is a modular code system made up of several codes, each with their own set of computer software requirements. The code system can be operated with 100% FORTRAN language on UNIX Workstations. All of the modules are designed to use the any FORTRAN 77 compiler and C compiler. External data storage must be provided for up to 9 scratch files, of which 5 must be direct (random) access. User-supplied input and output data files must be supplied on sequential-access devices, i.e., tapes or the equivalent. Library calls are used for job timing, etc., but they can be deleted.

12. OPERATING SYSTEM

MASH currently only operates under the IBM RISC UNIX operating system using the standard libraries. Since the code system is all FORTRAN, operation under other UNIX operating systems should be possible with little conversion effort.

13. CONTRIBUTORS

MASH was created by:

M. B. Emmett, W. A. Rhoades, R. L. Childs, and J. O. Johnson
Oak Ridge National Laboratory

W. H. Scott, Jr., J. A. Stoddard, D. C. Kaul, and S. D. Egbert
Science Applications International Corporation

Note: There are numerous other contributors to the various codes which make up the MASH code system. They are recognized in the literature associated with each individual code.

14. POINT OF CONTACT

Dr. Jeffrey O. Johnson, Applied Physics Group Leader
Computational Physics and Engineering Division
Nuclear Analysis and Shielding Section
Oak Ridge National Laboratory
P. O. Box 2008, MS-6363
Oak Ridge, Tennessee 37831-6363
Ph. (423) 574-5262, Fax (423) 574-9619
E-mail: joj@ornl.gov

15. CONTENTS OF CODE PACKAGE

- Source Programs
- User's Manual

16. DATE OF ABSTRACT

June 1997

17. KEYWORDS

TRANSPORT, NEUTRONICS, SHIELDING, DISCRETE ORDINATES,
MONTE CARLO, CRAY

18. SPONSOR

MASH development was sponsored by:

Defense Special Weapons Agency, U. S. Army National Ground Intelligence
Center, and the U. S. Department of Defense

APPENDIX F
USER NOTES

USER NOTES

INTRODUCTION

In order to assess the quality of the computational shielding efforts at ORNL, it is first necessary to explore the philosophies used by ORNL to solve problems of the class under consideration. The solution of the air-over-ground problem using the discrete ordinates method requires expert and experienced code users. The same can be said for the solution of the adjoint Monte Carlo formulation for the dose components leaving a complicated shield geometry.

In this appendix, a series of questions and answers are given in regards to the application of the MASH code system to a particular problem. For illustrative purposes only, the problem alluded to in the discussion is the sample problem included in this manual. When references to the attached input listings are noted in the discussion, the reader should consult that section of this manual to see the example.

The questions come from a novice user of the MASH code system with a background in Nuclear Engineering and a basic understanding of the physics and underlying principles of the methodology. The responses to the questions are those of the editor of this manual only. They are not meant to represent the philosophy of ORNL as a whole. They are simply based on his experience in using the MASH code system.

The purpose of the following questions is to qualify the "rules of thumb" being followed at ORNL, and to try to stimulate critical thought along the lines of discovering flaws or weaknesses in any part of the methodology being followed.

QUESTIONS AND ANSWERS ON AIR-OVER-GROUND ENVIRONMENT CALCULATIONS WITH GRTUNCL/DORT

1. Q: What library of cross sections is currently being used? What weighting function was chosen for preparing this library? Why was it chosen? Do you have any comments or concerns about the quality of the library? Do you suspect any particular data to be weak?

A: The library currently being utilized in the MASH analysis is the reference DNA DABL69 69 group (46n/23 γ) cross-section library. This library has three weighting functions, only one of which was used for all materials. The standard weighting function is a smoothly varying function consisting of a 300 K Maxwellian, a 1.4 MeV fission spectrum, and a 14.07 MeV fusion peak spectrum overlaid on a 1/E slowing-down spectrum. This is the weighting function I use for all my analysis. A fission source through infinite air spectrum was used to collapse additional sets of hydrogen, oxygen, and nitrogen data, and inverse of energy times the total cross section of type-304 stainless steel spectrum, $1/(E\Sigma_T)$, was used to collapse the major constituents of steel for use in deep penetration problems

involving ferrous materials. Since the cross sections collapsed using the infinite air spectrum were extracted at a distance of 2000 meters, I did not use them for the APRF experiments being performed at 170 and 400 meters. Should I end up doing calculations at distances approaching 2000 meters, I would use these cross sections to mix my air material. Likewise, for most of the armored vehicle analysis (to date), the armor has not been sufficiently thick enough to consider the problem a "deep penetration" problem. Therefore, I use the standard weighted materials for my steel components. Additional information on the details of the library can be obtained from:

D. T. Ingersoll, R. W. Roussin, C. Y. Fu, and J. E. White, "DABL69: A Broad-Group Neutron/Photon Cross-Section Library for Defense Nuclear Applications," ORNL/TM-10568, Oak Ridge National Laboratory, (June 1989).

2. Q: What is your philosophy for choosing radial mesh spaces from the source? How far beyond the target vehicle do you think the calculation should go? Have you checked this out? Do you increase the mesh detail in the vicinity of the target? If so, how? If not, why not? What is your philosophy for choosing axial mesh spaces from lower ground body? How high do you think the calculation should go? Have you checked this out? Do you have a mesh size transition between the ground and the air? Do you increase the mesh detail in the vicinity of the target? If so, how? If not, why not? Please list example data.

A: My current philosophy for choosing radial and axial mesh utilizes a conservative variant of the "square-root of two" rule. In discrete ordinates as you know, you should not let your fluence change by more than a factor of two between mesh cells. Since in air transport, the dominant component of fluence attenuation is geometric attenuation ($1/R^2$), you can set your mesh by choosing an initial cell size for the source, and multiplying this cell by the square root of two (i.e., 1.414) to obtain the boundary for the next cell. I use a slightly conservative approach and use 1.3 as my factor. I allow the mesh cell size to increase until it reaches a maximum size of 20 to 30 meters. For radial mesh, this procedure only has to be performed once (for a centrally located point source). For axial mesh, this procedure has to be performed twice (above and below the source location) for a point source. Furthermore, tighter mesh are used at the air/ground interface. I gradually increase the ground axial mesh spacing from a starting value of 0.5 cm until I reach a maximum size of approximately 5 cm. I usually extend approximately twice the distance from the source to the target (i.e., 400 meters beyond the 400 meter test site for a total distance from source of 800 meters), with a minimum distance beyond the target of approximately 300 meters. This distance is beyond the longest mean free path in air and more than sufficient. Axially, I usually make the dimension equal to the radial dimension. Consequently, for an 800 meter radial distance, I have an 800 meter axial distance. This will incorporate all the skyshine contribution to the dose at the 400 meter test site. I have run cases with only a 400 meter height since the APRF source is at approximately 16 meters. The difference between using 400 and 800 meter source heights was less than 2% due to the contribution from low energy gammas not accounted for in the smaller axial case. Likewise, additional cases using more mesh beyond the target showed insignificant changes relative to the currently used 400 meter case. Near the target/experiment positions, I usually gradually decrease the radial mesh cell until the cell containing

the target is only approximately 10 meters wide in the radial direction. The fluence does not change that significantly over the 10 meter interval (at 400 meters) and consequently the single mesh point folding algorithm in DRC will not cause a significant perturbation. In the axial direction, I usually place the first few air intervals above the ground at approximately 1 meter intervals until I reach a few meters above the top of the vehicle or intersect the 1.3 rule coming from the source. If the 1.3 rule does not become a factor, I will gradually increase the axial mesh until it blends in smoothly with that mesh generated with the 1.3 rule. A sample GRTUNCL and DORT listing is attached for the analysis of the Two-meter box at APRF.

3. Q: Which fluence solution option do you use, diamond-difference with negative fluence fix-up, or others? Why? Do you check the solution against any of the other options?

A: I use the Θ -weighted fluence solution in DORT. According to W. A. Rhoades, this solution has shown the least sensitivity to irregular mesh problems and the most stability. It does not guarantee the fluence solution regardless of mesh, but appears to allow a little more freedom. This has been the only fluence solution option I have used. J. V. Pace, III has used zero-weighted in the past, but I do not know if he did any comparison studies.

4. Q: What angular quadrature set do you use? Who prepared it? What philosophy was used in preparing it?

A: The current angular quadrature set being used is a 240 angle set, derived from a symmetric S_8 quadrature set, by subdividing each angle into five angles in each of the polar directions. This still yields a symmetric quadrature set, except now there are more polar angles to reduce quadrature streaming effects (ray effects) in the secondary gamma ray component. I believe the originator of this quadrature set is J. V. Pace and it came out of his extensive air-over-ground work on the Hiroshima-Nagasaki dose re-assessment program.

5. Q: What is your philosophy concerning the allowable aspect ratios of the mesh spaces in the radial to axial directions? Do you have any concerns about the accuracy of the diamond-difference average when the aspect ratio is large? If the mesh is variable; do you have any concerns about cumulative truncation errors? Have you ever checked this problem out? Please list some of the aspect ratios used in the vicinity of the target.

A: I have not really developed a philosophy concerning the aspect ratios of the mesh spaces in the axial and radial directions. Based on the rules discussed in regards to questions 2 and 3, and the use of the Θ -weighted fluence option, I look for fluence profiles which appear reasonable for the problem and do not violate the principals governing discrete ordinates calculations. I realize the large radial mesh in the ground will cause the fluence profile to not conform, however, this aspect of the problem remains to be insignificant relative to the fluence profile in the air. I have relied extensively on the experience and expertise of J. V. Pace, III, and W. A. Rhoades since they have been performing air-over-ground analysis for many years

and have probably discovered and encountered most of the pitfalls associated with this particular type of analysis through executing many of the perturbations you are inquiring about now. Unfortunately, much of this expertise is inside their head and has not been documented. I believe my worst aspect ratio in the air in the vicinity of the target is ten (radial interval of 10 meters by an axial interval of 1 meter).

6. Q: For purposes of coupling to MORSE, the sidewise and backwards directions are important to the determination of the indirect dose to the target. For the forward-biased quadrature set being used, is there sufficient detail in these other directions to adequately determine this dose component? Has this been checked?

A: The current quadrature set is symmetric and therefore yields the same treatment of the sideways and backward directions as it does the forward directions. I believe there is sufficient detail to model these directions with the quadrature set currently being used. In an unrelated study, I performed a 20 group simulated box problem using a symmetric S_2 , S_4 , S_6 , S_8 , and S_{10} quadrature set. The results showed stability of the neutron dose for all quadrature sets above (and including) S_6 . I did not investigate the stability of the gamma ray dose.

7. Q: Do you have any opinion as to the value of doing a several-day calculation, with much more spatial detail, to provide a benchmark for the normal DORT runs?

A: The best way to answer many of these questions (and probably introduce a few more) would be to set up and execute a large air-over-ground problem with a consistent axial and radial mesh and with reasonable aspect ratios approaching one. Include sufficient mesh above and beyond the source and target to insure all skyshine and backward directed fluence is accounted for, and possibly, increase the angular quadrature to test the current quadrature set. Re-assess a problem for which the current air-over-ground has been performed and compare the two calculations. Such a calculation could (and probably would) prove useful towards lending credibility to the current problem setup being used.

8. Q: Do you have any concerns about the effects of non-uniform, partially wet and bumpy terrain? If so, do you have any suggestions of how to simulate this effect? Comment similarly with respect to trees and vegetation.

A: Preliminary scoping calculations investigated the effects of the APRF topography out to the 400 meter test site, and the effects of ground moisture and meteorological data (temperature, pressure, and relative humidity) on the air environment during measurements made at APRF. Integral and spectral MASH results showed differences less than 2% for the topography model analysis. Consequently, a simple topography model of the APRF source-to-400 meter test site was determined to be sufficient for the analysis. Partial wet conditions could not easily be simulated in the 2-D model. The mud puddles in close proximity to the target cause me a little concern (e.g., the free-field phantom was standing right behind and within 5 meters of a huge puddle of water). The only way of modeling the terrain, the trees and vegetation, and to some extent the puddles of water would be to go to a 3-D air-over-ground calculation. This could be performed with either TORT, MORSE, or possibly MCNP. Such an analysis would require a fairly accurate mapping of the environmental conditions at the time a particular measurement was made.

Furthermore, standardization of such a model would be extremely difficult in view of changes in between experiments, especially the mud puddles. A better solution would be to backfill the low area where standing water is a problem, and look to standardize the rest of the problem.

QUESTIONS AND ANSWERS ON ADJOINT MONTE CARLO CALCULATIONS WITH MORSE

1. Q: Where did the geometry model come from that is currently being used? How many bodies, etc.? Has the model been checked for missing regions, holes, etc.? Were any found? What geometry package was used to process the model?

A: The two-meter box geometry was modeled in the MORSE component of the MASH code system using the GIFT geometry package. J. M. Barnes modeled the box by using the engineering blue prints supplied by APRF. The box required 49 bodies, and twenty four regions to model it precisely as the drawings specified. A simpler representation could have been modeled with less bodies and retained the same amount of detail. The geometry was checked by the GIFT debugging tool, converted to MORSECG input and checked with JUNEBUG, and analyzed with the new geometry package being created by T. J. Burns. Results of a preliminary study determined all the details of the box (i.e., lift tabs, drain holes, etc.) made insignificant contributions to the calculation and therefore were omitted in the final computational geometry model. The hatches were retained in the computational model for potential open hatch experiments performed in the future. The walls and roof of the box were comprised of two plates of steel each 5.08-cm thick. This detail was retained in the geometry model for region dependent biasing in the Monte Carlo analysis.

2. Q: What is your philosophy for choosing the number of starters? How many were actually used? What was the number of secondaries created and followed? Have you checked any cases of a similar nature with considerably more starters?

A: The Monte Carlo (MORSE) calculation for the detector position generated and tracked 1,500,000 primary source particles (1500 batches of 1000 particles) sampled over the 69 energy groups. All starters were used, approximately one secondary particle was generated for each starter, and approximately one particle escaped (to be scored in DRC) for each starter. I do not believe any other cases were run with more starters than what I chose to run. My philosophy for choosing the number of starters depends to some extent on whether I am analyzing integral or spectral experimental data. For integral data, you can obtain a reasonable degree of convergence with much less histories than that required for spectral comparisons. In integral comparisons not all of the energy groups need to be converged; only those making a significant contribution to the total. For spectral comparisons, the majority of the energy groups should be converged (typically less than 5%) for confidence in the calculated spectrum. I have found that you can obtain statistics on your integral result less than 5%, and have statistics on your differential results (group fluences) greater than 10%. Care must be taken in this situation because you may analyze the same calculation, with the same number of starting particles,

using a different starting random number, and obtain an entirely different integral result with a statistical uncertainty less than 5%. In this case, even though your integral result is converged to within 5%, there is still too much deviation in the contributions from the individual groups. Consequently, your integral result is undersampled even though the fractional standard deviation (fsd) says it is converged. One final point should be made about the fsd's printed in the MORSE output. You can converge your MORSE calculation to within 1% for both your integral and differential data and still not obtain the correct answer. The final result regardless of the level of convergence is only as good as the accuracy of the MASH model.

3. Q: What philosophy do you use for source biasing? Why did you choose this? Please list example data. What exact geometry was used for the source and where was it positioned?

A: I did not use source biasing in this calculation except for energy biasing discussed in question 5 below.

4. Q: What source spectrum did you use? Why did you choose it?

A: The source spectrum was an angle (240 angles) and energy dependent (69 groups, 46n and 23 γ) source spectrum supplied by SAIC as a result of their recent analysis of the APRF reactor leakage. The input is supplied in the attached GRTUNCL input listing. Details about the source calculation can be obtained from:

D. C. Kaul and S. D. Egbert, "Radiation Leakage From The Army Pulse Radiation Facility (APRF) Fast Reactor," SAIC-89/1423, Science Applications International Corporation, San Diego, California, (May 1989).

5. Q: Do you use energy biasing? If so, describe the philosophy used to determine which groups should be biased and by how much. Please list example data.

A: An energy dependent relative importance factor is utilized over the 69 groups to increase the frequency of sampling the adjoint source particle from energy groups which have a significant effect on the dose response function. In this case, the response function is the free-in-air tissue dose response function. An example is given in the attached MORSE input stream. Obtaining a good source biasing function can be aided through the use of 1-D ANISN calculations which approximate the 3-D calculations as much as possible. The geometry for the source in the adjoint MORSE calculation is just a detector location (a point detector) located in the combinatorial geometry target description. The source in the DORT air-over-ground analysis was modeled as a small cylinder (5 cm in height x 5 cm in radius) positioned at R=0.0, and Z=16.143 meters.

6. Q: Do you use region biasing? If so, what philosophy do you use in picking the regions and region thicknesses? How do you set the bias factors and splitting

ratios? Why? What weight cutoffs do you use for Russian Roulette? Why? What kill fractions do you use, and why? Please give examples.

A: The secondary particle production probability (GWLO) was set to 1.0 for all regions and energy groups in the Monte Carlo calculations, and the in-group energy biasing option in MORSE was switched on. Region dependent and energy independent splitting and Russian Roulette parameters were utilized in the steel to improve the efficiency of the Monte Carlo calculations. This was accomplished by subdividing the 10.16-cm-thickness of steel into two equally thick concentric regions and assigning each of the steel regions different splitting and Russian Roulette parameters which would allow a sufficient number of source particles (and secondary particles) to escape to obtain reasonable statistics. This allowed nominally one escaping particle for each source particle generated. The process is pretty much a trial and error approach. The region thicknesses to some extent were (and will be) set by the geometry data. You do not want to add additional regions to the geometry (unless the geometry is relatively simple) for the sole purpose of performing region dependent biasing. For complicated geometries, this task is impossible. You have to choose an initial kill-to-survival ratio (i.e., 10 to 1, 5 to 1, etc.) and then utilize the geometry data, source data, and energy biasing data to generate a biasing scheme. In MASH, the object is to obtain escaping particles in the energy groups which will make a significant contribution to the dose. Therefore, you want to set up your biasing scheme to maximize your leakages. This will require you to constantly change your biasing parameters to insure you get approximately the same number of leakages as you had starters. You must be careful not to over-bias the problem and create a totally unreal distribution. You also must be careful that you do not end up with approximately the same number of leaking particles as source particles, but all in a very few groups. The only way to set up a biasing scheme for a coupled neutron and gamma ray adjoint calculation with source energy biasing and region dependent biasing is through trial and error because almost everything you do affects everything else. Furthermore, each calculation is sufficiently different enough to render you a novice each time you set up a biasing scheme.

7. Q: What criteria do you use to judge the quality of the resulting calculations? What FSD's do you look at? What values are deemed acceptable or unacceptable, and why? What do you do if you don't like the results?

A: I look at several aspects of the output to determine my confidence in a particular calculation. I will look at the balance tables printed at the end of each batch to see if they are all approximately the same. If they are, the calculation is fairly well behaved and you are not experiencing gross anomalies in the calculation to cause large swings in your batch results. I look at the balance tables (printed by group) to determine how the biasing (if used) is working, how the secondary particle production distribution is looking, and how the collisions are occurring within the different regions in the geometry (if there are different importance regions (relative to the biasing) specified. After the adjoint leakage tape has been folded with the forward fluence on the coupling surface, I look at the integral detector fsd's to determine whether the problem is converged. If the problem is symmetric, you can look at the effect of rotating the geometry through 0, 90, 180, and 270 degrees and look at the consistency among the four different answers you will receive. I then look at the individual group fsd's to see how well the group fluences are converged. If I have any misgivings, I may rerun the calculation and double the

number of starters to see if the results change. If they do not, then the original calculation probably had an adequate number of starters. If there are significant differences between the two calculations, I begin comparing the two calculations to find out whether it was a case of undersampling, or if some other problems exist. If I cannot resolve the problem as being a "Monte Carlo" problem, I will tear down the entire analysis from the cross section generation on up to make sure I did not make some input error or keypunch error which did not manifest itself in the form of an error message. As I stated earlier, I believe you must have differential (spectral) fsd's in the 5% to 10% range for all the groups contributing to the integral response; even though the integral results may yield 5% fsd's with 20% fsd's on the differential results. Once the fsd's get greater than 15%, I start to have my suspicions about the quality of that result. Unless cost is a factor, I will run the number of histories required to obtain adequate convergence of the differential results to insure adequate convergence of the integral results. This by no means is an iron-clad guarantee, but it helps reduce a source of discrepancy.

8. Q: Do you have any concerns about your current random number generator?

A: I utilize the IBM RISC 6000 random number generator and do not have any problems with this software.

9. Q: What is your philosophy for picking the size of the coupling surface? Have you compared small versus large surfaces? Describe what surface dimensions you use.

A: My current philosophy for picking the coupling surface is to make it a "glove" fit of the outside dimensions of your target geometry. This is primarily due to the single radius fluence coupling algorithm currently in use in DRC. When you use a large coupling surface, you will take into account the transport in the air from the radius at which the fluence is obtained to the edge of the coupling surface twice. This could yield differences greater than 5% if the coupling surface is large. For instance, in the two-meter box calculations, the coupling surface need only be slightly larger than the box itself since the transport through the air has already been accounted for in the forward DORT calculation. In my initial box calculations, I had a large coupling surface (approximately 20 meters on a side). DRC then folded fluences at 400 meters with escapes at distances between 390 meters and 410 meters. If the source would have been fairly isotropic, the size of the coupling surface would not have mattered. But for the APRF forward directed reactor source at 400 meters, the DRC coupling with a large coupling surface yielded answers lower than those obtained with a small coupling surface. The current coupling surface is only a few centimeters larger than the outside dimension of the box.

10. Q: Should a slightly different spectrum be used inside the vehicle? (To weight the library?) (For example, tuna-can tank DORT run to collapse cross-sections.)

A: Tailoring the cross-sections to fit the particular problem is always a good idea in any analysis when it is feasible to do so. However, for target vehicle analysis utilizing adjoint Monte Carlo and 2-D air-over-ground environments which are not truly indicative of reality, I am not sure the net effect would not be within the statistical uncertainty if not the uncertainty of the parameters utilized in the model.

Furthermore, you will be introducing another complicated step into a process that is already complicated for users who may or may not have the background to perform the task. I believe the analysis should be performed for the experimental comparisons exactly the way it will be performed once it is used in the fields. Then you have a true measure of its capabilities and limitations relative to how it will function on a day-to-day basis.

In summary, I must say that the only way to learn how to use MASH is to have a basic understanding of the underlying principals of the theory and then apply them to the problem. To fine tune a problem requires, to some extent, a trial and error approach using small test problems. You constantly tweak the input parameters and look at the effect on the summary counters. Understanding these effects takes experience and involves a constant learning process. Unfortunately, the information gleaned from one problem may not be applicable or helpful for another problem, even if they are similar. Eventually, you have to cut your losses and proceed with your setup as it is rather than continuously modifying it to obtain better efficiency.

INTERNAL DISTRIBUTION

1. J. M. Barnes
2. J. D. Drischler
3. D. T. Ingersoll
- 4-5 J. O. Johnson
6. R. A. Lillie
7. R. T. Santoro
- 8-9. CPED Reports Office
10. Laboratory Records Department
11. Laboratory Records, ORNL-RC
12. Document Reference Section
13. Central Research Library
14. ORNL Patent Section

EXTERNAL DISTRIBUTION

15. Director, Defense Special Weapons Agency
ATTN: WEP (Robert Kehlet)
6801 Telegraph Road
Alexandria, VA 22310-3398
- 16-17. Director, U.S. Army National Ground Intelligence Center
ATTN: IANG-TCN (Maj. Thaddeus Lewis)
220 7th Street NE
Charlottesville, VA 22902-5396
18. Defense Technical Information Center
002Cy ATTN: DTIC/FDAB
Cameron Station
Alexander, Virginia 22304-6145
- 19-20. Office of Scientific and Technical Information
P.O. Box 62
Oak Ridge, TN 37830